Handbook of Alternative Fuel Technologies

Handbook of Alternative Fuel Technologies

Sunggyu Lee
James G. Speight
Sudarshan K. Loyalka

CRC Press
Taylor & Francis Group
Boca Raton London New York

CRC Press is an imprint of the
Taylor & Francis Group, an **informa** business

CRC Press
Taylor & Francis Group
6000 Broken Sound Parkway NW, Suite 300
Boca Raton, FL 33487-2742

Printed in the United States of America on acid-free paper
10 9 8 7 6 5 4 3 2 1

International Standard Book Number-10: 0-8247-4069-6 (Hardcover)
International Standard Book Number-13: 978-0-8247-4069-6 (Hardcover)

Library of Congress Cataloging-in-Publication Data

Lee, Sunggyu.
Handbook of alternative fuel technologies / Sunggyu Lee, James G. Speight, and Sudarshan K. Loyalka.
p. cm.
Includes bibliographical references and index.
ISBN-13: 978-0-8247-4069-6 (alk. paper)
1. Fuel--Handbooks, manuals, etc. 2. Fuel switching--Handbooks, manuals, etc. 3. Power resources--Handbooks, manuals, etc. I. Speight, J. G. II. Loyalka, S. K. III. Title.

TP318.L388 2007
662'.6--dc22 2006024771

Visit the Taylor & Francis Web site at
http://www.taylorandfrancis.com

and the CRC Press Web site at
http://www.crcpress.com

Contents

Preface

Energy has always been the foremost resource that humans have relied on for survival and productive activities. Industrialization and technological advancement of modern society have also been possible through the effective use of energy. There is a strong correlation between the index for quality of life and energy consumption. Heightened economic strength of a country, technological prosperity of a society, higher production output of an industry, improved finances of a household, and increased activities of an individual are also realized by effective utilization of energy.

A number of important factors have historically dominated the trend, market, and type of energy utilization. These factors are: (1) resource availability, (2) convenience of energy utilization, (3) efficiency of conversion, (4) technological feasibility, (5) portability and ease of transportation, (6) sustainability, (7) renewability, (8) cost and affordability, (9) safety and health effects, and (10) environmental acceptance and impact. The technological success and prosperity of petrochemical industries in the 20th and early 21st centuries can largely be attributed to the vast utilization of fossil fuels, especially petroleum, as well as technological breakthroughs and innovations by process industries. Industry and consumers have seen and come to expect a wide array of new and improved polymeric materials and other chemical and petrochemical products. However, the fossil fuel resources upon which industry is heavily dependent are limited in available quantities and are expected to be close to depletion in the near future.

The unprecedented popularity and successful utilization of petroleum resources observed in the 20th century may have to decline in the 21st century owing to a lack of resource availability, thus making prospects for future sustainability seem grim. Public appetites for convenient fuel sources and superior high-performance materials are, however, growing. Therefore, additional and alternative sources for fuels and petrochemical feedstocks are not only to be developed further but are also needed for immediate commercial exploitation. Use of alternative fuels is no longer a matter for the future; it is a realistic issue of the present.

Additional and alternative sources for intermediate and final products, whether fuels or petrochemicals, directly contribute to the conservation of petroleum resources of the world by providing additional raw material options for generating the same products for consumers. Examples may include wood alcohol for methanol, corn fermentation for ethanol, biodiesel from soybean or algae, BTX (benzene, toluene, and xylenes) from coal, biogas or bioliquid from agricultural wastes, hydrogen as transportation fuel, bio-hydrogen from a variety of biological sources, jet fuel from shale oil or crop oil, Fischer–Tropsch fuel from coal or biomass, bisphenols from agricultural sources, liquid transportation fuels from a natural gas source by ZSM-type catalysis, ethylene/propylene via conversion of synthesis gas, use of coal-derived acetylene for petroleum-derived ethylene as a building block chemical, and liquid fuels from spent tires or mixed wastes, etc.

If usable energy or deliverable power is the final product to be desired, alternate sources for energy may strongly and directly affect the lifestyle of consumers, as well as their energy consumption patterns. A good example can be found in electric cars that are powered by powerful rechargeable batteries. These powerful batteries serve no use for conventional gasoline motors, whereas, in turn, premium gasoline is not needed in these electric cars. Another good example is the solar house whose climate control inside the house is provided only by solar energy. Other examples include LPG vehicles, dimethylether (DME) buses, hybrid cars, E-85 vehicles, hydrogen vehicles, solar-powered equipment and vehicles, wind energy powered equipment, and geothermal heating and cooling, etc.

During the past several decades, there has been a considerable increase in research and development in areas of environmentally acceptable alternative fuels. Synthetic fuels were of prime interest in the 1970s, due to a sudden shortage of petroleum supply kindled by an oil embargo in 1973, as well as public concern about dwindling petroleum reserves. Although synfuels seemed to be a most promising solution to the conservation of petroleum resources (or, at least, frugal use of the resources) and the development of additional sources for conventional liquid fuels, some of the focus has been shifted toward environmental acceptance of the fuel and the long-term sustainability of world prosperity in the last decade of the 20th century. Efforts have been made to reduce emissions of air pollutants associated with combustion processes whose sources include electric power generation and vehicular transportation. Air pollutants that have been targeted for minimization or elimination include SO_x, NO_x, CO_x, VOCs, particulate matters (PM), mercury, and selenium. These efforts have significantly contributed to the enhancement of air quality and associated technologies.

Concerns of global warming via greenhouse gases have further intensified the issue of environmental acceptance of fuel consumption. Combustion of fossil fuels inevitably generates carbon dioxide due to an oxidation reaction of hydrocarbon and carbonaceous materials. Carbon dioxide is known as a major greenhouse gas with emissions that need to be significantly reduced. Therefore, new developments in alternative fuels and energy have focused more on nonfossil sources or on mitigation and fixation of carbon dioxide in fossil fuel utilization. Renewable energy sources are certainly very promising due to their long-term sustainability and environmental friendliness. Of particular interest are solar (solar thermal and photovoltaic), wind, hydropower, tidal, and geothermal energies, in addition to biomass (wood, wood waste, plant/crop-based renewables, agricultural wastes, food wastes, and algae) and biofuels including bioethanol, biohydrogen, and biodiesel. It should be noted that hydropower is also regarded as a "conventional" energy source, as it has provided a significant amount of electrical energy for over a century. Government mandates, tax incentives, and stricter enforcement of environmental regulations are pushing environmentally friendly alternative fuels into the marketplace at an unprecedented rate.

The number of alternative-fueled vehicles in use in the world is expected to increase sharply. These alternative-fueled vehicles are powered by liquefied petroleum gas (LPG), liquefied natural gas (LNG), ethanol 85% (E85), methanol 85% (M85), electricity, neat methanol (M100), ethanol 95% (E95), dimethylether (DME), and hydrogen, among which hydrogen presently accounts for very little but is considered the

most promising by many. It should be noted that this list of alternative fuels in vehicles only represents the successful results of previous developments and does not include recent advances and breakthroughs in the field. Research and development efforts in alternative-fueled vehicles and utilization of renewable energy sources have intensified in the past few years. Alternative-fueled vehicles and emission-free cars are expected to gain more popularity, due in part to enforcement of stricter emission standards, the unmistakable fate of depletion for conventional transportation fuels, and numerous tax incentives for such vehicles. This intensified interest is coupled with the record-high prices of gasoline- and petroleum-based products experienced all over the world. Perhaps the key difference between the 1973 oil embargo era and the present is that this time around, efforts are likely to firmly latch-on to the roster of ongoing priorities most exigent to mankind.

Energy from wastes cannot be neglected as a valuable energy source. If effectively harnessed, energy from wastes, including municipal solid waste (MSW), agricultural refuses, plastics and spent tires, and mixed wastes can be employed to alleviate the current burden for energy generation from fossil fuel sources. Moreover, energy generation from wastes bears extra significance in reducing the volume of wastes, thus saving landfill space and utilizing resources otherwise of no value. Environmental aspects involving waste energy generation are to be fully addressed in commercial exploitation.

A great number of research articles, patents, reference books, textbooks, monographs, government reports, and industry brochures are published and referenced everyday. However, these literary sources are not only widely scattered and massive in volume, but they are also lacking in scientific consistency and technological comprehensiveness. Further, most of the published articles focus on the justification and potential availability of alternative fuel sources rather than environmental and technical readiness of the fuel as a principal energy source for the future postpetroleum era.

This handbook aims to present comprehensive information regarding the science and technology of alternative fuels and their processing technologies. Special emphasis has been placed on environmental and socioeconomic issues associated with the use of alternative energy sources, such as sustainability, applicable technologies, mode of utilization, and impacts on society.

Chapter 1 focuses on the current concerns in the area of consumption of conventional energy sources and highlights the importance of further development and utilization of alternative, renewable, and clean energy sources. This chapter presents past statistics as well as future predictions for each of the major conventional and alternative energy sources of the world.

Chapter 2 deals with the science and technology of coal gasification to produce synthesis gas. Synthesis gas is a crucially important petrochemical feedstock and also serves as an intermediate for other valuable alternative fuels such as methanol, dimethylether, ethanol, gasoline, diesel, and hydrogen. As the technology developed for gasification of coal has been widely modified and applied to processing of other fuel sources such as oil shale and biomass, details of various gasifiers and gasification processes are presented in this chapter.

Chapter 3 covers the science and technology of coal liquefaction for production of clean liquid fuels. All aspects of pyrolysis, direct liquefaction, indirect liquefaction,

and coal–oil coprocessing liquefaction are addressed in detail. This chapter has significant relevance to the production of alternative transportation fuels that can replace or supplement the conventional transportation fuels. The scientific and technological concepts developed for coal liquefaction serve as foundations for other fuel processes.

Chapter 4 deals with the science and technology of coal slurry fuels. Major topics in this chapter include slurry properties, hydrodynamics, slurry types, transportation, and environmental issues.

Chapter 5 discusses the liquid fuels obtained from natural gas. Special emphasis is also placed upon the Fischer–Tropsch synthesis whose chemistry, catalysis, and commercial processes are detailed.

Chapter 6 presents the science and technology of resids. Properties and characterization of resids as well as conversion of resids are detailed in this chapter.

Chapter 7 describes the occurrence, production, and properties of oil sand bitumen and the methods used to convert the bitumen to synthetic crude oil. Properties of the synthetic crude oil are also discussed.

Chapter 8 explores the science and technology of oil shale utilization. In particular, occurrence, extraction, and properties of oil shale kerogen are discussed. A variety of oil shale retorting processes as well as shale oil upgrading processes are described.

Chapter 9 focuses on the synthesis of methanol from synthesis gas. Chemical reaction mechanisms, catalysis, and process technologies of methanol synthesis are described.

Chapter 10 deals with the production of fuel ethanol from corn. The chapter elucidates the chemistry, fermentation, and unit operations involved in the production process. Moreover, the chapter discusses the environmental benefits of the use of ethanol as internal combustion fuel or as oxygenated additives.

Chapter 11 discusses the detailed process steps and technological issues that are involved in the conversion of lignocellulosic materials into fuel ethanol.

Chapter 12 deals with a variety of process options for energy generation from biomass. Biomass characterization, environmental benefits, and product fuel properties are also discussed.

Chapter 13 focuses on the energy generation from waste materials. Particular emphasis is placed on beneficial utilization of municipal solid wastes, mixed wastes, polymeric waste, and scrap tires.

Chapter 14 describes the occurrence, renewability, and environmentally beneficial utilization of geothermal energy. Geothermal power plants, district heating, and geothermal heat pumps are also discussed.

Chapter 15 deals with the science and technology of nuclear energy. The chapter describes nuclear reactor physics, nuclear fuel cycles, types of reactors, and electricity generation from nuclear reactors. Public concerns of safety and health are also discussed.

Chapter 16 presents the basic concepts of fuel cells. This chapter also describes a number of different types of fuel cells and their characteristics. Hydrogen production and storage are also discussed in this chapter.

This book is unique in its nature, scope, perspectives, and completeness. Detailed description and assessment of available and feasible technologies, environmental health and safety issues, government regulations, issues for research and development, and

alternative energy network for production, distribution, and consumption are covered throughout the book. For R & D scientists and engineers, this handbook serves as a single-volume comprehensive reference that will provide necessary information regarding chemistry, technology, and alternative routes as well as scientific foundations for further enhancements and breakthroughs.

This book can also be used as a textbook for a three credit-hour course entitled "Alternative Fuels," "Renewable Energy," or "Fuel Processing." The total number of chapters coincides with the total number of weeks in a typical college semester. This book may also be adapted as a reference book for a more general subject on fuel science and engineering, energy and environment, energy and environmental policy, and others. Professors and students may find this book a vital source book for their design or term projects for a number of other courses.

All chapters are carefully authored for scientific accuracy, style consistency, notational and unit consistency, and cross-reference convenience so that readers will enjoy the consistency and comprehensiveness of this book.

Finally, the authors are deeply indebted to their former graduate students, colleagues, and family members for their assistance, encouragement, and helpful comments.

Sunggyu Lee
James G. Speight
Sudarshan K. Loyalka

Authors

Sunggyu Lee is professor of chemical and biological engineering at the University of Missouri–Rolla. He is the author or coauthor of six books and over 400 archival publications. He received 23 U.S. patents in the field of chemical process technologies. He has advised more than 80 graduate students for their doctoral and master's degrees. He is also the editor of the *Encyclopedia of Chemical Processing*, published by Taylor & Francis. A specialist in chemical reaction kinetics and process engineering, and an active member of the American Institute of Chemical Engineers, Dr. Lee has designed more than 25 pilot, commercial, and demonstration plants, and advised companies such as B.F. Goodrich, Water Technologies Limited, and Northern Technology International Corporation. He received his B.S. (1974) and M.S. (1976) degrees in chemical engineering from Seoul National University, Korea, and his Ph.D. degree (1980) in chemical engineering from Case Western Reserve University, Cleveland, Ohio. He taught at the University of Akron for 17 years and also at the University of Missouri–Columbia for 9 years before joining the University of Missouri–Rolla in 2006.

James G. Speight has more than 38 years of experience in areas associated with the properties and recovery of reservoir fluids; the refining of conventional petroleum, heavy oil, and tar sand bitumen; the properties of fuels and synthetic fuels, including gas-to-liquids; natural gas; coal; and oil shale. He received his B.S. degree in chemistry and his Ph.D. in organic chemistry from the University of Manchester, England, where he was a research fellow in chemistry from 1965 to 1967. He served on the Alberta (Canada) Research Council from 1967 to 1980, and for the next four years was with Exxon Research and Engineering Company. At Western Research Institute he was chief scientific officer and executive vice president from 1984 to 1990 and chief executive officer from then until 1998, when he began focusing on consulting with CD&W, Inc., giving lectures on energy and environmental issues, and authoring work in his field. He has taught over 60 courses and has prepared more than 400 publications, reports, and presentations, including more than 25 books and bibliographies related to fossil fuel processing and environmental issues. He has been editor of *Petroleum Science and Technology* (founding editor); *Energy Sources. Part A: Recovery, Utilization, and Environmental Effects*; and *Energy Sources. Part B: Economics, Planning, and Policy.*

Academic posts include adjunct professor of chemical and fuels engineering, University of Utah and visiting professor at the University of Trinidad and Tobago, Technical University of Denmark (Lyngby), University of Petroleum (Beijing, China), University of Regina (Saskatchewan, Canada), and University of Akron (Ohio).

His awards include the Diploma of Honor, National Petroleum Engineering Society, 1995, for outstanding contributions to the petroleum industry; the Gold Medal, Russian Academy of Sciences, 1996, for outstanding work in the area of

petroleum science, 1996; Specialist Invitation Program Speakers Award, NEDO (New Energy Development Organization, Government of Japan), 1987 and 1996, for contributions to coal research; Doctor of Sciences degree, Scientific Research Geological Exploration Institute (VNIGRI), St. Petersburg, Russia, 1997, for exceptional work in petroleum science; Einstein Medal, Russian Academy of Sciences, 2001, in recognition of outstanding contributions and service in the field of geologic sciences; and the Gold Medal — Scientists Without Frontiers, Russian Academy of Sciences, 2005, in recognition of his continuous encouragement of scientists to work together across international borders.

Sudarshan K. Loyalka was educated at the Birla College of Engineering (now Birla Institute of Science and Technology), Pilani, India (B.S. Mech., 1964) and Stanford University, Palo Alto, California (M.S., 1965; Ph.D., 1967, in nuclear engineering). He has been on the faculty of the University of Missouri–Columbia since 1967 and is Curators' Professor of Nuclear and Chemical Engineering. His research interests are in transport theory, aerosol mechanics, the kinetic theory of gases, and neutron reactor physics and safety. He is a Fellow of both the American Physical Society (since 1982) and the American Nuclear Society (since 1985). He has published about 200 papers and has advised approximately 80 graduate students. Dr. Loyalka has received the David Sinclair Award (1995) of the American Association for Aerosol Research and the Glenn Murphy Award (1998) of the American Association for Engineering Education.

Contributors

Mihaela F. Ion
Nuclear Science and Engineering
University of Missouri–Columbia
Columbia, MO

H. Bryan Lanterman
DRS Technologies, Inc.
Alexandria, VA

Sunggyu Lee
Chemical and Biological Engineering
University of Missouri–Rolla
Rolla, MO

Sudarshan K. Loyalka
Nuclear Science and Engineering
University of Missouri–Columbia
Columbia, MO

James G. Speight
CD&W Inc.
Laramie, WY

1 Global Energy Overview

Sunggyu Lee

CONTENTS

1.1 WORLD ENERGY CONSUMPTION

World energy consumption has been steadily increasing for a variety of reasons, which include enhancements in quality of life, population increase, industrialization, rapid economic growth of developing countries, increased transportation of people and goods, etc. There are many types of fuel available worldwide, the demand for which strongly depends on application and use, location and regional resources, cost, "cleanness" and environmental impact factors, safety of generation and utilization, socioeconomic factors, global and regional politics, etc. The energy utilization cycle consists of three phases: generation, distribution, and consumption, all of which must be closely balanced for an ideal energy infrastructure. Any bottlenecking or shortage would immediately affect the entire cycle as a limiting factor. If there is a decrease in production of a certain type of fuel, the distribution and consumption of this specific fuel would also decrease; so that fuel switching from this type to another, as well as forced conservation becomes inevitable. Further, based on the supply and demand principle, the consumer price of this fuel type would undoubtedly rise. Even a breakdown in the transportation system of a certain fuel type would affect the consumer market directly, and consequences such as fuel shortage and price hike would be realized at least for a limited time in the affected region.

Table 1.1 summarizes world energy consumption for each of the principal fuel types from 1980 to 2003.[1] As shown, all these types have recorded steady increases for the period. Coal and hydroelectric power show the slowest increase in consumption for the period, whereas renewable and nuclear energy have recorded the steepest increases, indicating that these are the emerging energy sources with the greatest

TABLE 1.1
World Net Consumption of Primary Energy by Energy Type, 1980–2003

Energy Type	1980	1985	1990	1995	2000	2001	2002	2003
Petroleum (1000 barrels per day)	63,108	60,089	66,576	70,018	76,946	77,701	78,458	80,099
Dry natural gas (trillion cubic feet)	52.89	62.24	73.37	78.64	88.21	89.31	92.51	95.50
Coal (million short tons)	4,126	4,898	5,269	5,116	5,083	5,165	5,250	5,439
Hydroelectric power (billion kilowatt-hours)	1,722.8	1,953.6	2,151.7	2,461.3	2,651.8	2,559.6	2,619.1	2,654.4
Nuclear electric power (billion kilowatt-hours)	684.4	1,425.5	1,908.8	2,210.0	2,450.3	2,517.2	2,546.0	2,523.1
Geothermal, solar, wind, wood, and waste electric power (billion kilowatt-hours)	31.1	55.5	131.5	177.5	249.5	259.8	292.1	310.1

future in the world energy market. Coal and hydroelectric power, however, are more conventional and established, and the world will still have to depend on these for a long time. The higher rates of growth for renewable and nuclear energy consumption also show their strong potential as alternative fuels that ultimately will replace and supplement the conventional fuel types in a variety of applications and end uses.

Among the conventional fossil fuels, the increased consumption of natural gas outpaced the other fossil fuel types, i.e., coal and petroleum, for the period reported in Table 1.1. This is attributable to stronger demands for natural gas in industrial and residential heating, increased installations of natural-gas-based electric power plants, and new discoveries of large natural gas deposits. Several times in the 21st century, the world has experienced significant shortages and price hikes of natural gas, mainly due to imbalances between supply and demand.

1.2 U.S. ENERGY CONSUMPTION

Figure 1.1 shows the total U.S. energy consumption[2] in quadrillion Btu's. One quadrillion is 10^{15} which is equal to 1000 trillion. Based on the data, it is noted that U.S. total energy consumption has tripled over the past 50 years, i.e., from 1950 to 2000. Over the first 25 years of this period the increase was about 2.4 times, whereas it was about 1.3 times over the following 25 years. The slowdown of the pace of U.S. energy consumption was noticed immediately after the oil crisis of 1973. Many factors may have contributed to this: to name a few, increase in energy conversion efficiency, energy conservation across the board, energy efficient products, and even climates becoming milder due to global warming. However, if we consider separately the period from 1973 to 1988, for which total U.S. energy consumption was fairly

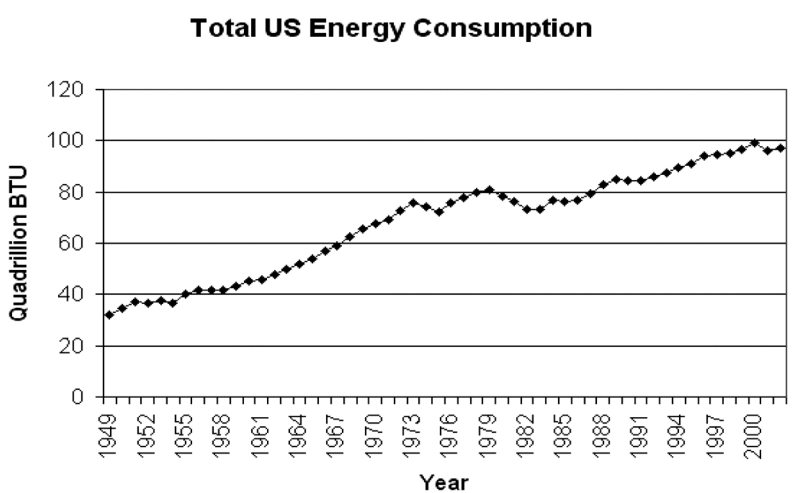

FIGURE 1.1 Total U.S. energy consumption. (From Web site by Maxwell School of Syracuse University, U.S. Energy Consumption, accessible through http://wilcoxen.cp.maxwell.syr.edu/pages/804.html. With permission.)

stable and did not change much, the recent rate of increase for the period from 1988 to 2000 was as steep as that for the initial 25 years, i.e., from 1950 to 1975. The period from 1973 to 1988 also coincides with the years when energy process development efforts in the U.S. were very active and public awareness of energy conservation was quite strong. During the 1990s, energy prices were stable, and research in energy process development took a backseat, partly due to the lack of immediate market competitiveness of alternative fuels. This was also the time when energy consumption sharply increased again in the U.S. as there was little fear of global energy crisis in the consumers' minds.

Figure 1.2 shows the past and projected data for U.S. energy consumption form 1980 to 2030.[15] The data are reported in quadrillion Btus. The information is obtained from the database developed by the Energy Information Administration (EIA), U.S. Department of Energy. The future projections show the following general trends:

1. Petroleum and coal will have steady increases in annual consumption.
2. Increases in consumption of natural gas and nuclear energy are likely to be mild.
3. Hydropower will remain at the current level.
4. Nonhydro renewable energy consumption will increase, but its market share will be still low.

The energy consumption pattern for the U.S. has been quite different from the rest of the world. Table 1.1 shows stronger growth was realized in renewable and nuclear energy sectors, which was not the case for the U.S. as shown in Figure 1.2. It should be also noted that the projections presented in Figure 1.2 were made in 2004 before another major crisis in petroleum. The record high petroleum crude oil price of 2006, as well as Hurricane Katrina of 2004 and its aftermath, will undoubtedly change the predictions of energy consumption in the U.S. from those presented

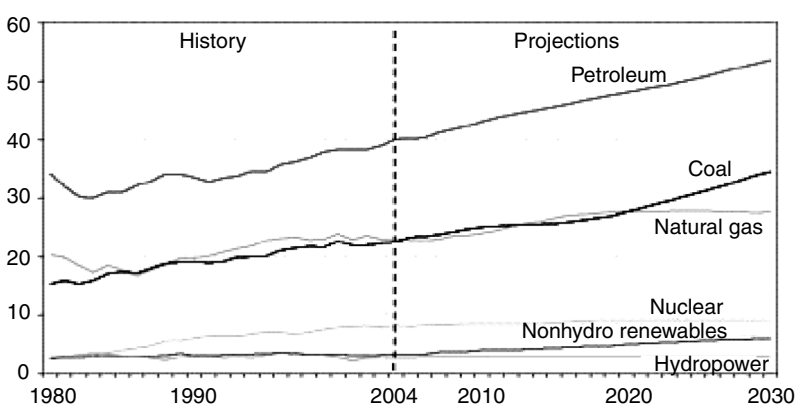

FIGURE 1.2 U.S. energy consumption by fuel types (1980–2030). (From Forecasts and Analyses, Energy Information Administration (EIA), U.S. Department of Energy, accessible through the Web site, http://www.eia.doe.gov/oiaf/forecasting.html. With permission.)

in Figure 1.2. In March 2003, the petroleum crude oil price on the global market was $31/bbl, whereas the price of crude oil topped $78/bbl in July 2006. In addition, the growth rate of ethanol as transportation fuel has been faster than anticipated. Further, a stronger case has recently been made for major R&D investments in the direction of a *hydrogen economy*. Therefore, a slower pace of petroleum consumption coupled with a substantially accelerated pace of renewable energy consumption will be part of the more likely scenarios for the future.

The energy crises of 1973 and 2005 were triggered by a shortage of petroleum crude supply in the global market, mainly driven by increased transportation fuel needs. The demand for alternative transportation fuels is growing stronger than ever. Cleaner-burning and more efficient fuels are going to be in high demands. Renewable energy that does not get depleted over the years will also receive strong attention. As an indication of this, ethanol from corn is gaining popularity very rapidly in the U.S. In 2006, many U.S. gas stations carry E85 (85% ethanol fuel) as a regularly available fuel product. People refer to this as a trend toward an *ethanol economy*.

1.3 PETROLEUM

Worldwide petroleum consumption data are summarized in Table 1.2 for the period from 1980 to 2003.[3] For this period, world petroleum consumption has grown at an average rate of 1.04% a year. Although this rate of increase may appear to be mild, it must be noted that petroleum resources are finite and can be depleted over years. Estimation of the years for which petroleum can be supplied and consumed at the current consumption rate has often been made by professionals and policymakers, but the numbers have been inconsistent and fluctuating from year to year. This uncertainty comes from the difficulty of estimating the future recoverable amount of petroleum from all the proved and unproved reserves. The Society of Petroleum Engineers (SPE) and the World Petroleum Council (WPC) have developed and approved several definitions of petroleum reserve-related terms to facilitate consistency among professionals using these terms[4]:

Proved reserves are those quantities of petroleum that, by analysis of geological and engineering data, can be estimated with reasonable certainty to be commercially recoverable, from a given date forward, from known reservoirs and under current economic conditions, operating methods, and government regulations. Proved reserves can be further categorized as *developed* or *undeveloped*.

Unproved reserves are based on geologic and engineering data similar to that used in estimates of proved reserves, but technical, contractual, economic, or regulatory uncertainties preclude such reserves being classified as proved. Unproved reserves may be further classified as *probable reserves* and *possible reserves*.

Probable reserves are those unproved reserves that an analysis of geological and engineering data suggests are more likely to be recoverable than not. If a probabilistic interpretation is to be given, there should be at least a

TABLE 1.2
World Petroleum Consumption, 1980–2003

Region/Country	1980	1985	1990	1995	2000	2001	2002	2003
Canada	1,873.0	1,526.0	1,746.5	1,818.5	2,027.0	2,042.9	2,079.4	2,193.3
Mexico	1,270.0	1,476.0	1,753.9	1,818.6	2,035.9	1,990.2	1,938.1	2,015.2
U.S.	17,056.0	15,726.0	16,988.5	17,724.6	19,701.1	19,648.7	19,761.3	20,033.5
North America	**20,203.8**	**18,732.4**	**20,495.0**	**21,369.3**	**23,771.8**	**23,689.7**	**23,786.7**	**24,250.3**
Argentina	499.0	415.1	413.0	453.4	510.9	474.4	438.3	450.0
Brazil	1,148.0	1,079.4	1,466.5	1,788.4	2,166.3	2,206.1	2,131.6	2,100.0
Venezuela	400.0	383.2	395.6	448.5	499.7	544.5	570.7	530.0
Central and South America	**3,613.4**	**3,225.7**	**3,760.6**	**4,459.1**	**5,230.0**	**5,343.2**	**5,261.6**	**5,243.4**
France	2,256.0	1,753.0	1,826.1	1,919.3	2,000.5	2,050.7	1,982.8	2,059.8
Germany	NA	NA	NA	2,882.2	2,771.8	2,814.6	2,721.2	2,677.4
East Germany	375.0	313.1	299.8	NA	NA	NA	NA	NA
West Germany	2,707.0	2,337.9	2,382.0	NA	NA	NA	NA	NA
Italy	1,934.0	1,705.0	1,873.8	1,942.1	1,853.8	1,836.8	1,870.1	1,874.4
Netherlands	792.0	610.0	734.5	767.3	855.4	893.1	899.2	920.0
Spain	990.0	858.0	1,010.1	1,189.4	1,433.2	1,492.3	1,506.9	1,544.3
Sweden	527.0	357.0	322.1	355.5	343.3	337.5	337.3	346.1
Turkey	314.0	359.0	477.0	608.3	666.9	618.6	657.7	652.9
U.K.	1,725.0	1,617.0	1,776.0	1,815.0	1,757.7	1,724.2	1,767.7	1,722.4
Western Europe	**14,322.0**	**12,295.1**	**13,306.2**	**14,160.7**	**14,667.8**	**14,833.1**	**14,819.1**	**14,950.6**

Former Czechoslovakia	355.0	300.1	284.3	NA	NA	NA	NA	NA
Former USSR	8,995.0	8,950.0	8,392.0	NA	NA	NA	NA	NA
Russia	NA	NA	NA	2,976.1	2,578.5	2,590.2	2,636.4	2,675.0
Eastern Europe and former USSR	**10,707.0**	**10,424.6**	**9,731.6**	**5,707.2**	**5,095.5**	**5,154.8**	**5,269.9**	**5,407.9**
Iran	590.0	790.0	1,002.5	1,140.2	1,248.3	1,285.3	1,350.3	1,425.0
Saudi Arabia	610.0	939.0	1,107.0	1,254.5	1,537.1	1,606.3	1,676.2	1,775.0
Middle East	**2,058.1**	**2,853.9**	**3,494.2**	**4,159.0**	**4,775.6**	**4,984.5**	**5,135.1**	**5,288.1**
Egypt	260.0	430.0	465.0	458.5	560.8	564.7	554.7	566.0
South Africa	312.0	350.0	375.0	421.1	457.9	458.2	475.4	484.0
Africa	**1,474.1**	**1,826.5**	**2,069.6**	**2,251.6**	**2,507.4**	**2,617.9**	**2,650.2**	**2,702.9**
Australia	594.0	639.0	736.8	814.1	871.9	877.9	875.8	875.6
China	1,765.0	1,885.0	2,296.4	3,363.2	4,795.7	4,917.9	5,160.7	5,550.0
India	643.0	894.9	1,168.3	1,574.7	2,127.4	2,183.7	2,263.4	2,320.0
Indonesia	408.0	465.0	651.1	807.3	1,036.7	1,077.0	1,125.6	1,155.0
Japan	4,960.0	4,436.0	5,218.1	5,676.1	5,607.0	5,530.0	5,464.6	5,578.4
South Korea	537.0	552.0	1,048.3	2,007.7	2,135.3	2,132.0	2,149.2	2,168.1
Singapore	202.0	227.0	363.0	512.2	660.3	686.6	698.0	705.0
Taiwan	380.0	378.0	541.5	736.9	865.3	881.7	893.7	915.0
Thailand	224.0	224.8	406.5	678.7	724.9	701.6	763.3	810.0
Asia and Oceania	**10,729.1**	**10,730.5**	**13,718.8**	**17,910.9**	**20,897.8**	**21,078.2**	**21,535.2**	**22,255.5**
World total	**63,107.6**	**60,088.8**	**66,576.0**	**70,017.8**	**76,945.9**	**77,701.3**	**78,457.7**	**80,098.8**

Note: In 1000 barrels per day; NA = not applicable.

50% probability that the quantities actually recovered will equal or exceed the sum of estimated proved plus probable reserves.

Possible reserves are those unproved reserves that an analysis of geological and engineering data suggests are less likely to be recoverable than probable reserves. If a probabilistic interpretation is to be given, there should be at least a 10% probability that the quantities actually recovered will equal or exceed the sum of estimated proved plus probable plus possible reserves.

The *Oil and Gas Journal (OGJ)* estimates that at the beginning of 2004, worldwide reserves of petroleum was 1.27 trillion barrels.[5] This estimate is 53 billion barrels higher than the prior year (2003), which reflected additional discoveries, improving technology, and changing economics.[5] If we use the world petroleum consumption rate of 2003 as a fixed rate, the worldwide petroleum reserve would be able to sustain the current level of consumption for an additional 43.4 years. Table 1.3 shows distribution of major petroleum reserves by countries.[5]

Currently, transportation, fuel, and petrochemical industries depend very heavily upon petroleum-based feedstocks. Therefore, alternative fuels replacing petrochemical feedstocks and supplementing petroleum derived materials must be developed and utilized more. Necessary infrastructure also needs to be developed and changed to make a transition from the current petroleum economy.

Table 1.2 also provides regionwide petroleum consumption data. It shows that consumption of petroleum in Western Europe for the past 23 years has been steadily constant, whereas in Asia, Oceania, and the Middle East, consumption has increased very rapidly, with the Asian and Oceanic regions alone accounting for 64.1%. This is

TABLE 1.3
Distribution of Major Petroleum Reserves

Nation	Reserve (billion barrels)
Saudi Arabia	262
Canada[a]	179
Iran	126
Iraq	115
Kuwait	99
United Arab Emirates	98
Venezuela	78
Russia	60
Libya	36
Nigeria	25
U.S.	22
China	18
Mexico	16
Qatar	15
World total	**1265**

[a] Mostly available in oil sands.

obviously due to the large number of rapidly developing economies in the region. As most of these countries are not major oil producers, this region will have to be most sensitive to the future of petroleum energy. The U.S. accounted for about 27% of the world total consumption in 1980, whereas for 2003 its portion decreased to 25%. On the other hand, consumption in Asia and Oceania increased form 17% in 1980 to 28% in 2003. Energy economists use the following terms for grouping nations based on their economic trends: *mature market economies* (western Europe, North America, and Japan), *emerging economies* (many Asian and African countries), and *transitional economies* (former Soviet Union [FSU] nations, eastern Europe).

Figure 1.3 shows the world petroleum crude oil production data in million barrels per day.[6] It also shows the breakdown of petroleum crude oil production between the Organization of Petroleum Exporting Countries (OPEC) nations and non-OPEC nations. It is worth noting that the production trends between the two groups during the period 1979 to 1993 were quite opposite, whereas from 1993 they are parallel.

In the U.S., 97% of the energy used in the transportation sector, which includes cars, trucks, trains, ships, and airplanes, comes from petroleum-based fuels. As such, petroleum is by far the most important transportation fuel. Serious R & D efforts are being made in many countries to develop vehicles that run on alternative energy, such as electricity, ethanol, and hydrogen.

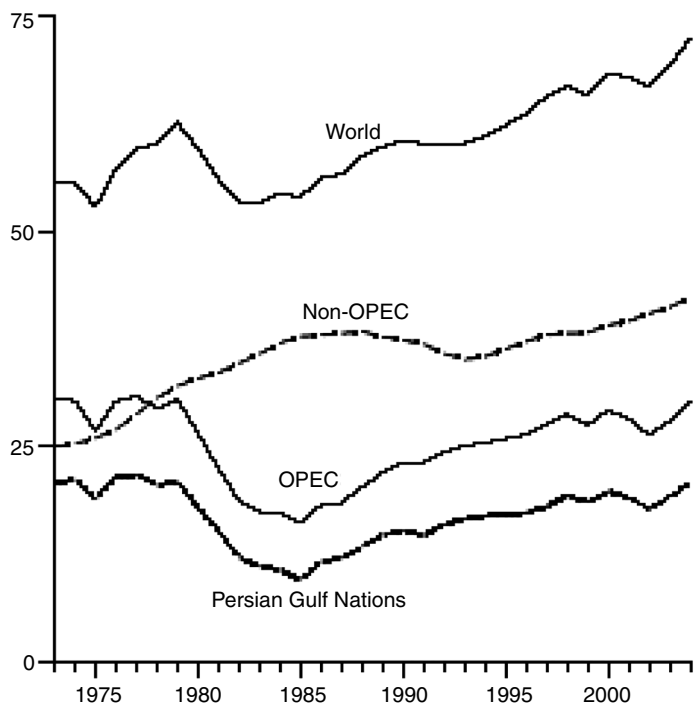

FIGURE 1.3 World petroleum crude oil production (in million barrels/day).

1.4 NATURAL GAS

In recent years, natural gas has gained popularity among many industrial sectors. It burns cleaner than coal or petroleum, thus providing environmental benefits. It is distributed mainly via pipelines and in a liquid phase (called *liquefied natural gas* [LNG]) transported across oceans by tankers.

Table 1.4 shows the worldwide consumption of dry natural gas by regions and countries for the period from 1980 to 2003.[7] As shown, the worldwide consumption of natural gas steadily increased at the rate of 2.6% per year. According to the *Oil and Gas Journal* (*OGJ*)[5] the world natural gas reserve as of January 1, 2004 is 6079 trillion cubic feet. Assuming that the current level of natural gas consumption for the world is maintained, the reserve would be enough to last for another 64 years, provided factors such as increased yearly consumption, discovery of new deposits, and advances in technology, such as utilization of natural gas hydrates, are not included. Even though this rough estimate may look somewhat better than that of petroleum, the fate of natural gas is more or less the same as that of petroleum.

Table 1.5 shows the worldwide distribution of natural gas for countries with major reserves.[5,8] Projection of the world reserves of natural gas has generally increased, at least by numbers due to new discoveries of major natural gas fields, whose estimated reserves offset more than the annual consumption. As shown in Table 1.5, Russia has about 27.6% of the world natural gas reserves, whereas the combined total for the Middle East accounts for 41.4% (at 2518 trillion cubic feet).[5,8] In terms of natural gas consumption, the U.S. accounts for 23.4% (based on statistics for 2003), whereas Asia and Oceania account for 13%. This is quite different from the consumption pattern for petroleum, which is the globally preferred transportation fuel. Energy provided by natural gas can be obtained by other sources or replaced by other types of energy depending upon a region's infrastructure and supply-and-demand system.

Natural gas is the third most-used energy source in the U.S. (23%) after petroleum and coal. The major consumers of natural gas are: manufacturers, public utilities, residential consumers (heating homes and cooking), and commercial users, mainly for heating buildings, as shown in Figure 1.4. Natural gas helps manufacture a wide variety of goods including plastics, fertilizers, photographic films, inks, synthetic rubber, fibers, detergents, glues, methanol, ethers, insect repellents, and much more.[9] It is also used in electric power generation as it burns cleaner and more efficiently than coal, and has less emission-related problems than other popular fossil fuels. However, natural gas has only a limited market share as a transportation fuel, even though it can be used in regular internal combustion engines. This is mainly due to its low energy density per volume unless it is compressed under very high pressure. Over half of U.S. homes use natural gas as the main heating fuel. Any major disruption in the natural gas supply would bring out unique but quite grave consequences in the nation's energy management, at least for the short term and for a certain affected region, as natural gas is heavily utilized by both electric power generating utilities and homes. The regional energy dependence problem has been somewhat mitigated by deregulation of utilities, which altered the business practices of electric utilities and natural gas industry. Deregulation allows customers

TABLE 1.4
World Dry Natural Gas Consumption (1980–2003)

Region/Country	1980	1985	1990	1995	2000	2001	2002	2003
Canada	1,883	2,165	2,378	2,791	2,952	2,912	3,060	3,212
U.S.	19,877	17,281	19,174	22,207	23,333	22,239	23,007	22,375
North America	**22,559**	**20,436**	**22,470**	**26,040**	**27,683**	**26,547**	**27,565**	**27,410**
Argentina	359	578	717	953	1,173	1,103	1,069	1,221
Venezuela	517	618	761	890	961	1,120	1,052	1,049
Central and South America	**1,241**	**1,755**	**2,024**	**2,581**	**3,304**	**3,537**	**3,557**	**3,820**
Belgium	371	306	341	443	554	547	563	547
France	981	1,110	997	1,183	1,403	1,473	1,586	1,545
Germany	NA	NA	NA	3,172	3,098	3,239	3,204	3,315
East Germany	493	580	357	NA	NA	NA	NA	NA
West Germany	2,128	1,966	2,312	NA	NA	NA	NA	NA
Iceland	0	0	0	0	0	0	0	0
Ireland	32	87	82	102	142	148	151	152
Italy	972	1,151	1,674	1,921	2,498	2,505	2,485	2,715
Netherlands	1,493	1,624	1,535	1,701	1,725	1,769	1,765	1,780
U.K.	1,702	1,991	2,059	2,690	3,373	3,338	3,313	3,360
Western Europe	**8,665**	**9,476**	**10,496**	**12,761**	**15,126**	**15,515**	**15,868**	**16,427**
Former Czechoslovakia	325	407	532	NA	NA	NA	NA	NA
Former USSR	13,328	20,302	24,961	NA	NA	NA	NA	NA
Hungary	344	395	394	407	425	472	473	515
Poland	418	443	427	416	473	482	479	528
Romania	1,251	1,336	1,261	901	600	696	646	636
Russia	NA	NA	NA	14,507	14,130	14,412	14,567	15,291
Eastern Europe and former USSR	**15,856**	**23,112**	**27,825**	**23,043**	**22,802**	**23,299**	**23,680**	**24,970**
Iran	232	600	837	1,243	2,221	2,478	2,798	2,790
Saudi Arabia	334	716	1,077	1,343	1,759	1,896	2,002	2,121
Middle East	**1,311**	**2,273**	**3,599**	**4,735**	**6,822**	**7,052**	**7,633**	**7,862**
Algeria	460	584	681	742	726	722	722	753
Egypt	30	175	286	439	646	867	941	954
Africa	**735**	**1,072**	**1,351**	**1,689**	**2,038**	**2,284**	**2,446**	**2,554**
Australia	322	463	625	710	797	841	839	886
China	505	457	494	582	933	1,046	1,128	1,181
Indonesia	195	513	547	1,061	1,081	1,182	1,197	1,229
Japan	903	1,468	1,851	2,207	2,845	2,843	2,943	3,055
Pakistan	286	365	482	646	856	774	809	840
Asia and Oceania	**2,523**	**4,120**	**5,605**	**7,790**	**10,433**	**11,078**	**11,756**	**12,462**
World total	**52,890**	**62,244**	**73,370**	**78,642**	**88,208**	**89,312**	**92,505**	**95,504**

Note: In billion cubic feet; NA = not applicable.

TABLE 1.5
Natural Gas Reserves

Nation	Reserves (trillion cubic feet)
Russia	1680
Iran	940
Qatar	917
Saudi Arabia	231
United Arab Emirates	212
U.S.	189
Algeria	160
Nigeria	159
Iraq	110
Australia	29[a]
World total	**6079**

[a] Downward adjustment made from 90 to 29 trillion ft^3, based on Australian government's report in 2005.

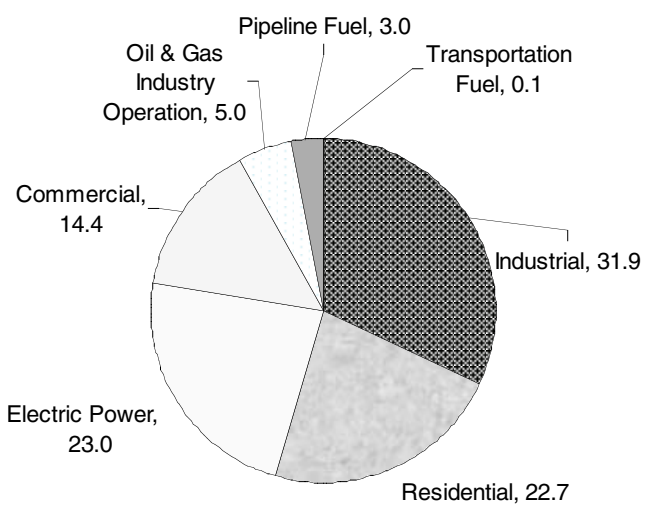

FIGURE 1.4 Principal uses of natural gas in the U.S.

to purchase their natural gas from suppliers other than their local utility, thus providing choices for consumers and eventually resulting in a better value for them.

Natural gas is distributed mainly via pipelines. In the U.S., more than one million miles of underground pipelines are connected between natural gas fields and major cities. This gas can be liquefied by cooling to 260°F (162°C), and is much more condensed in volume (615 times) when compared to natural gas at room temperature, making it easier to store or transport. LNG in special tanks can be transported by trucks or by ships as LNG has the fluidity and volume compactness of other liquid

fuels. In this regard, it has some of the necessary qualities for a transportation fuel. As a result, more than 100 LNG storage facilities are currently being operated in the U.S. and the number is still increasing.

Like all other fossil fuels, natural gas also generates carbon dioxide (a major greenhouse gas) upon combustion. Also, natural gas by itself is a greenhouse gas.[9,19] Therefore, in all phases of generation, storage, and transportation, preventive measures must be undertaken to ensure that accidental release of natural gas does not occur due to any leakages.

1.5 COAL

Coal is primarily consumed in electric power generation and in industrial sectors. In 2002, coal consumption accounted for 24% of the total energy consumption in the world.[10,11] About 65% of coal consumption was used for electric power generation, 31% for industrial consumers such as steel manufacturers and steam generators, and much of the remaining 4% for consumers in residential and commercial sectors. Coal was once an important transportation fuel for powering steam engines; however, coal nowadays is rarely used in transportation. Table 1.6 shows worldwide consumption of coal by regions and countries for the period from 1980 to 2003.[10]

According to the prediction for 2025 by the Energy Information Administration (EIA),[10] worldwide consumption of coal for electric power generation and industrial use would remain relatively stable, as shown in Table 1.7.[11] The slight increase in consumption by the industrial sector is mainly due to the rapid industrial growth of China, which has an abundant reserve and supply of coal, but limited reserve of oil and natural gas. International coal trade is projected to increase from 714 million tons in 2003 to 969 million tons in 2025, accounting for approximately 12 to 13% of total worldwide consumption of coal over this period.[11]

Total recoverable reserves of coal around the world are estimated at 1001 billion tons,[11] which would be enough to last approximately 184 years if maintained at the 2003 consumption level of 5.439 billion tons. The reserve amount was recently adjusted downward after applying more restrictive criteria, i.e., safe and economical recoverability. Even though coal deposits are distributed widely throughout the world, about 57% of the world recoverable coal reserves are located in three countries: U.S. (27%), Russia (17%), and China (13%). After these three, six countries account for 33% of the total reserves: India, Australia, South Africa, Ukraine, Kazakhstan, and Yugoslavia. Coal is also very unequally and unevenly distributed, just as are other fossil fuels such as petroleum and natural gas.

The U.S. consumed 1066 million tons of coal in 2002.[10,11] Consumption is projected to rise steadily to 1505 million tons in 2025. The strong dependence of the U.S. on coal for electric power generation is expected to continue. Dependence on coal consumption for U.S. electricity generation declined from 56% in the mid-1990s to 52% in 2002. It is projected to decline slightly from 52% in 2002 to 51% in 2015 and then return to 53% in 2025.[11] This prediction takes into account the expected addition of new coal-fired power plants, as well as the expected increase in the average utilization rate of coal-fired power generation capacity, from 70% in 2002 to 83% in 2025.[11]

TABLE 1.6
World Coal Consumption, 1980–2003

Region/Country	1980	1985	1990	1995	2000	2001	2002	2003
Canada	41.32	54.30	59.08	58.46	69.62	69.58	68.22	69.43
U.S.	702.73	818.05	904.50	962.10	1,084.09	1,060.15	1,066.35	1,094.13
North America	**749.33**	**880.12**	**972.17**	**1,032.86**	**1,168.91**	**1,146.33**	**1,151.38**	**1,183.97**
Central and South America	**19.40**	**28.36**	**26.54**	**32.94**	**37.10**	**35.47**	**34.22**	**35.07**
Germany	NA	NA	NA	297.52	269.81	278.15	280.12	273.05
East Germany	297.20	351.51	315.20	NA	NA	NA	NA	NA
West Germany	238.28	227.08	212.42	NA	NA	NA	NA	NA
Greece	25.63	41.91	58.95	64.43	72.41	75.49	76.81	76.04
Spain	36.08	53.71	52.08	47.83	49.72	45.63	50.53	45.62
Turkey	19.84	45.61	59.99	67.27	88.67	80.11	72.50	71.02
U.K.	133.56	116.29	119.38	78.97	63.91	70.09	64.16	68.76
Western Europe	**937.45**	**1,065.26**	**1,037.19**	**737.53**	**717.21**	**718.54**	**717.04**	**712.54**
Bulgaria	40.74	43.65	41.67	32.77	32.26	34.69	31.72	34.59
Czechoslovakia	NA	NA	NA	79.15	70.09	68.03	64.65	65.34
Former Czechoslovakia	134.05	140.29	119.48	NA	NA	NA	NA	NA
Former USSR	751.33	778.87	848.47	NA	NA	NA	NA	NA

Kazakhstan	NA	NA	NA	72.36	54.82	63.01	65.71	58.50
Poland	221.12	238.41	202.18	184.90	158.71	152.00	149.45	152.58
Romania	44.97	60.35	51.97	49.85	35.65	38.17	38.38	40.31
Russia	NA	NA	NA	270.04	252.51	241.65	240.17	250.73
Ukraine	NA	NA	NA	109.60	72.64	70.62	68.79	67.17
Eastern Europe and former USSR	**1,225.11**	**1,294.08**	**1,289.06**	**855.11**	**724.04**	**715.16**	**704.21**	**717.52**
Middle East	**1.08**	**4.81**	**5.68**	**9.28**	**13.84**	**14.84**	**15.96**	**15.55**
South Africa	104.77	141.77	139.08	162.26	176.06	173.52	172.11	187.76
Africa	**112.50**	**150.72**	**151.70**	**174.90**	**189.56**	**188.16**	**186.80**	**202.60**
Australia	74.30	86.29	103.72	112.24	141.00	140.98	145.25	144.08
China	678.52	920.95	1,124.13	1,494.74	1,282.29	1,356.60	1,412.96	1,531.09
India	129.83	193.47	255.79	331.92	406.07	413.56	430.63	430.62
Japan	98.11	119.38	126.43	141.56	156.88	166.88	171.92	175.58
North Korea	49.34	60.08	53.67	35.51	32.71	33.76	31.99	33.53
South Korea	25.68	45.19	47.80	56.01	72.48	76.04	79.71	81.38
Taiwan	6.59	12.10	18.94	29.03	49.49	52.87	56.32	60.67
Asia and Oceania	**1,081.61**	**1,474.41**	**1,786.93**	**2,273.06**	**2,231.89**	**2,346.18**	**2,440.53**	**2,572.08**
World Total	**4,126.48**	**4,897.76**	**5,269.29**	**5,115.68**	**5,082.54**	**5,164.68**	**5,250.14**	**5,439.33**

Note: In million short tons; NA = not applicable.

TABLE 1.7
Projected Energy Market Share of Coal (as percentages)

Market	2002	2015	2025
Electric power generation	39	39	38
Industrial sector	20	22	22
Other sectors	4	3	3
Total energy market	24	25	24

Coal has been studied extensively for conversion into gaseous and liquid fuels, as well as hydrocarbon feedstocks. Largely thanks to its relative abundance and stable fuel price on the market, coal has been a focal target for synthetic conversion into other forms of fuels, i.e., synfuels. R&D work has seen research ups and downs due to external factors, including the comparative fossil fuel market, as well as the international energy outlook of the era. Coal can be gasified, liquefied, pyrolyzed, and coprocessed with other fuels including oil, biomass, scrap tires, and municipal solid wastes.[12] Secondary conversion of coal-derived gas and liquids can generate a wide array of petrochemical products, as well as alternative fuels.

In 2003, coal was the second largest leading source of carbon dioxide emissions from the consumption and flaring of fossil fuels, accounting for 37% of the total.[17] The leading primary source of carbon dioxide emission was from the consumption of petroleum, accounting for 42% of the total. In third place was natural gas at 21%.[17]

1.6 NUCLEAR ENERGY

Table 1.8.[13] shows worldwide nuclear electric power generation data and Table 1.9 shows worldwide electricity generation data, from 1980 to 2003. Approximately 30.3% of the world nuclear electric power generation in 2003 was in the U.S., followed by France (16.6%), Japan (9.4%), Germany (6.2%), Russia (5.5%), and South Korea (4.9%). The market share of world electric power generation in 2003 by nuclear energy is 15.9%, while that for the U.S. is 19.6%. Dependence of electric power generation on nuclear energy in 2003 was by far the heaviest for France at 78%. It should be also noted during the same period that there were 19 countries which had more than 20% of their electric power generated using nuclear power plants.

According to the International Energy Outlook 2005, electric power generation using nuclear power plants from around the world is projected to increase from 2560 billion kilowatt-hours in 2002 to 3032 billion kilowatt-hours in 2015 and 3270 billion kilowatt-hours in 2025.[14] The outlook for nuclear energy in general improved substantially over recent years, due to a number of reasons that include:

1. Higher fossil fuel prices
2. Higher capacity utilization rates reported for many existing nuclear facilities

3. Expectation that most existing plants in the mature markets and transitional economies will be granted extensions in operating lives
4. Enforcement of Kyoto protocol
5. Anticipation for hydrogen economy and need for cost-effective electrical energy

However, predicting the trend for nuclear energy is still very difficult, owing to considerable uncertainties originating from political and socioeconomic factors.

1.7 RENEWABLE ENERGY

All fossil fuels are nonrenewable, and as such they will eventually be depleted. As they are based on finite resources and their distributions are heavily localized in certain areas of the world, they will become expensive. Further, energy generation from fossil fuels require combustion, thus damaging the environment with pollutants and greenhouse gas emission. In order to sustain the future of the world with a clean environment and nondepletive energy resources, renewable energy is the obvious choice. Renewable energy sources include: solar energy, wind energy, geothermal energy, biomass, and hydrogen. Most renewable energy, except for geothermal energy, comes directly or indirectly from the sun.[16] Benefits of renewable energy are numerous and they include:

1. Environmental cleanness without pollutant emission
2. Nondepletive nature
3. Availability throughout the world
4. No cause for global warming
5. Waste reduction
6. Stabilization of energy costs
7. Creation of jobs

Table 1.10 shows U.S. energy consumption by energy source from 2000 to 2004.[18] As can be seen in this comparative listing, the share of renewable energy is still very minute, about 6% of the total energy consumption. With increases in the prices of petroleum and natural gas, as was experienced in 2005 and 2006, the relative competitiveness of renewable and alternative fuels is drastically improving. Further, technological advances in the alternative renewable energy areas, as well as public awareness backed by strong governmental supports and incentives, make the outlook of alternative and renewable energy very promising.

Worldwide generation of geothermal, solar, wind, wood, and waste electric power increased at an average annual rate of 6.8% from 1993 to 2003.[17] The U.S. led the world with 94 billion kilowatt-hours, followed by Germany with 31 billion, Japan with 28 billion, Spain with 16.3 billion, and Brazil with 16.2 billion.[17] These five countries accounted for about 60% of the world geothermal, solar, wind, wood, and waste electric power generation in 2003.

TABLE 1.8
World Net Nuclear Electric Power Generation for 1980–2003

Region/Country	1980	1985	1990	1995	2000	2001	2002	2003
Canada	35.88	57.10	69.24	92.95	69.16	72.86	71.75	70.79
U.S.	251.12	383.69	576.86	673.40	753.89	768.83	780.06	763.73
North America	**287.00**	**440.79**	**648.89**	**774.38**	**830.86**	**849.97**	**861.07**	**844.49**
Argentina	2.22	5.43	7.03	7.07	5.99	6.54	5.39	7.03
Brazil	0	2.92	1.94	2.39	4.94	14.27	13.84	13.40
Central and South America	**2.22**	**8.36**	**8.97**	**9.46**	**10.93**	**20.81**	**19.23**	**20.43**
Belgium	11.91	32.69	40.59	39.29	45.75	44.03	44.99	45.01
Finland	6.63	17.98	18.26	18.26	21.36	21.63	21.18	21.60
France	63.42	211.19	298.38	358.37	394.40	400.02	414.92	419.02
Germany	NA	NA	NA	145.44	161.13	162.74	156.60	157.00
East Germany	11.89	12.74	5.33	NA	NA	NA	NA	NA
West Germany	43.70	125.90	139.82	NA	NA	NA	NA	NA
Italy	2.07	6.60	0	0	0	0	0	0
Netherlands	3.95	3.67	3.33	3.82	3.73	3.78	3.72	3.82
Slovenia	NA	NA	NA	4.56	4.55	5.04	5.31	4.96
Spain	5.19	28.04	51.56	52.68	59.10	60.52	59.87	58.79
Sweden	25.33	55.81	64.78	66.44	54.45	68.50	64.20	62.16
Switzerland	12.88	20.06	22.42	23.65	25.12	25.47	25.87	26.12
U.K.	32.29	53.77	62.46	84.52	80.81	85.38	83.64	84.49
Western Europe	**219.25**	**572.49**	**711.29**	**797.01**	**850.39**	**877.11**	**880.30**	**882.96**

Armenia	NA	NA	NA	0	1.84	1.99	2.09	1.82
Bulgaria	5.81	12.38	13.53	16.40	17.27	18.24	20.22	16.04
Czechoslovakia	NA	NA	NA	11.62	12.91	14.01	17.80	24.58
Former Czechoslovakia	4.50	11.90	23.40	NA	NA	NA	NA	NA
Former USSR	72.88	169.96	201.31	NA	NA	NA	NA	NA
Hungary	0	6.11	13.04	13.32	13.47	13.42	13.26	10.46
Lithuania	NA	NA	NA	10.64	8.42	11.36	14.14	15.48
Romania	0	0	0	0	5.23	5.04	5.11	4.54
Russia	NA	NA	NA	94.34	122.46	125.36	134.14	138.39
Slovakia	NA	NA	NA	10.87	15.67	16.25	17.06	16.97
Ukraine	NA	NA	NA	66.98	71.06	71.67	73.38	76.70
Eastern Europe and USSR	**83.19**	**200.34**	**251.28**	**224.26**	**268.32**	**277.33**	**297.19**	**304.98**
Middle East	**0**	**0**	**0**	**0**	**0**	**0**	**0**	**0**
South Africa	0	5.32	8.45	11.30	13.01	10.72	11.99	12.66
Africa	**0**	**5.32**	**8.45**	**11.30**	**13.01**	**10.72**	**11.99**	**12.66**
China	0	0	0	12.38	15.90	16.60	25.17	41.66
India	3.00	4.70	5.61	6.46	14.06	18.23	17.76	16.37
Japan	78.64	149.66	192.16	276.69	305.95	303.87	280.34	237.19
South Korea	3.28	15.78	50.24	63.68	103.52	106.53	113.15	123.19
Pakistan	0.002	0.33	0.36	0.50	0.38	1.98	1.80	1.81
Taiwan	7.81	27.79	31.55	33.93	37.00	34.09	38.01	37.37
Asia and Oceania	**92.73**	**198.25**	**279.93**	**393.64**	**476.80**	**481.30**	**476.22**	**457.58**
World total	**684.38**	**1,425.54**	**1,908.81**	**2,210.04**	**2,450.31**	**2,517.24**	**2,546.01**	**2,523.11**

Note: In billion kilowatt-hours; NA = not applicable.

TABLE 1.9
World Net Electricity Generation for 1980–2003

Region/Country	1980	1985	1990	1995	2000	2001	2002	2003
Canada	367.91	448.07	468.65	544.11	587.86	570.87	582.15	566.28
Mexico	63.60	93.13	116.57	144.91	193.91	198.63	203.66	209.20
U.S.	2,289.60	2,473.00	3,041.50	3,356.21	3,807.64	3,745.47	3,867.20	3,891.72
North America	**2,721.60**	**3,014.78**	**3,627.43**	**4,046.01**	**4,590.30**	**4,515.91**	**4,653.94**	**4,668.11**
Argentina	41.85	45.50	48.29	64.92	85.26	86.50	81.15	83.29
Brazil	138.28	190.64	219.62	271.79	342.45	323.04	340.07	359.19
Venezuela	32.01	46.22	57.61	71.60	83.24	87.73	85.05	87.44
Central and South America	**308.23**	**405.36**	**497.17**	**626.75**	**781.10**	**767.55**	**790.31**	**828.66**
Austria	40.73	43.32	48.09	53.76	58.73	59.19	62.01	55.75
Belgium	50.75	53.43	66.52	69.55	78.31	74.40	76.52	78.77
Finland	38.71	47.32	51.85	60.97	66.84	70.96	71.30	79.61
Former Yugoslavia	57.15	72.09	78.69	NA	NA	NA	NA	NA
France	250.81	325.04	397.58	469.05	511.82	522.30	529.09	536.92
Germany	NA	NA	NA	503.93	536.07	549.48	548.63	558.14
East Germany	98.81	113.83	104.01	NA	NA	NA	NA	NA
West Germany	371.05	407.93	422.00	NA	NA	NA	NA	NA
Italy	176.37	173.31	202.06	225.05	256.04	258.01	261.14	270.06
Netherlands	62.94	59.60	67.70	76.19	84.35	88.21	91.12	91.00
Norway	82.85	101.80	120.37	120.80	138.18	117.96	128.85	105.56
Portugal	14.97	18.60	27.12	31.59	41.35	44.12	43.44	44.32
Spain	109.18	125.51	143.92	157.42	211.07	221.98	230.08	247.31
Sweden	94.34	134.33	141.55	143.52	141.37	157.07	140.66	127.92
Turkey	23.32	34.37	55.25	82.85	118.97	116.57	123.33	133.63
U.K.	265.14	275.22	298.95	308.24	353.20	361.39	360.14	369.87
Western Europe	**1,844.50**	**2,106.19**	**2,355.89**	**2,527.95**	**2,847.47**	**2,901.62**	**2,922.53**	**2,973.66**

Czechoslovakia	NA	NA	NA	57.56	68.77	70.04	71.76	78.18
Estonia	NA	NA	NA	8.17	8.00	7.98	8.02	9.02
Former Czechoslovakia	72.70	76.83	81.88	NA	NA	NA	NA	NA
Former USSR	1,294.00	1,545.01	1,636.14	NA	NA	NA	NA	NA
Poland	113.77	128.13	126.67	129.26	134.69	135.22	133.98	141.25
Russia	NA	NA	NA	817.30	832.98	842.63	864.69	883.35
Ukraine	NA	NA	NA	183.37	160.13	163.27	163.87	169.92
Eastern Europe and former USSR	**1,603.19**	**1,886.24**	**1,974.79**	**1,569.24**	**1,564.12**	**1,590.83**	**1,624.61**	**1668.18**
Iran	21.26	35.32	55.86	80.23	114.28	122.53	132.68	142.35
Saudi Arabia	20.45	44.31	64.90	97.85	120.70	129.14	136.89	145.11
Middle East	**92.41**	**164.98**	**229.85**	**325.49**	**439.53**	**462.95**	**491.65**	**506.19**
Egypt	18.26	32.30	41.41	52.68	72.08	76.60	81.62	84.26
South Africa	93.07	133.26	156.03	176.07	196.46	197.82	205.67	215.88
Africa	**189.18**	**251.92**	**307.40**	**354.28**	**417.29**	**431.80**	**451.63**	**471.06**
Australia	87.72	111.02	146.36	164.08	195.80	204.67	209.62	215.76
China	285.47	390.68	590.34	956.09	1,300.37	1,409.62	1,570.38	1,806.76
India	119.26	174.93	275.49	396.02	529.12	548.02	563.53	556.80
Indonesia	12.79	26.40	43.02	56.83	87.63	96.08	102.27	109.46
Japan	549.11	639.60	821.78	947.55	1,010.89	989.31	1,036.21	1,017.50
South Korea	34.57	54.14	100.40	189.83	249.15	265.88	287.99	326.16
Malaysia	10.19	15.00	23.95	43.02	65.41	67.45	70.01	79.28
Pakistan	14.51	26.49	36.35	51.85	63.40	68.86	72.44	76.92
Taiwan	42.01	52.55	83.34	113.24	149.78	151.11	158.54	165.96
Thailand	13.58	22.91	43.65	75.58	90.53	96.60	102.87	114.71
Asia and Oceania	**1,268.05**	**1,646.47**	**2,337.58**	**3,184.25**	**3,973.10**	**4,139.41**	**4,428.40**	**4,736.56**
World total	**8,027.15**	**9,475.96**	**11,330.10**	**12,633.97**	**14,612.92**	**14,810.07**	**15,363.07**	**15,852.41**

Note: In billion kilowatt-hours; NA = not applicable.

TABLE 1.10
U.S. Energy Consumption by Energy Source for 2000–2004

Energy Source	2000	2001	2002	2003	2004[p]
Total [a]	98.961	96.464	97.952	98.714	100.278
Fossil fuels	84.965	83.176	84.070	84.889	86.186
Coal	22.580	21.952	21.980	22.713	22.918
Coal coke net imports	0.065	0.029	0.061	0.051	0.138
Natural gas[b]	23.916	22.861	23.628	23.069	23.000
Petroleum[c]	38.404	38.333	38.401	39.047	40.130
Electricity net imports	0.115	0.075	0.078	0.022	0.039
Nuclear electric power	7.862	8.033	8.143	7.959	8.232
Renewable energy	6.158	5.328	5.835	6.082	6.117
Conventional hydroelectric	2.811	2.242	2.689	2.825	2.725
Geothermal energy	0.317	0.311	0.328	0.339	0.340
Biomass[d]	2.907	2.640	2.648	2.740	2.845
Solar energy	0.066	0.065	0.064	0.064	0.063
Wind energy	0.057	0.070	0.105	0.115	0.143

Note: In quadrillion British thermal units (Btus).

[a] Ethanol blended into motor gasoline is included in both Petroleum and Biomass, but is counted only once in total consumption.

[b] Includes supplemental gaseous fuels.

[c] Petroleum products supplied, including natural gas plant liquids and crude oil burned as fuel.

Ethanol from corn has been increasingly used as gasoline-blending fuel. One new brand is E85, which contains 85% ethanol and 15% gasoline. Many gas stations in the U.S. have started to stock E85 fuels regularly and many automakers are offering multiple lines of automobiles that can be operated on either conventional gasoline or E85. Phase-down of MTBE (methyl tertiary–butyl ether), once the most popular oxygenated blend fuel, in many U.S. states also accelerated the use of ethanol as an oxygenated gasoline blend fuel. Public awareness of clean burning and energy efficient hydrogen has also propelled unprecedented interest in hydrogen technology and fuel cell research and development. Many experts predict the future to be a hydrogen economy. For the hydrogen economy to be realized, a long list of technological advances must be accomplished, which include technologies for inexpensive generation, safe distribution and storage, safe and efficient materials for hydrogen handling, hydrogen internal combustion engine, hydrogen fuel cells, loss prevention, etc.

Energy generation utilizing biomass and municipal solid wastes (MSW) are also promising in regions where landfill spaces are very limited. Technological advances in the fields have made this option efficient and environmentally safe.

REFERENCES

1. International Energy Annual 2003 posted in May–June 2005, Energy Information Administration (EIA), U.S. Department of Energy, accessible through the Web site, http://www.eia.doe.gov/pub/international/iealf/table11.xls.
2. Web site by Maxwell School of Syracuse University, U.S. Energy Consumption, accessible through http://wilcoxen.cp.maxwell.syr.edu/pages/804.html.
3. International Energy Annual 2003 posted on June 28, 2005, Energy Information Administration (EIA), U.S. Department of Energy, accessible through the Web site, http://www.eia.doe.gov/pub/international/iealf/table12.xls.
4. Society of Petroleum Engineers (SPE), Petroleum Reserve Definitions, accessible through the Web site, http://www.spe.org/spe/jsp/basic/01104_1216900.html.
5. *Oil and Gas Journal*, Worldwide Report, December 22, 2003.
6. Web site by Energy Information Administration (EIA), International Section, accessible through http://www.eia.doe.gov/emeu/international/contents.html.
7. International Energy Annual 2003 posted on May 25, 2005, Energy Information Administration (EIA), U.S. Department of Energy, accessible through the Web site, http://www.eia.doe.gov/pub/international/iealf/table13.xls.
8. International Energy Annual 2003 posted on May 25, 2005, Energy Information Administration (EIA), U.S. Department of Energy, accessible through the Web site, http://www.eia.doe.gov/pub/international/iea2003/table81.xls.
9. Lee, S., *Methane and Its Derivatives*, Marcel Dekker, New York, 1997.
10. International Energy Outlook 2005 (IEO2005), Coal, posted in July 2005, Energy Information Administration (EIA), U.S. Department of Energy, accessible through the Web site, http://www.eia.doe.gov/oiaf/ieo/coal.html.
11. International Energy Annual 2002, DOE/EIA-0219, Energy Information Administration (EIA), U.S. Department of Energy, Washington, D.C., March 2004.
12. Speight, J.G., *The Chemistry and Technology of Coal*, revised edition, Marcel Dekker, New York, 1994.
13. International Energy Annual 2003 posted on June 24, 2005, Energy Information Administration (EIA), U.S. Department of Energy, accessible through the Web site, http://www.eia.doe.gov/pub/international/iealf/table27.xls.
14. International Energy Outlook 2005 (IEO2005), Electricity, posted in July 2005, Energy Information Administration (EIA), U.S. Department of Energy, accessible through the Web site, http://www.eia.doe.gov/oiaf/ieo/electricity.html.
15. Forecasts and Analyses, Energy Information Administration (EIA), U.S. Department of Energy, accessible through the Web site, http://www.eia.doe.gov/oiaf/forecasting.html.
16. National Renewable Energy Laboratory (NREL), Renewable Energy Basics, accessible through the Web site, http://www.nrel.gov/learning/re_basics.html.
17. International Energy Annual 2003, World Energy Overview: 1993–2003, posted in May–July 2005, Energy Information Administration (EIA), U.S. Department of Energy, accessible through the Web site, http://www.eia.doe.gov/iea/overview.html.
18. Fuel Overview, Energy Information Administration (EIA), U.S. Department of Energy, accessible through the Web site, http://www.eia.doe.gov/fueloverview.html#C.
19. Speight, J.G. and Lee, S., *Environmental Technology Handbook*, 2nd Edition, Taylor & Francis, Philadelphia, PA, 2000.

2 Gasification of Coal

Sunggyu Lee

CONTENTS

2.1 BACKGROUND

Conversion of coal by any of the processes to produce a mixture of combustible gases is termed *coal gasification*, even though a large number of chemical reactions other than so-called gasification reactions are involved. Even though the product gases of coal gasification involve combustible chemical species, the purpose of gasification is not limited to generation of gaseous fuel, because the product gas can be easily processed to generate other valuable chemical and petrochemical feedstock. Commercial gasification of coal generally entails the controlled partial oxidation of the coal to convert it into desired gaseous products. The coal can be heated either directly by combustion or indirectly by another heat source. A gasifying medium is typically passed over (or through) the heated coal to provide intimate molecular contact for chemical reaction. The gaseous reactants react with carbonaceous matters of coal (i.e., coal hydrocarbons) or with other primary decomposition products of coal to produce gaseous products. Not all the gaseous products generated by such processes are desirable from the standpoints of fuel quality, further processing, and environmental issues. Therefore, coal gasification is always performed in connection with downstream processes, not only for final applications but also for gas-cleaning purposes. The primary emphases of coal gasification may be on electricity generation via *integrated gasification combined cycle* (IGCC) types, on syngas production for pipeline applications, on *hydrogen production*, or on synthesis of *liquid fuels* and petrochemicals as alternative sources of raw materials. With the advent of a hydrogen economy, the role of coal gasification in generation of hydrogen may become even more important.[75]

Conversion of coal from its solid form to a gaseous fuel (or, gaseous chemical) is widely practiced today. During earlier years (1920–1940), coal gasification was being employed to produce *manufactured gas* in hundreds of plants worldwide, and such plants were called *manufactured gas plants* (MGPs). This technology became obsolete

in the post–World War II era because of the abundant supply of petroleum and natural gas at affordable prices. With the advent of the *oil embargo* in the early 1970s and subsequent increases and fluctuations in petroleum prices, as well as the natural gas and petroleum shortage experienced during the beginning of the 21st century, the interest in coal gasification as well as its further commercial exploitation was revived. Recently, surging interest in fuel cell technology also prompted keen interest in coal gasification as a means of obtaining reliable and inexpensive hydrogen sources. Many major activities in research, development, and the demonstration of coal gasification have recently resulted in significant improvements in conventional technology, and thus made coal gasification more competitive in modern fuel markets.[1]

The concept of electric power generation based on coal gasification received its biggest boost in the 1990s when the U.S. Department of Energy's Clean Coal Technology Program provided federal cost sharing for the first true commercial-scale IGCC plants in the U.S. Tampa Electric Company's Polk Power Station near Mulberry, FL, is the nation's first "greenfield" (built as a brand new plant, not a retrofit) commercial gasification combined cycle power station.[75] The plant, dedicated in 1997, is capable of producing 313 MW of electricity and removing more than 98% of sulfur in coal that is converted into commercial products. On the other hand, the Wabash River Coal Gasification Repowering Project was the first full-size commercial gasification combined cycle plant built in the U.S., located outside West Terre Haute, IN. The plant started full operations in November 1995. The plant is capable of producing 292 MW of electricity and is still one of the world's largest single-train IGCCs operating commercially.[75]

Coal gasification includes a series of reaction steps that convert coal containing C, H, and O, as well as impurities such as S and N, into *synthesis gas* and other forms of hydrocarbons. This conversion is generally accomplished by introducing a gasifying agent (air, oxygen, and/or steam) into a reactor vessel containing coal feedstock where the temperature, pressure, and flow pattern (moving bed, fluidized, or entrained bed) are controlled. The proportions of the resultant product gases (CO, CO_2, CH_4, H_2, H_2O, N_2, H_2S, SO_2, etc.) depend on the type of coal and its composition, the gasifying agent (or gasifying medium), and the thermodynamics and chemistry of the gasification reactions as controlled by the process operating parameters.

Coal gasification technology can be utilized in the following energy systems of potential importance:

1. Production of fuel for use in electric power generation units
2. Manufacturing synthetic or substitute natural gas (SNG) for use as pipeline gas supplies
3. Producing hydrogen for fuel cell applications
4. Production of synthesis gas for use as a chemical feedstock
5. Generation of fuel gas (low-Btu or medium-Btu gas) for industrial purposes

Coal is the largest recoverable fossil fuel resource in the U.S. as well as in the world. Synthesis gas production serves as the starting point for production of a variety of chemicals. The success of the Tennessee Eastman Corp. in producing acetic anhydride from coal shows the great potential of using coal as petrochemical

feedstock.[2] A major concern for such a technology involves the contaminants in coal. Coal contains appreciable amounts of sulfur, which is of principal concern to the downstream processes because many catalysts that might be used in the production of chemicals are highly susceptible to *sulfur poisoning*. Coals also contain nonnegligible amounts of alkali metal compounds that contribute to the fouling and *corrosion* of the reactor vessels in the form of slag. Further, coal also contains a number of trace elements that may also affect downstream processes and potentially create environmental and safety risks. If coal gasification is to be adopted to produce certain target chemicals, the choice of the specific gasification technology becomes very critical because a different process will produce a different quality (or composition) of synthesis gas as well as alter the economics of production.

Synthesis gas (SG) is a very important starting material for both fuels and petrochemicals. Synthesis gas is also called *syn gas* or *syngas*. It can be obtained from various sources including petroleum, natural gas, coal, biomass, and even municipal solid wastes (MSWs). Syngas is conveniently classified, based on its principal composition, as: (1) H_2-rich gas, (2) CO-rich gas, (3) CO_2-rich gas, (4) CH_4-rich gas, etc. Principal fuels and chemicals directly made from syngas include hydrogen, carbon monoxide, methane, ammonia, methanol, dimethylether, gasoline, diesel fuel, ethylene, isobutylene, mixture of C_2-C_4 olefins, C_1-C_5 alcohols, ethanol, ethylene glycol, etc.[74]

Secondary fuels and chemicals synthesized via methanol routes include formaldehyde, acetic acid, gasoline, diesel fuel, methyl formate, methyl acetate, acetaldehyde, acetic anhydride, vinyl acetate, dimethylether, ethylene, propylene, isobutylene, ethanol, C_1-C_5 alcohols, propionic acid, methyl *tert*-butyl ether (MTBE), ethyl *tert*-butyl ether (ETBE), *tert*-amyl methyl ether (TAME), benzene, toluene, xylenes, ethyl acetate, a methylating agent, etc. The synthesis route of such chemicals via methanol as an intermediate is called *indirect synthesis*.

2.2 SYNGAS CLASSIFICATION BASED ON ITS HEATING VALUE

Depending on the heating values of the resultant synthesis gases produced by gasification processes, product gases are typically classified as three types of gas mixtures[3]:

1. *Low-Btu gas* consisting of a mixture of carbon monoxide, hydrogen, and some other gases with a heating value typically less than 300 Btu/scf.
2. *Medium-Btu gas* consisting of a mixture of methane, carbon monoxide, hydrogen, and various other gases with a heating value in the range of 300–700 Btu/scf.
3. *High-Btu gas* consisting predominantly of methane with a heating value of approximately 1000 Btu/scf. It is also referred to as *SNG*.

Coal gasification involves the reaction of coal carbon (precisely speaking, macromolecular coal hydrocarbons) and other pyrolysis products with oxygen, hydrogen, and water to provide fuel gases.

2.2.1 Low-Btu Gas

For production of low-Btu gases, air is typically used as a combusting (or gasifying) agent. As air, instead of pure oxygen, is used, the product gas inevitably contains a large concentration of undesirable constituents such as nitrogen or nitrogen-containing compounds. Therefore, it results in a low heating value of 150–300 Btu/scf. Sometimes, this type of gasification of coal may be carried out *in situ*, i.e., underground, where mining of coal by other techniques is not economically favorable. For such *in situ* gasification, low-Btu gas may be a desired product. Low-Btu gas contains 5 principal components with around 50% v/v nitrogen, some quantities of hydrogen and carbon monoxide (combustible), carbon dioxide, and some traces of methane. The presence of such high contents of nitrogen classifies the product gas as low Btu. The other two noncombustible components (CO_2 and H_2O) further lower the heating value of the product gas. The presence of these components limits the applicability of low-Btu gas to chemical synthesis. The two major combustible components are hydrogen and carbon monoxide; their ratio varies depending on the gasification conditions employed. One of the most undesirable components is hydrogen sulfide (H_2S), which occurs in a ratio proportional to the sulfur content of the original coal. It must be removed by gas-cleaning procedures before product gas can be used for other useful purposes such as further processing and upgrading.

2.2.2 Medium-Btu Gas

In the production of medium-Btu gas, pure oxygen rather than air is used as combusting agent, which results in an appreciable increase in the heating value, by about 300–400 Btu/scf. The product gas predominantly contains carbon monoxide and hydrogen with some methane and carbon dioxide. It is primarily used in the *synthesis of methanol*, higher hydrocarbons via *Fischer–Tropsch synthesis*, and a variety of other chemicals. It can also be used directly as a fuel to generate steam or to drive a gas turbine. The *H_2-to-CO ratio* in medium-Btu gas varies from 2:3 (CO-rich) to more than 3:1 (H_2-rich). The increased heating value is attributed to higher contents of methane and hydrogen as well as to lower concentration of carbon dioxide, in addition to the absence of nitrogen in the gasifying agent.

2.2.3 High-Btu Gas

High-Btu gas consists mainly of pure methane (>95%) and, as such, its heating value is around 900–1000 Btu/scf. It is compatible with natural gas and can be used as a synthetic or substitute natural gas (SNG). This type of syngas is usually produced by catalytic reaction of carbon monoxide and hydrogen, which is called the *methanation reaction*. The feed syngas usually contains carbon dioxide and methane in small amounts. Further, steam is usually present in the gas or added to the feed to alleviate carbon fouling, which alters the catalytic effectiveness. Therefore, the pertinent chemical reactions in the methanation system include:

$$3H_2 + CO = CH_4 + H_2O$$
$$2H_2 + 2CO = CH_4 + CO_2$$

$$4H_2 + CO_2 = CH_4 + 2H_2O$$
$$2CO = C + CO_2$$
$$CO + H_2O = CO_2 + H_2$$

Among these, the most dominant chemical reaction leading to methane is the first one. Therefore, if methanation is carried out over a catalyst with a syngas mixture of H_2 and CO, the desired H_2-to-CO ratio of the feed syngas is around 3:1. The large amount of H_2O produced is removed by condensation and recirculated as process water or steam. During this process, most of the exothermic heat due to the methanation reaction is also recovered through a variety of energy integration processes. Whereas all the reactions listed above are quite strongly exothermic except the forward water gas shift (WGS) reaction, which is mildly exothermic, the heat release depends largely on the amount of CO present in the feed syngas. For each 1% of CO in the feed syngas, an adiabatic reaction will experience a 60°C temperature rise, which may be termed as *adiabatic temperature rise*.

A variety of metals exhibit catalytic effects on the methanation reaction. In the order of catalytic activity, Ru > Ni > Co > Fe > Mo. Nickel is by far the most commonly used catalyst in commercial processes because of its relatively low cost and also of reasonably high catalytic activity. Nearly all the commercially available catalysts used for this process are, however, very susceptible to sulfur poisoning and efforts must be taken to remove all hydrogen sulfide (H_2S) before the catalytic reaction starts. It is necessary to reduce the sulfur concentration in the feed gas to lower than 0.5 ppm in order to maintain adequate catalyst activity for a long period of time. Therefore, the objective of the catalyst development has been aimed at enhancing the *sulfur tolerance* of the catalyst.

Some of the noteworthy commercial methanation processes include Comflux, HICOM, and direct methanation. Comflux is a Ni-based, pressurized fluidized bed (PFB) process converting CO-rich gases into SNG in a single stage, where both methanation and WGS reaction take place simultaneously. The HICOM process developed by British Gas Corporation is a fixed bed process, which involves a series of methanation stages using relatively low H_2-to-CO ratio syngas. Direct methanation is a process developed by the Gas Research Institute (GRI), which methanates equimolar mixtures of H_2 and CO, producing CO_2 rather than H_2O (steam) in addition to methane:

$$2\ H_2 + 2\ CO = CH_4 + CO_2$$

The catalyst developed is claimed to be unaffected by sulfur poisoning and, as such, the process can be used to treat the raw, quenched gas from a coal gasifier with no or little pretreatment.[76]

2.3 COAL GASIFICATION REACTIONS

In coal gasification, four principal reactions are crucial:

1. Steam gasification
2. Carbon dioxide gasification

3. Hydrogasification
4. Partial oxidation reaction

In most gasifiers, several of these reactions, along with the WGS reaction, occur simultaneously. Table 2.1 shows the *equilibrium constants* for these reactions as functions of temperature. The same data are plotted in Figure 2.1, as $\log_{10} K_p$ vs. $1/T$. From the figure, the following are evident and significant:

1. The plots of $\log_{10} K_p$ vs. $1/T$ are nearly linear for all reactions.
2. The exothermicity of reaction is on the same order as the slope of the plot of $\log_{10} K_p$ vs. $1/T$ for each reaction.
3. By the criterion of $K_p > 1$ (i.e., $\log_{10} K_p > 0$), it is found that hydrogasification is thermodynamically favored at lower temperatures, whereas CO_2 and steam gasification reactions are thermodynamically favored at higher temperatures.
4. The equilibrium constant for the WGS reaction is the weakest function of the temperature among all the compared reactions, as clearly evidenced in the plot. This also means that the equilibrium of this reaction can be reversed relatively easily by changing the imposed operating conditions.

2.3.1 Steam Gasification

The steam gasification reaction is endothermic, i.e., requiring heat input for the reaction to proceed in its forward direction. Usually, an excess amount of steam is also needed to promote the reaction.

TABLE 2.1
Equilibrium Constants for Gasification Reactions

		$\text{Log}_{10} K_p$					
T, K	1/T	I	II	III	IV	V	VI
300	0.003333	23.93	68.67	15.86	20.81	4.95	8.82
400	0.0025	19.13	51.54	10.11	13.28	3.17	5.49
500	0.002	16.26	41.26	6.63	8.74	2.11	3.43
600	0.001667	14.34	34.4	4.29	5.72	1.43	2
700	0.001429	12.96	29.5	2.62	3.58	0.96	0.95
800	0.00125	11.93	25.83	1.36	1.97	0.61	0.15
900	0.001111	11.13	22.97	0.37	0.71	0.34	0.49
1000	0.001	10.48	20.68	0.42	0.28	0.14	1.01
1100	0.000909	9.94	18.8	1.06	1.08	0.02	1.43
1200	0.000833	9.5	17.24	1.6	1.76	0.16	1.79
1300	0.000769	9.12	15.92	2.06	2.32	0.26	2.1
1400	0.000714	8.79	14.78	2.44	2.8	0.36	2.36

Note: Reaction I: $C + \frac{1}{2} O_2 = CO$; Reaction II: $C + O_2 = CO_2$; Reaction III: $C + H_2O = CO + H_2$; Reaction IV: $C + CO_2 = 2\ CO$; Reaction V: $CO + H_2O = CO_2 + H_2$; Reaction VI: $C + 2\ H_2 = CH_4$.

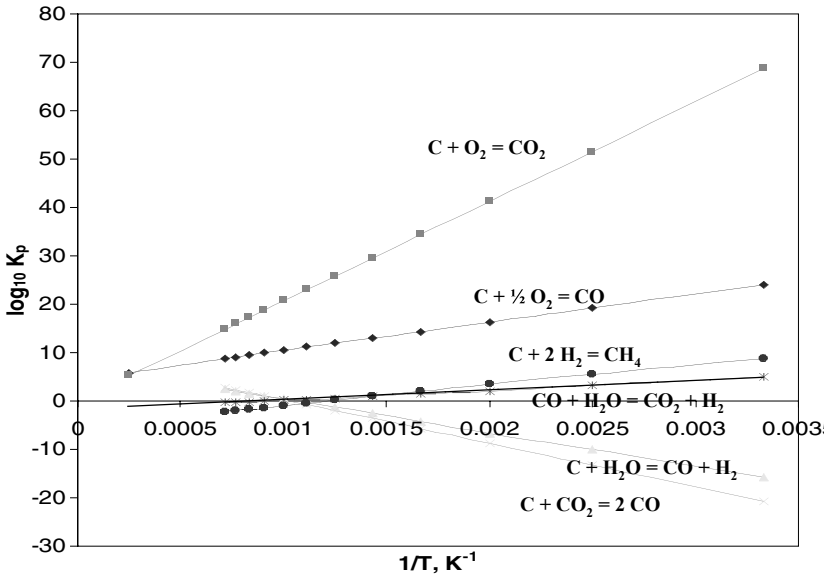

FIGURE 2.1 Equilibrium constant (*K*p) for gasification reactions.

$$C\ (s) + H_2O\ (g) = CO\ (g) + H_2\ (g) \qquad \Delta H°_{298} = 131.3\ \text{kJ/mol}$$

However, excess steam used in this reaction hurts the thermal efficiency of the process. Therefore, this reaction is typically combined with other gasification reactions in practical applications. The H_2-to-CO ratio of the product syngas depends on the synthesis chemistry as well as process engineering. Two reaction mechanisms[77,78] have received most attention for the carbon-steam reactions over a wide range of practical gasification conditions.

Mechanism A[77]

$$C_f + H_2O = C(H_2O)_A$$
$$C(H_2O)_A \rightarrow CO + H_2$$
$$C_f + H_2 = C(H_2)_B$$

In the given equations, C_f denotes free carbon sites that are not occupied, $C(H_2O)_A$ and $C(H_2)_B$ denote chemisorbed species in which H_2O and H_2 are adsorbed onto the carbon site, "=" means the specific mechanistic reaction is reversible, and "→" means the reaction is predominantly irreversible. In Mechanism A, the overall gasification rate is inhibited by hydrogen adsorption on the free sites, thus reducing the availability of the unoccupied active sites for steam adsorption. Therefore, this mechanism may be referred to as *inhibition by hydrogen adsorption.*

Mechanism B[78]

$$C_f + H_2O = C(O)_A + H_2$$
$$C(O)_A \rightarrow CO$$

On the other hand, in Mechanism B, the gasification rate is affected by competitive reaction of chemisorbed oxygen with hydrogen, thus limiting the conversion of chemisorbed oxygen into carbon monoxide. Therefore, this mechanism may be referred to as *inhibition by oxygen exchange.*

Both mechanisms are still capable of producing the rate expression for steam gasification of carbon in the form of[4]:

$$r = k_1 p_{H2O}/(1 + k_2 p_{H2} + k_3 p_{H2O})$$

which was found to correlate with the experimental data quite well. This type of rate expression can be readily derived by taking pseudo–steady state approximation on the adsorbed species of the mechanism.

It has to be clearly noted here that the mechanistic chemistry discussed in this section is based on the reaction between carbon and gaseous reactants, not for reactions between coal and gaseous reactants. Even though carbon is the dominant atomic species present in coal, its reactivity is quite different from that of coal or coal hydrocarbons. In general, coal is more reactive than pure carbon, for a number of reasons, including the presence of various reactive organic functional groups and the availability of catalytic activity via naturally occurring mineral ingredients. It may now be easy to understand why anthracite, which has the highest carbon content among all ranks of coal, is most difficult to gasify or liquefy. Alkali metal salts are known to catalyze the steam gasification reaction of carbonaceous materials, including coals. The order of catalytic activity of alkali metals on coal gasification reaction is Cs > Rb > K > Na > Li. In the case of catalytic steam gasification of coal, carbon deposition reaction may affect the catalysts' life by fouling the catalyst active sites. This carbon deposition reaction is more likely to take place whenever the steam concentration is lacking.

2.3.2 Carbon Dioxide Gasification

The reaction of coal with CO_2 may be approximated or simplified as the reaction of carbon with carbon dioxide, for modeling purposes. Carbon dioxide reacts with carbon to produce carbon monoxide and this reaction is called *Boudouard reaction.* This reaction is also endothermic in nature, similar to the steam gasification reaction.

$$C\ (s) + CO_2\ (g) = 2\ CO\ (g) \qquad \Delta H°_{298} = 172.5\ kJ/mol$$

The reverse reaction is a carbon deposition reaction that is a major culprit of carbon fouling on many surfaces, such as process catalyst deactivation. This gasification reaction is thermodynamically favored at high temperatures (T > 680°C),

which is also quite similar to the steam gasification. The reaction, if carried out alone, requires high temperature (for fast reaction) and high pressure (for higher reactant concentrations) for significant conversion. However, this reaction in practical gasification applications is almost never attempted as a solo chemical reaction, because of a variety of factors including low conversion, slow kinetic rate, low thermal efficiency, unimpressive process economics, etc.

There is general agreement that experimental data on the rate of carbon gasification by CO_2 fit an empirical equation of the form[4]:

$$r = k_1 p_{CO2}/(1 + k_2 p_{CO} + k_3 p_{CO2})$$

where p_{CO} and p_{CO2} are partial pressures of CO and CO_2 in the reactor. This rate equation is shown to be consistent with at least two mechanisms whereby carbon monoxide retards the gasification reaction.[4]

Mechanism A

$$C_f + CO_2 \rightarrow C(O)_A + CO$$
$$C(O)_A \rightarrow CO$$
$$CO + C_f = C(CO)_B$$

Mechanism B

$$C_f + CO_2 = C(O)_A + CO$$
$$C(O)_A \rightarrow CO$$

In both mechanisms, carbon monoxide retards the overall reaction rate. The retardation is via carbon monoxide adsorption to the free sites in the case of Mechanism A, whereas it is via reaction of chemisorbed oxygen with gaseous carbon monoxide to produce gaseous carbon dioxide in Mechanism B.

As mentioned earlier when discussing steam gasification, the CO_2 gasification rate of coal is different from that of the carbon-CO_2 rate for the very same reason. Generally, the carbon-CO_2 reaction follows a global reaction order on the CO_2 partial pressure that is around one or lower, i.e., $0.5 < n < 1$, whereas the coal-CO_2 reaction follows a global reaction order on the CO_2 partial pressure that is one or higher, i.e., $1 < n < 2$. The observed higher reaction order for the coal reaction is also based on the high reactivity of coal for the multiple reasons described earlier.

2.3.3 Hydrogasification

Direct addition of hydrogen to coal under high pressure forms methane. This reaction is called *hydrogasification* and may be written as:

$$\text{Coal} + H_2 = CH_4 + \text{Carbonaceous matter}$$

Or,

$$C\ (s) + 2\ H_2\ (g) = CH_4\ (g) \qquad \Delta H°_{298} = -74.8\ kJ/mol$$

This reaction is exothermic and is thermodynamically favored at low temperatures ($T < 670°C$), unlike both steam and CO_2 gasification reactions. However, at low temperatures, the reaction rate is inevitably too slow. Therefore, high temperature is always required for kinetic reasons, which in turn requires high pressure of hydrogn, which is also preferred from equilibrium considerations. This reaction can be catalyzed by K_2CO_3, nickel, iron chlorides, iron sulfates, etc. However, use of catalyst in coal gasification suffers from serious economic constraints because of the low raw material value, as well as difficulty in recovering and reusing the catalyst. Therefore, catalytic coal gasification has not been practiced much.

2.3.4 Partial Oxidation

Combustion of coal involves reaction with oxygen, which may be supplied as pure oxygen or as air, and forms carbon monoxide and carbon dioxide. Principal chemical reactions between carbon and oxygen involve:

$$C\ (s) + O_2\ (g) = CO_2\ (g) \qquad \Delta H°_{298} = -393.5\ kJ/mol$$
$$C\ (s) + 1/2\ O_2\ (g) = CO\ (g) \qquad \Delta H°_{298} = -111.4\ kJ/mol$$

If sufficient air or oxygen is supplied, combustion proceeds sequentially through vapor-phase oxidation and ignition of volatile matter to eventual ignition of the residual char. Certainly, it is not desirable to allow the combustion reaction to continue too long, because it is a wasteful use of carbonaceous resources.

Even though the combustion or oxidation reactions of carbon may be expressed in terms of simple stoichiometric reaction equations, partial oxidation involves a complex reaction mechanism that depends on how fast and efficiently combustion progresses. The reaction pathway is further complicated because of the presence of both gas-phase homogeneous reactions and heterogeneous reactions between gaseous and solid reactants. The early controversy involving the carbon oxidation reaction centered on whether carbon dioxide is a primary product of the heterogeneous reaction of carbon with oxygen or a secondary product resulting from the gas-phase oxidation of carbon monoxide.[4] Oxidation of carbon involves at least the following four carbon-oxygen interactions, of which only two are stoichiometrically independent:

$$C + 1/2\ O_2 = CO$$
$$CO + 1/2\ O_2 = CO_2$$
$$C + CO_2 = 2\ CO$$
$$C + O_2 = CO_2$$

Based on a great deal of research work, including isotope labeling studies, it is generally agreed concerning the carbon-oxygen reaction that[4]:

1. CO_2, as well as CO, is a primary product of carbon oxidation.
2. The ratio of the primary products, CO to CO_2, is generally found to increase sharply with increasing temperature.
3. There is disagreement in that the magnitude of the ratio of the primary products is a sole function of temperature and independent of the type of carbon reacted.

Further details on the carbon oxidation can be found from a classical work done by Walker et al.[4]

Combustion or oxidation of coal is much more complex in its nature than oxidation of carbon. Coal is not a pure chemical species; rather, it is a multifunctional, multispecies, heterogeneous macromolecule that occurs in a highly porous form (typical porosity of 0.3–0.5) with a very large available internal surface area (typically in the range of 250–700 m^2/g). The internal surface area of coal is usually expressed in terms of specific surface area, which is an intensive property that is a measure of the internal surface area available per unit mass. Therefore, coal combustion involves a very complex system of chemical reactions that occur both simultaneously and sequentially. Further, the reaction phenomenon is further complicated by transport processes of simultaneous heat and mass transfer. The overall rate of coal oxidation, both complete and partial, is affected by a number of factors and operating parameters, including the reaction temperature, O_2 partial pressure, coal porosity and its distribution, coal particle size, types of coal, types and contents of specific mineral matter, heat and mass transfer conditions in the reactor, etc.

Kyotani et al.[5] determined the reaction rate of combustion for 5 different coals in a very wide temperature range between 500 and 1500°C to examine the effects of coal rank (i.e., carbon content) and catalysis by coal mineral matter. Based on their experimental results, the combustion rates were correlated with various char characteristics. It was found that in a region where chemical reaction rate is controlling the overall rate, i.e., typically in a low-temperature region where the kinetic rate is much slower than the diffusional rate of reactant, the catalytic effect of mineral matter is a determining factor for coal reactivity. It was also found that for high-temperature regions where the external mass transfer rate controls the overall rate, the reactivity of coal decreased with increasing coal rank. When the external mass transfer rate limited (or controlled) the overall rate of reaction, the mechanistic rate of external mass transfer is the slowest of all mechanistic rates, including the surface reaction rate and the pore diffusional rate of reactant and product. Such a controlling regime is experienced typically at a high-temperature operation, as the intrinsic kinetic rate is far more strongly correlated against the temperature than the external mass transfer rate is.

2.3.5 Water Gas Shift (WGS) Reaction

Even though the WGS reaction is not classified as one of the principal gasification reactions, it cannot be omitted in the analysis of chemical reaction systems that involve synthesis gas. Among all reactions involving synthesis gas, this reaction equilibrium is least sensitive to the temperature variation. In other words, its equilibrium constant is least strongly dependent on the temperature. Therefore, this

reaction equilibrium can be reversed in a variety of practical process conditions over a wide range of temperatures. WGS reaction in its forward direction is mildly exothermic as:

$$CO\ (g) + H_2O\ (g) = CO_2\ (g) + H_2\ (g) \qquad \Delta H°_{298} = -41.2\ kJ/mol$$

Even though all the participating chemical species are in the form of a gas, scientists believe that this reaction predominantly takes place at the heterogeneous surfaces of coal and also that the reaction is catalyzed by carbon surfaces. As the WGS reaction is catalyzed by many heterogeneous surfaces and the reaction can also take place homogeneously as well as heterogeneously, a generalized understanding of the WGS reaction has been very difficult to achieve. Even the kinetic rate information in the literature may not be immediately useful or applicable to a practical reactor situation.

Syngas product from a gasifier contains a variety of gaseous species other than carbon monoxide and hydrogen. Typically, they include carbon dioxide, methane, and water (steam). Depending on the objective of the ensuing process, the composition of syngas may need to be preferentially readjusted. If the objective of the gasification were to obtain a high yield of methane, it would be preferred to have the molar ratio of hydrogen to carbon monoxide at 3:1, based on the following methanation reaction stoichiometry:

$$CO\ (g) + 3\ H_2\ (g) = CH_4\ (g) + H_2O\ (g)$$

If the objective of generating syngas is the synthesis of methanol via vapor-phase low-pressure process, the stoichiometrically consistent ratio between hydrogen and carbon monoxide would be 2:1. In such cases, the stoichiometrically consistent syngas mixture is often referred to as *balanced gas*, whereas a syngas composition that is substantially deviated from the principal reaction's stoichiometry is called *unbalanced gas*.

If the objective of syngas production is to obtain a high yield of hydrogen, it would be advantageous to increase the ratio of H_2 to CO by further converting CO (and H_2O) into H_2 (and CO_2) via WGS reaction. However, if the final gaseous product is to be used in fuel cell applications, carbon monoxide and carbon dioxide must be removed to acceptable levels by a process such as acid gas removal or other adsorption processes. In particular, for hydrogen proton exchange membrane (PEM) fuel cell operation, carbon monoxide and sulfurous species must be thoroughly removed from the hydrogen gas.

The WGS reaction is one of the major reactions in the steam gasification process, where both water and carbon monoxide are present in ample amounts. Even though all four chemical species involved in the WGS reaction are gaseous compounds at the reaction stage of most gas processing, the WGS reaction, in the case of steam gasification of coal, predominantly takes place heterogeneously, i.e., on the solid surface of coal. If the product syngas from a gasifier needs to be reconditioned by the WGS reaction, this reaction can be catalyzed by a variety of metallic catalysts. Choice of specific kinds of catalysts has always depended on the desired outcome, the prevailing temperature conditions, composition of gas mixture, and process economics. Many investigators have studied the WGS reaction over a variety of

catalysts including iron, copper, zinc, nickel, chromium, and molybdenum. Significant efforts have been made in developing a robust catalyst system that has superior sulfur tolerance and wider applicable temperature range.

2.4 SYNGAS GENERATION VIA COAL GASIFICATION

2.4.1 Classification of Gasification Processes

In the earlier section, the different types of synthesis gas were classified. Similarly, there are a large number of widely varying gasification processes. The gasification processes can be classified basically in two general ways: (1) by the Btu content of the product gas,[6] and (2) by the type of the reactor hardware configuration, as well as by whether the reactor system is operated under pressure or not.

The following processes for conversion of coal to gases are grouped according to *the heating value of the product gas.*

Medium- or High-Btu Gas Gasification Processes

1. Lurgi gasifier
2. Synthane gasifier
3. Atgas molten iron coal gasifier

Low- or Medium-Btu Gas Gasification Processes

1. Koppers-Totzek gasifier
2. Texaco gasifier
3. Shell gasifier
4. Kellogg's molten salt gasifier
5. CO_2-acceptor gasification process
6. U-gas process

Low-Btu Gas Only Gasification Process

1. Underground *in situ* gasification process

Based on the reactor configuration, as well as by the method of contacting gaseous and solid streams, gasification processes can also be categorized into the following four types[3]:

1. *Fixed or moving bed:* In the fixed bed reactor, coal is supported by a grate and the gasifying media (steam, air, or oxygen) pass upward through the supported bed, whereby the product gases exit from the top of the reactor. Only noncaking coals can be used in the fixed bed reactor. On the other hand, in the moving bed reactor, coal and gaseous streams move countercurrently, i.e., coal moves downward by gravity while gas passes upward through the coal bed. The temperature at the bottom of the reactor is higher than that at the top. Because of the lower temperature at the top for coal devolatilization, relatively large amounts of liquid hydrocarbons are also produced in this type of gasifier. In both types of reactor, the

residence time of the coal is much longer than that in a suspension reactor, thus providing ample contact time between reactants. Ash is removed from the bottom of the reactor as dry ash or slag. Lurgi and Wellman-Galusha gasifiers are examples of this type of reactor. It should be clearly understood that a moving bed reactor is classified as a kind of fixed bed reactor, because solids in the bed stay together regardless of the movement of the hardware that supports the bed.

2. *Fluidized bed:* It uses finely pulverized coal particles. The gas (or gasifying medium) flows upward through the bed and fluidizes the coal particles. Owing to the ascent of particles and fluidizing gas, larger coal surface area is made available, which positively promotes the gas-solid chemical reaction, which in turn results in enhancement in carbon conversion. This type of reactor allows intimate contact between gas and solid coal fines, at the same time providing relatively longer residence times than entrained flow reactor. Dry ash is either removed continuously from the bed, or the gasifier is operated at such a high temperature that it can be removed as agglomerates. Such beds, however, have limited ability to handle caking coals, owing to operational complications in fluidization characteristics. Winkler and Synthane processes use this type of reactor.
3. *Entrained bed:* This type of reactor is also referred to as *entrained flow reactor*, because there is no bed of solids. This reactor system uses finely pulverized coal particles blown into the gas stream before entry into the reactor, with combustion and gasification occurring inside the coal particles suspended in the gas phase. Because of the entrainment requirement, high space velocity of gas stream and fine powdery coal particles are very essential to the operation of this type of process. Because of the very short residence time (i.e., high space velocity) in the reactor, a very high temperature is required to achieve good conversion in such a short period of reaction time. This can also be assisted by using excess oxygen. This bed configuration is typically capable of handling both caking and noncaking coals without much operational difficulty. Examples of commercial gasifiers that use this type of reactor include the Koppers-Totzek gasifier and Texaco gasifier.
4. *Molten salt bath reactor:* In this reactor, coal is fed along with steam or oxygen in the molten bath of salt or metal operated at 1,000–1,400°C. Ash and sulfur are removed as slag. This type of reactor is used in Kellogg and Atgas processes.[7]

2.4.2 Historical Background of Coal Gasification and Its Commercialization

It was known as early as the 17th century that gas could be produced by simply heating the coal, i.e., pyrolysis of coal in modern terms. Around 1750, in England, coal was subjected to pyrolysis to form gases that were used for lighting.[8] With the invention of the Bunsen gas burner (at atmospheric pressure), the potential of heating was opened to gas combustion. In 1873, cyclic carbureted water gas process was developed by Thaddeus S. C. Lowe for gas production. In this process, water gas

(H_2 + CO) was produced by reacting hot coke (i.e., smokeless char) with steam via a simplified reaction of C + H_2O = CO + H_2. Heat for the reaction was supplied by combustion energy by introducing air intermittently to burn a portion of the coke. The development of coal-to-gas processes was a major breakthrough in Europe during those days, because coal was the principal fuel available besides wood. By the early 1920s, there were at least five *Winkler fluid bed processes* being operated, all of which were air-blown, producing 10 million scf/h of producer gas. Some of them were later converted to use oxygen instead of air in order to produce nitrogen-free syngas.

The *Lurgi process* was developed to manufacture town gas by complete gasification of brown coal in Germany. In 1936, the first commercial plant based on this process went operational. It produced 1 million scf/d of town gas from low-rank lignite coal. By 1966, there were at least ten Lurgi plants at a number of places in Europe and Asia producing synthesis gas.

In 1942, Heinrich Koppers in Germany developed the *Koppers-Totzek (K-T) suspension gasification process* based on the pilot plant work initiated four years earlier. The first industrial plant was built in France around 1949, which produced 5.5 million scf/d of synthesis gas that was later used to produce ammonia and methanol. By the early 1970s, there were at least 20 K-T plants built all over the world. All of them used oxygen as primary gasification medium, thus producing nitrogen-free syngas.

Winkler, Lurgi, and Koppers-Totzek processes all employed steam and oxygen (or air) to carry out gasification. Most of these developments were originated and perfected in Europe. However, very little development of these processes had taken place in the U.S. until the energy crisis of the 1970s, mainly because of the discovery of natural gas as a convenient fuel and also because of the relatively stable supply of liquid petroleum until then. After the oil embargo of 1973, very active research and development efforts were conducted for cleaner use of coal resources in coal gasification, coal liquefaction, clean coal technology, IGCC, etc. Since then, most coal power plants have significantly upgraded their quality of operation in terms of energy efficiency, by-products, emission control, and profitability.

2.4.3 General Aspects of Gasification

The kinetic rates and extents of conversion for various gasification reactions are typically functions of temperature, pressure, gas composition, and the nature of the coal being gasified. The rate of reaction is intrinsically higher at higher temperatures, whereas the equilibrium of the reaction may be favored at either higher or lower temperatures depending on the specific type of gasification reaction. The effect of pressure on the rate also depends on the specific reaction. Thermodynamically, some gasification reactions such as carbon-hydrogen reaction producing methane are favored at high pressures (>70 atm) and relatively lower temperatures (760–930°C), whereas low pressures and high temperatures favor the production of syngas (i.e., carbon monoxide and hydrogen) via steam or carbon dioxide gasification reaction.

Supply and recovery of heat is a key element in the gasification process from the standpoints of economics, design, and operability. Partial oxidation of char with steam and oxygen leads to generation of heat and synthesis gas. Another way to

produce a hot gas stream is via the cyclic reduction and oxidation of iron ore. The type of coal being gasified is also important to the gasification and downstream operations. Only suspension-type gasifiers such as entrained flow reactor can handle any type of coal, but if caking coals are to be used in fixed or fluidized bed, special measures must be taken so that coal does not agglomerate (or cake) during gasification. If such agglomeration does happen, it would adversely affect the operability of the gasification process. In addition to this, the chemical composition, the volatile matter (VM) content, and the moisture content of coal also play important roles in the coal processing during gasification. The S and N contents of coal seriously affect the quality of the product gas, as well as the gas-cleaning requirements. The sulfur content of coal typically comes from three different sources of coal sulfur, namely, pyritic sulfur, organic sulfur, and sulfatic sulfur. The first two are more dominant sulfur forms, whereas weathered or oxidized coals have more sulfatic forms than fresh coals. Sulfurous gas species can be sulfur dioxide, hydrogen sulfide, or mercaptans, depending on the nature of the reactive environment. If the reactive environment is oxidative, the sulfur dioxide is the most dominant sulfur-containing species in the product gas.

2.4.4 Gasification Processes

2.4.4.1 Lurgi Gasification

The Lurgi gasification process is one of the several processes for which commercial technology has been fully developed.[9]

Since its development in Germany before World War II, this process has been used in a large number of commercial plants throughout the world. This process produces low- to medium-Btu gas as product gas. It may be classified as a fixed bed process in which the reactor configuration is similar to that of a typical fixed bed reactor. The older version of Lurgi process is *dry ash gasification* process that differs significantly from the more recently developed *slagging gasification process*.

The dry ash Lurgi gasifier is a pressurized vertical reactor that accepts crushed noncaking coals only.[10] The coal feed is supported at the base of the reactor by a revolving grate through which the steam and oxygen mixture is introduced and the ash removed. This process takes place at around 24 to 31 atm and in the temperature range of 620 to 760°C. The residence time in the reactor is about 1 h. Steam introduced from the bottom of the reactor provides the necessary hydrogen species, and the heat is supplied by the combustion of a portion of the char. The product gas from a high-pressure reactor has a relatively high methane content compared to a nonpressurized gasifier. The high methane content of the product gas is a result of the relatively low gasification temperature. If oxygen is used as an injecting (and gasifying) medium, the exiting gas has a heating value of approximately 450 Btu/scf. The crude gas leaving the gasifier contains a substantial amount of condensable products including tar, oil, phenol, etc., which are separated in a devolatilizer, where gas is cleaned to remove unsaturated hydrocarbons and naphtha. The gas is then subjected to methanation ($CO + 3H_2 = CH_4 + H_2O$) to produce a high-Btu gas (pipeline quality).

Recent modification of the Lurgi process called *slagging Lurgi gasifier* has been developed to process caking coals.[3] Therefore, the operating temperature of this gasifier is kept higher and the injection ratio of steam is reduced to 1–1.5 mol/mol of oxygen. These two factors cause the ash to melt easily and, therefore, the molten ash is removed as a slag. Coal is fed to the gasifier through a lock hopper system and distributor. It is gasified with steam and oxygen injected into the gasifier near the bottom. The upward movement of hot product gases provides convective heat transfer and makes the preheating and devolatilization of coal easier. Both volatile matter liberated from coal and devolatilized char react with gasifying media, i.e., steam and oxygen. The molten slag formed during the process passes through the slag tap hole. It is then quenched with water and removed through a slag lock hopper. The amount of unreacted steam passing through the system has to be minimized in this process for high energy efficiency. Also, the high operating temperature and fast removal of product gases lead to higher output rates in a slagging Lurgi gasifier than a conventional dry ash Lurgi unit.

The conventional Lurgi gasification is widely recognized for its role as the gasifier technology for South Africa's Sasol complex. A typical product composition for oxygen-blown operation is given in Table 2.2. As can be seen, the H_2-to-CO ratio is higher than 2:1. It is also noted that a relatively large amount of CO_2 is present.

2.4.4.1.1 Lurgi Dry-Ash Gasifier

In this gasifier, coal sized between 1.5 in. and 4 mesh reacts with steam and oxygen in a slowly moving bed. The process is operated semicontinuously. A schematic of a Lurgi pressure gasifier is shown in Figure 2.2.[11] The gasifier is equipped with the following hardware parts[12]:

1. An automated *coal lock chamber* for feeding coal from a coal bin to the pressurized reactor. This device is often called a *coal lock hopper.*
2. A *coal distributor* through which coal is uniformly distributed into the moving bed.
3. A *revolving grate* through which the steam and oxygen are introduced into the reacting zone (coal bed) and the ash is removed.
4. An *ash lock chamber* for discharging the ash from the pressurized reactor into an ash bin, where the ash is cooled by water quenching.
5. A *gas scrubber* in which the hot gas is quenched and washed before it passes through a waste heat boiler.

The gasifier shell is water-cooled and steam is produced from the water jacket. A motor-driven distributor is located at the top of the coal bed, which evenly distributes the feed coal coming from the coal lock hopper. The grate at the bottom of the reactor is also driven by a motor to discharge the coal ash into the ash lock hopper. The section between the inlet and outlet grates has several distinct zones. The topmost zone preheats the feed coal by contacting with the hot crude product gas that is ready to leave the reactor. As the coal gets heated, devolatilization and gasification reactions proceed at temperatures ranging from 620 to 760°C. Devolatilization of coal is accompanied by gasification of the resulting char. The interaction

TABLE 2.2
Typical Lurgi Gas Products

Species	Mole Percentage
CO	16.9
H_2	39.4
CH_4	9.0
C_2H_6	0.7
C_2H_4	0.1
CO_2	31.5
H_2S + COS	0.8
N_2 +Ar	1.6

Source: From Lloyd, W.G., *The Emerging Synthetic Fuel Industry*, Thumann, A., Ed., Atlanta, GA: Fairmont Press, 1981, pp.19–58. With permission.

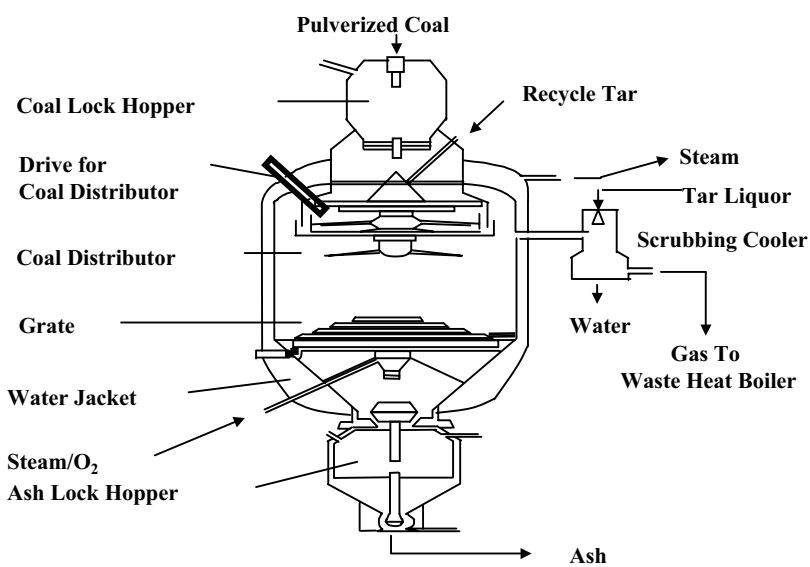

FIGURE 2.2 Lurgi nonslagging pressure gasifier.

between devolatilization and gasification is a determining factor in the kinetics of the process, as well as of the product compositions.

The bottom of the bed is the combustion zone, where coal carbon reacts with oxygen to yield mainly carbon dioxide. The exothermic heat generated by this reaction provides the heat for gasification and devolatilization, both of which are endothermic reactions. By utilizing the exothermic heat of combustion in the gasification and devolatilization, both of which are endothermic, energy integration within the gasifier is accomplished. More than 80% of the coal fed is gasified, the

remainder being burned in the combustion zone. The portion of feed coal burned for *in situ* heat generation may be called *sacrificial coal*. The temperature of the combustion zone must be selected in such a way that it is below the ash fusion point but high enough to ensure complete gasification of coal in subsequent zones. This temperature is also determined by the steam-to-oxygen ratio.

The material and energy balance of the Lurgi gasifier is determined by the following process variables:

1. Pressure, temperature, and steam-to-oxygen ratio.
2. The nature of coal: The type of coal determines the nature of gasification and devolatilization reaction. Lignite is the most reactive coal, for which reaction proceeds at 650°C. On the other hand, coke is the least reactive, for which minimum temperature required for chemical reaction is around 840°C. Therefore, more coal is gasified per unit mole of oxygen for lignite compared to other types (ranks) of coal. The higher the coal rank (i.e., the carbon content of coal), the lower the coal reactivity.
3. The ash fusion point of the coal, which limits the maximum operable temperature in the combustion zone, which in turn determines the steam-to-oxygen ratio.
4. Both the amount and chemical composition of the volatile matter of the coal, which influence the quality and quantity of tar and oils produced.

The Lurgi gasifier has relatively high thermal efficiency because of its medium-pressure operation and the countercurrent gas-solid flow. At the same time, it consumes a lot of steam and the concentration of carbon dioxide in the crude product gas is high, as shown in Table 2.2. Also, the crude gas leaving the gasifier contains a substantial amount of carbonization products such as tar, oil, naphtha, ammonia, etc. These carbonization products are results of devolatilization, pyrolytic reactions, and secondary chemical reactions involving intermediates. This crude product gas is passed through a scrubber, where it is washed and cooled down by a waste heat boiler.

2.4.4.1.2 Slagging Lurgi Gasifier

This gasifier is an improved version of the Lurgi dry-ash gasifier. A schematic[11] of slagging Lurgi gasifier is shown in Figure 2.3. The temperature of the combustion zone is kept higher than the ash fusion point. This is achieved by using a smaller amount of steam than dry-ash Lurgi gasifier, thus lowering the steam/oxygen ratio. The ash is removed from the bottom as slag, not as dry ash. Therefore, the process can handle *caking coals*, unlike the conventional dry-ash gasifier. The main advantage of this gasifier over the conventional dry-ash gasifier is that the yield of carbon monoxide and hydrogen is high and the coal throughput also increases many times. The steam consumption is also minimized.[13]

2.4.4.2 Koppers-Totzek Gasification

This gasification process uses entrained flow technology, in which finely pulverized coal is fed into the reactor with steam and oxygen.[14,15] The process operates at

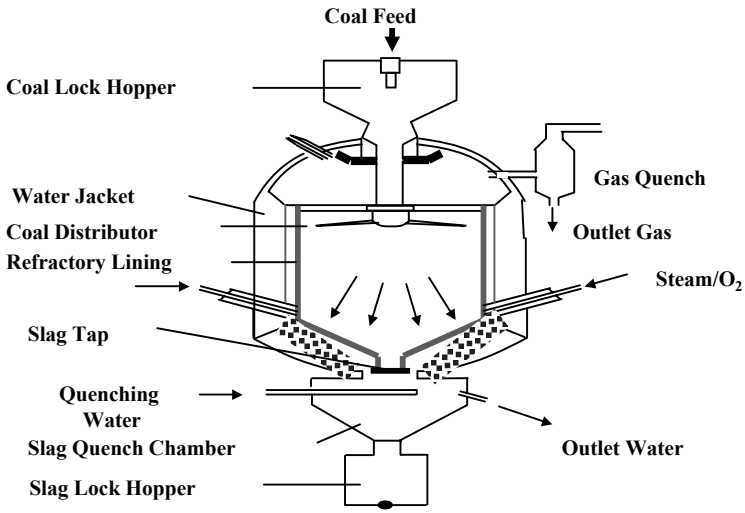

FIGURE 2.3 A schematic of slagging Lurgi gasifier.

atmospheric pressure. As with all entrained flow reactors, the space time in the reactor is very short. The gasifier itself is a cylindrical, refractory-lined coal burner with at least two burner heads through which coal, oxygen, and steam are charged. The burner heads are spaced either 180° (with the two-headed design) or 90° apart (with the four-headed arrangements) and are designed such that steam covers the flame and prevents the reactor refractory walls from becoming excessively hot. The reactor typically operates at a temperature of about 1400–1500°C and atmospheric pressure. At this high temperature, the reaction rate of gasification is extremely high, i.e., by orders of magnitude higher than that at a temperature in a typical fixed bed reactor. About 90% of carbonaceous matter is gasified in a single pass, depending on the type of coal. Lignite is the most reactive coal, for which reactivity approaches nearly 100%.[3]

In contrast to moving bed or fluidized bed reactors, this gasifier has very few limitations on the nature of feed coal in terms of caking behavior and mineral matter (ash) properties. Because of very high operating temperatures, the ash agglomerates and drops out of the combustion zone as molten slag and subsequently gets removed from the bottom of the reactor. The hot effluent gases are quenched and cleaned. This gas product contains no tar, ammonia, or condensable hydrocarbons and is predominantly synthesis gas. It has a heating value of about 280 Btu/scf and can be further upgraded by reacting with steam to form additional hydrogen and carbon dioxide via WGS reaction.

2.4.4.2.1 Koppers-Totzek Gasifier

This gasifier is one of the most significant entrained bed gasifiers in commercial operation today. It accepts almost any type of coal, including caking coal, without any major operational restrictions. It has the highest operating temperature (around 1400–1500°C) of all the conventional gasifiers. There are two versions in terms of process equipment design, a two-headed and a four-headed burner type. A schematic of a Koppers-Totzek

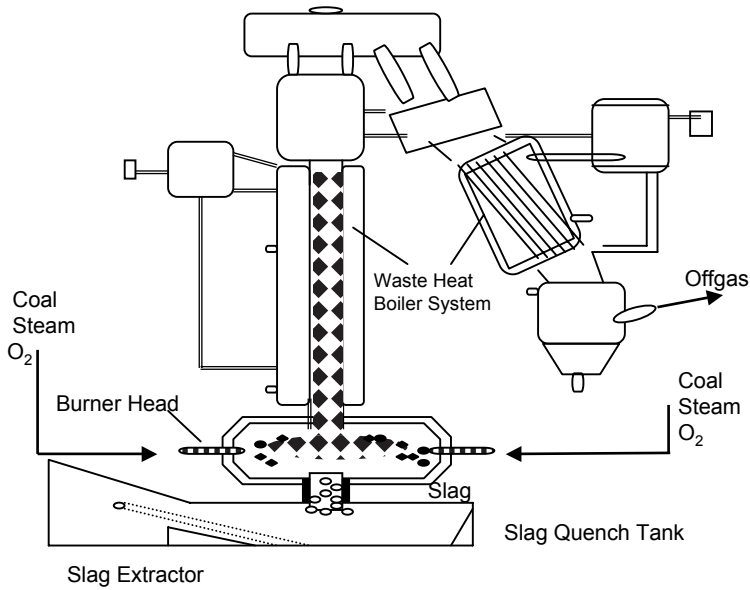

FIGURE 2.4 A schematic of Koppers-Totzek gasifier (two-headed burner design).

two-headed gasifier[16] is shown in Figure 2.4. The original version designed in 1948 in Germany was two-headed, with the heads mounted at the ends, i.e., 180° apart. The gasifier as such is ellipsoidal in shape and horizontally situated. Each head contains two burners. The shell of the gasifier is water-jacketed and has an inner refractory lining. Design of four-headed gasifiers began in India around 1970. In this design, burner heads are spaced 90°, instead of 180° as in two-headed ones. All the burner heads are installed horizontally. The capacity of a four-headed burner gasifier is larger than its two-headed counterpart.[17]

2.4.4.2.2 Features of the Koppers-Totzek Process

The Koppers-Totzek process has been very successfully operated commercially and some of the process features are summarized as follows:

1. *High capacity:* These process units are designed for coal feed rates up to 800 tons per day, or about 42 million scf/d of 300-Btu gas.
2. *Versatility:* The process is capable of handling a variety of feedstocks, including all ranks of solid fuels, liquid hydrocarbons, and pumpable slurries containing carbonaceous materials. Even feedstocks containing high sulfur and ash contents can be readily used in this process. Therefore, this process is not limited only to coal.
3. *Flexibility:* The changeover from solid fuel feed to liquid fuels involves only a change in the burner heads. Multiple feed burners permit wide variations in turndown ratio (defined as the numeric ratio between the highest and the lowest effective system capacity). This process is capable of instantaneous shutdown with full production resumable in a remarkably short time, only 30 min.

4. *Simplicity of construction:* There is no complicated mechanical equipment or pressure-scaling device required. The only moving parts in the gasifiers are the moving screw feeders for solids or pumps for liquid feedstocks.
5. *Ease of operation:* Control of the gasifiers is achieved primarily by maintaining carbon dioxide concentration in the clean gas at a reasonably constant value. Slag fluidity at high process temperatures may be visually monitored. Gasifiers display good dynamic responses.
6. *Low maintenance:* Simplicity of design and a minimum number of moving parts require little maintenance between the scheduled annual maintenance events.
7. *Safety and efficiency*: The process has a track record of over 50 years of safe operation. The overall thermal efficiency of the gasifier is 85 to 90%. The time on stream (TOS) or availability is better than 95%.

2.4.4.2.3 Process Description of Koppers-Totzek Gasification

The Koppers-Totzek gasification process, whose flow schematic is shown in Figure 2.5, employs partial oxidation of pulverized coal in suspension with oxygen and steam. The gasifier is a refractory-lined steel shell encased with a steam jacket for producing low-pressure process steam as an energy recovery scheme. A two-headed gasifier is capable of handling 400 tons per day of coal. Coal, oxygen, and steam are brought together in opposing gasifier burner heads spaced 180° apart (in the two-headed case). In the case of four-headed gasifiers, these burners are 90° apart. The

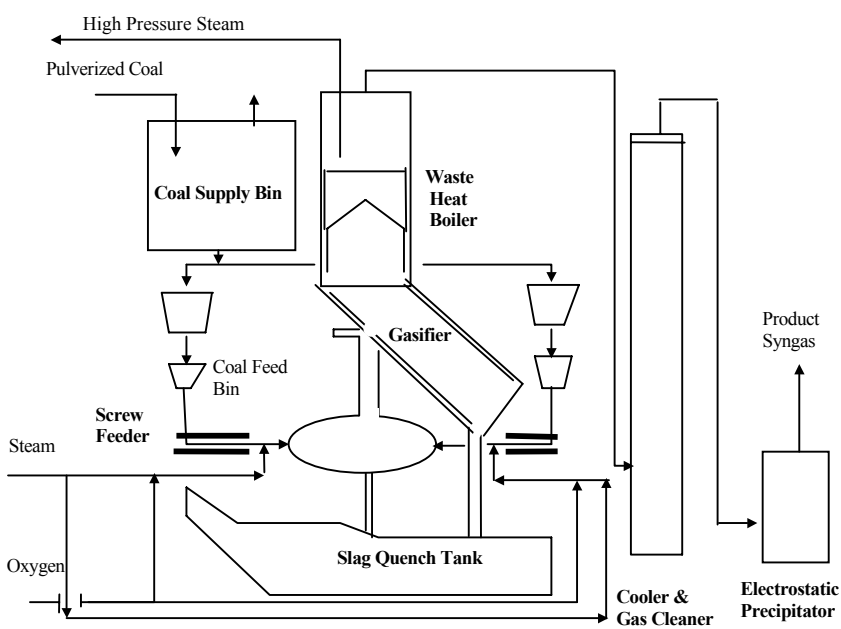

FIGURE 2.5 A schematic of the Koppers-Totzek gasification process.

four-head design can handle up to 850 tons of coal per day. Exothermic reactions due to coal combustion produce a flame temperature of approximately 1930°C, which is lowered by heat exchange with a steam jacket. Gasification of coal is almost complete and instantaneous. The carbon conversion depends on the reactivity of coal, approaching 100% for lignites. The lower the rank of coal, the higher the conversion.

Gaseous and vapor hydrocarbons evolving from coal at moderate temperature are passed through a zone of very high temperature, in which they decompose so rapidly that there is no coagulation of coal particles during the plastic stage. Thus, any coal can be gasified irrespective of the caking property, ash content, or ash fusion temperature. As a result of the endothermic reactions occurring in the gasifier between carbon and steam and radiation to the refractory walls, the reactor temperature decreases from 1930°C (flame temperature) to 1500°C. At these conditions, only gaseous products are produced with no tars, condensable hydrocarbons, or phenols formed. Typical compositions of Koppers-Totzek gaseous products are shown in Table 2.3.

Ash in the coal feed becomes molten in the high-temperature zone. Approximately 50% of the coal ash drops out as slag into a slag quench tank below the gasifier. The remaining ash is carried out of the gasifier as fine fly ash. The gasifier outlet is equipped with water sprayers to drop the gas temperature below the ash fusion temperature. This cooling prevents slag particles from adhering to the tubes of the waste heat boiler, which is mounted above the gasifier.

The raw gas from the gasifier passes through the waste heat boiler, where high-pressure steam up to 100 atm is produced via waste heat recovery. After leaving the waste heat boiler, the gas at 175–180°C is cleaned and cooled in a highly efficient scrubbing system, which reduces the entrained solids to 0.002–0.005 grains/scf or less and further lowers the temperature from 175 to 35°C. If the gas coming out of the Koppers-Totzek process is to be compressed to high pressures for chemical synthesis, electrostatic precipitators (ESPs) are used for further cleaning. Several gasifiers can share common cleaning and cooling equipment, thus reducing the capital cost.

TABLE 2.3
Typical Raw Product Gas Compositions of Koppers-Totzek Gasifier (oxygen-blown type)

Component	Percentage
CO	52.5
H_2	36.0
CO_2	10.0
H_2S + COS	0.4
N_2 + Ar	1.1

Note: Average heating value = 286 Btu/scf; all percentages are in volume percent.

Source: From Lloyd, W.G., *The Emerging Synthetic Fuel Industry*, Thumann, A., Ed., Atlanta, GA: Fairmont Press, 1981, pp. 19–58.

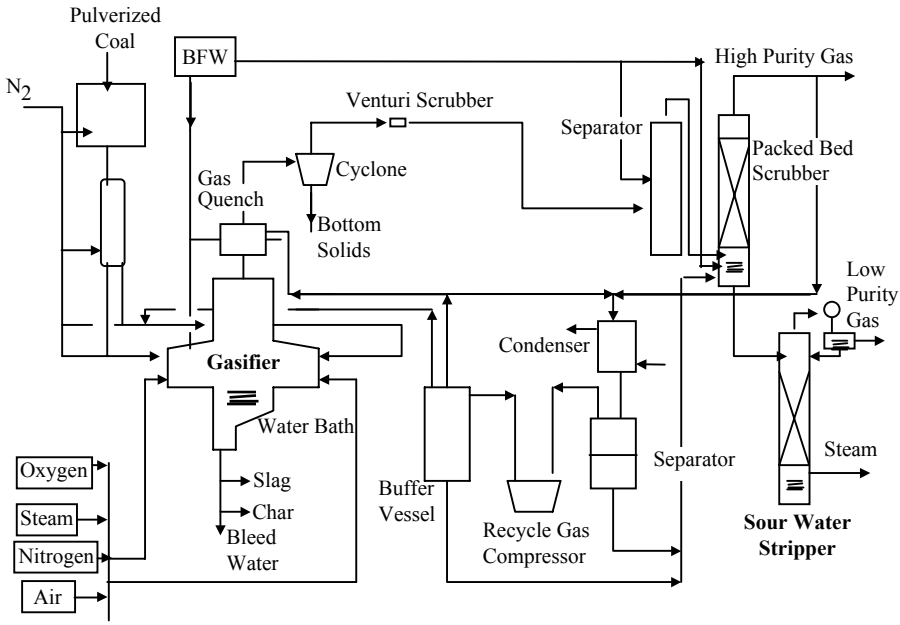

FIGURE 2.6 A schematic of shell gasification process.

The cool, cleaned gas leaving the gas cleaning system still contains sulfur compounds that must be removed to meet the final gas specifications. The type of the desulfurization system chosen depends on the end uses and the pressure of the product gas. For low pressures and low-Btu gas applications, there are a number of chemically reactive processes, such as *amine and carbonate processes*. At higher pressures, physical absorption processes such as *Rectisol process* can be used. The choice of the process also depends on the desired purity of the product gas and its selectivity with respect to the concentration of carbon dioxide and sulfides. Advances in gas cleaning have been quite significant in recent years, owing to more stringent environmental regulations.[18]

2.4.4.3 Shell Gasification

The Shell coal gasification process was developed by Royal Dutch and Shell group in the early 1970s. It uses a pressurized, slagging entrained flow reactor for gasifying dry pulverized coal.[19] Similar to the Koppers-Totzek process, it has the potential to gasify widely different ranks of coals, including low-rank lignites with high moisture content. Unlike other gasifying processes, it uses *pure oxygen* as the gasifying medium, for gasification via partial oxidation. Shell Global Solutions licenses two versions of gasification technologies, i.e., one for liquid feedstock applications and the other for coal and petroleum coke. A schematic of the Shell coal gasification process is given in Figure 2.6. The process has the following features[20]:

1. Almost 100% conversion of a wide variety of coals, including high-sulfur coals, lignites, and coal fines

2. High thermal efficiency in the range of 75 to 80%
3. Efficient heat recovery through production of high-pressure superheated steam
4. Production of clean gas without any significant amount of by-products
5. High throughput
6. Environmental compatibility

Coal before feeding to the gasifier vessel, is crushed and ground to less than 90-μm size. This pulverized and dried coal is fed through diametrically opposite diffuser guns into the reaction chamber.[21] The coal is then reacted with the pure oxygen and steam, where flame temperature reaches as high as 1800–2000°C. A typical operating pressure is around 30 atm. Raw product gas typically consists of mainly carbon monoxide (62–63%) and hydrogen (28%), with some quantities of carbon dioxide. A water-filled bottom compartment is provided in which molten ash is collected. Some amount of ash is entrained with the synthesis gas, which is then recycled along with the unconverted carbon. A quench section is provided at the reactor outlet to lower the gas temperature. Removal of particulate matter from the raw product gas is integrated with the overall process. This removal system typically consists of *cyclones and scrubbers*. The main advantage of this section is elimination of solid-containing wastewater, thus eliminating the need for filtration.

2.4.4.4 Texaco Gasification

The Texaco process also uses entrained flow technology for gasification of coal. It gasifies coal under relatively high pressure by injection of oxygen (or air) and steam with concurrent gas/solid flow. Fluidized coal is mixed with either oil or water to make it into *pumpable slurry*. This slurry is pumped under pressure into a vertical gasifier, which is basically a pressure vessel lined inside with refractory walls. The slurry reacts with either air or oxygen at high temperature. The product gas contains primarily carbon monoxide, carbon dioxide, and hydrogen with some quantity of methane. Because of high temperature, oil or tar is not produced. This process is basically used to manufacture *CO-rich synthesis gas*.[3] A schematic of the Texaco gasification process is shown in Figure 2.7.

This gasifier evolved from the commercially proven Texaco partial oxidation process[10] used to gasify crude oil and hydrocarbons. Its main feature is the *use of coal slurry feed*, which simplifies the coal-feeding system and operability of the gasifier. The gasifier is a simple, vertical, cylindrical pressure vessel with refractory linings in the upper partial oxidation chamber. It is also provided with a slag quench zone at the bottom, where the resultant gases and molten slag are cooled down. In the latter operation, large amounts of high-pressure steam can be obtained, which boosts the thermal efficiency of the process. Another important factor that affects the gasifier thermal efficiency is the water content of the coal slurry. This water content should be minimized because a large amount of oxygen must be used to supply the heat required to vaporize the slurry water. This gasifier favors high-energy dense coals so that the water-to-energy ratio in the feed is small. Therefore, eastern U.S. bituminous coals are preferable to lignites for this gasifier. The gasifier operates at around 1100–1370°C and a pressure of 20–85 atm.

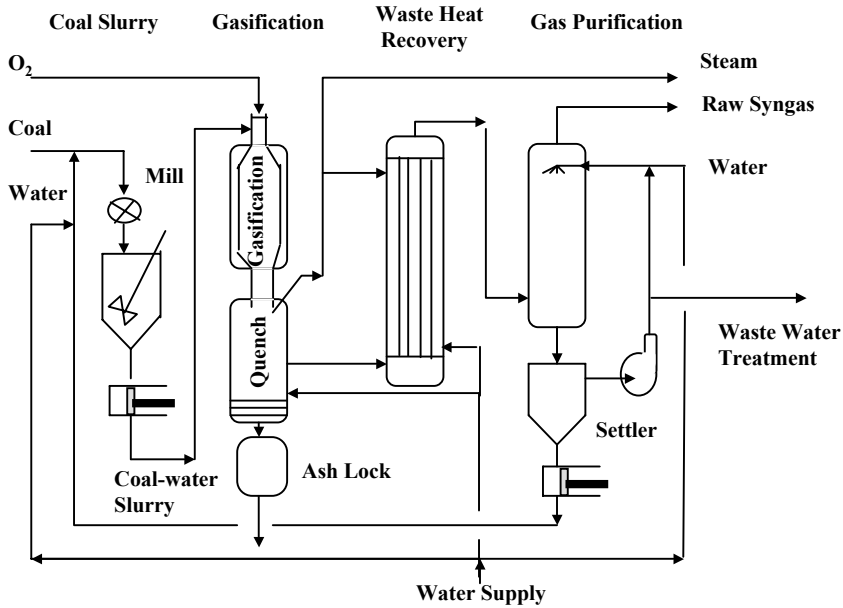

FIGURE 2.7 A schematic of Texaco gasification process.

The product gases and molten slag produced in the reaction zone pass downward through a water spray chamber and a slag quench bath, where the cooled gas and slag are then removed for further treatment. The gas, after being separated from slag and cooled, is treated to remove carbon fines and ash. These fines are then recycled to the slurry preparation system, while the cooled gas is treated for acid gas removal and elemental sulfur is recovered from the hydrogen sulfide (H_2S)-rich stream.

2.4.4.5 *In Situ* Gasification

In situ gasification, or underground gasification, is a technology for recovering the energy content of coal deposits that cannot be exploited either economically or technically by conventional mining (or *ex situ*) processes. Coal reserves that are suitable for *in situ* gasification have low heating values, thin seam thickness, great depth, high ash or excessive moisture content, large seam dip angle, or undesirable overburden properties. A considerable amount of investigation has been performed on *underground coal gasification (UCG)* in the former USSR and in Australia, but it is only in recent years, that the concept has been revived in Europe and North America as a means of fuel gas production. In addition to its potential for recovering deep, low-rank coal reserves, the UCG process may offer some advantages with respect to its resource recovery, minimal environmental impact, operational safety, process efficiency, and economic potential. The aim of *in situ* gasification of coal is to convert coal hydrocarbons into combustible gases by combustion of coal seam in the presence of air, oxygen, or steam.

The basic concepts of underground coal gasification may be illustrated by Figure 2.8.[22] The basic principles of *in situ* gasification are still very similar to those involved

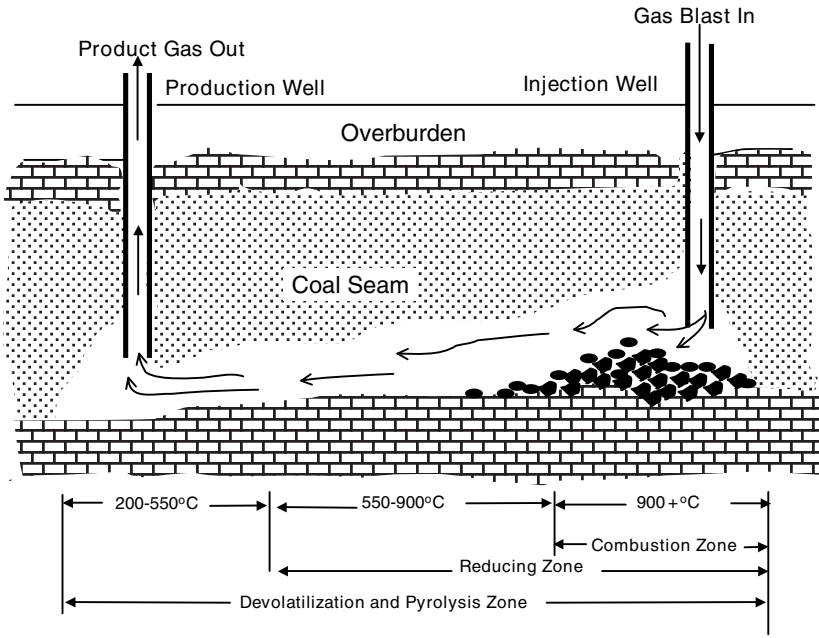

FIGURE 2.8 A schematic of *in situ* underground gasification process.

in the above-ground (*ex situ*) gasification of coal. Combustion process itself could be handled in either *forward* or *reverse* mode. Forward combustion involves movement of the combustion front and injected air in the same direction, whereas in reverse combustion, the combustion front moves in the opposite direction to the injected air. The process involves drilling and subsequent linking of the two boreholes to enable gas flow between the two. Combustion is initiated at the bottom of one borehole called *injection well* and is maintained by the continuous injection of air.

As illustrated in Figure 2.8, in the initial reaction zone, carbon dioxide is generated by reaction of oxygen (air) with the coal, which further reacts with coal to produce carbon monoxide by the Boudouard reaction ($CO_2 + C = 2CO$) in the reduction zone. Further, at such high temperatures, the moisture present in the seam may also react with carbon to form carbon monoxide and hydrogen via the steam gasification reaction ($C + H_2O = CO + H_2$). In addition to all these basic gasification reactions, coal decomposes in the pyrolysis zone owing to high temperatures to produce hydrocarbons and tars, which also contribute to the product gas mix. The heating value from the air-blown *in situ* gasifier is roughly about 100 Btu/scf. The low heat content of the gas makes it uneconomical for transportation, making it necessary to use the product gas on site. An extensive discussion on *in situ* gasification can be found in references by Thompson[23] and by Gregg and Edgar.[24] A noteworthy R&D effort in underground coal gasification has also been conducted by the Commonwealth Scientific and Industrial Research Organization (CSIRO), Australia. CSIRO researchers have developed a model to assist with the implementation of this technology.[25] A number of other trials and trial schemes were evaluated in Europe, China, India, South Africa, and the U.S.

2.4.4.5.1 Potential Possibility of Using Microbial Processes for In Situ Gasification

Juntgen[26] in his review article has explored the possibilities of using microbiological techniques for *in situ* conversion of coal into methane. Microorganisms have been found that grow on coal as a sole carbon source. Both forms of sulfur, namely organic and inorganic (pyritic and sulfatic), are claimed to be removable by biochemical techniques, and microorganisms are able to grow, in principle, in narrow pore structures of solids. The conversion of large-molecular-weight aromatics, including polynuclear aromatics (PNAs), is also potentially feasible. An important precursor of developing such new process techniques for *in situ* coal conversion in deep seams is the knowledge of coal properties, both physical and chemical, under the prevailing conditions. The two most important coal properties, which dictate the *in situ* processes, are the *permeability* of coal seam, including the overburden and the *rank* of coal. For microbial conversion of coal, microporosity also becomes an important parameter. The permeability of coal seam in great depths is usually quite small due to high rock overburden pressure. However, accessibility is very important for performing *in situ* processes. There are several ways to increase the permeability of the coal seams at great depths.[26] Some of these ideas are very similar to those used in *in situ* oil shale retorting as discussed in Chapter 8.

The main advantage of using microbiological techniques is that the reaction takes place at ambient temperatures. Progress made in developing these types of processes is quite notable. A remarkable effect of such reactions in coal is that the microorganisms can penetrate into fine pores of the coal matrix, and can also create new pores if substances contained in the coal matrix are converted into gaseous compounds.

However, the most difficult and complex problem associated with microorganism-based reactions is the transition from solely oxidative processes to methane-forming reactions. There are at least three reaction steps involved: (1) the aerobic degradation of coal to biomass and high-molecular-weight products, (2) an anaerobic reaction leading to the formation of acetate, hydrogen, and carbon monoxide, and (3) the conversion of these products to methane using methanogenic bacteria. Methanogenic bacteria belong to a group of primitive microorganisms, the *Archaea*. They give off methane gas as a by-product of their metabolism, and are common in sewage treatment plants and hot springs, where the temperature is warm and oxygen is absent. Advantages of these processes over other conversion processes are lower conversion temperature and more valuable products.[26] However, an intensive investigation must be conducted to adapt reaction conditions and product yields to conditions prevailing in coal seams at great depth, where transport processes play a significant role in the overall reaction.

2.4.4.5.2 Underground Gasification System

The underground gasification system involves three distinct sets of operations: pregasification, gasification, and further processing and utilization. Pregasification operations provide access to the coal deposit and prepare it for gasification. Connection between the inlet and outlet through the coal seam is achieved via shafts and boreholes. Linking can be achieved through several means, such as pneumatic, hydraulic, or electric linking, and using explosives, etc. Sometimes, partial linking

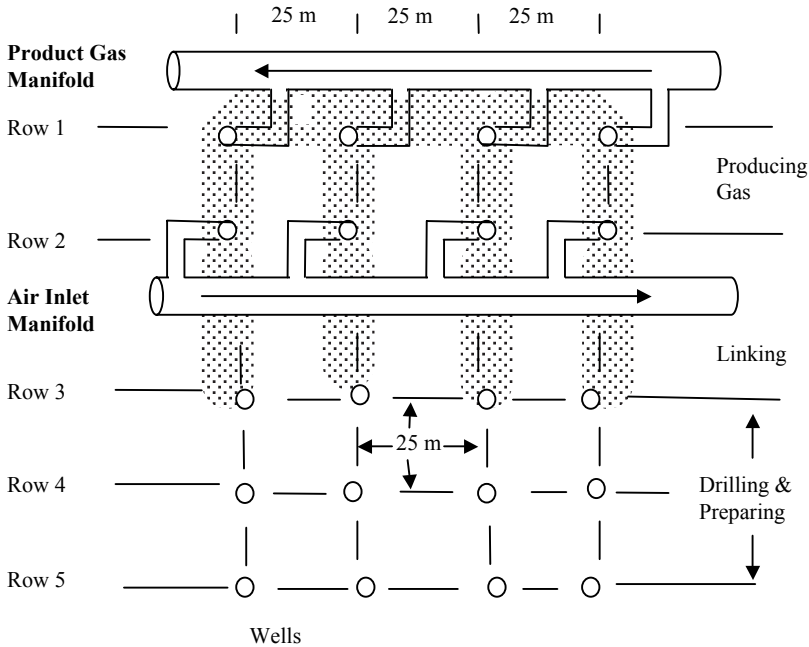

FIGURE 2.9 Plane view of linked-vertical-well underground gasification plant operated near Moscow.

may also be accomplished by taking advantage of the natural permeability of the coal seam. Among all the linking methods, only directionally drilled boreholes provide positive connections between inlet and outlet sections and all other methods permit a certain degree of uncertainty to play a role in the system. A schematic view of a *linked-vertical-well underground gasification* plant operated near Moscow[22] is shown in Figure 2.9.

The gasification operations that allow reliable production of low-Btu gas consist of input of gasifying agents such as air or oxygen and steam (or alternating air and steam), followed by ignition. Ignition can be managed either by electrical means or by burning solid fuels. Ignition results in contact between gasifying agents and coal organics at the flame front. The flame front may advance in the direction of gas flow *(forward burning)* or in the direction opposite to the gas flow (*backward burning*). During these operations, the major technical difficulties and challenges are in the area of process control. Owing to the unique nature of underground gasification, there inherently exists problems of controllability and observability.

The next, and most important, operation is the utilization of the product gas, and it requires a coupling between the gas source and the energy demand. The product gas can be either used as an energy source to produce electricity on site or can be upgraded to a high-Btu pipeline-quality gas for transmission. In some other applications, it could be utilized near the deposit as a hydrogen source, as a reducing agent, or as a basic raw material for manufacture of other chemicals. With realization of the hydrogen economy, the product gas may have good potential as a hydrogen

source. Generally speaking, there are no major technical problems involved with the utilization of product gas, apart from potential environmental concerns.

2.4.4.5.3 Methods for Underground Gasification

There are two principal methods that have been tried successfully, *shaft methods* and *shaftless methods* (and combinations of the two).[24,25,27] Selection of a specific method to be adopted depends on such parameters as the natural permeability of the coal seam, the geochemistry of the coal deposit, the seam thickness, depth, width and inclination, closeness to metropolitan developments, and the amount of mining desired. Shaft methods involve driving of shafts and drilling of other large-diameter openings that require underground labor, whereas shaftless methods use boreholes for gaining access to the coal seam and do not require labor to work underground.

2.4.4.5.3.1 Shaft Methods

1. *Chamber or warehouse method:* This method requires the preparation of underground galleries and the isolation of coal panels with brick wall. The blast of air for gasification is applied from the gallery at the previously ignited face of one side of the panel, and the gas produced is removed through the gallery at the opposite side of the panel. This method relies on the natural permeability of the coal seam for airflow through the system. Gasification and combustion rates are usually low, and the product gas may have variable composition from time to time. To enhance the effectiveness, coal seams are precharged with dynamites to rubblize them in advance of the reaction zone by a series of controlled explosions.
2. *Borehole producer method:* This method typically requires the development of parallel underground galleries and are located about 500 ft. apart within the coal bed. From these galleries, about 4-in.-diameter boreholes are drilled about 15 ft. apart from one gallery to the opposite one. Electric ignition of the coal in each borehole can be achieved by remote control. This method was originally designed to gasify substantially flat-lying seams. Variations of this technique utilize hydraulic and electric linking as alternatives to the use of boreholes.
3. *Stream method:* This method can be applied to steeply pitched coal beds. Inclined galleries following the dip of the coal seam are constructed parallel to each other and are connected at the bottom by a horizontal gallery or "fire-drift." A fire in the horizontal gallery initiates the gasification, which proceeds upward with air coming down one inclined gallery and gas leaving through the other. One obvious advantage of the stream method is that ash and roof material drop down, tend to fill void space, and do not tend to choke off the combustion zone at the burning coal front. However, this method is structurally less suitable for horizontal coal seams because of roof collapse problems.

2.4.4.5.3.2 Shaftless Methods

In shaftless methods, all development, including gasification, is carried out through a borehole or a series of boreholes drilled from the surface into the coal seam. A general

approach has been to make the coal bed more permeable between the inlet and outlet boreholes by a chosen linking method, ignite the coal seam, and then gasify it by passing air and other gasifying agents from the inlet borehole to the outlet borehole.

2.4.4.5.3.3 Percolation or Filtration Methods

This is the most direct approach to accomplish shaftless gasification of a coal seam using multiple boreholes. The distance required between boreholes depends on the seam permeability. Lower-rank coals such as lignites have a considerable natural permeability and, as such, can be gasified without open linking. However, higher-rank coals such as anthracites are far less permeable, and it becomes necessary to connect boreholes by some efficient linking techniques that will increase the permeability and fracture of the coal seam so that an increased rate of gas flow can be attained. Air or air/steam is blown through one borehole, and product gas is removed from another borehole. Either forward or reverse combustion can be permitted by this method. As the burn-off (a combination of combustion and gasification) progresses, the permeability of the seam also increases and compressed air blown through the seam helps enlarge cracks or openings in the seam. When the combustion of a zone nears completion, the process is transferred to the next pair of boreholes and continues. In this operation, coal ash and residues should be structurally strong enough to prevent roof collapse.

2.4.4.5.4 Potential Problem Areas with In Situ Gasification

There are several issues why the *in situ* gasification processes may not be able to produce a high-quality and constant quantity of product gas, recover a high percentage of coal energy in the ground, and control the groundwater contamination. Potential problem areas in commercial exploitation of this technology are discussed in the following text.

2.4.4.5.4.1 Combustion Control

Combustion control is essential for controlling the product gas quality as well as the extent of coal conversion. The reactive contacting between the coal and the gasifying agent should be such that the coal is completely *in situ* gasified, all oxygen in the inlet gas is consumed, and the production of fully combusted carbon dioxide and water is minimized. In a typical *in situ* coal gasification process, as the processing time goes by, the heating value of the product gas decreases. This may be attributable to increasingly poor contact of gas with the coalface, because of large void volumes and from roof collapse. The problem of efficient contacting needs to be solved satisfactorily in this process.

2.4.4.5.4.2 Roof Structure Control

After the coal is burned off, a substantial roof area is left unsupported. Uncontrolled roof collapse causes nontrivial problems in the combustion control, and also seriously hinders successful operation of the overall gasification process. Further, it potentially results in the leakage of reactant gases, seepage of groundwater into the coal seam, loss of product gas, and surface subsidence above the coal deposit.

2.4.4.5.4.3 Permeability, Linking, and Fracturing

An underground coal bed usually does not have a sufficiently high permeability to permit the passage of oxidizing gases through it without a serious pressure drop.

Also, intentional linking methods such as pneumatic, hydraulic, and electric, as well as fracturing with explosives, do not result in a uniform increase in permeability throughout the coal bed. They also tend to disrupt the surrounding strata and worsen the leakage problems. Therefore, the use of boreholes is proved to provide a more predictable method of linking and is a preferred technique.

2.4.4.5.4.4 Leakage Control

This is one of the most important problems because the loss of substantial amount of product gas can adversely affect the recovered amount of the product gas as well as the gasification economics. Further, the inlet reactant gases should not be wasted. Influx of water can also affect the control of the process. Leakage varies from site to site and also depends on a number of factors including geological conditions, depth of coal seam, types of boreholes and their seals, and permeability of coal bed.

Based on the above considerations, it is imperative that *in situ* gasification never be attempted in a severely fractured area, in shallow seams, or in coal seams adjoining porous sedimentary layers. It is also essential to prevent roof collapse and to properly seal inlet and outlet boreholes after operation.

2.4.4.5.5 Monitoring of Underground Processes

Proper monitoring of the underground processes is a necessary component of successful operation and design of an underground gasification system. *A priori* knowledge of all the parameters affecting the gasification is required so that adequate process control philosophy can be adopted and implemented for controlling the operation. These factors include the location, shape, and temperature distribution of the combustion front, the extent and nature of collapsed roof debris, the permeability of coal seam and debris, the leakage of reactant and product gases, the seepage of groundwater, and the composition and yield of the product gases.

2.4.4.5.6 Criteria for an Ideal Underground Gasification System

The following are the criteria for successful operation of an ideal underground coal gasification system:

1. The process must be operable on a large scale.
2. The process must ensure that no big deposits of coal are left ungasified or partially gasified.
3. The process must be controllable so that desired levels, in terms of quality and quantity, of product gases are consistently produced.
4. The mechanical features must ensure that they should be able to control undesirable phenomena such as groundwater inflow and leakage (as outflow) of reactants and products.
5. The process should require little or no underground labor, either during operation or even during the installation of the facilities.

2.4.4.6 Winkler Process

This is the oldest commercial process employing fluidized bed technology.[28] The process was developed in Europe in the 1920s. There are more than 15 plants in

operation today all over the world with the largest having an output of 1.1 million scf/d. In this process, pulverized coal is dried and fed into a fluidized bed reactor by means of a *variable speed screw feeder*. The gasifier operates at atmospheric pressure and a temperature of 815–1000°C. Coal particles react with oxygen and steam to produce offgas rich in carbon monoxide and hydrogen. The relatively high operating temperature leaves very little tar and liquid hydrocarbons in the product gas stream. The gas stream that may carry up to 70% of the generated ash is cleaned by water scrubbers, cyclones, and electrostatic precipitators (ESPs). Unreacted char carried over by the fluidizing gas stream is further converted by secondary steam and oxygen in the space above the fluidized bed. As a result the maximum temperature occurs above the fluidized bed. To prevent ash fines from melting at a high temperature and forming deposits in the exit duct, gas is cooled by a radiant boiler before it leaves the gasifier. Raw hot gas leaving the gasifier is passed through a waste heat recovery section. The gas is then compressed and goes through WGS reaction. The product gas has a heating value of about 275 Btu/scf. The thermal efficiency of the process runs approximately 75%.

2.4.4.6.1 Process Description

In the early 1920s, Winkler, an employee of Davy Power Gas Inc., conceived the idea of using a fluidized bed for gasifying the coal. The first commercial unit was built in 1926. Since then, more than 30 producers and 15 installations have put this process into operation for coal gasification.

In earlier facilities, dryers were used, prior to the introduction of coal into the gas generator, to reduce the coal moisture to less than 8%. It was later realized that as long as the feed coal could be sized, stored, and transported without plugging, dryers could be omitted. Without dryers, moisture in the coal is vaporized in the generator with the heat provided by using additional oxygen for combustion reaction. Drying the coal in the generator also offers an additional advantage, i.e., elimination of an effluent stream, the dryer stack, which would require further treatment of particulate and sulfur removal.

2.4.4.6.2 Gasifier (Gas Generator)

A schematic of a Winkler fluidized bed gasifier[22] is shown in Figure 2.10. Pulverized coal is fed to the gasifier through variable-speed feeding screws. These screws not only control the coal feed rate, but also serve to seal the gasifier by preventing steam from wetting the coal and blocking the pathway by agglomeration. A high-velocity gas stream flows upward from the bottom of the gasifier. This gas stream fluidizes the bed of coal, as well as intimately mixes the reactants, thus bringing them into close contact. Fluidization helps the gas-to-solid mass transfer. This also helps in attaining an isothermal condition between the solid and the gas stream, which permits the reactions to reach equilibrium in the shortest possible time. Gasification chemistry in the Winkler gasifier is based on a combination of combustion reaction and WGS reaction.

$$C + O_2 = CO_2$$

$$C + 1/2\ O_2 = CO$$

$$C + H_2O = H_2 + CO$$

$$CO + H_2O = CO_2 + H_2$$

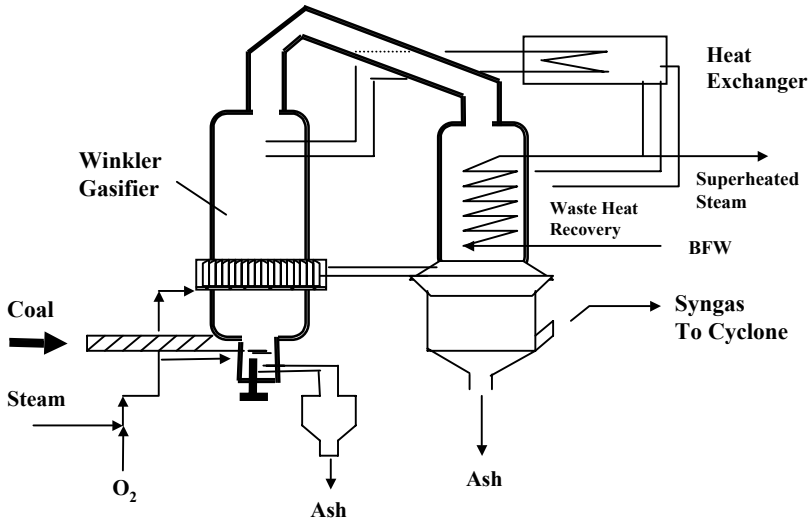

FIGURE 2.10 A schematic of Winkler gasification process.

In the preceding reactions, carbon was used instead of coal only for illustrative purposes. Therefore, the actual reactions in the gasifier are much more complex. Owing to the relatively high temperatures of the process, nearly all the tars and heavy hydrocarbons are reacted.[29]

As a result of the fluidization, the ash particles get segregated according to particle size and specific gravity. About 30% of the ash leaves through the bottom, whereas 70% is carried overhead. The lighter particles carried upward along with the produced gas are further gasified in the space above the bed. Therefore, the quantity of gasifying medium injected into this bed must be adjusted proportionally to the amount of unreacted carbon being carried over. If it is too little, ungasified carbon gets carried out of the generator, resulting in a slightly lower thermal efficiency, and if it is too much, product gas is unnecessarily consumed by combustion. The maximum temperature in the generator occurs in the space above the fluidized bed because of this secondary (further) gasification.

A radiant boiler installed immediately above the bed cools the hot product gas down to 150–205°C before it leaves the generator. This helps prevent the fly ash from getting sintered on the refractory walls of the exit duct. The sensible heat recovered by the radiant boiler generates superheated steam and is used to preheat the boiler feed water (BFW), as an energy integration scheme. The typical gas composition from a Winkler gasifier is shown in Table 2.4. As can be seen from the data, the product gas is rich in carbon monoxide, making the resultant gas a CO-rich syngas.

2.4.4.6.3 Features of the Winkler Process

The following are the chief characteristics of the Winkler process:

1. A variety of coal feeds of widely different ranks, ranging from lignite to coke, can be gasified. Petrologically, younger lignite is more reactive than older counterparts of bituminous and anthracite. With more reactive coal,

the required gasification temperature decreases, whereas the overall gasification efficiency increases. For less reactive coals, however, the energy losses through unburned solids inevitably increase.

2. Coal with high ash content can be gasified without difficulty. Although high-ash-content coals result in increased residues and incombustible materials, usually they are less expensive; and thus, sources of feed coal can be greatly expanded. Winkler gasifier is not sensitive to variations in the ash content during operation.
3. Winkler gasifier can also gasify liquid fuels in conjunction with coal gasification. The addition of supplementary liquid feeds results in an increase in production and heating value of the product gas, thereby boosting the process economics favorably.
4. Winkler gasification is very flexible in terms of the capacity and turndown ratio. It is limited at the lower end by the minimum flow required for fluidization and at the upper end by the minimum residence time required for complete combustion of residues.
5. Shutdown can be very easily facilitated by stopping the flows of oxygen, coal, and steam, and can be achieved within minutes. Even for hard coals (with low permeability), which are difficult to ignite, the heat loss during shutdown may be reduced by brief injection of air into the fuel bed.
6. Maintenance of the gas generator is straightforward, because it consists only of a brick-lined reactor with removable injection nozzle for the gasification medium.

From a more recent study, the high-temperature Winkler (HTW) process was chosen to be well suited for gasification of the lignite found in the Rhine area of Germany. The suitability was based on its temperature for gasification and the fluidized bed reactor configuration.[71] The study also discusses the selection criteria of gasification processes. Rhinebraun AG has operated a demonstration plant of HTW process at Berrenrath, Germany since 1986.[79] A variety of feedstocks other than coal, namely plastic wastes, household refuse, and sewage sludge, were successfully processed.[79]

TABLE 2.4
Typical Winkler Gas Products

Component	O_2-Blown (%)	Air-Blown (%)
CO	48.2	22.0
H_2	35.3	14.0
CH_4	1.8	1.0
CO_2	13.8	7.0
N_2 + Ar	0.9	56.0

Note: Heating value, Btu/scf: O_2-blown = 288; air-blown = 126.

Source: From Lloyd, W.G., *The Emerging Synthetic Fuel Industry*, Thumann, A., Ed., Atlanta, GA: Fairmont Press, 1981, pp.19–58.

2.4.4.7 Wellman-Galusha Process

This process has been in commercial use for more than 40 years. It is capable of producing low-Btu gas; to be specific, using air (as a gasifying medium) for fuel gas or using oxygen (as a gasifying medium) for synthesis gas. There are two types of gasifiers for this process, namely, *the standard type without agitator* and *the modified type with agitator*. The rated capacity of the agitated type is about 25% more than that of a standard type gasifier of the same size. The agitated type can handle volatile caking bituminous coals, whereas the nonagitated type would have technical difficulties with this type of coal.[3] A schematic of a *Wellman-Galusha agitated gasifier*[11] is shown in Figure 2.11.

This gasifier can be classified under the categories of a fixed bed or moving bed type reactor. The gasifier shell is water-jacketed and, hence, the inner wall of the reactor vessel does not require a refractory lining. The gasifier operates at about 540–650°C and at atmospheric pressure. Pulverized coal is fed to the gasifier from the top through a lock hopper and vertical feed pipes, whereas steam and oxygen are injected at the bottom of the bed through tuyeres. The fuel valves are operated to maintain constant flow of coal to the gasifier, which also helps in stabilizing the bed, thus maintaining the quality of the product gas. The injected air or oxygen passes over the water jacket and generates the steam required for the process. A rotating grate is located at the bottom of the gasifier to remove ash from the bed uniformly. An air-steam mixture is introduced underneath the grate and is evenly distributed through the grate into the bed. This gasifying medium passes through the ash, combustion, and gasifying zones in this specific order, while undergoing a variety of chemical reactions. The product gas contains hydrogen, carbon monoxide, carbon dioxide, and nitrogen (if air is used as an injecting medium), which being

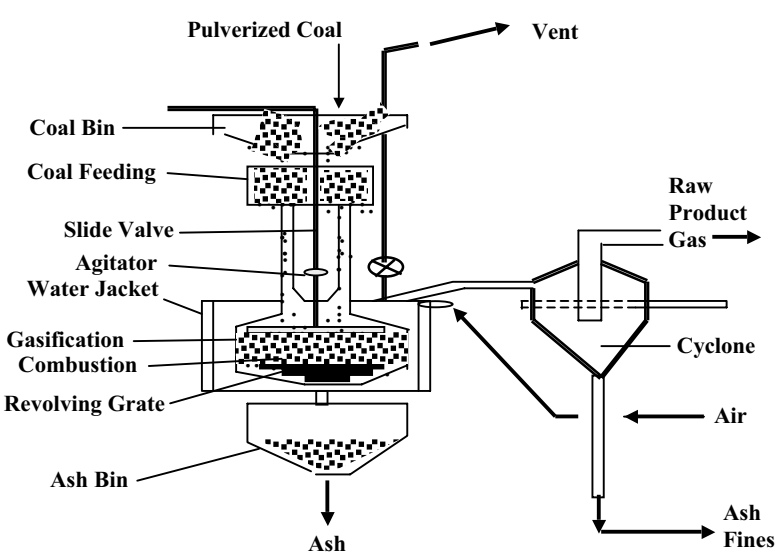

FIGURE 2.11 A schematic of agitated Wellman-Galusha gasifier.

TABLE 2.5
Typical Wellman-Galusha Products (air-blown)

Component	Percentage
CO	28.6
H_2	15.0
CH_4	2.7
N_2	50.3
CO_2	3.4

Note: Heating value (dry) = 168 Btu/scf.

Source: From Lloyd, W.G., *The Emerging Synthetic Fuel Industry*, Thumann, A., Ed., Atlanta, GA: Fairmont Press, 1981, pp.19–58.

hot, dries and preheats the incoming coal before leaving the gasifier. The typical product composition of a Wellman-Galusha gasifier is presented in Table 2.5.

The product gas is passed through a cyclone separator, where char particles and fine ash are removed. It is then cooled and scrubbed in a direct-contact countercurrent water cooler and treated for sulfur removal. If air is used as an oxidant as illustrated in Table 2.5, low-Btu gas is obtained owing to the presence of a large amount of nitrogen; if oxygen is used, then medium-Btu gas would be produced.

Unlike the standard Wellman-Galusha gasifier, the agitated version is equipped with a slowly revolving horizontal arm that spirals vertically below the surface of the coal bed to minimize channeling. This arm also helps in providing a uniform bed for gasification.

2.4.4.8 The U-GAS Process

The process was developed by the Institute of Gas Technology (IGT), Des Plaines, IL, to produce gaseous product from coal in an efficient and environmentally acceptable manner. The product gas may be used to produce low-Btu gas, medium-Btu gas, and SNG for use as fuels, or as chemical feedstocks for ammonia, methanol, hydrogen, oxo-chemicals, etc., or for electricity generation via an *IGCC*. Based on extensive research and pilot plant testing, it has been established that the process is capable of handling large volumes of gas throughput, achieving a high conversion of coal to gas without producing tar or oil, and causing minimum damage to the environment.

The U-GAS process is based on a single-stage, fluidized bed gasifier, as shown in Figure 2.12. The gasifier accomplishes four principal functions in a single stage, namely: (1) decaking coal, (2) devolatilizing coal, (3) gasifying coal, and (4) agglomerating and separating ash from char. Coal of about 0.25-in. diameter is dried and pneumatically injected into the gasifier through a lock hopper system. In the fluidized bed reactor, coal reacts with steam and oxygen at a temperature of 950–1100°C. The temperature of the bed is determined based on the type of coal feed and is controlled

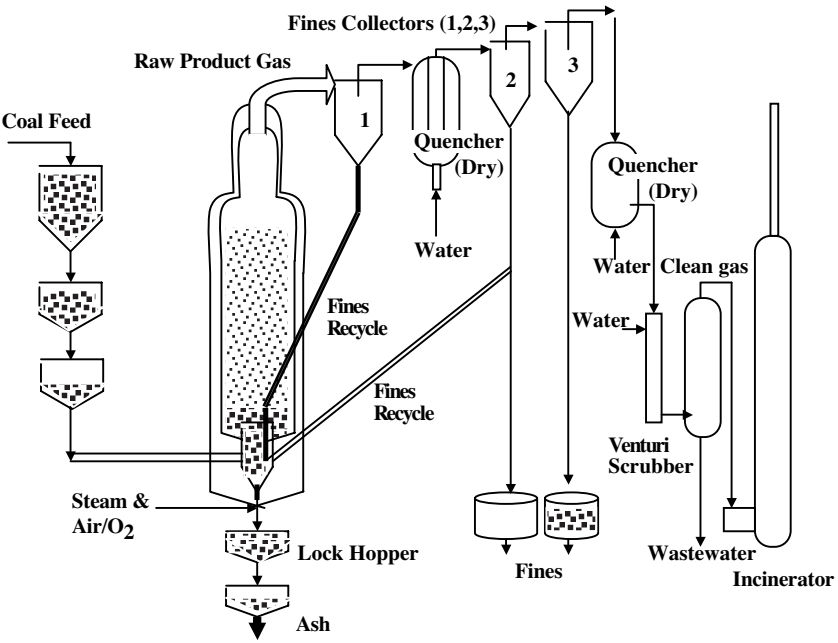

FIGURE 2.12 A schematic of U-gas process.

to prevent slagging conditions of ash. The pressure may be flexible, typically ranging from 50 to 350 psi, and is largely determined based on the ultimate use of the final product gas. Oxygen may be substituted with air. In the gasifier, coal is rapidly gasified producing H_2, CO, CO_2, and small amounts of CH_4. The fluidized bed is always maintained under reducing conditions and, as such, all sulfur species present in coal is converted into H_2S. Simultaneously with gasification, the ash is agglomerated into spherical particles that grow in size and are separated from the bed into water-filled ash hoppers, from which they are withdrawn as slurry. A portion of fluidizing gas enters the gasifier section through an inclined grid, whereas most of the remaining entering gas flows upward at a high velocity through the ash-agglomerating zone and forms a relatively hot zone within the bed.

Coal fines elutriated from the bed are collected by two external cyclones. Fines from the first cyclone are returned to the bed, whereas those from the second cyclone are sent to the ash-agglomerating zone. Raw product gas is virtually free of tar and oils, thus simplifying the ensuing energy recovery and gas purification steps. The pilot plant operated by the IGT has a gasifier made of a mild-steel, refractory-lined vessel with an I.D. of 3 ft. and a height of about 30 ft.

An IGCC process based on the IGT U-GAS process was developed by Tampella Power Company, Finland, which later became Carbona Inc. The choice of the IGT process is based on its excellent carbon conversion, as well as its versatility with a wide range of coals and peat. Enviropower Inc. originally licensed the U-gas technology and developed it as Enviropower gasification technology. Later, Enviropower's gasification business was taken over by Carbona Inc. Carbona has developed

the technology applicable to biomass gasification and is developing a pressurized fluidized bed gasification plant for the 55 MW cogeneration project with Ignifluid Boilers India Ltd. (IBIL), Chennai, India. The plant is designed for multifuel operation, including biomass.[70]

2.4.4.9 Catalytic Coal Gasification

In recent years, the study of catalytic gasification has received attention because it requires less thermal energy input but yields higher carbon conversion. Studies on the catalysis of coal gasification have twofold objectives: (1) to understand the kinetics of coal gasification that involves active mineral matter and (2) to design possible processes using these catalysts. The use of catalysts lowers the gasification temperature, which favors product composition under equilibrium conditions as well as high thermal efficiency. However, under normal conditions a catalytic process cannot compete with a noncatalytic one unless the catalyst is quite inexpensive or highly active at low temperatures. Recovery and reuse of catalyst in the process is undesirable and unattractive in coal gasification because of the expensive separation efforts and the low cost of coal and coal gas. Research on catalysis covers mainly three subjects: basic chemistry, application-related problems, and process engineering. Juntgen[30] published an extensive review article on catalytic gasification. Nishiyama[31] also published a review article, which features some possibilities for a well-defined catalytic research effort. The article contains the following observations:

1. Salts of alkali and alkaline earth metals as well as transition metals are active catalysts for gasification.
2. The activity of a particular catalyst depends on the gasifying agent as well as the gasifying conditions.
3. The main mechanism of catalysis using alkali and alkaline earth metal salts in steam and carbon dioxide gasification involves the transfer of oxygen from the catalyst to carbon through the formation and decomposition of the C-O complex, i.e., C(O).

The mechanism of hydrogasification reactions catalyzed by iron or nickel is still not very clear. But a possible explanation is that the active catalyst appears to be in the metallic state and there are two main steps for the mechanism. These are hydrogen dissociation and carbon activation.[32–36] For the latter case, carbon dissolution into and diffusion through a catalyst particle seems logical. Gasification proceeds in two stages, each of which has a different temperature range and thermal behavior, so that a single mechanism cannot explain the entire reaction. Thus, the catalyst is still assumed to activate the hydrogen.

Calcium as a catalyst has also been studied by several investigators.[37–45] This catalyst has a very high activity in the initial period when it is well dispersed in the other promoter catalyst, but with increasing conversion, the activity drops. The chemical state and dispersion are studied by chemisorption of carbon dioxide, x-ray diffraction (XRD), and some other analytical techniques. They confirmed the existence

of two or more states of calcium compounds, as well as the formation of a surface oxygen complex.

Compared to other heterogeneous catalytic systems, the catalysis in gasification is complex because the catalyst is very short-lived and effective only while in contact with the substrate, which itself changes during the course. As such, the definition of the activity for such systems is not very straightforward. For an alkali metal catalyst, the rate increases owing to the change in the catalyst dispersion and also to the increase in the ratio of catalyst/carbon in the later stage of gasification. Other possible explanations for the rate increase could be the change in surface area by pore opening, and the change in chemical state of the catalyst. At the same time, there are some changes that deactivate the catalyst, for example, agglomeration of catalyst particles, coking, and chemical reaction with sulfur or other trace elements. Coking causes fouling on the catalyst surface as well as sintering the catalyst, whereas reaction with sulfur poisons the catalytic activity.

The activity of the catalyst also depends on the nature of the substrate and gasifying conditions. The main properties of the substrate related to the activity are: (1) reactivity of the carbonaceous constituents, (2) catalytic effect of minerals, and (3) effect of minerals on the activity of added catalyst. The following general trends have been observed in reference to the factors affecting the activity of the catalysts:

1. Nickel catalysts are more effective toward lower-rank coals because they can be more easily dispersed into the coal matrix owing to higher permeability of the coal, whereas the efficiency of potassium catalyst is independent of the rank. In any case, the coal rank alone, as given by the carbon content, cannot predict catalyst activity.
2. The internal surface area of coal char relates to the overall activity of the catalyst. It can be related to the number of active sites in cases when the amount of catalyst is large enough to cover the available surface area. For an immobile catalyst, the conversion is almost proportional to the initial surface area.
3. Pretreatment of coal before the catalytic reaction often helps in achieving higher reaction rates. Although the pretreatment of coal may not be directly applicable as a practical process, a suitable selection of coal types or processing methods could enhance the activity of catalysts.
4. The effect of coal mineral matter on the catalyst effectiveness is twofold. Some minerals such as alkali and alkaline-earth metals catalyze the reaction, whereas others such as silica and alumina interact with the catalyst and deactivate it. In general, demineralization results in enhancement of activity for potassium catalysts, but only slightly so for calcium and nickel catalysts.

The method of catalyst loading is also important for activity management. The catalyst should be loaded in such a way that a definite contact between both solid and gaseous reactants is ensured. It was observed that when the catalyst was loaded from an aqueous solution, a hydrophobic carbon surface resulted in finer dispersion of the catalyst when compared to a hydrophilic surface.

The most common and effective catalysts for steam gasification are oxides and chlorides of alkali and alkaline-earth metals, separately or in combination.[46] Xiang et al. studied the catalytic effects of the Na–Ca composite on the reaction rate, methane conversion, steam decomposition, and product gas composition, at reaction temperatures of 700–900°C and pressures from 0.1 to 5.1 MPa. A kinetic expression was derived with the reaction rate constants and the activation energy determined at elevated pressures. Alkali metal chlorides such as NaCl and KCl are very inexpensive, and hence preferred as catalyst raw materials for catalytic gasification. However, their activities are quite low compared to the corresponding carbonates because of the strong affinity between alkali metal ion and chloride ion. Takarada et al.[47] have attempted to make Cl-free catalysts from NaCl and KCl by an ion exchange technique. The authors' ion-exchanged alkali metals to brown coal from an aqueous solution of alkali chloride using ammonia as a pH-adjusting agent. Cl ions from alkali chloride were completely removed by water washing. This Cl-free catalyst markedly promoted the steam gasification of brown coal. This catalyst was found to be catalytically as active as alkali carbonate in steam gasification. During gasification, the chemical form of active species was found to be in the carbonate form and was easily recovered. Sometimes, an effective way of preparing the catalyst is physical mixing K-exchanged coal with the higher-rank coals.[48] This direct contact between K-exchanged and higher-rank coal resulted in enhancement of gasification rate. Potassium was found to be a highly suitable catalyst for catalytic gasification by the physical mixing method. Weeda et al.[49] studied the high-temperature gasification of coal under product-inhibited conditions whereby they used potassium carbonate as a catalyst to enhance the reactivity. They performed temperature-programmed experiments to comparatively characterize the gasification behavior of different samples. However, the physical mixing method is likely to be neither practical nor economical for large-scale applications. Some researchers[50] have recovered the catalysts used, in the form of a fertilizer of economic significance. They used a combination of catalysts consisting of potassium carbonate and magnesium nitrate in the steam gasification of brown coal. The catalysts along with coal ash were recovered as potassium silicate complex fertilizer.

In addition to the commonly used catalysts such as alkali and alkaline-earth metals for catalytic gasification, some less-known compounds made of rare earth metals as well as molybdenum oxide (MoO_2) have been successfully tried for steam and carbon dioxide gasification of coal.[51–53] Some of the rare earth compounds used were $La(NO_3)_3$, $Ce(NO_3)_3$, and $Sm(NO_3)_3$. The catalytic activity of these compounds decreased with increasing burn-off (i.e., conversion) of the coal. To alleviate this problem, coloading with a small amount of Na or Ca was attempted and the loading of rare earth complexes was done by the ion exchange method.

Coal gasification technology could benefit from the development of suitable and effective catalysts that will help catalyze steam decomposition and carbon/steam reaction. Batelle Science & Technology International[54] has developed a process in which calcium oxide was used to catalyze the hydrogasification reaction. It was also shown that a reasonably good correlation exists between the calcium content and the reactivity of coal chars with carbon dioxide. Other alkali metal compounds, notably chlorides and carbonates of sodium and potassium, can also enhance the gasification rate by as much as 35–60%. In addition to the oxides of calcium, iron,

and magnesium, zinc oxides are also found to substantially accelerate gasification rates by 20–30%.

Some speculative mechanisms have been proposed by Murlidhara and Seras[54] as to the role of calcium oxide in enhancing the reaction rate. For instance, coal organic matter may function as a donor of hydrogen, which then may be abstracted by calcium oxide by a given mechanism as described in Scheme 1. Scheme 2 explains the mechanism of generating oxygen-adsorbed CaO sites and subsequent desorption of nascent oxygen, which in turn reacts with organic carbon of coal to form carbon monoxide. Scheme 3 explains direct interaction between CaO and coal organics, which results in liberation of carbon monoxide. The scheme further explains an oxygen exchange mechanism that brings the reactive intermediates back to CaO.

Scheme 1:

$$\text{Organic} \rightarrow \text{Organic}^{*} + H_2$$
$$CaO + 2H_2 \rightarrow CaH_2 + H_2O$$
$$\text{Organic}^{*} + CO_2 \rightarrow 2CO$$
$$CO_2 + CaH_2 \rightarrow CaO + CO + H_2$$

Scheme 2:

$$CaO + CO_2 \rightarrow CaO(O) + CO$$
$$CaO(O) \rightarrow CaO + (O)$$
$$C + (O) \rightarrow CO$$

Scheme 3:

$$CaO + 2C \rightarrow CaC_x + CO$$
$$CaC_x + \text{Organic (oxygen)} \rightarrow CaO + \text{Organic}^{*}$$

Exxon (currently, ExxonMobil) has reported that impregnation of 10–20% of potassium carbonate lowers the optimum temperature and pressure for steam gasification of bituminous coals, from 980 to 760°C and from 68 to 34 atm, respectively.[55] In their commercial-scale plant design, the preferred form of make-up catalyst was identified as potassium hydroxide. This catalyst aids the overall process in several ways. First, it increases the rate of gasification, thereby allowing a lower gasification temperature. Second, it prevents swelling and agglomeration when handling caking coals, which is another benefit of a lower gasification temperature. Most importantly, it promotes the methanation reaction because it is thermodynamically more favored at a lower temperature. Therefore, in this process, the production of methane is thermodynamically and kinetically favored in comparison to synthesis gas. A catalyst recovery unit is provided after the gasification stage to recover the used catalyst.

2.4.4.10 Molten Media Gasification

Generally speaking, molten media may mean one of the following: molten salt, molten metal, or molten slag. When salts of alkali metals and iron are used as a medium to carry out the coal gasification, it is referred to as *molten media gasification*. The molten medium not only catalyzes the gasification reaction, but also supplies the necessary heat and serves as a heat exchange medium.[3,56] There have been several distinct commercial processes developed over the years:

1. Kellogg-Pullman molten salt process
2. Atgas molten iron gasification process
3. Rockwell molten salt gasification
4. Rummel-Otto molten salt gasification

Schematics of a Rockwell molten salt gasifier and a Rummel–Otto single-shaft gasifier are shown in Figure 2.13[11] and Figure 2.14,[22] respectively.

2.4.4.10.1 Kellogg Molten Salt Process

In this process, gasification of coal is carried out in a bath of molten sodium carbonate (Na_2CO_3) through which steam is passed.[57] The molten salt produced by this process offers the following advantages:

1. The steam–coal reaction, being basic in nature, is strongly catalyzed by sodium carbonate, resulting in complete gasification at a relatively low temperature.
2. Molten salt disperses coal and steam throughout the reactor, thereby permitting direct gasification of caking coals without carbonization.
3. A salt bath can be used to supply heat to the coal undergoing gasification.
4. Owing to the uniform temperature throughout the medium, the product gas obtained is free of tars and tar acids.

Crushed coal is picked up from lock hoppers by a stream of preheated oxygen and steam and carried into the gasifier. In addition, sodium carbonate recycled from the ash rejection system is also metered into the transport gas stream and the combined coal, salt, and carrier are admitted to the gasifier. The main portion of the preheated oxygen and steam is admitted into the bottom of the reactor for passage through the salt bath to support the gasification reactions. Along with the usual gasification reactions, sulfur entering with the coal accumulates as sodium sulfide (Na_2S) to an equilibrium level. At this level, it leaves the reactor according to the following reaction:

$$Na_2CO_3 + H_2S \rightarrow Na_2S + CO_2 + H_2O$$

Ash accumulates in the melt and leaves along with the bleed stream of salt, where it is rejected and sodium carbonate is recycled. The bleed stream of salt is

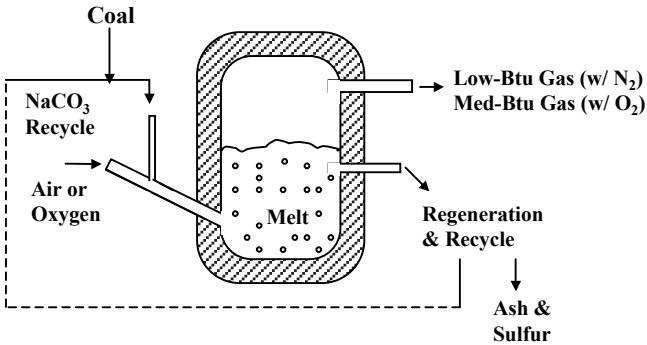

FIGURE 2.13 A schematic of Rockwell molten salt gasifier.

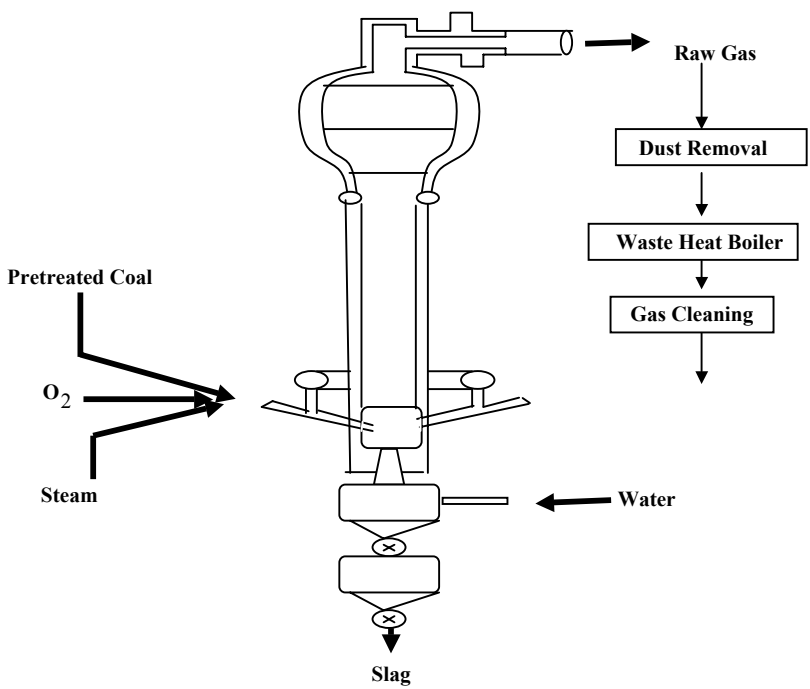

FIGURE 2.14 Rummel-Otto single-shaft gasifier.

quenched in water to dissolve sodium carbonate (Na_2CO_3) and permit rejection of coal ash by filtration. The dilute solution of sodium carbonate is further carbonated for precipitation and recovery of sodium bicarbonate ($NaHCO_3$). The filtrate is recycled to quench the molten salt stream leaving the reactor. The sodium bicarbonate filtrate cake is dried and heated to regenerate to sodium carbonate for recycle to the gasifier. The gas stream leaving the gasifier is processed to recover the entrained salt and the heat, and is further processed for conversion to the desired product gas such as synthesis gas, pipeline gas, or SNG.

2.4.4.10.2 Atgas Molten Iron Coal Gasification

This process is based on the molten iron gasification concept in which coal is injected with steam or air into a molten iron bath. Steam dissociation and thermal cracking of coal volatile matter generate hydrogen and carbon monoxide, i.e., principal ingredients of synthesis gas. The coal sulfur is captured by the iron and transferred to a lime slag from which elemental sulfur can be recovered as a by-product. The coal dissolved in the iron is removed by oxidation to carbon monoxide with oxygen or air injected near the molten iron surface. The Atgas process uses coal, steam, or oxygen to yield product gases with heating values of about 900 Btu/scf.

The Atgas molten iron process has several inherent advantages over the gas-solid contact gasification in either fixed or fluidized bed reactors.[58] They are:

1. Gasification is carried out at low pressures; hence, the mechanical difficulty of coal feeding in a pressurized zone is eliminated.
2. Coking properties, ash fusion temperatures, and generation of coal fines are not problematic.
3. The sulfur content of coal does not cause any environmental problem as it is retained in the system and recovered as elemental sulfur from the slag. Elemental sulfur by-product helps the overall process economics.
4. The system is very flexible with regard to the physical and chemical properties of the feed coal. Relatively coarse size particles can be handled without any special pretreatment.
5. Formation of tar is suppressed owing to very high-temperature operation.
6. The product gas is essentially free of sulfur compounds.
7. Shutdown and start-up procedures are greatly simplified compared to fixed bed or fluidized bed reactors.

Coal and limestone are injected into the molten iron through tubes using steam as a carrier gas. The coal goes through devolatilization with some thermal decomposition of the volatile constituents, leaving the fixed carbon and sulfur to dissolve in iron whereupon carbon is oxidized to carbon monoxide. The sulfur, in both organic and pyritic forms (FeS_2), migrates from the molten iron to the slag layer where it reacts with lime to produce calcium sulfide (CaS).

The product gas, which leaves the gasifier at approximately 1425°C, is cooled, compressed, and fed to a shift converter (WGS reactor) in which a portion of carbon monoxide is reacted with steam via WGS reaction to attain a CO-to-H_2 ratio of 1:3. The carbon dioxide produced is removed from the product gas, and the gas is cooled again. It then enters a methanator in which carbon monoxide and hydrogen react to form methane via $CO + 3H_2 = CH_4 + H_2O$. Excess water is removed from the methane-rich product. The final gaseous product has a heating value around 900 Btu/scf.

2.4.4.11 Plasma Gasification

Plasma gasification is a nonincineration thermal process that uses extremely high temperatures in an oxygen-free or oxygen-deprived environment to completely decompose input material into very simple molecules. The extreme heat, aided by

the absence of an oxidizing agent such as oxygen, decomposes the input material into basic molecular structure species. The plasma gasification or plasma pyrolysis process was originally developed for treatment of waste materials. However, the process can be very effectively applied to coal gasification or oil shale pyrolysis, capitalizing on its high thermal efficiency, as long as the input energy for plasma generation can be obtained effectively via energy integration or some other inexpensive source of energy. When the plasma gasification is applied to carbonaceous materials such as coal and oil shale kerogen, by-products are normally a combustible gas and an inert slag. Product gas can be cleaned by conventional technologies, including cyclone, scrubbers, and ESPs. Cyclone/scrubber effluents can normally be recycled for further processing.

Plasma is often mentioned as the fourth state. Electricity is fed to a plasma torch that has two electrodes, creating an arc through which inert gas is passed. The inert gas heats the process gas to a very high temperature, as high as 25,000°F. The temperature at a location several feet away from the torch can be as high as 5,000–8,000°F, at which temperature the carbonaceous materials are completely destroyed and broken down into their elemental forms. Furthermore, there is no tar or furan involved or produced in this process. Ash or mineral matter would become completely molten and flow out of the bottom of the reactor. Therefore, the plasma reactor is not specific to any particular kind of coal for gasification. Figure 2.15 illustrates how the plasma torch operates.[59]

When applied to waste materials such as municipal solid waste (MSW), plasma gasification possesses unique advantages for the protection of air, soil, and water resources through extremely low limits of air emissions and leachate toxicity. Because the process is not based on combustion of carbonaceous matters, generation of *greenhouse chemicals*, in particular carbon dioxide, is far less than from any other conventional gasification technology. Furthermore, air emissions are typically orders of magnitude below the current regulations. The slag is monolithic and the leachate

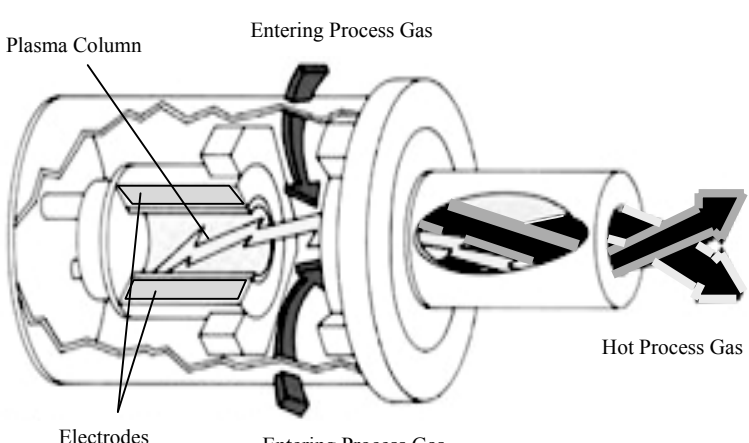

FIGURE 2.15 Plasma torch. (From Recovered Energy, Inc. Web site, http:www.recoveredenergy.com/d_plasma.html, 2004. With permission.)

levels are orders of magnitude lower than the current EP-toxicity standard, which is one of the four criteria for hazardous waste classification.[72] Slag weight and volume reduction ratios are typically very large; for example, in the case of biomedical wastes they are 9:1 and 400:1, respectively. Even though the data for a variety of coals are not readily available in the literature, both the mass reduction ratio and the volume reduction ratio for coals are believed to be significantly higher than those for nonplasma gasification technology, thus substantially reducing the burden of waste and spent ash disposal problem.

Activities in Canada and Norway are noteworthy in the technology development of plasma gasification. Resorption Canada Limited (RCL)[60] is a private Canadian entity that was federally incorporated to develop and market industrial processes based on plasma arc technology. They have amassed extensive operating experience in this technology, covering a wide variety of input materials including environmental, biomedical, and energy-related materials and resources.

2.5 MATHEMATICAL MODELING OF COAL GASIFIERS

As research and development continues on new and efficient coal gasification concepts, mathematical modeling provides insight into their operation and commercial potential. The influence of design variables and processing conditions on the gasifier performance must be *a priori* determined before any commercial processes are designed. Such models are then used as tools for design modifications, scaling, and optimization.

Coal gasification is performed in different types of reactors in which, depending on the type of gas–solid contact, the bed can be moving, fluidized, entrained, or made up of molten salts. Of these, a moving bed configuration may be the most widely used because of its high coal conversion rates and thermal efficiency.

Different approaches have been used to model various types of reactors. There are mainly two kinds of models. The first kind is the thermodynamic or equilibrium model, which is easier to formulate; but it generates only certain restrictive information such as offgas compositions in a limiting case. The other type of model is the kinetic model, which predicts kinetic behavior inside the reactor. The time-dependent behavior of the process can be either steady state or dynamic in nature. Adanez and Labiano[61] have developed a mathematical model of an atmospheric moving bed countercurrent coal gasifier and studied the effect of operating conditions on the gas yield and composition, process efficiency, and longitudinal temperature profiles. The model was developed for adiabatic reactors. It assumes that the gasifier consists of four zones with different physical and chemical processes taking place. They are the zones for: (1) coal preheating and drying, (2) pyrolysis, (3) gasification, and (4) combustion, followed by the ash layer, which acts as a preheater of the reacting (i.e., entering) gases. In reality, however, there is no physical distinction between the zones, and the reactions occurring in each zone vary considerably. The model uses the *unreacted shrinking core model* to define the reaction rate of the coal particles.[73] The unreacted shrinking core model assumes that the dimension (as often represented by the particle size) of unreacted core (of the remaining coal particle) is progressively shrinking as the coal gets reacted. The most critical parameter in

the operation of these moving bed gasifiers with dry ash extraction is the longitudinal temperature profile, because the temperature inside the reactor must not exceed the ash-softening (or ash-oozing) point at any time, in order to avoid ash fusion or oozing. The model also takes into account the effect of coal reactivity, particle size, and steam/oxygen ratio. To partially check the validity of the model, predicted data on the basis of the model were compared to real data on the product gas composition for various coals, and good agreement was attained. The authors have concluded that the reactivity of the coals and the emissivity of the ash layer must be known accurately, as they have a strong influence on the temperature profiles, the maximum temperature in the reactor, and its capacity for processing coal.

Lim et al.[62] have developed a mathematical model of a spouted bed gasifier based on simplified first-order reaction kinetics for the gasification reactions. The spouted bed gasifier has been under development in Canada and Japan.[63,64] The spout is treated as a plug flow reactor (PFR) of a fixed diameter with cross-flow into the annulus. The annulus is treated as a series of steam tubes, each being a plug flow reactor with no axial dispersion. The model calculates the composition profile of various product gases in the spout as a function of the height, radial composition profiles, and average compositions in the annulus at different heights, the average compositions exiting the spout and annulus, and the flow rates and linear velocities in the spout and annulus. The model has been further developed as a two-region model including an enthalpy balance.[80]

Monazam et al.[65] have developed a similar model for simulating the performance of a cross-flow coal gasifier. Gasification in a cross-flow gasifier is analogous to the batch gasification in a combustion pot. Therefore, the model equations for kinetics as well as mass and energy balances formulated were based on a batch process. In the cross-flow coal gasifier concept, operating temperatures are much higher than 1000°C and, as such, the diffusion through the gas film and ash layer is a critical factor. The model also assumes shrinking unreacted core model for kinetic formulations. Simulation results of the model were compared to the experimental data obtained in batch and countercurrent gasification experiments, and good agreement was attained. It was also concluded that the performance of the gasifier depends on the gas-solid heat transfer coefficient, whereas the particle size and the bed voidage had a significant effect on the time required for complete gasification.

Watkinson et al.[66] have developed a mathematical model to predict the gas composition and yield from coal gasifiers. Gas composition depends on the contacting pattern of blast and fuel, temperature and pressure of the operation, composition of the blast, and form of fuel feeding. The authors have presented a calculation method and the predicted data have been compared to the operating data from nine different types of commercial and pilot-scale gasifiers, including Texaco, Koppers-Totzek, and Shell, Winkler-fluidized bed, and Lurgi dry ash as well as Lurgi slagging moving bed gasifier. The model consists of elemental mass balances for C, H, O, N, and S, chemical equilibria for four key chemical reactions, and an optional energy balance. The four key reactions were partial oxidation, steam gasification, Boudouard reaction, and WGS reaction. Predictions were most accurate for entrained flow systems, less accurate for fluidized bed gasifiers, and uncertain for moving bed reactors. This was due to the lower temperatures and uncertain

volatile yields in the latter ones resulting in deviation between the calculated and experimentally reported values.

Lee et al.[67] developed a single-particle model to interpret kinetic data of coal char gasification with H_2, CO_2, and H_2O. Their model yields asymptotic analytical solutions taking into account all the major physical factors that affect and contribute to the overall gasification rate. Some of the factors taken into account involved changing magnitudes of internal surface area, porosity, activation energy, and effective diffusivity as functions of conversion (or burnoff). Their model closely describes the characterizing shape of the conversion vs. time curves as determined by CO_2 gasification studies. The curve shape under certain restrictions leads to a "universal curve" of conversion vs. an appropriate dimensionless time. The model developed is mathematically very simple, and all the parameters in the model equation have physical significance. Therefore, the model is applicable to a wide variety of coals having different physicochemical and petrological properties. The number of adjustable parameters in this model is only two. Their model predictions were compared against experimental data obtained using a novel thermobalance reactor, and excellent agreement was attained.[67]

Gururajan et al.[68], in their review, critically examined many of the mathematical models developed for fluidized bed reactors. The review is primarily concerned with the modeling of bubbling fluidized bed coal gasifiers. They also discuss the rate processes occurring in a fluidized bed reactor and compare some of the reported models in the literature with their presentation.

When a coal particle is fed into a gasifier, it undergoes several physicochemical transformations, which include: (1) drying, (2) devolatilization, and (3) gasification of the residual char in different gaseous atmospheres. These heterogeneous reaction-transport phenomena are accompanied by a number of supplementary reactions that are homogeneous in nature. Detailed kinetic studies are an important prerequisite for the development of a mathematical model. Mathematical models for a bubbling fluidized bed coal gasifier can be broadly classified into two kinds, i.e., thermodynamic (or equilibrium) and kinetic (or rate) models. Thermodynamic models predict the equilibrium compositions and temperature of the product gas based on a given set of steam/oxygen feed ratios, the operating pressure, and the desired carbon conversion. These models are independent of the type of the gasifier and based on the assumption of complete oxygen consumption. Therefore, they cannot be used to investigate the influence of operating parameters on the gasifier performance. The kinetic model, on the other hand, predicts the composition and temperature profiles inside the gasifier for a given set of operating conditions and reactor configurations and hence can be used to evaluate the performance of the gasifier. They are developed by combining a suitable hydrodynamic model for the fluidized bed with appropriate kinetic schemes for the reactive processes occurring inside the gasifier. Various rate models may be classified into four groups on the basis of hydrodynamic models used.[68] They are:

1. Simplified flow models
2. Davidson-Harrison type models
3. Kunii-Levenspiel type models
4. Kato-Wen type models

The same review[68] also examined and compared the different types of models. Although many investigators have compared their model predictions with experimental data, a detailed evaluation of the influence of model assumptions on its predictions has not been reported. Although efforts have been made to compare the predictions of different models, an attempt to evaluate the model with experimental data from different sources has not been made.

Gururajan et al. in their review article[68] have developed a model of their own for a bottom feeding bubbling fluidized bed coal gasifier based on the following assumptions:

1. The bubble phase is in plug flow and does not contain any particles, whereas the emulsion phase is completely mixed and contains the particles in fluidized conditions.
2. Excess gas generated in the emulsion phase passes into the bubble phase. The rate of this excess per unit bed volume is constant.
3. The coal particles in the feed are spherical, homogeneous, and uniform in size.
4. Only WGS reaction occurs in the homogeneous gas phase.
5. External mass transfer and intraparticle diffusion are assumed to be negligible in the char gasification reactions.
6. Entrainment, abrasion, agglomeration, or fragmentation of the bed particles is assumed to be negligible.
7. The gasifier is at a steady state and is isothermal.

All the model equations are derived on the basis of the preceding assumptions. The model predictions were compared with the experimental data from three pilot-scale gasifiers reported in the literature.[68] They concluded that the predictions were more sensitive to the assumptions regarding the combustion/decomposition of the volatiles and the products of char combustion than to the rate of char gasification. Hence, in pilot-scale gasifiers, owing to the short residence time of coal particles, the carbon conversion and the product gas yields are mainly determined by the fast-rate coal devolatilization, volatiles combustion/decomposition and char combustion, and also by the slow-rate char gasification reactions. This explains why models based on finite-rate char gasification reactions are able to fit the same pilot-scale gasification data.

A better understanding of coal devolatilization, decomposition of the volatiles, and char combustion under conditions prevailing in a fluidized bed coal gasifier is very important for the development of a model with good predictive capability. There is a strong need to investigate the kinetics of gasification of coal and char in synthesis gas atmospheres and to obtain experimental data for the same coal and char in a pilot-scale plant.

It is well known that there are many physical changes occurring when the coal char particles are gasified. There have been many attempts to unify these dynamic changes through various normalizing parameters such as half-life, coal rank, reactivity, or surface area. According to the study by Raghunathan and Yang,[69] the experimental char conversion vs. time data from different experiments can be unified

into a single curve where time is considered to be normalized time, $t/t_{1/2}$, $t_{1/2}$ being the half-life of the char-gas reaction. This unification curve with only one parameter is then fitted into the rate models commonly used, e.g., the *grain model* and the *random pore model*. With the aid of reported correlations for unification curves, a master curve is derived to approximate the conversion–time data for most of the gasification systems. Also, as the half-life (more precisely, half-conversion time) is simply related to the average reactivity, it can be generally used as a reactivity index for characterizing various char-gas reactions. Further, conversions up to 70% can be predicted with reasonable accuracy over a wide range of temperatures.

A great deal of effort has been devoted to mathematically modeling a variety of gasifiers and reaction conditions in order to obtain design- and performance-related information. Numerous simplified models and asymptotic solutions have been obtained for coal gasification reactors along with a large database of digital simulation of such systems.

2.6 FUTURE OF COAL GASIFICATION

The roles of coal gasification have been changing constantly based on the societal demands of the era. We observed in the past century that the principal roles and foci of coal-derived syngas shifted from domestic heating fuel, to feedstock for Fischer–Tropsch (F-T), to petrochemical feedstocks, to starting materials for alternative fuels, to IGCC, and to hydrogen sources. With the advent of hydrogen economy, coal gasification has again taken center stage as a means for producing hydrogen for fuel cell applications.[75] Further, coal gasification technology can also be easily applied to biomass and solid waste gasification with minor modifications. Unlike coal, biomass is not only renewable, but also available inexpensively, often free of charge. Coal can also be coprocessed together with a variety of other materials, including petroleum products, scrap tires, biomass, municipal wastes, sewage sludge, etc. With advances in flue gas desulfurization, coal gasification can be more widely utilized in process industries. In electric power generation, IGCC has contributed tremendously to improvement of power generation efficiency, thus keeping the cost of electric power competitive against all other forms of energy. Keen interest in methanol and dimethylether is rekindled due to the ever-rising cost of conventional clean liquid fuel. In order to use coal gasification technology in hydrogen production, the steam gasification process, which is essentially very similar to the hydrocarbon reformation process, needs to be refined further. Therefore, more advances are expected in the areas of product gas cleaning, separation and purification, feedstock flexibility, and integrated or combined process concepts.

REFERENCES

1. Howard-Smith, I. and Weimer, G., Coal conversion technology, *Chem. Technol. Rev.,* 66: 1–333, 1976, Park Ridge, NJ: Noyes Data Corp.
2. Wilson, J., Halow, J., and Ghate, M.R., *CHEMTECH,* 123–128, February 1988.

3. Speight, J.G., *The Chemistry and Technology of Coal*, New York: Marcel Dekker, 1983, pp. 461–516.
4. Walker, P.L., Rusinko, F., and Austin, L.G., Gas reactions in carbon, *Advances in Catalysis*, Eley, D.D., Selwood, P.W., and Weisz, P.B., Eds., Vol. XI, New York: Academic Press, 1959, pp. 133–221.
5. Kyotani, T., Kubota, K., and Tomita, A., *Fuel Process. Technol.*, Vol. 36, 209–217, 1993.
6. Bodle, W.W. and Vyas, K.C., Clean Fuels from Coal, Symposium Papers, Chicago, IL: Institute of Gas Technology, September 10–14, 1973, pp. 49–91.
7. Braunstein, H.M. and Pfuderer, H.A., Environmental Health and Control Aspects of Coal Conversion: An Information Overview, Report ORNL-EIS-94, Oak Ridge National Laboratory, Oak Ridge, TN, 1977.
8. Vyas, K.C. and Bodle, W.W., Clean Fuels from Coal — Technical Historical Background and Principles of Modern Technology, Symposium II papers, IIT Research Institute, 1975, pp. 53–84.
9. Rudolph, P.E.H, The Lurgi Process — The Route to SNG from Coal, presented at the Fourth Pipeline Gas Symposium, Chicago, IL, October 1972.
10. Cooper, B.R. and Ellington, W.A., *The Science and Technologies of Coal and Coal Utilization*, New York: Plenum, 1984, pp.163–230.
11. Lloyd, W.G., Synfuels technology update, in *The Emerging Synthetic Fuel Industry*, Thumann, A., Ed., Atlanta, GA: Fairmont Press, 1981, pp.19–58.
12. Moe, J.M., SNG from Coal via the Lurgi Gasification Process, in Clean Fuels from Coal, Symposium Papers, Chicago, IL: Institute of Gas Technology, September 10–14, 1973, pp. 91–110.
13. Johnson, B.C., The Grand Forks slagging gasifier, in *Coal Processing Technology*, Vol. IV, A CEP technical manual, New York: AIChE, 1978, pp. 94–98.
14. Michels, H.J. and Leonard, H.F., *Chem. Eng. Prog.*, 74(8): 85, 1978.
15. Van der Bergt, M.J., *Hydrocarbon Process.*, 58(1): 161, 1979.
16. Sams, D.A. and Shadman, F., *AIChE J.,* 32(7): 1132–1137, 1986.
17. Farnsworth, J., Leonard, H.F., and Mitsak, M., Production of Gas from Coal by the Koppers-Totzek Process, in Clean Fuels from Coal, Symposium Papers, Chicago, IL: Institute of Gas Technology, September 10–14, 1973, pp. 143–163.
18. Gas Processing Developments, *Hydrocarbon Process.*, 41–65, May 2001.
19. *EPRI J.*, 41–44, December 1983.
20. *Oil Gas J.*, 51, April 29, 1985.
21. *Hydrocarbon Processing,* 96, April 1984.
22. Probstein, R.F. and Hicks, R.E., *Synthetic Fuels*, New York: McGraw-Hill, 1982.
23. Thompson, P.N., *Endeavor,* 2: 93, 1978.
24. Gregg, D.W. and Edgar, T.F., *AIChE J.*, 24: 753, 1978.
25. Commonwealth Scientific and Industrial Research Organization Web site, http://www.em.csiro.au/ 2004.
26. Juntgen H., *Fuel,* 66: 443–453, April 1987.
27. Nadkarni, R.M., Underground Gasification of Coal, in *Clean Fuels from Coal*, Symposium papers, Chicago, IL: Institute of Gas Technology, September 10–14, 1973, pp. 611–638.
28. Odell, W., U.S. Bureau of Mines Information, 7415, 1974.
29. Banchik, I.N., The Winkler Process for the Production of Low Btu Gas from Coal, in *Clean Fuels from Coal*, Symposium II Papers, IIT Research Institute, 1975, pp. 359–374.

30. Juntgen, H., Application of catalysts to coal gasification processes, incentives and perspectives, *Fuel,* 62: 234–238, 1983.
31. Nishiyama, Y., *Fuel Process. Technol.*, 29: 31–42, 1991.
32. Asami, K. and Ohtuska, Y., *Ind. Eng. Chem. Res.*, 32: 1631–1636, 1993.
33. Yamashita, H., Yoshida, S., and Tomita, A., *Energy Fuels,* 5: 52–57, 1991.
34. Matsumoto, S., *Energy Fuels,* 5: 60–63, 1991.
35. Srivastava, R.C., Srivastava, S.K., and Rao, S.K., *Fuel,* 67: 1205–1207, 1988.
36. Haga, T. and Nishiyama, Y., *Fuel,* 67: 748–752, 1988.
37. Ohtuska, Y. and Asami, K., Steam gasification of high sulfur coals with calcium hydroxide, *Proc. 1989 Int. Conf. Coal Sci.*, 1: 353–356, 1989.
38. Salinas Martinez, C. and Lineras-Solano, A., *Fuel,* 69: 21–27, 1990.
39. Joly, J.P., Martinez-Alonso, A., and Marcilio, N.R., *Fuel,* 69: 878–894, 1990.
40. Muhlen, H.J., *Fuel Process. Technol.*, 24: 291–297, 1990.
41. Levendis, Y.A., Nam, S.W., and Gravalas, G.R., *Energy Fuels*, 3: 28–37, 1989.
42. Zheng, Z.G., Kyotani, T., and Tomita, A., *Energy Fuels,* 3: 566–571, 1989.
43. Muhlen, H.J., *Fuel Process. Technol.*, 24: 291–297, 1986.
44. Haga, T., Sato, M., and Nishiyama, Y., *Energy Fuels,* 5: 317–322, 1991.
45. Pareira, P., Somorajai, G.A., and Heinemann, H., *Energy Fuels,* 6: 407–410, 1992.
46. Xiang, R., You, W., and Shu-fen, L., *Fuel,* 66: 568–571, 1987.
47. Takarada, T., Nabatame, T., and Ohtuska, Y., *Ind. Eng. Chem. Res.*, 28: 505–510, 1989.
48. Takarada, T., Ogirawa, M., and Kato, K., *J. Chem. Eng. Jpn.,* 25: 44–48, 1992.
49. Weeda, M., Tromp, J.J., and Moulijn, J.A., *Fuel,* 69: 846–850, 1990.
50. Chin, G., Liu, G., and Dong, Q., *Fuel,* 66: 859–863.1987.
51. Carrasco-Marin, F., Rivera, J., and Moreno, C., *Fuel,* 70: 13–16, 1991.
52. Lopez, A., Carrasco-Marin, F., and Moreno, C., *Fuel,* 71: 105–108, 1992.
53. Toshimitsu, S., Nakajima, S., and Watanabe, Y., *Energy Fuels,* 2: 848–853, 1988.
54. Murlidhara, H.S. and Seras, J.T., Effect of calcium on gasification, in *Coal Processing Technology*, Vol. IV, A CEP technical manual, New York: AIChE, 1978, pp. 22–25.
55. Gallagher, J.E. and Marshall, H.A., SNG from coal by catalytic gasification, in *Coal Processing Technology*, Vol. V, A CEP technical manual, New York: AIChE, 1979, pp. 199–204.
56. Cover, A.E. and Schreiner, W.C., in Clean Fuels from Coal, Symposium Papers, Chicago, IL: Institute of Gas Technology, September 10–14, 1973, pp. 273–279.
57. Cover, A.E., Schreiner, W.C., and Skaperdas, G.T., Kellogg's coal gasification process, *Chem. Eng. Prog.* 69(3): 31–36, 1973.
58. LaRosa, P. and McGarvey, R.J., in Clean Fuels from Coal, Symposium Papers, Chicago, IL: Institute of Gas Technology, September 10–14, 1973, pp. 285–300.
59. Recovered Energy, Inc. Web site, http:www.recoveredenergy.com/d_plasma.html, 2004.
60. Resorption Canada Limited (RCL) Web site, http://www.plascoenergygroup.com.
61. Adanez, J. and Labiano, F.G., *Ind. Eng. Chem. Res.*, 29: 2079–2088, 1990.
62. Lim, C.J., Lucas, J.P., and Watkinson, A.P., *Can. J. Chem. Eng.*, 69: 596–606, 1991.
63. Foong, S.K., Cheng, G., and Watkinson, A.P., *Can. J. Chem. Eng.*, 59: 625–630, 1981.
64. Watkinson, A.P., Lim, C.J., and Cheng, G., *Can. J. Chem. Eng.*, 65: 791–798, 1987.
65. Monazam, E., Johnson, E., and Zondlo, J., *Fuel Sci. Technol. Int.*, 10(1): 51–73, 1992.
66. Watkinson, A.P., Lucas, J.P., and Lim, C.J., *Fuel,* 70: 519–527, April 1991.
67. Lee, S., Angus, J.C., Gardner, N.C., and Edwards, R.V., *AIChE J.,* 30(4): 583–593, 1984.
68. Gururajan, V.S., Agarwal, P.K., and Agnew, J.B., *Trans. IChemE.*, 70(Part A): 211–238, 1992.

69. Raghunathan, K. and Yang, Y.K., *Ind. Eng. Chem. Res.*, 28: 518–523, 1989.
70. Skrifvars, B.-J. and Kilpinen, P., Biomass Combustion Technology in Finland, The IFRF (Int. Flame Research Foundation), *Industrial Combustion Magazine*, Tech 02, March 1999, also accessible through http://www.magazine.ifrf.net/9903biomass1/turku/.
71. Teggers, H. and Schrader, L., The high-temperature Winkler process — a way for the generation of synthesis gas from lignite, *Energiewirtschaftliche Tagesfragen*, 31: 397–399, 1981.
72. Speight, J.G. and Lee, S., *Environmental Technology Handbook*, Philadelphia, PA: Taylor & Francis, 2000.
73. Levenspiel, O., *Chemical Reaction Engineering*, 3rd ed., New York: John Wiley & Sons, 1999.
74. Lee, S., *Methane and Its Derivatives*, New York: Marcel Dekker, 1997.
75. U.S. Department of Energy, Fossil Energy homepage, Gasification Technology R&D, April 2006, accessible through http://www.fossil.energy.gov/programs/powersystems/gasification/index.html.
76. Lee, A.L., Evaluation of Coal Conversion Catalysts, Final Report submitted to U.S. Department of Energy, GRI-87-0005, Gas Research Institute, Chicago, IL, 1987.
77. Gadsby, J., Hinshelwood, C.N., and Skykes, K.W., *Proc. R. Soc.*, A187, 129, 1946.
78. Johnstone, H.F., Chen, C.Y., and Scott, D.S., *Ind. Eng. Chem.*, 44: 1564, 1952.
79. Addhoch, W., Sato, H., Wolff, J., and Radtke, K., High Temperature Winkler Gasification of Municipal Solid Waste, paper presented at 2000 Gasification Technologies Conference, San Francisco, CA, October 8–11, 2000, accessible through http://www.gasification.org/docs/2000_Papers/Gtc00320.pdf.
80. Lucas, J.P., Lim, C.J., and Watkinson, A.P., *Fuel,* 77(7): 683–694, 1998.

3 Clean Liquid Fuels from Coal

Sunggyu Lee

CONTENTS

3.1 BACKGROUND

There are three principal routes by which liquid fuels can be produced from solid coal: coal pyrolysis, direct liquefaction, and indirect liquefaction. Liquid-like fuels can also be obtained via coal slurry technology.

Even though coal has a reasonably high heating value of approximately 8,000–14,000 Btu/lb, its solid state is one of the main reasons it is inconvenient to handle as a consumer fuel. To make this solid fuel user-friendlier, research has been ongoing to convert it into pipeline-quality gaseous fuel or clean liquid fuel. During World War II, production of approximately 100,000 bbl/d of liquid fuel from coal was reported for the German war effort. The German liquefaction process used a high-temperature and high-pressure technology, and the product liquid fuels were of environmentally poor quality by modern environmental standards as cleaning and refining was minimal.

The current process objectives of coal liquefaction are mainly focused on easing the severity of operating conditions, minimizing the hydrogen requirement, and making the liquid product more environmentally acceptable. Due to the recent trend toward higher and fluctuating petroleum prices in the world market, the relative process economics of coal liquefaction are changing much more favorably. Considering the vast amount of coal reserves throughout the world and the global distribution of major deposits, this alternative is even more attractive and also very practical.

There are inherent technological advantages with coal liquefaction, as coal liquefaction can produce clean liquid fuels that can be sold as *transportation fuels*. It had long been believed that if the crude oil price stays at a level higher than about $35 per barrel for a sustainably long period, production of gasoline and diesel by liquefaction of coal would become economically competitive. Such a claim was made when the crude oil price was substantially lower than $35 per barrel. The crude oil price has been sharply rising in the 21st century, and it hit the $78 mark in July 2006.[41] Financial experts are warning that such a high crude oil price is here to stay, rather than a temporary phenomenon. Even after considering the changes in various economic factors involving energy industries, production of transportation fuels or fuel oils via coal liquefaction is certainly an outstanding option for the future. Further, the products of coal liquefaction can be refined and formulated to possess the properties of conventional *transportation fuels*, requiring neither major infrastructural changes in distribution nor lifestyle changes for consumers.

3.2 COAL PYROLYSIS FOR LIQUID FUEL

Pyrolysis of coal yields condensable tar, oil, and water vapor and noncondensable gases, through a process called *destructive distillation*, which involves cleavages of C–C bonds in coal macromolecular structure. The C–C bond cleavage reactions are largely responsible for the molecular weight reduction in coal hydrocarbons that ultimately converts solid fuel into liquid or gas. The solid residue of coal pyrolysis that is left behind is called *char*. Therefore, char contains substantially less amounts of volatile hydrocarbons than coal and is lower in H contents as well. As implied, the ratio of H/C is an effective indicator of the nature of coal product. For instance,

formation of coal char from coal is in the direction of the H/C ratio decreasing, whereas conversion of coal into coal liquid is in the direction of the H/C ratio increasing. The condensed pyrolysis product must be further hydrogenated to remove sulfur and nitrogen species as well as to improve the liquid fuel quality. Nitrogen and sulfur species not only generate air pollutants (in forms of NO_x and SO_x) when combusted but also poison and deactivate the upgrading catalyst. As the term implies, pyrolysis involves thermal decomposition reactions that induce mainly the cleavage of C–C bonds and partial breakdown of C–S and C–H bonds inside the macromolecular structure of coal, thus producing lower molecular weight products such as liquid hydrocarbons.

A number of coal pyrolysis processes are commercially available. Table 3.1 lists various coal pyrolysis processes and their process operating conditions and yields.[1] The factors affecting the process efficiency and product yield include the coal rank, coal particle size, reactor type, process mechanics, hydrogen partial pressure, reactor pressure, processing temperature, coal residence time, etc. A quick glance at Table 3.1 implies that higher liquid yields are obtained with shorter residence times, and also that hydrogen atmosphere helps the liquid product yield.[2] A shorter residence time, if properly managed, does not allow a sufficient reaction time to thermally crack the liquid hydrocarbons further (to gaseous hydrocarbons), thereby leaving more liquid hydrocarbons in the product stream. Adding hydrogen to coal hydrocarbons improves the H/C ratio high enough to increase the fluidity and to produce a liquid fuel. High tar content in supercritically extracted coal products may be attributable to the supercritical solvent's excellent low-temperature solubility that extracts and dissolves the tar *as is*. In this special case of low-temperature operation, extraction of large molecular weight hydrocarbons is taking place mainly due to the superior solvent properties of supercritical fluids, rather than the C–C bond breakage reaction of coal pyrolysis.

3.2.1 COED Process

The COED (Char-Oil-Energy-Development) process was originally developed by the FMC Corporation. The process has been improved, and the improved version has become the COED/COGAS process. The process is based on a fluidized bed technology that is carried out in four successive fluidized bed pyrolysis stages at progressively higher temperatures. Figure 3.1 shows a schematic of the COED/COGAS process.[1] The optimal temperatures for four stages vary, depending on the properties of the feed coal. The temperatures of the stages are selected to be just below the maximum temperature to which the particular feed coal can be heated without agglomerating and plugging the fluid bed.[1] Typical operating temperatures are 315–345°C, 425–455°C, 540°C, and 870°C in the first, second, third, and fourth stage, respectively.[2] Heat for the process is provided by combusting a portion of the product char with a steam-oxygen mixture in the fourth stage. Hot gases flow countercurrently to the char and provide the hot fluidizing medium for pyrolysis stages. The gases leaving both the first and second stages are passed to cyclones that remove the fines, but the vapors leaving the cyclones are quenched in a Venturi scrubber to condense the oil, and the gases and oil are separated in a decanter. The gas is desulfurized and then steam-reformed to produce hydrogen and fuel gas. The oil from the decanter is

TABLE 3.1
A Comparative Summary of Pyrolysis and Hydropyrolysis Processes

Process	Developer	Reactor Type	Reaction Temperature (°C)	Reaction Pressure (psi)	Coal Residence Time	Yield (%)		
						Char	Oil	Gas
Lurgi–Ruhrgas	Lurgi–Ruhrgas	Mechanical mixer	450–600	15	20 sec	45–55	15–25	30
COED	FMC Corp.	Multiple fluidized bed	290–815	20–25	1–4 h	60.7	20.1	15.1
Occidental coal pyrolysis	Occidental	Entrained flow	580	15	2 sec	56.7	35.0	6.6
TOSCOAL	Tosco	Kiln-type retort vessel	425–540	15	5 min	80–90	5–10	5–10
Clean coke	U.S. Steel Corp.	Fluidized bed	650–750	100–150	50 min	66.4	13.9	14.6
Union Carbide process	Union Carbide	Fluidized bed	565	1000	5–11 min	38.4	29.0	16.2

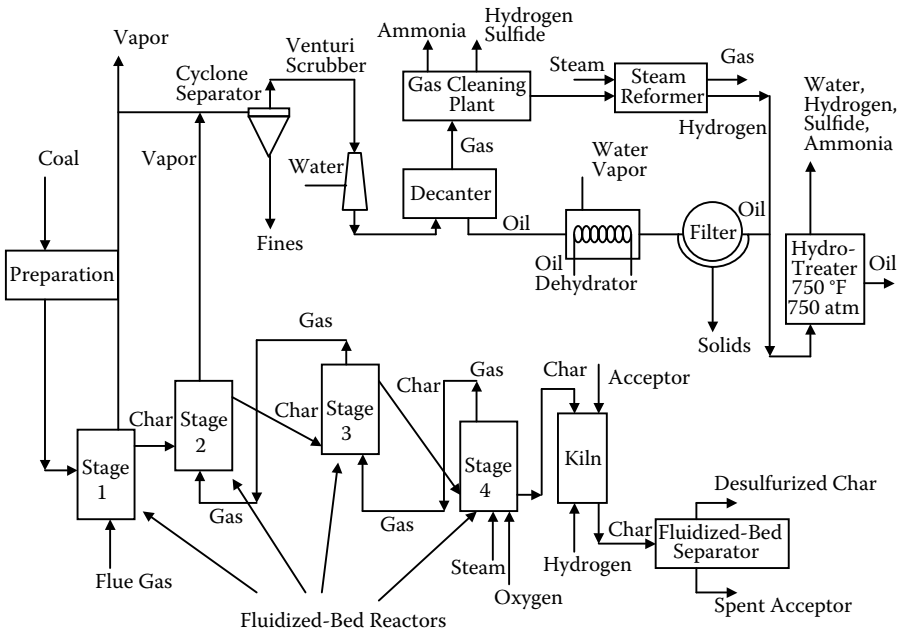

FIGURE 3.1 A schematic of the COED/COGAS process. (From Speight, J.G., *The Chemistry and Technology of Coal*, Marcel Dekker, New York, 1983. With permission.)

dehydrated, filtered, and hydrotreated to remove nitrogen, sulfur, and oxygen to form a heavy synthetic crude oil of approximately 25° API.

The API gravity is frequently correlated with the specific gravity of oil at 60°F using the following formula:

$$°\text{API gravity} = (141.5/\text{SG at } 60°\text{F}) - 131.5$$

where SG at 60°F is the specific gravity of oil at 60°F. For example, if the specific gravity of an oil is 1.0, the °API gravity would be 10, i.e., 10°API gravity. As shown, a lower value in the API gravity means it is a heavier oil.

The properties of synthetic crude oils from coal by the COED process are shown in Table 3.2.[1]

The char is desulfurized in a shift kiln, where it is treated with hydrogen to produce hydrogen sulfide (H_2S), which is subsequently absorbed by an acceptor such as dolomite or limestone.[1] The COGAS process involves the gasification of the COED char to produce a synthesis gas ($CO + H_2$). This COED/COGAS process is significant from both liquefaction and gasification standpoints.

3.2.2 TOSCOAL Process

A schematic of the TOSCOAL process is shown in Figure 3.2.[1] In this process, crushed coal is fed to a rotating drum which contains preheated ceramic balls at temperatures between 425 and 540°C. The hydrocarbons, water vapor, and gases are

TABLE 3.2
Synthetic Crude Oil Products from Coal by COED Process

Properties	Coal	
	Illinois No.6	Utah King
Analysis of hydrocarbon types (vol%)		
Paraffins	10.4	23.7
Olefins	—	—
Naphthenes	41.4	42.2
Aromatics	48.2	34.1
°API gravity	28.6	28.5
ASTM distillation (°F)		
Initial boiling point (IBP)	108	260
50% distilled	465	562
End point	746	868
Fractionation yields (wt%)		
IBP–180°F	2.5	
180–390°F	30.2	5
390–525°F	26.7	35
390–650°F	51.0	65
650–EP	16.3	30
390–EP	67.3	95

Source: From Speight, J.G., *The Chemistry and Technology of Coal*, Marcel Dekker, New York, 1983. With permission.

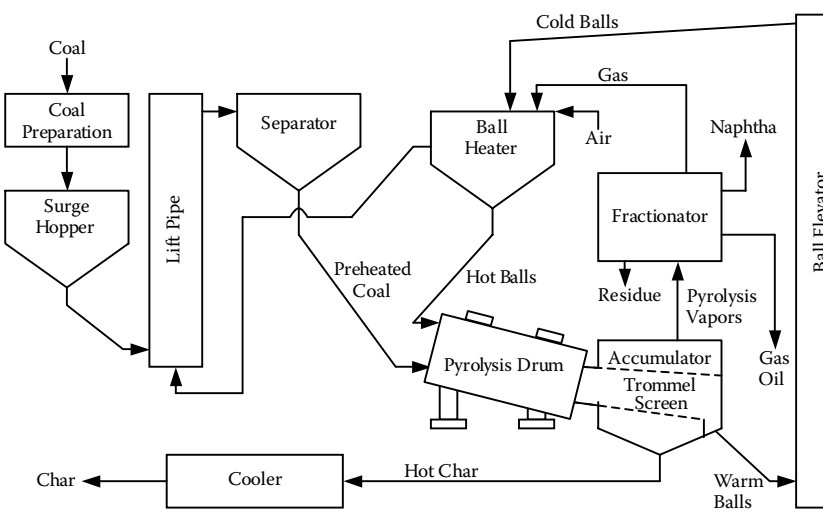

FIGURE 3.2 A schematic of TOSCOAL process.

TABLE 3.3
Liquid Products from Wyodak Coal (as Mined) via TOSCOAL Process

Temperature°C	425	480	520
Yield (wt%)			
Gas ($\leq C_3$)	6.0	7.8	6.3
Oil ($\geq C_4$)	5.7	7.2	9.3
Char	52.5	50.6	48.4
Water	35.1	35.1	35.1
Recovery percentage	99.3	100.7	99.1

Source: From Carlson, F.B. et al., Reprints of Clean Fuels from Coal II Symposium, Institute of Gas Technology, Chicago, IL, 1975, p. 504.

drawn off, and the residual char is separated from the ceramic balls in a revolving drum which has holes in it. The ceramic balls are reheated in a separate furnace by burning some of the product gas.[2] The TOSCOAL process is analogous to the TOSCO process for producing overhead oil from oil shale.[38] In this process analogy, the char replaces the spent shale, whereas the raw coal replaces raw oil shale.[1,38] It is noted that TOSCO is an acronym of the Oil Shale Corporation.

Table 3.3 shows the properties of liquids produced by the TOSCOAL process from Wyodak coal (as mined). As shown, the recovery efficiency is nearly 100%. It should be noted that the recovery efficiency is from the total material balance concept, not the conversion efficiency toward coal liquid or coal gas. As such, the high recovery rate of water comes from the nature of the feed coal. Wyodak coal is the coal from the Tongue River Member of the Fort Union Formation, Powder River Basin, WY. It is subbituminous in rank and has a typical heating value of 8,200–8,300 Btu/lb. It contains on the average 5–6% ash and less than 0.5% sulfur. It is not a coincidence that the processing temperature for the TOSCOAL process is similar to that for the TOSCO oil shale process.[38]

3.2.3 Lurgi–Ruhrgas Process

The Lurgi–Ruhrgas (L–R) process was developed as a low-pressure process for liquid production from lower rank coals. This process developed in Europe is currently in commercial use. A schematic of this process is given in Figure 3.3.[1]

In the L–R process, crushed coal is fed into a mixer and heated rapidly to 450–600°C by direct contact with hot recirculating char particles which have been previously heated in a partial oxidation process in an entrained-flow reactor.[1] Cyclone removes the fines from the product gases and the liquid products are collected by a series of condensers. The liquid products are hydrotreated to yield upgraded products. The high gas yield is due to the relatively long residence time, and the gaseous products include both primary and secondary products. The term *secondary product* is used here to clearly indicate that the product is not formed directly from the coal,

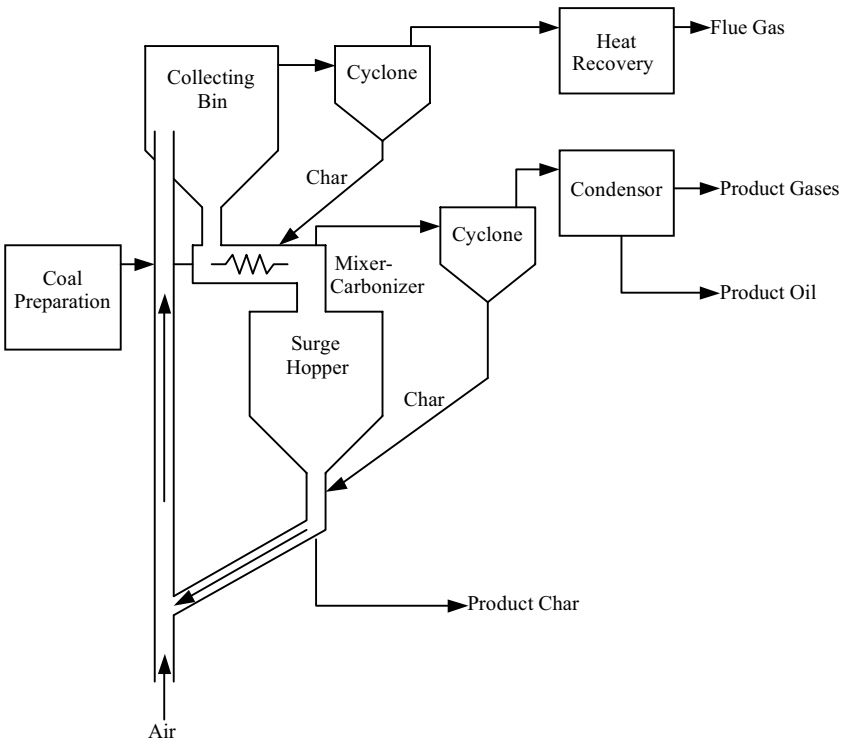

FIGURE 3.3 A schematic of the Lurgi-Ruhrgas process.

but rather by thermal decomposition of other primary products that are derived directly from coal. Therefore, the reactions involved in the secondary product formation include gas-phase, gas-liquid, and gas-solid reactions.

3.2.4 Occidental Flash Pyrolysis Process

A schematic of the occidental flash pyrolysis process is given in Figure 3.4.[1] In this process, hot recycle char provides the heat for the flash pyrolysis of pulverized coal in an entrained flow reactor at a temperature not exceeding 760°C. The process operates with a short residence time, thereby increasing the coal throughput and also increasing the production of liquid products while minimizing the production of gaseous products. At a short residence time at a high temperature, pyrolytic decomposition of coal hydrocarbons into liquid-range hydrocarbons actively takes place, but their further conversion into gaseous hydrocarbons is less appreciable. Like other processes, cyclones remove fine char particles from the pyrolysis overhead before quenching in the two-stage collector system.[1] The first stage consists of quenching at approximately 99°C to remove the majority of heavier hydrocarbons, whereas the second stage is for quenching at approximately 25°C to cause water and light oils (i.e., lower molecular weight hydrocarbons) to be removed.

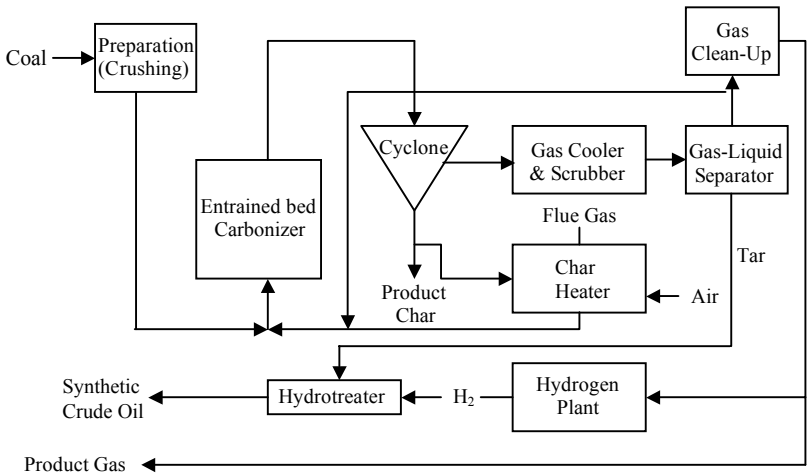

FIGURE 3.4 A schematic of the occidental flash pyrolysis process. (From Speight, J.G., *The Chemistry and Technology of Coal* (Rev. Ed.), Marcel Dekker, New York, 1994.

3.2.5 Clean Coke Process

A schematic of the clean coke process is shown in Figure 3.5.[1] The process involves feeding oxidized clean coal into a fluidized bed reactor at temperatures up to 800°C when the coal reacts to produce tar, gas, and low-sulfur char. Alternatively, the coal can be processed by noncatalytic hydrogenation at 455–480°C and pressures of up to 340 bars of hydrogen. With direct hydrogenation of coal, the process accomplishes the addition of hydrogen to the coal hydrocarbons while cracking the high-molecular-weight hydrocarbons into lower molecular hydrocarbons, thus increasing the H/C ratio of the fuel to a level of the liquid hydrocarbon fuel. The liquid products from both the carbonization and hydrogenation stages are combined for further processing to yield synthetic liquid fuels.

3.2.6 Coalcon Process

A schematic of the Coalcon process is shown in Figure 3.6.[1] This process is based on a dry noncatalytic fluidized bed of coal particles suspended in hydrogen gas. Hot, oxygen-free flue gas is used to heat the coal to approximately 325°C and also to carry the coal to a feed hopper. A fractionator is employed to subdivide the overhead stream into four streams, viz., (1) gases (H_2, CO, CO_2, and CH_4), (2) light oil, (3) heavy oil, and (4) water. Most of the char is removed from the bottom of the reactor, quenched with water, and cooled.[1] The char can then be used as a feed to a Koppers-Totzek gasifier and reacted with oxygen and steam to produce hydrogen for the process.[1]

3.3 DIRECT LIQUEFACTION OF COAL

Direct liquefaction of coal is defined to mean *hydroliquefaction,* to distinguish it from pyrolysis, coprocessing, and indirect liquefaction. Hydroliquefaction more

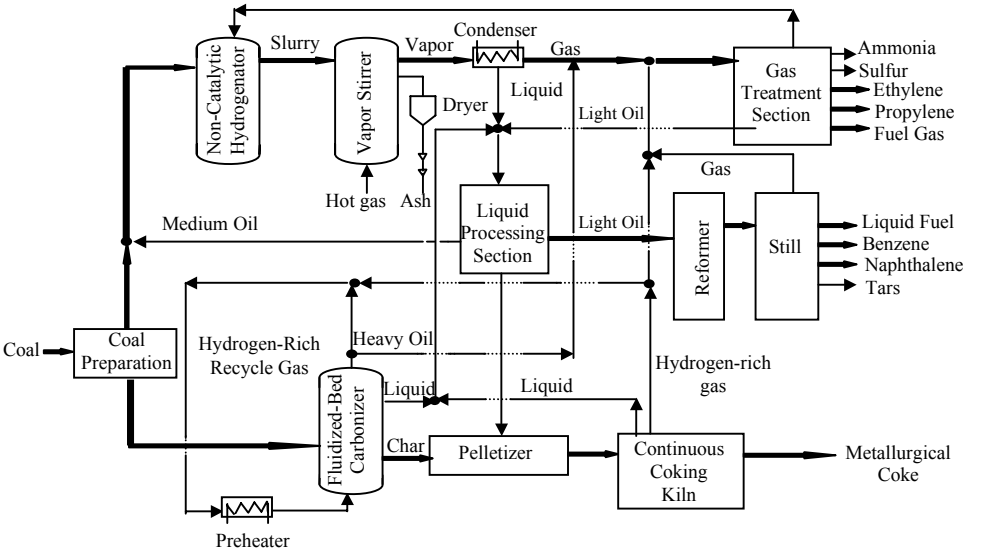

FIGURE 3.5 A schematic of the clean coke process. (From Speight, J.G., *The Chemistry and Technology of Coal* (Rev. Ed.), Marcel Dekker, New York, 1994.)

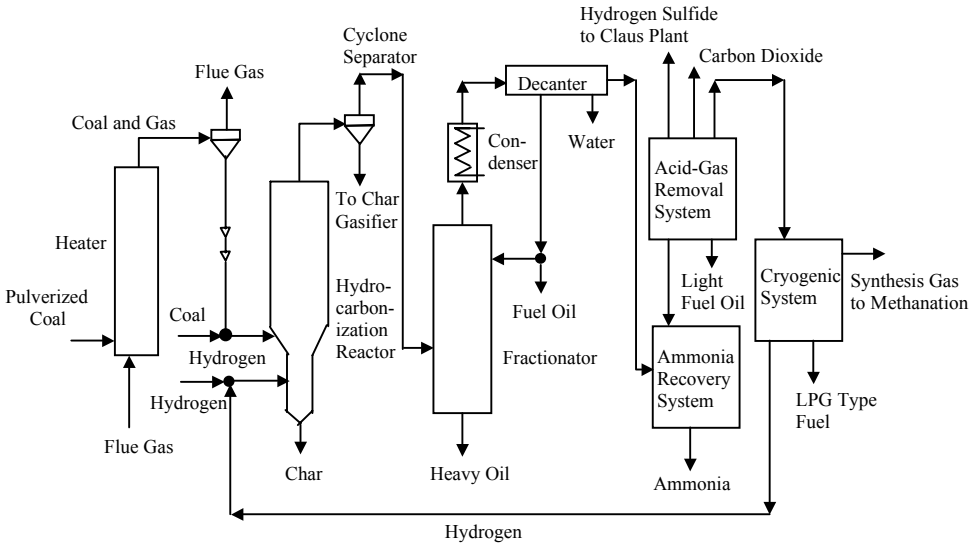

FIGURE 3.6 A schematic of Coalcon process. (From Speight, J.G., *The Chemistry and Technology of Coal* (Rev. Ed.), Marcel Dekker, New York, 1994.)

specifically means that liquefaction process is carried out under hydrogen environment. Direct liquefaction may be categorized into single or two stages. In two-stage processes, the coal is first hydrogenated in a liquid-phase stage transforming it into a deashed, liquid product; and then in a second vapor-phase hydrogenation stage, the liquid products are catalytically converted to clean, light distillate fuels. Direct liquefaction has a relatively long history, and various processes have been successfully operated on large scales. Large-scale operations of coal liquefaction, in turn, contributed tremendously to the advances of chemical process industries in all aspects of machinery, design, and knowledge. Recent processes that are ready for demonstration or full commercialization include H-Coal, SRC-I, SRC-II, EDS, ITSL, CC-ITSL, and CTSL. In this section, several significant direct coal liquefaction processes are reviewed.

3.3.1 Bergius-IG Hydroliquefaction Process

The Bergius process was operated very successfully in Germany before and during World War II and was a two-stage process.[2] It is currently not in use, but it contributed immensely to the development of catalytic coal liquefaction technology. The process involves the catalytic conversion of coal (slurried with heavy oil) in the presence of hydrogen and an iron oxide catalyst, at 450–500°C and 200–690 bars (197–681 atm, or 20–69 MPa). The products were usually separated into light oils, middle distillates, and residuum. Middle distillates, or mid-distillates, are a general classification of refined petroleum products that includes heating oil, distillate fuel oil, jet aviation fuel, and kerosene. Generally speaking, the typical boiling range of mid-distillates is 300–750°F, and that for residuum is 600–1000°F.

These oils, except for residuum, were catalytically cracked to motor fuels and light hydrocarbons in a vapor-phase hydrogenation stage, which serves as the second stage of the process. Some argue that the severe conditions used in the original process might have been due to the fact that German coals are much more difficult to liquefy than U.S. coals. It is truly remarkable, from a technological standpoint, that the process, under the severe process conditions of a hydrogen atmosphere, was very successfully operated on a large scale in the 1940s.

The residence time for catalytic conversion was about 80–85 min., which was quite long, and hydrogen consumption was also quite significant — approximately 11% by mass of the daf (dry ash-free) coal.

3.3.2 H-Coal Process

The H-Coal process is a direct catalytic coal liquefaction process developed in 1963 by Hydrocarbon Research, Inc. (HRI), currently Hydrocarbon Technologies Inc. (HTI). The process development proceeded through several stages from conceptual, to bench-scale (25 lb/d), to process development unit (PDU) (3 tons/d), and to a pilot plant in Catlettsburg, KY (200–600 tons/d).[42] This pilot plant project received $300 million in funds from the U.S. Department of Energy (DOE), the Commonwealth of Kentucky, EPRI, Mobil, AMOCO, CONOCO, Ruhrkohle, Ashland Oil, SUN Oil, Shell, and ARCO.

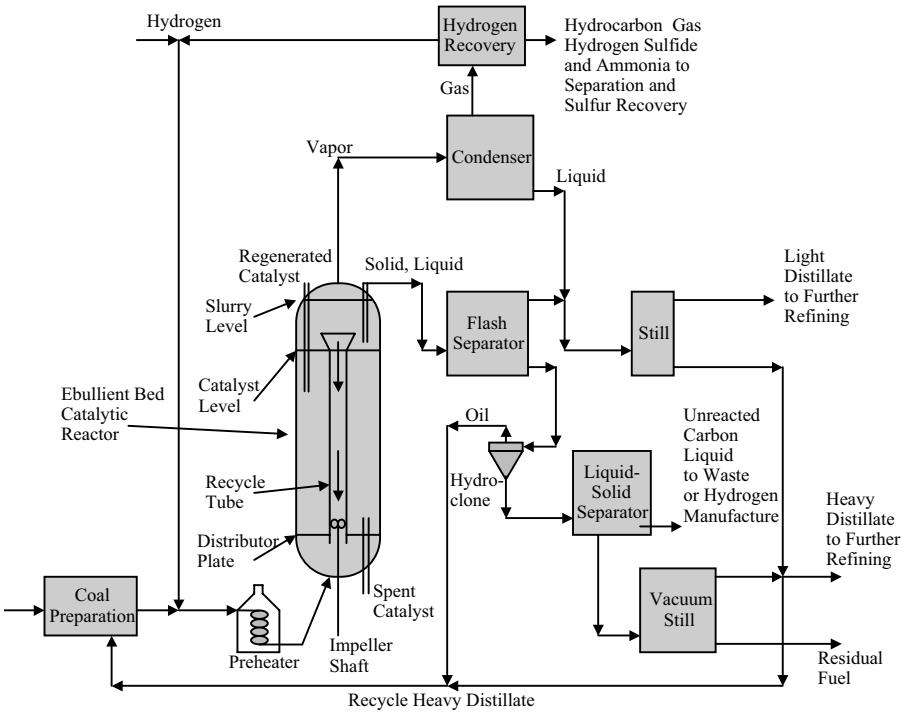

FIGURE 3.7 A schematic of the H-coal process.

A schematic of the H-Coal process is shown in Figure 3.7.[1,4] Pulverized coal, recycle liquids, hydrogen, and catalyst are brought together in the ebullated-bed reactor to convert coal into hydrocarbon liquids and gaseous products. The catalyst pellets are 0.8 to 1.5-mm diameter extrudates, and pulverized coal is of –60 mesh. The term *–60 mesh* denotes the particle fraction that passes through the 60-mesh screen, i.e., the particle size in this fraction is smaller than the hole opening of the 60-mesh screen. Coal slurried with recycle oil is pumped to a pressure of up to 200 bars and introduced into the bottom of the ebullated-bed reactor. The H-Coal process development has contributed very significantly to the field of chemical reaction engineering in the areas of multiple phase reactions as well as design of ebullated and liquid-entrained reactors. The ebullated bed reactor is similar to a liquid entrained reactor, but much larger gas bubbles help fluidize the solid particles in a gas–liquid–solid fluidized bed reactor. Therefore, relatively large coal particles can be used in the ebullated bed reactor.

The process temperature conditions, 345–370°C, may be altered appropriately to produce different product slates.[1] Table 3.4 shows typical product compositions from the H-Coal process.[1] A higher reaction temperature of 445–455°C has also been successfully demonstrated for the process.[4]

Advantages and disadvantages of the H-Coal process are summarized in Table 3.5. Like most other single-stage processes, H-Coal process is best suited for high-volatile bituminous coal.

TABLE 3.4
Product Compositions from the H-Coal Process

	Illinois		Wyodak
	Synthetic Crude	Low-sulfur Fuel Oil	Synthetic Crude
Product (wt%)			
C_1–C_3 hydrocarbons	10.7	5.4	10.2
C_4–200°C Distillate	17.2	12.1	26.1
200–340°C Distillate	28.2	19.3	19.8
340–525°C Distillate	18.6	17.3	6.5
525°C + Residual Oil	10.2	29.5	11.1
Unreacted ash-free coal	5.2	6.8	9.8
Gases	15.0	12.8	22.7
Total (100+H_2 reacted)	104.9	103.2	106.2
Conversion (%)	94.8	93.2	90.2
H_2 consumption (scf/ton)	18,600	12,200	23,600

Source: From Speight, J.G., *The Chemistry and Technology of Coal* (Rev. Ed.), Marcel Dekker, New York, 1994.

TABLE 3.5
Advantages and Shortcomings of the H-Coal Process

Advantages	Disadvantages
1. Coal dissolution and upgrading to distillates are accomplished in one reactor.	1. High reaction temperature (445–455°C) results in high gas yields (12–15%) due to excessive thermal cracking.
2. Products have a high H/C ratio and low heteroatom content.	2. Hydrogen consumption is relatively high. Some distillate product is gasified to supplement hydrogen need.
3. High throughput of coal occurs due to fast reaction rates of catalytic hydrogenation.	3. Product contains considerable vacuum gas oil (345–525°C, bp), which is difficult to upgrade by standard refinery process.
4. Ash is removed by vacuum distillation, followed by gasification of vacuum tower bottoms to generate the hydrogen required for the process.	4. Due to the considerable amount of vacuum gas oil, it has utility solely as a boiler fuel.

3.3.3 Solvent Refined Coal (SRC-I)

In 1962, the Spencer Chemical Co. began to develop a process that was later taken up by Gulf Oil Co., which in 1967 designed a 50-ton/d SRC pilot plant at Fort Lewis, WA.[4] The plant was operated in the SRC-I mode from 1974 until late 1976. In 1972, Southern Services Co. (SSC) and Edison Electric Institute (EEI) designed and constructed a 6-ton/d SRC-I pilot plant at Wilsonville, AL.

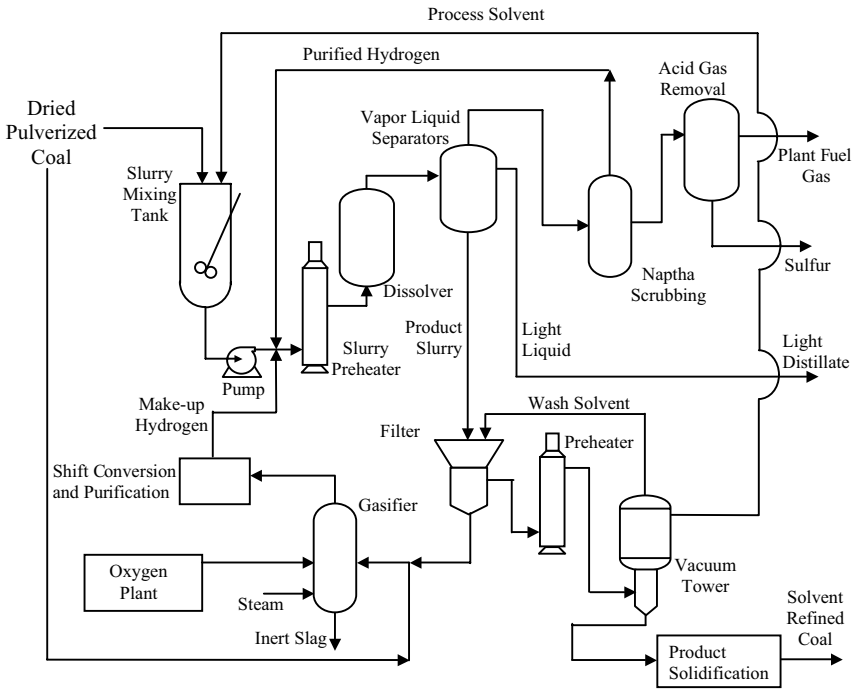

FIGURE 3.8 A schematic of SRC-I process. (From Speight, J.G., *The Chemistry and Technology of Coal* (Rev. Ed.), Marcel Dekker, New York, 1994. With permission.)

The principal objective of the original SRC-I process was to produce a solid boiler fuel with a melting point of about 150°C and a heating value of 16,000 Btu/lb. In the interest of enhancing commercial viability, the product slate was expanded to include liquids that were products of a Coker/Calciner, an Expanded-Bed Hydrocracker, and a Naphtha Hydrotreater.[4]

SRC-I is a thermal liquefaction process in which solvent, coal, and hydrogen are reacted in a "dissolver" reactor to produce a nondistillable resid, which upon deashing can be used as a clean boiler fuel. Reaction conditions are slightly less severe than H-Coal process. The absence of a catalyst diminishes the hydrogenation rates and the resid has an H/C ratio about the same as the coal feed. Again, this process is also ideally suited for bituminous coals, especially those containing high concentrations of pyrite. The pyrite is considered to be the liquefaction catalyst. A schematic of SRC-I process is shown in Figure 3.8.[1]

Advantages and disadvantages of SRC-I are given in Table 3.6.

Nondistillable SRC-I resid products cannot be deashed by vacuum distillation. Extraction-type separation processes were developed specifically for this process.[4] Typical of these is Kerr–McGee's Critical Solvent Deashing (CSD). This deashing process uses a light aromatic solvent to precipitate the heaviest (toluene-insoluble) fraction of the resid, all of the ash, and unconverted coal. This process recovers a heavy but solid-free recycle solvent. The CSD was also used for the two-stage liquefaction (TSL) processing that is discussed later in this chapter.

TABLE 3.6
Advantages and Disadvantages of SRC-I

Advantages	Disadvantages
1. A good boiler fuel with high heating value is obtained.	1. Distillate solvent is of poor quality.
2. Reaction conditions are less severe.	2. Solvent is frequently incorporated into the resid product.
3. The process is noncatalytic and easy to operate.	3. Due to 2, solvent balance cannot be achieved.
	4. Nondistillable SRC-I resid cannot be recovered by vacuum distillation.

3.3.4 Exxon Donor Solvent (EDS) Process

A schematic of the EDS process is shown in Figure 3.9.[1] The EDS process utilizes a noncatalytic hydroprocessing step for the liquefaction of coal to produce liquid hydrocarbons. Its salient feature is the hydrogenation of the recycle solvent, which is used as a hydrogen donor to the slurried coal in a high-pressure reactor. This process is also considered to be a single-stage process, as both coal dissolution and resid upgrading take place in one thermal reactor. The liquefaction reaction is carried out noncatalytically. The recycle solvent, however, is catalytically hydrogenated in a separate fixed-bed reactor.[4] This solvent is responsible for transferring hydrogen to the slurried coal in the high-pressure liquefaction reactor. Reaction conditions are similar to those of SRC-I and H-Coal.

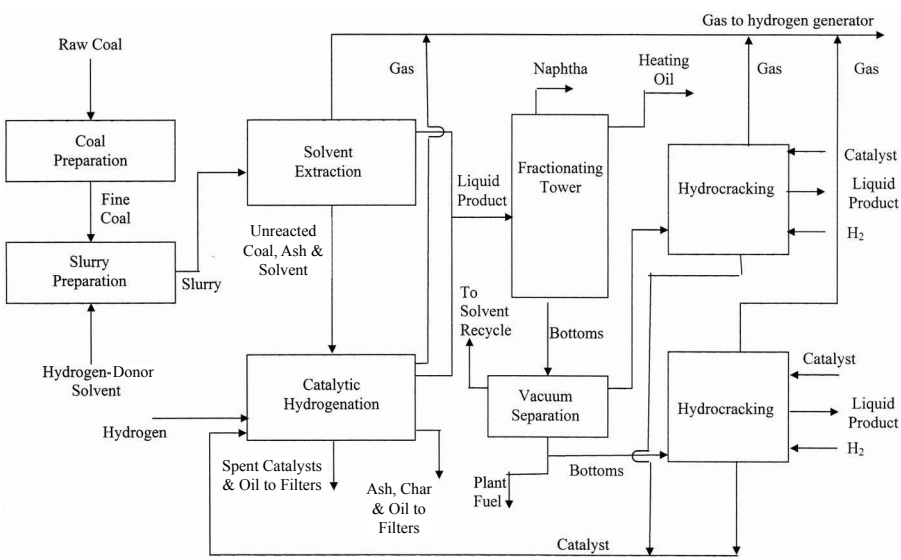

FIGURE 3.9 A schematic of the Exxon Donor Solvent (EDS) process.

EDS solvent must be well hydrogenated to be an effective hydrogen donor. The recycle solvent "donates" hydrogen to effect rapid hydrogenation of primary liquefaction products. Thermal hydrogenation and cracking follow this step to produce distillates.[4] The product quality is slightly inferior to that of H-Coal, due to the absence of a hydrotreating catalyst. Distillate yields are also lower than the H-Coal process. Overall, its process economics are still about equal to the H-Coal process because of the less expensive thermal reactor and the simple solids removal process.

The EDS process development started with bench-scale research in the mid-1960s and then progressed to a pilot plant study in the 1970s and 1980s with a 1 ton/d scale. The initial program of process development was completely under Exxon's own responsibility, whereas the later part of development was cosponsored as a joint venture between Exxon and the U.S. DOE. In 1980, a large-scale (250 tons/d) demonstration type of installation, which was named the Exxon Coal Liquefaction Plant (ECLP), was constructed and put in operation. The plant was shut down and dismantled in 1982.

3.3.5 SRC-II Process

The SRC-II process uses direct hydrogenation of coal in a reactor at high pressure and temperature to produce liquid hydrocarbon products instead of the solid products in SRC-I. The 50-ton/d pilot plant at Fort Lewis, WA, which operated in the SRC-I mode from 1974 to 1976, was modified to run in the SRC-II mode, producing liquid products for testing.[4] The pilot plant was successfully operated from 1978 until 1981.

The SRC-II process is a thermal process, and uses the mineral matter in the coal as the only catalyst. The mineral matter concentration in the reactor is kept high by recycle of the heavy oil slurry. The recycled use of mineral matter and the more severe reaction conditions distinguish the SRC-II operation from the SRC-I process and also account for the lighter products. The net product is –540°C distillate, which is recovered by vacuum distillation. The term, –540°C distillate, denotes the fraction which comes out below 540°C of distillation temperature. The vacuum bottoms including ash are sent to gasification to generate process hydrogen. The SRC-II process is limited to coals that contain catalytic mineral matter and therefore excludes all lower-rank coals and some bituminous coals. Pulverized coal of particle size smaller than 0.125 in., and the solvent-to-coal ratio of 2.0 are used for SRC-II, whereas the solvent-to-coal ratio is 1.5 for SRC-I. The liquid product quality is inferior to that of the H-coal process. A schematic of the SRC-II process is shown in Figure 3.10.

3.3.6 Nonintegrated Two-Stage Liquefaction (NTSL)

Even though single-stage processes like EDS, SRC-I, SRC-II, and H-coal, are technologically sound, their process economics suffers for the following reasons:

1. The reaction severity is high, with temperatures of 430–460°C and liquid residence times of 20–60 min. These severe operating conditions were considered necessary to achieve coal conversions of over 90% (to tetrahydrofuran (THF) or quinoline solubles).

2. Distillate yields are low, only about 50% for mmaf (mineral matter and ash free) bituminous coals and even lower for subbituminous coals.
3. Hydrogen efficiency is low due to high yields of hydrocarbon gases.
4. The costs associated with the SRC-I process or the like may be too high to produce a boiler fuel.

Based on these reasons, a coal liquefaction process is best applied to make higher value-added products, such as transportation fuels.[4] To produce higher value-added products from the SRC-I process, the resid must first be hydrocracked to distillate liquids. Efforts made by Mobil and Chevron on fixed-bed hydrocracking were not entirely successful, due to the plugging of the fixed bed ashes and rapid deactivation of the catalyst by coking.

The SRC-I resid was successfully hydrotreated by LC-Fining (Lummus–Cities–Fining), a variation of ebullated-bed technology developed by Cities Services R&D.[5] As a result, hydrocracking part was added to the SRC-I process to form Nonintegrated Two-Stage Liquefaction (NTSL). This rather unique name was given, because the hydrocracking part did not contribute solvent to the SRC-I part. In other words, the NTSL process was a combination of two separate processes, viz., coal liquefaction and resid upgrading. A schematic of NTSL process is shown in Figure 3.11. Even with the addition of the hydrocracking section, NTSL was a somewhat inefficient

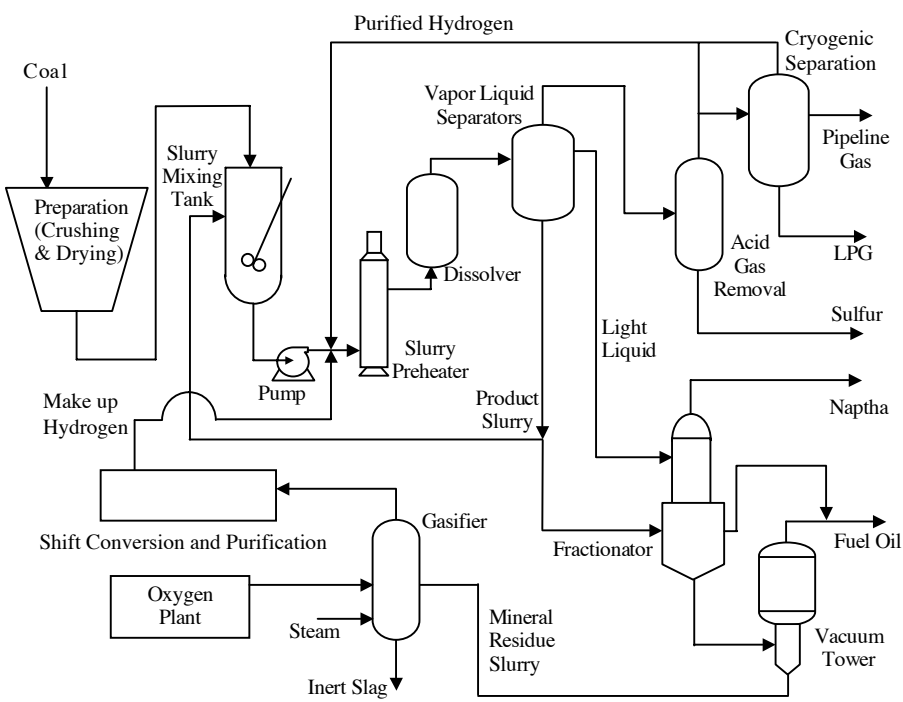

FIGURE 3.10 A schematic of the SRC-II process. (From Speight, J.G., *The Chemistry and Technology of Coal* (Rev. Ed.), Marcel Dekker, New York, 1994.)

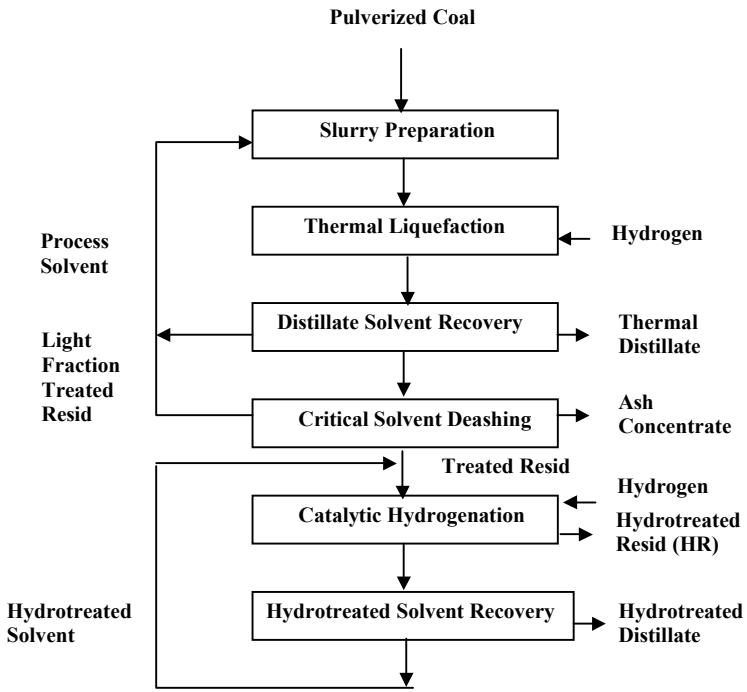

FIGURE 3.11 A block diagram of NTSL process. (From Schindler, H.D., Coal Liquefaction — A Research and Development Needs Assessment, COLIRN Panel Assessment, DOE/ER-0400,UC-108, Final Report, Vol. II., March 1989.)

process due to the shortcomings listed earlier. SRC-I product is a less reactive feed to hydrocracking, thus requiring high-temperature (over 430°C) and low-space velocity (i.e., low productivity) for complete conversion to distillates. In order to keep the temperature and reactor size at reasonable levels, resid conversion was held below 80%. NTSL operation data at the Wilsonville facility are presented in Table 3.7. Yields were higher than those for H-coal, but hydrogen consumption was still high due to the extensive thermal hydrogenation step in the SRC-I dissolver, which was renamed the Thermal Liquefaction Unit (TLU).[4] NTSL was short-lived and a newer integrated approach was later developed.

3.3.7 Thermal Integrated Two-Stage Liquefaction (ITSL)

Thermal coal dissolution studies by Consol, Mobil, and Wilsonville in the late 1970s had shown that coal conversion to tetrahydrofuran-solubles is essentially complete in an extremely short time, 1–5 min. Within this short dissolution period, hydrogenation from the gas phase is negligible, and almost all hydrogen comes from the solvent in the liquid phase.[4] If hydrogen transfer from the solvent is insufficient to satisfy the liquefaction needs, the product will have a high concentration of toluene-insolubles, causing precipitation and plugging in the reactor or in downstream equipment. With a well-hydrogenated solvent, however, short contact time (SCT)

TABLE 3.7
NTSL at Wilsonville Facility (Illinois No. 6 Coal)

Operating Conditions	
Run ID	241CD
Configuration	NTSL
Catalyst	Armak
Thermal stage	
Average reactor temperature (°F)	805
Coal space velocity (lb/h/ft^3 @ > 700°C)	20
Pressure (psig)	2170
Catalytic stage	
Average reactor temperature (°F)	780
Space velocity (lb feed/h/lb catalyst)	1.7
Catalyst age (lb resid/lb catalyst)	260–387
Yields (wt% mmaf coal)	
C_1– C_3 gas	7
C_4 + distillate	40
Resid	23
Hydrogen consumption	4.2
Hydrogen efficiency	
lb C_4 + distillate/lb H_2 consumed	9.5
Distillate selectivity	
lb C_1-C_3/lb C_4 + distillate	0.18
Energy content of feed coal rejected to ash concentrate (%)	20

Source: From Schindler, H.D., Coal Liquefaction — A Research and Development Needs Assessment, COLIRN Panel Assessment, DOE/ER-0400,UC-108, Final Report, Vol. II., March 1989.

liquefaction is the preferred thermal dissolution procedure because it eliminates the inefficient thermal hydrogenation inherent in the SRC-I. Cities Services R&D successfully hydrocracked the SRC-I resids by LC-Fining at relatively low temperatures of 400–420°C. Gas yield was low and hydrogen efficiency was high. A combination of this process with SCT is certainly a good idea and provides a successful example of process integration. The low-temperature LC-Fining provides the liquefaction solvent to the first stage SCT, thus the two stages become integrated. This combination has the potential to liquefy coal to distillate products in a more efficient process than any of the single stage processes.[4]

3.3.7.1 Lummus ITSL (1980–1984)

A combination of SCT and LC-Fining was made by Lummus in the ITSL process.[6] A process flow diagram of Lummus ITSL process is given in Figure 3.12. Coal is slurried with recycled solvent from LC-Fining and is converted to quinoline-solubles (or THF-solubles) in the SCT reactor. The resid is hydrocracked to distillates in the LC-Fining stage, where recycle solvent is also generated. The ash is removed by the

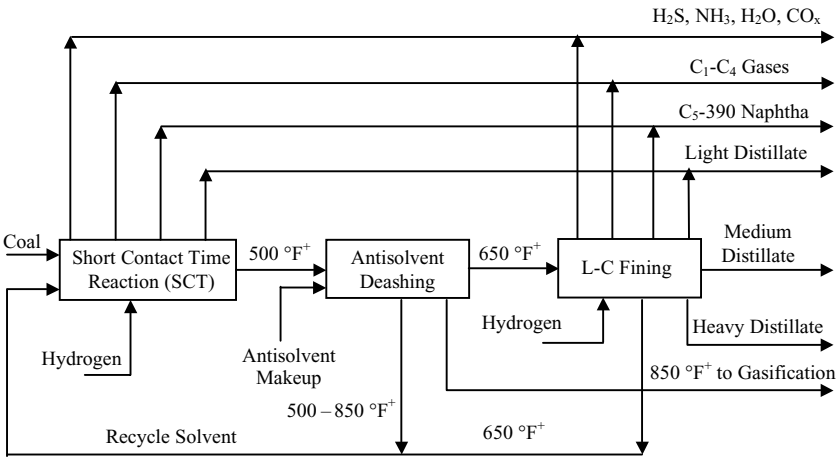

FIGURE 3.12 A schematic of integrated two-stage liquefaction (ITSL). (From Speight, J.G., *The Chemistry and Technology of Coal*, Marcel Dekker, New York, 1983.)

Lummus Antisolvent Deashing (ASDA) process, which is similar to deasphalting operation with petroleum. The net liquid product is either –340°C or –450°C distillate. The recycle solvent is hydrogenated +340°C atmospheric bottoms. It is the recycle of these full-range bottoms, including resid, that couples the two reaction stages and results in high yields of all distillate product.[4]

Some of the features of the Lummus ITSL are summarized as follows:

1. The SCT reactor is actually the preheater for the dissolver in the SRC-I process, thus eliminating a long residence-time high-pressure thermal dissolution reactor.
2. Coal conversion in the SCT reactor was 92% of mmaf coal for bituminous coals and 90% for subbituminous coals.
3. Molecular hydrogen gas consumption was essentially zero, and the hydrogen transferred from the solvent was equivalent to 1.2–2.0% of the coal weight. Gaseous hydrocarbon yield was reduced to 1% for bituminous coal and to 5–6% for subbituminous coal.
4. The SCT resid was more reactive to hydrocracking than SRC-I resid.
5. The LC-Fining second reactor as a hydrotreater (HTR) accomplishes two principal tasks: (1) to make essentially all of the distillate product and (2) to generate recycle solvent capable of supplying the hydrogen required by the SCT reactor.
6. All distillate products were produced as a result of full recycle of unconverted resid to the first stage.
7. A second-stage HTR temperature of 400°C provides sufficient hydrogenation and cracking activity to accomplish both tasks.
8. Catalyst deactivation was much slower than other processes operated at higher temperatures.
9. The SCT resid was more reactive, not only for conversion to distillate, but also for heteroatom removal. Product quality surpassed those achieved

by the preceding processes. Chevron successfully refined the ITSL products for specification transportation fuels.

10. The ash was removed by antisolvent deashing (ASDA), which used process-derived naphtha as antisolvent to precipitate the heaviest components of the resid and the solids.
11. The ASDA had the advantage of low pressure (100–1000 psi) and low temperature (260–282°C) operation.

Data for typical product yields by the Lummus ITSL process are given in Table 3.8,[4] and the product quality of the Lummus ITSL distillates is shown in Table 3.9.[4]

3.3.7.2 Wilsonville ITSL (1982–1985)

The Advanced Coal Liquefaction R&D Facility at Wilsonville, AL, sponsored by the DOE, the Electric Power Research Institute (EPRI), and AMOCO, was operated by Catalytica, Inc. under the management of Southern Company Services, Inc. The Hydrotreater (HTR) design was supplied by Hydrocarbon Research, Inc., and the deashing technology was provided by Kerr–McGee.

The Wilsonville facility began operations as a 6-ton/d single-stage plant for SRC-I in 1974. In 1978, a Kerr-McGee Critical Solvent Deashing (CSD) unit replaced the filtration equipment that had been used for solids removal from the SRC product. In 1981, an H-Oil ebullated-bed hydrotreater was installed for upgrading the recycle solvent and product. In 1985, a second ebullated-bed reactor was added in the hydrotreater area to allow operation with close-coupled reactors. A schematic for the Integrated Two-Stage Liquefaction (ITSL) configuration used at Wilsonville facility for bituminous coal runs is shown in Figure 3.13. A distillate yield of 54–59% of mmaf coal was confirmed, as shown in Table 3.10. It is noted that the hydrogen

TABLE 3.8
Lummus ITSL Product Yields

Product	lb/100 lb mmaf Coal	
	Illinois 6	Wyodak
H_2S, H_2O, NH_3, CO_x	15.08	23.08
C_1–C_4	4.16	7.30
Total gas	**19.24**	**30.38**
C_5–390°F	6.92	1.25
390–500°F	11.46	8.49
500–650°F	17.26	22.46
650–850°F	23.87	21.36
Total distillate product	**59.51**	**53.56**
Organics rejected with ash	26.09	20.22
Grand total	**104.84**	**104.16**
Molecular hydrogen consumption	4.84	4.16
Hydrogen efficiency, lb distillates/lb H_2	12.28	12.86
Distillate yield, bbl/ton mmaf coal	**3.52**	**3.08**

TABLE 3.9
Lummus ITSL Distillate Product Quality (Illinois No. 6 Coal)

°API	C	H	O	N	S	HHV, Btu/lb
Naphtha						
36.8	86.79	11.15	1.72	0.18	0.16	19,411
45.4	86.01	13.16	0.62	0.12	0.09	20,628
Light distillates (390–500°F)						
15.5	88.62	9.51	1.50	0.28	0.09	18,673
22.9	87.75	11.31	0.73	0.13	0.08	19,724
Medium distillates (500–650°F)						
7.5	90.69	8.76	0.27	0.25	0.03	18,604
12.9	89.29	10.26	0.28	0.12	0.05	19,331
Heavy distillates (650–850°F)						
–1.5	91.47	7.72	0.26	0.50	0.05	18,074
1.8	90.77	8.47	0.45	0.23	0.08	18,424

Source: From Schindler, H.D., Coal Liquefaction — A Research and Development Needs Assessment, COLIRN Panel Assessment, DOE/ER-0400,UC-108, Final Report, Vol. II., March 1989.

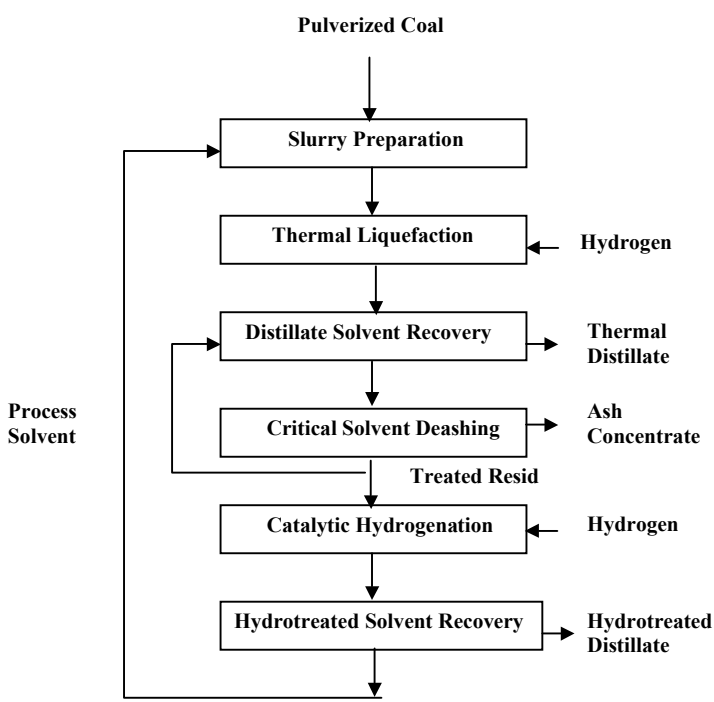

FIGURE 3.13 A block diagram of the ITSL process. (From Schindler, H.D., Coal Liquefaction — A Research and Development Needs Assessment, COLIRN Panel Assessment, DOE/ER-0400,UC-108, Final Report, Vol. II., March 1989. With permission.)

TABLE 3.10
ITSL and NTSL Operation Data at Wilsonville Facility (Illinois No. 6 Coal)

Operating Conditions						
Run ID	241CD	7242BC	243JK/244B	247D	250D	250G(a)
Configuration	NTSL	ITSL	ITSL	RITSL	CC-ITSL	CC-ITSL
Catalyst	Armak	Shell324M	Shell324M	Shell324M	Amocat IC	Amocat IC
Thermal Stage						
Average reactor temperature (°F)	805	860	810	810	824	829
Coal space velocity, lb/h/ft^3 @ > 700°C	20	43	28	27	20	20
Pressure, psig	2170	2400	1500–2400	2400	2500	2500
Catalytic stage						
Average reactor temperature (°F)	780	720	720	711	750	750
Space velocity, lb feed/h/lb catalyst	1.7	1.0	1.0	0.9	2.08	2.23
Catalyst usage, lb resid/lb catalyst	260–387	278–441	380–850	446–671	697–786	346–439
Yields (wt% mmaf Coal)						
C_1–C_3 gas	7	4	6	6	7	8
C_4+ distillate	40	54	59	62	64	63
Resid	23	8	6	3	2	5
Hydrogen consumption	4.2	4.9	5.1	6.1	6.1	6.4
Hydrogen efficiency						
lb C_4+ distillate/lb H_2 consumed	9.5	11	11.5	10.2	10.5	9.8
Distillate selectivity						
lb C_1–C_3/lb C_4+ distillate	0.18	0.07	0.10	0.10	0.11	0.12
Energy content of feed coal rejected to Ash Concentrate (%)	20	24	20–23	22	23	16

Source: From Schindler, H.D., Coal Liquefaction — A Research and Development Needs Assessment, COLIRN Panel Assessment, DOE/ER-0400,UC-108, Final Report, Vol. II., March 1989.

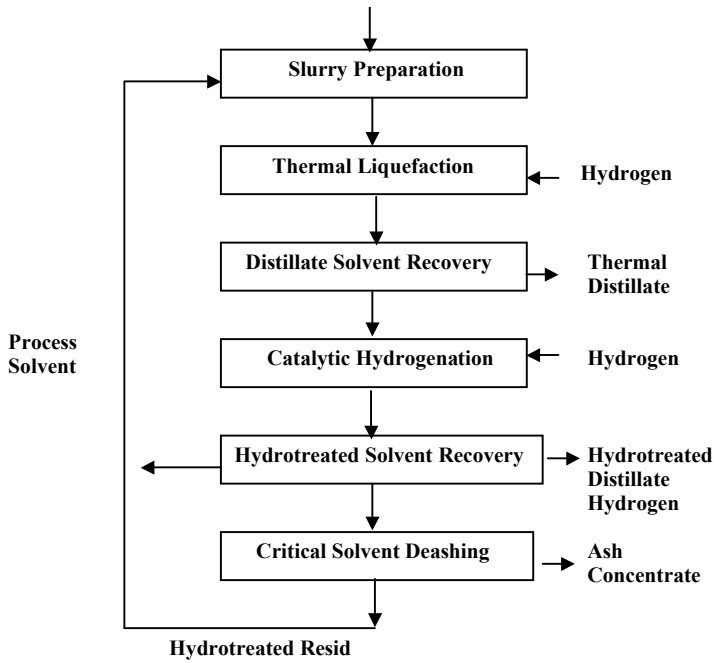

FIGURE 3.14 A block diagram of the RITSL process. (From Schindler, H.D., Coal Liquefaction — A Research and Development Needs Assessment, COLIRN Panel Assessment, DOE/ER-0400,UC-108, Final Report, Vol. II., March 1989.)

efficiency for the ITSL based on the distillate productivity per hydrogen consumption is substantially increased from that for the NTSL result.

Lummus enhanced the ITSL process by increasing the distillate yield by placing the deasher after the second stage, with no detrimental effect of ashy feed on catalyst activity. This enhanced process is called *reconfigured two-stage liquefaction* (RITSL), as illustrated in Figure 3.14. The process improvements were experimentally confirmed at Wilsonville facility. The enhancements included higher distillate yield, lower resids, and less energy rejects.

With the deasher placed after the second stage reactor and the two stages operating at about the same pressure, the two reactors were close-coupled to minimize holding time between the reactors and to eliminate pressure letdown and repressurizing between stages.[4] This enhancement was called *close-coupled ITSL* (or CC-ITSL). The improved results were evidenced by higher distillate yield, lower resids, and lower energy reject.

3.3.8 Catalytic Two-Stage Liquefaction (CTSL)

Beginning in 1985, all PDU programs in the U.S. have used two catalyst stages. The two-stage liquefaction was found much more effective than the single stage. As mentioned earlier, all single-stage liquefaction processes have faced difficulties in converting subbituminous coal into soluble liquids, though they can handle bituminous coals satisfactorily.

3.3.8.1 HRI's CTSL Process

In 1982, Hydrocarbon Research, Inc. (currently, Hydrocarbon Technologies, Inc. (HTI), a division of Headwaters, Inc.) initiated the development of a catalytic two-stage concept, overcoming the drawbacks of H-coal, which is inherently a high-temperature catalytic process.[42] The first-stage temperature was lowered to 400°C to more closely balance hydrogenation and cracking rates and to allow the recycle solvent to be hydrogenated *in situ* to facilitate hydrogen transfer to coal dissolution. The second stage was operated at higher temperatures (435–440°C) to promote resid hydrocracking and generate an aromatic solvent, which is then hydrogenated in the first stage.[4] The lower first-stage temperature provides better overall management of hydrogen consumption and reduced hydrocarbon gas yields.[4,7] A schematic of this process is shown in Figure 3.15.[4]

The HRI's CTSL had three major changes in comparison to the H-coal process. The first was the two-stage processing; the second was incorporation of a pressure filter to reduce resid concentration in the reject stream (filter cake) below the 45–50% in the vacuum tower bottoms of the H-coal process; and the third change is in the catalyst itself. The H-coal process used a cobalt-molybdenum (CoMo)-on-alumina catalyst, American Cyanamid 1442 B, which had been effective in hydrocracking petroleum resids. In coal liquefaction, hydrogenation must occur first, followed by thermal cracking of hydroaromatics, whereas in petroleum applications the contrary is true. Therefore, the H-coal catalyst was found unsuitable due to its porosity distribution, which was designed for smaller molecules. For CSTL, the H-coal catalyst was replaced by a nickel-molybdenum (NiMo) catalyst of a bimodal pore distribution with

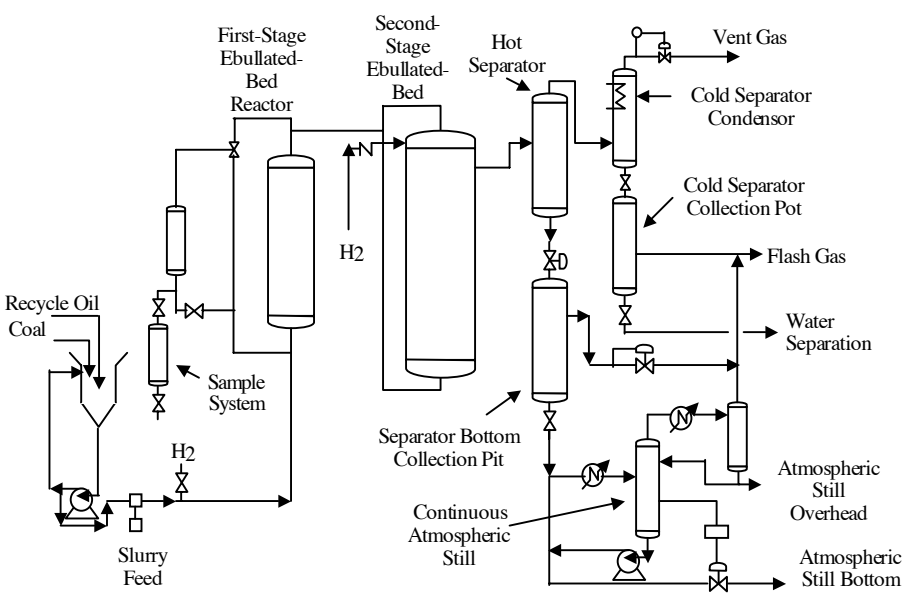

FIGURE 3.15 A schematic of HRI's CTSL.

TABLE 3.11
CTSL vs. H-Coal Demonstration Runs on Illinois No.6 Coal

	H-Coal	CSTL	
	PDU-5	(227-20)	(227-47)
Yields (wt% mmaf coal)			
C_1–C_3	11.3	6.6	8.6
C_4–390°F	22.3	18.2	19.7
390–650°F	20.5	32.6	36.0
650–975°F	8.2	16.4	22.2
975°F + Oil	20.8	12.6	2.7
Hydrogen consumption (wt% mmaf coal)	6.1	6.3	7.3
Coal conversion (wt% mmaf coal)	93.7	94.8	96.8
975°F+ conversion (wt% mmaf coal)	72.9	82.2	94.1
C_4-975°F (wt% mmaf coal)	51.0	67.2	77.9
Hydrogen efficiency	8.4	10.7	10.7
C_4 + distillate product quality			
EP (°F)	975	975	750
°API	26.4	23.5	27.6
% Hydrogen	10.63	11.19	11.73
% Nitrogen	0.49	0.33	0.25
% Sulfur	0.02	0.05	0.01
bbl/ton	3.3	4.1	5.0

Source: From Speight, J.G., *The Chemistry and Technology of Coal*, Marcel Dekker, New York, 1983.

larger micropores (115–125 Angstroms) as opposed to 60–70 Angstroms for the H-coal catalyst. The nickel promoter is also more active for hydrogenation than cobalt. Table 3.11 shows a comparison between H-coal and HRI CTSL.[4]

As shown in the table, the two-stage catalytic reaction produces a liquid with low heteroatom concentrations and a high H/C ratio, thus making the product closer to petroleum than other coal liquids made by earlier processes. Their later-version enhanced process is named the *HTI coal process*.[42] The modern version of this process uses HTI's proprietary GelCat™ catalyst, which is a dispersed, nano-scale, iron-based catalyst.[42]

3.3.8.2 Wilsonville CTSL

A second ebullated-bed reactor was added at the Wilsonville Advanced Coal Liquefaction Facility in 1985. Since then, the plant has been operated in the CTSL mode. As in ITSL, Wilsonville preferred to have most of the thermal cracking take place in the first reactor and solvent hydrogenation in the second reactor.[4] Therefore, the first reactor was at higher temperature (426–438°C), whereas the second reactor was kept lower at 404–424°C. A flow diagram of Wilsonville CTSL is shown in Figure

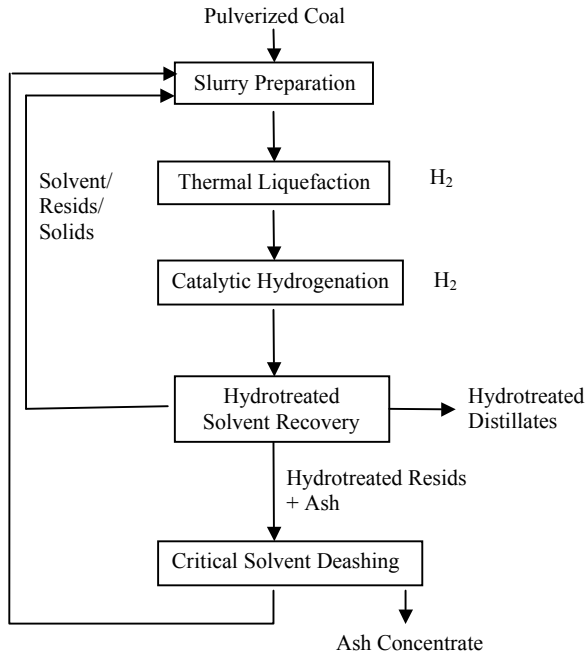

FIGURE 3.16 A flow diagram of CSTL with a solids recycle at Wilsonville.

3.16.[4] Run data of Wilsonville CTSL are summarized in Table 3.12. Distillate yields of up to 78% and reduced organic rejection to 8–15% were achieved at Wilsonville operating over 4 tons of coal per day.

3.3.9 Evolution of Liquefaction Technology

An extensive review by COLIRN (Coal Liquefaction Research Needs) panel assessment[4] was published by the DOE. Substantial technological innovations and enhancements have been realized for the last several decades of the 20th century, especially in the areas of process configurations and catalysts. Table 3.13 summarizes the history of process development improvements in the form of yields and distillate quality.[4,8]

Distillate yields have increased from 41 to 78%, resulting in equivalent liquid yields of about 5 bbl/ton of mmaf bituminous coal. The distillate quality was comparable to or better than No. 2 fuel oil with good hydrogen content and low heteroatom content.

3.4 INDIRECT LIQUEFACTION OF COAL

The indirect liquefaction of coal involves the production of synthesis gas mixture from coal as a first stage and the subsequent catalytic production of hydrocarbon fuels and oxygenates from the synthesis gas as a second stage. Indirect liquefaction can be classified into two principal areas[9]:

TABLE 3.12
CTSL Operation Data at Wilsonville Facility

Operating Conditions			
Run ID	253A	254G	251-IIIB
Configuration	CTSL	CTSL	CTSL
Coal	Illinois No.6	Ohio No. 6	Wyodak
Catalyst	Shell 317	Shell 317	Shell 324
First stage			
Average reactor temperature (°F)	810	811	826
Inlet hydrogen partial pressure (psi)	2040	2170	2510
Feed space velocity (lb/h/lb catalyst)	4.8	4.3	3.5
Pressure (psig)	2600	2730	2600
Catalyst age (lb resid/lb catalyst)	150–350	1003–1124	760–1040
Catalytic stage			
Average reactor temperature (°F)	760	790	719
Space velocity (lb feed/h/lb catalyst)	4.3	4.2	2.3
Catalyst age (lb resid/lb catalyst)	100–250	1166–1334	371–510
Yield (wt.% of mmaf Coal)			
C_1–C_3 gas	6	8	11
C_4+ distillate	70	78	60
Resid	~1	~1	2
Hydrogen consumption	6.8	6.9	7.7
Hydrogen efficiency			
lb C_4+ distillate/lb H_2 consumed	10.3	11.3	7.8
Distillate selectivity			
lb C_1–C_3/lb C_4+ distillate	0.08	0.11	0.18
Energy content of feed coal rejected to ash concentrate (%)	20	10	15

1. Conversion of syngas to light hydrocarbon fuels via Fischer–Tropsch synthesis (FTS).
2. Conversion of syngas to oxygenates such as methanol, higher alcohols, dimethylether (DME), and other ethers.

3.4.1 Fischer–Tropsch Synthesis (FTS) for Liquid Hydrocarbon Fuels

The FTS process is currently being operated commercially. The SASOL plant in South Africa has been in operation since 1956. A generalized flowsheet for the SASOL plant is shown in Figure 3.17.[44]

3.4.1.1 Reaction Mechanism and Chemistry

FTS follows a simple polymerization reaction mechanism, the monomer being a C_1-species derived from CO. This polymerization reaction follows a molecular-weight distribution (MWD) described mathematically by Anderson,[10] Schulz,[11] and Flory.[12]

TABLE 3.13
History of Liquefaction Process Development for Bituminous Coal

Process	Configuration	Distillate (wt% mmaf Coal)	Yield (bbl/ton mmaf Coal)	°API Gravity	Nonhydrocarbon (wt%)		
					S	O	N
SRC II (1982)	One-stage noncatalytic	41	2.4	12.3	0.33	2.33	1.0
H-Coal (1982)	One-stage catalytic	52	3.3	20.2[a]	0.20	1.0	0.50
RITSL, Wilsonville (1985)	Integrated two-stage, thermal–catalytic	62	3.8	20.2[b]	0.23	1.9	0.25
CTSL, Wilsonville (1986)	Integrated close-coupled two-stage catalytic–catalytic	70	4.5	26.8[b]	0.11	< 1	0.16
CTSL, Wilsonville (1987)	Integrated close-coupled two-stage low–ash coal	78	5.0	—[c]	—[c]	—[c]	—[c]
CTSL, HRI (1987)	Catalytic–catalytic	78	5.0	27.6	0.01	—	0.25

[a] Light product distribution, with over 30% of product in gasoline boiling range; less than heavy turbine fuel.

[b] Higher boiling point distribution, with 30% of product in gasoline fraction and over 40% in turbine fuel range.

[c] Data unavailable

Source: From Schindler, H.D., Coal Liquefaction — A Research and Development Needs Assessment, COLIRN Panel Assessment, DOE/ER-0400,UC-108, Final Report, Vol. II., March 1989.

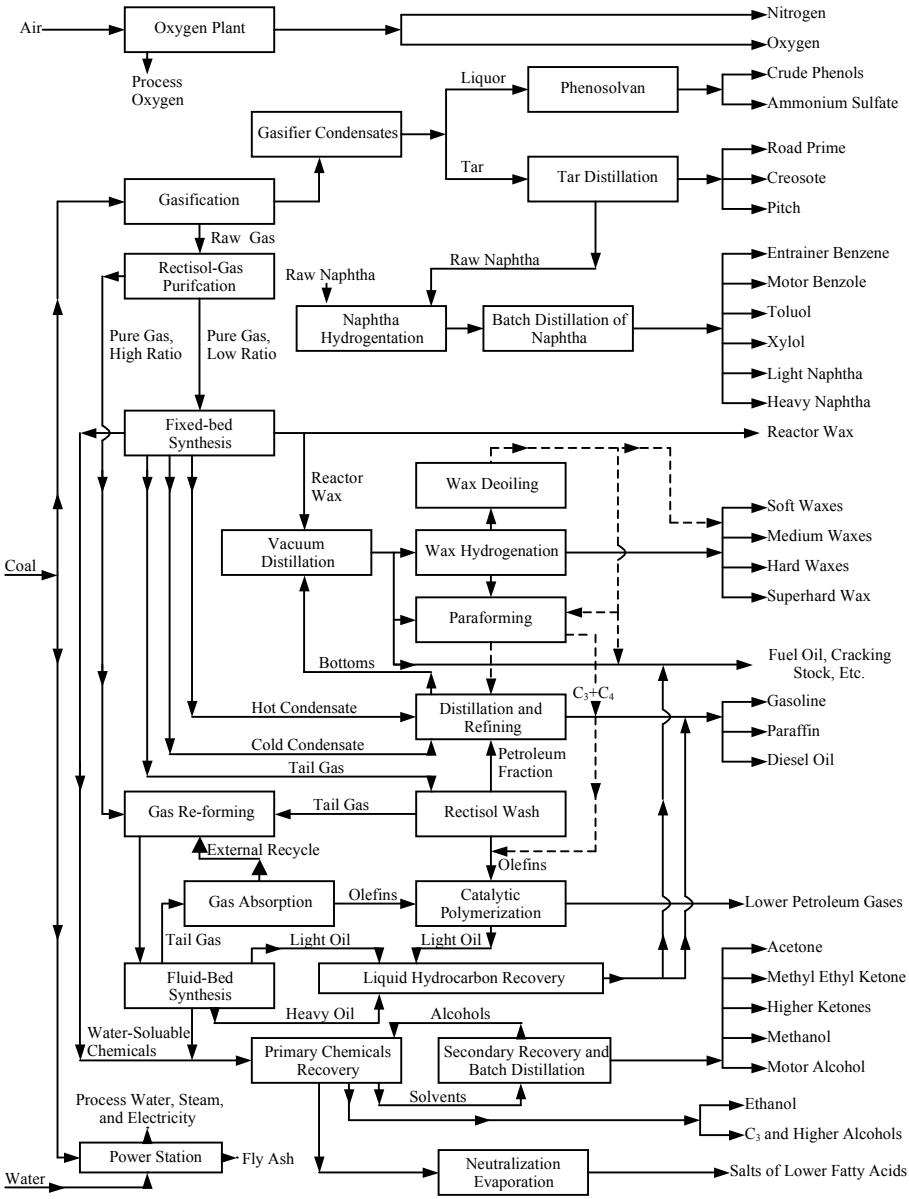

FIGURE 3.17 A generalized flowsheet for the SASOL plant. (From Hoogendorn, J.C. and Salomon, J.M., *Br. Chem. Eng.*, 2: 238, 1957. With permission.)

Recognizing these two independent groups' work, the description of the FTS product distribution is usually referred to as the Anderson–Schulz–Flory (ASF) distribution, which is generally accepted and frequently used. The ASF distribution equation is written as:

$$\log(w_n/n) = n \log x + \log[(1-x)^2/x]$$

where w_n, n, and x are the mass fraction, the carbon number, and the probability of chain growth, respectively. This equation can predict the maximum selectivity attainable by an FTS with an optimized process and catalyst, as shown in Table 3.14.

From a linear plot of log (w_n/n) versus n, the chain growth probability can be computed either from the slope (log x) or from the intercept, log $((1-x)^2/x)$. These predicted values are valid whether the products are hydrocarbons only (i.e., paraffins and olefins) or hydrocarbons plus alcohols (i.e., a mixture of paraffins, olefins, and alcohols).

3.4.1.2 Fischer–Tropsch Catalysis

According to the ASF equation, catalysts with a small value of x (i.e., a lower chain growth probability) produce a high fraction of methane. On the other hand, a large x value indicates the production of heavier hydrocarbons. The latest FTS processes aim at producing high-molecular-weight products and very little methane, and then cracking these high MW substances to yield lower hydrocarbons. There have been numerous attempts to surpass or exceed the ASF distribution so that one could produce liquid fuels in yields that exceed those predicted by the ASF equation.

Inexpensive iron catalysts are used for the FTS. These catalysts are prepared by fusing iron oxides such as millscale oxides. In practice, either an alkali salt or one or more nonreducible oxides are added to the catalyst.[4] A great deal of literature data are available; however, very few share the common grounds in their catalyst pretreatment, catalyst ingredients, catalyst preparation, and reactor design and configuration, making direct comparison of the results very difficult, if not impossible.

In FTS, removal of wax formed by the reaction is crucial as it can disable the catalytic activity. The SASOL plants furnish a major portion of South Africa's requirements for fuels and chemicals. Data on the existing SASOL plants are given in Table 3.15.

An approximate distribution of products from SASOL-2 operation is given in Table 3.16.[13]

TABLE 3.14
Maximum Selectivities Attainable by FTS

Product	Maximum Selectivity (wt%)
Methane	100
Ethylene	30
Light olefins (C_2-C_4)	50
Gasoline (C_5-C_{11})	48

Source: From Schindler, H.D., Coal Liquefaction — A Research and Development Needs Assessment, COLIRN Panel Assessment, DOE/ER-0400,UC-108, Final Report, Vol. II., March 1989.

TABLE 3.15
SASOL Plants

Plant	Location	Start Date	Coal t/d	Liquids bbl/d	Cost $ billion
SASOL-1	Sasolburg, S. Africa	1935	6,600	6,000	—
SASOL-2	Secunda, S. Africa	1981	30,000	40,000	2.9
SASOL-3	Secunda, S. Africa	1982	30,000	40,000	3.8

Source: From Schindler, H.D., Coal Liquefaction — A Research and Development Needs Assessment, COLIRN Panel Assessment, DOE/ER-0400,UC-108, Final Report, Vol. II., March 1989.

TABLE 3.16
Product Distribution of SASOL-2

Product	Tons/Year
Motor fuels	1,650,000
Ethylene	204,000
Chemicals	94,000
Tar products	204,000
Ammonia (as N)	110,000
Sulfur	99,000
Total saleable products	2,361,000

Source: From Wender, I., Review of Indirect Liquefaction, in Coal Liquefaction, USDOE Contract DE-AC01-87-ER 30110, Ed., Schindler, H.D. (Chairman of COLIRN), Final Report, March 1989.

3.4.1.3 Fischer–Tropsch Processes Other than SASOL

There have been a great number of publications and patents on other FTS catalysts, mainly cobalt, ruthenium, nickel, rhodium, and molybdenum. However, none of these has been commercially verified either by SASOL or by other efforts.

Modern gasifiers, as discussed in Chapter 2, produce syngas with low (0.6–0.7) H_2/CO ratios. Iron is known as a good water gas shift (WGS) catalyst, whereas neither cobalt nor ruthenium is active for the reaction. In the absence of water gas shift reaction, the oxygen in CO is rejected as water gas so that a syngas with an H_2/CO ratio of two is needed to produce olefins or alcohols.[13] For synthesis of paraffins, an H_2/CO ratio of larger than two is required. When water is formed in the FTS, it can react with CO to form more H_2 by the WGS reaction, so that syngas with a low H_2/CO ratio can still be used with these catalysts. This is the reason why the water gas shift reaction is very important in the FTS.

Recent efforts involve slurry Fischer–Tropsch (F-T) reactors. Mobil, in the 1980s, studied upgrading a total vaporous F-T reactor effluent over ZSM-5 catalyst. Shell,

in 1985, announced its SMDS (Shell Middle-Distillate Synthesis) process for the production of kerosene and gas oil from natural gas.[14] This two-stage process involves the production of long-chain hydrocarbon waxes and subsequent hydroconversion and fractionation into naphtha, kerosene, and gas oil. UOP characterized F-T wax and its potential for upgrading.[14] Dow has developed molybdenum catalysts with a sulfur tolerance up to about 20 ppm. The catalyst system is selective for the synthesis of C_2-C_4 hydrocarbons, especially when promoted with 0.5–4.0 wt% potassium.[13]

Using a precipitated iron catalyst, the slurry F-T reactor operating with a finely divided catalyst suspended in an oil reactor medium, has been shown to yield high single-pass syngas conversion with low H_2/CO ratios.[13–16] A great number of studies involving three-phase slurry reactors have been published. Development of F-T synthesis process has scientifically contributed to the design and analysis of multiphase reactor systems.

Most recently, China and South Africa announced a major collaborative project in indirect coal liquefaction.[43] Shenhua group, China's largest coal producer, and SASOL of South Africa are main entities involved in this venture. The new Chinese plants, once completed, would have a total annual production capacity of 60 million tons of oil.[43]

3.4.2 Conversion of Syngas to Methanol

The synthesis of methanol from syngas is a well-established technology. Because liquid hydrocarbon of methanol is synthesized from coal via syngas as an intermediate, the coal-to-methanol synthesis process is classified as an indirect coal liquefaction process. Synthesis gas is produced via gasification of coal, by biomass gasification, or via steam reforming of natural gas. Therefore, the profitability of a methanol plant is made on a case-by-case basis to account for location-specific factors such as energy resources, consumption infrastructure, environmental impact, and capital cost. Methanol plants exist where there are large reserves of competitively priced natural gas or coal, or where there are large captive uses for product methanol by neighboring chemical plants.

The advent of methanol synthesis has given a boost to the value of natural gas. Conventional steam reforming produces hydrogen-rich syngas at low pressure. However, this process is well suited to the addition of carbon dioxide, which utilizes the excess hydrogen and hence increases the methanol productivity.[17]

The global methanol demand increased about 8%/year from 1991 to 1995, then 3–4%/year over the next 10-year period following 1995. In 2005, the global demand for methanol amounted to about 32 million tons per year, with growth rates at or near GDP. Due to the decline and phaseout of MTBE in recent years, the regional demand for methanol has suffered in some countries, especially in North America and Europe. Nonetheless, the global demand of methanol is still expected to grow steadily at or near the GDP growth rate. Asia, especially China, will be the main driver for growth regarding the demand of methanol and its derivatives. Average growth rates for Asia are expected to be 3.8% for methanol, 4.8% for acetic acid, and 4.4% for formaldehyde.[39] The breakdown of the methanol demand is given in Table 3.17.[39] A detailed analysis of methanol market is published annually by Chemical Market Associates,

TABLE 3.17
Methanol Demand by Chemicals and End Uses

Chemicals and End Uses	%
Formaldehyde	36
Methyl t-butyl ether (MTBE)	25
Acetic acid	11
Solvents	4
Methyl methacrylate (MMA)	3
Gas and fuels	3
Dimethyl terephthalate (DMT)	2
Others (manufacturing other chemicals)	16
Total	100

Source: From a Web site by Lurgi on Methanol market and Technology, 2006; accessible through http://www.lurgi.de/lurgi_headoffice_kopie/english/nbsp/menu/products/gas_to_petrochemicals_and_fuels/methanol/markets/index.html. With permission.

Inc. (CMAI).[40] This report provides information on supply, demand, production, history, and forecasts for methanol capacity, trade, and pricing.

All industrially produced methanol is made by the catalytic conversion of synthesis gas containing carbon monoxide, carbon dioxide, and hydrogen as the main components. Modern commercial methanol processes can be classified into vapor-phase low-pressure synthesis and liquid-phase low-pressure synthesis.[17,18,20] The former is more conventional and dominates in the current marketplace. This low-pressure vapor-phase process replaced its earlier version of high-pressure technology and is more suited for H_2 -rich synthesis gas of typical H_2/CO ratio ranging between 2 and 3.[17,19] The latter technology of liquid-phase synthesis is more recent in its development and more suitable for CO-rich synthesis gas of the typical H_2/CO ratio ranging from 0.6 to 0.9. As discussed in Chapter 2, CO-rich syngas is produced typically by modern coal gasifiers.

Methanol productivity can be enhanced by synthesis gas enrichment with additional carbon dioxide to a certain limit.[17] There is an optimal concentration of carbon dioxide, which is dependent upon the process type (vapor phase vs. liquid phase), synthesis gas feed compositions, and operating temperature and pressure conditions. However, if too much CO_2 is present in the syngas, it accelerates catalyst deactivation, shortens its lifetime, and produces water, which adversely affects the catalyst matrix stability resulting in crystallite growth via hydrothermal synthesis phenomena.[17] Although this statement is generally true for vapor phase synthesis of methanol, it was also found that a high concentration of CO_2 helps the catalyst structural stability by formation of $ZnCO_3$ on the original $Cu/ZnO/Al_2O_3$ catalyst. As a different approach, a special catalyst has also been designed to operate under high CO_2 conditions. The catalyst's crystallites are located on energetic stable sites that lower the tendency to migrate. This stability also minimizes the influence of water formed on the catalyst matrix, which is only slightly affected. This catalyst preserves its

higher activity due to a lower deactivation rate over long-term operations.[17] The basic reactions involved in methanol synthesis are:

$$CO_2 + 3H_2 = CH_3OH + H_2O \qquad \Delta H°_{298} = 52.81 \text{ kJ/mol} \qquad (3.1)$$

$$CO + 2H_2 = CH_3OH \qquad \Delta H°_{298} = 94.08 \text{ kJ/mol} \qquad (3.2)$$

$$CO + H_2O = CO_2 + H_2 \qquad \Delta H°_{298} = 41.27 \text{ kJ/mol} \qquad (3.3)$$

Of the three reactions, only two are stoichiometrically independent. In other words, material balance of the above reaction system would only require any two of the three stoichiometric equations. The chemical mechanism of the methanol synthesis over the $Cu/ZnO/Al_2O_3$ catalyst has been somewhat controversial.[13,15,17] The controversy involved whether the synthesis of methanol over the $Cu/ZnO/Al_2O_3$ goes predominantly via CO_2 hydrogenation (Equation 3.1) or via CO hydrogenation (Equation 3.2). Along with the synthesis reaction, the second companion reaction was automatically in the middle of the controversy. In this case, the controversy was whether water gas shift reaction proceeds forward or backward under normal synthesis conditions over the very same catalyst. However, more experimental evidences point toward the theory that methanol synthesis over the $Cu/ZnO/Al_2O_3$ proceeds predominantly via the CO_2 hydrogenation and the forward water gas shift reaction,[14,17,18,21,22] as:

$$CO_2 + 3H_2 = CH_3OH + H_2O$$

$$CO + H_2O = CO_2 + H_2$$

More detailed discussions on the methanol synthesis technology are available in Chapter 9.

3.4.3 Conversion of Methanol to Gasoline or Target Hydrocarbons

Methanol itself can be used as a transportation fuel just as liquefied petroleum gas (LPG) and ethanol. However, direct use of methanol as a motor fuel in passenger vehicles would require nontrivial engine modifications and substantial changes in the lubrication system. Even though methanol has a high octane rating and is by molecular formula an excellent candidate of oxygenated hydrocarbon, its use as gasoline blending chemical is also limited due to its high Reid vapor pressure (RVP) that is a measure of affected volatility of blended gasoline. This is one of the reasons why the conversion of methanol to gasoline is quite appealing.[23,24]

The Mobil Research and Development Corporation developed the methanol-to-gasoline (MTG) process. The process technology is based on the catalytic reactions using the zeolites of the ZSM-5 class.[25,26] MTG reactions can be written as:

$$n\ CH_3OH \rightarrow (\ -CH_2-\ )_n + nH_2O$$

The detailed reaction path is described in Reference 26. The following simplified steps describe the overall reaction path:

$$2CH_3OH = (CH_3)_2O + H_2O$$
$$(CH_3)_2O \rightarrow \text{light olefins} + H_2O$$
$$\text{light olefins} \rightarrow \text{heavy olefins}$$
$$\text{heavy olefins} \rightarrow \text{paraffins}$$
$$\text{aromatics}$$
$$\text{naphthenes}$$

The MTG reactions are exothermic and go through the dimethylether (DME) intermediate route. As shown, the conversion of methanol to dimethylether is via dehydration process.

Based on the shape-selective pore structure of the ZSM-5 class catalysts, the product hydrocarbons can be tailor-made to fall predominantly in the gasoline boiling range. The product distributions are influenced by the temperature, pressure, the space velocity, the reactor type, and Si /Al ratio of the catalyst.[27] Paraffins are dominated by isoparaffins, whereas aromatics are dominated by highly methyl-substituted aromatics. C_9^+ aromatics are dominated by symmetrically methylated isomers, reflecting the shape selective nature of the catalyst. The C_{10} aromatics are mostly durene (1,2,4,5- tetramethylbenzene), which has an excellent octane number but the freezing point is very high at 79°C. Too high a durene content in the gasoline may impair automobile driving characteristics, especially in cold weather, due to its tendency to crystallize at a low temperature.[9] Mobil's test found no drivability loss at minus 18°C using a synthetic gasoline containing 4 wt% of durene.[9] Mobil also developed a heavy gasoline treating (HGT) process to convert durene into other high-quality gasoline components by isomerization and alkylation.[27]

Basically, three types of chemical reactors were developed for the MTG process: (1) adiabatic fixed bed, (2) fluidized bed, and (3) direct heat exchange. The first two were developed by Mobil and the last by Lurgi.

The adiabatic fixed-bed concept uses a two-stage concept, viz., (1) the first stage DME reactor and (2) the second stage DME conversion to hydrocarbons. The first commercial plant of 14,500 bbl/d gasoline capacity was constructed in New Zealand. The plant had been running successfully from its 1985 start-up until its recent shutdown. The synthesis gas is generated via steam reforming of natural gas obtained from the offshore Maui fields. This plant was also successfully run in New Zealand and reduced the durene content to 2 wt%. The successful operation of MTG in New Zealand was a very important milestone in history, as it made possible the chemical synthesis of gasoline from unlikely fossil fuel sources like natural gas and coal. Petroleum crude is no longer the sole source for gasoline. Although the plant for methanol-to-gasoline in New Zealand ceased its operation in the late 1990s, a major plant complex for methanol-to-olefins is being planned in Nigeria for 2009 operation.[40]

TABLE 3.18
Typical Process Conditions and Product Yields for the MTG Process

Conditions	Fixed Bed Reactor	Fluid Bed Reactor
Methanol/water charge (w/w)	83/17	83/17
Dehydration reactor inlet T (°C)	316	—
Dehydration reactor outlet T (°C)	404	—
Conversion reactor inlet T (°C)	360	413
Conversion reactor outlet T (°C)	415	413
P (kPa)	2170	275
Recycle ratio (mol/mol charge)	9.0	—
Space velocity (WHSV)	2.0	1.0
Yields (wt% of MeOH charged)		
MeOH + dimethyl ether	0.0	0.2
HCs	43.4	43.5
Water	56.0	56.0
CO, CO_2	0.4	0.1
Coke, other	0.2	0.2
Total	**100.0**	**100.0**
Hydrocarbon product (wt%)		
Light gas	1.4	5.6
Propane	5.5	5.9
Propylene	0.2	5.0
Isobutane	8.6	14.5
n-Butane	3.3	1.7
Butenes	1.1	7.3
C_5+ Gasoline	79.9	60.0
Total	**100.0**	**100.0**
Gasoline (including alkylate), RVP-62kPa (9 psi)	85.0	88.0
LPG	13.6	6.4
Fuel gas	1.4	5.6
Total	**100.0**	**100.0**
Gasoline octane number (RON)	93	97

Source: From U.S. DOE Working Group on Research Needs for Advanced Coal Gasification Techniques (COGARN) (S.S. Penner, Chairman), Coal Gasification: Direct Application and Synthesis of Chemicals and Fuels, DOE Contract No. DE-AC01-85 ER30076, DOE Report DE/ER-0326, June 1987.

A fluidized bed MTG concept was concurrently developed by Mobil. The heat of reaction can be removed from the reactor either directly using a cooling coil or indirectly using an external catalyst cooler. The process research went through several stages involving a bench-scale fixed fluidized bed, 4 bpd, 100 bpd cold-flow models, and a 100 bpd semiwork plant. Table 3.18 shows typical MTG process conditions and product yields.[9]

During the MTG development, Mobil researchers found that the hydrocarbon product distribution can be shifted to light olefins by increasing the space velocity, decreasing the methanol partial pressure, and increasing the reaction temperature.[28] Typical yields[9] from 4 bpd operation were: C_1-C_3 paraffins, 4 wt%; C_4 paraffins, 4 wt%; C_2–C_4 olefins, 56 wt%; and C_5^+ gasoline, 35 wt%. Using olefins from the methanol-to-olefins (MTO) or F-T processes, diesel and gasoline can be made via a process converting olefins to diesel and gasoline. Using acid catalysts, catalytic polymerization is a standard process and is being used at SASOL to convert C_3-C_4 olefins into gasoline and diesel (G+D). Recently, Mobil developed an olefins-to-gasoline-and-diesel (MOGD) process using their commercial zeolite catalyst.[29,30] Lurgi also developed its own version of the methanol-to-propylene (MTP) process.[4]

Recently, an innovative process enhancement has been made by Lee and coworkers under the sponsorship of the Electric Power Research Institute (EPRI).[31] Their process, called the DTG (DTH, DTO) process, is based on the conversion of dimethylether (DME) to hydrocarbon over ZSM-5 type catalyst.[31,32] This process is based on the novel, economical, single-stage synthesis process of dimethylether (DME) from syngas, which produces methanol as an intermediate for dimethylether. By producing DME in a single stage, the intermediate methanol formation is no longer limited by chemical equilibrium, thus increasing the reactor productivity, in terms of total hydrogenation extent, substantially. This is especially true for the synthesis of methanol in the liquid phase. Furthermore, by feeding DME directly to the ZSM-5 reactor instead of methanol, the stoichiometric conversion and hydrocarbon selectivity increase substantially due to less water formation and involvement. The difference between MTG and DTG, therefore, is in the placement of methanol dehydration reaction step (i.e., DME formation reaction). In the MTG, methanol-to-DME conversion takes place in the gasoline reactor, whereas methanol-to-DME conversion, in the DTG, takes place in the syngas reactor. Therefore, methanol is an intermediate of the syngas conversion reactor for DTG, whereas DME is an intermediate for gasoline synthesis reactor for MTG. The DTG process is not yet tested on a large scale.

The Topsoe Integrated Gasoline Synthesis Process (TIGAS) uses combined steam reforming and autothermal reforming for syngas production with a multifunctional catalyst system to produce an oxygenates mixture rather than methanol.[13]

3.4.4 Higher Alcohol Synthesis

Mixtures of C_1-C_6 alcohols can be used as transportation fuels either as is or as an additive to gasoline. In the U.S., however, selling new unleaded fuels or fuel additives in unleaded fuels has been prohibited by the Clean Air Act. Exceptions have been granted in the form of EPA waivers, and good examples have been the waivers granted to requests by DuPont, ARCO, SUN, and American Methyl in the late 1970s through the mid-1980s. Some of the more significant ones that are still impacting the current fuel market in the U.S. are related to the MTBE blending and the use of 10% ethanol in gasoline. Due to the public health and environmental problems cited in a number of states in the U.S. and Europe, MTBE is going to be phased out completely in these countries by 2007.

Technical advantages of using C_1-C_6 alcohol blends with gasoline can be summarized as:

1. Enhancement of octane number
2. Enhancement in hydrocarbon solubility in comparison to methanol-gasoline blends
3. Enhanced water tolerance compared to unblended gasoline
4. Enhanced control of fuel volatility

Despite some obvious technological benefits, certain EPA restrictions, especially volatility specifications (evaporative index [EI] or Reid vapor pressure [RVP]), have imposed serious economic penalties on alcohol blends (except ethanol), thus making them difficult to be accepted by refiners and blenders. Fuels containing higher alcohol blends have been in use in Germany at ca. 3–5 mol% for automobile transportation.

Higher alcohol synthesis (HAS) has been practiced in Germany since 1913 after BASF successfully developed cobalt- or osmium-catalyzed synthesis of a mixture of alcohols and other oxygenates at 10–20 MPa and 300–400°C.[4] This was followed by the F-T Synthol process for alcohol mixtures in 1923–1924. It was also found that higher alcohols were coproducts of methanol synthesis over ZnO/Cr_2O_3 catalysts, alkalized ZnO/Cr_2O_3 catalysts, and alkalized Cu-based catalysts. Later, the Synthol process was further developed and enhanced to a process at a lower temperature of <200°C, medium pressure of 20 MPa, and inexpensive but potent iron catalysts. Later, the process incorporated several additional reactor stages with intermediate CO_2 removal and gas recycle.[33] In 1984, Dow Chemical Co. announced a new process for higher alcohol synthesis based on MoS_2 catalysis, and Union Carbide Corporation also revealed a new process.[4] [The two companies merged in 2000 for unrelated business reasons.] The Dow Chemical process is also known as Dow HAS. On the other hand, the technology for higher alcohol based on alkali-promoted ZnO/Cr_2O_3 methanol synthesis catalysts for the high-pressure methanol synthesis was further developed by Snamprogetti, Enichem, and Haldor Topsoe A/S (SEHT). This is often referred to as the SEHT HAS process.

3.5 COAL AND OIL COPROCESSING

Coprocessing is defined as the simultaneous reaction treatment of coal and petroleum resid, or crude oil, with hydrogen to produce distillable liquids. More strictly speaking, this technology should be classified under direct liquefaction as a variation. Petroleum liquids have been often used as a liquefaction solvent, mainly for start-up or whenever coal-derived liquids were unavailable. However, some serious considerations have been recently given to the processing possibilities of hydrocracking petroleum resid while liquefying coal in the same reactor. In this sense, coprocessing has an ultimate objective of cobeneficiation.

An early coprocessing patent was granted to UOP, Inc. in 1972 for a process whereby coal is solvent extracted with petroleum.[34] Another early patent on coprocessing was issued to Hydrocarbon Research, Inc. (HRI) in 1977 for the single-stage ebullated-bed COIL process based on the HRI's H-Oil and H-Coal technology.[35]

Consol R & D tested the use of a South Texas heavy oil for coal hydroextraction but found that, even after hydrogenation, the petroleum made a very poor liquefaction solvent.[9] The Canada Centre for Mineral and Energy Technology (CANMET) developed the CANMET hydrocracking process for petroleum resids. They found that small additions of coal (<5 wt%) to the petroleum feedstock significantly improved distillate product yields. A 5000 bpd plant using this process was started up in 1985 by Petro-Canada near Montreal, Quebec.[36,37]

In summary, coprocessing has several potential economic and technological advantages relative to coal liquefaction or hydroprocessing of heavy petroleum residua. Synergisms and cobeneficiating effects can be obtained, especially in the area of: (1) replacement of recycle oil, (2) sharing hydrogen between hydrogen-rich and hydrogen-deficient materials, (3) aromaticity of the product, (4) demetalation and catalyst life extension, and (5) overall energy efficiency.[37] For the current technology, temperatures of 400–440°C, 2000 psig hydrogen pressure, and alumina-supported cobalt, molybdenum, nickel, or disposable iron catalysts are frequently used. Various efforts in developing more selective and resilient catalysts are being executed.

REFERENCES

1. Speight, J.G., *The Chemistry and Technology of Coal* (Rev. Ed.), Marcel Dekker, New York, 1994.
2. Probstein, R.F. and Hicks, R.E., *Synthetic Fuels*, McGraw-Hill, New York, 1982.
3. Carlson, F.B., Yardumian, L.H., and Atwood, M.T., Reprints of Clean Fuels from Coal II Symposium, Institute of Gas Technology, Chicago, IL, 1975, p. 504.
4. Schindler, H.D., Coal Liquefaction — A Research and Development Needs Assessment, COLIRN Panel Assessment, DOE/ER-0400,UC-108, Final Report, Vol. II., March 1989.
5. Potts, J.D., Hastings, K.E., Chillingworth, R.S., and Unger, K., Expanded-Bed Hydroprocessing of Solvent Refined Coal (SRC) Extract, Interim Technical Report FE-2038-42, February 1980.
6. Schindler, H.D., Chen, J.M., and Potts, J.D., Integrated Two-Stage Liquefaction, Final Tech. Report, DOE Contract DE-AC22-79 ET14804, June 1993.
7. Comolli, A.G. and McLean, J.B., The Low-Severity Catalytic Liquefaction of Illinois No. 6 and Wyodak coals, Pittsburgh Coal Conference, Pittsburgh, PA, September 16–20, 1985.
8. Weber, W. and Stewart, N., *EPRI Monthly Review*, January 1987.
9. U.S. DOE Working Roup on Research Needs for Advanced Coal Gasification Techniques (COGARN) (S.S. Penner, Chairman), Coal Gasification: Direct Application and Synthesis of Chemicals and Fuels, DOE Contract No. DE-AC01-85 ER30076, DOE Report DE/ER-0326, June 1987.
10. Anderson, R.B., *The Fischer-Tropsch Synthesis*, Academic Press, Orlando, FL, 1984.
11. Schulz, G.V., *Z. Phys. Chem.,* 32, 27, 1936.
12. Flory, P.J., *J. Am. Chem. Soc*., 58, 1877, 1936.
13. Wender, I., Review of Indirect Liquefaction, in Coal Liquefaction, USDOE Contract DE-AC01-87-ER 30110, Schindler, H.D., Ed., (Chairman of COLIRN), Final Report, March 1989.

14. van der Burgt, M.J., The Shell Middle Distillate Synthesis Process, the 5th Synfuels Worldwide Symposium, Washington, D.C., McGraw-Hill, New York, November 1985.
15. Humbach, J. and Schoonover, N.W., Proc. Ind. Liquefaction Contractor's Meeting, Pittsburgh, PA, PETC, 1985, pp. 29–38.
16. Koelbel, H. and Ralek, M., *Catal. Rev.: Sci. Eng.*, 21, 225, 1980.
17. Lee, S., *Methanol Synthesis Technology*, CRC Press, Boca Raton, FL, 1990.
18. Cybulski, A., *Catal. Rev.: Sci. Eng.*, 36(4), 557–615, 1994.
19. Oxturk, S. and Shah, Y., Comparison of gas and liquid methanol synthesis process, *Chem. Eng. J.*, 37, 177–192, 1988.
20. Lee, S., Research Support for Liquid Phase Methanol Synthesis Process Development, EPRI Report AP-4429, Palo Alto, CA, February 1986, pp. 1–312.
21. Chanchlanii, K., Hudgins, R., and Silveston, P., Methanol synthesis from H_2, CO, and CO_2 over Cu/ZnO catalysts, *J. Catal.*, 136, 59–75, 1992.
22. Sizek, G., Curry-Hyde, H., and Wainwright, M., Methanol synthesis over ZnO promoted copper surfaces, *Appl. Catal. Gen.*, 115, 15–28, 1994.
23. Mills, G.A., *Fuel*, 73(8), 1243–1279, 1994.
24. Fox, J.M., *Catal. Rev.: Sci. Eng.*, 35(20), 169–212, 1993.
25. Chang, C.D., *Catal. Rev.: Sci. Eng.*, 25, 1, 1983.
26. Chang, C.D. and Silvestri, A.J., *J. Catal.*, 47, 249, 1977.
27. Chang, C.D. and Silvestri, A.J., The MTG Process: Origin and Evolution, presented at the 21st State-of-the-Art ACS Symposium on Methanol as a Raw Material for Fuels and Chemicals, Marco Island, FL, June 1986, pp. 115–18.
28. Socha, R.F., Chu, C.T.W., and Avidan, A.A., An Overview of Methanol-to-Olefins Research at Mobil: from Conception to Demonstration Plant, presented at the 21st State-of-the-Art ACS Symposium on Methanol as a Raw Material for Fuels and Chemicals, Marco Island, FL, June 1986, pp. 115–18.
29. Tabak, S.A., Avidan, A.A., and Krambeck, F.J., MTO-MOGD Process, presented at the 21st State-of-the-Art ACS Symposium on Methanol as a Raw Material for Fuels and Chemicals, Marco Island, FL, June 1986, pp. 115–118.
30. Tabak, S.A. and Krambeck, F.J., *Hydrocarbon Process.*, 64, 72, September 1985.
31. Lee, S., Gogate, M.R., Fullerton, K.L., and Kulik, C.J., U.S. Patent No. 5,459,166, October 17, 1995.
32. Lee, S., Gogate, M.R., and Kulik, C.J., *Fuel Sci. Technol. Int.*, 13(8), 1039–1058, 1995.
33. Xiaoding, X., Doesburg, E.B.M., and Scholten, J.J.F., *Catalysis Today*, Vol. 2, 1987, pp. 125–170.
34. Gatsis, J.G., U.S. Patent No. 3,705,092, December 5, 1972.
35. Chervenak, M.C. and Johanson, E.S., U.S. Patent No. 4,054,504, October 18, 1977.
36. Kelly, J.F. and Fouda, S.A., CANMET Coprocessing: An Extension of Coal Liquefaction and Heavy Oil Hydrocracking Technology, presented at the DOE Direct Liquefaction Contractors' Review Meeting, Albuquerque, NM, October 1984.
37. Lee, S., *Alternative Fuels*, Taylor & Francis, Philadelphia, PA, 1997.
38. Lee, S., *Oil Shale Technology*, CRC Press, Boca Raton, FL, 1991.
39. A Web site by Lurgi on Methanol market and Technology, 2006; accessible through http://www.lurgi.de/lurgi_headoffice_kopie/english/nbsp/menu/products/gas_to_petrochemicals_and_fuels/methanol/markets/index.html.
40. Chemical Market Associates, Inc., 2006 World Methanol Analysis, CMAI, Houston, TX, 2006.
41. *USA Today*, July 14, 2006.

42. A Web site by Hydrocarbon Technologies Inc., HTI Direct Coal Liquefaction Technology, 2006; accessible through http://www.htigrp.com/data/upfiles/pdf/DCL%20Technology%2023Feb05.pdf.
43. Silverstein, K., Coal Liquefaction Plants Spark Hope, Daily Issue Alert, November 1, 2004; accessible through http://www.utilipoint.com/issuealert/article.asp?id=2314.
44. Hoogendom, J.C. and Salomon, J.M., *Br. Chem. Eng.,* 2:238, 1957.

4 Coal Slurry Fuel

Sunggyu Lee

CONTENTS

4.1 INTRODUCTION

Coal slurry fuels consist of finely ground coal dispersed into one or more liquids such as water, oil, or methanol. Slurry fuels have the advantages of being convenient to handle (similar to heavy fuel oil) as liquid fuel and processing high energy density, as illustrated in Table 4.1.[1,2] Coal slurries have been investigated as potentially efficient replacement for oil in boilers and furnaces, fuel in internal combustion engines, and recently energy feedstock for cofiring of coal fines in utility boilers. Coal slurry is used around the world in countries such as the U.S., Russia, Japan, China, and Italy.

Coal slurry fuels have been investigated since the 19th century, but economic constraints have kept it from becoming a major energy source. Typically, interest in coal slurry develops whenever regional or short-term oil availability is in doubt, such as periods during both world wars and again in the energy crises of 1973 and 1979.[3] Much of the work during these time periods was focused on coal-oil fuels, which could quickly and readily replace oil or liquid fuel in furnaces and boilers. However, recent research, since 1980, has concentrated more on coal-water slurry fuels (CWSFs) for the complete replacement of oil in industrial steam boilers, utility boilers, blast furnaces, process kilns, and diesel engines.[4,34]

TABLE 4.1
Fuel Energy Densities

Fuel	Density (lb/gal)	Btu/lb	Btu/gal	Btu/ft^3
Coal in bulk (7% moisture)	6.2–9.4	12,500	76,000–116,500	573,000–872,000
Residual oil	8.2	18,263	150,000	1,122,000
60% Coal/40% water blend	9.8	8,000	78,700	589,000
70% Coal/30% water blend	10.2	9,373	95,600	715,000

Source: From Kesavan, S., Stabilization of Coal Particle Suspensions using Coal Liquids, M.S. thesis, University of Akron, 1985. With permission.

The initial development of coal slurry was noted over a hundred years ago by Smith and Munsell.[5] By World War I, a full-scale slurry test was successfully made on a U.S. Navy Scout ship. The test revealed some technical problems such as high ash content (of raw material coal), visible fluid track left in the ship's wake, and stability problems with the slurry (such as settling and sedimentation).[6]

In the 1930s, the Cunard ship company used coal-oil slurries on both land and sea trials in an attempt to reduce oil imports and further develop new markets for coal.[7–9] At about the same time in Japan, tests were conducted on coal-in-oil fuels at their National Fuel Laboratory.[10] Similar tests were also performed in Germany on a mixture of powdered coal (55 wt%) and tar oil (45 wt%) called "Fliesskhloe." The German tests showed that the coal-oil mixture burned well and had thermal efficiencies of 70–75%.[11] Although the systems worked well from technological standpoints, economic limitations hindered further development.

Development during the Second World War consisted of two comprehensive programs at the Bureau of Mines and Kansas State College. The programs explored methods of preparation, flow, stability, and burning processes of coal-oil slurry.[6] After the war, development on coal-oil slurries ceased until the 1970s. On the other hand, work on coal-water fuels started in the USSR in the 1950s,[12,13] and similar work was conducted in the U.S. and Germany on storage, pumping, and combustion properties.[14]

The energy crisis of 1973 again propelled research and development of coal-oil slurry. A consortium of companies led by General Motors (GM) was formed in 1973 to develop the technology.[15] In 1975, the Department of Energy (DOE) joined support of the project, and by 1976 the program had expanded into switching utility gas and oil boilers to coal-oil mixtures. The initial comprehensive investigations were completed in 1977, and the DOE transferred GM projects to places such as New England Power and Service Co. (NEPSCO) and Pittsburgh Energy Technology Center (PETC).[6]

However, recent research, since 1980, has centered on coal-water slurry fuels for replacement of oil.[4,75] The economic incentive for replacing oil with coal-oil slurries disappeared as oil prices stabilized in 1980s and 1990s. This spurred development of coal-water slurries for complete replacement of oil or coburning of coal fines in a slurry. Record-high oil prices in the 21st century will rekindle interest in coal slurry fuel as a potential transportation fuel and as an alternative fuel for diverse

applications. A significant amount of development has been accomplished on coal slurry rheology, characterization, atomization, combustion mechanisms, and transport techniques.[34]

4.2 COAL SLURRY CHARACTERIZATION

Coal-slurry mixtures can be made from a combination of various liquids, the most common liquid ingredients being oil, water, and methanol. Detailed descriptions for various types of coal slurries are as follows:

1. *Coal-Oil Mixtures (COM)*: a suspension of coal in fuel oil, also referred to as coal-oil dispersions (COD).
2. *Coal-Oil-Water (COW)*: a suspension of coal in fuel oil with less than 10 wt% water in which oil is the main ingredient.
3. *Coal-Water-Oil (CWO)*: a suspension of coal in fuel oil with more than 10 wt% water in which water is the main ingredient.
4. *Coal-Water Fuels (CWF), Coal-Water Mixtures (CWM), Coal-Water Slurries (CWS), or Coal-Water Slurry Fuels (CWSF)*: a suspension of coal in water.
5. *Coal-Methanol Fuel (CMF)*: a suspension of coal in methanol.
6. *Coal-Methanol-Water (CMW)*: a suspension of coal in methanol and water.

The CMF and CMW slurries possess favorable properties; however, the cost of methanol has all but eliminated them from further development. COM, once actively investigated, has now been shelved for economic reasons. CWF has been investigated for complete oil replacement in boilers and furnaces and internal combustion engines, but low oil prices in the past decades have reduced the economic advantage and somewhat cooled the interest. However, CWF developed from waste streams and tailings were being investigated for cofiring in boilers and furnaces.[16] The comparative economics of coal-water slurry against the conventional fuel in the 21st century is undoubtedly far more favorable.[34] Furthermore, CWF provides a valuable mode of coal transportation through a long pipeline.

Important slurry characteristics are stability, pumping, atomizability, and combustion characteristics. These properties control the hydrodynamics and rheology of the coal slurry system. A coal slurry must have low viscosity at pumping shear rates (10–200 sec^1) and at atomization shear rates (5,000–30,000 sec^1). This allows for low pumping power requirements and increased boiler and furnace efficiencies through smaller droplets sizes.[17] There are several types of pumps that are developed for coal slurry pumping.

In order to understand coal slurry hydrodynamics and rheology, an understanding of dispersed systems is required. Solid-liquid dispersed systems are classified into two, based on their particle sizes, namely, *colloidal* and *coarse-particle* systems. Colloidal dispersed systems consist of particles smaller than 1 μm and coarse particle dispersion systems (suspension) consist of particles larger than 1 μm. In colloidal dispersion systems, sedimentation is prevented by Brownian motion (thermal activity). However, suspensions are thermodynamically unstable and will tend to precipitate owing to the overwhelming gravitational force on large-size particles.

4.2.1 Particle Size Distribution

Typical coal slurry fuels have a particle size distribution (PSD) with 10–80% of the particles smaller than 74 μm (-200 mesh). Micronized CWF has a PSD with a mean particle diameter of less than 15 μm and 98% of the particles are smaller than 44 μm (-325 mesh). This type of slurry is typically produced by coal beneficiation systems in the removal of mineral matter, mainly pyrites (FeS_2) and ash.

The sizing of coal is a multistep process consisting of coal crushing, pulverization, and finishing steps. Finishing steps encompass coarse, fine, and ultrafine crushing of coal. Coal crushing reduces the coal size to 20–7.6 cm and 5–3.2 cm, depending on the application, and coarse pulverization further reduces the coal size to <3.2 mm. The finishing processes can be carried out by wet or dry grinding. They reduce the particle size to <1 mm for coarse, <250 μm for fine, and <44 μm for ultrafine grinding. In slurry preparation, wet grinding is often used to minimize oxidation of the coal, which is normally detrimental to many beneficiation or treatment processes.

Coal slurries are most economical when they have the maximum amount of coal (i.e., highest solid loading) at the lowest possible viscosity. To obtain the highest possible loading, a bimodal or multimodal PSD is utilized, as shown in Figure 4.1.[2] The finer coal particles fit into the interstices of the larger coal particles, forming a higher concentrated network of particles. These particles may also act as a lubricant, leading to a lower viscosity.[18] A unimodal slurry has a peak solid loading of ~65% at which time the viscosity becomes infinite, whereas idealized multimodal systems offer a theoretically possible loading in excess of 80%, as shown in Figure 4.2.[19] The lowest viscosity of a coal-water mixture occurs at a fine-to-coarse ratio of 35 ± 5:65 ± 5, regardless of the ratio of the mean diameters.[18] Multimodal systems are commonly used, because they can easily be generated by a common grinding scheme. A typical multimodal distribution formulated for minimum viscosity is shown in Figure 4.3.[19]

The settling of coal particles is a complex phenomenon from a theoretical point of view, involving hydrodynamic and physiochemical forces. The falling movement of fine coal in slurries has a Reynolds number (Re) <<1, which leads to the use of *Stokes' equation* for hindered settling rate as shown in Equation 4.1 and Equation 4.2.[3]

$$v = \frac{d^2 g(\rho_1 - \rho_2)}{18\mu} f(\phi) \tag{4.1}$$

$$f(\phi) = \frac{v}{v_t} \leq 1 \tag{4.2}$$

where

v = hindered settling rate
v_t = single-particle settling velocity
μ = viscosity of dispersing medium
ρ_1 = density of dispersed medium
ρ_2 = density of dispersing medium
d = diameter of dispersed particles
g = gravitational acceleration
$f(\phi)$ = is a function of volume fraction of suspended solids

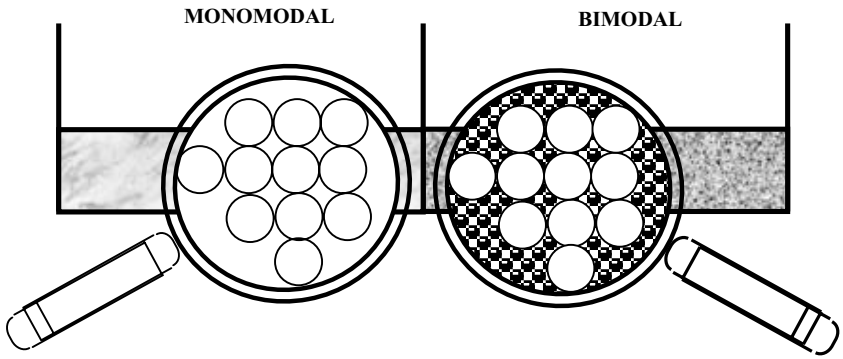

FIGURE 4.1 PSD for unimodal and bimodal distributions. (Reference: Kesavan, S., Stabilization of Coal Particle Suspensions using Coal Liquids, M.S. thesis, University of Akron, 1985.)

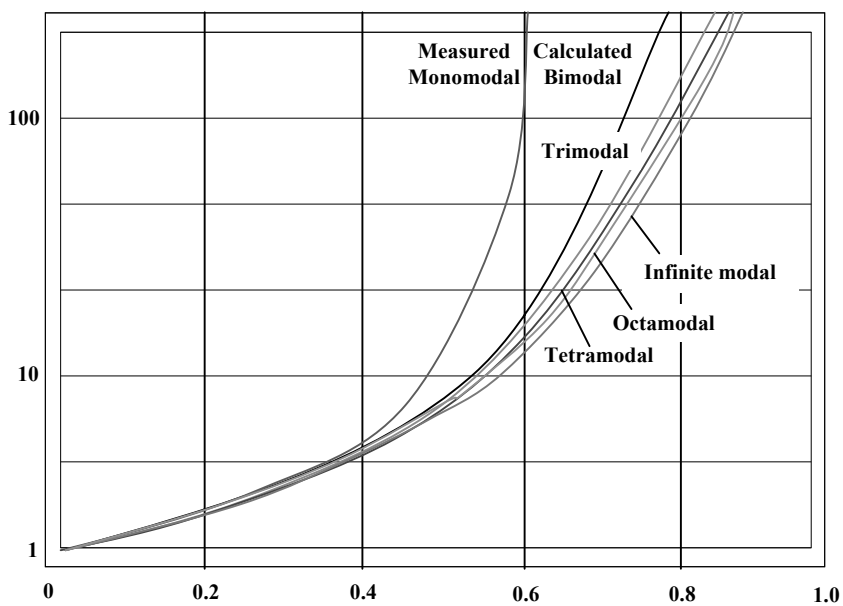

FIGURE 4.2 PSD effect on viscosity. (Source: Hunter, R.J., *Foundations of Colloidal Science*, Vol. 1, Oxford University Press, Oxford, 1987.)

Stokes' law suggests that to reduce the sedimentation velocity, the particle diameter should be reduced, the viscosity of the dispersing medium should be increased, and the difference in density between the solid and the liquid phase should be decreased. However, optimal slurry processing demands high loading at low viscosity for transportation and atomization requirements. Therefore, the low-viscosity slurry inherently promotes the sedimentation of the fines. To alleviate this obvious difference in the property requirements of the resultant slurry, various additives and surfactants have been developed.

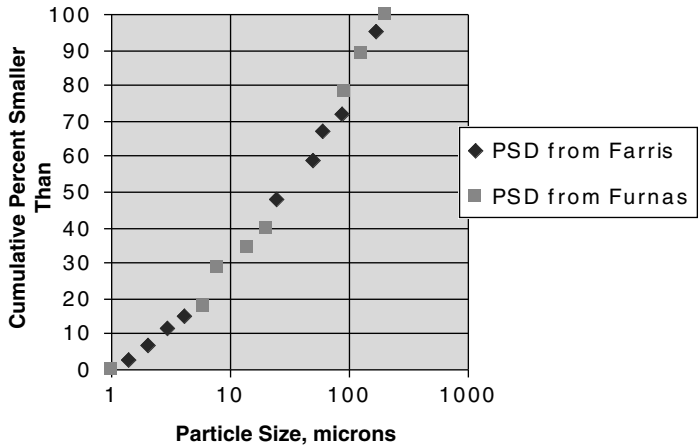

FIGURE 4.3 PSD formulated for minimal viscosity. (From Hunter, R.J., *Foundations of Colloidal Science*, Vol. 1, Oxford University Press, Oxford, 1987.)

4.2.2 Rheology

Rheology is the study of a system's response to a mechanical perturbation in terms of elastic deformations and viscous flow.[20,21] In most rheological systems, elastic response is associated with solids, whereas viscous response is associated with liquids. Therefore, a suspension system such as coal slurry exhibits behaviors of both elastic and viscous responses. These responses in coal slurry are a function of the type of coal, coal concentration, PSD, properties of dispersing phase, and additive package.[4,22]

Coal slurries, in general, exhibit non-Newtonian behavior; however, they do exhibit a wide range of responses including Newtonian, dilatant, pseudoplastic (shear thinning), and plastic flow characteristics. Each of these responses is shown graphically in Figure 4.4, as a plot of the shear stress vs. the rate of shear.[23] Newtonian is the simplest response and exhibits a linear functionality between shear stress and shear rate. Typically, slurries exhibit pseudoplastic or shear-thinning behaviors, meaning that as the shear stress is increased, the shear rate increases at a slower rate. This behavior is typical of a material that has a fragile internal structure that degrades with shearing stresses. The material does not have a yield point, but the apparent viscosity continually decreases with applied stress. An extension of this behavior is thixotropy, which exhibits shear thinning that requires significant periods of time to reform the internal structure. The period of time can range anywhere from minutes to several days. Dilatant behavior is the opposite of shear thinning, as the resistance to flow increases with the shear stress. In plastic behavior, a sufficient stress, higher than the yield stress, must be applied for flow to begin. Once the suspension yields, then the shear stress is linear with shearing rate. The important rheological characteristics are yield stress, viscosity, and plasticity (thixotropy).[24] These values are determined experimentally.

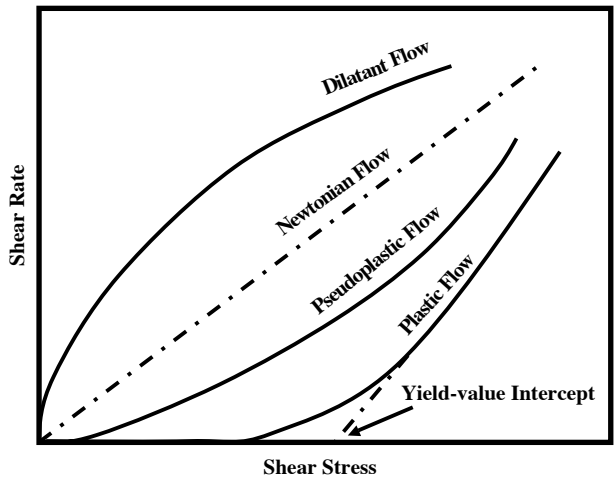

FIGURE 4.4 Rheograms of various flow behaviors. (Reference: Evans, D.F. and Wennerstrom, H., *The Colloidal Domain Where Physics, Chemistry, Biology, and Technology Meet*, VCH, New York, 1994.)

Viscosity has proved to be very difficult to model because it exhibits both elastic and viscous responses. The *Einstein equation* for viscosity in dilute suspensions is given by Equation 4.3.

$$\mu_r = \frac{\mu}{\mu_0} = 1 + 2.5\phi \tag{4.3}$$

where

μ_0 = viscosity of dispersing phase
μ_r = relative viscosity
μ = absolute viscosity
ϕ = volume fraction of solids

This equation works well for dilute systems. To describe higher concentrations, a number of investigators have developed relations in the form of $\mu_r = f(\phi)$ that asymptotically reduce to Einstein's equation at low concentrations.[4] Modeling of these systems, however, utilizes only one parameter, the volume fraction of solids. This type of model is called a *one-parameter model*. This assumes that the particles are inert and, as such, interactions between particles are negligible.

The viscosity of the suspending medium not only affects the sedimentation velocity but also the rate of agglomeration. An empirical expression for $f(\phi)$ is given by:

$$f\left(\phi\right) = e^{-5.9\phi} \tag{4.4}$$

This equation illustrates how rapidly an increase in solids' volume fraction, ϕ, can reduce the sedimentation rate. However, the increased stability compromises slurry properties such as viscosity, combustion characteristics, and overall handling.[25]

Physicochemical forces are important in coal slurry, because of the small size of the particles (most coal particles in slurry are smaller than 50 μm). Although bulk properties such as density and viscosity of coal and water are important, surface properties have a large effect on the slurry properties.

4.2.3 Stability

Slurry stability is classified into three broad categories, namely, *sedimentative* (static), *mechanical* (dynamic), and *aggregative*. The stability of a slurry is a crucial factor in its processability and applicability, which ultimately determine the value of the slurry. The factors that affect slurry stability are density, particle size, solid concentration, surface properties (relative hydrophilic nature), surface charge (zeta potential), morphology of coal, and type of slurrying liquid.[26]

The stability of a slurry against gravity is called "sedimentative stability." A statically unstable slurry will settle, but as the system becomes more stable, the degree of settling decreases. Static stability in a fluid requires a *yield stress* in the fluid sufficient to support the largest particle. The stability in a dynamic system is called *dynamic stability*. Dynamic stability involves the superposition of mechanical stresses; some examples are pumping and mixing.[27] The third stability type, *aggregative stability*, is a function of interparticle forces.

4.2.4 Suspension Types

A suspension can be classified into three broad categories, namely, aggregatively stable, flocculated, and coagulated, as shown in Figure 4.5.[3] In an *aggregatively stable* suspension, repulsion forces do not allow particles to adhere to each other. They tend to settle owing to gravity, leading to a highly classified and compact sediment with coarse particles at the bottom and finest particles on the top.

In the second suspension type, *flocculated*, the particles weakly interact to form porous clusters called *flocs*. They tend to settle slowly because of increased drag forces from the floc structure. The formed sediments are very loose and occupy a large fraction of the original slurry volume. The slurry is easily brought back to original uniform concentrations with mild agitation.

In the last suspension type, *coagulated*, the particles interact strongly. The strong attractive interparticle forces promote the formation of compact and tightly bound clusters, which are difficult to break loose without significant agitation. These unstable slurries have fast settling rates and often display non-Newtonian behavior like thixotropic (time-dependent behavior), pseudoplasticity (shear thinning), or plastic behavior.

4.2.5 Interparticle Interactions

Recent studies have shown that stability in slurries is achieved by promoting networks through weak interparticle interactions.[26] The properties of coal slurries are governed by the nature of the forces between particles. Six important particle–particle

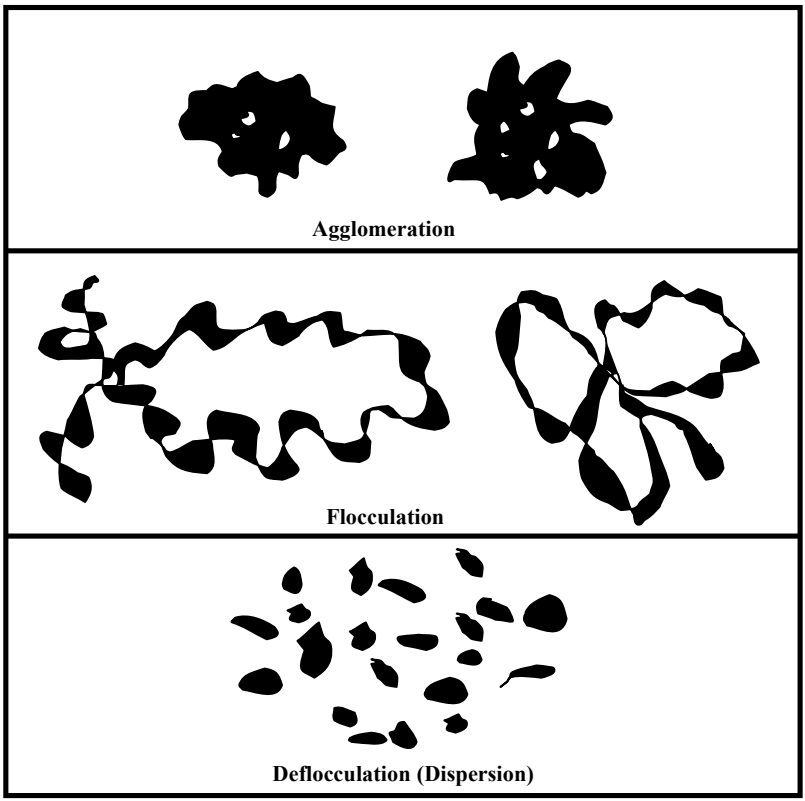

FIGURE 4.5 Illustrations of suspension types. (From Papachristodoulou, G. and Trass, O., *Can. J. Chem. Eng.*, 65, 177–201, 1987.)

interactions may exist in aqueous dispersions.[26] A more comprehensive analysis of these phenomena can be found in literature.[28,29]

1. Interaction between *electrical double layers* (EDL)
2. van der Waals (VDW) attraction
3. Steric interactions
4. Polymer flocculation
5. Hydration- and solvation-induced interactions
6. Hydrophobic interactions

When a substance is brought into contact with an aqueous polar medium, it acquires a surface electrical charge through mechanisms such as ionization, ion adsorption, or ion dissolution. The surface charge influences the distribution of nearby ions in solution, i.e., ions of opposite charge are attractive whereas ions of like charges are repulsive. This, coupled with the mixing effects of thermal motion, leads to the formation of the EDL. The EDL consists of a surface charge with a neutralizing excess of counterions, and, further from the surface, co-ions distributed in a diffuse manner as shown in Figure 4.6.[26] The EDL is important because the interaction

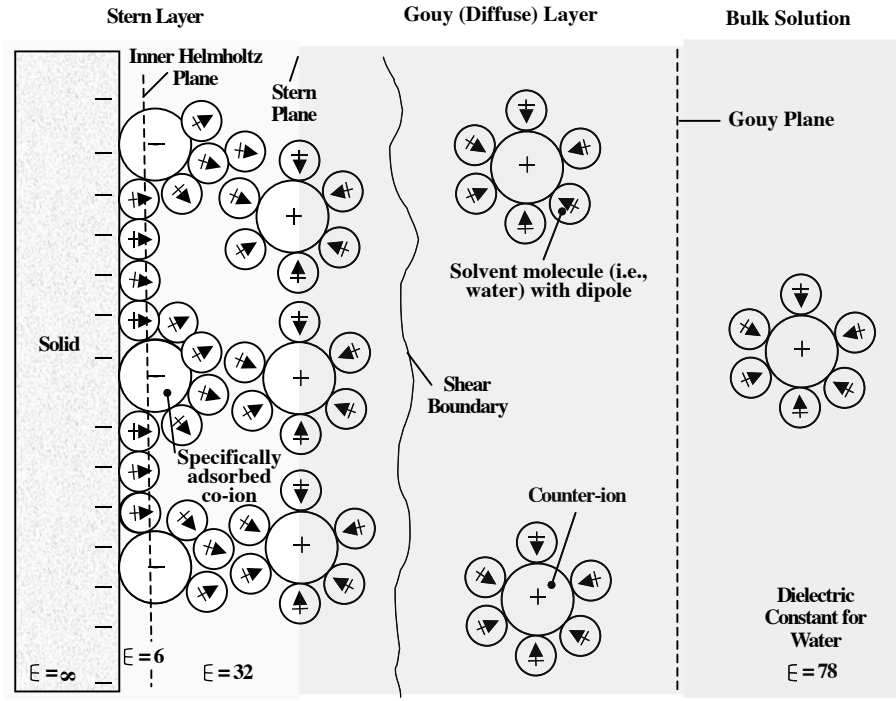

FIGURE 4.6 A schematic representation of EDL in the vicinity of a liquid–solid interface. (Source: Rowell, R.L., The Cinderella Synfuel, *CHEMTECH*, April 1989, pp. 244–248.)

between charged particles is governed by the overlap of their diffuse double layers. This creates a potential (Stern potential) at the interface of the Stern plane and the diffuse layer. Unfortunately, direct measurement of the Stern potential is impossible; however, it is possible to measure the zeta potential (ζ), which corresponds to the shear plane adjacent to the Stern plane as shown in Figure 4.7.[26] Although the zeta potential may not necessarily give a good indication of Stern potential, in certain cases an expression such as Equation 4.5 can be formulated for the repulsive energy (V_R) of interaction between particles based on surface roughness, shape, and other factors.[30]

$$V_R = 2\pi\varepsilon a\zeta^2 e^{(-\kappa h)} \tag{4.5}$$

where

a = radius of two particles
ζ = zeta potential
κ = inverse Debye length
ε = permissivity of the medium
h = distance between particles

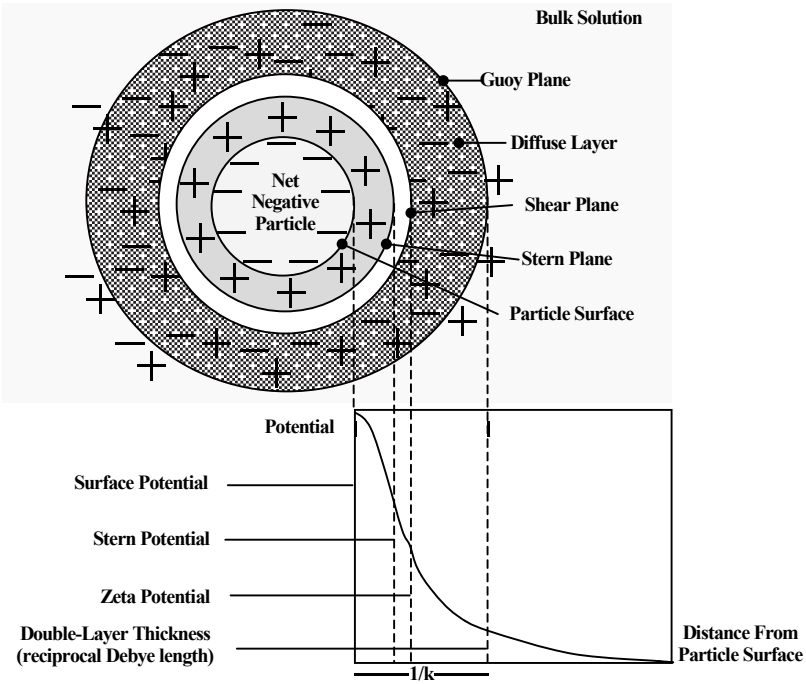

FIGURE 4.7 Distribution of electric potential in the double-layer region surrounding a charged particle. (Reference: Rowell, R.L., The Cinderella Synfuel, *CHEMTECH*, April 1989, pp. 244–248.)

The attractive force, van der Waals force, encourages aggregation between particles when the distance between particles is very small. These forces are due to spontaneous electric and magnetic polarizations giving a fluctuating electromagnetic field within the dispersed solids and aqueous medium separating the particles.[26] Two common methods are used for predicting these forces, namely, Hamaker approach and Lifshitz approach. The Hamaker approach adds up the forces pairwise between the two bodies, whereas the Lifshitz method directly computes the attractive forces based on the electromagnetic properties of the media. Fundamental concepts of the Hamaker approach are explained in this chapter, though the more rigorous Lifshitz method is not covered.

The simpler method, Hamaker, for identical spheres is represented by:

$$V_A = -\frac{A_{12}a}{12h} \tag{4.6}$$

where A_{12} is the Hamaker constant.

Now, it is possible to predict the interactions of the EDL and van der Waals forces by:

$$V_T = V_A + V_R \tag{4.7}$$

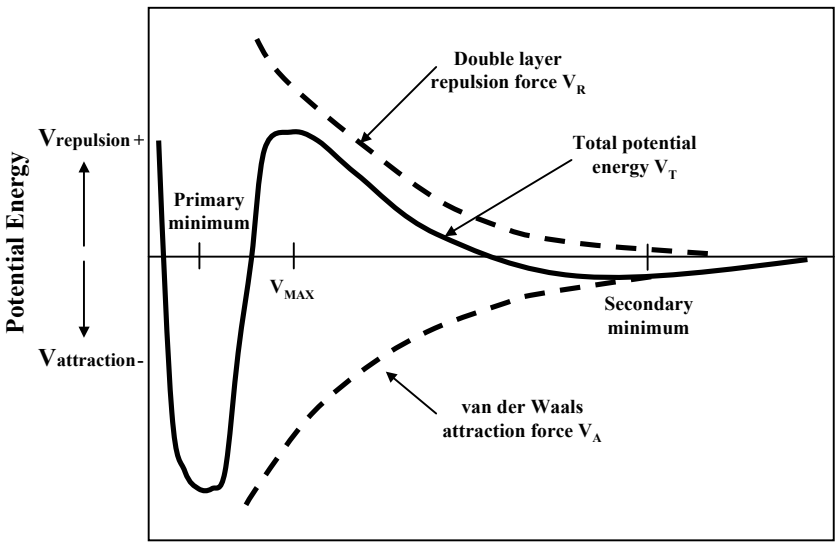

FIGURE 4.8 Particle–particle interaction potential energy. (From Rowell, R.L., The Cinderella Synfuel, *CHEMTECH*, April 1989, pp. 244–248.)

This forms the basis of the DVLO (Derjaguin–Landua–Verwey–Overbeek) theory of colloid stability.[24] The energy interactions for EDL and van der Waals forces are shown in Figure 4.8.[26] The subsequent total energy curve allows for prediction of aggregation at close distances (primary minimum) and the possibility of a weak and reversible aggregation in the secondary minimum.[26] The form of the curve depends on the size of the particles and surface charge.[31] For example, coarse particles are more likely to be vulnerable to aggregation at the secondary minimum.

Kinetic effects are important, because thermodynamic prediction may not yield sufficient information. Coagulation rates are described in terms of the stability ratio. The stability ratio, *W*, can be thought of as the efficiency of interparticle collisions resulting in coagulations as shown in Equation 4.8 for two identical particles brought together by diffusion.[26]

$$W = 2\int_0^{\infty} \frac{\exp\left(\frac{V_T}{kT}\right)}{\left(2+s\right)^2} ds \tag{4.8}$$

where $s = h/a$.

The other types of interparticle interactions (steric interactions, polymer flocculation, hydration- and solvent-induced interactions, and hydrophobic interactions) represent special cases. The most significant of these are steric interactions and polymer flocculations. Steric interactions develop when molecules (usually polymers or macromolecues) are adsorbed onto the particle surface at high coverages. The polymer molecules protrude from the surface of the particle into solution. When

particles approach one another, the polymer chains overlap and often dehydrate, increasing the stability of the slurry.[32] Polymer flocculation occurs when the particle surface has low coverage of a high-molecular-weight polymer. The polymers bridge the particles and form flocs.[32,34]

Hydration- and solvation-induced interactions become important when interparticle distance is on the order of a solvent molecule, i.e., very short. For aqueous systems, these solvation effects are clearly visible in structuring of the water near the interfacial surface (with their bound water), which interacts with hydrated ions from solution. The net effect is an increased stability or net repulsion between particles as it becomes necessary for the ions to lose their bound water to allow the approach to continue.[26]

Hydrophobic interactions are analogous to hydration and solvation effects, because stability can be enhanced by the attraction between two hydrophobic particles. Therefore, hydrophobic particles tend to associate with each other. The hydrophobic forces are greater than the van der Waals force and have a longer range.[26]

4.3 COAL-WATER SLURRY

Coal-water slurries attracted technologists' attention initially as a replacement fuel for oil in furnaces and boilers and recently for cofiring of boilers and furnaces in the use of coal fines.[34] CWM and CWSF have received a great deal of attention for use as a fuel because of the relative ease of handling (similar to fuel oil and not explosive, unlike coal dust), storage in tanks, and injection into furnaces and boilers. CWMs typically have extremely high loadings in the range of 60–75 wt% coal, which leads to high energy densities per unit mass. Possible applications include gas turbines, diesel engines, fluid bed combustors, blast furnaces, and gasification systems.[2] CWM with a lower coal loading of 50 wt% may be used for the internal combustion engine, especially when nonexplosive fuel is needed, for example, in military vehicles and helicopters. However, coal slurries for cofiring purposes are limited by economics to the use of minimal additives as well as lower coal concentrations (50 wt%).[35]

The physical properties of coal slurry are extremely important in the processing of the fuel. A slurry must be stable and exhibit low viscosity in the shear rates of pumping and atomization. The flow characteristics of coal-water slurry depend on: (1) physicochemical properties of the coal, (2) the volume fraction, ϕ, of the suspended solids, (3) the particle size range and distribution (PSD), (4) interparticle interactions (affected by the nature of surface groups, pH, electrolytes, and chemical additives), and (5) temperature.[36,75] Rheological and hydrodynamic behavior of coal-water slurries varies from coal to coal. Each coal has a unique package of PSD, concentration, and additives to reach the desired processability.

A parameter that measures how well a coal will slurry, i.e., *slurry capability* (or, slurriability), is the equilibrium moisture content of coal. The equilibrium moisture content is a measure (index) of the hydrophilic nature of the coal. The equilibrium moisture content of a coal sample can be readily determined by proximate analysis. The more hydrophilic a coal is, the more water it will hold and the less likely it is to produce a highly concentrated slurry.[37,75] The coal-water slurry viscosity increases

with the hydrophilicity of the coal. Therefore, a hydrophobic coal can more easily form a slurry of low viscosity at high solid loadings.

Conventional high-rank coals (black coal), except anthracite, have a hydrophobic nature from the lack of acid groups and will form a slurry of ~80 wt% (dry coal weight basis). Anthracite coals have low reactivity and are not very volatile, leading to poor ignition stability.[2] However, low-rank coals (brown coal) are hydrophilic from an abundance of oxygen functional groups and will form slurries of only 20–25 wt% (dry coal weight basis).[38] These slurries have low concentrations but form slurries that are nonagglomerating and have high reactivities. Difference in coal slurry stability between types of coals is a function of the relative balance between acid and base groups on the coal surface.[39]

CWMs are loaded to the highest possible concentration at acceptable viscosities. However, viscosity increases with coal concentration (loading), though reducing the viscosity compromises the stability of the slurry.[3] The viscosity of the slurry increases gradually with increasing solid loading until a critical point is reached at which interparticle friction becomes important. Beyond this point, the viscosity increases very sharply until the slurry ceases to flow.[34,75] To properly stabilize coal-water slurries, i.e., to enhance the stability of the coal dispersion, additives such as surfactants and electrolytes are added.

Surfactants are used as dispersants to wet and separate coal particles by reducing the interfacial tension of the coal-water system. Surfactants are short-chain molecules containing both a hydrophobic group and a hydrophilic oxide (nonionic) or a charged ionic group (ionic). These molecules attach themselves to the coal particles through adsorption or ionic interaction. Generally speaking, dispersants are ionic. Some examples of such dispersants are sodium, calcium, and ammonium lignosulfates, and the sodium and ammonium salts of naphthalene formaldehyde sulfonates.[4]

Ionic surfactants adsorb onto the alkyl groups at hydrophobic sites on the coal particle. This gives the coal particles a negative charge, which affects the EDL, enhancing the repulsive forces and thus preventing agglomeration.[17] Anionic surfactants decrease the viscosity of the slurry up to a critical loading. At this point the coal adsorption sites are saturated and the remaining surfactant forms micelles in the slurry, leading to an enhanced structure and increased viscosity.

Nonionic surfactants function by two different methods depending on the nature of the coal. On a hydrophilic coal surface the hydrophobic end of the surfactant is toward the aqueous phase. The water then acts as a lubricating material between coal particles. The second method is via attachment of surfactant on a hydrophilic coal. The hydrophilic end of the surfactant attaches to the coal molecule, leaving the hydrophobic end into the aqueous medium. This increases the amount of water near the surface of the coal particle, producing a hydration layer or solvation shell. This prevents agglomeration by cushioning coal particles and lowers the viscosity.[17]

The ionic strength of water in the CWM is an important parameter in the rheological and hydrodynamic characteristics of a slurry. Because coal is a mixture of macromolecular carbonaceous materials and mineral matters rather than a uniformly homogeneous substance, the ionic strength of the water will affect the interaction with coal. In a hydrophobic colloidal system dispersed by electrically repulsive forces, the electrolyte concentration (and its ionic strength) has a considerable effect

on the stability against flocculation of particles.[17] The cation concentration causes an increase in the viscosity of the slurry with decreasing pH.[40] Electrolytes strongly affect the degree of particle dispersion and, thus, rheology in CWM that uses anionic dispersant.[40] The addition of electrolyte to a slurry using nonionic dispersants has no appreciable effect on the viscosity.[40]

In highly concentrated slurries,[76] minimal settling is expected, but viscosity-reducing additives increase the settling rate. To stabilize the dispersion, flocculating agents are added, which produce a gel. Some examples of this are nonionic amphoteric polymers of polyoxyethylene, starches, natural gums, salts, clays, and water-soluble polymeric resins.[2,76]

Polymers have been used for drag reduction, i.e., viscosity reduction.[41,76] Both ionic and nonionic polymer solutions show reduction in viscosity, although the reduction is more pronounced for anionic polymers.

4.4 COAL-OIL SLURRY

Coal-oil slurries have been investigated for over 100 years. Typically, interest peaks in times of high prices and shortages of oil. The most recent interest was fueled by the energy crises of 1973 and 1979, when tremendous effort was expended in finding a quick viable alternative to oil in boilers and furnaces. Since the mid 1980s, however, most slurry investigation has been directed toward CWM.

In general, coal-oil slurries exhibit non-Newtonian behavior, mostly pseudoplastic except at low coal loadings where the slurry is Newtonian (provided the oil is also Newtonian). The viscoelastic properties of the dispersion depend on coal concentration, PSD, coal type, oil type, and chemical additives. Rheological properties of COM are highly sensitive to coal concentration. At this critical concentration, a dramatic increase in viscosity occurs with incremental changes in concentration.

The standard PSD in COMs is listed in Table 4.2.[3] COMs are classified as lyophobic because the dispersed particles are not compatible with the dispersion medium. These systems are thermodynamically unstable and will separate into two continuous phases.

TABLE 4.2
COM Particle Size Distribution (PSD)

Percentage[a]	Particle Size (μm)
100	< 200
80	< 74
65	< 44
15	< 10–20
1	< 1 (colloidal)

[a] Passing through mesh size.

Source: From Papachristodoulou, G. and Trass, O., *Can. J. Chem. Eng.*, 65, 177–201, 1987. With permission.

Ultrafine COMs with 95% of particles smaller than 325 mesh (44 μm) and slurry concentrations of 50 wt% have been investigated. These slurries reduce abrasiveness, exhibit improved combustion characteristics, and do not contain additives.[4,42] However, the grinding cost becomes higher, and coal concentration is typically limited to 50 wt%.

Common chemical additives for COMs are surfactants and polymers. The surfactants add stability to the mixture by preventing agglomeration and enhancing flocculation. Cationic polymers are the most effective surfactants for stabilization,[43] though anionic polymers are used more frequently to reduce the drag.[44,76]

In many instances, water is added to coal-oil slurries forming COW or CWO, depending on the water concentration. Water, a flocculating agent, is added to increase the stability of the slurry as well as for cost savings. Water increases the viscosity of the resultant slurry through the formation of aggregates and particle bridging,[44] although the combustion properties are more or less retained.

4.5 ADVANCED TRANSPORTATION OF COAL SLURRY

The transportation of coal slurries can be accomplished by truck and railroad tanks, slurry tankers, and slurry pipelines. Historically, transportation schemes of coal-water slurries have received the most attention and development. Although all transportation schemes and options have been investigated, few new processing developments have occurred in truck, railroad, or slurry tankers. In these cases, the slurry stability has been enhanced to minimize settling during transportation or the slurry has been dewatered to maximize energy density and cost-effectiveness of transportation. On the other hand, coal-water pipeline systems across the world have undergone almost constant development since the 1950s. Coal pipelines can be broken into four different systems: (1) conventional fine coal, (2) conventional coarse coal, (3) stabilized flow, and (4) coal-water mixture. These systems differ by the particle size of coal in the slurry, as shown in Table 4.3.[45]

Only two systems in the U.S. are conventional fine-coal slurry pipelines. The first was the Ohio pipeline by the Consolidation Coal Company, which was built in 1957 and operated for several years until another competitive transportation mode, the unit train, became available. The slurry traveled at moderate velocities and had

TABLE 4.3
Summary of Particles Sizes in Coal-Water Slurry Pipeline Systems

Coal-Water Slurry Systems	Particle Sizes
Conventional fine coal	Less than 1 mm
Conventional coarse coal	50–150 mm
Coal-water mixtures	–30 and –150 μm (less than 200 mesh)
Stabilized-flow coal	Less than 0.2 mm (fine) and less than 50 mm (coarse)

Source: From Hsu, B.D., Leonard, G.L., and Johnson, R.N., *J. Eng. Gas Turbines Power*, 110, 516–520, July 1988. With permission.

a coal content of 50 wt%. The second pipeline system built, Black Mesa pipeline, followed the same basic design of the earlier Consolidation pipeline. The pipeline began operation in 1970 and is still operating today. The pipeline operates at 4–6 mph, and is optimized for minimal erosion and settling at a 50% coal loading.[45,46] The success of this pipeline has significantly impacted other solid transporting slurry pipelines in the world.

In conventional coarse-coal slurry transportation, run of mine (ROM) coal is transported at high velocities in coal loadings ranging from 35 to 60%, depending on the coal particle size (50–150 mm).[45] In this pipeline, coal slurry preparation costs are minimal; however, energy requirements for the pipeline transportation are high. This type of system is limited to short distances where other transportation modes such as rail, barge, truck, or conveyor can be used.

Stabilized flow coal slurry systems use smaller particles to support the coarse coal particles. The particle size distribution for the fine coal is <0.2 mm and for the coarse coal, <50 mm.[45] This PSD was utilized to enhance the stability of the slurry for long transportation distances. Coal concentrations of up to 70 wt% can be used. The coarse coal is easier to dewater than fine coals because of the particle size.

Coal-water mixture pipeline systems are designed for direct use at the final destination site, most likely in utility boilers and furnaces. The coal concentration is between 70 and 75 wt% with bimodal and polymodal particle size distributions of coal particles smaller than 200 mesh.[45] CWMs use approximately 1% surfactants and dispersants for slurry stability. These pipelines have yet to be investigated over long distances.

Many different coal processing configurations exist for coal use at the end of a coal slurry pipeline. The options include direct use of CWM, dewatering and conveying to a plant (Figure 4.9), piping to an offshore platform and dewatering into ship (Figure 4.10), dewatering into a railcar or truck, and piping into an offshore buoy system into a ship.[33–48]

Table 4.4 is a comparison of coal content in coal slurries for the pipeline systems discussed.[45] Each coal transportation mode has its own merits, and therefore a decision has to be made on an individual basis. The transport systems are evaluated in Table 4.5.[45]

As mentioned earlier, one of the most significant and successful coal slurry pipelines is the Black Mesa Pipeline, which is a 273-mi. (440-km) long, 18-in. (457-mm)

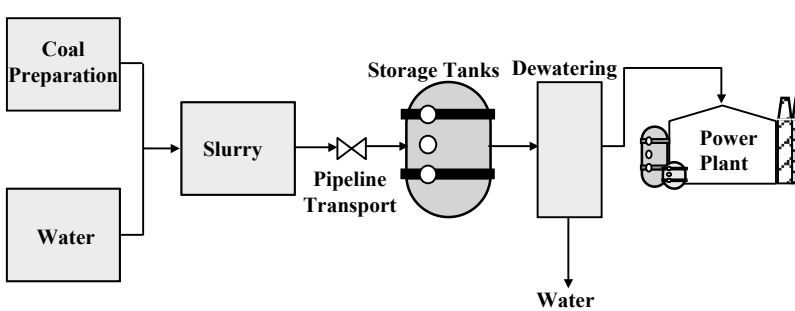

FIGURE 4.9 Domestic combustion pipeline scheme. (From Hsu, B.D., Leonard, G.L., and Johnson, R.N., *J. Eng. Gas Turbines Power*, 110, 516–520, July 1988.)

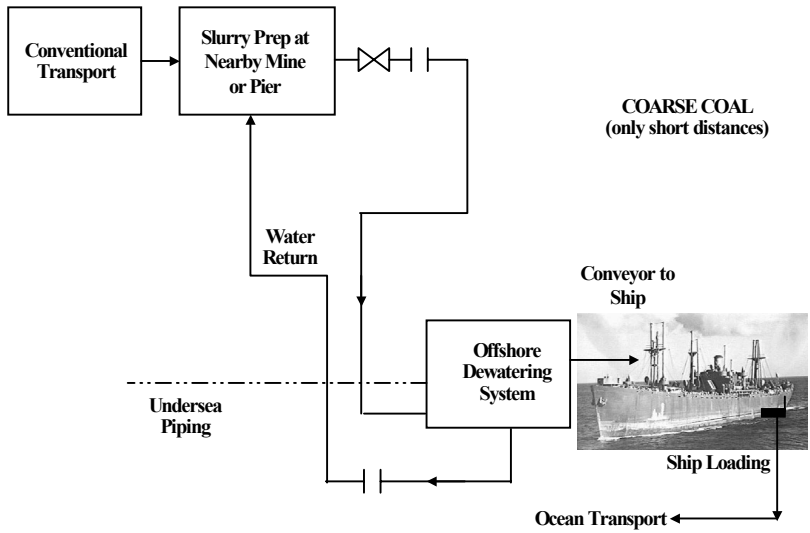

FIGURE 4.10 Offshore coarse coal pipeline scheme with dewatering. (From Hsu, B.D., Leonard, G.L., and Johnson, R.N., *J. Eng. Gas Turbines Power*, 110, 516–520, July 1988.)

TABLE 4.4
Comparison of Coal Content in Coal Slurries

Coal-Water Slurry Systems	Percentage of Coal in Mixture
Conventional fine coal	50 (overland and ship loading)
	75 (aboard ship)
Conventional coarse coal	30–60 (overland-short distances only and ship loading)
	90–92 (aboard ship)
Coal-water mixtures	70 (overland)
	85–90 (ship loading and aboard ship)
Stabilized-flow coal	70–75 (overland, ship loading, and aboard ship)

Source: From Hsu, B.D., Leonard, G.L., and Johnson, R.N., *J. Eng. Gas Turbines Power*, 110, 516–520, July 1988. With permission.

diameter coal-water slurry pipeline, originating from Black Mesa in northeastern Arizona. The system transports coal from Peabody Western Coal Company's open pit mine to the Mohave Generating Station, which is a 1580-MW steam-powered electric generating plant located in Laughlin, NV. Black Mesa Pipeline began its commercial operation in November 1970 and has transported over 120 million tons (as-mined) with an availability factor of 98%. The pipeline delivers coal at a rate of 570 to 600 M/T (or, 630–660 short tons) per hour, and the nominal capacity is over 5 million tons (4.5 million tonnes) per year. Black Mesa Pipeline has helped development of other solid transportation pipelines in the world, which include slurry pipeline transportation of limestone, copper concentrates, iron concentrates, gilsonite, and phosphate. Some

TABLE 4.5
Coal-Water Slurry Pipeline System Selection

	System Characteristics		
Objective	**Length (mi)**	**Type**	**Best Pipeline Selection**
Rapid implementation	<5	Domestic	Coarse coal
		Export	Coarse coal
	50–100	Domestic	Conventional fine coal
		Export	Conventional fine coal
	>100	Domestic	Conventional fine coal
		Export	Conventional fine coal
Lowest cost and water use	<5	Domestic	Coarse coal
		Export	Coarse coal
	50–100	Domestic	Stabilized flow
		Export	Stabilized flow
	>100	Domestic	Stabilized flow
		Export	Stabilized flow
Oil displacement	All	Domestic	CWM
		Export	CWM

Source: From Hsu, B.D., Leonard, G.L., and Johnson, R.N., *J. Eng. Gas Turbines Power*, 110, 516–520, July 1988. With permission.

TABLE 4.6
Major Long-Distance Slurry Pipeline Projects

Material Transported	**System Name Location**	**Length (mi)**	**Annual Tonnage (millions)**	**Initial Operation**
Coal	Consolidation Ohio	108	1.3	1957
	Black Mesa Arizona	273	4.8	1970
Limestone	Calaveras California	17	1.5	1971
	Rugby England	57	1.7	1964
	Gladstone Australia	15	2.0	1981

of the major long-distance slurry pipeline projects for coal slurry and limestone slurry are shown in Table 4.6.

4.6 ENVIRONMENTAL ISSUES

Environmental issues play an important role in the implementation of coal slurry fuels. The transportation systems must take into account possible leaks and spills

encountered with slurry handling. Combustion processes must be thoroughly investigated to find the differing combustion mechanisms in coal slurry, specifically, the mineral matter and sulfur content of the coal.

In the transportation of coal slurries, spills, leaks, and catastrophic disasters are important factors in safe handling. Transportation of CWMs has been widely investigated for both short and long distances. Slurries of water are considered nontoxic and nonhazardous. Historically, in the U.S. when there have been handling accidents in pipeline systems, cleanup of the coal has not been necessary. The coal has been allowed to reenter the ground naturally. CWMs have the distinct advantage in that they are not readily combustible in accidents.

In the combustion of slurries many processes will not be able to handle the high sulfur and mineral matter content of coal. Therefore, combustion processes in utility boilers and furnaces may exhibit slagging, fouling, and erosion. Other applications such as cement and asphalt kilns and fluid bed combustors are able to easily handle the increases in inorganic material. The amount of ash that induces fouling in boilers varies from boiler to boiler. Table 4.7 shows the predicted acceptable ash levels for differing types of boilers.[2]

An important constituent in the coal is sulfur both in organic and inorganic forms. Sulfur is a precursor for ash formation and can form SO_x, precursor to acid rain, which has regulated emissions. In many instances, coal beneficiation techniques are used to clean the coal after grinding. These processes are broken into physical and chemical cleaning methods. Physical cleaning methods are based on differences in coal and mineral matter density or surface properties. Examples of physical cleaning processes are gravitational separation,[49] froth flotation,[50] selective agglomeration,[51] heavy medium separation,[52] high-gradient magnetic separation,[53] microbubble flotation,[54] and biological method.[55] Chemical cleaning methods have been widely investigated at the laboratory scale but are not commonly used on an industrial scale.[56]

Other environmentally regulated emissions from combustion of coal slurries are NO_x, hydrocarbons (VOCs), and particulate matter (PM). The burning of coal slurries reduces the amount of hydrocarbon emissions significantly in oil-designed boilers and furnaces. NO_x emissions are a function of fuel's nitrogen content, fuel composition, combustion temperature, and amount of excess air.[4] NO_x emissions are controllable by conventional methods such as low excess air, stage combustion, low-temperature

TABLE 4.7
Permissible Coal Ash Content for Utility Boilers

Ash Content (%)	Boiler Type
5–7	Coal designed/coal capable
2–3	Liberal oil design
<0.5	Compact oil designed

Source: From Kesavan, S., Stabilization of Coal Particle Suspensions using Coal Liquids, M.S. thesis, University of Akron, 1985. With permission.

combustion, and flue gas recirculation.[2] The particulate emissions are directly related to the ash content in the coal slurry and can be significantly higher than oil-burning furnaces. However, conventional particle control techniques are effective in removing the particulates.[4] Further, low-ash content coal is preferred as a slurry coal.

4.7 COMBUSTION

The combustion of coal in utility boilers (and furnaces) and internal combustion engines has been widely investigated throughout the 1970s and 1980s. The bulk of combustion research and development has been in the area of CWSFs.

Generally, COM combustion occurs in three stages: (1) heating of droplet, (2) combustion of volatile matter, and (3) combustion of char. For coal, char combustion rate is controlled (or limited) by the mass transfer rate of oxygen for particles larger than 100 μm, whereas smaller ones are limited by the kinetic reaction rate.[4] In other words, the rate-limiting step for char combustion reaction is the mass transfer rate of oxygen to coal-reactive sites for large coal particles, whereas that for smaller particles is the surface reaction rate. Carbon conversions in coal slurry combustion are comparable to those of fuel oil combustion.

COM and CWSF differ in burning characteristics such that CWSF heat is only generated by the coal, unlike COM, whose energy is provided by combustion of both coal and oil. There are potential problems associated with CWSF combustion such as flame stability, incomplete combustion, erosion, and slagging. Flame stability is a function of atomized droplet size, fuel stability, agglomeration properties, burner swirl, burner throat construction, and preheat air temperature.[2] Incomplete combustion is a result of inadequate preheating, delayed ignition (vaporization of water), insufficient excess oxygen supply, and agglomeration. Erosion occurs through excess velocities of particle-laden gases. Slagging is a function of inorganic content and slow char particle burnout. In cases of using CWSF in oil boilers and furnaces, the boiler duty is derated, unless modifications are made to the unit.

The combustion mechanism for CWSF shown in Figure 4.11[57] is similar to that of pulverized coal with the additional stage of water evaporation. The coal slurry droplet is injected into a hot gas stream and quickly dries. The particles in the droplet agglomerate from surface forces and become tightly bound while undergoing plastic deformation during pyrolysis. Ignition occurs and devolatilization produces fragmentation. The char further fragments during burnout.

Coal combustion is considered slow when compared to the combustion of oil.[58] The flame temperature is lowered because of the energy absorbed in order to vaporize the water. The atomization of the slurry strongly influences the combustion efficiency.[59] Fine atomization increases the rate of evaporation through surface area increase and reduces the size of the agglomerates. Smaller droplets produce more stable flames and greater carbon burnout.[2]

Coal-water slurry firing of conventional boilers has been performed over extended periods of time with few operational problems. The boilers were successfully started, reliably and safely operated, and complied with emission norms. The combustion efficiency was 95%, and thermal efficiency was 79%. However, in order

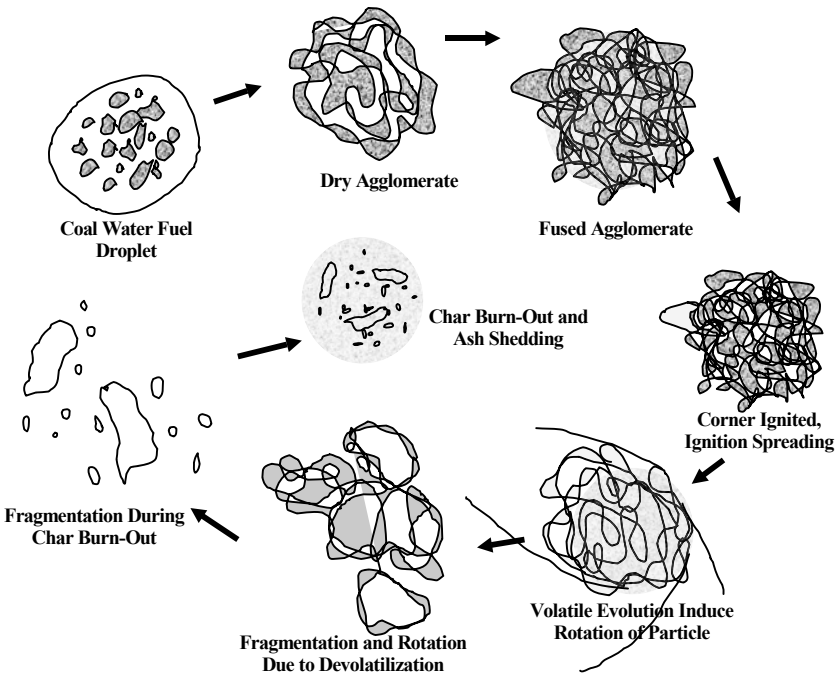

FIGURE 4.11 CWSF combustion mechanism. (Reference: Miller, S.F., Morrison, J.L., and Scaroni, A.W., The formulation and combustion of coal water slurry fuels from impounded coal fines, *Proc. 19th Int. Tech. Conf. on Coal Utilization and Fuel Systems*, 1994, pp. 643–650.)

to increase efficiency to over 99%, costly modification must be made and anticipated maintenance schedules are up to 6 times/year.[60,61]

Until recently, coal has only been used in external combustion engines (Rankine cycles). Attempts at coal utilization, dating back to the development of the diesel engine during the 1920s, on large-bore diesel engines were investigated. Problems such as fuel introduction, combustion efficiency, and engine wear could not be resolved at the time and the work was halted.[62]

Investigation in CWSF has brought about renewed interest in coal-fired internal combustion engines. Recent feasibility studies have shown that slurry engines have thermal efficiencies similar to those of oil engines, and the use of new materials has limited the erosive effects.[63] The presence of water in the fuel allows for controlling of NO_x emissions. Hydrocarbon and CO emissions are low, although CO_2 emission is higher than oil because of the high carbon content of the coal.[64,65] The particulates generated can easily be handled with particulate traps.[65]

The difficulties in the utilization of CWSF in diesel engines are fuel injection (atomization), ignition, erosion, and corrosion.[66] The fuel injection system efficiency is dependent on slurry properties, combustion chamber layout, fuel compatibility, ignition delays, and erosion. Initial ignition of CWM is difficult because the water must first be evaporated from the coal.[67] Operating combustion temperatures are

higher, the optimal range being 1000–1100 K.[62,67] This is to limit the ignition delay of coal from the evaporative effects of water and the slower burning of coal.[50,67] Erosion of parts in the injection system as well as in the cylinders is a major concern for the life of the engine. Engine wear is 6 times higher in a CWM-fired engine than a diesel-fired one, but can be reduced significantly to twice as much with special alloys and redesigned parts.[65] These findings hold great promise for the success of efforts to operate an internal combustion engine on CWSF.

4.8 RECENT ADVANCES AND THE FUTURE

Coal-water fuels have received the most process development recently. Coal slurry facilities have been built in Australia, Canada, China, Italy, Japan, Sweden, and the U.S. The most active countries have been Japan, China, and Russia. China has built several slurry production facilities and boiler units. Japan has done considerable research and technological development on slurry processes and has converted several boilers. Russia has built several pipelines, production facilities, and boilers.

In Australia, a group of companies comprising Ube Industries, Nissho Iwai Corp., and Coal & Allied Industries have been working since 1987 on developing the production, transportation, and marketing of CWM from Australia to Japan.[68] In 1991, the first bilateral trading of coal slurry began between China and Japan.[69] A coal-water slurry plant was built in Rizhao located in Shandong province by Yanzhou Coal Mining Bureau, Nisshon Iwai Corp., and JWG Corporation. The plant has a capacity of 250,000 tons/year. The coal is mined, and then transported by train to Rizhao. The coal is processed into CWM and shipped to an overseas terminal. Once in the relay terminal, the CWM is transferred to coastal shipping and then finally to end users. The manufacture, transportation, and combustion of coal slurry have involved only minimal technical problems.[69]

In the U.S., the greatest potential use for CWM may be in the utilization of coal fines for cofiring boilers. Over 40 million tons of coal fines are discarded annually in the U.S. into slurry ponds, and some 2.3 billion tons of coal fines are estimated to reside in ponds in 1994.[16] Coal fines (-100 mesh) production has increased over the years with the increase in demand of cleaner coal. Increased demand for high-quality coal (often beneficiated) has led to rejecting 20–50% of coal mined as coal fines.[70] The environmental impact of coal fines is nonproductive use of land, loss of aesthetics, danger of slides, dam failure, significant permitting costs, and possible water pollution.[70]

Recently, GPU Energy (PENELEC), New York State Electric and Gas Corporation (NYSEG), Pennsylvania Electric Energy Development Authority (PEEDA), Pennsylvania Electric Energy Research Council (PEERC), and the Electric Power Research Institute (EPRI) commissioned a project to investigate the utilization of CWM developed for coal fines. The project investigated laboratory-scale as well as full-scale cofiring of a 32-MW boiler.[72]

CWM will reduce the coal-handling problems and eliminate the need for costly dryers and their associated environmental hazards. CWM will also eliminate the need for addition of oil at start-up, which is used to stabilize the combustion. Moreover, the equipment life of pulverizer will also be extended by reducing the

equipment load. Using CWM from coal fines has the ability to stabilize the cost of fuel to the boiler because it is a lower-cost fuel, and fuel ratio can be controlled up to 50%.[71,74] Environmentally, the addition of coal slurry reduces the NO_x emissions.[74]

To be economically more competitive, the lowest-cost slurry must be developed, which may lead to a "low-tech slurry," i.e., one without stabilizers, dispersants, or the need for further grinding. This slurry can be developed from coal pond fines, from fine coal fraction of existing coal supplies, or using advanced coal technologies in the future to deep-clean fine coal.[65] The slurry has been tested with solid loadings ranging between 54 and 67 wt% coal, and the test has demonstrated excellent handling and storage properties.[73]

However, slurry developed from coal fines is highly variable. The slurriability is a function of PSD, ash level, and extent of oxidation. Therefore, slurry preparation can vary from a minimal processing to a significant processing. Minimal processing is from coals derived from wet, fine coal that has been cleaned. Significant processing can come from coal fines that have high ash content and oxidation levels. High oxidation makes the coals more wettable through oxygen bonds, which in turn increases the viscosity and stability of the slurry. Typically, weathered coals are more oxidized.

Currently, slurry produced from coal fines at Homer City is being cofired along with powdered coal in the 32-MW boiler #14 of the Seward Station. The plant has been operating without disruption. The NO_x production has decreased by 10–20%, while CO_2, SO_2, and particulates have remained essentially the same as for powder coal, but the CO level is highly variable.[73]

Coal slurry development finds itself adjusting once again to process economics. Since the mid 1980s, COM, once the most investigated slurry, has become uneconomical and development has focused on CWM. In regions where coal is plentiful but transportation is lacking, such as China and Russia, slurry development continues on production, pipelines, and combustion. In other places such as Japan where natural resources and storage spaces are limited, the ease of transportation that CWM makes possible is now being exploited. In the U.S., coal slurry development is now centered on coal utilization. CWM enables the use of higher amounts of coal after beneficiation and greatly reduces the environmental liability in discarded coal fines. Coal slurry development continues in internal combustion engines in injection systems, atomizer design, and materials for construction.[74] Coal slurry process development will continue and may be poised to represent a major form of coal energy.

REFERENCES

1. Choudhury, R., Slurry fuels, *Prog. Energy Combust. Sci.*, 18, 409–427, 1992.
2. Kesavan, S., Stabilization of Coal Particle Suspensions using Coal Liquids, M.S. thesis, University of Akron, Akron, OH, 1985.
3. Papachristodoulou, G. and Trass, O., Coal slurry fuel technology, *Can. J. Chem. Eng.*, 65, 177–201, 1987.
4. Smith, H.R. and Munsell, H.M., Liquid Fuels, U.S. Patent No. 219181, 1879.
5. Lord, N.W., Ouellette, R.P., and Farah, O.G., *Coal-Oil Mixture Technology*, Ann Arbor Science, Ann Arbor, MI, 1982.
6. Manning, A.B. and Taylor, R.A.A., Colloidal fuel, *J. Inst. Fuel*, 9, 303, 1936.

7. Manning, A.B. and Taylor, R.A.A., Colloidal fuel, *Trans. Inst. Chem. Eng.*, 14, 45, 1936.
8. Adams, R.A., Holmes, F.C.V., and Perrin, A.W., Colloidal Fuel Using Cracked Oil and High Carbon Residue, U.K. Patent No. 396,432 August 2, 1933.
9. Barkley, J.F., Hersberger, A.B., and Burdick, L.R., *Trans. Am. Soc. Mech. Eng.*, 66, 185, 1944.
10. Nakabayashi, Y., Outline of COM R&D in Japan, *Proc. 1st Int. Symp. on Coal-Oil Mixture Combustion, M78-97*, St. Petersburg, FL, May 1978.
11. Basta, N. and D'Anastaio, M., The Pulse Quickens For Coal-Slurry Projects, *Chemical Engineering*, September 17, 1984, pp. 22–25.
12. Bergman, P.D., Kirkland, L., and George, T.J., Why Coal Slurries Stir Worldwide Interest, *Coal Mining and Processing*, 19, 10, 1982, pp. 24–42.
13. Marnell, P., Direct firing of coal water suspensions, state of the art review, *Proc. Coal Technol. '80,* Industrial Presentation Inc., Houston, TX, 1980.
14. Brown, A., Jr., Powdered COM Program, Final Report of the General Motors Corporation, October 1977.
15. Miller, B.G., Coal-water slurry fuel utilization in utility and industrial boilers, *Chem. Eng. Prog.*, 85(3), 29–38, March 1989.
16. Meyer, C.W., Stabilization of coal/fuel oil slurries, *Proc. 2nd Int. Symp. on coal-Oil Mixture Combustion*, Vol. 2, CONF-791160, Danvers, MA, November 1979.
17. Williams, R.A., Characterization of process dispersions, *Colloid and Surface Engineering: Applications in the Process Industries*, Williams, R.A., Ed., Butterworth Heinemann, Boston, MA, 1992.
18. Barnes, H.A., Hutton, J.F., and Walters, K., *An Introduction to Rheology*, Elsevier, New York, 1989.
19. Hunter, R.J., *Foundations of Colloidal Science*, Vol. 1, Oxford University Press, Oxford, U.K., 1987.
20. Shaw, D.J., *Introduction to Colloid and Surface Chemistry*, 4th ed., Butterworth Heinemann, Boston, MA, 1991.
21. Napper, D.H., *Polymeric Stabilization of Colloidal Dispersions*, Academic Press, 1983.
22. Gregory, J., Flocculation of polymers and polyelectrolytes, *Solid Liquid Dispersions*, Tadros, T.F., Ed., Academic Press, pp. 163–181, 1987.
23. Evans, D.F. and Wennerstrom, H., *The Colloidal Domain Where Physics, Chemistry, Biology, and Technology Meet*, VCH, New York, 1994.
24. Vossoughi, S., and Al-Husaini, O.S., Rheological characterization of the coal/oil/water slurries and the effect of polymer, *Proc. 19th Int. Tech. Conf. on Coal Utilization and Fuel Systems*, Clearwater, FL, March 21–24, 1994, pp. 115–122.
25. Ross, S. and Morrison, I.D., *Colloidal Systems and Interfaces*, John Wiley & Sons, New York, 1988.
26. Rowell, R.L., The Cinderella Synfuel, *CHEMTECH*, April 1989, pp. 244–248.
27. Turian, R.M., Fakhreddine, M.K., Avramidis, K.S., and Sung, D.-J., Yield stress of coal-water mixtures, *Fuel*, 72, 9, 1305–1315, 1993.
28. Roh, N.-S., Shin, D.-H., Kim, D.-C., and Kim, J.-D., Rheological behavior of coal-water mixtures 1. Effects of coal type, loading and particle size, *Fuel*, 74, 8, 1220–1225, 1995.
29. Woskoboenko, F., Siemon, S.R., and Creasy, D.E., Rheology of Victorian brown coal slurries, 1. Raw coal-water, *Fuel*, 66, 1299–1304, September 1987.
30. Roh, N.-S., Shin, D.-H., Kim, D.-C., and Kim, J.-D., Rheological behavior of coal-water mixtures 2. Effect of surfactants and temperature, *Fuel*, 74, 9, 1313–1318, 1995.

31. Kaji, R., Muranaka, Y., Miyadera, H., and Hishinuma, Y., Effect of electrolyte on the rheological properties of coal-water mixtures, *AIChE J.*, 33, 1, 11–18, 1987.
32. Rowell, R.L., Vasconcellos, S.R., Sala, R.J., and Farinato, R.S., Coal-oil mixtures 2. Surfactant effectiveness on coal oil mixture stability with a sedimentation column, *Ind. Eng. Chem., Proc. Des. Dev.*, 20, 283–288, 1981.
33. Veal, C.J. and Wall, D.R., Coal-oil dispersions — overview, *Fuel*, 60, 873–882, 1982.
34. Kawatra, S.K., Coal-water slurries, in *Encyclopedia of Chemical Processing*, Lee, S., Ed., Vol. 1, Taylor & Francis, New York, 2005, pp. 495–503.
35. Bertram, K.M. and Kaszynski, G.M., A comparison of coal-water slurry pipeline systems, *Energy*, 11, 11/12, 1167–1180, 1986.
36. Brolick, H.J. and Tennant, J.D., Innovative transport modes: coal slurry pipelines, ASME Fuels and Combustion Division Pub. *FACT*, 8, 85–91, 1990.
37. Manford, R.K., Coal-water slurry: a status report, *Energy*, 11, 11/12, 1157–1162, 1986.
38. Ng, K.L., Coal Unloading System Using a Slurry System, 281–287.
39. Hapeman, M.J., Review and Update of the Coal Fired Diesel Engine, 47–50.
40. Likos, W.E. and Ryan, III, T.W., Experiments with coal fuels in a high-temperature diesel engine, *J. Eng. Gas Turbines Power*, 110, 444–452, July 1988.
41. Rao, A.K., Melcher, C.H., Wilson, R.P., Jr., Balles, E.N., Schaub, F.S., and Kimberly, J.A., Operating results of the cooper-bessemer JS-1 engine on coal-water slurry, *J. Eng. Gas Turbines Power*, 110, 431–436, July 1988.
42. Urban, C.M., Mecredy, H.E., Ryan, III, T.W., Ingalls, M.N., and Jetss, B.T., Coal-water slurry operation in an EMD diesel engine, *J. Eng. Gas Turbines Power*, 110, 437–443, July 1988.
43. Hsu, B.D., Progress on the investigation of coal-water slurry fuel combustion in a medium speed diesel engine: Part 1 — ignition studies, *J. Eng. Gas Turbines Power*, 110, 415–422, July 1988.
44. Hsu, B.D., Progress on the investigation of coal-water slurry fuel combustion in a medium speed diesel engine: Part 2 — preliminary full load test, *J. Eng. Gas Turbines Power*, 110, 423–430, July, 1988.
45. Hsu, B.D., Leonard, G.L., and Johnson, R.N., Progress on the investigation of coal-water slurry fuel combustion in a medium speed diesel engine: Part 3 — accumulator injector performance, *J. Eng. Gas Turbines Power*, 110, 516–520, July 1988.
46. Wenglarz, R.A. and Fox, R.G., Jr., Physical aspects of deposition from coal-water fuels under gas turbine conditions, *J. Eng. Gas Turbines Power*, 112, 9–14, January 1990.
47. Wenglarz, R.A. and Fox, R.G., Jr., Chemical aspects of deposition/corrosion from coal-water fuels under gas turbine conditions, *J. Eng. Gas Turbines Power*, 112, 1–8, January 1990.
48. Dwyer, J.G., Australian coal water mixtures (CWM) plant development at Newcastle, NSW, *Proc. 19th Int. Tech. Conf. on Coal Utilization and Fuel Systems*, 1994, pp. 35–38.
49. Hamieh, T., Optimization of the interaction energy between particles of coal water suspensions, *Proc. 19th Int. Tech. Conf. on Coal Utilization and Fuel Systems*, 1994, pp. 103–114.
50. Vossoughi, S. and Al-Husaini, O.S., Rheological characterization of the coal/oil/water slurries and the effect of polymer, *Proc. 19th Int. Tech. Conf. on Coal Utilization and Fuel Systems*, 1994, pp. 123–131.
51. Tobori, N., Ukigia, T., Sugawara, H., and Arai, H., Optimization of additives for CWM commercial plant with a production rate of 500 thousand tons per year, *Proc. 19th Int. Tech. Conf. on Coal Utilization and Fuel Systems*, 1994, pp. 123–133.

52. Addy, S.N. and Considine, T.J., Retrofitting oil-fired boilers to fire coal water slurry: an economic evaluation, *Proc. 19th Int. Tech. Conf. on Coal Utilization and Fuel Systems*, 1994, pp. 341–352.
53. Kaneko, S., Suganuma, H., and Kabayashi, Y., Fundamental study on the combustion process of CWM, *Proc. 19th Int. Tech. Conf. on Coal Utilization and Fuel Systems*, 1994, pp. 403–414.
54. Takahashi, Y. and Shoji, K., Development and scale-up of CWM preparation process, *Proc. 19th Int. Tech. Conf. on Coal Utilization and Fuel Systems*, 1994, pp. 485–495.
55. Tu, J., Cefa, K., Zhou, J., Yao, Q., Fan, H., Cao, X., Qiu, Y., Huang, Z., Wu, X., and Liu, J., The comparing research on the ignition of the pulverized coal and the coal water slurry, *Proc. 19th Int. Tech. Conf. on Coal Utilization and Fuel Systems*, 1994, pp. 517–528.
56. Battista, J.J., Bradish, T., and Zawadzki, E.A., Test results from the co-firing of coal water slurry fuel in a 32 MW pulverized coal boiler, *Proc. 19th Int. Tech. Conf. on Coal Utilization and Fuel Systems*, 1994, pp. 619–630.
57. Miller, S.F., Morrison, J.L., and Scaroni, A.W., The formulation and combustion of coal water slurry fuels from impounded coal fines, *Proc. 19th Int. Tech. Conf. on Coal Utilization and Fuel Systems*, 1994, pp. 643–650.
58. Schimmeller, B.K., Jacobsen, P.S., and Hocko, R.E., Industrial use of technologies potentially applicable to the cleaning of slurry pond fines, *Proc. 19th Int. Tech. Conf. on Coal Utilization and Fuel Systems*, 1994, pp. 805–817.
59. Crippa, E.R., 50,000 HP coal slurry diesel engine, *Proc. 19th Int. Tech. Conf. on Coal Utilization and Fuel Systems*, 1994, pp. 821–828.
60. Bradish, T.J., Battista, J.J., and Zawadzki, E.A., Co-firing of water slurry in a 32 MW pulverized coal boiler, *Proc. 18th Int. Tech. Conf. on Coal Utilization and Fuel Systems*, 1993, pp. 303–313.
61. Yanagimacho, H., Matsumoto, O., and Tsuri, M., CWM production in China and CWM properties in all stages from production to combustion in the world's first bilateral CWM trade, *Proc. 18th Int. Tech. Conf. on Coal Utilization and Fuel Systems*, 1993, pp. 327–337.
62. Morrison, D.K., Melick, T.A., and Sommer, T.M., Utilization of coal water fuels in fire tube boilers, *Proc. 18th Int. Tech. Conf. on Coal Utilization and Fuel Systems*, 1993, pp. 339–347.
63. Pisupati, S.V., Britton, S.A., Miller, B.G., and Scarani, A.W., Combustion performance of coal water slurry fuel in an off-the -shelf 15,000 lb steam/h fuel oil designed industrial boiler, *Proc. 18th Int. Tech. Conf. on Coal Utilization and Fuel Systems*, 1993, pp. 349–360.
64. Morrison, J.L., Miller, B.G., and Scaroni, A.W., Preparing and handling coal water slurry fuels: potential problems and solutions, *Proc. 18th Int. Tech. Conf. on Coal Utilization and Fuel Systems*, 1993, pp. 361–368.
65. Battista, J.J. and Zawadzki, E.A., Economics of coal water slurry, *Proc. 18th Int. Tech. Conf. on Coal Utilization and Fuel Systems*, 1993, pp. 455–466.
66. Ohene, F., Luther, D., and Simon, U., Fundamental investigation of non-Newtonian behavior of coal water slurry on atomization, *Proc. 18th Int. Tech. Conf. on Coal Utilization and Fuel Systems*, 1993, pp. 607–617.
67. Kihm, K.D. and Kim, S.S., Investigation of dynamic surface tension of coal water slurry (CWS) fuels for application to atomization characteristics, *Proc. 18th Int. Tech. Conf. on Coal Utilization and Fuel Systems*, 1993, pp. 637–648.
68. Tu, J., Yao, Q., Cao, X., Cen, K., Ren, J., Huang, Z., Liu, J., Wu, X., and Zhao, X., Studies on thermal radiation ignition of coal water slurry, *Proc. 18th Int. Tech. Conf. on Coal Utilization and Fuel Systems*, 1993, pp. 659–668.

69. Hamich, T. and Siffert, B., Physical-chemical properties of coals in aqueous medium, *Proc. 18th Int. Tech. Conf. on Coal Utilization and Fuel Systems*, 1993, pp. 771–782.
70. Fullerton, K.L., Lee, S., and Kesavan, S., Laboratory scale dynamic stability testing for coal slurry fuel development, *Proc. 18th Int. Tech. Conf. on Coal Utilization and Fuel Systems*, 1993, pp. 799–808.
71. Hamich, T. and Siffert, B., Rheological properties of coal water highly concentrated suspensions, *Proc. 18th Int. Tech. Conf. on Coal Utilization and Fuel Systems*, 1993, pp. 809–820.
72. Zang, Z.-X., Zhang, L., Fu, X., and Jiang, L., Additive for coal water slurry made from weak slurrability coal, *Proc. 18th Int. Tech. Conf. on Coal Utilization and Fuel Systems*, 1993, pp. 821–833.
73. Everett, D.H., *Basic Principles of Colloid Science*, Royal Society of Chemistry, London, 1988.
74. Sadler, L.Y. and Sim, K.G., Minimize Solid-Liquid Mixture Viscosity By Optimizing Particle Size Distribution, *Chemical Engineering Progress*, 87(3), 1991, pp. 68–71.
75. Kawatra, S.K. and Bakshi, A.K., The on-line pressure vessel rheometer for concentrated coal slurries, *Coal Prep.*, 22(1), 2002.
76. Zakin, J., Zhang, Y., and Yunying, Q., Drag reducing agents, in *Encyclopedia of Chemical Processing*, Lee, S., Ed., Vol. 2, Taylor & Francis, New York, 2005, pp. 767–785.

5 Liquid Fuels from Natural Gas

James G. Speight

CONTENTS

5.1 INTRODUCTION

Natural gas is the gaseous mixture found in petroleum reservoirs. It consists predominantly of methane. Similar to petroleum and coal, this gas is derived from the remains of plants, animals, and microorganisms that lived millions and millions of years ago.

Natural gas, in itself, might be considered very uninteresting as it is colorless and odorless in its pure form. This gas is a combustible mixture of hydrocarbon gases, and although the major constituent is methane, ethane (C_2H_6), propane (C_3H_8), butane (C_4H_{10}), and pentane (C_5H_{12}) are also present. However, its composition varies widely. It is combustible and, when burned, produces energy. Unlike other fossil fuels, however, natural gas is clean burning and emits lower levels of potentially harmful by-products into the air.

Liquid fuels, on the other hand, are usually more complex mixtures of hydrocarbons than natural gas. Thus, for the purposes of this chapter, the term *liquid fuel* includes all liquids ordinarily and practically usable in internal combustion engines. Diesel and all types of aviation fuels also come under this definition.

Natural gas can also be used to produce alternative fuels. The term *alternative fuel* includes methanol, ethanol, and other alcohols; mixtures containing methanol and other alcohols with gasoline or other fuels; biodiesel; fuels (other than alcohol) derived from biological materials; and any other fuel that is substantially not a petroleum product.

The production of liquid fuels from sources other than petroleum broadly covers those produced from tar sand (oil sand), bitumen, coal, oil shale, and natural gas. These so-called synthetic liquid fuels (termed *synfuels*) have characteristics similar to those of petroleum-generated liquid fuels, but differ because the constituents of synfuels do not occur naturally in the source materials used for their production (Han and Chang, 1994). Thus, liquid fuels that are derived from sources other than natural crude petroleum are synfuels. For much of the 20th century, the emphasis was on liquid products derived from coal upgrading or by extraction or hydrogenation of organic matter in coke liquids, coal tars, tar sands, or bitumen deposits. It is only recently that potential of natural gas as a source of liquid fuels has been recognized, and attention is now focused on this new source of liquid fuel.

Projected shortages of petroleum make it clear that in the present century alternative sources of liquid fuels are necessary. Although such sources (for example, natural gas) are available, the exploitation technologies are in general not as mature as for petroleum. The feasibility of upgrading natural gas to valuable chemicals, especially liquid fuels, has been known for years. However, the high cost of steam reforming and the partial oxidation processes used for the conversion of natural gas to synthesis gas has hampered the widespread exploitation of natural gas. Other viable sources of liquid fuels include tar sand (also called oil sand or bituminous sand) (Berkowitz and Speight, 1975; Speight, 1990 and references cited therein) and coal (Speight, 1994 and references cited therein).

Natural gas, which typically has 85–95% methane, has been recognized as a plentiful and clean alternative feedstock to crude oil. Currently, the rate of discovery of proven natural gas reserves is increasing faster than the rate of natural gas production. Many of the large natural gas deposits are located in areas where abundant crude oil resources are located, such as the Middle East. However, huge reserves of natural gas are also found in many other regions of the world, providing oil-deficient countries access to a plentiful energy source. It is frequently located in remote areas far from any consumption centers, and pipeline costs can account for as much as one third of the total cost. Thus, tremendous strategic and economic incentives exist for gas conversion into liquids, especially if this can be accomplished on-site or at a point close to the wellhead so that transportation costs are minimized.

However, despite reduced prominence, coal continues to be a viable option for the production of liquid fuels in the future. World petroleum production is expected ultimately to level off and then decline, and despite the apparent surplus natural gas, its production too is expected to suffer a similar decline. Gasification of coal into synthesis gas (syngas) is utilized to synthesize liquid fuels in much the same manner as natural gas steam-reforming technology. It is more important, however, to exploit the available natural gas reserves to the maximum and by conversion of natural gas to liquid fuels.

Liquid fuels possess certain inherent advantages in terms of being more readily stored, transported, and metered than natural gas. They are also generally easy to process or clean by chemical and catalytic means, and are more compatible with 20th century fuel infrastructures, because most fuel-powered conveyances are designed to function only with relatively clean, low-viscosity liquids. Therefore, production of synfuels from alternative feedstocks is based on adjusting the hydrogen–carbon ratio to the desired intermediate level.

Thus, the purpose of this chapter is to describe the occurrence and production of liquid fuels from natural gas.

5.2 OCCURRENCE AND RESOURCES

Natural gas occurs in the porous rock of the earth's crust either alone or with accumulations of petroleum (Speight, 1993 and references cited therein). In the latter case, the gas forms the gas cap, which is the mass of gas trapped between the liquid petroleum and the impervious cap rock of the petroleum reservoir. When the pressure in the reservoir is sufficiently high, natural gas may be dissolved in the petroleum and is released upon penetration of the reservoir during drilling operations.

It is a fossil fuel and, similar to petroleum, is produced by the transformation of the remains of plants, animals, and microorganisms that lived millions and millions of years ago.

There is an abundance of natural gas in North America, but it is a nonrenewable resource and essentially irreplaceable. Therefore, understanding the availability of natural gas supply is important as the use of natural gas is increased. The British Petroleum (BP) report of 2003 shows the current estimates of natural gas availability worldwide (BP Statistical Review of World Energy, 2003). Thus, there is a vast amount of natural gas estimated to be still underground.

However, it is important to compare the different methodologies and systems of classification used in such estimates, as it is important to delve into the assumptions behind each study in order to gain a complete understanding of the estimate itself with a particular focus on proven and potential resources.

Constant revisions are being made to these estimates. New technology combined with increased knowledge of particular areas or reservoirs mean that these estimates are in a constant state of flux. Further complicating the scenario is the fact that there are no universally accepted definitions for the terms used differently by geologists, engineers, and resource accountants.

Most of the natural gas found in North America is concentrated in relatively distinct geographical areas, or basins. States located on top of a major basin have the highest level of natural gas reserves. U.S. natural gas reserves are mostly concentrated around Texas and the Gulf of Mexico.

5.3 COMPOSITION

Natural gas is colorless and odorless in its pure form. It is a combustible mixture of hydrocarbon gases. Although natural gas is formed primarily of methane, it can

TABLE 5.1
Typical Composition of Natural Gas

Constituent	Formula	v/v (%)
Methane	CH_4	70–90
Ethane	C_2H_6	0–5
Propane	C_3H_8	0–5
Butane	C_4H_{10}	0–5
Pentane	C_5H_{12}	0–5
Hexane (and higher)	$\geq C_6H_{14}$	Trace–5
Benzene (and higher)	$\geq C_6H_6$	Trace
Carbon dioxide	CO_2	0–8
Oxygen	O_2	0–0.2
Nitrogen	N_2	0–5
Hydrogen sulfide	H_2S	0–5
Rare gases	He, Ne, A, Kr, Xe	Trace
Water	H_2O	Trace–5

also include ethane, propane, butane, and pentane. The composition of natural gas can vary widely (Table 5.1) before it is refined. In its purest form, natural gas is almost pure methane (CH_4). Ethane, propane, and the other hydrocarbons are also commonly associated with natural gas (Table 5.1).

Natural gas is considered *dry* when it is almost pure methane, with most of the other commonly associated hydrocarbons having been removed. When other hydrocarbons are present it is considered *wet*.

Natural gas is commonly associated with petroleum reservoirs. Once brought to the surface from underground, the gas is refined to remove impurities such as water, other gases, sand, and various other compounds. Some of the constituent hydrocarbons (such as propane and butane) are removed and sold separately. After refining, the clean natural gas is transmitted through a network of pipelines to its point of consumption.

5.4 NATURAL GAS LIQUIDS

The term *natural gas liquid*, often referred to as *natural gasoline*, is used to designate the hydrocarbons having higher molecular weight than methane that also occur in natural gas (Speight, 1993, p. 141). Mixtures of liquefied petroleum gas, pentanes, and higher-molecular-weight hydrocarbons fall into this category. Care should be taken not to confuse *natural gasoline* with the term *straight-run gasoline* (often also incorrectly referred to as *natural gasoline*), which is gasoline distilled unchanged from petroleum.

Current estimates (December 2001) of natural gas liquids in the U.S. indicate that the reserves total up to 7993 million barrels.

5.5 CONVERSION OF NATURAL GAS TO LIQUIDS

Two routes can be used for the conversion of natural gas to liquid fuels via indirect technology, once the synthesis gas has been produced (Figure 5.1); both routes have been commercialized. One route involves use of the Fischer–Tropsch technology to produce liquid fuels directly or by further processing. The other route involves production of methanol, which is then converted to liquid fuels.

In general, the proven technology to upgrade methane is via steam reforming to produce syngas (carbon monoxide plus hydrogen). Such a gas mixture is clean, and when converted to liquids produces liquid fuels free of heteroatom compounds (except for some trace amount) that contain sulfur and nitrogen.

The direct methane conversion technology, which has received considerable attention, involves the oxidative coupling of methane to produce higher hydrocarbons such as ethylene. These olefin products (i.e., hydrocarbons containing the –C=C- function) may be upgraded to liquid fuels via catalytic oligomerization processes, as currently practiced in the petroleum and petrochemical industries (Speight, 1999 and references cited therein).

A second trend in synfuels is the increased attention to oxygenate compounds as alternative fuels, as a result of the growing environmental concern about burning fossil-based fuels. The environmental impact of the oxygenates, such as methanol, ethanol, and methyl *tert-butyl* ether (MTBE) requires very serious consideration, as the environmental issues regarding their use are not fully understood or resolved.

Thus, the use of natural gas for production of synfuels and chemicals offers a clean and economic alternative to conventional fuels and chemicals. For production of chemicals, the most promising scenarios involve manufacturing olefins, and also the resulting polymer products, at a remote location and shipping them to developed markets.

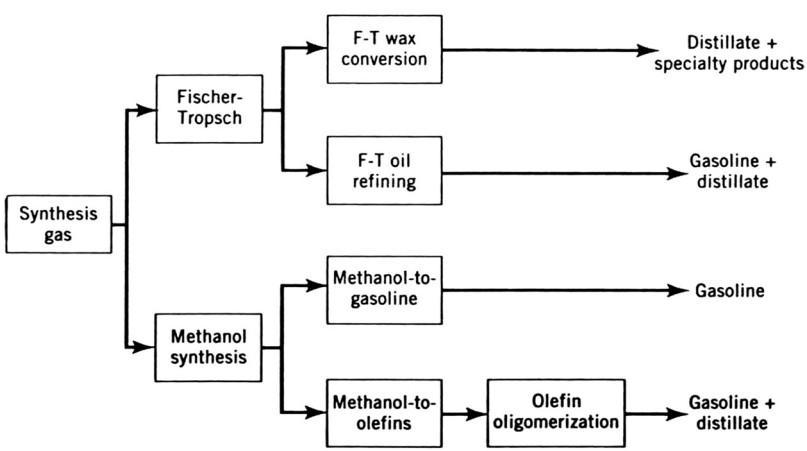

FIGURE 5.1 Natural gas to liquid fuels.

TABLE 5.2
Occurrence of Natural Gas

	Trillion Cubic Feet ($ft^3 \times 10^9$)	Percentage (%)
South and Central America	250.00	4.55
North America	252.47	4.59
Africa	418.07	7.60
Asia Pacific	445.26	8.10
Middle East	1979.49	35.98
Europe and Asia	2155.33	39.18
Total	5500.61	100.00

There are approximately 5500 trillion cubic feet (tcf) of proven natural gas reserves in the world (Table 5.2). The Middle East, Europe, and Asia together account for approximately 75% of these reserves.

Indirect liquefaction of coal and conversion of natural gas to synfuels is defined by technology that involves an intermediate step to generate syngas. Several technologies have been, and continue to be, evaluated by various companies, which include gas-to-liquids (GTL), methanol-to-gasoline (MTG), methanol-to-olefins (MTO), methanol-to-propylene (MTP), olefins-to-gasoline and distillates (MOGD), dimethyl ether (DME) processes, large-scale methanol processes, and power generation from methanol.

The commercially proven technologies by Shell (middle distillate synthesis process [MDS process]) and Sasol for the production of middle distillates via GTL processes show great potential for fuel alternatives and higher-value products.

Fischer–Tropsch naphtha and gas oils produced by various GTL processes are attractive for steam-cracking applications because of their high concentration of normal paraffin components. The high paraffinic content of the Fischer–Tropsch liquids allows them to be cracked at very high severities that are not usual for conventional feedstocks. When compared to conventional naphtha-cracking yields, the yields for Fischer–Tropsch naphtha show a higher selectivity to ethylene and less to heavier products such as butanes.

5.5.1 Syngas Production

Syngas is a mixture of carbon monoxide (CO) and hydrogen (H_2) that is manufactured by steam-reforming natural gas. A certain amount of carbon dioxide (CO_2) is also almost always produced.

$$CH_4 + H_2O \rightarrow CO + 3H_2$$

This gas is an extremely important precursor for the synthesis of methanol, hydrogen, ammonia, and other products. In particular, methane can be converted to syngas and gasoline produced from this mixture by the Fischer–Tropsch process.

Using this technology, gasoline is currently produced at Sasol, South Africa, and Malaysia. Methanol can be produced from syngas using the MTG process.

$$CO + 2H_2 \rightarrow CH_3OH$$

Syngas produced using existing methods account for about 60% of the total conversion cost of natural gas to gasoline. Thus, natural gas is an excellent choice for an abundant alternative energy source.

The trend to increase the number of hydrogenation (hydrocracking and/or hydrotreating) processes in refineries, coupled with the need to process the heavier oils, which require substantial quantities of hydrogen for upgrading, has resulted in vastly increased demands for this gas. A part of the demand for hydrogen can be satisfied by hydrogen recovery from catalytic reformer product gases, but other external sources are required (Bland and Davidson, 1967). Most of the external hydrogen is manufactured either by steam-methane reforming or by oxidation processes (Campbell, 1997). However, other processes, such as steam-methanol interaction or ammonia dissociation, may also be used as sources of hydrogen. Electrolysis of water produces high-purity hydrogen, but the power costs may be prohibitive.

Steam-methane reforming is a continuous catalytic process that has been employed for syngas production, and in some refineries for hydrogen production, over a period of several decades. The major reaction is the formation of carbon monoxide and hydrogen from methane and steam:

$$CH_4 + H_2O \rightarrow CO + 3H_2$$

But higher-molecular-weight feedstocks (such as propane and other hydrocarbon constituents of natural gas) may also yield carbon monoxide and hydrogen, which can be adjusted to fit the required ratio for syngas:

$$C_3H_8 + 3H_2O \rightarrow 3CO + 7H_2$$

that is,

$$C_nH_m + nH_2O \rightarrow nCO + (0.5m + n)H_2$$

In the actual process, the feedstock is first desulfurized by passing it through activated carbon, which may be preceded by caustic and water washes. The desulfurized material is then mixed with steam and passed over a nickel-based catalyst (730–845°C [1350–1550°F] and 400 psi). Effluent gases are cooled by the addition of steam or condensate to about 370°C (700°F), at which point (if hydrogen is the desired product) carbon monoxide reacts with steam in the presence of iron oxide in a shift converter to produce carbon dioxide and hydrogen. The carbon dioxide is removed by amine washing and the remaining hydrogen is usually a high-purity (>99%) material.

Another syngas generation process is a continuous, noncatalytic process that produces carbon monoxide and hydrogen by partial oxidation of gaseous or liquid

hydrocarbons. A controlled mixture of preheated feedstock and oxygen is fed to the top of the reactor, where carbon dioxide and steam are the primary products. A secondary reaction between the feedstock and the gases forms carbon monoxide and hydrogen.

If necessary for hydrogen production only, the effluent is then led to a shift converter with high-pressure steam, where carbon monoxide is converted to carbon dioxide with the concurrent production of hydrogen at the rate of 1 mol of hydrogen for every mole of carbon dioxide. Reactor temperatures vary from 1095 to 1480°C (2000–2700°F) and pressures from atmospheric to more than 1500 psi. Gas purification depends on the use of the gas.

5.5.2 Fischer–Tropsch Process

The hydrocarbon resources of the world are not evenly distributed. Substantial proportion of known reserves are situated in remote locations far from areas of high consumption. Transportation of liquid hydrocarbons from source to consumer is a task for which a large and flexible infrastructure exists. However, when natural gas deposits in remote locations are to be exploited, the transportation task becomes a major challenge, particularly if geography, economics, or a combination of both precludes the possibility of a pipeline.

There are two routes for the production of synfuels from natural gas (via syngas): (1) the hydrocarbon route and (2) the methanol route. Both routes are often referred to as the Fischer–Tropsch synthesis (Friedel and Anderson, 1950). The first step for both routes is the conversion of natural gas into syngas (a mixture of hydrogen and carbon monoxide with some carbon dioxide). The proportions of these components in the mixture vary according to the individual synthesis process selected, and also according to the product slate desired. Typical values of the principal characteristic, the H_2-to-CO ratio, for different processes cover a wide range from below 1 to nearly 3. The range of H_2-to-CO ratios required for the different synthesis processes means that considerable effort is required to match the syngas generation and synthesis process so as to ensure the optimum overall conversion rate. In addition, varying amounts of pure hydrogen may be required for hydrogenation of the crude product from the synthesis.

5.5.2.1 General Process Description

Fischer–Tropsch synthesis is a well-known process for conversion of syngas to synfuels and raw materials for the chemical industry. The process is versatile in its raw materials consumption, i.e., it can use any type of coal, natural gas, or similar types of carbon-containing feedstock as its material, and similarly the product distribution can also be changed. The increase of mineral oil prices has caused intense efforts to develop the Fischer–Tropsch process on a commercial scale. The details of the Fischer–Tropsch reactions and process are still not completely understood, even though the reaction was discovered 90 years ago.

Synfuels produced by the Fischer–Tropsch process are nowadays more expensive than natural-oil-based hydrocarbon fuels. However, under certain conditions and in

the next century, the process economics may become favorable. The process deserves special attention where: (1) coal reserves are significant and available at a cheaper rate and (2) natural gases are abundant. In the long run, production of hydrocarbon synthesis based on coal will exceed that of oil.

Syngas (a mixture of CO and H_2) can be obtained from coal or coke, natural gas, or similar type of carbon containing feedstock by steam-reforming or gasification processes (as described earlier). Catalysts are used for the production of hydrocarbons. Metals such as ruthenium (Ru), iron (Fe), and cobalt (Co) are usually deposited on an inert support, such as silica, alumina, or aluminosilicates, to increase the surface area of the catalyst (Espinoza et al., 1999; Steynberg et al., 1999). Addition of promoters to improve properties of the catalyst or selectivity are mostly applied. Typical reaction conditions of the Fischer–Tropsch process are P = 10–40 bar and T = 200–300°C.

5.5.2.2 Chemistry

In the Fischer–Tropsch synthesis, hydrocarbons (C_xH_y) are synthesized from carbon monoxide (CO) and hydrogen (H_2) (in other words, syngas). The Fischer–Tropsch process is an established technology and already applied on a large scale.

The number of chemical reactions involved in the manufacture of syngas is very large. The most important of these (limited to methane because it is the major constituent of natural gas), given the objective of producing carbon monoxide and hydrogen from the methane, are reforming (reaction 1) and partial oxidation (reaction 3), resulting in hydrogen-to-carbon-monoxide ratios of 3 and 2, respectively. If a source of carbon dioxide is available (or for natural gas rich in carbon dioxide), reforming with carbon dioxide (reaction 2) provides a hydrogen-to-carbon-monoxide ratio of 1. The figures for higher hydrocarbons in natural gas are correspondingly lower. The final hydrogen to carbon monoxide ratio is influenced further by the carbon monoxide shift reaction (reaction 5).

1. Reforming (strongly endothermic)

$$CH_4 + H_2O \rightarrow CO + 3H_2 \quad (1)$$

$$CH_4 + CO_2 \rightarrow 2CO + 2H_2 \quad (2)$$

2. Combustion (strongly exothermic)

$$2CH_4 + O_2 \rightarrow 2CO + 4H_2 \quad (3)$$

$$CH_4 + 2O_2 \rightarrow CO_2 + 2H_2O \quad (4)$$

3. Shift conversion (mildly exothermic)

$$CO + H_2O \rightarrow CO_2 + H_2 \quad (5)$$

Carbon

$$CH_4 \rightarrow 2H_2 + C \quad (6)$$

$$2\,CO \rightarrow CO_2 + C \quad (7)$$

The reforming reactions (reaction 1 and reaction 2) are strongly endothermic and must be supported by the strongly exothermic reactions of partial oxidation (reaction 3) and/or complete combustion (reaction 4). The latter reaction is, however, in principle less desirable as neither H_2 nor CO is produced.

Thus, in the Fischer–Tropsch reaction (exothermic) 1 mol of carbon monoxide reacts with 2 mol of hydrogen to form a hydrocarbon chain extension ($–CH_2–$). The oxygen from the CO is released as product water:

$$CO + 2H_2 \rightarrow –CH_2 + H_2O \qquad \Delta H = –165\ kJ/mol$$

The reaction implies a hydrogen to carbon monoxide ratio of at least 2 for the synthesis of the hydrocarbons. When the ratio is lower, it can be adjusted in the reactor with the catalytic water gas shift reaction:

$$CO + H_2O \rightarrow CO_2 + H_2 \qquad \Delta H = –42\ kJ/mol$$

When catalysts with water gas shift activity are used, water produced in the reaction can react with carbon monoxide to form additional hydrogen. In this case a minimal H_2 to CO ratio of 0.7 is required and the oxygen from the CO is released as CO_2:

$$2CO + H_2 \rightarrow CH_2 + CO_2 \qquad \Delta H = –204\ kJ/mol$$

The reaction affords mainly aliphatic straight-chain hydrocarbons (C_xH_y). Besides these straight-chain hydrocarbons, branched hydrocarbons, unsaturated hydrocarbons (olefins), and primary alcohols are also formed in minor quantities. The kind of liquid obtained is determined by the process parameters (temperature, pressure, etc.), the kind of reactor, and the catalyst used. Typical operation conditions for the Fischer–Tropsch synthesis are a temperature range of 200–350°C and pressures of 15–40 bar, depending on the process.

The Fischer–Tropsch process is a very complicated process that requires a well-defined choice of reactors, catalysts, and operating conditions to synthesize the desired products. Even then, a mixture of compounds is obtained. The Fischer–Tropsch synthesis was originally operated in packed-bed reactors. These reactors have several drawbacks that can be overcome by a slurry reactor. In these slurry reactors, the synthesis gas is bubbled through a suspension of catalyst particles (typically 30–50 μm) in an inert liquid. The heat of reaction is removed by circulating the slurry through external or internal heat exchangers. The slurry reactor can be operated at higher temperatures and at low H_2 to CO ratios without any problems due to efficient heat transfer and uniform temperatures. The application of very small catalyst particles caused no occurrence of intraparticle heat and mass transfer resistances.

Economic studies have shown that the Fischer–Tropsch synthesis in a slurry bubble column has several advantages over the fixed bed reactors. As the Fischer–Tropsch process offers a number of advantages in slurry phase over the two-phase processes, special attention is paid to the effects of an inert-liquid phase on the reaction rate, mass transfer, and product distribution.

5.5.2.3 Products

The subsequent chain growth in the Fischer–Tropsch process is comparable with a polymerization process, resulting in a distribution of chain lengths of the products. In general, the product range includes the light hydrocarbons methane (CH_4), ethane (C_2H_6), propane (C_3H_8), and butane (C_4H_{10}); naphtha (C_5H_{12} to $C_{12}H_{26}$); kerosene-diesel fuel ($C_{13}H_{28}$ to $C_{22}H_{46}$); low-molecular-weight wax ($C_{23}H_{48}$ to $C_{32}H_{66}$); and high-molecular-weight wax ($>C_{33}H_{68}$). Linear alpha-olefins are also produced, but the distribution of the products depends on the catalyst and the process operation conditions (temperature, pressure, and residence time).

The (theoretical) chain length distribution can be described by means of the Anderson–Schulz–Flory equation (Schulz, 1935, 1936; Flory, 1936; Friedel and Anderson, 1950),

$$\text{Log } W_n/n = 2 \log (\ln \alpha) + n\log \alpha$$

where W_n is the weight fraction of chains with *n* carbon atoms and the chain growth probability factor (α) that is defined by

$$\alpha = k_p/(k_p + k_t)$$

where k_p is the propagation rate and k_t is the termination rate.

5.5.2.4 Catalysts

Several types of catalysts can be used for the Fischer–Tropsch synthesis (Ponec, 1982; Snel, 1987; van der Laan and Beenackers, 1999). The most important catalysts are based on iron (Fe) or cobalt (Co). Cobalt catalysts have the advantage of a higher conversion rate and a longer life (over 5 years). It is more reactive for hydrogenation and produces less unsaturated hydrocarbons and alcohols compared to iron catalysts. Iron catalysts on the other hand, have a higher tolerance for sulfur, are cheaper, and produce more olefin products and alcohols. The lifetime of the iron catalysts is, however, short and in some commercial installations may be measured in weeks.

5.5.2.5 Commercial Processes

The three main industrially proven processes involve various versions of tubular steam reforming, catalytic autothermal reforming, and noncatalytic partial oxidation.

In tubular steam reforming, the methane–steam reaction (reaction 1) takes place over a catalyst in a tube that is externally heated. A large steam surplus is required to suppress carbon formation in the catalyst. This tends to drive the carbon monoxide shift reaction (reaction 5) to the right, resulting in a hydrogen-rich syngas. The heat

is supplied largely by the undesirable complete combustion reaction of methane to carbon dioxide and water (reaction 4) outside the tubes.

In catalytic autothermal reforming, oxygen is added to the feed. The heat requirement for the methane–steam reaction (reaction 1) is largely met by the methane–oxygen partial oxidation reaction (reaction 3), thus producing a lower hydrogen-to-carbon-monoxide ratio in the syngas. As in tubular reforming, considerable amounts of steam are required to suppress carbon formation. The absence of the metallurgical limitations of the catalyst tubes of a steam reformer allows higher operating temperatures, thus reducing methane slip. At these higher temperatures, the carbon monoxide shift equilibrium is also more favorable to carbon monoxide than in the case of the tubular steam reformer.

In noncatalytic partial oxidation, the reaction of methane with oxygen (reaction 3) is dominant. The absence of any catalyst means that the process is tolerant of a small degree of carbon formation and allows even higher operating temperatures. It is thus possible to operate partial oxidation without any steam addition, and the resulting syngas is rich in carbon monoxide.

The art of selecting the right syngas generation process (or combination of processes) consists of ensuring correct gas specification as required by the selected synthesis, and simultaneously minimizing certain inherent inefficiencies of the individual processes. In case of tubular reforming, this inherent inefficiency lies in the use of external complete combustion, requiring an expensive heat recovery train and still involving substantial losses in the stack gas. In the case of autothermal reforming and partial oxidation, the inefficiency lies in the energy requirement and investment for the oxygen plant (Fleshman, 1997).

Lurgi GmbH is currently involved in the design and supply of syngas production units for two major synfuel projects: one based on Sasol's Synthol process and the other using Shell's SMDS synthesis (Sie et al., 1991). There is a substantial difference in the hydrogen to carbon monoxide ratios required by the two processes, and this has led to the selection of different syngas production routes.

The Synthol process has been operated on a commercial scale since the 1950s by Sasol and has undergone some evolution. The initial process, the Arge Process, involved low temperatures (200–250°C), medium pressures, and a fixed catalyst bed. This process primarily produced a linear paraffin wax, which had use as petrochemical feedstock and also for transport fuels after further processing. This was the only process available until the 1950s and 1960s. Subsequently, the Sasol Synthol process was developed; it involved higher temperatures (300–360°C) and medium pressures, but used a circulating fluidized bed to produce light olefins for production of chemicals and gasoline components. This process has recently been updated to the Advanced Synthol process.

The latest development of Fischer–Tropsch technology is the Sasol slurry-phase reactor, an integral part of the Sasol slurry-phase distillate (SSPD) process, which conducts the synthesis reaction at low temperatures (200–250°C) and pressures. The process involves bubbling hot syngas through a liquid slurry of catalyst particles and liquid reaction products. Heat is removed from the reactor via coils within the bed, producing steam. Liquid products are removed from the reactor, and the liquid hydrocarbon wax separated from the catalyst. The gas streaming from the top of the

reactor is cooled to recover light hydrocarbons and reaction water. The Sasol slurry-phase technology has undergone several developments primarily concerned with catalyst formulations. Initial development used an iron-based catalyst, but recent developments have used a cobalt-based catalyst, giving greater conversion.

The Shell middle-distillate synthesis (SMDS) process is a two-step process (Figure 5.2) that involves Fischer–Tropsch synthesis of paraffinic wax called the heavy paraffin synthesis (HPS). The wax is subsequently hydrocracked and isomerized (in the presence of hydrogen) to yield a middle-distillate boiling-range product in the heavy paraffin conversion (HPC) (Sie et al., 1991; Eisenberg et al., 1998). In the heavy paraffin synthesis stage, wax is maximized by using a proprietary catalyst having high selectivity toward heavier products and by the use of a tubular, fixed bed reactor. The heavy paraffin conversion stage employs a commercial hydrocracking catalyst in a trickle flow reactor. The heavy paraffin conversion step allows for production of narrow-range hydrocarbons not possible with conventional Fischer–Tropsch technology.

The products manufactured are predominantly paraffinic, free from sulfur, nitrogen, and other impurities; and have excellent combustion properties. The very high cetane number and smoke point indicate clean-burning hydrocarbon liquids having reduced harmful exhaust emissions. This process has also been proposed for producing chemical intermediates, paraffinic solvents, and extra-high-viscosity-index lube oils.

The Lurgi combined reforming process was originally developed for large-scale methanol production, and it is this application that is described here. In the context of production of liquid fuels, it is suitable as a building block for the MTG or the MOGD process. For the high-pressure Synthol process, carbon dioxide needs to be purged from the system. The conventional tubular steam-reforming process as used for methanol syngas production produces a hydrogen to carbon monoxide ratio of over 4 and a stoichiometric ratio of 2.6–2.9 (i.e., a hydrogen-rich gas) depending on the quality of the natural gas feedstock.

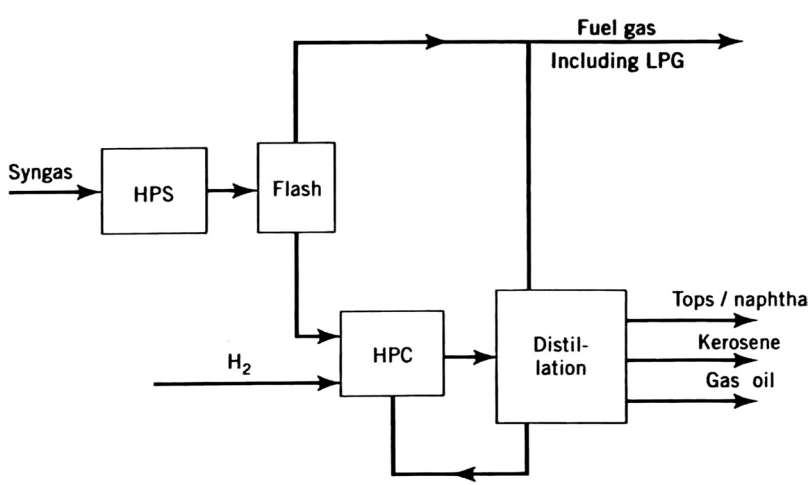

FIGURE 5.2 Shell middle-distillate synthesis (SMDS) process.

Autothermal reforming or partial oxidation produces carbon-monoxide-rich gases with hydrogen to carbon monoxide ratios in the range 1.5–3.5 and a stoichiometric number of about 1.8.

Approximately half the feed is processed in the tubular primary reformer. The other half, together with the primary reformer effluent, is autothermally reformed with pure oxygen in the secondary reformer. Besides matching hydrogen-rich and carbon-monoxide-rich process steps to produce an optimum stoichiometric ratio, the combined reforming process has other beneficial effects, such as the following:

- The methane slip of the overall reforming process is governed by the temperature of the secondary reformer, which is not subject to the same limitations of tube metallurgy as the tubular reformer. The combined process can thus provide a lower methane slip.
- Less syngas of the optimized quality is required per ton of methanol, reducing both the syngas compressor load and the capital cost of the synthesis unit.
- The operating temperature of the primary reformer need no longer be chosen to minimize methane slip. The reformer can also be operated under mild conditions. The higher operating pressure thus made possible enables the syngas compressor load to be further reduced.
- The reduced throughput through the primary reformer together with the lower operating temperature combine to reduce the tubular reformer to about 25% of the size required for the single-stage process. This reduces the stack gas losses referred to earlier by the same amount.

The Shell Gasification Process (SGP) process is a much older process, the basic development having been made in the 1950s. More than 150 units have been built in the last 50 years. With natural gas feedstock, the unit produces synthesis gas with a hydrogen-to-carbon-monoxide ratio of 1.7–1.8 and a carbon dioxide content of 1.7–3 volume percent, depending on the steam addition rate.

In the unit, the gas feed is preheated with the raw gas to a temperature of about 380°C for desulfurization prior to being fed to the SGP reactor with oxygen. The partial oxidation reaction takes place at about 1300–1400°C in the refractory-lined reactor. The sensible heat of the hot gas is used to generate high-pressure steam, with or without superheat as required. The noncatalytic partial oxidation reactor produces small amounts of soot that are washed out in a scrubber. The carbon is concentrated in the reaction water, which is discharged for wastewater treatment.

Comparison of the syngas quality with that produced by combined reforming shows a considerably lower hydrogen to carbon monoxide ratio of 1.86 with against 3.14 for combined reforming, making the SGP process a better match than, for instance, the SMDS process. Also, the amount of natural gas required to produce syngas is about 3.5% in this case. These advantages may be offset by higher oxygen requirements.

One feature common to all Fischer–Tropsch processes is the inherent lack of selectivity. The actual selectivity depends on the desired product slate, as well as on

the catalyst and the operating conditions. In all cases, however, substantial quantities of gaseous hydrocarbons, including methane, are produced.

In principle, it is desirable to recycle these gaseous hydrocarbons to produce more syngas. On the other hand, it is necessary to purge inert gases, principally argon and nitrogen. The other aspect of selectivity that requires recognition is that a proportion of higher-molecular-weight products, including waxes, is produced and may require hydrotreating for conversion to a saleable product (Dickenson et al., 1997).

The Syntroleum process is a cost-effective refinement of GTL technology that has been in use for several decades. A major advantage is that the process uses compressed air instead of pure oxygen to facilitate the conversion reaction, substantially reducing the capital costs and vastly improving the safety of the process plants.

The Syntroleum process consists of three major reaction steps: (1) natural gas is first partially oxidized with air to produce syngas, (2) syngas is then reacted in a Fischer–Tropsch reactor to produce liquid hydrocarbons of various chain lengths, and (3) higher-boiling fraction of the products is separated and hydrocracked to produce transportation fuels. The synfuels produced are middle distillates consisting of naphtha, kerosene, diesel, and other hydrocarbon-based products.

5.5.3 Other Processes

In the ExxonMobil AGC-21 process, there are three key steps (Lopez et al, 2003):

1. In the first step, syngas is generated by contacting methane with steam and a limited amount of oxygen in a high-capacity catalytic reactor.
2. Hydrocarbons are synthesized in the second step at high alpha as described by a Shulz-Flory distribution in a novel slurry reactor using new, high-productivity catalysts operating at high levels of syngas conversion. The full-range, primarily normal paraffin product contains significant 650°F+ waxy material that is solid at room temperature and melts above 250°F, and is unsuitable for pipelining or transporting in conventional crude carriers.
3. The final step, accomplished with proprietary catalysts in a packed bed reactor, converts wax to high-quality liquids that make excellent feeds for refineries and chemical plants, and directly marketable products in some instances, such as lube basestocks or specialty solvents.

The chemistry of each step is straightforward, yet becomes more complex as processes go to high yield and selectivity. Oxygen, methane, and steam ratios are carefully controlled to produce syngas (carbon monoxide and hydrogen) at stoichiometric proportions of about 2.1 to 1, hydrogen to carbon monoxide.

Methanol is produced catalytically from syngas and by-products, such as ethers and formic acid esters, and higher hydrocarbons, are formed during side reactions and are found in the crude methanol product. For many years methanol was produced from coal, but after World War II low-cost natural gas and light petroleum fractions replaced coal as the feedstock. Following this, one of the most significant developments in synfuels technology, since the discovery of the Fischer–Tropsch process, is the Mobil MTG process (Chang, 1983). Methanol is efficiently transformed into

hydrocarbons ranging from ethane to decane by a reaction that is catalyzed by synthetic zeolites.

$$nCH_3OH \rightarrow C_nH_{2n+2} + nH_2O$$

Olefins and aromatic compounds are also produced, but the reaction chemistry is more complex than suggested by this simple equation. For accuracy and economics, chemical equations should be derived for each particular aspect of the process.

In the process (which can use a fixed bed reactor or a fluid bed reactor), the methanol feed, vaporized by heat exchange with reactor effluent gases, is converted in a first-stage reactor containing an alumina catalyst to an equilibrium mixture of methanol, dimethyl ether (DME), and water. This is combined with recycled light gas, which serves to remove reaction heat from the highly exothermic MTG reaction, and enters the reactors containing zeolite catalyst, where reaction temperature conditions are 360–415°C at a pressure of approximately 300–350 psi.

As the MTG process produces primarily gasoline, a variation of that process has been developed that allows for production of gasoline and distillate fuel. The combined process (MTO and MOGO) produces gasoline and distillate in various proportions and, if needed, can be terminated at a point to produce olefin by-products.

In the MTO process, methanol is converted over a zeolite catalyst to give high yields of olefins with some ethylene and low-boiling light saturated hydrocarbons. Generally, catalyst and process variables that increase methanol conversion decrease olefins yield. In the MTO process, typical conversions exceed 99.9%. The coked catalyst is continuously withdrawn from the reactor and burned in a regenerator.

The MOGD-process, low-molecular-weight olefins produce oligomers in the gasoline-boiling range using a zeolite catalyst. Other distillate products are also produced. Gasoline to distillate product ratios can vary, depending on process conditions, from 0.2 to >100.

The direct conversion of natural gas (methane) to liquid fuels involves conversion of methane to the desired liquid fuels while bypassing the syngas step. Direct upgrading routes that have been extensively studied include direct partial oxidation to oxygenates, oxidative coupling to higher hydrocarbons, and pyrolysis to higher hydrocarbons.

In a series of patents, the Rentech process takes advantage of the synergism between iron-based Fischer–Tropsch synthesis and plasma-based syngas production. For example, in one process (Yakobson et al., 2002), the plasma-based syngas production is a front-end conversion process in which hydrocarbon feedstock, such as natural gas, is fed to a high-or low-temperature plasma torch or electrical arc reactor. The arc converts the feedstock into a hydrogen and carbon monoxide syngas. This syngas can then be converted by the Fischer–Tropsch process into liquid hydrocarbons. During Fischer–Tropsch synthesis using iron-based catalysts, a portion of the syngas is converted into carbon dioxide. By recycling the carbon dioxide extracted from the process, tail gas is returned to the plasma torch, where it can be efficiently converted into carbon monoxide, which in turn is fed to the Fischer–Tropsch reactor. The plasma can reform natural gas with only the addition of carbon dioxide from the Fischer–Tropsch reactor, producing a syngas consisting almost exclusively of carbon monoxide and hydrogen. In addition to the carbon dioxide

produced in the Fischer–Tropsch reactor, the reactor tail gas components can be converted into additional carbon monoxide and hydrogen for the Fischer–Tropsch reactor feedstock. This synergy between iron-based Fischer–Tropsch synthesis and plasma-based syngas production allows for significantly improved carbon conversion efficiency and is an excellent technique for reducing carbon dioxide emissions while producing cleaner fuels that are sulfur and aromatic free. Additionally, plasma-based syngas production offers distinct advantages over other methods of producing syngas as it does not need an air separation plant and has essentially no moving parts.

Oxygen-permeable membranes can potentially replace the expensive cryogenic oxygen plants for oxygen production. When combined with an appropriate catalyst on the oxygen-lean side, the membrane can be used to convert natural gas to synthesis gas via a partial oxidation reaction:

$$2CH_4 + O_2 \rightarrow CO + 2H_2$$

5.6 THE FUTURE

Fischer–Tropsch diesel has a high cetane number and can be manufactured free of both aromatics and sulfur. It can be used in existing distribution infrastructure and diesel engines, and compared to petroleum diesel has lower emissions of oxides of nitrogen and particulate matter. The near-zero sulfur content of Fischer–Tropsch diesel may also enable exhaust aftertreatment, resulting in further emission reductions. Thus, this diesel could help displace the diesel fuel that is typically used to power medium- and heavy-duty vehicles and meet specifications for extremely low-sulfur diesel fuel. If approved, Fischer–Tropsch diesel could be designated as an alternative fuel as early as winter 2004.

The syngas production routes described earlier are based on proven technologies and provide us with reliable starting points for the development of processes that offer the potential for further reduction of both capital and operating costs.

For some syntheses, the use of straight catalytic autothermal reforming can be an advantage. Lurgi has used this process both for methanol production and treating Fischer–Tropsch tail gases. Whereas in a secondary reformer configuration the hot hydrogen-rich primary reformer effluent is self-igniting, ignition of a straight autothermal reformer requires the use of a noble-metal-promoted ignition catalyst. Velocities in the ignition-catalyst area must be kept high to eliminate any possibility of backburning. These high velocities lead over a period of time to mechanical attrition of the expensive ignition catalyst. As part of the ongoing development of its reforming processes, the process arrangement has been modified to bring the operating conditions closer to that of a secondary reformer, thus dispensing with the need for the ignition catalyst.

The HCT reforming technology is based on the use of the so-called HCT reformer tube. In principle, this is a normal centrifugally cast reformer tube, catalyst filled, heated from outside, and normally designed for downflow of the process gas through the catalyst bed. But on the inside it encloses a double helix made of tubes of suitable material embedded in the catalyst. The reformed process gas passes this double helix in a counterflow to the process gas flow through the catalyst bed, thus

transferring a part of its sensible heat to the reforming process. Calculations and practical experience have shown that based on an inlet temperature of 450°C and reaction-end temperature of 860°C, this internal heat transfer covers up to 20% of sensible and reaction heat of the process gas. In addition to the resultant saving of fuel, an investment saving of about 15% can be expected, the bulk of which is attributable to the smaller convection bank required.

REFERENCES

Anderson, R.B., *The Fischer Tropsch Synthesis*, Academic Press, New York, 1984.

Berkowitz, N. and Speight, J.G., *Fuel,* 54:138, 1975.

Bland, W.F. and Davidson, R.L., *Petroleum Processing Handbook*, McGraw-Hill, New York, 1967.

BP (British Petroleum), BP Statistical Review of World Energy, British Petroleum, London, see also http://www.bp.com/centres/energy/index.asp, 2003.

Campbell, W.M., in *Handbook of Petroleum Refining Processes*, Meyers, R.A., Ed., McGraw-Hill, New York, 1997, chap. 6.1.

Chang, C.D., *Catal. Rev.: Sci. Eng.*, 25: 1, 1983.

Dickenson, R.L., Biasca, F.E., Schulman, B.L., and Johnson, H.E, *Hydrocarbon Process.*, 76(2): 57, 1997.

Eisenberg, B., Fiato, R.A., Mauldin, C.H., Ray, G.R., and Soled, R.L., *Stud. Surf. Sci. Catal.*, 119: 943, 1998.

Espinoza, R.L., Steynberg, A.P., Jager, B., and Vosloo, A.C., *Appl. Catal. Gen.*, 186: 13, 1999.

Fleshman, J.D., in *Handbook of Petroleum Refining Processes*, Meyers, R.A., Ed., McGraw-Hill, New York, 1997, chap. 6.2.

Flory, P.J., *J. Am. Chem. Soc.*, 58: 1877, 1936.

Friedel, R.A. and Anderson, R.B., *J. Am. Chem. Soc.*, 72: 2307, 1950.

Han, S. and Chang, C.D., Synthetic (liquid) fuels, in *Kirk-Othmer Encyclopaedia of Chemical Technology*, Kroschwitz, J.I. and Howe-Grant, M., Eds., 4th ed., Vol. 12, John Wiley & Sons, New York, 1994, p. 155.

Lopez, A.M., Fiato, R.A., Ansell, I.L., Quinlan, C.W., and Ramage, M.P., *Hydrocarbon Asia*, July/August, 2003, p. 56.

Ponec, V., in *Metal Support and Metal Additive Effects in Catalysis*, Imelik, B., Ed., Elsevier, Amsterdam, The Netherlands, 1982, p. 63 et seq.

Schulz, G.V., *Z. Phys. Chem.*, B30: 379, 1935.

Schulz, G.V., *Z. Phys. Chem.*, B32: 27, 1936.

Sie, S.T., Senden, M.M.G., and van Wechum, H.M.H., *Catalysis Today*, 8, 1991, p. 371.

Snel, R., *Catal. Rev.: Sci. Eng.*, 29: 361, 1987.

Speight, J.G., in *Fuel Science and Technology Handbook*, Speight, J.G., Ed., Part V, Marcel Dekker, New York, 1990.

Speight, J.G., *Gas Processing: Environmental Aspects and Methods*, Butterworth-Heinemann, Oxford, 1993.

Speight, J.G., *The Chemistry and Technology of Coal*, 2nd ed., Marcel Dekker, New York, 1994.

Speight, J.G., *The Chemistry and Technology of Petroleum*, 3rd ed., Marcel Dekker, New York, 1999.

Steynberg, A.P., Espinoza, R.L., Jager, B., and Vosloo, A.C., *Appl. Catal. Gen.*, 186: 41, 1999.

Van der Laan, G.P. and Beenackers, A.A.C.M., *Catal. Rev.: Sci. Eng.*, 41: 255, 1999.

Yakobson, D.L., Vavruska, J.S., Bohn, E., and Blutke, A., U.S. Patent No. 6,380,268, April 30, 2002.

6 Resids

James G. Speight

CONTENTS

6.1 INTRODUCTION

Approximately 2000 years ago, Arab scientists developed methods for the distillation of petroleum, and interest in the thermal product of petroleum (nafta; naphtha) was aroused when it was discovered that this material could be used as an illuminant and as a supplement to asphalt incendiaries in warfare. The discovery also led to the production of resids, which may have been used when the supply of bitumen or natural asphalt from natural seepages became limited.

A *residuum* (plural *residua*, also shortened to *resid*, plural *resids*) is the residue obtained from petroleum after nondestructive distillation has removed all the volatile materials. The temperature of the distillation is usually maintained below that at which the rate of thermal decomposition of petroleum constituents is minimal.

Residua are black, viscous materials and are obtained by distillation of a crude oil under atmospheric pressure (atmospheric residuum) in an atmospheric distillation unit (atmospheric tower, atmospheric pipe still) or under reduced pressure (vacuum residuum) in a vacuum distillation unit (vacuum tower, vacuum pipe still) (Figure 6.1). They may be liquid at room temperature (generally, atmospheric residua) or almost solid (generally, vacuum residua), depending on the nature of the petroleum from which the resid was obtained (Table 6.1) or depending on the cut point of the distillation (Table 6.2).

Resids contain very-high-molecular-weight molecular polar species called *asphaltenes* that are soluble in carbon disulfide, pyridine, aromatic hydrocarbons, and chlorinated hydrocarbons (Gruse and Stevens, 1960; Speight, 1999; Van Gooswilligen, 2000). They are the nonvolatile fractions of petroleum that are isolated from the atmospheric distillation unit and form the vacuum distillation unit. Resids

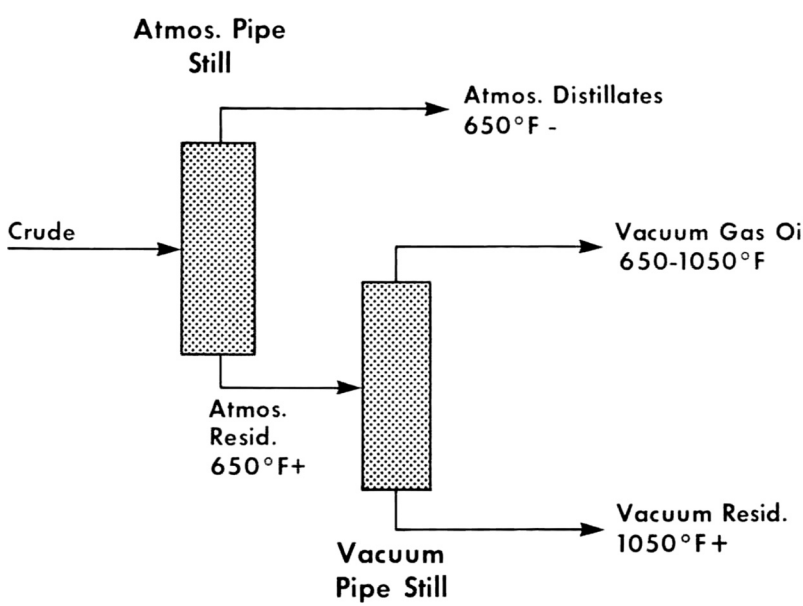

FIGURE 6.1 Schematic of resid production.

TABLE 6.1
Properties of Atmospheric and Vacuum Resids from Different Crude Oils

Crude oil origin	Kuwait		Khafji		Bachaquero		West Texas		Safaniya		Alaska (North Slope)		Tia Juana (ight)	
Residuum type	Atmos-pheric	Vacuum	Atmos-pheric	Vacuum	Atmos-pheric	Vacuum	Atmos-pheric	Vacuum	Atmos-pheric	Vacuum	Atmos-pheric	Vacuum	Atmos-pheric	Vacuum
Fraction of crude, vol%	42	21	—	—	34	—	—	—	40	22	58	22	49	18
Gravity, °API	13.9	5.5	14.4	6.5	17	2.8	9.4	18.4	11.1	2.6	15.2	8.2	17.3	7.1
Viscocity SUS, 210°F	—	—	—	—	—	—	—	—	—	—	1281	—	165	—
SPS, 122°F	553	500,000	—	—	—	—	313	86	—	—	—	—	172	—
SPS, 210°F	—	—	429	—	—	—	—	—	—	—	—	—	—	—
cSt, 100°F	—	—	—	—	—	—	—	—	—	—	—	—	890	—
cSt, 210°F	55	1900	—	—	—	—	—	—	—	—	42	1950	35	7959
Pour Point, °F	65	—	—	—	—	—	—	—	—	—	75	—	—	—
Sulfur, wt%	4.4	5.45	4.1	5.3	2.4	3.7	3.3	2.5	4.3	5.3	1.6	2.2	1.8	2.6
Nitrogen, wt%	0.26	0.39	—	—	0.3	0.6	0.5	0.6	0.4	0.4	0.36	0.63	0.3	0.6
Metals, ppm														
Nickel	14	32	37	53	450	100	27	11	26	46	18	47	25	64
Vanadium	50	102	89	178	—	900	57	20	109	177	30	82	185	450
Asphaltenes, wt%														
Pentane insolubles	—	11.1	—	12.0	10	—	—	—	17.0	30.9	4.3	8.0	—	—
Hexane insolubles	—	—	—	—	—	—	—	—	—	—	—	—	—	—
Heptane insolubles	2.4	7.1	—	—	—	—	—	—	—	—	31.5	—	—	—
Resin, wt%	—	39.4	—	—	—	—	—	—	—	—	—	—	—	—
Carbon residue, wt%														
Ramsbottom	9.8	—	—	—	—	—	—	—	—	—	8.4	17.3	—	—
Conradson	12.2	23.1	—	21.4	12	27.5	16.9	6.6	14.0	25.9	—	—	9.3	21.6

Source: From Speight, J.G., *The Desulfurization of Heavy Oils and Residua*, 2nd ed., Marcel Dekker, New York, 2000. With permission.

TABLE 6.2
Properties of Tia Juana Crude Oil and Resids Produced Using Deferent Cut Points

Boiling range									
°F	Whole crude	>430	>565	>650	>700	>750	>850	>950	>1050
°C	Whole crude	>220	>295	>345	>370	>400	>455	>510	>565
Yield on crude, vol%	100.0	70.2	57.4	48.9	44.4	39.7	31.2	23.8	17.9
Gravity, °API	31.6	22.5	19.4	17.3	16.3	15.1	12.6	9.9	7.1
Specific gravity	0.8676	0.9188	0.9377	0.9509	0.9574	0.9652	0.9820	1.007	1.0209
Sulfur, wt%	1.08	1.42	1.64	1.78	1.84	1.93	2.12	2.35	2.59
Carbon residue (Conradson), wt%	—	6.8	8.1	9.3	10.2	11.2	13.8	17.2	21.6
Nitrogen, wt%	—	—	—	0.33	0.36	0.39	0.45	0.52	0.60
Pour point, °F	–5	15	30	45	50	60	75	95	120
Viscosity:									
Kinematic, cSt	10.2	83.0	315	890	1590	3100	—	—	—
@ 100°F	10.2	83.0	315	890	1590	3100	—	—	—
@ 210°F	—	9.6	19.6	35.0	50.0	77.0	220	1010	7959
Furol (SFS) sec									
@ 122°F	—	—	70.6	172	292	528	—	—	—
@ 210°F	—	—	—	—	25.2	37.6	106	484	3760
Universal (SUS) sec @ 210°F	—	57.8	96.8	165	234	359	1025	—	—
Metals:									
Vanadium, ppm	—	—	—	185	—	—	—	—	450
	—	—	—	25	—	—	—	—	64
	—	—	—	28	—	—	—	—	48

Source: From Speight, J.G., *The Desulfurization of Heavy Oils and Residua*, 2nd ed., Marcel Dekker, New York, 2000. With permission.

derive their characteristics from the nature of their crude oil precursor, with some variation possible by choice of the end point of the distillation.

When a residuum is obtained from a crude oil and thermal decomposition has commenced, it is more usual to refer to this product as *pitch*. The differences between parent petroleum and the residua are due to the relative amounts of various constituents present, which are removed or remain by virtue of their relative volatility.

The chemical composition of a residuum from an asphaltic crude oil is complex and subject to the method of production (i.e., the temperature at which the distillation is carried out). Physical methods of fractionation usually indicate high proportions of asphaltenes and resins, even in amounts up to 50% (or higher) of the residuum. In addition, the presence of ash-forming metallic constituents, including such organometallic compounds as those of vanadium and nickel, is also a distinguishing feature of residua and heavy oils. Furthermore, the deeper the *cut* into the crude oil, the greater the concentration of sulfur and metals in the residuum and the greater the deterioration in physical properties (Speight, 2000, and references cited therein).

Even though a resid is a manufactured product, the constituents do occur naturally as part of the native petroleum, assuming that thermal decomposition has not taken place during distillation. Resids are specifically produced during petroleum refining, and the properties of the various residua depend upon the cut point or boiling point at which the distillation is terminated.

6.2 RESID PRODUCTION

Resid production involves distilling everything possible from crude petroleum until a nonvolatile residue remains. This is usually done by stages (Speight and Ozum, 2002) in which distillation at atmospheric pressure removes the lower-boiling fractions and yields an atmospheric residuum (*reduced crude*) that may contain higher-boiling (lubricating) oils, wax, and asphalt.

The *atmospheric distillation* tower is divided into a number of horizontal sections by metal trays or plates, and each is the equivalent of a still. The greater the number of trays, the greater the degree of redistillation and, hence, the better the fractionation or separation of the mixture fed into the tower. A tower for fractionating crude petroleum may be 13 ft. in diameter and 85 ft. high with 16 to 28 trays. The feed to a typical tower enters the vaporizing or flash zone, an area without trays. The majority of the trays are usually located above this area. The feed to a bubble tower, however, may be at any point from top to bottom with trays above and below the entry point, depending on the kind of feedstock and the characteristics desired in the products.

However, the usual permissible temperature in the vaporizing zone to which the feedstock can be subjected is usually considered to be 350°C (660°F). The rate of thermal decomposition increases markedly above this temperature; if decomposition occurs within a distillation unit, it can lead to coke deposition in the heater pipes or in the tower itself with the resulting failure of the unit. Some distillation units use temperatures in the vaporizing zone up to 393°C (740°F) and reduce the residence time in the hot zone. Caution is advised when using a higher temperature because units that are unable to continually attain the petroleum flow-through as specified

in the design can suffer from resid decomposition (owing to longer residence times in the vaporizing zone) and poorer-quality asphalt.

Distillation of the reduced crude under vacuum removes the oils (and wax) as overhead products, and the asphalt remains as a bottom (or residual) product. The majority of the polar functionalities and high-molecular-weight species in the original crude oil, which tend to be nonvolatile, are concentrated in the vacuum residuum (Speight, 2000), thereby conferring desirable or undesirable properties on the asphalt.

At this stage, the residuum is frequently and incorrectly referred to as *pitch* and has a softening point (ASTM D-36, ASTM D-61, ASTM D-2319, ASTM D-3104, ASTM D-3461) related to the amount of oil removed, and increases with increasing overhead removal. In character with the elevation of the softening point, the pour point is also elevated: the more the oil distilled from the residue, the higher the softening point.

Vacuum distillation has seen wide use in petroleum refining because the boiling point of the heaviest cut obtainable by distillation at atmospheric pressure is limited by the temperature in the vaporizing zone (about 350–390°C [660–740°F]) at which the residue starts to decompose or *crack*, unless *cracking distillation* is preferred. When the feedstock is required for the manufacture of lubricating oils, further fractionation without cracking is desirable, and this can be achieved by distillation under vacuum conditions.

The fractions obtained by vacuum distillation of reduced crude include:

1. *Heavy gas oil*, an overhead product, used as catalytic cracking stock or, after suitable treatment, a light lubricating oil
2. *Lubricating oil* (usually three fractions: light, intermediate, and heavy), obtained as a sidestream product
3. *Vacuum residuum*, the nonvolatile product that may be used directly as asphalt or to asphalt

The residuum may also be used as a feedstock for a coking operation or blended with gas oils to produce a heavy fuel oil.

6.3 PROPERTIES

Resids exhibit a wide range of physical properties, and there are several relationships between various physical properties (Speight, 1999). Whereas properties such as viscosity, density, boiling point, and color of petroleum may vary widely, the ultimate or elemental analysis varies, as already noted, over a narrow range for a large number of samples. The carbon content is relatively constant, though the hydrogen and heteroatom contents are responsible for the major differences between petroleum. The nitrogen, oxygen, and sulfur can be present in only trace amounts in some petroleum, which as a result consists primarily of hydrocarbons.

The properties of resids are defined by a variety of standard tests that can be used to define quality (Table 6.3). And remembering that the properties of residua vary with cut point (Table 6.2), i.e., the vol% of the crude oil helps the refiner produce asphalt of a specific type or property.

TABLE 6.3
Analytical Inspections for Petroleum and Resids

Petroleum	Heavy Feedstocks
Density (specific gravity)	Density (specific gravity)
API gravity	API gravity
Carbon (wt%)	Carbon (wt%)
Hydrogen (wt%)	Hydrogen (wt%)
Nitrogen (wt%)	Nitrogen (wt%)
Sulfur (wt%)	Sulfur (wt%)
	Nickel (ppm)
	Vanadium (ppm)
	Iron (ppm)
Pour point	Pour point
Wax content	
Wax appearance temperature	
Viscosity (various temperatures)	Viscosity (various temperatures)
Carbon residue of residuum	Carbon residue[a]
	Ash (wt%)
Distillation profile	Fractional composition
All fractions plus vacuum residue	Asphaltenes, wt%
	Resins (wt%)
	Aromatics (wt%)
	Saturates (wt%)

[a] Conradson carbon residue or microcarbon residue.

Properties such as the API gravity and viscosity also help the refinery operator to gain an understanding of the nature of the material that is to be processed. The products from high-sulfur feedstocks often require extensive treatment to remove (or change) the corrosive sulfur compounds. Nitrogen compounds and the various metals that occur in crude oils will cause serious loss of catalyst life. The carbon residue indicates the amount of thermal coke that may be formed to the detriment of the liquid products.

6.3.1 Elemental (Ultimate) Analysis

The analysis of resids for the percentages of carbon, hydrogen, nitrogen, oxygen, and sulfur is perhaps the first method used to examine the general nature and perform an evaluation. The atomic ratios of the various elements to carbon (i.e., H/C, N/C, O/C, and S/C) are frequently used for indications of the overall character of the resid. It is also of value to determine the amounts of trace elements, such as vanadium and nickel, in a resid because these materials can have serious deleterious effects on process and product performance.

Resids are not composed of a single chemical species, but are rather complex mixtures of organic molecules that vary widely in composition and are composed of carbon, hydrogen, nitrogen, oxygen, and sulfur as well as trace amounts of

metals, principally vanadium and nickel. The heteroatoms, although a minor component compared to the hydrocarbon moiety, can vary in concentration over a wide range depending on the source of the asphalt and hence can be a major influence on asphalt properties.

Generally, most resids contain 79–88% w/w carbon, 7–13% w/w hydrogen, trace–8% w/w sulfur, 2–8% w/w oxygen, and trace–3% w/w nitrogen. Trace metals such as iron, nickel, vanadium, calcium, titanium, magnesium, sodium, cobalt, copper, tin, and zinc occur in crude oils. Vanadium and nickel are bound in organic complexes and, by virtue of the concentration (distillation) process by which asphalt is manufactured, are also found in resids.

Thus, elemental analysis is still of considerable value in determining the amounts of elements in resids, and the method chosen for the analysis may be subject to the peculiarities or character of the resid under investigation and should be assessed in terms of accuracy and reproducibility. The methods that are designated for elemental analysis are:

1. *Carbon* and *hydrogen content* (ASTM D-1018, ASTM D-3178, ASTM D-3343, ASTM D-3701, ASTM D-5291, ASTM E-777, IP 338)
2. *Nitrogen content* (ASTM D-3179, ASTM D-3228, ASTM D-3431, ASTM E-148, ASTM E-258, ASTM D-5291, and ASTM E-778)
3. *Oxygen content* (ASTM E-385)
4. *Sulfur content* (ASTM D-124, ASTM D-129, ASTM D-139, ASTM D-1266, ASTM D-1552, ASTM D-1757, ASTM D-2622, ASTM D-2785, ASTM D-3120, ASTM D-3177, ASTM D-4045 and ASTM D-4294, ASTM E-443, IP 30, IP 61, IP 103, IP 104, IP 107, IP 154, IP 243)

The most pertinent property in many contexts is the *sulfur content* which, along with the API gravity, represents the two properties that have the greatest influence on the value of a resid.

The sulfur content varies from about 2% to about 6% for residua (Speight, 2000 and references cited therein). In fact, the nature of the distillation process by which residua are produced (i.e., removal of distillate without thermal decomposition) dictates that the majority of the sulfur, which is predominantly in the higher-molecular-weight fractions, be concentrated in the resid (Gary and Handwerk, 1984).

6.3.2 Metallic Content

Resids contain relatively high proportions of metals either in the form of salts or as organometallic constituents (such as the metallo-porphyrins), which are extremely difficult to remove from the feedstock. Indeed, the nature of the process by which residua are produced virtually dictates that all the metals in the original crude oil be concentrated in the residuum (Speight, 1999). Those metallic constituents that may actually *volatilize* under the distillation conditions and appear in the higher-boiling distillates are the exceptions here.

Determination of metals can be carried out by direct methods (ASTM, 2003) and also by indirect methods in which the sample is combusted so that only inorganic

ash remains. The ash can then be digested with an acid, and the solution examined for metal species by atomic absorption (AA), spectroscopy, or by inductively coupled argon plasma (ICP) spectrometry.

6.3.3 Density and Specific Gravity

Density is defined as the mass of a unit volume of material at a specified temperature and has the dimensions of grams per cubic centimeter (a close approximation to grams per milliliter). *Specific gravity* is the ratio of the mass of a volume of the substance to the mass of the same volume of water and is dependent on two temperatures, namely, those at which the masses of the sample and the water are measured. The *API gravity* is also used.

For clarification, it is necessary to understand the basic definitions that are used: (1) *density* is the mass of liquid per unit volume at 15.6°C (60°F), (2) *relative density* is the ratio of the mass of a given volume of liquid at 15.6°C (60°F) to the mass of an equal volume of pure water at the same temperature, and (3) *specific gravity* is the same as the relative density, and the terms are used interchangeably.

Although there are many methods for the determination of density owing to the different nature of petroleum itself, the accurate determination of the API gravity of petroleum and its products (ASTM D-287) is necessary for the conversion of measured volumes to volumes at the standard temperature of 60°F (15.56°C). Gravity is a factor governing the quality of crude oils. However, the gravity of a petroleum product is an uncertain indication of its quality. Correlated with other properties, gravity can be used to give approximate hydrocarbon composition and heat of combustion. This is usually accomplished though use of the API gravity that is derived from the specific gravity:

$$\text{API gravity, deg} = (141.5/\text{sp gr } 60/60°\text{F}) - 131.5$$

and is also a critical measure of the quality of petroleum.

API gravity or density or relative density can be determined using one of two hydrometer methods (ASTM D-287, ASTM D-1298). The use of a digital analyzer (ASTM D-5002) is finding increasing popularity for the measurement of density and specific gravity.

Most resids have a specific gravity of petroleum higher than 1.0 (10 API), with most resids having an API gravity on the order of 5 to 10 API.

6.3.4 Viscosity

Viscosity is the single most important fluid characteristic governing the motion of resids and is actually a measure of the internal resistance to motion of a fluid by virtue of the forces of cohesion between molecules or molecular groupings. It is generally the most important property for monitoring resid behavior in pipes when the resid is moved from one unit to another.

A number of instruments are commonly used with resids for this purpose. The vacuum capillary (ASTM D-2171) is commonly used to classify paving asphalt at

60°C (140°F). Kinematic capillary instruments (ASTM D-2170, ASTM D-4402) are commonly used in the 60 to 135°C (140 to 275°F) temperature range for both liquid and semisolid asphalts in the range of 30 cSt to 100,000 cSt. Saybolt tests (ASTM D-88) are also used in this temperature range and at higher temperatures (ASTM E-102). At lower temperatures, the cone-and-plate instrument (ASTM D-3205) has been used extensively in the viscosity range 1,000 P to 1,000,000 P.

The viscosity of resids varies markedly over a very wide range and is dependent on the cut point at which the distillation is terminated. Values vary from less than several hundred centipoises at room temperature to many thousands of centipoises at the same temperature. In the present context, the viscosity of vacuum resids is at the higher end of this scale, where a relationship between viscosity and density has been noted.

6.3.5 Carbon Residue

The carbon residue presents indications of the *coke-forming propensity* of a resid. There are two older well-established methods for determining the carbon residue: the Conradson method (ASTM D-189) and the Ramsbottom method (ASTM D-524). A third, more modern, thermogravimetric method (ASTM D-4530) is also in use.

Resids have high carbon residues, and resids that contain metallic constituents will have erroneously high carbon residues. The metallic constituents must first be removed from the resid, or they can be estimated as ash by complete burning of the coke after carbon residue determination.

The *carbon residue* of a resid serves as an indication of the propensity of the sample to form carbonaceous deposits (thermal coke) under the influence of heat. The produced are also often used to provide thermal data that give an indication of the composition of the asphalt (Speight, 1999; Speight, 2001).

Tests for Conradson carbon residue (ASTM D-189, IP 13), the Ramsbottom carbon residue (ASTM Test Method D524, IP 14), the microcarbon carbon residue (ASTM D4530, IP 398), and asphaltene content (ASTM D-2006, ASTM D-2007, ASTM D-3279, ASTM D-4124, ASTM D-6560, IP 143) are often included in inspection data for resids. All three methods are applicable to resids. The data give an indication of the amount of coke that will be formed during thermal processes as well of the amount of asphaltenes in the resid.

The produced by the microcarbon test (ASTM D4530, IP 398) are equivalent to those by Conradson Carbon method (ASTM D-189 IP 13). However, this micro-carbon test method offers better control of test conditions and requires a smaller sample. Up to 12 samples can be run simultaneously.

Other test methods (ASTM D-2416, ASTM D-4715) that indicate the relative coke-forming properties of tars and pitches might also be applied to resids. Both test methods are applicable to resids having an ash content ≤0.5% (ASTM D-2415). The former test method (ASTM D-2416) gives results close to those obtained by the Conradson carbon residue test (ASTM D-189 IP 13). However, in the latter test method (ASTM D-4715), a sample is heated for a specified time at 550 ± l0°C (1022 ± 18°F) in an electric furnace. The percentage of residue is reported as the coking value.

Resids that contain ash-forming constituents will have an erroneously high carbon residue, depending on the amount of ash formed.

6.3.6 Heat of Combustion

The gross heat of combustion of crude oil and its products is given with fair accuracy by the equation:

$$Q = 12{,}400 - 2100d^2$$

where d is the 60/60°F specific gravity; deviation is generally less than 1%.

For thermodynamic calculation of equilibria useful in petroleum science, combustion data of extreme accuracy are required because the heats of formation of water and carbon dioxide are large in comparison to those in the hydrocarbons. Great accuracy is also required of the specific heat data for the calculation of free energy or entropy. Much care must be exercised in selecting values from the literature for these purposes because many of those available were determined before the development of modern calorimetric techniques.

6.3.7 Molecular Weight

For resids that have little or no volatility, *vapor pressure osmometry* (*VPO*) has been proved to be of considerable value.

The molecular weights of resids are not always (in fact, rarely) used in the determination of process behavior. Nevertheless, there may be occasions when the molecular weight of asphalt is desired.

Currently, of the methods available, several standard methods are recognized as being useful for determining the molecular weight of petroleum fractions, and these methods are:

ASTM D-2224: Test Method for Mean Molecular Weight of Mineral Insulating Oils by the Cryoscopic Method (discontinued in 1989 but still used by some laboratories for determining the molecular weight of petroleum fractions up to and including gas oil).

ASTM D-2502: Test Method for Estimation of Molecular Weight (Relative Molecular Mass) of Petroleum Oils from Viscosity Measurements.

ASTM D-2503: Test Method for Estimation of Molecular Weight (Relative Molecular Mass) of Hydrocarbons by Thermoelectric Measurement of Vapor Pressure.

ASTM D-2878: Method for Estimating Apparent Vapor Pressures and Molecular Weights of Lubricating Oils.

ASTM D-3593: Test Method for Molecular Weight Averages or Distribution of Certain Polymers by Liquid Size Exclusion (Gel Permeation Chromatography — GPC) Using Universal Calibration has also been adapted to the investigation of molecular weight distribution in petroleum fractions.

Each method has proponents and opponents because of assumptions made in the use of the method or because of the mere complexity of the sample and the nature of the inter- and intramolecular interactions. Before application of any one

or more of these methods, consideration must be given to the mechanics of the method and the desired end result.

Methods for molecular weight measurement are also included in other more comprehensive standards (ASTM D-128, ASTM D-3712), and there are several indirect methods that have been proposed for the estimation of molecular weight by correlation with other, more readily measured physical properties (Speight, 1999, 2001).

The molecular weights of the individual fractions of resids have received more attention and have been considered to be of greater importance than the molecular weight of the resid itself (Speight, 1999, 2001). The components that make up the resid influence the properties of the material to an extent that is dependent on the relative amount of the component, the molecular structure of the component, and the physical structure of the component that includes the molecular weight.

Asphaltenes have a wide range of molecular weights, from 500 to at least 2500, depending on the method (Speight, 1994). Asphaltenes associate in dilute solution in nonpolar solvents, giving higher molecular weights than is actually the case on an individual-molecule basis. The molecular weights of the resins are somewhat lower than those of the asphaltenes and usually fall within the range of 500 to 1000. This is due not only to the absence of association but also to a lower absolute molecular size. The molecular weights of the oil fractions (i.e., the resid minus the asphaltene fraction and minus the resin fraction) are usually less than 500, often 300 to 400.

A correlation connecting molecular weight, asphaltene content, and heteroatom content with the carbon residues of whole residua has been developed and has been extended to molecular weight and carbon residue (Schabron and Speight, 1997a, 1997b).

6.3.8 Other Properties

Resids may be liquid or solid at ambient temperature and, in the latter case, the *melting point* is a test (ASTM D-87 and D-127) that is widely used to know the melting point to prevent solidification in pipes.

The *softening point* of a resid is the temperature at which the resid attains a particular degree of softness under specified conditions of test.

There are several tests available to determine the softening point of resids (ASTM D-36, ASTM D-61, ASTM D-2319, ASTM D-3104, ASTM D-3461, IP 58). In the test method (ASTM D-36, IP 58), a steel ball of specified weight is laid on the layer of sample contained in a ring of specified dimensions. The softening point is the temperature, during heating under specified conditions, at which the asphalt surrounding the ball deforms and contacts a base plate.

The *pour point* is the lowest temperature at which the resid will pour or flow under prescribed conditions. For residua, the pour points are usually high (above 0°C; 32°F) and are more an indication of the temperatures (or conditions) required to move the material from one point in the refinery to another.

The thermal cracking of resid is a first-order reaction, but there is an induction period before the coke begins to form.

The focus in such studies has been on the asphaltene constituents and the resin constituents (Speight, 2002, and references cited therein). Several chemical models (Wiehe, 1993, 1994, and references cited therein; Gray, 1994, and references cited

therein; Speight, 1994, and references cited therein) describe the thermal decomposition of asphaltene constituents and, by inference, the constituents of the resin fraction. The prevalent thinking is that the polynuclear aromatic fragments become progressively more polar as the paraffinic fragments are stripped from the ring systems by scission of the bonds (preferentially) between the carbon atoms alpha and beta to the aromatic rings.

6.4 COMPOSITION

Determination of the composition of resids has always presented a challenge because of the complexity and high molecular weights of the molecular constituents. The principle behind composition studies is to evaluate resids in terms of composition and process behavior.

Physical methods of fractionation usually indicate high proportions of asphaltenes and resins even in amounts up to 50% (or higher) of the residuum. In addition, the presence of ash-forming metallic constituents, including such organometallic compounds as those of vanadium and nickel, is also a distinguishing feature of resids. Furthermore, the deeper the cut into the crude oil, the greater the concentration of sulfur and metals in the residuum, and the greater the deterioration in physical properties (Speight 2000, and references cited therein).

6.4.1 Chemical Composition

The chemical composition of resids is, in spite of the large volume of work performed in this area, largely speculative (Altgelt and Boduszynski, 1994; Speight, 1999). Acceptance that petroleum is a continuum of molecular types that continues from the low-boiling fractions to the nonvolatile fractions (Speight, 1999, and references cited therein) is an aid to understanding the chemical nature of the heavy feedstocks.

6.4.1.1 Hydrocarbon Compounds

On a molecular basis, resids contain hydrocarbons as well as the organic compounds of nitrogen, oxygen, and sulfur; and metallic constituents. Even though free hydrocarbons may be present and the hydrocarbon skeleton of the various constituents may appear to be the dominating molecular feature, it is, nevertheless, the nonhydrocarbon constituents (i.e., nitrogen, oxygen, and sulfur) that play a large part in determining the nature and, hence, the processability of resids.

In the *asphaltene fraction* (a predominant fraction of resids), free condensed naphthenic ring systems may occur, but general observations favor the occurrence of combined aromatic–naphthenic systems that are variously substituted by alkyl systems. There is also general evidence that the aromatic systems are responsible for the polarity of the asphaltene constituents. Components with two aromatic rings are presumed to be naphthalene derivatives, and those with three aromatic rings may be phenanthrene derivatives. Currently, and because of the consideration of the natural product origins of petroleum, phenanthrene derivatives are favored over anthracene ones. In addition, trace amounts of pericondensed polycyclic aromatic

hydrocarbons such as methylchrysene, methyl- and dimethylperylenes, and benzofluorenes have been identified in crude oil. Chrysene and benzofluorene homologues seem to predominate over those of pyrene.

The polycyclic aromatic systems in the *asphaltene fraction* are complex molecules that fall into a molecular weight and boiling range where very little is known about model compounds (Speight, 1994, 1999). There has not been much success in determining the nature of such systems in resids. In fact, it has been generally assumed that as the boiling point of a petroleum fraction increases, so does the number of condensed rings in a polycyclic aromatic system. To an extent, this is true, but the simplicities of such assumptions cause omission of other important structural constituents of the petroleum matrix, the alkyl substituents, the heteroatoms, and any polycyclic systems that are linked by alkyl chains or by heteroatoms.

6.4.1.2 Sulfur Compounds

Sulfur compounds are perhaps the most important nonhydrocarbon constituents of resids and occur as a variety of structures (Speight, 1999, and references cited therein). During the refining sequences involved in converting crude oils to salable products, a great number of the sulfur compounds that occur in petroleum are concentrated in the resids.

The major sulfur species are alkyl benzothiophene, dibenzothiophene, benzonaphtho-thiophene, and phenanthro-thiophene derivatives.

6.4.1.3 Nitrogen Compounds

The presence of nitrogen in resids is of much greater significance in refinery operations than might be expected from the relatively small amounts present.

Nitrogen in resids may be classed arbitrarily as *basic* and *nonbasic*. The basic nitrogen compounds (Speight, 1999, and references cited therein), which are composed mainly of pyridine homologues and occur throughout the boiling ranges, have a decided tendency to exist in the higher-boiling fractions and residua (Gary and Handwerk, 1984). The nonbasic nitrogen compounds, which are usually of the pyrrole, indole, and carbazole types, also occur in the higher-boiling fractions and residua.

Typically, about one third of the compounds are basic, i.e., pyridine and its benzologs, whereas the remainder are present as neutral species (amides and carbazole derivatives). Although benzo- and dibenzoquinoline derivatives found in petroleum are rich in sterically hindered structures, hindered and unhindered structures have also been found.

Porphyrins (nitrogen–metal complexes) are also constituents of petroleum and usually occur in the nonbasic portion of the nitrogen-containing concentrate (Reynolds, 1991 and 1997). Pyrrole, the chief constituent of the porphyrin molecule, is marked by high stability because of its aromatic character.

The presence of vanadium and nickel in resids, especially as metal porphyrin complexes, has focused much attention in the petroleum refining industry on the occurrence of these metals in feedstocks (Reynolds, 1991 and 1997). Only a part of the total nickel and vanadium in crude oil is recognized to occur in porphyrin structures.

6.4.1.4 Oxygen Compounds

The total oxygen content of petroleum is usually less than 2% w/w, although larger amounts have been reported, and it does increase with the boiling point of the fractions. In fact, resids may have oxygen contents of up to 8% w/w. Although these high-molecular-weight compounds contain most of the oxygen, little is known concerning their structure, but those of lower molecular weight have been investigated with considerably more success and have been shown to contain carboxylic acids ($R\text{-}CO_2H$) and phenols (Ar-OH, where Ar is an aromatic moiety).

6.4.1.5 Metallic Compounds

The occurrence of metallic constituents in crude oil is of considerably greater interest to the petroleum industry than might be expected from the very small amounts present.

Distillation concentrates the metallic constituents in the resids (Table 6.2); some can appear in the higher-boiling distillates but the latter may, in part, be due to entrainment. The majority of the vanadium, nickel, iron, and copper in resids may be precipitated along with the asphaltenes by low-boiling alkane hydrocarbon solvents. Thus, removal of the asphaltenes with *n*-pentane reduces the vanadium content of the oil by up to 95%, with substantial reductions in the amounts of iron and nickel.

6.4.2 Fractionation

Understanding the chemical transformations of the macromolecular constituents during conversion is limited by the diversity (over a million chemical structures) of the complex macromolecules in a resid.

One way to sample this molecular diversity is to separate the resid and its conversion products into fractions using solubility or insolubility in low-boiling liquid hydrocarbons as well as adsorption followed by desorption on solids such as silica gel, alumina, or clay (Figure 6.2). Following the application of such a procedure, it can be shown that, in the simplest sense, resids from the same crude differ in the relative amounts of these fractions that are present (Figure 6.3), as they often do when produced from different crude oil. Thus, the *physical composition* (or *bulk composition*), refers to the composition of a resid, is determined by these various physical techniques (Speight, 1999, and references cited therein).

There are also two other operational definitions that should be noted at this point, and these are the terms *carbenes* and *carboids*. Both these fractions are by definition insoluble in benzene (or toluene), but the *carbenes* are soluble in carbon disulfide whereas the *carboids* are insoluble in carbon disulfide. Only traces, if any, of these materials occur in natural resids. On the other hand, resids that have received some thermal treatment (such as visbroken resids) may have considerable quantities of these materials present as they are also considered to be precursors to coke.

Resids, especially vacuum resids (*vacuum bottoms*), are the most complex fractions of petroleum. Few molecules are free of heteroatoms and the molecular weight of the constituents extends from 400 to >2000 and, at the upper end of this molecular weight range, characterization of individual species is virtually impossible. Separations by

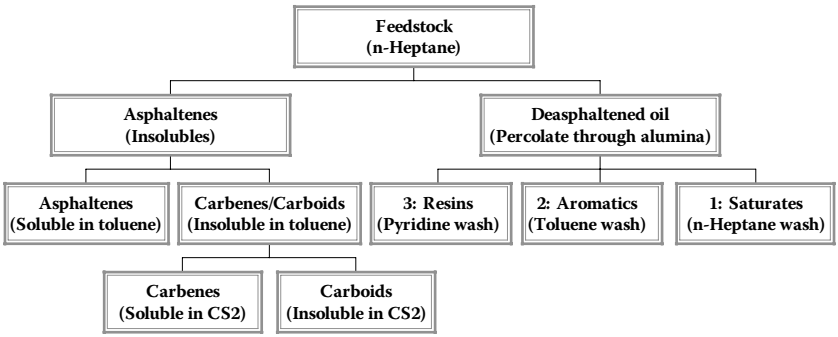

FIGURE 6.2 Resid fractionation.

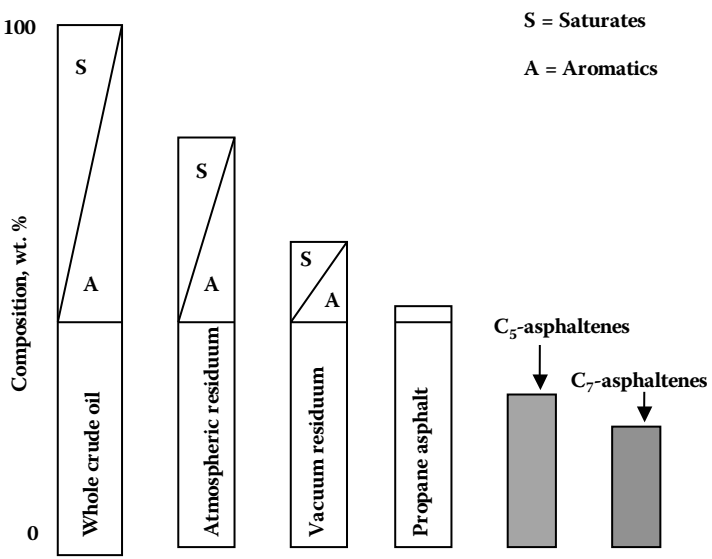

FIGURE 6.3 Comparison of petroleum and resid composition showing the asphaltene content.

group type become blurred by the shear frequency of substitution and by the presence of multiple functionalities in single molecules.

Resids can be separated into a variety of fractions using a myriad of different techniques that have been used since the beginning of petroleum science (Speight, 1999). In general, the fractions produced by these different techniques are called *saturates*, *aromatics*, *resins*, and *asphaltenes* (Figure 6.2). And much of the focus has been on the asphaltenes fraction because of its high sulfur content and high coke-forming propensity (Speight, 1994, 1999).

The methods employed can be conveniently arranged into a number of categories: (1) fractionation by precipitation; (2) fractionation by distillation; (3) separation by chromatographic techniques; (4) chemical analysis using spectrophotometric techniques (infrared, ultraviolet, nuclear magnetic resource, x-ray fluorescence, emission, neutron activation), titrimetric and gravimetric techniques, elemental analysis; and

(5) molecular weight analysis by mass spectrometry, vapor pressure osmometry, and size exclusion chromatography.

6.4.2.1 Asphaltene Separation

By definition, the *asphaltene fraction* is that portion of the feedstock that is precipitated when a large excess (40 volumes) of a low-boiling liquid hydrocarbon (e.g., *n*-pentane or *n*-heptane) is added to 1 volume of the crude oil (Speight, 1994, 1999). *n*-Heptane is the preferred hydrocarbon, with *n*-pentane still being used (Speight, et al., 1984; Speight, 1994; ASTM, 2003).

The asphaltene fraction (ASTM D-2006, ASTM D-2007, ASTM D-3279, ASTM D-4124, ASTM D-6560, IP 143) has the highest molecular weight and is the most complex fraction in petroleum. The asphaltenes content gives an indication of the amount of coke that can be expected during processing (Speight, 1999; Speight, 2001, Speight and Ozum, 2002).

In any of the methods for the determination of the asphaltene content, the resids mixed with a large excess (usually >30 volumes hydrocarbon per volume of sample) of low-boiling hydrocarbon such as *n*-pentane or *n*-heptane. For an extremely heavy residuum, a solvent such as toluene may be used prior to the addition of the low-boiling hydrocarbon, but an additional amount of the hydrocarbon (usually >30 volumes hydrocarbon per volume of solvent) must be added to compensate for the presence of the solvent. After a specified time, the insoluble material (the asphaltene fraction) is separated (by filtration) and dried. The yield is reported as a percentage (% w/w) of the original sample.

It must be recognized that, in any of these tests, different hydrocarbons (such as *n*-pentane or *n*-heptane) will give different yields of the asphaltene fraction, and if the presence of the solvent is not compensated by use of additional hydrocarbon, the yield will be erroneous. In addition, if the hydrocarbon is not present in large excess, the yields of the asphaltene fraction will vary and will be erroneous (Speight, 1999).

The *precipitation number* is often equated to the asphaltene content, but there are several obvious issues that argue against this. For example, the method to determine the precipitation number (ASTM D-91) advocates the use of naphtha for use with black oil or lubricating oil, and the amount of insoluble material (as a % v/v of the sample) is the precipitating number. In the test, 10 ml of sample is mixed with 90 ml of ASTM precipitation naphtha (that may or may not have a constant chemical composition) in a graduated centrifuge cone and centrifuged for 10 min at 600 to 700 rpm. The volume of material on the bottom of the centrifuge cone is noted until repeat centrifugation gives a value within 0.1 ml (the precipitation number). Obviously, this can be substantially different in regard to asphaltene content.

In another test method (ASTM D-4055), pentane insoluble materials above 0.8 μm in size can be determined. In the test method, a sample of oil is mixed with pentane in a volumetric flask, and the oil solution is filtered through a 0.8-μm-membrane filter. The flask, funnel, and the filter are washed with pentane to completely transfer the particulates onto the filter, which is then dried and weighed to give the yield of pentane-insoluble materials.

Another test method (ASTM D-893) that was originally designed for the determination of pentane- and toluene-insoluble materials in used lubricating oils can also be applied to resids. However, the method may need modification by first adding a solvent (such as toluene) to the resid before adding pentane.

6.4.2.1.1 Carbon-Disulfide-Insoluble Constituents

The component of highest carbon content is the fraction termed *carboids* and consists of species that are insoluble in carbon disulfide or in pyridine. The fraction called *carbenes* contains molecular species that are soluble in carbon disulfide and soluble in pyridine but are insoluble in toluene (Figure 6.2).

Resids are hydrocarbonaceous materials composed of constituents (containing carbon, hydrogen, nitrogen, oxygen, and sulfur) that are completely soluble in carbon disulfide (ASTM D-4). Trichloroethylene and 1,1,1-trichloroethane have been used in recent years as solvents for the determination of asphalt solubility (ASTM D-2042).

The carbene and carboid fractions are generated by thermal degradation or by oxidative degradation and are not considered to be naturally occurring constituents of asphalt. The test method for determining the toluene-insoluble constituents of tar and pitch (ASTM D-4072 and ASTM D-4312) can be used to determine the amount of carbenes and carboids in resids.

6.4.2.2 Fractionation of Deasphaltened Oil

After removal of the asphaltene fraction, further fractionation of resids is also possible by variation of the hydrocarbon solvent.

However, fractional separation has been the basis of most resid composition analysis (Figure 6.2). The separation methods that have been used divide a resid into operationally defined fractions. Three types of resid separation procedures are now in use: (1) chemical precipitation in which *n*-pentane separation of asphaltenes is followed by chemical precipitation of other fractions with sulfuric acid of increasing concentration (ASTM D-2006); (2) adsorption chromatography using a clay-gel procedure in which, after removal of the asphaltenes, the remaining constituents are separated by selective adsorption or desorption on an adsorbent (ASTM D-2007 and ASTM D-4124); and (3) size-exclusion chromatography, in which gel permeation chromatographic (GPC) separation of asphalt constituents occurs based on their associated sizes in dilute solutions (ASTM D-3593).

The fractions obtained in these schemes are defined operationally or procedurally. The solvent used for precipitating them, for instance, defines the amount and type of asphaltenes in a resid. Fractional separation of a resid does not provide well-defined chemical components. The materials separated should only be defined in terms of the particular test procedure (Figure 6.2). However, these fractions generated by thermal degradation are not considered to be naturally occurring constituents of resid. The test method for determining the toluene-insoluble constituents of tar and pitch (ASTM D-4072, ASTM D-4312) can be used to determine the amount of carbenes and carboids in resid.

Many investigations of relationships between composition and properties take into account only the concentration of the asphaltenes, independently of any quality

criterion. However, a distinction should be made between the asphaltenes that occur in straight-run residua and those that occur in cracked residua. Because asphaltenes are a solubility class rather than a distinct chemical class, vast differences occur in the makeup of this fraction when it is produced by different processes.

For example, liquefied gases, such as propane and butane, precipitate as much as 50% by weight of the resid. The precipitate is a black, tacky, semisolid material, in contrast to the pentane-precipitated asphaltenes, which are usually brown, amorphous solids. Treatment of the propane precipitate with pentane then yields the insoluble, brown, amorphous asphaltenes and soluble, near-black, semisolid resins, which are, as near as can be determined, equivalent to the resins isolated by adsorption techniques.

Separation by adsorption chromatography essentially commences with the preparation of a porous bed of finely divided solid, the adsorbent. The adsorbent is usually contained in an open tube (column chromatography); the sample is introduced at one end of the adsorbent bed and induced to flow through the bed by means of a suitable solvent. As the sample moves through the bed, the various components are held (adsorbed) to a greater or lesser extent depending on the chemical nature of the component. Thus, those molecules that are strongly adsorbed spend considerable time on the adsorbent surface rather than in the moving (solvent) phase, but components that are slightly adsorbed move through the bed comparatively rapidly.

There are three ASTM methods that provide for the separation of a feedstock into four or five constituent fractions (Speight, 2001, and references cited therein). It is interesting to note that as the methods have evolved, there has been a change from the use of pentane (ASTM D-2006 and D-2007) to heptane (ASTM D-4124) to separate asphaltenes. This is, in fact, in keeping with the production of a more consistent fraction that represents the higher-molecular-weight complex constituents of petroleum (Girdler, 1965; Speight et al., 1984).

Two of the methods (ASTM D-2007 and D-4124) use adsorbents to fractionate the deasphaltened oil, but the third method (ASTM D-2006) advocates the use of various grades of sulfuric acid to separate the material into compound types. Caution is advised in the application of this method because the method does not work well with all feedstocks. For example, when the sulfuric acid method (ASTM D-2006) is applied to the separation of heavy feedstocks, complex emulsions can be produced.

6.5 USE OF DATA

It has been asserted that more needs to be done in correlating analytical data obtained for resids with processability (Speight et al., 1984; Boduszynski, 1988; Reynolds, 1991). Currently, used coke yield predictors are simplistic and feedstock specific (Beret and Reynolds, 1990; Gary and Handwerk, 1984).

Standard analyses on resids, such as determinations of elemental compositions and molecular weight, have not served to be reliable predictors of processability, and determining average structural features also does not appear to be very helpful.

The data derived from any one, or more, of the evaluation techniques described here give an indication of resid behavior. The data can also be employed to give the refiner a view of the differences between different residua, thereby indicating the means by which the resids should be processed, as well as for the prediction of

product properties (Dolbear et al., 1987; Adler and Hall, 1988; Wallace and Carrigy, 1988; Al-Besharah et al., 1989).

Because of resid complexity, there are disadvantages in relying on the use of bulk properties as the sole means of predicting behavior. Therefore, fractionation of resids into components of interest and study of the components appears to be a better approach than obtaining data on whole residua. By careful selection of a characterization scheme, it may be possible to obtain a detailed overview of feedstock composition that can be used for process predictions.

The use of composition data to model resid behavior during refining is becoming increasingly important in refinery operations (Speight, 1999).

In the simplest sense, resids can be considered composites of four major operational fractions and this allows different resids to be compared on a relative basis to provide a very simple but convenient feedstock map (Figure 6.4). However, such a map does not give any indication of the complex interrelationships of the various fractions, although predictions of feedstock behavior are possible using such data. It is necessary to take the composition studies one step further using subfractionation of the major fractions to obtain a more representative indication of petroleum composition.

Further development of this concept (Long and Speight, 1989, 1990, 1997) involved the construction of a different type of compositional map, using the molecular weight distribution and the molecular-type distribution as coordinates. The separation involved the use of an adsorbent such as clay, and the fractions were characterized by *solubility parameter* as a measure of the polarity of the molecular types. The molecular weight distribution can be determined by gel permeation chromatography.

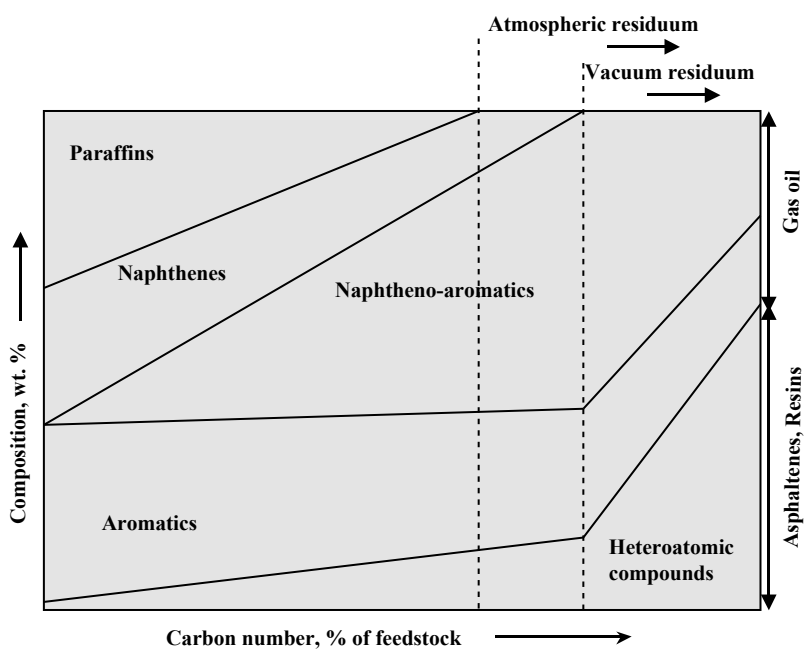

FIGURE 6.4 Simplified representation and resid composition.

Using these two distributions, a map of composition can be prepared with molecular weight and solubility parameter as the coordinates for plotting the two distributions. Such a composition map can provide insights into many separation and conversion processes used in resid processing.

6.6 RESID CONVERSION

Resid quality is a relevant issue with regard to the selection and efficiency of the conversion technology. High levels of metals (vanadium and nickel) are a well-known characteristic of many resids. The Conradson carbon and asphaltene content of resids are also high, and so represent challenges for the upgrading technology.

6.6.1 Visbreaking

Visbreaking is a low-conversion thermal process, used originally to reduce the resid viscosity to meet the specification for heavy fuel oil applications. Currently, the visbreaking process converts resids (15–20% v/v conversion) to produce some liquid fuel boiling range liquids, with visbroken resid being used to meet heavy fuel oil specifications.

The process is not designed to produce coke formation and therefore operates with the induction period prior to coke formation.

A visbreaker reactor may be similar to a delayed coker with a furnace tube followed by a soaker drum. However, the drum is much smaller in volume to limit the residence time, with the entire liquid product flowing overhead. Alternatively, the entire visbreaker may be a long tube coiled within a furnace. Differences in resid properties can cause coke to form in the vessel, and some coke removal protocols may be necessary.

Visbreaking may be applied to atmospheric resids, vacuum resids, and also to solvent deasphalter bottoms (asphalt). A common operation involved visbreaking the atmospheric residue in combination with a thermal cracker to minimize fuel oil while producing additional light distillates.

However, visbreaking is typically applied to vacuum resids and is frequently used as a mild vacuum residue conversion process when feedstock for fluid catalytic cracking is sought. The lower-boiling distillates are recovered for processing to transportation fuels, and the higher-boiling distillates are recovered as feedstock for the fluid catalytic cracking unit. A high-temperature coil visbreaker allows a high-boiling distillate to be recovered from the fractionator. For lower-boiling distillates and with soaking drum technology, a separate vacuum flasher is usually required.

Conversion in a visbreaker is limited by the requirement to produce a stable fuel oil. As the resid is thermally cracked, reactions occur which increase the asphaltene content which, coupled with the reduction (by thermal cracking) of the resins holding the asphaltene constituents in solution, leads to precipitation of the asphaltenes.

6.6.2 Coking

Coking is a high-temperature (450–500°C [842–932°F]) process and is the most popular conversion choice for resids that usually have a high content of polynuclear

aromatic systems (low hydrogen, high heteroatoms, high Conradson carbon). Coking converts the polynuclear aromatic systems to coke (a relatively low-value product) and overhead (relatively high-value distillates) that can be upgraded further to liquid fuels and other products.

Delayed coking is the oldest and most popular choice for resid conversion. The resid is heated by flow through a long tube in a furnace and then reacted by flow into the bottom of a high, cylindrical, insulated drum. The drums are used in pairs with one onstream and the other offstream. Volatile (overhead) products pass to a fractionator and coke accumulates in the drum. High-boiling liquid products may be recycled to the furnace and pass through the coke drum again.

When the drum fills up with coke, the hot feed is switched offstream and the second drum is switched onstream. The coke is removed from the offstream drum using high-pressure water, after which time the onstream–offstream cycle (usually about 16 h) will be reversed.

The *fluid coking and flexicoking* processes are also employed for resid conversion. In the *fluid coking* process, the hot resid is sprayed on a hot, fluidized bed of coke particles in a reactor. The volatile products (overhead) pass to a fractionator while the coke particles are removed from the bottom of the reactor and transferred to another vessel, the burner or regenerator. Here the excess coke is partially burned with air to provide the heat for the process, and the coke then is recirculated back to the reactor.

In the flexicoking process, which is very similar to the fluid coking process, a third vessel (the gasifier) is added to the fluid coking flow. The gasifier coke is used to gasify excess coke with steam and air to produce a low-Btu gas containing hydrogen, carbon monoxide, nitrogen, and hydrogen sulfide. After removal of the hydrogen sulfide, the low-Btu gas is burned as a clean fuel within the refinery or in a nearby power plant.

6.6.3 Resid Catalytic Cracking

Resid catalytic cracking has much better selectivity to desired products (high-gasoline and low-gas yields) than for coking or hydroconversion.

In fluid catalytic cracking, feed is sprayed on zeolite catalyst in a short-contact-time riser reactor. The vaporized product flows to a fractionator while the catalyst with coke and adsorbed hydrocarbons flows to a fluidized bed regenerator in which the coke and hydrocarbons are burned off the catalyst. Fluid catalytic cracking requires much more higher-quality feeds than coking or hydroconversion. This is because of expensive zeolite catalysts, intolerance to sodium, nickel, vanadium, and basic nitrogen, as well as limitations on the amount of coke that can be burned in the regeneration step by cooling capacity. As a result, the feed in resid catalytic cracking is at worst an excellent-quality atmospheric resid, but mixtures of vacuum gas oil and atmospheric resids are more common. The total feed is limited to Conradson Carbon Residues of 3 to 8 wt%, depending on the cooling capacity.

6.6.4 Hydroconversion

Hydroconversion combines thermal cracking with hydrogenation. The addition of hydrogen increases the coke induction period by lowering the solubility parameter

by hydrogenating polynuclear aromatic systems, but primarily by terminating free radicals and reducing the frequency of aromatics from combining to form larger polynuclear aromatic systems. Thus, hydroconversion of vacuum resids to volatile liquids can be over 85% as opposed to 50–60% for coking. However, one has to deal with the cost of hydrogen and catalyst, high-pressure vessels, poisoning of catalysts, the difficulty of asphaltenes in diffusing through small pores, and the intolerance to coke and sediment formation. The active catalyst needs to be a transition metal sulfide because the high level of sulfur in resid feeds will poison other hydrogenation catalysts.

Atmospheric and vacuum residue desulfurization units are commonly operated to desulfurize the residue as a preparatory measure for feeding low-sulfur vacuum gas-oil feed to cracking units (fluid catalytic cracking units and hydrocracking units), low-sulfur residue feed to delayed coker units, and low-sulfur fuel oil to power stations. Two different types of processing units are used for the direct catalytic hydroprocessing of residue.

These units are either (1) a down-flow, trickle phase reactor system (fixed catalyst bed) or (2) liquid recycle and back mixing system (ebullating bed).

6.6.4.1 Fixed Bed Units

Because metal removal is one of the fastest reactions and as the metals accumulate in the pores of supported catalysts, it is common to have a guard bed in front of the fixed bed. When insufficient metal removal occurs in the guard bed, the feed is switched to a second guard bed with fresh catalyst and the catalyst is replaced in the first guard bed. Thus, the fixed bed is protected from metal deposition. To hydrogenate the largest macromolecules in the resid, the asphaltenes, some or all of the catalysts need to have pores 50–100 μm in diameter. Even with these precautions, it is difficult to get longer than 1-year run lengths on fixed bed hydroconversion units with vacuum resid feeds and conversions to volatile liquids of 50% or more. This is because of catalyst deactivation with coke or by coke and sediment formation downstream of the reactor.

6.6.4.2 Ebullating Bed Units

The LC Finer and H-Oil units use the mechanically ebullate the catalyst so that it can be mixed and replaced onstream. The conversion is greatly dependent on the feed, but conversions of vacuum resids to volatile liquids on the order of 70% are possible. Often, these units are limited by the deposition of coke and sediment downstream of the reactor in hot and cold separators.

6.6.4.3 Dispersed Catalyst Processes

If one cannot diffuse the asphaltenes to the catalyst, why not diffuse the catalyst to asphaltenes? Dispersed catalysts also can be continuously added in low enough amounts (i.e., 100 ppm) to consider them throwaway catalysts with the carbonaceous by-product. However, economics usually dictates some form of catalyst recycle to minimize catalyst cost. Nevertheless, by designing the reactor to maximize the

solubility of the converted asphaltenes, the conversion of vacuum resids to gas and volatile liquids can be above 95%, with greater than 85% volatile liquids. However, the last 5 to 10% conversion may not be worth the cost of hydrogen and reactor volume to produce hydrocarbon gases and very aromatic liquids from this incremental conversion.

6.6.5 Solvent Deasphalting

Solvent deasphalting, though not strictly a conversion process, is a separation process that represents a further step in the minimization of resid production.

The process takes advantage of the fact that maltenes are more soluble in light paraffinic solvents than asphaltenes. This solubility increases with solvent molecular weight and decreases with temperature. As with vacuum distillation, there are constraints with respect to how deep a solvent deasphalting unit can cut into the residue or how much deasphalted oil can be produced.

In the case of solvent deasphalting, these constraints are typically: (1) the quality of the deasphalted oil required by conversion units, and (2) the residual fuel oil stability and quality.

Solvent deasphalting has the advantage of processing the flexibility to meet a wide range of deasphalted oil quality. The process has very good selectivity for the rejection of asphaltene constituents and metal constituents, along with varied selectivity (depending on the feedstock) for other coke precursors, but less selectivity for sulfur constituents and for nitrogen constituents. The disadvantages of the process are that it performs no conversion, produces a very high-viscosity by-product pitch, and where high-quality deasphalted oil is required, the solvent deasphalting process is limited in the quality of feedstock that can be economically processed.

The viability of the solvent deasphalting process is dependent on the potential for upgrading the deasphalted oil and the differential between the value of the cutter stocks and the price of high-sulfur residual fuel oil. If there is an outlet for asphalt (from the unit) and the conversion capacity exists to upgrade the deasphalted oil, solvent deasphalting can be a highly attractive option for resid conversion.

6.6.6 Future Processes

We are still on the steep part of the learning curve as to the characterization, phase behavior, and conversion chemistry of petroleum resids. As a result, there is much room for improvement in regard to resid conversion processes. However, the rate of construction of new resid conversion units in refineries has been decreasing. Future growth appears to be at or near heavy crude production sites, to decrease heavy crude viscosity and improve the quality to ease transportation, and open markets for crude oils or resids that are of marginal value. There remains room for improving coking and hydroconversion processes by reducing hydrocarbon gas formation, by inhibiting the formation of polynuclear aromatic systems not originally present in the resid, and by separating an intermediate quality (low in cores) fraction before or during conversion. Both these processes would benefit if a higher-valued by-product, such as carbon fibers or needle coke, could be formed from the polynuclear

aromatic systems. In addition, the challenge for hydroconversion is to take advantage of the nickel and vanadium in the resid to generate an *in situ* dispersed catalyst and to eliminate catalyst cost. Finally, resid catalytic cracking needs to move to poorer-quality and lower-cost feeds by making more tolerant catalysts, by processing only the saturates and small-ring aromatics portion, and by improved methods to remove heat from the regenerator.

REFERENCES

Adler, S.B. and Hall, K.R., *Hydrocarbon Process.*, 71(11): 71, 1988.

Al-Besharah, J.M., Mumford, C.J., Akashah, S.A., and Salman, O., *Fuel*, 68: 809, 1989.

Altgelt, K.H. and Boduszynski, M.M., *Compositional Analysis of Heavy Petroleum Fractions*, Marcel Dekker, New York, 1994.

ASTM, *ASTM Annual Book of Standards*, American Society for Testing and Materials, West Conshohocken, Pennsylvania, 2003.

Beret, S. and Reynolds, J.G., *Fuel Sci. Technol. Int.*, 8: 191, 1990.

Boduszynski, M.M., *Energy Fuels*, 2: 597, 1988.

Boduszynski, M.M., *Liquid Fuel Technol.*, 2: 211, 1984.

Dolbear, G.E., Tang, A., and Moorehead, E.L., in *Metal Complexes in Fossil Fuels*, Filby, R.H. and Branthaver, J.F., Eds., Symposium Series No. 344, American Chemical Society, Washington, D.C., 1987, p. 220.

Gary, J.H. and Handwerk, G.E., *Petroleum Refining: Technology and Economics*, 2nd ed., Marcel Dekker, New York, 1984.

Girdler, R.B., *Proc. Assoc. Asphalt Paving Technologists*, 34: 45, 1965.

Gray, M.R., *Upgrading Petroleum Residues and Heavy Oils*, Marcel Dekker, New York, 1994.

Gruse, W.A., and Stevens, D.R., *Chemical Technology of Petroleum*, McGraw-Hill, New York, 1960, chap. 15.

Long, R.B. and Speight, J.G., *Revue de l'Institut Français du Pétrole*, 44: 205, 1989.

Long, R.B. and Speight, J.G., *Revue de l'Institut Français du Pétrole*, 45: 553, 1990.

Long, R.B. and Speight, J.G., in *Petroleum Chemistry and Refining*, Taylor & Francis, Washington, D.C., 1997, chap. 1.

Reynolds, J.G., *Fuel Sci. Technol. Int.*, 9: 613, 1991.

Reynolds, J.G., in *Petroleum Chemistry and Refining*, Speight, J.G., Ed., Taylor & Francis, Washington, D.C., 1997, chap. 3.

Schabron, J.F. and Speight, J.G., *Revue de l'Institut Français du Pétrole*, 52: 73, 1997a.

Schabron, J.F. and Speight, J.G., *Prepr. Div. Fuel Chem. Am. Chem. Soc.*, 42(2): 386, 1997b.

Speight, J.G., in *Asphaltenes and Asphalts, I. Developments in Petroleum Science*, 40, Yen, T.F. and Chilingarian, G.V., Eds., Elsevier, Amsterdam, The Netherlands, 1994, chap. 2.

Speight, J.G., *The Chemistry and Technology of Petroleum*, 3rd ed., Marcel Dekker, New York, 1999.

Speight, J.G., *The Desulfurization of Heavy Oils and Residua*, 2nd ed., Marcel Dekker, New York, 2000.

Speight, J.G., *Handbook of Petroleum Product Analysis*, John Wiley & Sons, New York, 2002.

Speight, J.G. and Ozum, B., *Petroleum Refining Processes*, Marcel Dekker, New York, 2002.

Speight, J.G., Long, R.B., and Trowbridge, T.D., *Fuel*, 63: 616, 1984.

Van Gooswilligen, G., in *Modern Petroleum Technology*, Vol. 1 and 2: Downstream, Lucas, A.G., Ed., John Wiley & Sons, New York, 2000.

Wallace, D., and Carrigy, M.A., *Proceedings of the Third UNITAR/UNDP International Conference on Heavy Crude and Tar Sands*, Meyer, R.F., Ed., Alberta Oil Sands Technology and Research Authority, Edmonton, Alberta, Canada, 1988.
Wiehe, I.A., *Ind. Eng. Chem. Res.*, 32: 2447, 1993.
Wiehe, I.A., *Energy Fuels*, 8: 536, 1994.

7 Liquid Fuels from Oil Sand

James G. Speight

CONTENTS

7.1 INTRODUCTION

Liquid fuels are produced from several sources, the most common being petroleum. However, other sources such as oil sand (Berkowitz and Speight, 1975; Speight, 1990, and references cited therein) and coal are also viable sources of liquid fuels. Coal, to a lesser extent, can also be used as a source of liquid fuels (Speight, 1994, and references cited therein).

When liquid fuels are produced from a source such as oil sand, the initial product is often referred to as *synthetic crude oil* or *syncrude*, which is, in the present context, a liquid fuel that does not occur naturally.

The purpose of this chapter is to describe the occurrence, production, and properties of oil sand bitumen, and the methods used to convert the bitumen to synthetic crude oil. Properties of the synthetic crude oil are also given.

Oil sand (also known as *tar sand* and *bituminous sand*) is a sand deposit that is impregnated with an organic material called *bitumen*. The term *natural asphalt* is

also used for the organic material that impregnates various sand deposits, but the term is less precise than bitumen.

The names *oil sand* and *tar sand* are scientifically incorrect because oil sand does not contain oil and tar is most commonly produced from bituminous coal, besides being generally understood to refer to the product from coal, although it is advisable to specify coal tar if there is the possibility of ambiguity.

Thus, technically, *oil sand* should be called *bituminous sand* because the hydrocarbonaceous material is bitumen (soluble in carbon disulfide) and not oil. The term *oil sand* is used in reference to the synthetic crude oil that can be manufactured from the bitumen.

Oil sand is a mixture of sand, water, and bitumen, and the sand component is predominantly quartz in the form of rounded or subangular particles, each of which (as far as is known for the Athabasca deposit) is wet with a film of water. Surrounding the wetted sand grains and somewhat filling the void among them is a film of bitumen. The balance of the void volume is filled with connate water and sometimes, a small volume of gas. High-grade oil sand contains about 18% by weight of bitumen, which may be equivalent in consistency (viscosity) to an atmospheric or vacuum petroleum residuum.

The definition of bitumen has been very loosely and arbitrarily based on API gravity or viscosity; it is quite arbitrary and too general to be technologically accurate. There have been attempts to rationalize the definition based on viscosity, API gravity, and density, but they also suffer from a lack of technical accuracy. For example, 10° API is the generally used line of demarcation between oil sand bitumen and heavy oil. But one must ask if the difference between 9.9° API gravity oil and 10.1° API oil is really significant. Both measurements are within the limits of difference for standard laboratory test methods. Similarly, the use of viscosity data is also open to question because the difference between oil having a viscosity of 9,950 cp and oil having a viscosity of 10,050 cp is minimal and, again, both measurements are within the limits of difference for standard laboratory test methods.

More appropriately, oil sand *bitumen* in oil sand deposits is a highly viscous hydrocarbonaceous material, and it is not recoverable in its natural state through a well by conventional oil well production methods, including currently used enhanced recovery techniques, as specified in the U.S. government regulations. Thus, it is not surprising that the properties of bitumen from oil sand deposits are significantly different from those of conventional crude oil (recoverable by primary and secondary techniques) and heavy oil (recoverable by enhanced oil recovery techniques).

Chemically, the material should perhaps be called *bituminous sand* rather than *oil sand* because the organic matrix is bitumen, a hydrocarbonaceous material that consists of carbon and hydrogen, with smaller amounts of nitrogen, oxygen, sulfur, and metals (especially nickel and vanadium).

The bitumen in various oil sand deposits represents a potentially large supply of energy. However, many of the reserves are available only with some difficulty, and optional refinery scenarios will be necessary for conversion of these materials to liquid products because of the substantial differences in character between conventional petroleum, heavy oil, and oil sand bitumen (Table 7.1). On the other hand, because of the diversity of available information and the continuing attempts to

TABLE 7.1
The Properties of Bitumen and Conventional Crude Oil

Property	Bitumen	Conventional Crude Oil
Gravity, °API	8	35
Viscosity		
Centipoise @ 100°F (38°C)	500,000	10
Centipoise @ 210°F (99°C)	1,700	
SUS @ 100°F (38°C)	35,000	30
SUS @ 210°F (99°C)	500	
Pour point (°F)	50	0
Elemental analysis (percentage by weight)		
Carbon	83	86
Hydrogen	10.6	13.5
Sulphur	4.8	0.1
Nitrogen	0.4	0.2
Oxygen	1	0.2
Fractional composition (percentage by weight)		
Asphaltenes	19	5
Resins	32	10
Aromatics	30	25
Saturates	19	60
Metals (parts per million)		
Vanadium	250	10
Nickel	100	5
Carbon residue (percentage by weight)	14	5
Heating value Btu/lb	17,500	19,500

delineate the various world oil sand deposits, it is virtually impossible to present accurate numbers that reflect the extent of the reserves in terms of the barrel unit. Indeed, investigations into the extent of many of the world's deposits are continuing at such a rate that the numbers vary from one year to the next. Accordingly, the data quoted here are approximate.

Current commercial recovery operations of bitumen in oil sand formations involve use of a mining technique. This is followed by bitumen upgrading and refining to produce a synthetic crude oil. Other methods for the recovery of bitumen from oil sand are based either on mining, combined with some further processing or operation on the oil sands *in situ*.

The API gravity of oil sand bitumen varies from 5° API to approximately 10° API, depending on the deposit; viscosity is very high, and volatility is low. The viscosity of bitumen is high, being on the order of several thousand to one million centipoises, with higher viscosities being recorded. Bitumen volatility is low, and there are very little of the naphtha and kerosene constituents present.

The lack of mobility of bitumen requires a mining step followed by the hot water process that is, to date, the only successful commercial process to be applied to

bitumen recovery from mined oil sand. Many process options have been tested with varying degrees of success, and one of these options may even supersede the hot water process at some future date.

In addition, bitumen is relatively hydrogen deficient and therefore requires substantial hydrogen addition during refining. Bitumen is currently commercially upgraded by a combination of carbon rejection (coking) and product hydrotreating. Coking, the process of choice for residua, is also the process of choice for bitumen conversion. Bitumen is currently converted commercially by delayed coking and fluid coking. In each case, the bitumen is converted to distillate oils, coke, and light gases. The coker distillate is a partially upgraded material and is a suitable feed for hydrodesulfurization to produce a low-sulfur synthetic crude oil.

Over the next decades, the potential for the production of liquid fuels from oil sand is high, and the liquid fuels produced from these reserves offer a means of alleviating shortfalls in the supply of liquid fuels.

The only commercial operations for the recovery and upgrading of bitumen occur in northeast Alberta, Canada, near the town of Fort McMurray, where bitumen from the Athabasca deposit is converted to a synthetic crude oil. Therefore, most of the data available for inspection of bitumen and determination of behavior originate from studies of these Canadian deposits. The work on bitumen from other sources is fragmented and spasmodic. The exception is the bitumen from deposits in Utah, where ongoing programs have been in place at the University of Utah for more than three decades. The data for the bitumen show a very wide range of properties (Smith-Magowan et al., 1982).

7.2 OCCURRENCE AND RESERVES

The occurrence and reserves of oil sand bitumen that are available for production of liquid fuels are known to an approximation, but the definitions by which these reserves are estimated need careful consideration. Best estimates are all that are available.

Thus, the world reserves of conventional petroleum (arbitrarily defined as having a gravity equal to or greater than 20° API) are reported to be composed of approximately 1,195 billion barrels ($1{,}195 \times 10^9$ bbl) or 30% by volume of the total reserves (of petroleum plus heavy oil plus bitumen). Heavy oil (arbitrarily defined as having a gravity greater than 10° API but less than 20° API) is reported to be 690 billion barrels (690×10^9 bbl) or 15% by volume of the total reserves. Oil sand bitumen (arbitrarily defined as having a gravity equal to or less than 10° API) is reported to be 1,920 billion barrels ($1{,}920 \times 10^9$ bbl) or 55% by volume of the total reserves. However, the bitumen reserves contain *extra heavy oil*, which term is sometimes used to describe bitumen. The API gravity of this material is less than 10° API, but the viscosity may fall into a different range when compared to bitumen viscosity. And in such reserves estimations, there is often no mention of the method of recovery on which the definition of oil sand bitumen hinges.

Therefore, estimations of bitumen availability must be placed in the correct definitional context and, more particularly, in the context of the available recovery method.

Oil sand deposits are widely distributed throughout the world in a variety of countries, and the various deposits have been described as belonging to two types:

(1) stratigraphic traps and (2) structural traps, although gradations between the types of deposit invariably occur (Walters, 1974; Phizackerley and Scott, 1978; Meyer and Dietzman, 1981). In terms of specific geological and geochemical aspects of the formation, the majority of the work has, again, been carried out on the Athabasca deposit. For this reason, the focus of this chapter is on the work carried out on the Canadian oil sand deposits.

Nationally, the largest oil sand deposits are in Alberta and Venezuela, with smaller oil sand deposits occurring in the U.S. (mainly in Utah), Peru, Trinidad, Madagascar, the former Soviet Union, the Balkan states, and the Philippines. Oil sand deposits in northwestern China (Xinjiang Autonomous Region) are larger; at some locations, the bitumen appears on the land surface around the town of Karamay.

In Canada, the Athabasca deposit along with the neighboring Wabasca, Peace River, and Cold Lake deposits have been estimated to contain approximately 2 trillion barrels (2×10^{12} bbl) of bitumen. The Venezuelan deposits may at least contain 1 trillion barrels (1.0×10^{12} bbl) of bitumen. Deposits of oil sand, each containing approximately 20 million barrels (20×10^{6} bbl) of bitumen, have also been located in the U.S., Albania, Italy, Madagascar, Peru, Romania, Trinidad, Zaire, and the former USSR. The oil sand deposits in the U.S. are contained in a variety of separate deposits in various states (Marchant and Koch, 1984) but, as many of these deposits are small, information on most is limited.

The Californian deposits are concentrated in the coastal region west of the San Andreas Fault. The largest deposit is the Edna deposit, which is located midway between Los Angeles and San Francisco. The deposit occurs as a stratigraphic trap, extends over an area of about 7000 acres, and occurs from outcrop to 100-ft (30-m) depth. The Sisquoc deposit (Upper Pliocene) is the second largest in California, and the total thickness of the deposit is about 185 ft (56 m), occurring over an area of about 175 acres with an overburden thickness between 15 and 70 ft (4.6 and 21 m). The third California deposit at Santa Cruz is located approximately 56 m (90 km) from San Francisco. The Kentucky oil sand deposits are located at Asphalt, Davis-Dismal Creek, and Kyrock. Oil sand deposits in New Mexico occur in the Triassic Santa Rosa sandstone. Finally, the oil sand deposits in Missouri occur over an area estimated at 2000 mi^2, and the individual bitumen-bearing sands are approximately 50 ft (15 m) in thickness, except where they occur in channels that may actually be as much as 250 ft (76 m) thick.

Oil sand deposits in Venezuela occur in the Officina/Tremblador tar belt, which is believed to contain bitumen-impregnated sands of a similar extent to those of Alberta, Canada. The organic material is bitumen having an API gravity less than 10°.

The Bemolanga (Madagascar) deposit is the third largest oil sand deposit presently known and extends over some 150 mi^2 in western Madagascar with a recorded overburden from 0 to 100 ft (0 to 30 m). The average pay zone thickness is 100 ft (30 m) with a total bitumen in-place quoted at approximately 2 billion barrels (approximately 2×10^{9} bbl).

The largest oil sand deposit in Europe is that at Selenizza, Albania. This region also contains the Patos oil field, throughout which there occurs extensive bitumen impregnation.

The Trinidad Asphalt Lake (situated on the Gulf of Paria, 12 mi west-south-west of San Fernando and 138 ft [43 m] above sea level) occupies a depression in the Miocene sheet sandstone.

The Romanian deposits are located at Derna and occur (along with Tataros and other deposits) in a triangular section, east and northeast of Oradia between the Sebos Koros and Berrettyo rivers.

Oil sands occur at Cheildag, Kobystan, and outcrop in the south flank of the Cheildag anticline; there are approximately 24 million barrels (24×10^6 bbl) of bitumen in place. Other deposits in the former USSR occur in the Olenek anticline (northeast of Siberia), and it has been claimed that the extent of bitumen impregnation in the Permian sandstone is on the same order of magnitude (in area and volume) as that of the Athabasca deposits. Oil sands have also been reported from sands at Subovka, and the Notanebi deposit (Miocene sandstone) is reputed to contain 20% bitumen by weight. On the other hand, the Kazakhstan occurrence, near the Shubar-Kuduk oil field, is a bituminous lake with a bitumen content that has been estimated to be of the order of 95% by weight of the deposit.

Oil sand occurrences also exist in the southern Llanos of Colombia, Burgan in Kuwait, and at the Inciarte and Bolivar coastal fields of the Maracaibo Basin, but very little is known about the deposits. There are also small deposits in the Leyte Islands (Philippines), the Mefang Basin in Thailand, Chumpi, and near Lima (Peru). Oil sand deposits have also been recorded in Spain, Portugal, Cuba, Argentina, Thailand, and Senegal, but most are poorly defined and are considered to contain (in-place) less than 1 million barrels (1×10^6 bbl) of bitumen.

The fact that commercialization has taken place in Canada does not mean that commercialization is imminent for other oil sand deposits. There are considerable differences between the Canadian deposits and the deposits in the U.S. and the rest of the world that could preclude across-the-board application of the principles applied to the Canadian oil sand deposits to the other oil sand deposits.

7.3 BITUMEN PROPERTIES

Bitumen can be assessed in terms of sulfur content, carbon residue, nitrogen content, and metals content. Properties such as the API gravity and viscosity also help the refinery operator to gain an understanding of the nature of the material that is to be processed. The products from high-sulfur feedstocks often require extensive treatment to remove (or change) the corrosive sulfur compounds. Nitrogen compounds and the various metals that occur in crude oils will cause serious loss of catalyst life. The carbon residue presents an indication of the amount of thermal coke that may be formed to the detriment of the liquid products.

7.3.1 Elemental (Ultimate) Composition

The elemental analysis of oil sand bitumen has been widely reported and of the data that are available, the proportions of the elements vary over fairly narrow limits (Speight, 1990, and references cited therein):

Carbon, 83.4 ± 0.5%
Hydrogen, 10.4 ± 0.2%
Nitrogen, 0.4 ± 0.2%
Oxygen, 1.0 ± 0.2%
Sulfur, 5.0 ± 0.5%
Metals (Ni and V), >1000 ppm

Bitumen from oil sand deposits in the U.S. has a similar ultimate composition to the Athabasca bitumen. However, to note anything other than the hydrogen-to-carbon atomic ratio (which is an indicator of the relative amount of hydrogen needed for upgrading), or the amount of nitrogen, is beyond the scope of general studies.

7.3.2 Chemical Composition

The precise chemical composition of bitumen, despite the large volume of work performed in this area, is largely speculative. In very general terms (and as observed from elemental analyses), heavy oil and bitumen are complex mixtures of (1) hydrocarbons, (2) nitrogen compounds, (3) oxygen compounds, (4) sulfur compounds, and (5) metallic constituents. However, this general definition is not adequate to describe the composition of bitumen as it relates to conversion to liquid products.

It is therefore convenient to divide the hydrocarbon components of bitumen into the following four classes:

1. Paraffins, which are saturated hydrocarbons with straight or branched chains, but without any ring structure. The occurrence of such chemical species in heavy oil and bitumen is rare.
2. Naphthenes, which are saturated hydrocarbons containing one or more rings, each of which may have one or more paraffinic side chains (more correctly known as *alicyclic hydrocarbons*).
3. Aromatics, which are hydrocarbons containing one or more aromatic nuclei, such as benzene, naphthalene, and phenanthrene ring systems, which may be linked up with (substituted) naphthene rings and paraffinic side chains.
4. Heteroatom compounds, which include organic compounds of nitrogen, oxygen, sulfur, and porphyrins (metallo-organic compounds). These are by far the major class of compound contained in bitumen and play a major role in conversion processes.

On a molecular basis, bitumen is a complex mixture of hydrocarbons with varying amounts of organic compounds containing sulfur, oxygen, and nitrogen, as well as compounds containing metallic constituents, particularly vanadium nickel, iron, and copper (Reynolds, 2000). Compared to the more conventional crude oils in which the hydrocarbon content may be as high as 97% by weight, bitumen (depending upon the source) may contain as little as 50% by weight hydrocarbons, with the remainder being compounds that contain nitrogen, oxygen, sulfur, and metals.

7.3.3 Fractional Composition

Fractional composition is an important property of bitumen, and bitumen can be separated into a variety of fractions called saturates, aromatics, resins, and asphaltenes (Speight, 1999, 2000, and references cited therein). Much of the focus has been on the constituents of the asphaltene fraction because of its high sulfur content, high coke-forming propensity, and the complexity of the cracking reactions (Chakma, 2000; Yen, 2000).

Data that define the composition are extremely important to refining processes. The data give the refiner an indication of the potential behavior of the bitumen in refinery processes and the potential yields of products that might be expected. The data also provide guidelines for the mining operation that is deigned to produce an average feedstock for further processing and so maintain a product balance.

7.3.4 Thermal Reactions

The thermal reactions of bitumen have received considerable attention and provide valuable information about the potential chemical conversion that can be performed (Speight, 1970, 1978, and references cited therein).

Bitumen constituents can be thermally decomposed under conditions similar to those employed for visbreaking (viscosity breaking; about 470°C [880°F]) to afford, on the one hand, light oils that contain higher paraffins and, on the other hand, coke:

$$\text{Bitumen} \rightarrow H_2, + CO, + CO_2, + H_2S, + SO_2, + H_2O,$$
$$+ CH_2{=}CH_2, + CH_4, + CH_3\,CH_3,$$
$$+ (CH_3)_3CH, + CH_3(CH_2)_nCH_3, \text{ etc.}$$

The reaction paths are extremely complex; spectroscopic investigations indicate an overall dealkylation of the aromatics to methyl (predominantly) or ethyl (minority) groups. In fact, the thermal decomposition of heavy oil and bitumen constituents affords a light oil and a hydrocarbon gas composed of the lower paraffins. Coke is also produced. The constituents of bitumen may also be hydrogenated to produce resins and oils at elevated temperatures (>250°C).

7.3.5 Physical Properties

The specific gravity of bitumen shows a fairly wide range of variation. The largest degree of variation is usually due to local conditions that affect material lying close to the faces, or exposures, occurring in surface oil sand deposits. There are also variations in the specific gravity of the bitumen found in beds that have not been exposed to weathering or other external factors.

Bitumen gravity primarily affects the upgrading requirements needed because of the low hydrogen content of the produced bitumen. The API gravity of known U.S. oil sand bitumen ranges downward from about 14° API (0.973 specific gravity) to approximately 2° API (1.093 specific gravity). Although only a vague relationship exists between density (gravity) and viscosity, very-low-gravity bitumen generally has very high viscosity.

TABLE 7.2
Distillation Data (cumulative percentage by weight distilled) for Bitumen and Crude Oil

Cut Point		Cumulative Percentage by Weight Distilled		
°C	°F	Athabasca	PR Spring	Leduc (Canada)
200	390	3	1	35
225	435	5	2	40
250	480	7	3	45
275	525	9	4	51
300	570	14	5	
325	615	26	7	
350	660	18	8	
375	705	22	10	
400	750	26	13	
425	795	29	16	
450	840	33	20	
475	885	37	23	
500	930	40	25	
525	975	43	29	
538	1000	45	35	
538+	1000+	55	65	

Bitumen is relatively nonvolatile (Bunger et al., 1979; Speight, 2000), and nondestructive distillation data (Table 7.2) show that oil sand bitumen is a high-boiling material. There is usually little or no gasoline (naphtha) fraction in bitumen, and the majority of the distillate falls in the gas oil–lubrication distillate range (greater than 260°C [500°F]). In excess of 50% by weight of each, bitumen is nondistillable under the conditions of the test; this amount of nonvolatile material responds very closely to the amount of asphaltenes plus resins of the feedstock.

The pour point is the lowest temperature at which the bitumen will flow. The pour point for oil sand bitumen can exceed 300°F — far greater than the natural temperature of oil sand reservoirs. The pour point is important to consider because for efficient production, a thermal extraction process to increase the reservoir temperature to beyond the pour point temperature must supply supplementary heat energy.

7.4 BITUMEN RECOVERY

Current commercial operations involve mining oil sand, after which the sand is transported to a processing plant, extract the bitumen, and dispose of the waste sand.

The Athabasca deposit in Canada is the site of the only commercial oil sand mining operation. The Suncor mining and processing plant, located 20 mi north of Fort McMurray, Alberta, started production in 1967. The Syncrude Canada mining and processing plant, located 5 mi (8 km) away from the Suncor plant, started production in 1978. In both projects, about half of the terrain is covered with muskeg,

an organic soil resembling peat moss, which ranges from a few inches to 23 ft (7 m) in depth. The major part of the overburden, however, consists of Pleistocene glacial drift and Clearwater Formation sand and shale. The total overburden varies from 23 to 130 ft (7 to 40 m) in thickness. The underlying oil sand strata averages about 150 ft (45 m), although typically 16 to 33 ft (5 to 10 m) must be discarded because of a bitumen content below the economic cut-off grade designated by either plant and generally on the order of 5% by weight.

Both Suncor and Syncrude are individually projecting production targets of 500,000 bbl/d of synthetic crude oil (mostly in the liquid fuel boiling range) within the next 5 to 10 years.

There are two approaches to open-pit mining of oil sand. The first uses a few mining units of custom design, e.g., bucket-wheel excavators and large draglines in conjunction with belt conveyors. In the second approach, a multiplicity of smaller mining units of conventional design is employed, e.g., scrapers and truck-and-shovel operations have been considered. Each method has advantages and risks. Both Suncor and Syncrude Canada, Ltd., with Suncor converting to large-scale truck and shovel technology in 1993, originally adopted the first approach.

Underground mining options have also been proposed but for the moment have been largely discarded because of the fear of collapse of the formation onto any operators or equipment. This particular option should not, however, be rejected out of hand because a novel aspect or the requirements of the developer (which remove the accompanying dangers) may make such an option acceptable.

Once the oil sand is mined, there remains the issue of recovering the bitumen. This is accomplished by application of the hot water process. To date, the hot water process is the only successful commercial process to be applied to bitumen recovery from mined oil sand in North America. Many process options have been tested with varying degrees of success, and one of these options may even supersede the hot water process. The hot water process utilizes the linear and nonlinear variation of bitumen density and water density, respectively, with temperature so that the bitumen, which is heavier than water at room temperature, becomes lighter than water at approximately 80°C (180°F). Surface-active materials in the oil sand also contribute to the process.

The oil sands deposits in the U.S. and the rest of the world have received considerably less attention than the Canadian deposits. Nevertheless, approaches to recover the bitumen from the U.S. oil sands have been made. In the present context, an attempt has been made to develop the hot water process for the Utah sands (Hatfield and Oblad, 1982; Miller and Misra, 1982). The process differs significantly from that used for the Canadian sands because of the oil-wet Utah sands, in contrast to the water-wet Canadian sands. This necessitates disengagement by hot water digestion in a high-shear force field under appropriate conditions of pulp density and alkalinity. The dispersed bitumen droplets can also be recovered by aeration and froth flotation.

The other above-ground method of separating bitumen from oil sands after the mining operation involves direct heating of the oil sand without previous separation of the bitumen (Gishler, 1949). Thus, the bitumen is not recovered as such but is an upgraded overhead product. Although several processes have been proposed to

accomplish this, the common theme is to heat the oil sand to separate the bitumen as a volatile product. At this time, however, it must be recognized that the volatility of the bitumen is extremely low, and what actually separates from the sand is a cracked product with the coke remaining on the sand.

The coke that is formed as a result of the thermal decomposition of the bitumen remains on the sand, which is then transferred to a vessel for coke removal by burning in air. The hot flue gases can be used either to heat incoming oil sand or as refinery fuel.

A later proposal suggested that the Lurgi process might have applicability to bitumen conversion (Rammler, 1970). A more modern approach has also been developed, which also cracks the bitumen constituents on the sand (Taciuk, 1981). The processor consists of a large, horizontal, rotating vessel that is arranged in a series of compartments. The two major compartments are a preheating zone and a reaction zone. Product yields and quality are reported to be high.

7.5 LIQUID FUELS FROM OIL SAND

Liquid fuels are produced from oil sand bitumen in the form of synthetic crude oil (syncrude) that undergoes further refining at a conventional refinery to produce the liquid fuels.

Synthetic crude oil is a complex mixture of hydrocarbons, somewhat similar to petroleum but differing in composition from petroleum insofar as the constituents of synthetic crude oil are not found in nature.

As a feedstock, the quality of oil sand bitumen is low compared to that of conventional crude oil and heavy oil. The high carbon residue of bitumen dictates that considerable amounts of coke will be produced during thermal refining (Table 7.3, Figure 7.3). Thus, production of liquid fuels from oil sand bitumen has included options for coke use.

Technologies for the production of liquid fuels from bitumen can be broadly divided into *carbon rejection* processes and *hydrogen addition* processes (Figure 7.1).

Carbon rejection processes redistribute hydrogen among the various components, resulting in fractions with increased hydrogen-to-carbon atomic ratios and fractions with lower hydrogen-to-carbon atomic ratios. On the other hand, hydrogen addition

TABLE 7.3
Predicted Coke Yields from Various Feedstocks

API Gravity of Feedstock	Carbon Residue Percentage by Weight	Coke Yield	
		Delayed Coking	Fluid Coking
2	30	45	35
6	20	36	23
10	15	28	17
16	10	18	12
26	5	9	3

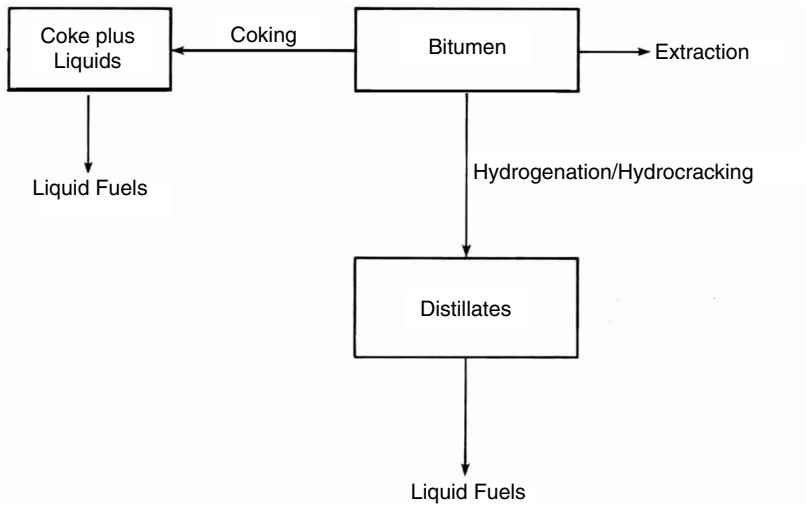

FIGURE 7.1 Production of liquid fuels from oil bitumen by carbon rejection processes and hydrogen addition processes.

processes involve reaction heavy crude oils with an external source of hydrogen and result in an overall increase in hydrogen-to-carbon ratio. Within these broad ranges, all upgrading technologies can be subdivided as follows:

1. Carbon rejection: for example, visbreaking, steam cracking, fluid catalytic cracking, and coking. Carbon rejection processes offer attractive methods of conversion of bitumen because they enable low operating pressure, though involving high operating temperature, without requiring expensive catalysts.
2. Hydrogen addition: Catalytic hydroconversion (hydrocracking), hydrovisbreaking, and donor solvent processes. Bitumen hydrotreating processes (with the attendant process parameters; Table 7.4) offer desulfurization to low-sulfur feedstocks for other processes or hydrocracking to kerosene and gas oil.
3. Separation processes: Distillation and deasphalting. Solvent deasphalting allows removal of sulfur and nitrogen compounds as well as metallic constituents in the high-carbon asphalt and would be more appropriate for use in combination with other processes.

Currently, the overall upgrading process by which bitumen is converted to liquid fuels is accomplished in two steps. The first step is the *primary upgrading* or *primary conversion* process (Figure 7.2), which improves the hydrogen-to-carbon ratio by either carbon removal or hydrogen addition, cracking bitumen to produce distillable products that are more easily processed downstream to liquid fuels.

The *secondary upgrading* process involves hydrogenation of the primary products and is the means by which sulfur and nitrogen are removed from the primary

TABLE 7.4
Hydrotreating Processing Parameters

Parameter	Naphtha	Bitumen
Temperature (°C)	300–400	340–450
Pressure (atm.)	35–70	50–200
LHSV	4.0–10.0	0.2–1.0
H^2 recycle rate (scf/bbl)	400–1000	3000–5000
Catalysts' life (years)	3.0–10.0	0.5–1.0
Sulfur removal (%)	>95	<80
Nitrogen removal (%)	>95	<40

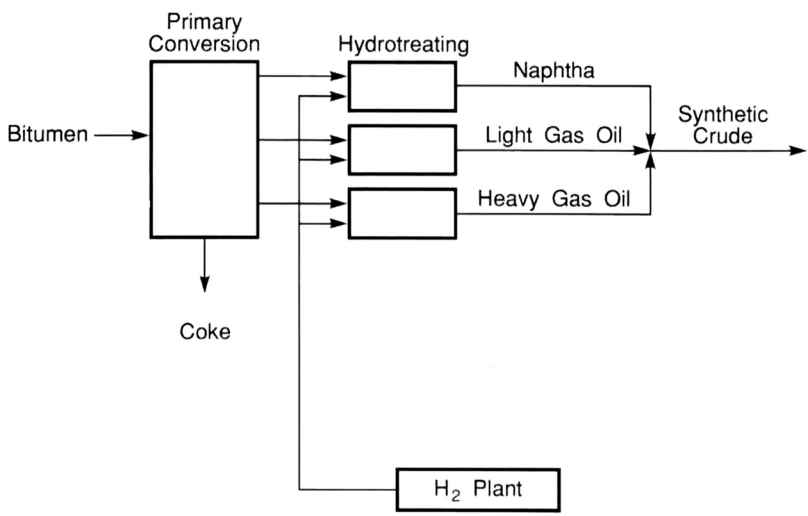

FIGURE 7.2 Bitumen conversion to liquid fuels by primary upgrading and secondary processes.

products. The upgraded or synthetic crude can then be refined to a variety of liquid fuels such as gasoline, diesel fuel, and jet fuel.

Bitumen is hydrogen deficient, and is upgraded by carbon removal (coking) or hydrogen addition (hydrocracking). There are two methods by which bitumen conversion can be achieved: (1) by direct heating of mined oil sand and (2) by thermal decomposition of separated bitumen. The latter is the method used commercially, but the former deserves mention here because the potential for commercialization remains open.

Although this improvement in properties may not appear to be dramatic, it usually leads to major advantages for refinery operators. Any incremental increase in the units of hydrogen-to-carbon ratio can save amounts of costly hydrogen during upgrading. The same principles are also operative for reductions in the nitrogen, sulfur, and oxygen contents. This latter occurrence also improves catalyst life and

activity as well as reducing the metals content. In short, *in situ* recovery processes (although less efficient in terms of bitumen recovery relative to mining operations) may have the added benefit of leaving some of the more obnoxious constituents (from the processing objective) in the ground.

The low proportion of volatile constituents (i.e., those constituents boiling below 200°C [392°F]) in bitumen precludes refining by distillation, and it is recognized that refining by thermal means is necessary to produce liquid fuel streams. A number of factors have influenced the development of facilities that are capable of converting bitumen to a synthetic crude oil.

Visbreaking has been considered as one process for the primary upgrading step (Table 7.5). However, a visbreaking product is still high in sulfur and nitrogen, with some degree of unsaturation. This latter property enhances gum formation with the accompanying risk of pipeline fouling and similar disposition problems in storage facilities and fuel oil burners. A high-sulfur content in finished products is environmentally unacceptable. In addition, high levels of nitrogen cause problems in the downstream processes, such as in catalytic cracking, where nitrogen levels in excess of 3000 parts per million will cause rapid catalyst deactivation; metals (nickel and vanadium) cause similar problems.

The higher-boiling constituents (i.e., those boiling in the range 200 to 400°C [390 to 750°F]) can be isolated by distillation but, in general terms, more than 40% by weight of oil sand bitumen boils above 540°C (1000°F). Nevertheless, the low proportion of volatile constituents (i.e., those constituents boiling below 200°C

TABLE 7.5
Examples of Product Yields and Properties for Visbreaking Athabasca Bitumen and Similar API Feedstocks

	Arabian Light Vacuum Residuum	Arabian Light Vacuum Residuum	Iranian Light Vacuum Residue	Athabasca Bitumen
Feedstock				
API gravity	7.1	6.9	8.2	8.6
Carbon residue[a]	20.3		22.0	13.5
Sulfur (wt%)	4.0	4.0	3.5	4.8
Product yields[b] (vol%)				
Naphtha (<425 °F, <220 °C)	6.0	8.1	4.8	7.0
Light gas oil (425–645 °F, 220–340 °C)	16.0	10.5	13.1	21.0
Heavy gas oil (645–1000 °F, 340–540 °C)		20.8	[b]	35.0
Residuum	76.0	60.5	79.9	34.0
API gravity	3.5	0.8	5.5	
Carbon residue[a]				
Sulfur (wt%)	4.7	4.6	3.8	

[a] Conradson

[b] A blank product yield line (or cell) indicates that the yield of the lower-boiling product has been included in the yield of the higher-boiling product.

[390°F]) in bitumen precludes complete refining by distillation although a vacuum distillation unit has been included in the latest plant (Syncrude) operation. However, it is recognized that refining by thermal means (i.e., thermal cracking) is necessary to produce liquid fuel streams. A number of factors have influenced the development of facilities that are capable of converting bitumen to a synthetic crude oil. A visbreaking product would be a hydrocarbon liquid that was still high in sulfur and nitrogen with some degree of unsaturation.

Thus, a product of acceptable quality could be obtained by distillation to an appropriate cut point, but the majority of the bitumen would remain behind to be refined by whichever means would be appropriate, remembering, of course, the need to balance fuel requirements and coke production. It is, therefore, essential that any bitumen-upgrading program convert the nonvolatile residuum to a lower-boiling, low-viscosity, low-molecular-weight product that also has a high hydrogen-to-carbon ratio.

7.5.1 Coking Processes

Coking processes are the primary upgrading processes by which bitumen conversion to distillable products is accomplished.

In the early stages of oil sand development, coking became the process of choice for bitumen conversion, and bitumen is currently converted commercially by delayed coking (Suncor) and by fluid coking (Syncrude). In each case, the charge is converted to distillate oils, coke, and light gases. The coke fraction and product gases can be used for plant fuel. The coker distillate is a partially upgraded material in itself and is a suitable feed for hydrodesulfurization to produce a low-sulfur synthetic crude oil.

Delayed coking (Table 7.6) is a semibatch process in which feed bitumen is heated before being fed to coking drums that provide sufficient residence time for the cracking reactions to occur.

The Suncor plant (in operation since 1967) involves a delayed coking technique followed by hydrotreating of the distillates to produce synthetic crude oil that has properties which are substantially different from the original bitumen and which are close to the properties of conventional petroleum (Table 7.7). The selection of delayed coking over less severe thermal processes, such as visbreaking, was based (at the time of planning, from 1960 to 1964) on the high yields of residuum produced in these alternate processes. The yields of coke from the residuum would have exceeded the plant fuel requirements, especially if the distillate had to be shipped elsewhere for hydrogen treating as well as a more favorable product distribution and properties. Alternate routes for the disposal of the excess coke would be needed.

In the Suncor operation, bitumen conversion to liquids is on the order of 75% by volume, with fluid coking giving a generally higher yield of liquids compared to delayed coking (Table 7.3, Figure 7.3). The remainder appears as coke (approximately 15% by weight) and gases.

Fluid coking is a continuous process employing two vessels with fluid coke. It provides a better yield of overhead products than delayed coking. Feed oil flows to the reactor vessel, where cracking and formation of coke occur; coke is combusted in the burner. Fluid transfer lines between these vessels provide the coke circulation

TABLE 7.6
Examples of Product Yields and Product Properties for Delayed Coking of Athabasca Bitumen and Similar API Feedstocks

	Kuwait Residuum	West Texas Residuum	Tia Juana Residuum	Alaska NS Residuum	Arabian Light Residuum	Athabasca Bitumen
Feedstock						
API gravity	6.7	8.9	8.5	7.4	6.9	7.3
Carbon residue[a]	19.8	17.8	22.0	18.1		17.9
Sulfur (wt%)	5.2	3.0	2.9	2.0	4.0	5.3
Product yields (vol%)						
Naphtha (95–425°F, 35–220°C)	26.7	28.9	25.6	12.5	19.1	20.3
Light gas oil (425–645°F, 220–340°C)	28.0	16.5	26.4	[b]	[b]	[b]
Heavy gas oil (645–1000°F, 340–540°C)	18.4	26.4	13.8	51.2	48.4	58.8
Coke	30.2	28.4	33.0	27.2	32.8	21.0
Sulfur (wt%)	7.5	4.5		2.6	5.6	8.0

[a] Conradson.

[b] A blank product line (or cell) indicates that the yield of the lower-boiling product has been included in the yield of the higher-boiling product.

TABLE 7.7
Properties of Synthetic Crude Oil from Athabasca Bitumen

Property		Bitumen	Synthetic Crude Oil	Crude Oil
Gravity, °API		8	32	35
Sulfur (percentage by weight)		4.8	0.2	0.1
Nitrogen (percentage by weight viscosity)		0.4	0.1	0.2
Centipoise @ 100°F		500,000	10	10
Distillation profile (percentage by weight; cumulative)				
°C	°F			
0	30	0	5	5
30	85	0	30	30
220	430	1	60	40
345	650	17	90	70
550	1020	45	100	90
Residuum		100		100

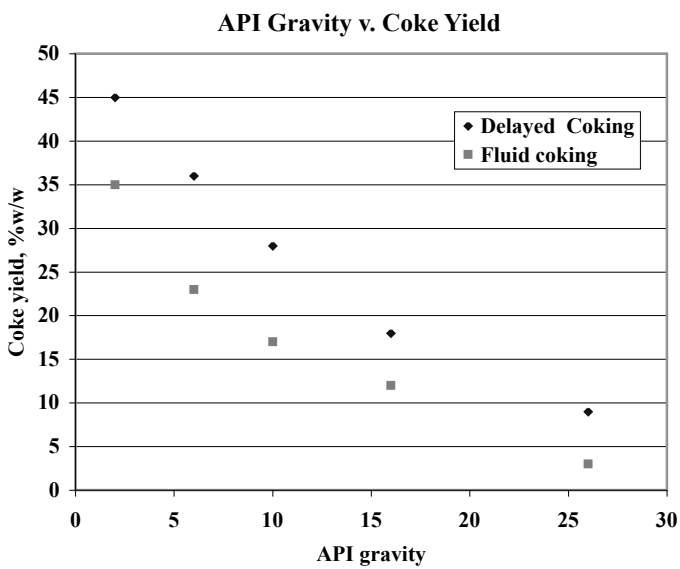

FIGURE 7.3 Comparison of coke produced by delayed coking and fluid coking processes.

necessary for heat balance. The proportion of coke burned is just sufficient to satisfy heat losses and provide the heat for the cracking reactions.

In the fluid coking process, whole bitumen (or topped bitumen) is preheated and sprayed into the reactor, where it is thermally cracked in the fluidized coke bed at temperatures typically between 510 and 540°C (950 and 1000°F) to produce light

products and coke. The coke is deposited on the fluidized coke particles while the light products pass overhead to a scrubbing section in which any high-boiling products are condensed and recombined with the reactor fresh feed. The uncondensed scrubber overhead passes into a fractionator, in which liquid products of suitable boiling ranges for downstream hydrotreating are withdrawn. Cracked reactor gases containing butanes and lower-molecular-weight hydrocarbon gases pass overhead to a gas recovery section. The propane material ultimately flows to the refinery gas system, and the condensed butane and butenes may (subject to vapor pressure limitations) be combined with the synthetic crude. The heat necessary to vaporize the feed and to supply the heat of reaction is supplied by hot coke that is circulated back to the reactor from the coke heater. Excess coke that has formed from the fresh feed and deposited on hot circulating coke in the fluidized reactor bed is withdrawn (after steam stripping) from the bottom of the reactor.

Sulfur is distributed throughout the boiling range of the delayed coker distillate, as with distillates from direct coking. Nitrogen is more heavily concentrated in the higher-boiling fractions but is present in most of the distillate fractions. Raw coker naphtha contains significant quantities of olefins and diolefins that must be saturated by downstream hydrotreating. The gas oil has a high aromatic content typical of coker gas oils.

7.5.2 Product Upgrading

The primary liquid product is then hydrotreated (secondary conversion or refining) to remove sulfur and nitrogen (as hydrogen sulphide and ammonia, respectively) and to hydrogenate the unsaturated sites exposed by the conversion process. It may be necessary to employ separate hydrotreaters for light distillates and medium-to-heavy fractions; for example, the heavier fractions require higher hydrogen partial pressures and operating temperatures to achieve the desired degree of sulfur and nitrogen removal. Commercial applications have therefore been based on the separate treatment of two or three distillate fractions at the appropriate severity to achieve the required product quality and process efficiency.

Hydrotreating is generally carried out in down-flow reactors containing a fixed bed of cobalt molybdate catalysts. The reactor effluents are stripped of the produced hydrogen sulfide and ammonia. Any light ends are sent to the fuel gas system, and the liquid products are recombined to form synthetic crude oil.

Finishing and stabilization (hydrodesulfurization and saturation) of the liquid products is achieved by hydrotreating the liquid streams as two or three separate streams. This is necessary because of the variation in conditions and catalysts necessary for treatment of a naphtha fraction relative to the conditions necessary for treatment of gas oil. It is more efficient to treat the liquid product streams separately and then to blend the finished liquids to a synthetic crude oil. To take advantage of optimum operating conditions for various distillate fractions, the Suncor coker distillate is treated as three separate fractions: naphtha, kerosene, and gas oil. In the operation used by Syncrude, the bitumen products are separated into two distinct fractions: naphtha and mixed gas oils. Each plant combines the hydrotreated fractions to form synthetic crude oil, which is then shipped by pipeline to a refinery. The

upgraded or synthetic crude oil has properties that are quite different from the original feedstock and are closer to the properties of a conventional high-API gravity crude oil (Table 7.7), and the product can be sent by pipeline to a refinery for further upgrading.

7.5.3 Other Processes

There are several other processes that have received some attention for bitumen upgrading. These processes include partial upgrading (a form of thermal deasphalting), flexicoking, the Eureka process, and various hydrocracking processes.

Direct coking of tar sand with a fluid bed technique has also been tested (Gishler, 1949). In this process, tar sand is fed to a coker or still, where the tar sand is heated to approximately 480°C (approximately 895°F) by contact with a fluid bed of clean sand from which the coke has been removed by burning. Volatile portions of the bitumen are distilled. Residual portions are thermally cracked, resulting in the deposition of a layer of coke around each sand grain. Coked solids are withdrawn down a standpipe, fluidized with air, and transferred to a burner or regenerator (operating at approximately 800°C, approximately 1470°F), where most of the coke is burned off the sand grains. The clean, hot sand is withdrawn through a standpipe. A portion (20 to 40%) is rejected, and the remainder is recirculated to the coker to provide the heat for the coking reaction. The products leave the coker as a vapor, which is condensed in a receiver. Reaction off-gases from the receiver are recirculated to fluidize the clean, hot sand that is returned to the coker.

An early process involved a coker for bitumen conversion and a burner to remove carbon from the sand. A later proposal suggested that the Lurgi process might be applicable to bitumen conversion (Rammler, 1970). Another approach has also been developed that also cracks the bitumen constituents on the sand. The processor consists of a large, horizontal, rotating vessel that is arranged in a series of compartments. The two major compartments are a preheating zone and a reaction zone (Taciuk, 1981).

Partial coking or thermal deasphalting process provides a minimal upgrading of bitumen. In partial coking, the hot water process froth is distilled at atmospheric pressure, and minerals and water are removed. A dehydrated mineral-free bitumen product is obtained that contains most of the asphaltenes and coke precursors. The process has been carried out in batch equipment in laboratory tests over periods ranging from 30 min to 4 h. Thermal cracking begins as the liquid temperature passes 340°C (645°F). The distillation is continued into the range 370 to 450°C (700 to 840°F). With slow heating (10°C [50°F] temperature rise per hour), the coke production rate is approximately 1% by weight of feed per hour. As the coke forms about the entrained mineral particles, 1 to 4% by weight coke up to 50% by volume of the feed is recovered as distillate. After this treatment, the residue may be filtered to yield an essentially ash-free production suitable for applications such as metallurgical coke or production of bituminous paints, for which the original mineral content would have disqualified it.

In flexicoking, a gasifier vessel is added to the system to gasify excess coke with a gas-air mixture to a low-heating-value gas that can be desulfurized and used as a

plant fuel. The Eureka process is a variant of delayed coking and uses steam stripping to enhance yield and produce a heavy pitch rather than coke by-product.

Another option includes the presence of steam as an agent to reduce coke formation. For example, thermal cracking of Athabasca bitumen at various reaction conditions with and without the presence of steam showed that the presence of steam decreased coke yield and decreased sulfur removal, and reduced the H/C ratio of the liquid products (Dutta et al., 2000).

Hydrocracking has also been proposed as a means of bitumen upgrading, i.e., asphaltene conversion to liquid fuels (Solari, 2000). The overall liquid yield of direct hydrogenation or hydrocracking of bitumen is substantially higher than that of coking, and significant amounts of sulfur and nitrogen are removed. Currently, however, large quantities of external fuel or hydrogen plant feedstock are required.

Most hydrocracking processes start with an upflow reactor system in which the 524°C (975°F) material is cracked or converted. To prevent coking, the processes operate at high pressure with direct contact between bitumen feed and circulating hydrogen. Hydrocracking processes include, predominantly, the H-Oil process (Table 7.8) and the LC-Fining process (Table 7.9). In fact, LC-Fining is now an onstream process for bitumen conversion to liquid fuels.

TABLE 7.8
H-Oil Process Feedstock and Product Data for Athabasca Bitumen and Low-API Feedstocks

	Arabian Medium Vacuum Residuum	Arabian Medium Vacuum Residuum	Athabasca Bitumen
Feedstock			
API gravity	4.9	4.9	8.3
Sulfur (wt%)	5.4	5.4	4.9
Nitrogen (wt%)			0.5
Carbon residue (wt%)			
Metals (ppm)	128.0	128.0	
Ni			
V			
Residuum (>525°C, >975°F) wt%			50.3
% conversion	0.7	0.9	
Products (wt%)			
Naphtha (C5–204°C, 400°F)	17.6	23.8	16.0
Sulfur (wt%)			1.0
Distillate (204–343°C, 400–650°F)	22.1	36.5	43.0
Sulfur (wt%)			2.0
Vacuum gas oil (343–534°C, 650–975°F)	34.0	37.1	26.4
Sulfur (wt%)			3.5
Residuum (>534°C, >975°F)	33.2	9.5	16.0
Sulfur (wt%)			5.7

TABLE 7.9
LC-Fining Process Feedstock and Product Data for Athabasca and Low-API Feedstocks

	Gach Saran Vacuum Residuum	Arabian Heavy Vacuum Residuum	AL/AH[a] Vacuum Residuum	Athabasca Bitumen
Feedstock				
API gravity	6.1	7.5	4.7	9.1
Sulfur (wt%)	3.5	4.9	5.0	5.5
Nitrogen (wt%)				0.4
Carbon residue (wt%)				
Metals				
Ni			39.0	
V			142.0	
Products (wt%[b])				
Naphtha (C5–205°C, C5–400°F)[b]	9.7	14.3	23.9	11.9
Sulfur (wt%)				1.1
Nitrogen (wt%)				
Distillate (205–345°C, 400–650°F)[b]	14.1	26.5	64.8	37.7
Sulfur (wt%)				0.7
Nitrogen (wt%)				
Heavy distillate (345–525°C, 650–975°F)[b]	24.1	31.1	11.9	30
Sulfur (wt%)				1.1
Nitrogen (wt%)				
Residuum (<>525°C, >975°F)[b]	47.5	21.3	5.0	12.9
Sulfur (wt%)				3.4
Nitrogen (wt%)				
Carbon residue (wt%)				

[a] AL/AH: Arabian light crude oil blended with Arabian heavy crude oil.
[b] Distillation ranges may vary by several degrees because of different distillation protocols.

The hydrocracker products, as expected, have higher hydrogen and lower sulfur and nitrogen contents than those from the coking route and require less secondary upgrading. However, disadvantages of the hydrogen route include relatively high hydrogen consumption and high-pressure operation. Processes that use conventional (e.g., Co-Mo or Ni-Mo) catalysts are susceptible to metals poisoning, which may limit applicability to, or economics of, operation on feeds high in metals such as bitumen.

7.5.4 The Future

Of the Canadian oil sand deposits, the Athabasca deposit is the only oil sand deposit with reserves shallow enough to be mined. There are currently three oil sand plants mining in the Athabasca deposit: Suncor Energy, Syncrude Canada, and Albian Sands Energy Inc. Many other companies have plans underway to construct oil sand plants.

As of May 2003, there had been 23 billion dollars (Cdn $\$23 \times 10^9$) spent on oil sand development with another 30 billion dollars forecast over the next 10 years. If all of those projects carry through to completion, bitumen production should be 2,000,000 bbl/d (a conservative estimate of 1,500,000 bbl of liquid fuels).

Because 90% of the Canadian oil sand deposits lie deep below the surface and cannot be recovered by open pit (surface) mining techniques, *in situ* processes are being developed to access the deeper deposits. One of the most promising *in situ* techniques is referred to as SAG-D (steam-assisted gravity drainage). This involves injecting steam though a series of wells into the deposit, after which the hot bitumen migrates by draining to the production wells.

The future of upgrading bitumen lies in the development of new processes and the evolution of refinery operations to meet the challenge of these heavy feedstocks. In fact, the essential step required of refineries is the upgrading of heavy oil and bitumen, particularly residua. In fact, the increasing supply of heavy crude oil is a matter of serious concern for the petroleum industry. To satisfy the changing pattern of product demand, significant investments in refining conversion processes will be necessary to profitably utilize these heavy crude oils. The most efficient and economical solution to this problem will depend to a large extent on individual country and company situations. However, the most promising technologies will likely involve the conversion of vacuum bottom residual oils, asphalt from deasphalting processes, and superheavy crude oils into useful low-boiling and middle-distillate products.

New processes for bitumen conversion will probably be used in place of the current visbreaking (or hydrovisbreaking) and coking processes, with some degree of hydrocracking as a primary conversion step. Other processes may replace or augment the deasphalting processes in many refineries. An exception, which may become the rule, is the upgrading of bitumen from oil sand deposits in Canada. The bitumen is subjected to either delayed coking (Suncor) or fluid coking (Syncrude) as the primary upgrading step, without prior distillation or topping. After primary upgrading, the product streams are hydrotreated and combined to form a synthetic crude oil that is shipped to a conventional refinery for further processing. Conceivably, other heavy oils and bitumen might be upgraded in the same manner and, depending on the upgrading facility, upgraded further for sales.

The limitations of processing these heavy oil and bitumen depend to a large extent on the amount of higher-molecular-weight constituents (i.e., asphaltene constituents) that contain the majority of the heteroatom constituents. These constituents are responsible for high yields of thermal and catalytic coke. The majority of the metal constituents in crude oils are associated with asphaltenes. Some of these metals form organometallic complexes. The rest are found in organic or inorganic salts that are soluble in water or in crude. In recent years, attempts have been made to isolate and to study the vanadium present in petroleum porphyrins, mainly in asphaltene fractions.

When catalytic processes are employed, complex molecules (such as those that may be found in the original asphaltene fraction) or those formed during the process are not sufficiently mobile (or are too strongly adsorbed by the catalyst) to be saturated by hydrogenation. The chemistry of the thermal reactions of some of these constituents dictates that certain reactions, once initiated, cannot be reversed, and

they proceed to completion. Coke is the eventual product. These deposits deactivate the catalyst sites and eventually interfere with the hydroprocess.

For future oil sand development, the government of the Province of Alberta, Canada, has announced a standard royalty formula for the oil sand industry, having embraced the principles and, to a large degree put into the practice, the fiscal recommendations of the National Task Force on Oil Sands Strategies. The Canadian Government plans to extend the mining tax regulation to include *in situ* operations. More than \$3.4 billion ($\$3.4 \times 10^9$) in new projects and expansions have been waiting for the resolution of fiscal terms to allow the industry to move forward with a number of projects that are in the initial stages of development. It is anticipated that such a move will encourage further development of the Canadian oil sand resources.

In another move to the future, Shell has constructed an upgrader at Scotford, near Fort Saskatchewan, Alberta. The upgrader uses hydrogenation technology to process bitumen into a wide range of premium-quality low-sulfur liquid fuels. Diluted bitumen is transported by pipeline to the upgrader.

There have been numerous forecasts of world production and demand for conventional crude, all covering varying periods of time. However, even after considering the impact of the conservation ethic, the development of renewable resources, and the possibility of slower economic growth, nonconventional sources of liquid fuels could well be needed to make up for the future anticipated shortfalls in conventional supplies.

This certainly applies to North America, which has additional compelling reasons to develop viable alternative fossil fuel technologies. Those reasons include, of course, the security of supply and the need to quickly reduce the impact of energy costs on the balance of payments. There has been the hope that the developing technology in North America will eventually succeed in applying the new areas of nuclear and solar energy to the energy demands of the population. However, the optimism of the 1970s has been succeeded by the reality of the 1980s, and it is now obvious that these energy sources will not be the answer to energy shortfalls for the remainder of the present century. Energy demands will most probably need to be met by the production of more liquid fuels from fossil fuel sources.

In the U.S., oil sand economics is still very much a matter for conjecture. The estimates that have been published for current and proposed Canadian operations are, in a sense, not applicable to operations in the U.S. because different production techniques may be required.

There is very little doubt that unlocking energy from oil sand is a complex and expensive proposition. With conventional production, the gamble is taken in the search, and the expenses can be high with no guarantee of a commercial find. With oil sand deposits, the bitumen is known to be there, but getting it out has been the problem and has required gambling on the massive use of untried technology. There is no real market for the bitumen extracted from the oil sand, and the oil sand itself is too bulky to be shipped elsewhere with the prospect of any degree of economic return. It is therefore necessary that the extraction and upgrading plants be constructed in the immediate vicinity of the mining operation.

To develop the present concept of liquid fuels from oil sands, it is necessary to combine three operations, each of which contributes significantly to the cost of the

venture: (1) a mining operation capable of handling 2 million tons, or more, of oil sand per day, (2) an extraction process to release the bitumen from the sand, and (3) an upgrading plant to convert the bitumen oil to a synthetic crude oil.

For Suncor (formerly Great Canadian Oil Sands Ltd.), being the first of the potential oil sand developers carried with it a variety of disadvantages. The technical problems were complex and numerous, with the result that Suncor (on stream: 1967) had accumulated a deficit of $67 million by the end of 1976, despite having reported a $12 million profit for that year. Since that time, Suncor has reported steady profits and has even realized the opportunity to expand operations to 60,000 bbl/day of synthetic crude oil. However, with hindsight it appears that such a situation may have some distinct advantages. The early start in oil sand processing gave Suncor a relatively low capital cost per daily barrel for a nonconventional synthetic crude oil operation. Total capital costs were about $300 million that, at a production rate of 50,000 bbl/d, places the capital cost at about $6000 per daily barrel.

It is perhaps worthy of mention here that a conventional refinery (150 to 300×103 bbl/d) may have cost at that time $100 to 400 million and have an energy balance (i.e., energy output/energy input) in excess of 90%. An oil sand refinery of the Suncor-Syncrude type may have an energy balance of the order of 70 to 75%.

The second oil sand processing plant, erected by the Syncrude Canada Ltd., faced much stiffer capital costs. In fact, it was the rapidly increasing capital costs that nearly killed the Syncrude project. Originally estimated at less than $1 billion (i.e., $\$1 \times 109$), capital needs began to escalate rapidly in early 1975. The cost was more than one of the four partners wanted to pay, and the number of participants dropped to three. Because the company dropping out held one of the largest interests, the loss was keenly felt and for a while the project was in jeopardy. It was finally kept alive through the participation of the Canadian government and the governments of the provinces of Ontario and Alberta. The Canadian government took a 15% interest in the project, the Province of Alberta a 10% interest, and the Province of Ontario a 5% interest. The balance remained with three of the original participants: Imperial Oil Ltd., Gulf Oil Canada Ltd., and Canada-Cities Service Ltd. After that initial setback, progress became rapid, and the project (located a few miles north of the Suncor plant) was brought to completion (onstream: 1978). The latest estimate of the cost of the plant is in the neighborhood of $2.5 billion. At a design level of 120,000–130,000 bbl/days, the capital cost is in excess of $20,000 per daily barrel.

For both the Suncor and Syncrude plants, the investment is broken down into four broad areas: (1) mining (28 to 34%), (2) bitumen recovery (approximately 12%), (3) bitumen upgrading (28 to 30%), and (4) offsites, including the power plant (16 to 24%).

Obviously, there are many features to consider when development of oil sand resources for the production of liquid fuels is given consideration. It is more important to recognize that what are important features for one resource might be less important in the development of a second resource. Recognition of this facet of oil sand development is a major benefit that will aid in the production of liquid fuels in an economic and effective manner.

REFERENCES

Berkowitz, N. and Speight, J.G., *Fuel*, 54: 138, 1975.

Bunger, J.W., Thomas, K.P., and Dorrence, S.M., *Fuel*, 58: 183, 1979.

Chakma, A., Kinetics and mechanisms of asphaltene cracking during petroleum recovery and processing operations, in *Asphaltenes and Asphalts 2. Developments in Petroleum Science*, 40B, Yen, T.F. and Chilingarian, G.V., Eds., Elsevier, Amsterdam, The Netherlands, 2000, chap. 6.

Dutta, R.P., McCaffrey, W.C., Gray, M.R., and Muehlenbachs, K., *Energy Fuels*, 14: 671, 2000.

Gishler, P.E., *Can. J. Res.*, 27: 104, 1949.

Gray, M.R., *Upgrading Petroleum Residues and Heavy Oils*, Marcel Dekker, New York, 1994.

Hatfield, K.E. and Oblad, A.G., *Proceedings of the 2nd International Conference on Heavy Crude and Tar Sands*, Meyer, R.F., Wynn, J.C., and Olson, J.C., Eds., McGraw-Hill, New York, 1982, p. 1175.

Marchant, L.C. and Koch, C.A., *Proceedings of the 3rd International Conference on the Future of Heavy Crude and Tar Sands*, Meyer, R.F., Wynn, J.C., and Olson, J.C., Eds., McGraw-Hill, New York, 1984, p. 1029.

Meyer, R.F., Ed., Heavy Crude and Oil sands — Hydrocarbons for the 21st Century, Petróleos de Venezuela S.A., Caracas, Venezuela, 1991.

Meyer, R.F. and Dietzman, W.D., in *The Future of Heavy Crude Oil and Tar Sands*, Meyer, R.F. and Steele, C.T., Eds., McGraw-Hill, New York, 1981, p. 16.

Miller, J.C. and Misra, M., *Fuel Process. Technol.*, 6: 27, 1982.

Phizackerley, P.H. and Scott, L.O., in *Bitumens, Asphalts, and Tar Sands*, Chilingarian, G.V. and Yen, T.F., Eds., Elsevier, Amsterdam, The Netherlands, 1978, p. 57.

Rammler, R.W., *Can. J. Chem. Eng.*, 48: 552, 1970.

Reynolds, J.G., Understanding metals in fossil fuels: a perspective of contributions by Yen, T.F., in *Asphaltenes and Asphalts 2. Developments in Petroleum Science*, 40B, Yen, T.F. and Chilingarian, G.V., Eds., Elsevier, Amsterdam, The Netherlands, 2000, chap. 3.

Smith-Magowan, D., Skauge, A., and Hepler, L.G., *Can. J. Pet. Technol.*, 21(3): 28, 1982.

Solari, R.B., Asphaltene hydroconversion, in *Asphaltenes and Asphalts 2. Developments in Petroleum Science*, 40B, Yen, T.F. and Chilingarian, G.V., Eds., Elsevier, Amsterdam, The Netherlands, 2000, chap. 7.

Speight, J.G., *Fuel*, 49: 134, 1970.

Speight, J.G., The thermal cracking of athabasca bitumen, in *Bitumens, Asphalts and Tar Sands: Developments in Petroleum Science*, 7, Chilingarian, G.V. and Yen, T.F., Eds., Elsevier, Amsterdam, The Netherlands, 1978, chap. 6.

Speight, J.G., in *Fuel Science and Technology Handbook*, Speight, J.G., Ed., Part II, Marcel Dekker, New York, 1990, chap. 12–16.

Speight, J.G., *The Chemistry and Technology of Coal*, 2nd ed., Marcel Dekker, New York, 1994.

Speight, J.G., *The Chemistry and Technology of Petroleum*, 3rd ed., Marcel Dekker, New York, 1999.

Speight, J.G., *The Desulfurization of Heavy Oils and Residua*, 2nd ed., Marcel Dekker, New York, 2000.

Taciuk, W., *Energy Proc. Canada.*, 74(4): 27, 1981.

Walters, E.J., in *Oil Sands: Fuel of the Future*, Hills, L.V., Ed., Canadian Society of Petroleum Geologists, Calgary, Alberta, Canada, 1974, p. 240.

Yen, T.F., The realms and definitions of asphaltenes, in *Asphaltenes and Asphalts 2. Developments in Petroleum Science*, 40B, Yen, T.F. and Chilingarian, G.V., Eds., Elsevier, Amsterdam, The Netherlands, 2000, chap. 3.

8 Shale Oil from Oil Shale

Sunggyu Lee

CONTENTS

8.1 OIL SHALE AS A SYNTHETIC FUEL (SYNFUEL) SOURCE

Interest in retorting oil from oil shale to produce a competitively priced synfuel had intensified since the oil embargo of the 1970s. Commercial interest, once very high in the 1970s and 1980s, substantially declined in the 1990s owing to the stable and low oil price. However, interest in oil shale as a clean liquid fuel source is being renewed in the 21st century, mainly triggered by the sky-rocketing petroleum prices as well as the shortage of oil in the global market. However, it should be noted that oil shales have been used as liquid and solid fuels in certain areas for a long time, and its research also has quite a long history.

Mixed with a variety of sediments over a lengthy geological time period, shale forms a tough, dense rock ranging in color from light tan to black. Shales are often called *black shale* or *brown shale*, depending on the color. Oil shales have also been given various names in different regions. For example, the Ute Indians, on observing that some outcroppings burst into flames upon being hit by lightning, referred to it as *the rock that burns*.

Oil shales are widely distributed throughout the world, with known deposits in every continent. In this regard, oil shale is quite different from petroleum, which is more concentrated in certain regions of the world. Table 8.1 shows some published information regarding worldwide oil shale reserves.[65] Depending on the data source and the year of reporting, the statistical values vary somewhat. Shales have been used in the past as a source of liquid fuel throughout the world, including Scotland, Sweden, France, South Africa, Australia, the USSR, China, Brazil, and the U.S. However, the oil shale industry has experienced several fluctuations on account of political, socioeconomic, market, and environmental reasons.

It is believed (evidence is lacking though supporting) that oil shales have been used directly as solid fuels in various regions, especially in areas with rich shales readily available near the earth's surface. For instance, an oil shale deposit at Autun, France, was commercially exploited as early as 1839.[62] As early as the 1850s, shale oil was being promoted as a replacement for wood, which America depended on for its energy. Logically, the oil shale industry in the U.S. was an important part of the U.S. economy prior to the discovery of crude oil in 1859. As Colonel Drake drilled his first oil well in Titusville, Pennsylvania, shale oil and its commercial production were gradually forgotten about and virtually disappeared with the availability of vast supplies of inexpensive liquid fuel, i.e., petroleum. Similarly, Scotland had a viable shale industry from 1850 to 1864, when the low price of imported crude oil forced it to cease operation. It is interesting to note that British Petroleum (BP) was

TABLE 8.1
Oil Shale Reserves of the World

IFP (1973)		BP (1978)		WEC (2002)		USGS (2003)		USDOE (2005)	
U.S.	66	U.S.	63	U.S.	78	U.S.	70	U.S.	72
Brazil	24	Brazil	23	Russia	7.4	Russia	15	Brazil	5.4
USSR	3.4	USSR	3.3	Brazil	2.5	Zaire	3.3	Jordan	4.2
Congo	3.0	Zaire	2.9	Jordan	1.0	Brazil	2.7	Morocco	3.5
Canada	1.3	—	—	Australia	1.0	Italy	2.4	Australia	2.1
Italy	1.1	—	—	Estonia	0.5	Morocco	1.8	China	1.5
China	0.8	—	—	China	0.5	Jordan	1.1	Estonia	1.1
Sweden	0.1	—	—	France	0.2	Australia	1.0	Israel	0.3
Germany	0.1	—	—	—	—	Estonia	0.5	—	—
Burma	0.1	—	—	—	—	China	0.5	—	—
—	—	—	—	—	—	Canada	0.5	—	—
—	—	—	—	—	—	France	0.2	—	—

Note: Figures are percentages; IFP = Institut Français du PÈtrole, BP = British Petroleum, WEC = World Energy Council, USGS = United States Geological Survey.

Source: From Laherrere, J., Review on Oil Shale Data, September 2005, www.oilcrisis.com/laherrere/OilShaleReview200509.pdf.

originally formed as a shale oil company. Likewise in Russia, oil shale from Estonia once supplied fuel gas for Leningrad.

In 1912, the president of the U.S., by executive order, established the Naval Petroleum and Oil Shale Reserves. The Office of Fossil Energy of the U.S. Department of Energy has been overseeing U.S. strategic interests in oil shale since that time. U.S. interest in oil shale revived briefly in the 1920s as domestic reserves of crude oil declined. But, subsequent discoveries of large quantities of oil deposits in Texas again killed the hopes of an embryonic oil shale industry. Serious interest in oil shale commercialization and development revived once again in the 1970s and the 1980s, as the Arab oil embargo affected world energy supply and, consequently, the world economy.

In 1974, Unocal developed their *Union B* retort process, and in 1976 planned for a commercial-scale plant at Parachute Creek to be built when investment would be economical. Many other companies, like Exxon, Shell, Dow Chemical, Sohio, TOSCO ARCO, AMOCO, Paraho, and others, initiated their own versions of oil shale development. In 1981, Unocal began construction of their Long Ridge 50,000 bbl/d plant based on their *Union B* retorting technology. AMOCO completed their *in situ* retorting demonstration of 1,900 and 24,400 bbl of shale oil in 1980 and 1981, respectively. In 1980, Exxon purchased ARCO's Colony interest and in 1981 began Colony II construction, aiming at a production level of 47,000 bbl/d based on the TOSCO II process. In 1982, Exxon announced the closure of their Colony II project due to low demand and high cost. This event was known as *Exxon Black Sunday*. Meanwhile, Shell continued with their *in situ* experiments at Red Pinnacle until 1983. To make matters worse, Congress abolished the Synthetic Liquid Fuels Program after 40 years of

operation and an investment of $8 billion. Paraho reorganized itself as New Paraho and began SOMAT asphalt production. In 1991, Occidental closed their C-b (Rio Blanco County, Colorado) tract project without actual operation. *Unocal* operated their last large-scale experimental mining and retorting facility in western U.S. from 1980 until the shutdown of its Long Ridge (San Miguel County, Colorado) project in 1991. Unocal produced a total of 4.5 million barrels of shale oil from oil shale with an average of about 34 gal of shale oil per ton of rock over the life of the project.[62] After Unocal's shutdown in 1992, there has been no oil shale production in the U.S. In the 1980s and 1990s, the stable crude oil price once again served as the principal reason for the diminishing interest in oil shale. Shell continued with some efforts in oil shale, particularly in the area of *in situ* heating technology at their property in Mahogany, Colorado. A notable experiment on *in situ* heating was done in 1997. Although oil shale activities in the U.S. have all but halted, some significant efforts continued in other countries such as Estonia, Australia, and Brazil.

There is again a sign of renewed interest in oil shale in the 21st century, as unstable and high energy prices, including those for natural gas and petroleum products, were experienced in most developed regions of the world at the onset of the new century. Examples of energy-related crises are: (1) California blackouts in 2001, (2) gasoline price surges in various regions of the U.S. in 2000 and 2001, (3) very high gasoline price owing to short supply of crude oil in 2004, (4) very high crude oil price in 2005 and 2006, and (5) sharp increases in residential energy costs in 2000, 2001, 2005 and 2006. However, it remains to be seen if the desire for energy self-sufficiency or independence will again swing the balance in favor of development of western U.S. oil shales.

At present, oil shale is commercially exploited in several countries, such as Brazil, China, Estonia, and Australia. Brazil has a long history of oil shale development and exploitation since the late 19th century. In 1935, shale oil was produced at a small plant in São Mateus do Sul in the state of Paraná.[63] A more serious developmental effort was imitated by Petrobras, which developed the *Petrosix process* for oil shale retorting. The Semiworks retort was developed in 1972 and operated on a limited commercial scale, and then a larger Industrial Module Retort was brought into service for commercial production in December 1991. The total annual production of shale oil in Brazil was 195,200 tons in 1999.[63]

In China, the total annual production of shale oil in Fushun, Liaoning province, amounted to 80,000 tons in 2001.[61] They used 80 new retorts, which are known as *Fushun retorts*. Fushun used to produce as much as 780,000 tons of shale oil a year using the earlier retorts, and the production was peaked in 1959.[61] Another major developmental effort is also being planned at Jilin province by China Power Investment Corp (CPIC), one of the country's major power producers. The estimated oil shale deposit in Jilin province is 17 billion tons, which is about 56% of the total deposits in China. Some reports[61] claim that China has the fourth largest oil shale deposits in the world after the U.S., Brazil, and Russia.

Estonia also has a long history of oil shale development and commercial exploitation. Its deposits are situated in the west of the Baltic Oil Shale Basin, and their oil shale is of high quality. Permanent mining of oil shale began in 1918 and continues to date.[63] The oil shale output in Estonia peaked at 31.35 million tons in 1980. In

1999, output was 10.7 million metric tons, out of which 1.3 million tons were retorted to produce 151,000 tons of shale oil.[63]

In the U.S., the Energy Security Act, S.932, was legislated under the Carter administration on June 30, 1980. This legislation was intended to help create 70,000 jobs a year to design, build, operate, and supply resources for synfuel plants and for production of biomass fuels. The act established the Synthetic Fuels Corporation. New directions under President Reagan along with relatively stable oil prices made the synfuel industry less attractive to the public. Under President Bush's administration, production and development of synfuels became strategically less important than clean coal technology (CCT) and acid rain control. Under the Clinton administration, when energy prices were very stable and low, this de-emphasizing trend further intensified in favor of national budget deficit reduction, which received public support and was based on projected long-term stability in energy supply and cost. Environmental protection received strong governmental and public support. In the 21st century, under President Bush, because of record-high energy prices and frequently experienced shortages, a renewed interest in energy self-sufficiency and development of commercial oil fields has been revived, but at the expense of some potential environmental disturbances. In 2004, the Office of Naval Petroleum and Oil Shale Reserves of the U.S. Department of Energy initiated a study on the significance of America's oil shale resources. The U.S. government also launched a new oil shale program with the *Oil Shale Development Act of 2005* to establish a leasing program in 2006. Likewise, interest in alternative energy also intensified worldwide.

Oil and gas, i.e., fluids from fossil fuels, accounted for one third of the total energy consumed in U.S. by the late 1920s. By the mid-1940s, oil and gas began to provide half of U.S. energy needs. They account for three fourths of U.S. energy needs today. The strong demand for oil and gas is likely to persist for a while, even though *bioenergy* and *hydrogen* fuels are rapidly gaining popularity, and are generally perceived as the principal energy sources for the future. Consequently, modern society's unprecedented appetite for fluid-type energy sources — without any new discoveries of major petroleum deposits in sight — will make it necessary to supplement supplies of domestic energy with synfuels such as those derived from oil shale or coal, as well as alternative fuel sources such as biomass, crops (e.g., soy and corn), and recycled materials. Hydrogen and ethanol will undoubtedly play very important roles as new gaseous and liquid fuels in the future energy market.

Market forces based on supply and demand will greatly affect the commercial development of oil shale. Besides competing with conventional crude oil and natural gas, shale oil will have to compete with coal-derived fuels for a similar market.[1] Liquid fuels derived from coal are methanol, additional products of indirect liquefaction, Fischer–Tropsch hydrocarbons, or oxygenates. Table 8.2 shows synfuel products and their corresponding market characteristics.

Table 8.3 summarizes various countries involved in major types of synfuel development.

Depending on the relative level of success in synfuel or alternative energy development, the energy consumption patterns in the 21st century may be significantly affected. More emphasis will be undoubtedly placed on clean and renewable energy development, as well as environmentally clean utilization of conventional fuel.

TABLE 8.2
Synfuel Products and Markets

Product	Technology Status	Market	Commercialization
Shale oil	Pilot plants up to 2000 tons/d	Mid-distillates (jet fuel; diesel fuel)	Regionally operated
Tar sands	Small; medium-scale plants	Synthetic crudes (transportation fuels)	In commercial production; production increases sharply
Coal liquids	Direct liquefaction in pilot plants (250 tons/d)	Light and mid-distillates; petrochemical feedstocks	Small-scale; specific application oriented; large-scale plants planned
Coal hydrocarbons	Indirect liquefaction of coal via Fischer–Tropsch synthesis; technology proved on large scales by SASOL	Petrochemical feedstocks	In commercial production
Methanol from natural gas	Low-pressure methanol synthesis technology actively used worldwide	Chemical and petrochemical feedstocks; gas turbine; MTBE/ETBE/TAME production; dimethylether production; fuel gasoline market; off-peak energy generation and storage	Very active and in large capacities; commercially used since the 1920s; in commercial production
Methanol from coal	Coal gasification proved in large-scale plants; liquid-phase methanol (LPMeOH) process proved for coal-derived syngas; single-stage synthesis process of dimethyether (DME) from coal-derived syngas developed	Chemical and petrochemical feedstock; dimethylether (DME) synthesis; once-through methanol (OTM); IGCC application	Large-scale plant commercialized in mid-1990s; large-scale plants are being planned

TABLE 8.3
Synfuel Developmental Efforts in Various Countries

Nation	Coal	Oil Shale	Tar Sand	Biomass
Australia	✓	✓		
Brazil	✓	✓		✓
Canada	✓		✓	✓
China	✓	✓		✓
Europe	✓			✓
Israel		✓		
Japan	✓			✓
Korea	✓			✓
Russia	✓	✓		✓
South Africa	✓			
U.S.A.	✓	✓		✓

Note: A prediction of production and development cannot be made, because of the high uncertainty in this field. More effort in synfuel production from agricultural sources (e.g., crops) are expected in various regions of the world.

8.2 CONSTRAINTS IN COMMERCIAL PRODUCTION OF SHALE OIL

During commercial exploitation of shale oils, one can be faced with various constraints that represent possible deterring factors. These constraints originate from a variety of sources: technological, economical (or financial), institutional, environmental, socio-economical, political, and water availability. The Office of Technology Assessment (OTA) analyzed the requirements for achieving each of the production goals by 1990, given the state of knowledge and the regulatory structure of the early 1980s.[2] Table 8.4 shows the factors that could hinder attainment of the goals, as assessed by OTA. In this table, their original target year of 1990 has been used without any alteration. Taking into consideration the fact that no serious commercialization activity was realized in the 1990s for a variety of reasons, the readers should use their own discretion in interpreting the given information. The constraints judged to be "moderate" will hamper, but not necessarily preclude, development; those judged to be "critical" could become more serious barriers; and when it was unclear whether or to what extent certain factors would impede development, they were called "possible" constraints. Even though the information contained in this table may be currently outdated, it is still relatively accurate and applicable to the present situation, considering the relative inactivity in this field during the last decade of the 20th century. Due to the high and fluctuating prices of energy, especially those of liquid fuels, in the 21st century, there is rekindled interest in our commercialization of oil shale processes throughout the world.

8.2.1 Technological Constraints

Oil shale can be retorted by either aboveground (*ex situ*) or underground (*in situ*) processing. In aboveground processing, shale is mined, transported to a processing

TABLE 8.4
Constraints to Implementing Shale Oil Production Targets (as of 1981)

	Severity of Impediment to 1990 Production Target (bbl/d)			
Potential Deterring Factors	**100,000**	**200,000**	**400,000**	**1,000,000**
Technological				
Readiness	None	None	None	Critical
Economic				
Availability of private capital	None	None	None	Moderate
Marketability of shale oil	Possible	Possible	Possible	Possible
Investor participation	None	Possible	Possible	Possible
Institutional				
Availability of land	None	None	Possible	Critical
Permitting procedures	None	None	Possible	Critical
Major pipeline capacity	None	None	None	Critical
Design and construction services	None	None	Moderate	Critical
Equipment availability	None	None	Moderate	Critical
Environmental				
Compliance with regulations	None	None	Possible	Critical
Water availability				
Availability of surplus surface water	None	None	None	Possible
Adequacy of existing supply systems	None	None	Critical	Critical
Socioeconomic				
Adequacy of community facilities and services	None	Moderate	Moderate	Critical

Source: From Office of Technology Assessment.

facility, and then heated in retorting vessels. Underground retorting processes can be classified into two large categories: (1) In *true in situ* (*TIS*) *processing*, an oil shale deposit is first fractured by explosives and then retorted underground, and (2) *A modified in situ* (*MIS*) *processing* is a more advanced *in situ* technology in which a portion of the deposit is mined and the rest rubblized by explosives and retorted underground. The crude shale oil can be burned as a boiler fuel, or it can be further converted into syncrude by adding hydrogen.

Critical issues that need to be answered include:

1. What are the advantages and disadvantages of different mining and processing methods?
2. Are the technologies ready for large-scale commercial applications?
3. What are the major areas of uncertainty in these technologies?
4. Are the technologies for process optimization available?
5. Are there sufficient scale-up data obtained from pilot and demonstration-scale plant operation?
6. What is the possibility of further technological breakthroughs in the process?
7. Are there sufficient data regarding the physical, chemical, and geological properties of oil shale and shale oil?

8.2.2 Economic and Financial Constraints

Even though an oil shale plant having a significant capacity is quite costly to build, the product oil will have to be competitive for the current and future energy price structure. World petroleum prices have been fluctuating for the past four decades, and the crude oil price has been sharply rising in the early part of the 21st century. However, long-term profitability of the industry could be impacted by future pricing strategies of competing fuels. This concern elevates the risk level of an oil shale industry. Considering the shortage of clean liquid fuel sources in the world energy market and the general trend of increasing prices, marketability of oil shale is improving, with good future prospects. This may be especially true in countries that do not produce sufficient petroleum but possess vast deposits of oil shale. In this regard, there are three issues possible: First, the involvement of the government can improve the economic scenario by providing the industry with incentives and credits in a variety of forms and tying the industry to the economic development of a region; second, specialization of products and diversification of by-products can contribute to the profitability of the industry; and third, securing captive use of shale oil in strategically developed energy-intensive industries also can contribute to the stability of the industry.

Even though a generalized cost breakdown of shale oil production is very difficult to make, a typical cost distribution for an oil shale project may be estimated as shown in Table 8.5. It can be seen from the table that the mining cost takes up a good share of the total operating cost. The cost to obtain shale oil crude, which includes the mining and retorting cost, is approximately 70% of the total operating cost. *Energy efficiencies* of most oil shale processes range from 58 to 63%, which can be further improved by utilizing efficient motors, adopting creative energy integration schemes, and exploiting waste energy. Table 8.6 shows some comparative information regarding the energy efficiencies of various synfuel processes. It should be noted that the efficiencies are very difficult to compare on a fair basis because efficiencies reported for the same process can be quite different from one another, depending on who reports it, how it is measured, on what basis it is calculated, etc. Improving energy efficiency without increasing the capital and operational cost is, therefore, a very important task that has to be undertaken by the process development team.

TABLE 8.5
Typical Cost Distribution for an Oil Shale Project

Cost Factor	Construction (%)	Operation (%)
Mining (shale crushing and spent shale disposal)	16	43
Retorting	37	28
Upgrading	22	29
Utilities and off-sites	25	—
Total	100	100

Source: From Taylor, R.B. *Chemical Engineering*, September 7, 1981.

TABLE 8.6
Energy Efficiencies of Various Synfuel Processes

Process	Efficiency (%)
Lurgi pressure gasification	70
Lurgi pressure gasification followed by shift methanation	63
Shale oil processes	58–63
Combined cycle	57
Fischer–Tropsch synthesis	40
Low-pressure methanol synthesis	49
Methanol synthesis followed by methanol-to-gasoline (MTG)	45

Issues related to the economics of oil shale processing are:

1. What are the economic and energy-supply benefits of oil shale development?
2. What are the environmental and ecological impacts of oil shale development?
3. What are the economic impacts of establishing an oil shale industry?
4. How many shale oil products can be used in the local region?
5. Is there enough capacity for pipeline transportation of shale oil?
6. Is there an upgrading facility operating in the vicinity, or is a separate upgrading facility going to be built as part of the project?
7. How much will an oil shale facility cost?
8. For how many years can the facility be operated in the original location?
9. What is the return on investment, especially for the long term?
10. At what level of petroleum crude price is shale oil competitive?
11. When the petroleum crude price goes up, what is the impact on the production cost of shale crude oil? Is it going to be more competitive? Is there any threshold value for the petroleum crude price for shale oil to be a strong competitor?
12. Overall, is oil shale economically competitive without any tax credits and incentives and at what level?

8.2.3 Environmental and Ecological Constraints

The oil shale deposits found in the *Green River Formation* in the states of Colorado, Wyoming, and Utah are the largest in terms of size of deposit and most studied in the U.S. The oil contained in these deposits is estimated at about 1800 billion barrels of recoverable shale oil. Owing to the vast resources and high oil content of shales, this region has long been the most attractive to oil shale industries. However, the technology used in mining and processing oil shale has aroused environmental and ecological concerns. The *Devonian-Mississippian eastern black shale* deposits are widely distributed between the Appalachian and Rocky Mountains. Even though these oil shales also represent a vast resource of fossil fuel, they are generally lower in grade (oil content per unit mass of shale rock) than Green River Formation oil shales.[9]

Several factors affecting the environmental constraints in commercially exploiting Green River Formation oil shale are discussed hereafter. This analysis is provided as an example and may also serve as a guideline for other similar projects. Therefore, similar analyses can be conducted for other oil shale deposits worldwide.

8.2.3.1 Region of Oil Shale Field and Population

The Upper Colorado region, which is the upper half of the Colorado River Basin, is traditionally "western rural" and consists of sparsely vegetated plains. The population density is also low, approximately three persons per square mile. The region is therefore less sensitive to disturbances on land, changes in traffic patterns, and construction and operation noises.

8.2.3.2 Water Availability

A rate-limiting factor in further development of the area is the availability of water, which may not be a problem in other regions. Water of the Colorado River could be made available for depletion by oil shale. An important factor that must be taken into consideration in any water use plan is the potential salt loading of the Colorado River. With oil shale development near the river, the average annual salinity is anticipated to increase, unless some preventive measures or treatment methods are implemented. The ecological damages associated with these higher salinity levels could be significant, and have been the subject of extensive ecological studies.

8.2.3.3 Other Fossil Energy and Mineral Resources

The Green River Formation oil shale area has extensive fossil fuel resources other than oil shale. Natural gas recoverable from this area is estimated at 85 trillion ft^3, crude oil reserves are estimated at 600 million barrels, and coal deposits at 6–8 billion tons. These nonshale energy resources are not trivial, and they can also be developed together with oil shale. Furthermore, 27 billion tons of alumina and 30 billion tons of nahcolite are present in the central Piceance Creek Basin. These minerals may be mined in conjunction with oil shale. Such an effort can potentially enhance the profitability of the combined venture.

8.2.3.4 Regional Ecology

Ecologically, the tristate region is very valuable. Owing to the sparse population density, the region has retained its natural character, of which the community is proud. Fauna include antelopes, bighorn sheep, mule deer, elks, black bears, moose, and mountain lions. However, there is little fishery habitat in the oil shale areas, even though the Upper Colorado region includes 36,000 acres in natural lakes.

8.2.3.5 Fugitive Dust Emission and Particulate Matter Control

Operations such as crushing, sizing, transfer conveying, vehicular traffic, and wind erosion are typical sources of fugitive dust. Control of airborne particulate matters

(PM) could pose a challenge. Compliance with regulations regarding particulate matter control must be factored in.

8.2.3.6 Hazardous Air Pollutants (HAPs)

Gaseous emissions such as H_2S, NH_3, CO, SO_2, NO_x, and trace metals are sources of air pollution. Such emissions are at least conceivable in oil-shale-processing operations. However, the level of severity is far less than that of other types of fossil fuel processing. The same argument can be made for the emission of carbon dioxide, which is a major greenhouse gas.

8.2.3.7 Outdoor Recreation and Scenery

Outdoor recreation in the tristate oil shale region has always been considered of high quality, because of the vastness of the essentially pristine natural environment and the scenic and ecological richness of the area. Maintaining the beauty of the area and preserving the high-quality natural resources must be taken into serious consideration, when oil shale in the region is commercially exploited. Such considerations generally hold true for other oil shale regions in the world.

8.2.3.8 Groundwater Contamination

Control of groundwater contamination is an important and nontrivial task. It is generally true for all types of oil shale operations including *ex situ* retorting, *in situ* pyrolysis, spent shale disposal and reburial, and upgrading. Without appropriate preventive measures, the groundwater could be contaminated by heavy metals, inorganic salts, organics such as polycyclic aromatic hydrocarbons (PAHs), etc. Both prevention and treatment must be fully investigated.

8.3 RESEARCH AND DEVELOPMENT NEEDS IN OIL SHALE

The synthetic crude reserves in oil shale, in terms of their crude oil production potential, are sufficient to meet U.S. consumption for several centuries at the current rate of liquid fuel utilization. Raw shale oil is the crude oil product of the retorting process and is highly *paraffinic*, i.e., containing mostly straight-chained hydrocarbons. However, it also contains fairly high levels of sulfur, nitrogen, and oxygen, as well as olefins; and it requires substantial upgrading before it can be substituted for refinery feed. Sulfur removal down to a few parts per million (ppm) is necessary to protect multimetallic reforming catalysts. Removing nitrogen from condensed heterocyclics, which also poisons cracking catalysts, requires an efficient technology that uses less hydrogen. The technologies developed for petroleum crude upgrading can be adopted for oil shale upgrading with relatively minor or no modifications.

This problem stresses the need for understanding the properties of oil shale and shale oil on a molecular level. Research needs can be broadly classified into six general categories: (1) chemical characterization of the organic and inorganic constituents,

(2) correlations of physical properties, (3) enhanced recovery processes of synfuels, (4) refining of crude shale oil, (5) process design with efficient energy integration schemes, and (6) environmental and toxicological problems.

8.3.1 Chemical Characterization

Improved analytical techniques must be developed to obtain the information needed to better understand oil shale chemistry, as well as to develop new technologies for utilizing shale. Most analytical methods developed and used for petroleum analytical chemistry have a long history of successful application, but their validity to the shale application is often questionable. Basic questions that need to be answered include:

1. In what forms do the organic heteroatoms exist?
2. How are they bonded into the basic carbon structure?
3. What can serve as the model compounds for sulfur and nitrogen sources in oil shale?
4. What is the aromaticity level of shale oil?
5. What is the ratio of alkanes to alkenes?
6. What are the effects of different retorting processes on the boiling range distribution of the shale oil crude?
7. What are the inorganic ingredients in oil shale and shale oil?

One way of characterizing oil shale is via separation of organics by extraction. The most commonly used techniques include gel permeation chromatography (GPC) for molecular weight distribution, gas chromatography (GC) using both packed column and glass capillary column for product oil distribution, simulated distillation using GC for boiling range determination, and molecular identification by liquid chromatography (LC).

Mass spectrometry (MS) can be extremely useful. In particular, GC–MS is good for product identification and model compound studies. Pyrolysis GC–MS can also be used for examining shale decomposition reactions.

Elemental analysis of oil shale is quite similar to that of petroleum and coal. More stringent requirements for C, H, O, N, and S analysis are needed for oil shale, as organic carbon in the shale should be distinguished from inorganic carbon in carbonate materials. Analysis for C, H, N, and S, which are very frequently used for coal analysis, can also be used for oil shale.

8.3.2 Correlation of Physical Properties

Physical properties of oil shale should be characterized via electrical and conductive measurements, scanning microscopy, spectroscopic probes, and all other conventional methods. Especially, the correlation between physical properties and pyrolysis conversion is useful for designing a pilot-scale or commercial retort. The ^{13}C-NMR work should be expanded to provide a detailed picture of the various chemical forms encountered. Electron spin resonance (ESR) studies of carbon radicals in oil shale could also provide invaluable clues about the conversion process.

Correlations of physical properties that can be used for a variety of oil shales are especially useful. Predictive forms of correlation are a powerful tool in engineering design calculations, as well.

8.3.3 Mechanisms of Retorting Reactions

Kinetics of oil shale retorting has been studied by various investigators. However, the details of reaction mechanism have not been generally agreed upon. This may be one of the reasons why problems associated with *in situ* pyrolysis require, primarily field experiments rather than small laboratory-scale experiments. The retorting process itself can be improved and optimized when its chemical reaction mechanisms are fully elucidated. Similarly, more efficient retort design can be accomplished.

8.3.4 Heat and Mass Transfer Problems

Oil shale rocks are normally low in both porosity and permeability. Therefore, it is very important to know the combined heat and mass transfer processes of a retort system. The processes of heat and mass transfer in a retort operation affect the process operating cost significantly, because the thermal efficiency is directly related to the total energy requirement and mass transfer conditions directly affect the recovery of oil and gas from a retort. The various process technologies may differ from one another only in their method of heat and mass transfer, and there is always room for further improvement. Therefore, understanding the transport processes in oil shale retorting is essential in mathematical modeling of a retort system, as well as in design of an efficient retort system. The analysis of heat and mass transfer requires a vast amount of information, such as physical properties of inorganic and organic ingredients of oil shale, bed and rock porosity, and its distribution; permeability; dolomite and other carbonate compositions in the shale, etc.

8.3.5 Catalytic Upgrading of Shale Oil Crudes

As mentioned earlier, prerefining of crude shale oil is necessary to reduce sulfur and nitrogen levels, and contamination by mineral particulates. Because large portions of nitrogen and sulfur species in shale oil are present as heteroaromatics, research opportunities of great significance exist in the selective removal of heteroaromatics, final product quality control, and molecular weight reduction.

Raw shale oil has a relatively high pour point of 75 to 80°F, compared to 30°F for Arabian Light. Olefins and diolefins may account for as much as one half of the low-boiling fraction of 600°F or lower, and lead to the formation of gums.

Raw shale oil typically contains 0.5 to l.0% oxygen, l.5 to 2.0% nitrogen, and 0.15 to l.0% sulfur. As can be seen, the nitrogen level in shale oil is very high, whereas the sulfur level is in a similar range to other fossil fuel liquids. Sulfur and nitrogen removal must be very complete as their compounds poison most of the catalysts used in refining; their oxides (SO_x and NO_x) are well-known air pollutants.

As raw shale oil is a condensed overhead product of pyrolysis, it does not contain the same kinds of macromolecules found in petroleum and coal residuum. Conventional catalytic cracking, however, is an efficient technique for molecular weight reduction. It is crucially important to develop a new cracking catalyst that is more resistant to basic poisons (nitrogen and sulfur compounds).[73] At the same time, research should also focus on reduction of molecular weight of shale oil crude with low consumption of hydrogen.

8.3.6 By-Product Minerals from U.S. Oil Shale

Many different kinds of carbonate and silicate minerals occur in oil shale formations. Trona beds [$Na_5(CO_3)(HCO_3)_3$] in Wyoming are a major source of soda ash (sodium carbonate [Na_2CO_3]), whereas nahcolite ($NaHCO_3$) is a potential by-product of oil shale mining from Utah and Colorado.

Precious metals and uranium are contained in good amounts in eastern U.S. shales. It is unlikely that in the near future recovery of these mineral resources will be possible as a commercially favorable recovery process has not yet been developed. However, it should be noted that there are many patents on recovery of alumina from Dawsonite-bearing beds by leaching, precipitation, calcination, etc. The chemical formula for dawsonite is $NaAl(CO_3)(OH)_2$.

8.3.7 Characterization of Inorganic Matters in Oil Shale

The analytical techniques applied to the characterization of inorganic constituents in oil shale include x-ray powder diffraction (XRD), thermogravimetric analysis (TGA), scanning electron microscopy (SEM), and transmission electron microscopy (TEM). Further, electron microprobe analysis (EMPA) may provide a useful tool for studying crystals at the molecular level and generate valuable information on the phases encountered. Most oil shale is also rich in inorganic matter, and these inorganic ingredients also go through the same process treatment as the organic constituents of the shale. The most significant of this inorganic matter include dolomite ($CaCO_3 \cdot MgCO_3$) and calcite ($CaCO_3$), both of which decompose upon heating and liberate gaseous carbon dioxide. This carbonate decomposition reaction is endothermic in nature, i.e., absorbing heat thereby reducing the process thermal efficiency of kerogen (oil shale hydrocarbon) pyrolysis.

8.4 PROPERTIES OF OIL SHALE AND SHALE OIL

To develop efficient retorting processes as well as to design a cost-effective commercial-scale retort, physical, chemical, and physicochemical properties of oil shales (raw material) and shale oils (crude liquid products) must be fully known. However, difficulties exist in the measurement of various physical and chemical properties of a variety of oil shales on a consistent basis. In this section, the properties that are essential in designing an efficient retort, as well as in understanding the oil shale retorting process, will be discussed. Even though a good deal of literature and data have been presented in this section, it is not solely intended to build a data bank of

oil shale properties; rather, appropriate utilization (and interpretation) of data and their measurements are stressed. More extensive treatment of property data can be found in References 7–9,12, and 26 given at the end of this chapter.

8.4.1 Physical and Transport Properties of Oil Shale

8.4.1.1 Fischer Assay

The nominal amount of condensable oil that can be extracted from oil shale is commonly denoted by the term *Fischer assay* of the oil shale. The Fischer assay is a simple and representative quantity that can be obtained quite easily for all kinds of oil shale by following *the standardized retorting procedure* under nitrogen atmosphere. The actual oil content in the oil shale, both theoretically and nominally, exceeds the Fischer assay. Depending on the treatment processes as well as the type of oil shale, oil yield from oil shale often exceeds the Fischer assay value by as much as 50%. Examples of such extraction processes include retorting in a hydrogen-rich environment, retorting in a CO_2 sweep gas environment, supercritical fluid extraction of oil shale, etc. The procedure for Fischer assay of oil shale is modified from a Fischer assay procedure for carbonization of coal at a low temperature. A brief description of the *Fischer assay procedure* is as follows: Take a crushed sample of oil shale of 100 g and subject it to a preprogrammed (such as linear ramping) heating schedule in an inert (such as nitrogen) environment. The oil shale is heated from 298 to 773 K very linearly over a 50-min. period while being purged with nitrogen. The linear heating rate is 9.5°C/min. Following the heat-up period, the sample is held at 773 K for an additional 20 to 40 min. and the oil collected, typically in a condenser tube, is measured. This recovered oil amount is then recorded in a unit of liters per ton (l/ton) or gallons per ton (gal/ton).

This procedure cannot recover all the organic matter originally contained in shale and leaves char associated with ash in the rock matrix, as well as larger-molecular-weight hydrocarbons blocking the pores. Nevertheless, the Fischer assay is used as a very convenient measure of recoverable organic hydrocarbon content and provides a common basis for comparison among various oil shales. If this value is higher than 100 l/ton, it is typically considered a *rich shale*; if less than 30 l/ton, a *lean shale*.

8.4.1.2 Porosity

Porosity of porous materials can be defined in a number of different ways, depending on what specific pores are looked at and how the void volumes are measured. They include: interparticle porosity, intraparticle porosity, internal porosity, porosity by liquid penetration, porosity by saturable volume, porosity by liquid absorption, superficial porosity, total open porosity, bed porosity (bed void fraction), packing porosity, etc.

Porosity of the mineral matrix of oil shale cannot be determined by the methods used for determining porosity of petroleum reservoir rocks, because the organic matter in the shale exists in solid form and is essentially insoluble. However, the results of a laboratory study at the Laramie Center[3] (currently, Western Research

TABLE 8.7
Porosities and Permeabilities of Raw and Treated Oil Shale

	Porosity			Permeability	
Fischer Assay	Raw	Heated to 815°C	Plane	Raw	Heated to 815°C
1.0[a]	9.0[b]	11.9	A[c]	—	0.36[d]
			B	—	0.56
6.5	5.5	12.5	A	—	0.21
			B	—	0.65
13.5	0.5	16.4	A	—	4.53
			B	—	8.02
20.0	<0.03	25.0	A	—	—
			B	—	—
40.0	<0.03	50.0	A	—	—
			B	—	—

[a] Fischer assay in gal/ton.

[b] Numbers in percentages of the initial bulk volume. Porosity was taken as an isotropic property, i.e., property that is independent of measurement direction.

[c] Plane A is perpendicular to the bedding plane, Plane B is parallel to the bedding plane.

[d] Units in milidarcy.

Source: From Chilingarian, G.V. and Yen, T.F., *Bitumens, Asphalts, and Tar Sands*, Elsevier, Amsterdam, 1978, chap. 1.

Institute, Laramie, WY) have shown that inorganic particles contain a micropore structure, about 2.36 to 2.66 vol%. Although the particles have an appreciable surface area, about 4.24 to 4.73 m^2/g for shale assaying of about 29 to 75 gal/ton, it seems to be limited mainly to the external surface rather than the pore structure. Measured porosities of the raw oil shales are shown in Table 8.7.[4]

As noted, except for the two low-yield oil shales, naturally occurring porosities in the raw oil shales are almost negligible, and they do not afford access to gases. Porosity may exist to some degree in the oil shale formation where fractures, faults, or other structural defects occurred. It is also believed that a good portion of the pores are either blind or very inaccessible. Crackling and fractures, or other structural defects often create new pores and also break up some of the blind pores. It should be noted here that *closed* or *blind* pores are normally not accessible by mercury porosimetry even at high pressures. Owing to the severity of mercury poisoning, the instrument based on pressurized mercury penetration through pores is no longer used.

8.4.1.3 Permeability

Permeability is the ability, or measurement of a rock's ability, to transmit fluids and is typically measured in darcies or millidarcies. Permeability is part of the proportionality constant in *Darcy's law*, which relates the flow rate of the fluid and the fluid viscosity to a pressure gradient applied to the porous media. Darcy's law is a

phenomologically derived constitutive equation based on the conservation of momentum that describes the flow of a fluid through a porous medium. A simple relationship relates the *instantaneous discharge rate* (local volumetric flow rate) through a porous medium to the *local hydraulic gradient* (change in hydraulic head over a distance, i.e., $\Delta h/L$, dh/dL, or ∇h) and the *hydraulic conductivity* (k) at that point.

$$Q = -kA\frac{h_a - h_b}{L}$$

Or, dividing both sides by the area (A) yields,

$$q = -k\ \nabla h$$

where q is the *Darcy flux*, i.e., that is the discharge rate per unit area, expressed in terms of [length/time]. Even though the final unit of the Darcy flux is the same as that of velocity, a clear conceptual difference between the two must be understood. Based on the analogy between Darcy's and Poiseuille's law, the hydraulic conductivity term can be factored out in terms of intrinsic permeability and the fluid properties as:

$$k = (k')\bullet(\rho g/\mu))$$

where k' is the *intrinsic permeability*, which has the dimension of [length^2]. Whereas the term $[\rho g/\mu]$ describes the penetrating fluid properties, the intrinsic permeability (k') summarizes the properties of the porous medium. The usual unit for permeability is the *darcy* (D), or more commonly the *milli darcy* or *mD* (1 darcy $\approx 10^{-12}$ m^2). Converted to SI units, precisely speaking, 1 D is equivalent to 0.986923 μm^2. The discussion presented here is a simplified one, in which unidirectional homogeneous fluid permeation without explicit inclusion of any external force terms is considered. However, it may be still evident that permeability should be expressed in a multidirectional manner; in other words, it is most adequately expressed as a *permeability tensor*. Exhaustive discussions about Darcy's law can be found in most textbooks on transport phenomena,[66] fluid mechanics, and hydraulogy.

The permeability of raw oil shale is essentially zero because the pores are filled with a nondisplaceable organic material. Tisot[4] showed that gas permeability, either perpendicular or parallel to the bedding plane, was not detected in most oil shale samples at a pressure differential across the cores of 3 atm of helium for 1 min. In general, oil shale constitutes a highly impervious system. Thus, one of the major challenges of any *in situ* retorting project is the creation of a suitable degree of permeability in the formation. This is why an appropriate rubblization technique is essential to the success of an *in situ* pyrolysis project.

Of practical interest is the dependency of porosity or permeability on temperature and organic content. Upon heating to 510°C, an obvious increase in oil shale porosity is noticed. These porosities, which vary from 3 to 6 l vol%[4] of the initial bulk oil shale volume, represented essentially the volumes occupied by the organic matter before the

retorting treatment. Therefore, oil shale porosity increases as the pyrolysis reaction proceeds. In the low-Fischer-assay oil shales, i.e., lean oil shales, structural breakdown of the cores is insignificant and the porosities are those of intact porous structures. However, in the high-Fischer-assay oil shales, i.e., rich oil shales, this is not the case because structural breakdown and mechanical disintegration due to retorting treatment become extensive and the mineral matrices no longer remain intact. Thermal decomposition of the mineral carbonates, such as magnesium and calcium carbonates ($MgCO_3$ and $CaCO_3$), actively occurring around 380-900°C also results in an increase in porosity. The increase in porosity from low- to high-Fischer-assay oil shales varies from 2.82 to 50%, as shown in Table 8.7.[75] These increased porosities constitute essentially the combined spaces represented by the loss of the organic matter and the decomposition of the mineral carbonates. Crackling of particles is also due to the devolatilization of organic matter, which increases the internal vapor pressure of large nonpermeable pores to such an extent that the mechanical strength of the particle can no longer retain the gas. Liberation of carbon dioxide from mineral carbonate decomposition also contributes to the pressure buildup in the oil shale pores.

Gas permeability[4] is low in both planes of the mineral matrices from the three low-Fischer-assay oil shales heated to 815°C. As noted in Table 8.l, the mineral matrix from the 13.5 gal/ton oil shale has the highest permeability of 8.02 mD. This value may be somewhat higher than the primary permeability of the mineral matrix as the permeabilities created by removing the organic matter via devolatilization and pyrolysis, as well as by thermally decomposing the mineral carbonates, are also included. Even though the oil shale cores used for these measurements have no visible fractures, minute fractures may have formed during heating up to 815°C, which probably contributed to some secondary permeability. Permeabilities after heating up to 815°C, for the oil shales that exceeded 13.5 gal/ton, are not given. In these oil shales, structural breakdown of the mineral matrices under a stress-free environment was so extensive as to preclude measurements of the permeabilities in high-Fischer-assay oil shales.[4] Dolomite ($CaCO_3 \cdot MgCO_3$) decomposition via half-calcination and full-calcination reactions becomes very active at temperatures higher than 380°C, when magnesium carbonate ($MgCO_3$) starts to decompose readily, releasing carbon dioxide. Once the temperature is raised beyond 890°C, decomposition of calcite ($CaCO_3$) via calcination reaction becomes quite active and thermodynamically favored. At these two temperatures (380 and 890°C), the equilibrium constant for decomposition of magnesium carbonate and calcium carbonate respectively becomes unity, or $K_p = 1$.

In the case of eastern U.S. shales, especially Devonian oil shales, decomposition of kerogen produces lighter hydrocarbons than those from other shales. This often results in a substantial increase in volatile pressure in the solid matrix, which leads to cracking and mechanical disintegration of solid structure. This is also the reason why the oil yield from eastern oil shale pyrolysis via a procedure similar to Fischer assay is not necessarily an accurate measure of the organic content of the shale.

8.4.1.4 Compressive Strength

The raw oil shales have high compressive strength, both perpendicular and parallel to the bedding plane.[2] After heating, the inorganic matrices of low-Fischer-assay oil shales

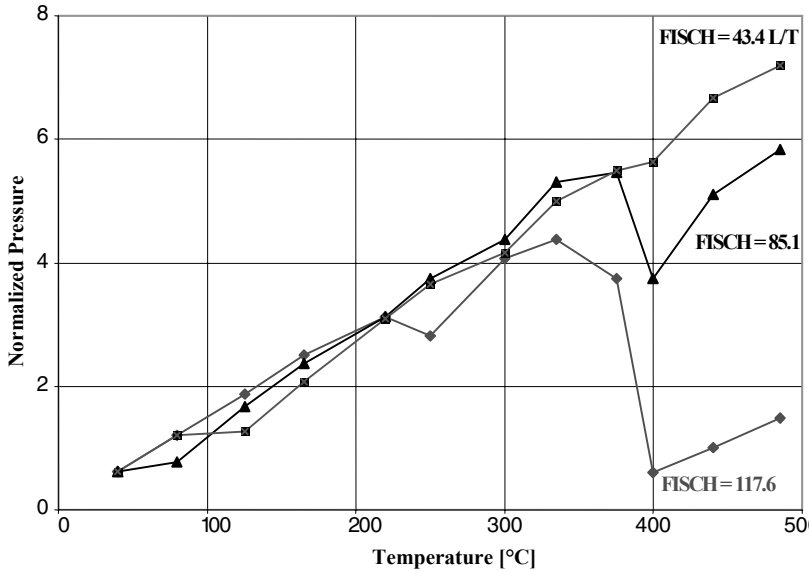

FIGURE 8.1 Variation of compressive strength of oil shale as a function of Fischer assay of oil shale. (From Wang, Y., M.S. thesis, University of Akron, Akron, OH, 1982.)

retain high compressive strength in both perpendicular and parallel planes. This indicates that a high degree of inorganic cementation exists between the mineral particles comprising each lamina and between adjacent laminae. With an increase in organic matter of oil shale, the compressive strength of the respective organic-free mineral matrices decreases and it becomes very low in those rich oil shales, as shown in Figure 8.1.[5]

It is also noteworthy that a structural transition point exists. Gradual expansion (volume swelling) of oil shale under a stress-free environment was noted immediately upon application of heat. Around 380°C, the samples are seen to undergo drastic changes in compressive strength. The greater loss of compressive strength at the yield point and the low recovery on reheating for the richer oil shales are both attributed to extensive *plastic deformation* effects. The degree of plastic deformation thus seems to be directly proportional to the amount of organic matter in oil shale. The discontinuities in the pressure plot at temperatures below the yield point presumably arise from the evolution of pore water from the oil shale matrix. The well-defined transition point at 380°C, therefore, represents a pronounced change in the compressive strength of richer oil shale. It is interesting to note that near this temperature most coals also exhibit similar plastic properties. Similarity in plastic properties between oil shale and coal may be attributed to the macromolecular structure of their organic matter.

8.4.1.5 Thermal Properties

The term *thermal* is used here to represent those parameters that are directly or indirectly related to the transport, absorption, or release of heat, i.e., thermal energy. Properties such as thermal conductivity, thermal diffusivity, enthalpy, density, and

heat capacity fall into this category. For materials that undergo thermal decomposition or phase transformation (this is the case with oil shales in general), it is necessary to characterize their thermal behavior by thermoanalytical techniques such as *thermogravimetric analysis* (*TGA*)[64] and *differential thermal analysis* (*DTA*).

8.4.1.5.1 Thermal Conductivity

Measurements of thermal conductivity of oil shale show that blocks of oil shale are anisotropic about the bedding plane. The measurements were made by techniques such as the transient probe method,[4] the thermal comparator technique,[7] and the line source method.[8] The range of temperature and shale grades investigated in some instances is, however, quite limited.[9,10] Some earlier studies did not focus on the anisotropic nature of the heat conduction. However, later studies have shown that the thermal conductivity as a function of temperature, oil shale assay and direction of heat flow, parallel to the bedding plane (parallel to the earth's surface for a flat oil shale bed), was slightly higher than with thermal conductivity perpendicular to the bedding plane. As layers of material were laid to form the oil shale bed over a long period of geological years, the resulting continuous strata have slightly higher resistance to heat flow perpendicular to the strata than parallel to the strata. A summary of the literature data on the thermal conductivity of Green River oil shale is given in Table 8.8.

TABLE 8.8
Comparison between Thermal Conductivity Values for Green River Oil Shales

Temperature Range (°C)	Fischer Assay, gal/ton	Plane	Thermal Conductivity (J/m-sec-°C)	Reference
38–593	7.2–47.9	—	0.69–l.56 (raw shales) 0.26–l.38 (retorted shales) 0.16–l.21 (burnt shales)	8
25–420	7.7–57.5	A Average	0.92–l.92 1.00–l.82 (burnt shales)	6
38–205	10.3–45.3	A B	0.30–0.47 0.22–0.28	11
20–380	5.5–62.3	A B	1.00–l.42 (raw shales) 0.25–l.75 (raw shales)	7

Note: A = Parallel to the bedding plane; B = Perpendicular to the bedding plane; Average = Average of both directions.

The results shown in Table 8.7 indicate that the thermal conductivities of retorted and burnt shales are lower than those of the raw shales from which they are obtained. This is attributable to the fact that mineral matter is a better conductor of heat than the organic matter; on the other hand, organic matter is still a far better conductor than the voids created by its removal.[8] Whereas the first of these hypotheses is well justified when one takes into account the contribution of the lattice conductivity to the overall value, the effect of the amorphous carbon formed from the decomposition of the organic matter could also be important in explaining the differences in thermal conductivity values for retorted shales and the corresponding burnt samples. The role of voids in determining the magnitude of the effective thermal conductivity is likely to be significant only for samples with high organic content. The data for thermal conductivity measured by Tihen[8] are presented in Figure 8.2. Other measurements[12] were made of the effect of oil shale assay on thermal conductivity. These data also show that thermal conductivity decreases with an increase in oil shale assay.[32]

The thermal conductivities of oil shales are, in general, only weakly dependent on temperature,[32] most studies report a gradual decrease with increasing temperature.[10,24] However, extreme caution needs to be exercised in the interpretation of results at temperatures close to the decomposition temperature of the shale organic matter. This is because the kerogen decomposition reaction (or pyrolysis reaction)

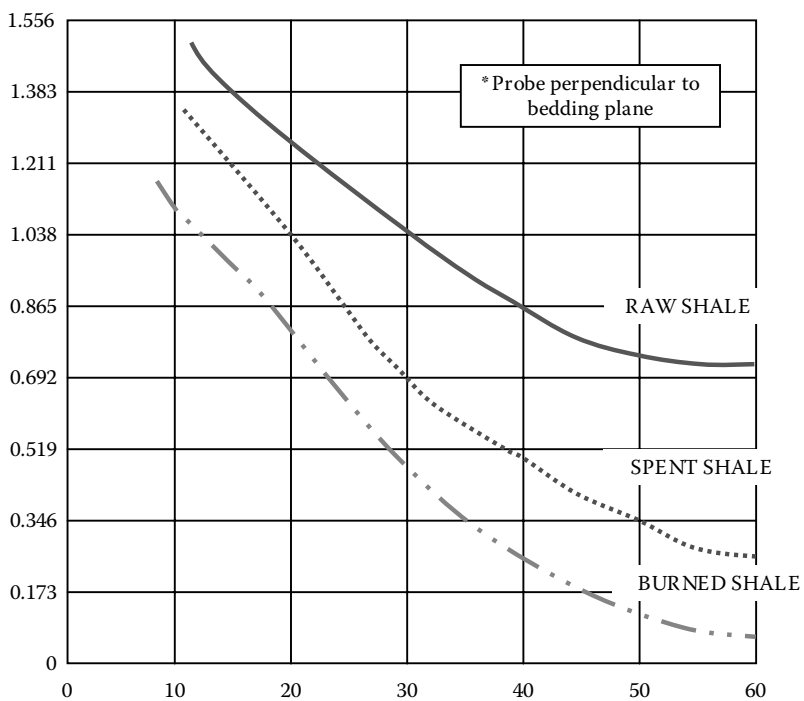

FIGURE 8.2 Thermal conductivity of raw, spent, and burnt oil shale (1 gal/t = 4.18 cm^3/kg). (From Smith, J.W., *U.S. Bur. Mines Rep. Invest.*, 7248, 1969.)

is endothermic in nature and, as such, the temperature transients can be confounded between the true rate of heat conduction and the rate of heat of reaction.

For example, thermal conductivity values reported at temperatures around 400°C normally include the thermal effects of decomposition of the shale organic matter and, therefore, they may not be the intrinsic values.

The thermal conductivity values of oil shales show an inverse dependence on organic matter content.[6,8] Equations that have been proposed by various authors, relating thermal conductivity to the three parameters, namely, temperature, organic content, and extent of kerogen conversion, are shown as follows:

$$K = c_1 + c_2x_1 + c_3x_2 + c_4x_3 + c_5x_1x_2 + c_6x_2x_3 + c_7x_3x_1 + c_8x_1x_2x_3 \quad (8.1)$$

where x_1, x_2, and x_3 denote the organic content, kerogen conversion, and temperature, respectively. The equation by Tihen et al.,[8] which was taken as the average for the perpendicular and parallel thermal conductivities of raw and spent shales, is given by:

$$\begin{aligned} K = {} & (1 - x_2)\{1.9376 - 4.739 \times 10^{-2}x_1 \\ & + 1.776 \times 10^{-3}(x_3 - 273) + 4.371 \times 10^{-4}x_1^2 \\ & - 4.885 \times 10^{-6}(x_3 - 273)^2 \\ & - 1.671 \times 10^{-5}x_1(x_3 - 273)\} + x_2\{1.680 - 5.204 \times 10^{-2}x_1 \\ & - 1.003 \times 10^{-4}(x_3 - 273) + 4.951 \times 10^{-4}x_1^2 \\ & - 1.468 \times 10^{-9}(x_3 - 273)^2 \\ & + 0.667 \times 10^{-5}x_1(x_3 - 273)\}, \text{ J/sec-m-°C} \end{aligned} \quad (8.2)$$

where x_1 and x_2 are the organic content and kerogen conversion in fractions, and x_3 is in degrees Kelvin.

Prats and O'Brien[6] proposed a second-order polynomial in $(x_3 - 25)$ of the form

$$K = c_1[1 - D_1(x_3 - 25) + D_2(x_3 - 25)^2] \exp(c_2F) \quad (8.3)$$

where F is Fischer assay in liters per ton, K is thermal conductivity in W/m-°C, and x_3 is the shale temperature in degrees Celsius. In Equation 8.3, c_1, c_2, D_1, and D_2 are empirically determined. By Equation 8.3, the thermal conductivity is a relatively simple function of the temperature and the organic content of shale. An even simpler equation was proposed for Baltic shales[38]as:

$$K = 1.30/F + 0.06 + 0.003\ T \quad (8.4)$$

where F is Fischer assay in liters per ton, T is temperature in degrees Celsius, and K is thermal conductivity in W/m-°C.

When using simple correlations, one has to realize their limitations, especially in the case of extrapolation or interpolation of experimental data. Most simple expressions normally have narrower ranges of validity.

The problem of thermal conduction through a bed of oil shale rubble is quite complex. It is similar to that of packed beds of randomly sized and oriented particles. It is also difficult to generalize the size distribution of fractured underground beds of oil shale as well as to accurately control the size and shape of particles when *in situ*, underground rubblization takes place. To improve process efficiency, various process ideas of rubblization and heating shales have been generated.

Thermal diffusivity, α, is defined as:

$$\alpha = \frac{k}{\rho C_p} \tag{8.5}$$

where k, ρ, and C_p denote the thermal conductivity, density, and heat capacity, respectively. Therefore, the thermal diffusivity has a dimension of L^2t^{-1} (as in the unit of cm^2/sec), similar to mass and momentum diffusivities. For an oil shale particle to reach a predetermined temperature throughout the particle dimension, the required time may be estimated by[9]:

$$t = \frac{\rho C_p L_{ch}^2}{k} \times 0.3 \tag{8.6}$$

where L_{ch} is the characteristic length of the oil shale particle. Equation 8.6 is based on the isothermality criterion of $t^*_{ch} = 0.3$, in which the characteristic time becomes 0.3. The underlying idea for the characteristic length may be explained by the *penetration depth*, or *a representative linear dimension* for conduction. For a sphere, the characteristic length may be calculated by:

$$L_{ch} = \frac{\text{volume}}{\text{surface area}} = \frac{\frac{4}{3}\pi R^3}{4\pi R^2} = \frac{R}{3} = \frac{D}{6} \tag{8.7}$$

The same calculation can be carried out for a regular cylinder whose diameter is the same as its length:

$$L_{ch} = \frac{\text{volume}}{\text{surface area}} = \frac{2\pi R^3}{[2\pi R(2R) + 2\pi R^2]} = \frac{R}{3} = \frac{D}{6} \tag{8.8}$$

An analogous calculation can be made for determination of a characteristic dimension for other geometries.[9]

As can be readily seen from Equation 8.6, the heat-up time required is proportional to the square of the characteristic dimension. In other words, a successful operation of *in situ* retort using the combustion retorting process depends quite strongly on how finely the rubblization of oil shale bed can be achieved. If the particle size of rubblized oil shale is large, the heat-up period would be quite long, thus making the retort inefficient.

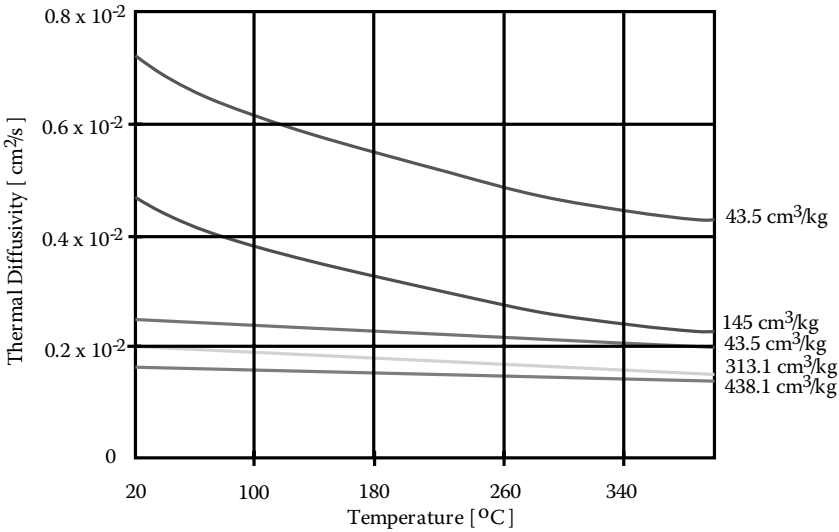

FIGURE 8.3 Dependence of oil shale thermal diffusivity perpendicular to the bedding plane on temperature and Fischer assay. (From Dubow, J. et al., *11th Oil Shale Symposium Proc.*, Colorado School of Mines, Golden, CO, 1978, p. 350.)

TABLE 8.9
Thermal Diffusivity of Green River Oil Shale

Temp Range (°C)	Fischer Assay (gal/ton)	Shale Type	Thermal Diffusivity (cm^2/s)	Measurement Technique	Reference
38–260	6.7–48.4	Raw shale	0.26–0.98	Transient line probe	8
38–482	Low	Retorted shale	0.13–0.88	Transient line probe	8
38–593	~0	Burnt shale	0.10–0.72	Transient line probe	8
25–350	5.0–82.2	Raw shale	0.10–0.90	Laser flash	33

The dependence of the thermal diffusivity of Green River oil shale perpendicular to the bedding plane on temperature and Fischer assay was measured by Dubow et al.,[12] and is shown in Figure 8.3. The thermal diffusivity values show the same broad trends as the thermal conductivities, with variations in temperature and shale grade.[32] As expected, the thermal diffusivity decreases with increasing temperature and organic content in the oil shale. Thus, the retorted and burnt shales show reduced thermal diffusivities relative to those for the raw shales,[32] as shown in Table 8.9. Oil shale samples containing large amounts of pyrites (FeS_2) are likely to show high thermal diffusivities, as the thermal diffusivity of pyrite itself is quite high.

8.4.1.5.2 Heat Capacity of Oil Shale

Earlier work by McKee and Lyder (1921)[14] on specific heat of U.S. oil shales is restricted to limited ranges of temperatures and shale grades. Later studies by Wang

et al. (1979)[15] reported heat capacity dependencies on temperatures and shale grade, characterized by the following type of equation:

$$c = c_1 + c_2 x_1 + c_3 x_2 + c_4 x_1 x_2 \tag{8.9}$$

Again, it is very difficult to generalize the heat capacity of oil shale in any simple functional form, because of the vast heterogeneity of oil shales even within the same formation, as well as among different formations.

Considerable increases in the values of heat capacity with increasing organic content have been observed,[14,15] although relative contributions of various oil shale constituents to the overall values are somewhat uncertain. Values of heat capacity for most oil shales are not available readily. Although actual measurement of heat capacity of a solid sample is not a complicated task, it may not be a bad idea to measure it when the information is needed.

The heat capacity correlation given by Sohn and Shih[16] is:

$$\begin{aligned} C_{px} = {} & \{(907.09 + 505.85\, x_1)\,(1 - x_2) + 827.06\, x_2\} \\ & + \{(0.6184 + 5.561\, x_1)\,(1 - x_2) + 0.92\, x_2\}(x_3 - 298)\ \text{J/kg°C} \end{aligned} \tag{8.10}$$

where x_1 is the organic content of shale in mass fraction, x_2 is the fractional conversion of kerogen, and x_3 is the temperature in degrees Kelvin.

8.4.1.5.3 Enthalpy and Heat of Retorting

Wise et al.[17] measured the enthalpy of raw, spent, and burnt oil shale from the Green River formation. Oil was removed from the spent shale by conventional retorting, but it still retained small amounts of char residue. However, virtually all organic matter was removed from the burnt shale, as shown in Figure 8.4. The

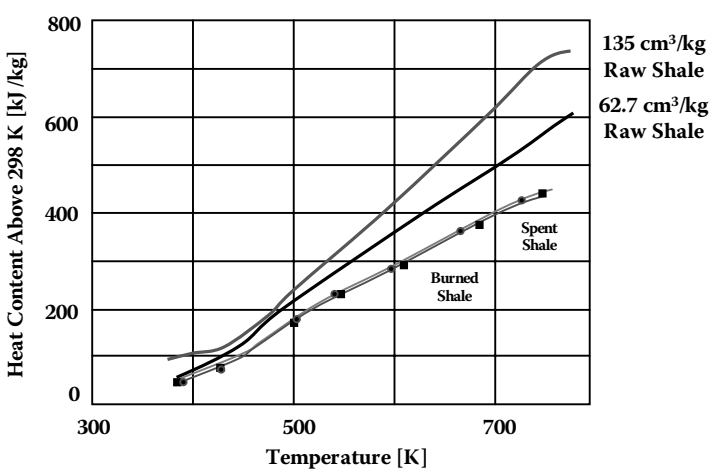

FIGURE 8.4 Heat capacity of raw, spent, and burnt oil shale. (From Johnson, W.F. et al., *Q. Colo. Sch. Mines*, 70(3), 237, 1975.)

enthalpy data may be represented by a function of temperature and Fischer assay of oil shale as:

$$\Delta H = a + bT + cT^2 + dT^3 + eT^4 + fT^2F \tag{8.11}$$

where T is the temperature and F is the oil shale Fischer assay. All the coefficients from a to f are also given Reference 17. The *specific heat* can be determined by differentiation of the enthalpy with respect to the temperature:

$$C_{px} = [\partial H_s/\partial T]_p \tag{8.12}$$

These data are in good agreement with earlier data by Shaw[18] and by Sohns et al.[19]

The available data for *heat of retorting* of Green River oil shales are listed in Table 8.10. The reported values for the heat of retorting (endothermic) show the expected increase with increasing shale assay and temperature. The disparity in the range of values observed by different investigators possibly reflects differences in the composition of shale samples. It should be borne in mind that the presence of minerals, which decompose at temperatures below the range at which the organic matter is thermally extracted, would increase the energy requirements for processing shales. Thus, it has been estimated that shales containing nahcolite and dawsonite would require an additional 117 cal/g (490 J/g) and 215 cal/g (890 J/g), respectively.[20] Heat requirements for retorting oil shales containing 17% analcite would be increased by about 6%.[21]

8.4.1.5.4 Density or Specific Gravity

The density of Green River oil shale was measured by Tisot[4] and found to be in the range of l.8 to 2.0 g/cm^3. Later, some efforts were made to correlate the oil yield from oil shale (such as the Fischer assay) with the specific gravity.[24] This idea may have some practical significance, as the oil yield is usually a constant fraction of the organic content and the oil shale density is dependent upon the organic content.

8.4.1.5.5 Self-Ignition Temperature (SIT)

The *self-ignition temperature* (SIT) is the temperature at which an oil shale sample spontaneously ignites in the presence of atmospheric oxygen, or under any other prescribed oxidative conditions. There is no standardized procedure generally

TABLE 8.10
Values Reported for Heat of Retorting of Green River Oil Shales

Heat of Retorting (kJ/kg)	Fischer Assay (gal/ton)	Ref.
238–878	23.5–46.7	19
581–699	8.0–32.8	20
335	25.6	22

Source: From Wang, Y., M.S. thesis, University of Akron, Akron, OH, 1982.

adopted for this measurement. However, if a consistent measurement of this temperature is made for oil shale, it can provide very valuable information regarding the fuel characteristics of the shale.

The spontaneous ignition temperature of oil shale has been measured and characterized under a variety of conditions by Allred.[25] The information regarding SIT is very important, as it governs not only the initiation of the combustion retorting process, but also the dynamics of oil shale retorting by the advancing oxidation zone. Branch also explains its importance in his article.[26] In the countercurrent combustion retorting process, the combustion front moves toward the injected oxidizer, whereas in the cocurrent process the front moves in the same direction as the oxidizer. Therefore, the spontaneous ignition temperature of the raw oil shale should be below the oil shale retorting temperature in the countercurrent process. In the cocurrent combustion process, char remaining in the shale after retorting is burned to sustain the retort by providing the necessary thermal energy.

The SITs of Colorado oil shale have been measured over a wide range of total pressure and oxygen partial pressure.[25] With nitrogen as a diluent, the ignition temperature was found to depend on the oxygen partial pressure, but not significantly on the total pressure. The temperature at which ignition could occur was also found to correlate to the temperature at which methane and other light hydrocarbons are devolatilized from the oil shale. As shown in Figure 8.5, in the case for raw Colorado oil shale, higher ignition temperatures were required for lower oxygen partial pressures, and the lowest ignition temperature of 450 K was considerably lower than the oil production temperature of about 640 K. More detailed information is available from the original text[24] or from other sources.[9,25,26] This experimental evidence strongly suggests that ignition of oil shale may be associated with oxidation of gaseous hydrocarbons that evolved from oil shale.

Joshi[27] took a different approach to studying the SIT. He defined the SIT as the temperature at which the shale bursts into flames in air within 360 sec of introduction

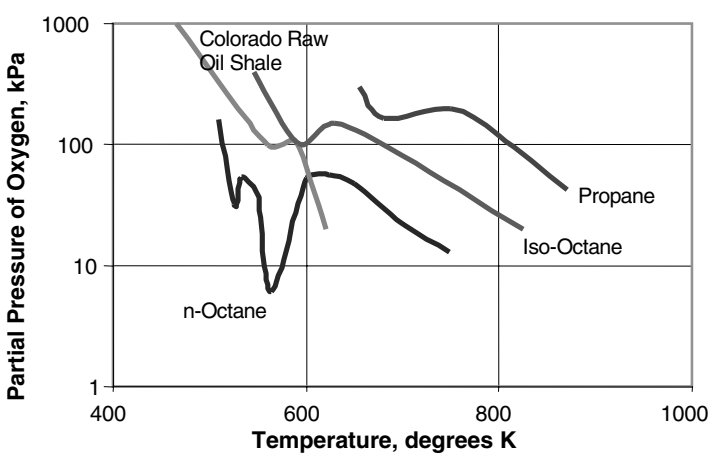

FIGURE 8.5 Self-ignition temperature of raw oil shale, *i*-octane, *n*-octane, and propane. (From Smith, J.W., *U.S. Bur. Mines Rep. Invest.*, 7248, 1969.)

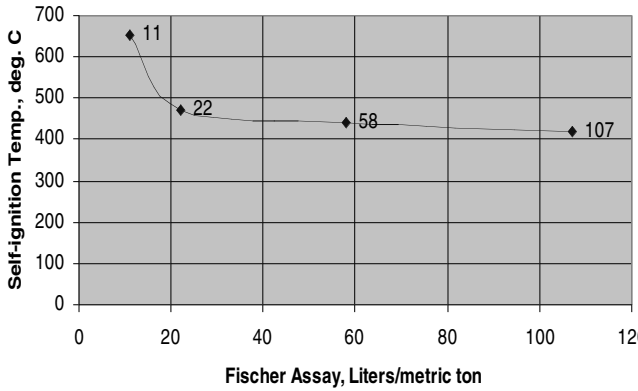

FIGURE 8.6 Self-ignition temperature of oil shale as a function of Fischer assay. (From Joshi, R., M.S. thesis, University of Akron, Akron, OH, 1983.)

into a preheated isothermal retorter. His SIT measurements were made at an oxygen partial pressure of 0.21 atm, i.e., under atmospheric conditions. Joshi's approach was different from that of Allred's in the sense that different oil shales can be characterized by the SIT. In other words, the SIT defined by Joshi can be used more like a physical property that is easy to measure. It was found that the SIT depends very strongly on the Fischer assay of oil shale. Generally speaking, the higher the Fischer assay, the lower the SIT. Figure 8.6 graphically illustrates the relation between SIT and Fischer assay for several different shales.

Joshi's results also suggest that the ignition of oil shale is associated with the oxidation of gaseous hydrocarbons evolved from oil shale. The ignition of the shale samples were always preceded by a slight exploding (crackling) sound, which strongly suggests that ignition occurred only when the vapor pressure of the gaseous hydrocarbons evolved reached a certain level. Further tests by Joshi[27] revealed that the SIT is also a function of particle size. Tests were carried out on particles of size –4 + 8 mesh to –60 mesh. It was also found that Colorado shale particles of size –40 + 60 mesh and smaller did not burst into flames under the defined conditions. The same phenomenon was observed for Cleveland shale no. 2 with the limiting particle size being –20 + 40 mesh, which did not burst into flames. It has been stated that as the particle size becomes smaller, the diffusional limitations of the product vapor decrease substantially in magnitude. As a result, there is a continuous diffusion of product vapor (gaseous hydrocarbons) from the rock matrix to the surface and from the surface to the boundary layer.

Consequently, heating induces a buildup of gaseous hydrocarbons inside the rock matrix, which ultimately causes cracking of the shale particles. The concentration of the gaseous hydrocarbons near the surface immediately after internal cracking is high enough to stimulate ignition. As mentioned earlier, the SIT data can be very useful, as ignition temperature governs the initiation of the combustion process and also the dynamics of *in situ* oil shale retorting. Further, these data are also valuable because they provide an indication of the explosivity of oil shale dust during oil shale-mining operations. However, this hazard is considerably less likely to take place in oil shale mining than during coal mining.[4,6]

8.4.2 Thermal Characteristics of Oil Shale and Its Minerals

Thermal or thermoanalytical methods, such as thermogravimetric analysis (TGA) and differential thermal analysis (DTA), are particularly useful for characterization of thermal behavior of oil shales and oil shale minerals. The use of both TGA and DTA has been well established in the areas of coal and polymer research, as a relatively simple procedure generates valuable information about the sample's thermal behavior.

8.4.2.1 Thermoanalytical Properties of Oil Shale

Figure 8.7 and 8.8 shows the effects of the surrounding atmosphere on the thermal behavior of Green River oil shale.[32] Figure 8.7 shows the DTA curve in an inert atmosphere of flowing N_2, whereas Figure 8.8 shows the DTA curve in the presence of air, i.e., in an oxidative atmosphere.

The peak corresponding to kerogen decomposition is seen to be endothermic in nature, i.e., absorbing heat. This endothermic nature is very much expected, as all pyrolysis reactions require input of thermal energy. In the presence of air, however, two exotherms are apparent as shown in Figure 8.8, the first peak at 439°C and the second at 500°C. Whereas the first exothermic peak may be attributed to the combustion of light hydrocarbon fractions from the shale organic matter, the second exotherm appears to be from the burn-off of carbonaceous char.[32]

Figure 8.9 shows the TGA curve of Stuart oil shale of Queensland, Australia.[78] The sample used in this experiment was obtained from Kerosene Creek member and

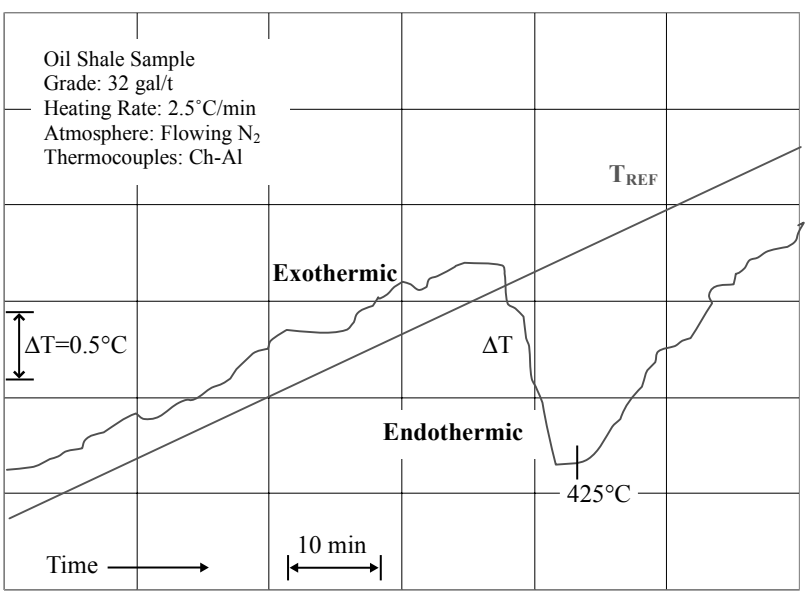

FIGURE 8.7 Effect of the surrounding atmosphere on the thermal behavior of Green River oil shale — DTA in an inert atmosphere of flowing nitrogen. (From Rajeshwar, K. et al., *J. Mater. Sci.,* 14, 2025–2052, 1979.)

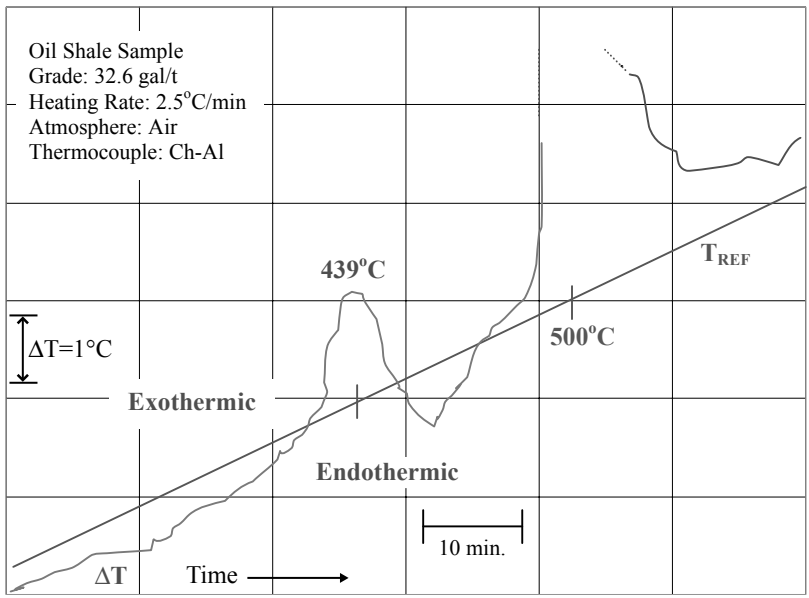

FIGURE 8.8 Effect of the surrounding atmosphere on the thermal behavior of Green River oil shale — DTA in the presence of air. (From Rajeshwar, K. et al., *J. Mater. Sci.*, 14, 2025–2052, 1979.)

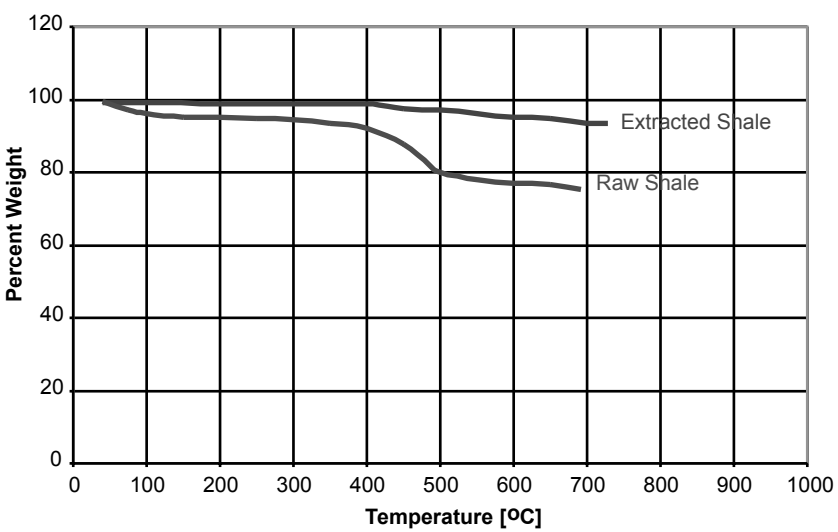

FIGURE 8.9 Thermogravimetric analysis of stuart shale before and after oil extraction. (From Kesavan, S.K. and Lee, S., *Fuel Sci. Technol. Int.*, 6(5), 505, 1988.)

supplied by Southern Pacific Petroleum NL. The total mass loss of the raw shale by the TGA from 25 to 600°C was 12.2%, which includes: (1) evaporative loss of moisture, (2) kerogen decomposition and devolatilization, and (3) thermal decomposition of

mineral carbonates and resultant CO_2 liberation. It is not surprising to observe a further mass loss from preextracted shale, which is attributable principally to decomposition of mineral carbonates.

8.4.2.2 Thermochemical Properties of Oil Shale Minerals

The identification and quantification of various carbonates existing in the Green River oil shales, such as ferroan (or ferroan dolomite), ankerite [calcium iron magnesium manganese carbonate, or $Ca(Fe, Mg, Mn)(CO_3)_2$], and dawsonite, were accomplished using thermal analysis techniques.[34] A quantitative determination method for nahcolite [$NaHCO_3$] and trona [$Na_3 (CO_3) ((HCO_3)\cdot 2H_2O)$] in Colorado oil shales was proposed by Dyni et al.[35]

Rajeshwar et al.[32] summarized the thermochemical properties of minerals commonly found in oil shale deposits, and their results are shown in Table 8.11.

DTA involves heating or cooling a test sample and an inert reference under identical conditions and recording any temperature difference between the sample and reference. This differential temperature (ΔT) is then plotted against time, or against temperature. Changes in the sample that lead to the absorption or release of heat can be detected relative to the inert reference. The DTA peak temperature is the temperature indicated at the time of maximum peak value of DTA curve, which is a characteristic property of the material[76] and is not dependent on the size of the material sample.

Regarding the decomposition of *dawsonite*, there are some conflicting theories.[32] One belief is that dawsonite decomposes at 370°C according to the following reaction:

$$NaAl(OH)_2CO_3 \rightarrow H_2O + CO_2 + NaAlO_2 \tag{8.13}$$

Another is based on the investigation of thermal behavior of dawsonite at temperatures between 290 to 330°C, and the chemical reaction that is taking place is believed to be[36]:

$$2NaAl(OH)_2CO_3 \rightarrow Na_2CO_3 + Al_2O_3 + H_2O + CO_2 \tag{8.14}$$

Yet another belief is that dawsonite decomposes in two steps.[37] In the first step, it has been found that between 300 to 375°C, crystalline dawsonite decomposes with the evolution of all the hydroxyl groups and two thirds of the carbon dioxide, leaving an amorphous residue. In the second step, the balance CO_2 is released between 360 to 650°C, producing crystalline $NaAlO_2$.

Plagioclase is a form of feldspar that has a chemical composition of $NaAlSi_3O_8$. Plagioclase is usually white in color, but can also be gray and greenish white. This mineral was found to be abundant in the moon rock samples.

The dominant mineral constituent of oil shale is dolomite. Dolomite is approximately a one-to-one mixture of magnecite ($MgCO_3$) and calcite ($CaCO_3$). Therefore, the chemical formula of dolomite is often expressed by either $CaCO_3\cdot MgCO_3$ or $CaMg(CO_3)_2$. Upon heating, dolomite undergoes a two-stage thermal decomposition reaction generally known as *calcination*.

TABLE 8.11
Thermochemical Properties of Common Minerals in Oil Shale Deposits

Minerals	Chemical Formula	Type of Chemical Reaction	DTA Peak Temperature (°C)
Calcite	$CaCO_3$	Dissociation	860–1010
Dolomite	$CaCO_3 \cdot MgCO_3$	Dissociation	790, 940
Analcite	$NaAlSi_2O_6 \cdot H_2O$	Dehydration; dissociation	150–400
Shortite	$Na_2Ca_2(CO_3)_3$	Dissociation	470
Trona	$Na_2CO_3 \cdot NaHCO_3 \cdot 2H_2O$	Dissociation; dehydration	170
Pyrite	FeS_2	Oxidation; dissociation	550
Potassium feldspar	$KAlSi_3O_8$	Dissociation	—
Gaylussite	$CaNa_2(CO_3)_2 \cdot 5H_2O$	Dehydration; crystallographic transformation; melting	145, 175, 325, 445, 720–982
Illite	$K_{0.6}(H_3O)_{0.4}Al_{1.3}Mg_{0.3}Fe^{2+}_{0.1}Si_{3.5}O_{10}(OH)_2 \cdot (H_2O)$ (empirical formula)	Dehydroxylation	100–150, 550, 900
Plagioclase	$NaAlSi_3O_8$–$CaAl_2Si_2O_8$	Dissociation	—
Nahcolite	$NaHCO_3$	Dissociation	170
Dawsonite	$NaAl(OH)_2CO_3$	Dehydroxylation; dissociation	300, 440
Gibbsite	γ-$Al(OH)_3$	Dehydroxylation	310, 550
Ankerite	$Ca(Mg, Mn, Fe)(CO_3)_2$	Dissociation	700, 820, 900
Siderite	$FeCO_3$	Oxidation; dissociation	500–600, 830
Albite	$NaAlSi_3O_8$	Dissociation	—
Quartz	SiO_2	Crystallographic transformation	~575

Source: From Branch. M.C., *Prog. Energy Combust. Sci.*, 5, 193, 1979.

$$CaCO_3 \cdot MgCO_3 \xleftrightarrow{\Delta} CaCO_3 \cdot MgO + CO_2 \tag{8.15}$$

$$CaCO_3 \cdot MgO \xleftrightarrow{\Delta} CaO \cdot MgO + CO_2 \tag{8.16}$$

The first reaction is called *half-calcination of dolomite,* whereas the entire reaction combining both reaction 15 and reaction 16 is called *full calcination of dolomite.* Equilibrium decomposition temperature, i.e., where Ka = 1, is 380°C for magnecite decomposition and 890°C for calcite decomposition, respectively.[9] It can be readily seen that dolomite decomposes quite actively in typical retorting conditions.

8.4.3 Electric Properties of Oil Shale

Electric properties also change as functions of temperature and other variables. Both alternating current (AC) and direct current (DC) methods can be employed in measuring electric properties of oil shale. In general, AC techniques are preferable in view of their capability to detect and resolve various polarization mechanisms in the material.

8.4.3.1 Electric Resistivity

Measurements on various types of oil shales in DC electric fields have shown an exponential decrease in resistivity values as a function of temperature.[5,32,39] The trend is typically characteristic of ionic solids, which conduct current by a thermally activated transport mechanism. The presence of various minerals in the oil shale rock matrix makes it difficult to conclusively identify the current-carrying ions in the material. However, the close correspondence of activation energies at high temperatures (>380°C) with those typically observed for carbonate minerals seems to indicate that *carbonate ions* could be a major current-carrying species.[5,32] However, estimates made from such data are at best speculative and must be used with due caution.[32] The chemical change in oil shale material due to heating could also influence its conduction property. Thus, changes in the resistivity (from 10^{10} Ω-cm at room temperature to 10 Ω-cm at 900°C) of Russian shales were attributed to the thermal decomposition of oil shale kerogen.[38,39] Figure 8.10 shows the frequency-dependent behavior of electric resistivity as a function of reciprocal temperature ($1/T$) for a sample (117 l/ton Fischer assay) of raw Green River oil shale. The minima in the resistivity curves are observed at temperatures ranging from 40 to 210°C, and are due to the gradual loss of free moisture and bonded water molecules to the clay particles in the shale matrix. Figure

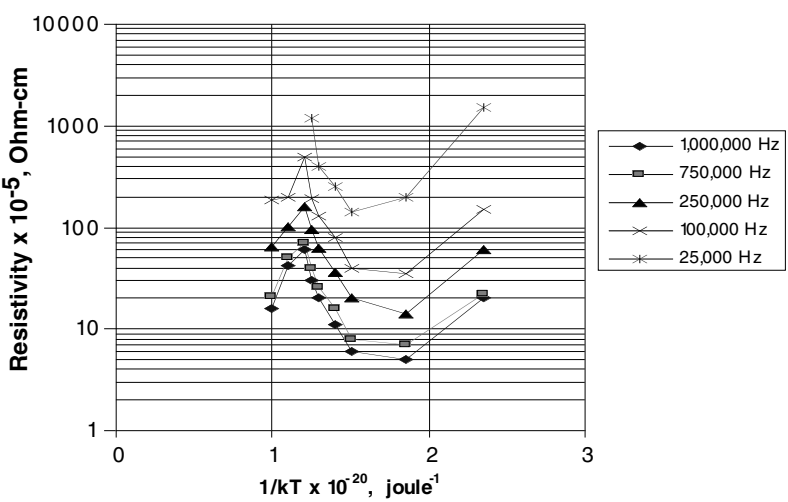

FIGURE 8.10 Frequency-dependent behavior of electrical resistivity as a function of reciprocal temperature for a 117 l/t shale sample. (From Rajeshwar, K. et al., *J. Mater. Sci.,* 14, 2025–2052, 1979.)

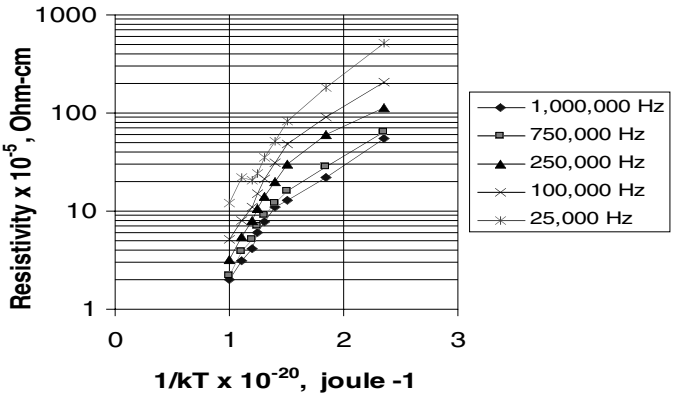

FIGURE 8.11 Frequency-dependent behavior of electrical resistivity as a function of reciprocal temperature for a 117 l/t shale sample reheated in a second cycle. (From Rajeshwar, K. et al., *J. Mater. Sci.,* 14, 2025–2052, 1979.)

8.11 shows the same behavior for the reheated materials; however, the trends for these curves are quite different from those for raw shales.

For these reheating experiments, the shales were cooled back to room temperature and reheated back to approximately 500°C. The curves of Figure 8.11 exhibit the usual Arrhenius behavior typical of ionic solids, as mentioned before. It can be seen that there is no minimum or peak in the resistivity data and that the results are attributable to thermally activated conduction.

8.4.3.2 Dielectric Constants

The dielectric constant (k) is a number that is a characteristic property relating the ability of a material to carry alternating current to the ability of vacuum to carry alternating current. The capacitance created by the presence of the material, therefore, is directly related to the dielectric constant of the material.

An extensive review of the dielectric constant of oil shales is presented in Rajeshwar et al.[32] The dielectric constant of oil shales also exhibits a functional dependency on temperature and frequency. Anomalously high dielectric constants are observed for oil shales at low temperatures, and these high values are attributed to electrode polarization effects, according to Scott et al.[40] A more likely explanation is the occurrence of interfacial polarization (e.g., Maxwell-Wagner type) in these materials arising from the presence of moisture and as a result of accumulation of charges at the sedimentary varves in the shale.

Figure 8.12 shows the variation of dielectric constant with the number of heating cycles for several grades of Green River oil shales.[41] Each heating cycle consisted of heating the sample at 110°C for 24 h and cooling back to room temperature prior to testing. A noticeable decrease in dielectric constant with each subsequent drying cycle is very evident.

Figure 8.13 shows the variation of dielectric constant with frequency and thermal treatment for Green River oil shales.[41] The degree of frequency dispersion at each

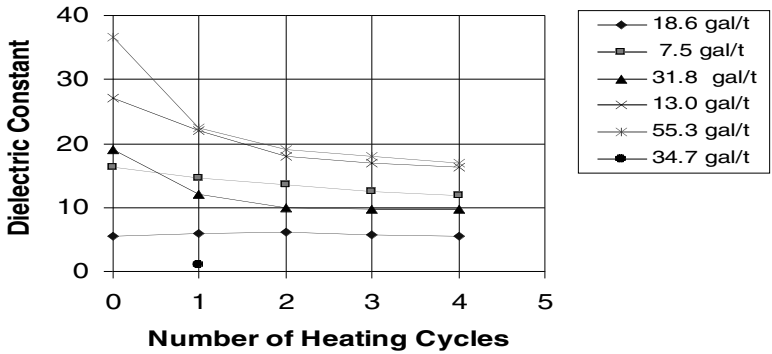

FIGURE 8.12 Variations of dielectric constant (ε′) with number of heating cycles for several grades of Green River shales. (From Rajeshwar, K. et al., *J. Mater. Sci.,* 14, 2025–2052, 1979.)

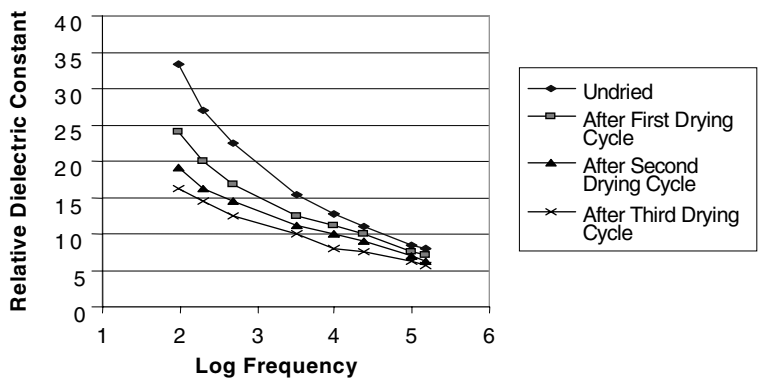

FIGURE 8.13 Variation of dielectric constant (ε′) with frequency and thermal treatment for Green River oil shales. (From Rajeshwar, K. et al., *J. Mater. Sci.,* 14, 2025–2052, 1979.)

heating cycle attests to an appreciable effect of moisture on the interfacial polarization mechanisms in oil shale.

Figure 8.14 and Figure 8.15 show the variation of dielectric constant of Green River oil shales as a function of frequency and temperature at low temperatures (<250°C) as well as at high temperatures (>250°C).[42] A general explanation may be that the dielectric constant decreases with increasing temperatures up to 250°C and thereafter increases again, attaining values comparable to those observed initially for the raw shales. The initial decrease may be due to the gradual release of absorbed moisture and chemically bonded water from the shale matrix. However, the subsequent increase may be due to more complex factors including: (1) increased orientational freedom of the kerogen molecules, (2) buildup of carbon in the shale, and (3) presence of a space charge layer in the material at high temperatures. Further details can be found from the work by Rajeshwar et al.[32]

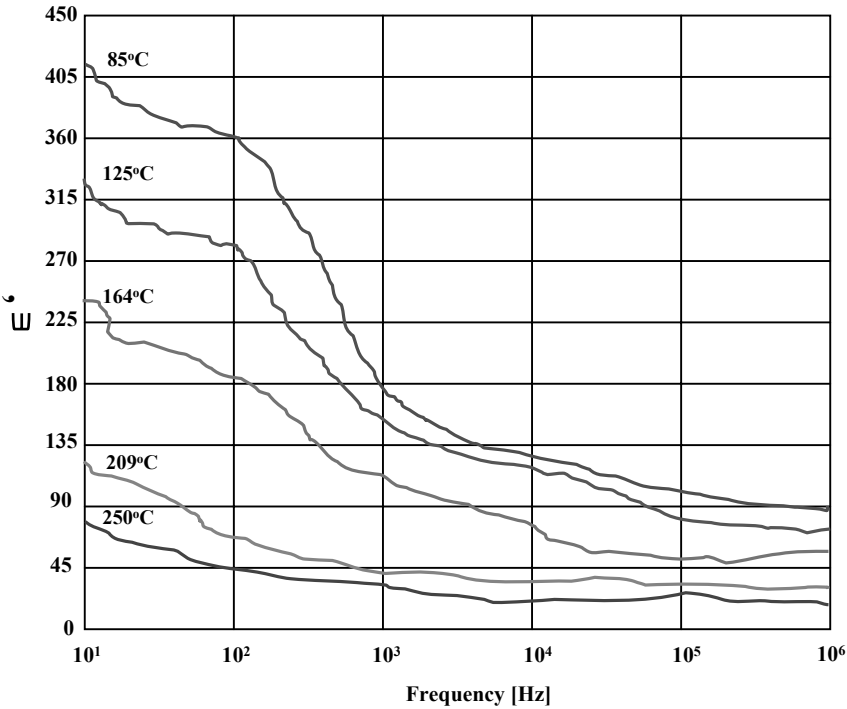

FIGURE 8.14 Frequency and temperature dependence of dielectric constant (ε′) at low temperatures (<250°C). (From Rajeshwar, K. et al., *J. Mater. Sci.,* 14, 2025–2052, 1979.)

8.4.4 Molecular Characterization of Kerogen

In applying chemical and engineering principles to the decomposition of oil shale, difficulties are encountered owing to the lack of structural and molecular understanding of kerogen. A *chemical model of kerogen structure* has been proposed by Yen[28] as $C_{220}H_{330}O_{18}N_2S_4$. If we use this formula as a representative chemical formula for kerogen molecule, its molecular weight becomes 3,414. Kerogen has a macromolecular structure that gives a fairly large molecular (formula) weight.

8.4.4.1 Derivation of Stoichiometric Coefficient

As the structure of kerogen cannot be represented as a uniquely defined chemical species, a stoichiometric equation for kerogen decomposition is often impractical. The kerogen decomposition reaction is frequently expressed by the following descriptive equation:

$$\text{Kerogen} \rightarrow \text{condensable oil vapors} + \text{gaseous products} + \text{residual char} \qquad (8.17)$$

This equation cannot be taken as a stoichiometric equation, as the atomic balance on constituent atoms is not established. The following analysis is therefore intended to provide a theoretical bridge between a qualitative expression and a stoichiometric equation.[23]

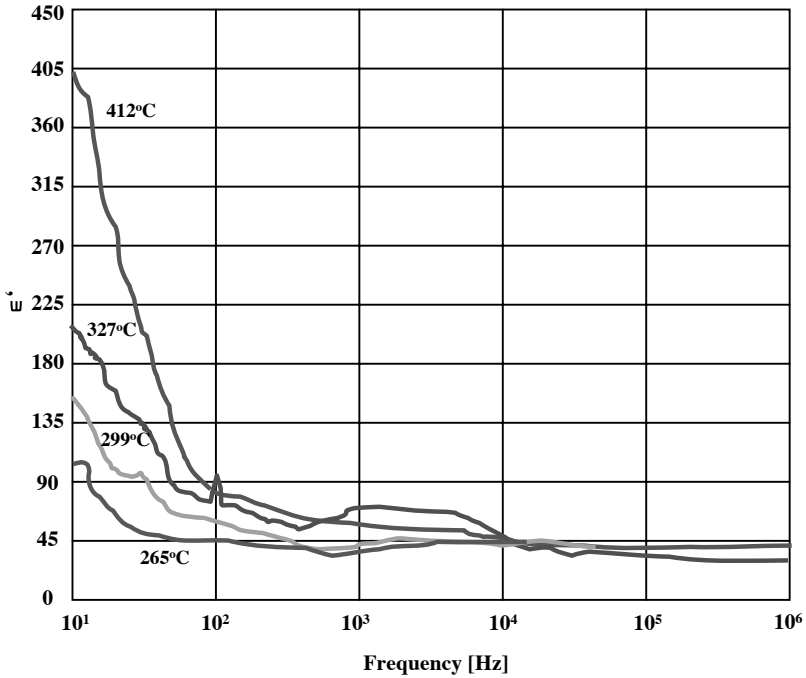

FIGURE 8.15 Frequency and temperature dependence of dielectric constant (ε′) at high temperatures (>250°C). (From Rajeshwar, K. et al., *J. Mater. Sci.,* 14, 2025–2052, 1979.)

The initial mass of organic carbon per cubic meter of particle volume is:

$$m_1 = \rho_s \omega \text{ , kg/m}^3$$
$$= \rho_s \omega .1000 / M_k \text{ , mol/m}^3 \quad (8.18)$$

where ρ_s is the density of oil shale particle in kg/m^3, ω is the mass fraction of kerogen in the particle, and M_k is the molecular weight (or formula weight) of kerogen in grams per mole. The total mass of oil recoverable (conventionally) from oil shale per cubic meter of particle volume is:

$$m_2 = F\left[\frac{l}{M/T}\right]\cdot \rho_s \left[\frac{kg}{m^3}\right]\cdot \rho_o \left[\frac{g}{cm^3}\right] = F\cdot \rho_s \cdot \rho_o \left[\frac{g}{m^3}\right]$$
$$= F\cdot \rho_s \cdot \rho_o / M_p \text{ mol/m}^3 \quad (8.19)$$

where F is the Fischer assay of oil shale in liters per metric ton, ρ_o is the density of shale oil (not oil shale) in g/cm^3, and M_p is the average molecular weight of condensable product in g/mol.

Assume that the kerogen decomposes into oil vapors and gaseous products completely at moderate decomposition temperatures. Then, the stoichiometric coefficient equivalent may be expressed by:

$$\alpha = \frac{F \cdot \rho_s \cdot \rho_o / M_p}{\rho_s \cdot \omega \cdot 1000 / M_k} = \frac{F \cdot \rho_s \cdot M_k}{\omega \cdot M_p \cdot 1000} \tag{8.20}$$

where α is a theoretically obtained stoichiometric coefficient (or its equivalent) for reaction (8.17).

8.4.4.2 Relation between Fischer Assay and Mass Fraction of Kerogen

An empirical correlation between the Fischer assay of oil shale and the weight percentage of kerogen is proposed by Cook[29]:

$$F = 2.216\ wp - 0.7714,\ \text{gal/ton} \tag{8.21}$$

where F is the Fischer assay estimated in gallons of oil recoverable per ton of shale and wp is the weight percentage of kerogen in the shale. However, caution must be exercised in using this equation, as the mass fraction of kerogen in oil shale is strongly dependent on the measurement technique. For certain oil shales, the maximum recoverable oil amount via supercritical extraction or CO_2 retorting is significantly higher than the Fischer assay value.[9]

It is also conceivable that such a correlation can be sensitive to the types of oil shale retorted, as well. Nonetheless, there is little doubt that the Fischer assay of any oil shale is strongly correlated against the kerogen content of the shale.

8.4.4.3 Nitrogen Compounds in Shale Oil

Nitrogen compounds in shale oil cause technological difficulties in the downstream processing of shale oil, in particular, poisoning the refining catalysts. Needless to say, these nitrogen compounds originate from oil shale and the amount and type depend heavily on the petrochemistry of the oil shale deposits. Although direct analysis and determination of molecular forms of nitrogen containing compounds in oil shale rock is very difficult, analysis of the shale oil extracted by retorting processes provides valuable information regarding the organonitrogen species in the oil shale. Poulson[70] reported the breakdown of organonitrogen compounds in shale oil based on a preliminary study of shale oil light distillates, and the results are shown in Table 8.12. The major compound classes Poulson identified were pyridines, quinolines, pyrroles, and indoles.[70]

TABLE 8.12
Predominant Classes of Nitrogen Compounds in a Shale Oil Light Distillate

Nitrogen Type	Total Nitrogen
Alkylpyridines	42
Alkylquinolines	21
Alkylpyrroles (N-H)	8
Alkylindoles (N-H)	7
Cyclic amides (pyridones, quinolines)	3
Anilides	2
Unclassified very weak bases (*N*-alkylpyrroles and *N*-alkylindoles?)	4
Other unclassified very weak bases (reduced to nontitratable types and not sulfoxides)	3
Nonbasic (nontitratable) nitrogen in original light distillate	8
Analytical loss	2
Total	**100**

Source: From Poulson, R.E. et al., *ACS Div. Pet. Chem. Prepr.*, 15(1), A49–A55, 1971.

8.4.5 Boiling Range Distributions of Various Shale Oils

Shale oils or oil shale crudes are obtained by various oil shale processes. The characteristics of shale oils are very important in devising a process for upgrading shale oils, as well as in identifying the market for them. In particular, distillation properties of shale oil are crucially important for its refining and upgrading.

8.4.5.1 Analytical Methods

In characterizing hydrocarbon mixtures for specification or for other purposes, a precise analytical distillation may be needed. Actual distillation may require 25 to 100 plates. It is extremely costly and tedious to carry out such a distillation on a reasonable scale. Instead, gas chromatography (GC) with a separating column at a constant temperature can be effectively used to obtain a *boiling point analysis*. However, this technique is somewhat restricted to a rather narrow boiling range, as lighter components elute too soon and tend to overlap, and heavy components emerge very late, producing relatively wide bands or still remain in the column.

A newer technique of temperature programming of the separating column makes a wide-range, single-stage analysis possible.[30] By using a column packing that separates according to the boiling point and by precise programming of the column temperature, the boiling range for various peaks can be determined from elution times or temperatures of emergence.

A standard method for *boiling range distribution* of petroleum fractions by gas chromatography has been adopted by the American Society for Testing and Materials,

West Conshohocken, PA (ASTM) and is given in the ASTM D2887[31] Procedure, which is briefly described in the following section:

8.4.5.1.1 ASTM D2887 Procedure[31]

1. Scope: This standard method determines the boiling range distribution of petroleum products. It is generally applicable to petroleum fractions with a final boiling point of 1000°F (538°C) or lower at atmospheric pressure.
2. Summary of the method: The sample is introduced into a gas chromatographic column, which separates hydrocarbons in the order of their boiling points. The column temperature is raised at a reproducible (preprogrammed) rate and the area under the chromatogram is recorded throughout the run. Boiling temperatures are assigned to the elution time axis from a calibration curve obtained under the same conditions by running a known mixture of hydrocarbons (ranging from C_m to C_n) covering the boiling range expected from the sample. From these data, the boiling range distribution of the sample may be obtained.
3. Initial and final boiling points: The *initial boiling point* (*IBP*) is the point at which a cumulative area count equals 0.5% of the total area under the chromatogram. On the other hand, the *final boiling point* (*FBP*) is the point at which a cumulative area count equals 99.5% of the total area under the chromatogram. The *normal boiling point* (*NBP*) is the point at which the vapor pressure reaches 760 mmHg, or 1 atm.
4. Apparatus for boiling range distribution: A gas chromatograph equipped with a thermal conductivity detector (TCD) is typically used for the experiment of gasoline fractions. For all other types of samples, either a TCD or a flame ionization detector (FID) may be used. The detector must have sufficient sensitivity to detect 1% dodecane ($C_{12}H_{26}$) with a peak height of at least 10% of full scale on the recorder under the conditions prescribed in this method and without loss of resolution. Practically any column can be used, provided that under the conditions of the test, separations are in order of boiling points and the column resolution (R) is at least 3 and not more than 8. As a stable baseline is essential for the accuracy of this method, matching dual columns are required to compensate for column bleed, which cannot be eliminated completely by conditioning alone.

The temperature programming must be done over a range that is sufficient to establish a retention time of at least 1 min for the IBP to elute the entire sample. A microsyringe is needed for sample injection and a flow controller is also required for holding carrier gas flow constant to ± 1% over the full operating temperature range. The carrier gas used is either helium or hydrogen for a TCD; whereas nitrogen, helium, or argon may be used with an FID. The calibration mixture to be used is a mixture of hydrocarbons of known boiling point covering the boiling range of the sample. At least one compound in the mixture must have a boiling point lower than the initial boiling point (IBP) of the test sample in order to obtain an accurate

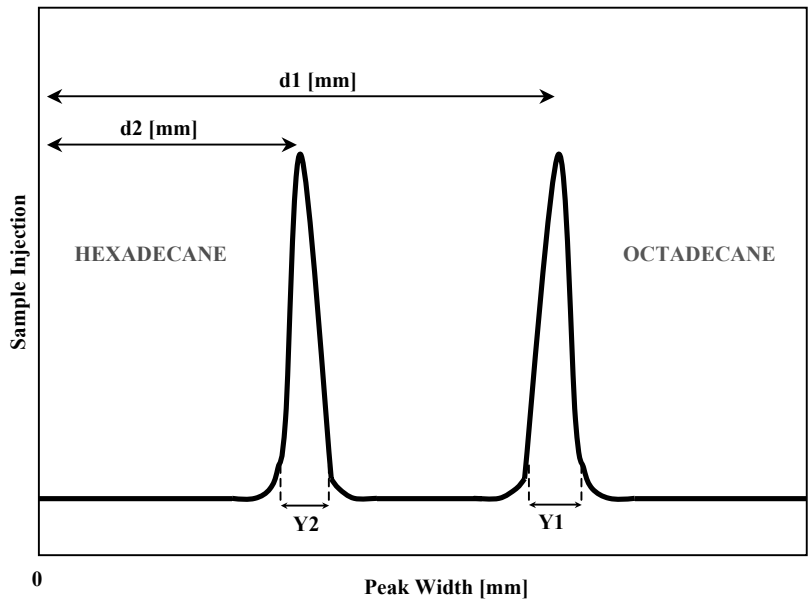

FIGURE 8.16 Column resolution (R). (Source: ASTM Standards D2887-73.)

distribution of boiling range. Both integral and differential plots can be constructed from the chromatographic data. Most shale oils show density functions that are close to a normal distribution.

To test column resolution, a mixture of 1% each of C_{16} and C_{18} *n*-paraffin in a suitable solvent such as octane (C_8) needs to be prepared. Inject the same volume of this mixture as used in analyses of samples and obtain the chromatogram. As shown in Figure 8.16, calculate resolution (R) from the distance between the C_{16} and C_{18} *n*-paraffin peaks at the peak maxima (d) and the width of the peaks at the baseline (Y_1 and Y_2).

$$R = [2(d_1 - d_2)]/(Y_1 + Y_2) \tag{8.22}$$

Resolution (R), based on Equation 8.22, must be at least 3 but not more than 8.

Table 8.13 and Table 8.14 show the typical operating conditions and the boiling points of *n*-paraffins, respectively. These tables provide very valuable information regarding the boiling range properties of paraffinic hydrocarbons.

8.5 OIL SHALE EXTRACTION AND RETORTING PROCESSES

The organic matter in oil shale typically contains both bitumen and kerogen. The bitumen fraction is soluble in most organic solvents, and it is not difficult to extract directly from oil shale. The readily soluble bitumen content in oil shale occupies

TABLE 8.13
Typical Operating Conditions

	1	2	3	4
Column length (ft)	4	5	2	2
Column ID (in)	0.188	0.090	0.188	0.188
Liquid phase	OV-1	SE-30	UC-W98	SE-30
Percent liquid phase (%)	3	5	10	10
Support material	S[a]	G[b]	G[b]	P[c]
Support mesh size	60/80	60/80	60/80	60/80
Initial column temperature (°C)	20	40	50	50
Final column temperature (°C)	360	350	350	390
Programming rate (°C/min)	10	6.5	8	7.5
Carrier gas	He	He	N_2	He
Carrier gas flow rate (ml/min)	40	30	60	60
Detector	TCD	FID	FID	TCD
Detector temperature (°C)	360	360	350	390
Injection port temperature (°C)	360	370	200	390
Sample size (μl)	4	0.3	1	5
Column resolution (R)	5.3	6.4	6.5	3

Note: OV-1 = methyl silicone polymer liquid phase; SE-30 = dimethyl silicone elastomer liquid phase; UC-W98 = silicone liquid phase; TCD = thermal conductivity detector; FID = flame ionization detector.

[a] Diatoport S, silane-treated.

[b] Chromosorb G (AW-DMS); AW = acid washed; DMS = treated with dimethylchlorosilane.

[C] Chromosorb P, acid-washed.

Source: From ASTM Standards D2887.

only a minor portion, whereas insoluble kerogen accounts for the major portion of oil shale organic matter. Furthermore, kerogen is nearly inert to most chemicals owing to its macromolecular and complex structure, therefore making most reactive processes less effective and making extraction more difficult.

Several different approaches are possible for the extraction of oil (organic matter) from the mineral matrix (inorganic rock matrix): (l) to drastically break the chemical bonds of the organics, (2) to mildly degrade or depolymerize the organics, and (3) to use solvents that have extraordinarily strong solvating power. The first approach is widely used in industrial applications, as high-temperature pyrolysis decisively cleaves the bonds of the organics. *Retorting* processes belong to this category and have a long history. The second approach may be achieved by a biochemical process or a controlled oxidative process. The third approach can be accomplished by potent extraction methods, such as a supercritical fluid extraction process that is based on the strong solvating power of a fluid in its supercritical region.

During the process of extraction of shale oil from oil shale, both chemical and physical properties of oil shale play important roles. The low porosity, low permeability, and tough mechanical strength of the oil shale rock matrix make the extraction

TABLE 8.14
Boiling Points of *n*-Paraffins

Carbon Number	Boiling Point (°C)	Carbon Number	Boiling Point (°C)	Carbon Number	Boiling Point (°C)
2	89	17	302	32	468
3	42	18	317	33	476
4	0	19	331	34	483
5	36	20	344	35	491
6	69	21	356	36	498
7	98	22	369	37	505
8	126	23	380	38	512
9	151	24	391	39	518
10	174	25	402	40	525
11	196	26	412	41	531
12	216	27	422	42	537
13	235	28	432	43	543
14	253	29	441	44	548
15	271	30	450		
16	287	31	459		

Note:
C_1 to C_{20} values taken from Selected Values of Hydrocarbons and Related Compounds, API Project 44, Loose-Leaf data sheet: Table 20a–e (Part 1), April 30, 1956.
C_{21} to C_{44} values taken from Vapor Pressures and Boiling Points of High Molecular Weight Hydrocarbons, C_{21} to C_{100}, report of Investigation of API Project 44, August 15, 1965.

Source: From ASTM Standards D2887.

process less efficient by making the mass transport of reactants and products much harder. Both heat and mass transfer conditions of a process also crucially affect the process economics as well as process efficiency.

The oil shale retorting processes can be classified as *ex situ* (or, above ground, off the sites) and *in situ* (or subsurface, within the existing formation) processes. As the names imply, *ex situ* processes are carried out above the ground after the shale is mined and crushed, whereas *in situ* processes are carried out under the ground, thus not requiring mining of shale entirely.

In this section, various processes developed and demonstrated for oil shale extraction are reviewed in terms of engineering and technological aspects.

8.5.1 *Ex Situ* Retorting Processes

In an *ex situ* process, oil shale rock is mined, either surface or underground, crushed, and then conveyed to a retorter that is subjected to temperatures around 500 to 550°C. At this temperature, chemical bonds of the organic compounds are broken and the kerogen molecules are pyrolyzed, yielding simpler and lighter molecules.

The advantages of *ex situ* processes are:

1. Efficiency of organic matter recovery has been demonstrated to be high, about 70 to 90% of the total organic content of the shale. Therefore, the amount of wasted organic matter, i.e., the unextracted portion or the organic residue, can be minimized by keeping the efficiency high.
2. Control of process operating variables is relatively straightforward. Therefore, the effects of undesirable process conditions can be minimized.
3. Once oil is formed, product recovery becomes relatively simple.
4. Process units can be used repeatedly for a large number of retorting operations.

However, the disadvantages of *ex situ* processes are:

1. Operating cost is usually high, as oil shale has to be first mined, crushed, transported, and then heated. Mining and transportation costs may become quite significant.
2. Spent shale disposal, underground water contamination, and revegetation problems are yet to be solved convincingly and effectively.
3. The process is somewhat limited to rich shale resources accessible to surface mining. In this regard, process economics plays an important role.
4. The capital investment for large-scale units may become very high as reusability is typically limited. Once the mine is depleted, a part of the investment may be lost forever.

The liberated compounds from oil shale retorting include gas and oil, which is collected, condensed, and upgraded into a liquid product that is roughly equivalent to crude oil. This oil can be transported by a pipeline or by a tanker to a refinery, where it is refined into the final product.

Various *ex situ* retorting processes are discussed in the following sections.

8.5.1.1 U.S. Bureau of Mines' Gas Combustion Retort

The first major experimental retort was built and operated by the U.S. Bureau of Mines (USBM). From 1944 to 1956, pilot plant investigations of oil shale retorting were carried out by USBM at facilities several miles west of Rifle, CO. Among the numerous types of retorts, the *gas combustion retort* gave the most promising results and was studied extensively.[43] This retort is made of a vertical, refractory-lined vessel through which crushed shale moves downward by gravity, countercurrent to the retorting gases. Recycled gases enter the bottom of the retort and are heated by the hot retorted shale as they pass upward through the vessel. Air and additional recycle gas (labeled as dilution gas) are injected into the retort through a distributor system at a location approximately one third of the way up from the bottom and are mixed with rising hot recycled gas. Figure 8.17 shows a schematic of a gas combustion retort. Combustion of the gases and of some residual carbon provides thermal energy to heat the shale immediately above the combustion zone to the retorting temperature.

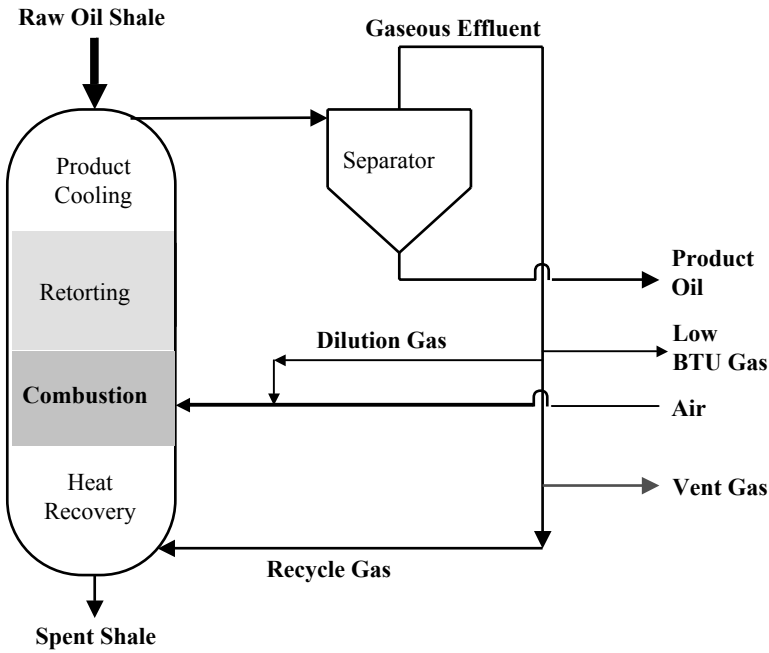

FIGURE 8.17 A gas combustion retort.

The incoming shale cools oil vapors and gases, and the oil leaves the top of the retort as a mist. The oil vapors and mists are subsequently chilled to produce liquid oil products that have to be upgraded.

This retort is similar to a *moving bed reactor* popularly used for coal gasification in its operating concepts.

8.5.1.2 The TOSCO II Oil Shale Process

The TOSCO II oil shale retorting process was developed by The Oil Shale Corp. An article by Whitcombe and Vawter[44] describes the process in detail and also presents economic projections for production of crude shale oil and hydrotreated shale oil. As an oil shale process, the TOSCO process is one of the few complete processes for production of shale oil.

8.5.1.2.1 Process Description

Oil shale is crushed and heated to approximately 480°C by direct contact with *heated ceramic balls*. At this temperature, the organic material (kerogen and bitumen) in oil shale rapidly decomposes to produce hydrocarbon vapor. Subsequent cooling of this vapor yields crude shale oil and light hydrocarbon gases. Figure 8.18 represents a schematic diagram of the process.

The pyrolysis reaction takes place in a retorting kiln (also referred to as the pyrolysis reactor or retort) shown in the central portion of the schematic. The feed streams to the retort are l/2-in. diameter ceramic balls heated to about 600°C and

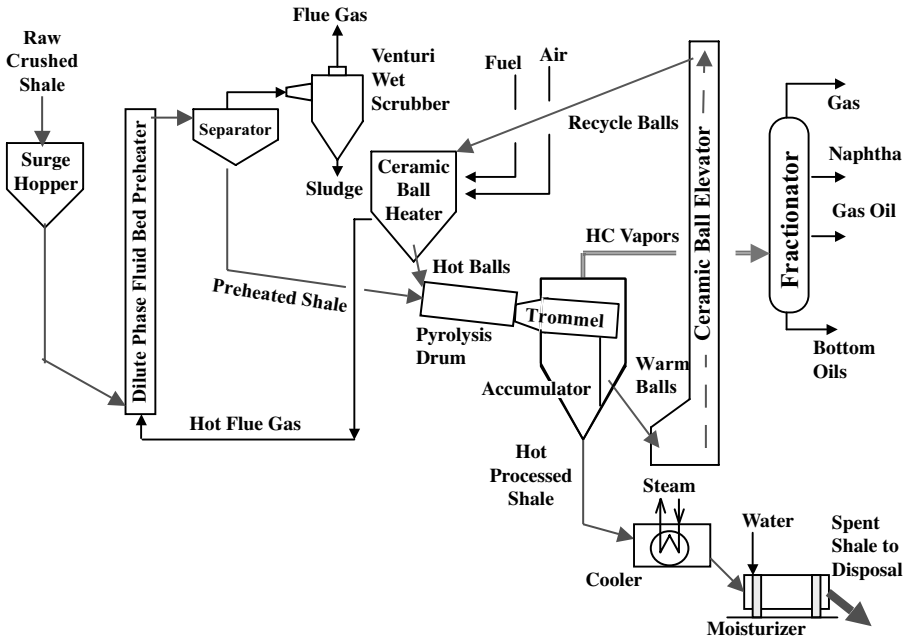

FIGURE 8.18 The TOSCO II process.

preheated (substantially lower than 450°C) shales crushed to a size of l/2 in. or smaller. The rotation of the retort mixes the feed materials and facilitates a high rate of heat transfer from the ceramic balls to the shale. At the discharge end of the retort, the ceramic balls and shale are at an isothermal (or near-isothermal) temperature by the time the shale is fully retorted.

The hydrocarbon vapor formed by the pyrolysis reaction flows through a cyclone separator to remove entrained solids, and then into a fractionation system, which is similar to the primary fractionator of a catalytic cracking unit. From this stage onwards, oil vapor produces heavy oil, distillate oils, naphtha, and light hydrocarbon gases.

The ceramic balls and spent shale are moved from the retort into a cylindrical trammel screen. Spent shale passes through the screen openings into a surge hopper. The ceramic balls move across the screen and into a bucket elevator for transport to the ball heater, where they are reheated by direct contact with flue gas. The ceramic balls are then recycled back to the retort.

Spent shale, discharged from the retort at 480°C, is first cooled in a rotating vessel containing tubes in which water is vaporized to produce high-pressure steam. The shale then flows into another rotating vessel in which it is further cooled by direct contact with water. The water flow is controlled so that the spent shale from the vessel contains 12% moisture by mass. The moisture is added to control dust emissions to make the spent shale suitable for compaction before disposal.

The preheating of oil shale is achieved by direct contact between the crushed shale and the flue gas effluent from the ball heater. The gaseous effluent from the process is the flue gas used to heat the ceramic balls and to preheat the shale. The

process includes a wet scrubber system to control the particulate content of the gas and an incinerator to control its hydrocarbon content in the flue gas. Emission of SO_x and NO_x are controlled by the choice of fuels used in the process, as well as the firing temperatures of process heaters. The process effectively uses the concept of energy integration for minimization of energy cost (in particular, heating shales by contacting hot ceramic balls, producing steam using the residual heat of the spent shale, and managing and recovering flue gas energy).

8.5.1.2.2 Process Yield of TOSCO

Tests in a pilot plant and semiworks have shown that the TOSCO II process recovers nearly 100% of the recoverable hydrocarbon in oil shale, as determined by the Fischer assay procedure. It is remarkable that the TOSCO process may be regarded as an effective scale-up of the Fischer assay procedure. Table 8.15 shows results from a 7-day, continuous operation of the semiworks plant.[44]

The average plant yield during this period was 161.1 kg of hydrocarbons per metric ton of oil shale processed, approximately 1.7% higher than by Fischer assay of the average shale sample used for the period.[44]

8.5.1.2.3 Gaseous and Crude Shale Oil Product from TOSCO Process

Table 8.16 shows a typical analysis of the C_4 and higher hydrocarbons produced by the TOSCO II retort. The effluent gas is practically free of nitrogen and contains a good amount of carbon dioxide produced by pyrolysis. However, a relatively high amount of hydrogen sulfide is also present, which has to be removed in the gas cleanup stage.

Table 8.17 shows the properties of shale oil (C_5 and heavier fractions) produced by the TOSCO II retorting process. The average sulfur level in the liquid oil product is 0.7%, whereas the average nitrogen content is 1.9%, which is high compared to that of conventional crude oils. The nitrogen content of conventional crude oil very seldom exceeds 1.0 percent by mass. The high level of nitrogen in shale oil may be attributed to the geological reason based on the original formation of this fossil fuel,

TABLE 8.15
TOSCO II Semiworks Plant Yield Data

Hydrocarbons	Plant Yield (kg/t)	Fischer Assay Yield (kg/t)
Total hydrocarbons	161.1	158.3
C_1–C_4	24.8	12.1
C_5 and heavier fractions	136.3	146.2
Other gaseous products		
$H_2 + CO$	2.25	1.85
$CO_2 + H_2O$	16.35	15.65

Source: From Whitcombe, J.A., and Vawter, R.G., Science and Technology of Oil Shale, Yen, Y.F., Ed., Ann Arbor Science MI, 1976, P.51, Table 4.1.

TABLE 8.16
Typical Analysis of C_4 and Lighter Gases from the TOSCO Semiworks Plant

Component/Fraction	Mass%
H_2	1.50
CO	3.51
CO_2	33.08
H_2S	5.16
CH_4	11.93
C_2H_4	8.67
C_2H_6	8.43
C_3H_6	11.08
C_3H_8	5.45
$C_4's$	11.19
Total	**100.00**

Source: From Whitcombe, J.A. and Vawter, R.G., The TOSCO-II oil shale process, in *Science and Technology of Oil Shale*, Yen, Y.F., Ed., Ann Arbor Science, Ann Arbor, MI, 1976, chap. 4.

TABLE 8.17
Properties of Crude Shale Oil from TOSCO II Retorting Process

Boiling Ranges and Components	Vol%	°API	Mass%	
			S	N
C_5–204	17	51	0.7	0.4
204–510	60	20	0.8	2.0
510 +	23	6.5	0.7	2.9
Total	100	21	0.7	1.9

Note: Boiling ranges are given in °C.

Source: From Whitcombe, J.A. and Vawter, R.G., The TOSCO-II oil shale process, in *Science and Technology of Oil Shale*, Yen, Y.F., Ed., Ann Arbor Science, Ann Arbor, MI, 1976, chap. 4.

i.e., oil shale deposits having come from protein-containing sources. The principal objective of the hydrotreating process is removal of nitrogen compounds that are poisonous to catalysts of many upgrading processes; including reforming, cracking, and hydrocracking.

8.5.1.2.4 TOSCO Process Units

Figure 8.19 represents a schematic of the TOSCO II process for commercial operation.[44] The commercial plant involves two hydrotreating units. The first one is the

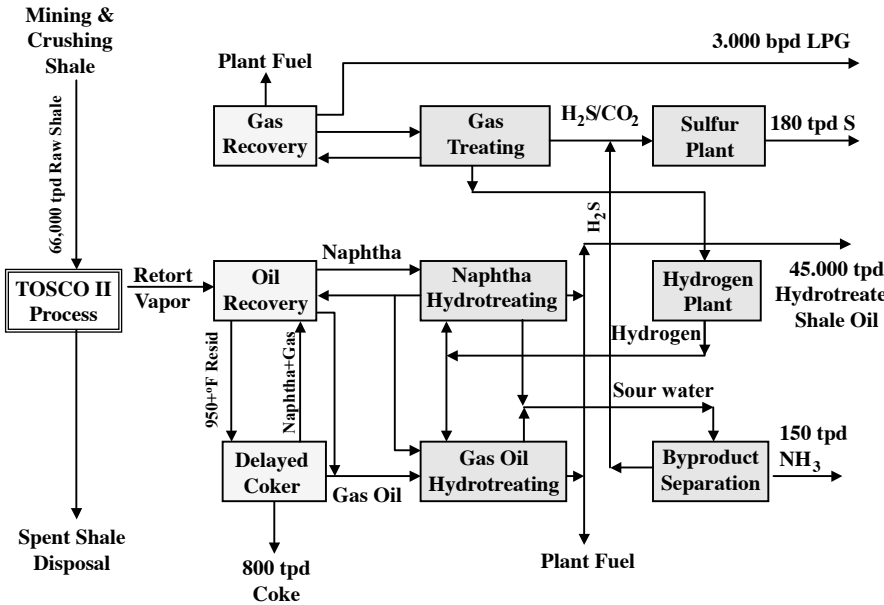

FIGURE 8.19 A block flow diagram — shale oil hydrotreating plant. (Source: Thumann, A., *The Emerging Synthetic Fuel Industry*, Fairmont Press, 1981.)

distillate hydrotreater that processes the 200–500°C oil formed in the retorter plus similar boiling range components formed in the coker. The second hydrotreater processes C_5 to 200°C naphtha formed in the retort, the coker, and the distillate hydrotreater. The distillate hydrotreater is designed to reduce the nitrogen content of the 200°C-plus product from the unit to a level lower than 1000 ppm. The naphtha hydrotreater is designed to reduce the nitrogen content about 1 ppm or below. Sulfur removal is nearly complete in each of the hydrotreating units.[44] The product compositions shown in Table 8.14 can be altered by changing the fuels chosen for burning in the process facilities. The production of C_5^+ fractions can be increased by burning the C_3^- products instead of hydrotreated oil. Table 8.18 shows the properties of the C_5–510°C fractions of hydrotreated shale oil, which is a blend of sulfur-free distillate products.

Refining such hydrotreated oils is relatively straightforward and requires an atmospheric distillation unit and a reformer. It would produce gasoline, sulfur-free light distillate fuels (No. l and No. 2 heating oils, as well as diesel fuel), and a sulfur-free heavier distillate fuel oil that is suitable for use as industrial fuel oil.[44]

8.5.1.2.5 Spent Shale Disposal

The typical spent shale produced by the TOSCO II process is a fine-grained dark material comprising approximately 80 mass% of the raw oil shale fed. It contains an average 4.5% of organic carbon via char formation in a hydrogen-deficient environment. The mineral constituents of spent shale consisting of principally dolomite, calcite, silica, and silicates are mostly unchanged by the retorting process treatment, except that some carbonate minerals such as dolomite decompose to oxides, liberating

TABLE 8.18
Properties of Typical Hydrotreated Shale Oil

Boiling Ranges and Components	Vol%	°API	Nitrogen (ppm)
C_5–204	43	50	1
204–361	34	35	800
361–EP	23	30	1200
Total	100	40[a]	

Note: Boiling ranges are given in °C.

[a] °API for the total amount of the product.

Source: From Whitcombe, J.A. and Vawter, R.G., The TOSCO-II oil shale process, in *Science and Technology of Oil Shale*, Yen, Y.F., Ed., Ann Arbor Science, Ann Arbor, MI, 1976, chap. 4.

carbon dioxide. During the retorting process, significant size reduction also takes place, yielding the particle (grain) size of most spent shale finer than 8 mesh.

The technology for spent shale disposal was seriously tested in 1965 after completion of the 1000 ton/d semiworks plant at Parachute Creek. Small revegetation test plots were constructed in 1966 to evaluate both plant growth factors and plant species. In 1967, the first field demonstration revegetation plot was constructed and seeded. Extensive off-site investigations have been carried out, including the spent shale permeability, quality analysis of water runoff from spent shale embankments, etc.

8.5.1.3 The Union Oil Retorting Process

In the Union Oil process, the heat needed for retorting is provided by *combustion of coke* inside the retort. The shale is fed from the bottom of the retort and conveyed (pumped) upward by means of a specially developed *rock pump*. The product oil is siphoned out from the bottom of the retort and fully recovered. The process is quite unique and innovative, utilizing well-designed rock pumps and adopting a number of designs for heating shales in the retort. According to a process described by Deering,[45] coke-containing spent shale derived from a gas-heated reduction zone is passed through a *combustion-gasification zone* countercurrently to an upflowing mixture of steam and oxygen-containing gas to effect partial combustion of the coke on the spent shale, i.e., $C + \frac{1}{2}O_2 = CO$. The resulting heat (exothermic heat) of combustion is used to support concurrent endothermic gasification reactions between steam and unburnt coke, i.e., $C + H_2O = CO + H_2$. Figure 8.20 shows a schematic of the Union Oil process. The oil shale feed rate can be varied considerably depending on the size of the retort and the desired retention time.

The recycled water gas ($CO + H_2O + H_2 + CO_2$) contains hydrogen, and it must pass through the combustion-gasification zone in which hydrogen-burning temperatures prevail. A significant aspect of the process is that the overall yield of hydrogen, even with such passage, is still not significantly affected. This retort uses lump shales of about the same size range that the Gas Combustion Retort uses. Another important feature of the process is that it does not require cooling water.

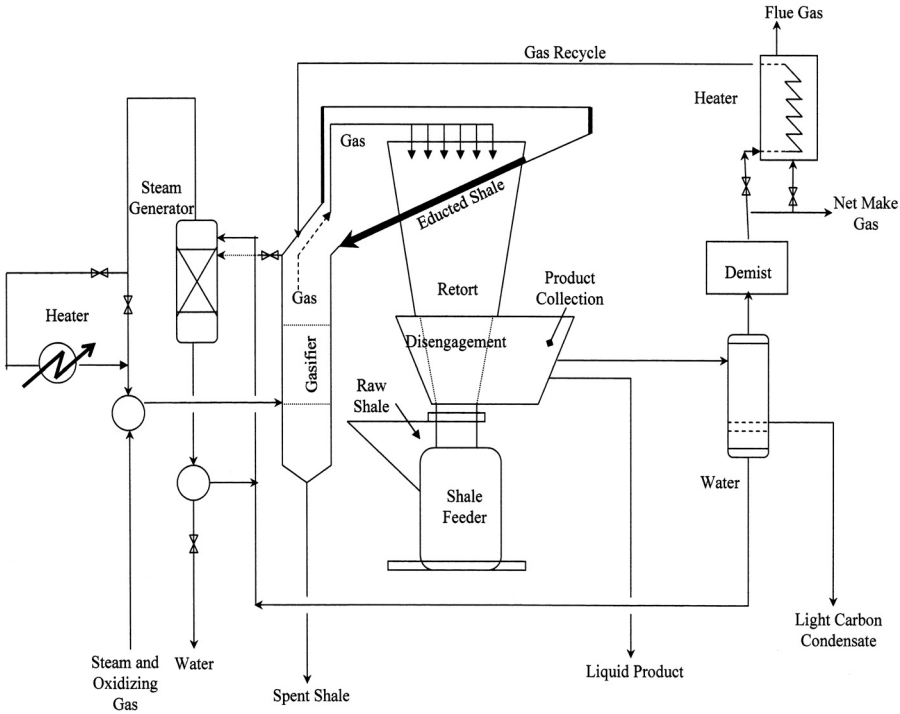

FIGURE 8.20 The Union Oil's retorting-gasification process (Based on U.S. patent 4,010,092).

The Union Oil Co. developed three different process designs as follows:

1. *The A retort* is the one in which internal combustion of gas and residual char from shale provides the energy required for the process. This design is based on direct heating.
2. *The B retort* is the one in which the oil shale is heated indirectly by a recycled stream of externally heated gas.
3. *The Steam-Gas Recirculation (SGR) retort* is the one in which the heat carrier for the process is generated in a separate vessel by gasifying the residual char with air and steam.

Union Oil had accumulated pilot plant experiences with the preceding three designs; which included a 2-ton/d prototype and a 50-ton/d pilot plant using the A retort design at Wilmington, CA, and a nominal 6-ton/d pilot retort using the B mode and a pilot using the SGR mode at the Union Research Center, Brea, CA. A larger-scale pilot plant was built near Parachute Creek in Western Colorado, where the oil shale could be mined readily from an outcrop of the Mahogany zone. The pilot plant had a capacity of l000 tons/d, and its operation was completely successful. Unocal ceased operation in 1991. This operational experience is undoubtedly very valuable for future commercialization of the process.

8.5.1.4 The Lurgi-Ruhrgas Process

The *Lurgi-Ruhrgas* (*LR*) process distills hydrocarbons from oil shale by bringing raw shale in contact with hot fine-grained solid heat carrier. The ideal heat carrier for this process is the spent shale. However, if rich shales are used in the process as raw shales, they typically deteriorate into a fine powder during process treatment and must be supplemented by more durable materials like sand for use as heat carriers. A schematic of the L-R process is presented in Figure 8.21.

The pulverized oil shale and heat carriers are brought into contact in a mechanical mixer such as a screw conveyer. In pilot plant tests, the shale was first crushed to a maximum size of one fourth to one third of an inch, but larger commercial units might process particles as large as half an inch.[45] The oil vapor and gaseous products are cleaned of dust in a hot cyclone, and the liquid oil is separated by condensation.

Retorted shale from the mixer passes through a hopper to the bottom of a lift pipe with the dust from the cyclone. Preheated air introduced at the bottom of the pipe carries the solids up to the surge bin. Solids are heated by the combustion of the residual char in the shale to approximately 550°C. In case residual char is not sufficient for this process, fuel gas is also added. In the surge bin, the hot solids separate from the combustion gases and return to the mixer, where they are brought in contact with fresh oil shale, completing the cycle. As an improvement, a new design of surge bin was introduced by Kennedy and Krambeck.[68] This improved surge bin has baffles that facilitate uniform flow of feed material through the surge bin.

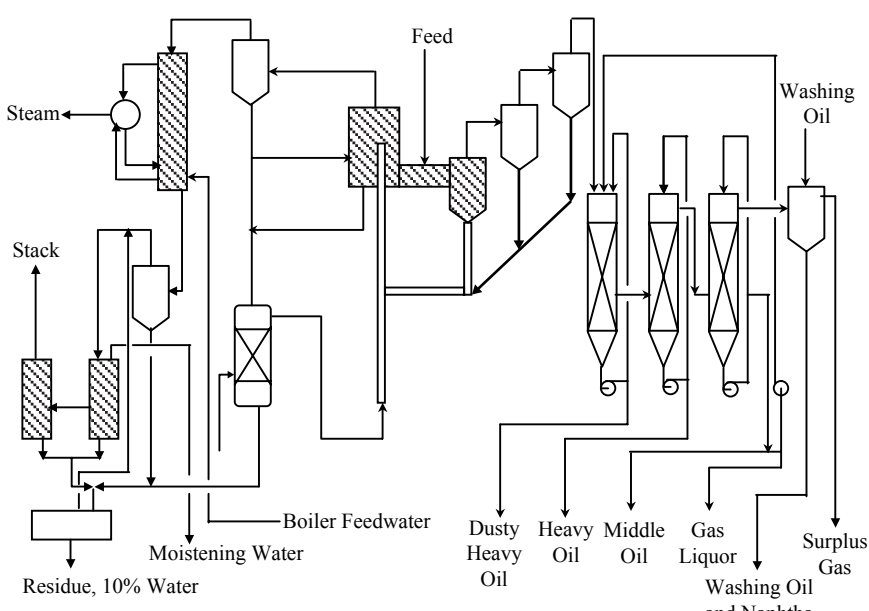

FIGURE 8.21 The Lurgi-Ruhrgas retort system (Source: Matar, S., *Synfuels: Hydrocarbons of the Future*, Pennwell Publishing Co., Tulsa, OK, 1982.)

Pilot plant tests have produced high yields, exceeding the Fischer assay value of the raw Colorado shale, at approximately 30 gal/ton of shale. As no combustion occurs in the mixer retort during this process, the product gas from the mixer has a relatively high calorific value (CV). The L-R process can operate with a wide range of particle sizes (very fine to medium) and, therefore, it can be modified for a variety of shale feedstocks. The process hardware is mechanically simple except for the mixer, which may be difficult to design because it must operate reliably in a harsh environment. However, the movement of dust through the system potentially causes two major problems of concern. One is the accumulation of combustible dust in the transfer lines, increasing the likelihood of fires and plugging. The other is entrainment of dust in the oil produced. (Even though most of the dust is removed in the hot cyclone, some is inevitably carried over to the retort product.) When the crude oil from the process is fractionated, the dust concentrates in the heaviest fraction, requiring an additional processing step. This heavy fraction can be diluted and filtered or recycled to the mixer.

The L-R process, originally developed in the 1950s for the low-temperature flash-carbonization of coal, was tested on European and Colorado oil shale in a 20 ton/d pilot plant at Herten, Germany. Two 850 ton/d pilot plants for carbonizing brown coal were built in Yugoslavia in 1963, and a large plant that uses the L-R process to produce olefins by cracking light oils was built in Japan.[45,46]

As an improvement over this process, *time domain reflectometry* (TDR) was evaluated and developed by Reeves and Elgezawi[67] to monitor volumetric water content (θ_v) in oil shale solid waste retorted and combusted by the Lurgi-Ruhrgas process. A TDR probe was designed and tested that could be buried and compacted in waste embankments and provide *in situ* measurements for θ_v in the high-saline and high-alkaline conditions exhibited by the spent oil shale solid waste.[67]

8.5.1.5 Superior's Multimineral Process

The multimineral process was developed by the Superior Oil Co. In addition to synthetic gas (syngas) and oil, it also produces minerals such as nahcolite ($NaHCO_3$), alumina (Al_2O_3), and soda ash.[47] A schematic of Superior Oil's multimineral retort process is shown in Figure 8.22. The process is basically a four-step operation for oil shale that contains recoverable concentrations of oil, nahcolite, and dawsonite (a sodium-aluminum salt [$Na_3Al(CO_3)_3 \cdot Al(OH)_3$]). Superior Oil had operated a pilot plant of this process in Cleveland, OH.

Nahcolite is in the form of discrete nodules that are more brittle than shale. It is recovered by secondary crushing and screening, followed by a specialized process called *photosorting* that recovers nahcolite product of >80% purity. After removal of nahcolite, shale is retorted using the *McDowell-Wellman* process.[45] The process was originally developed as a stirred-bed, low-Btu coal gasifier. The unique, continuously fed, circular-moving grate retort used in this process is a proven, reliable piece of hardware that provides accurate temperature control, separate process zones, and a water seal that eliminates environmental contamination.

Nahcolite has been tested as a dry scrubbing agent to absorb sulfurous and nitrous oxides. Dawsonite in shale is decomposed in the retort to alumina and soda

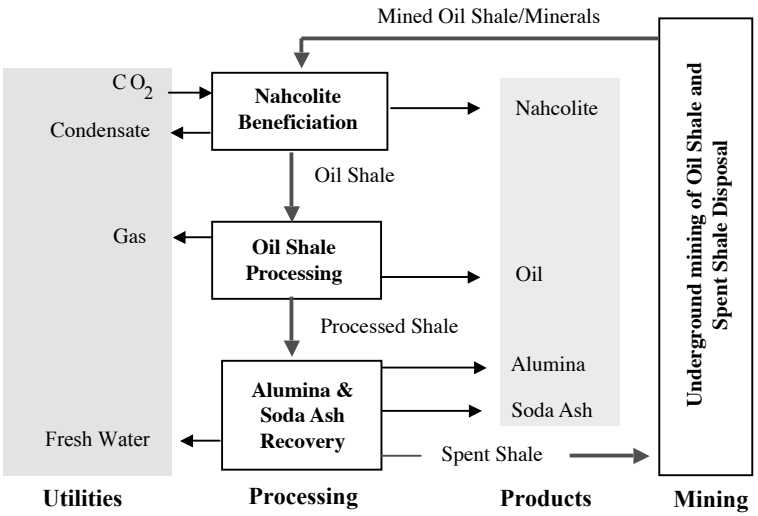

FIGURE 8.22 Superior oil's multimineral retort system.

ash. After shale is leached with recycled liquor and makeup water from the saline subsurface aquifer, the liquid is seeded and pH is lowered to recover the alumina. This alumina can be extracted and recovered at a competitive price with alumina from bauxite. Soda ash is recovered by evaporation, and can be used for a variety of industrial applications, such as neutralizing agents. The leached spent shale is then returned to the process. The by-products that this process generates may make the process economically even more attractive.

8.5.1.6 The Paraho Gas Combustion Process

The Paraho retort is a stationary, vertical, cylindrical, and refractory-lined kiln of mild steel developed by Paraho Development Corp. Raw shale enters at the top and is brought to the retorting temperature by a countercurrent flow of hot combustion gases. A schematic of the Paraho gas combustion retort system is shown in Figure 8.23. Shale is fed at the top along a rotating "pantsleg" distributor and moves downward through the retort. The rising stream of hot gas breaks down the kerogen to oil, gas, and residual char. The oil and gas are drawn off, and the residual char burns in the mixture of air and recycled gas. By injecting a part of the gas–air mixture through the bottom of the kiln, much of the sensible heat in the spent shale is recovered. The retort temperature is controlled by adjusting the compositions of the gas–air mixtures to the preheat and combustion zones.[45] Shale oil vapors flow upward and pass at a moderate temperature to an oil recovery unit. The end products are shale oil and low-Btu gas. A typical analysis of crude shale oil from this process is shown in Table 8.19. The shale oil produced can be upgraded to a crude feedstock.

The heavy naphtha cut (88–178°C) from the treated oil has a higher octane rating and lower sulfur than a comparable Arabian crude fraction. The diesel fraction (178–341°C) is identical to comparable fractions from other sources, so the heavy cut can be used as a feedstock for cracking units.[47]

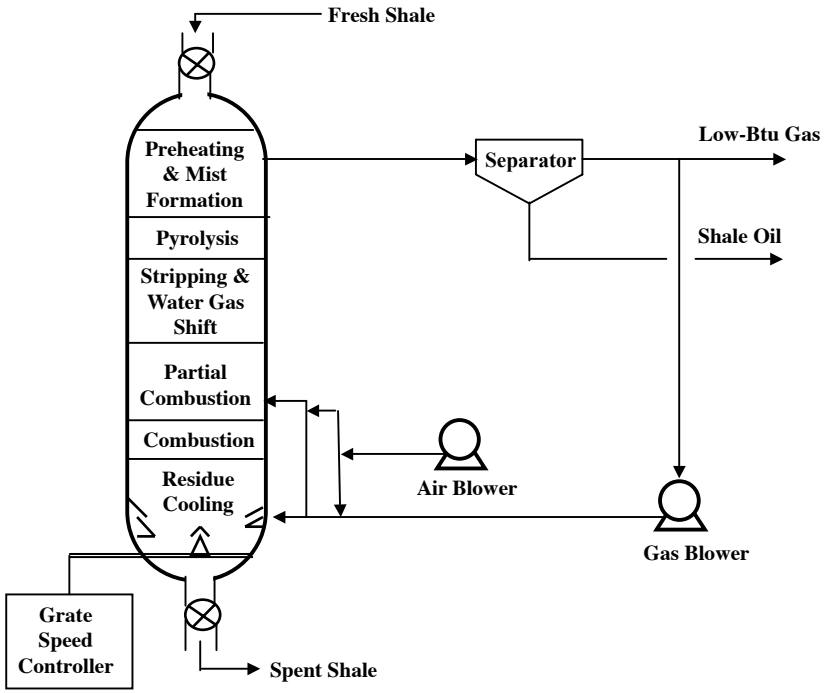

FIGURE 8.23 The Paraho process for shale oil extraction.

TABLE 8.19
Typical Analysis of Paraho Retort Shale Oil

API gravity (°API)	19.70
Nitrogen (wt%)	2.18
Conradson carbon (wt%)	4.50
Ash (wt%)	0.06
Sulfur (wt%)	0.74
Pour point (°C)	26.0
Viscosity, cp, 38°C	256.0

Research and development on the Paraho retort, initiated by the company in August 1973, continued until April 1976 under the sponsorship of 17 energy and engineering companies. In 1978, Paraho delivered 100,000 bbl of raw shale oil to the U.S. Navy for defense testing purposes.[45]

The Paraho process can handle shale particle sizes of at least 3 in., keeping crushing and screening costs to a minimum, yet achieving a high conversion of better than 90% of Fischer assay. By burning the residual char and also recovering sensible heat from the spent shale, a high thermal efficiency can be achieved. The process is mechanically simple, requiring little auxiliary equipment. Also, no water is required for product cooling.

In 1987, Paraho reorganized as New Paraho Corp. at Boulder, CO, and began production of shale oil modified asphalt[66] (SOMAT) asphalt additives, which is used in test strips in five states in the U.S. In 1991, New Paraho reported successful tests of SOMAT shale oil asphalt additives.

8.5.1.7 Petrosix Retorting Process

The Petrosix retorting process was developed in Brazil by Petrobras to use oil shale deposits in the Irati belt, which extends up to 1200 km.[47] The estimated deposit for this area is 630 billion barrels of oil, 10 million tons of sulfur, 45 million tons of liquefied gas and 22 billion m^3 of fuel gas.

This process has an external heater that raises the recycle gas temperature to approximately 700°C. The fuel for the heater can be gas, liquid, or solid. Shale is crushed in a two-stage stem that incorporates a fine rejection system. This retort has also three zones, i.e., high, middle, and low.

Crushed shale is fed by desegregation feeders to the retort top and then it is forced downward by gravity, countercurrent to the hot gas flow. In the middle zone, hot recycle gas is fed at 700°C. Shale oil in mist form is discharged from the upper zone and is passed to a battery of cyclones and onto an electric precipitator to coalesce. The shale is then recovered and some gas is recycled to the lower zone to adjust the retort temperature.[47] The remaining gas is treated in a light-ends recovery section sweetened (desulfurized), and discharged as liquefied petroleum gas (LPG). Figure 8.24 shows a schematic of the Petrosix retort process, and Table 8.20 shows some properties of shale oil produced by this process.[47]

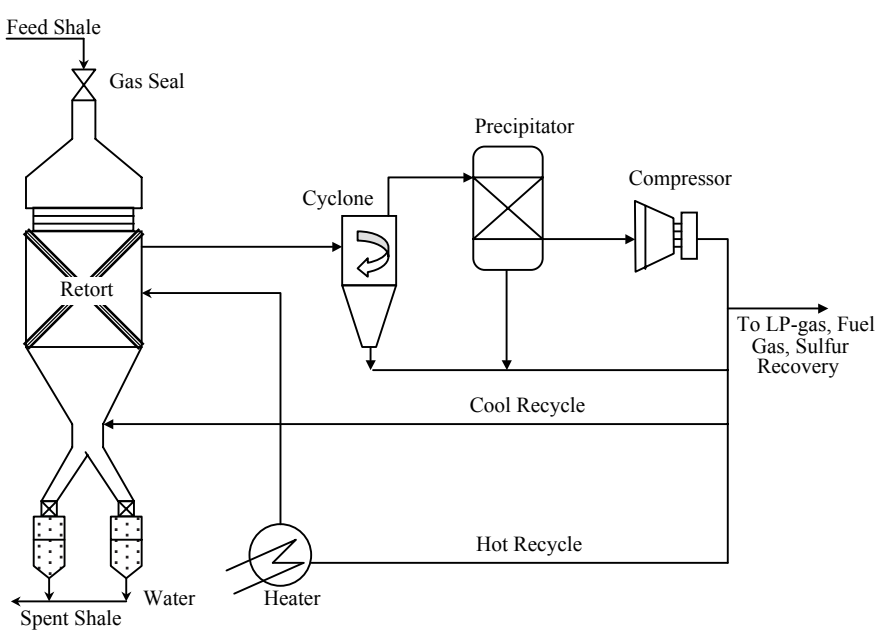

FIGURE 8.24 The Petrosix retort system.

TABLE 8.20
Typical Shale Oil Properties by Petrosix[47]

Gravity (°API)	19.60
Sulfur (wt%)	1.06
Nitrogen (wt%)	0.86
Pour Point (°F)	25.0

Source: From Matar, S., *Synfuels: Hydrocarbons of the Future*, Pennwell Publishing Co., Tulsa, OK, 1982.

The most up-to-date version of the Petrosix process has the primary characteristic of being easy to operate.[69] After the oil shale is taken out by open-cut mining, the shale goes to the grinder to reduce the particle size of the rocks (shales) that vary between 6 to 70 mm. These ground shale rocks (stones) are then transferred to a retort, where they are heated at a temperature of approximately 500°C, thereby releasing organic matter from the shale in the form of oil and gas.[69]

8.5.1.8 Chevron Retort System

A small pilot unit with a shale-feed capacity of 1 ton/d was developed by Chevron Research. This process used a catalyst and a fractionation system. The pilot operated on a staged, turbulent-flow bed process that reportedly used the shale completely. Figure 8.25 shows a schematic of this process, which is also called *shale oil hydrofining* process. The heart of this process is in the shale oil upgrading part rather than in the retorting part.

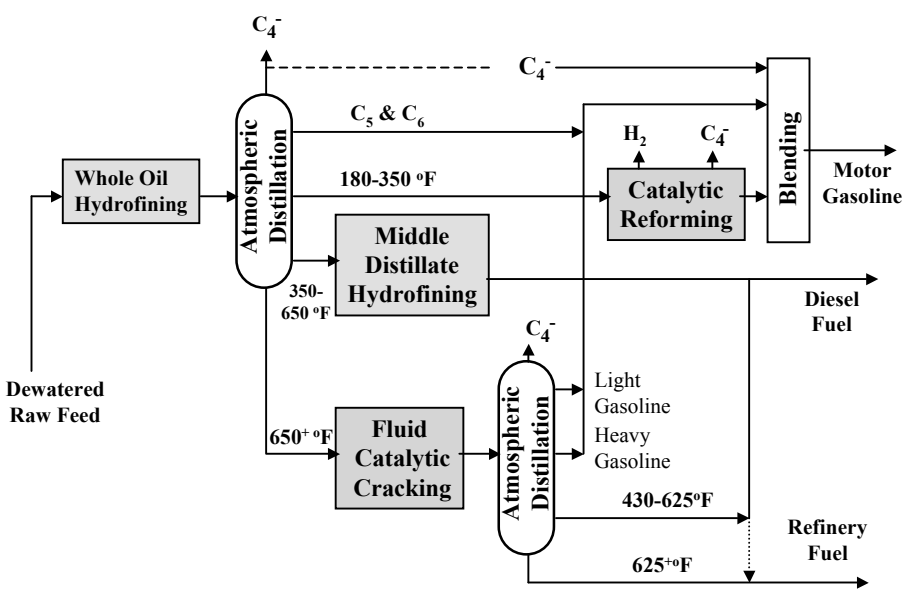

FIGURE 8.25 The Chevron shale oil hydrotreating system.

8.5.1.9 Moving Bed Retorting Process

A U.S. patent by Barcellos[60] describes a moving bed retorting process for obtaining oil, gas, sulfur, and other products from oil shale. The process comprises drying, pyrolysis, gasification, combustion, and cooling of pyrobituminous shale or similar rocks in a single passage of the shale continuously in a moving bed. The charge and discharge of oil shale is intermittent, and the maximum temperature of the bed is maintained within a range of about 1050–1200°C or even higher. The temperature employed in this process is much higher than any other retorting processes discussed in this chapter. At this high temperature, the shale is essentially completely freed from the organic matter, fixed carbon, and sulfur resulting in a clean solid residue, which can be disposed of without harming the ecology, according to the inventor's claim. The advantage of this process is claimed to be in its retorting efficiency, as the process operates at high temperatures. However, a main concern may be in its energy efficiency and minimization of waste energy. No pilot plant research data has been published for this process. No large-scale demonstration has been done on this process.

8.5.1.10 The Carbon Dioxide Retorting Process

Lee and Joshi[48] developed a retorting process that differs from other retorting processes in its chemistry by use of a different sweep gas, i.e., carbon dioxide. They claim that pyrolysis products of kerogen can be swept out far better in the carbon dioxide medium and, therefore, the richest oil shales can be retorted with significantly higher yields than their Fischer assay values when carbon dioxide is used as a process gas. Other advantages of the processes include the suppression of dolomite and calcite decomposition reaction because of the higher partial pressure of CO_2 in the system.

The *carbon dioxide retorting* process can be adopted in various retort designs with little or no system configuration change. The preliminary experimental data show that the CO_2 retorting process substantially enhances the oil yields from Colorado and Australian shales over the conventional process (Fischer assay). However, if the CO_2 retorting process is applied to a lean, low-permeability shale, like Ohio Devonian shale, the swollen kerogen blocks the porepaths, resulting in poorer oil yields than the case with nitrogen as sweep gas as in Fischer assay. This process is scientifically interesting in the sense that kerogen swells and softens in both subcritical and supercritical CO_2 medium. No large-scale demonstration has been done on this process concept.

8.5.2 *In Situ* Retorting Processes

Oil shale retorting can also be achieved underground, i.e., without mining the shale. Such a process is called an *in situ oil shale retorting process* or *subsurface retorting*. In a typical *in situ* process, the shale is fractured by either explosives or hydrostatic pressure. A portion of the oil shale organic matter is then burned to obtain heat necessary for retorting. The retorted shale oil is pumped out of the production zone in a manner similar to the extraction of crude petroleum.

The advantages of *in situ* processing include:

1. Oil can be recovered from deep deposits of oil shale formation.
2. Mining costs can be eliminated, or minimized.
3. There is no solid waste disposal problem, as all operations are conducted through well bores. Therefore, the process may be environmentally more desirable, as long as mineral leaching or harmful side effects of the processed shales are absent or controlled.
4. Shale oil can be extracted from leaner shale, e.g., deposits containing <15 gal/ton of oil.
5. The process is ultimately more economical owing to elimination or reduction of mining, transportation, and crushing costs.

However, the disadvantages of *in situ* processing are:

1. It is difficult to control subsurface combustion because of insufficient permeability within the shale formation.
2. Drilling cost is still high.
3. Recovery efficiencies are generally low.
4. It is difficult to establish the required permeability and porosity in the shale formation.
5. There is a concern for possible contamination of aquifers. If not controlled or treated, effects may linger for an extended period of time even after the project completion. Tests and control may require extensive efforts.

The *in situ* technology for production of shale oil from shales, in general, optimizes recovery process economics while minimizing environmental impact. This is why considerable emphasis has also been placed on these processes.

In situ retorting processes can be roughly classified into two types, i.e., *modified in situ* (MIS) and *true in situ* (TIS). MIS retorting, the brainchild of Occidental Petroleum, involves partial mining of the oil shale deposit to create a void space and rubblizing the rest into this space so as to increase the overall permeability of the shale. The underground rubblized shale is then ignited using an external or internal fuel source.[22] TIS retorting is similar to MIS, but no mining is done in this process. The shale deposits are rubblized to increase the permeability, and then the underground burning is begun.

A review of the oil shale literature indicates that all *in situ* oil shale processes can be classified into the following categories[49]:

1. Subsurface chimney
   A. Hot gases
   B. Hot fluids
   C. Chemical extraction
2. Natural fractures
   A. Unmodified
   B. Enlargements by leaching

3. Physical induction
   A. No subsurface voids

Other ways of classifying the *in situ* oil shale retorting processes are:

1. Formation of retort cavities
   A. Horizontal sill pillar
   B. Columnar voids
   C. Slot-shaped columnar voids
   D. Multiple zone design
   E. Multiple horizontal units
   F. Multiple adjacent production zones
   G. Multiple gallery-type retort zones
   H. Spaced-apart upright retort chambers
   I. Permeability control of rubble pile
   J. Formation of rich and lean zones
   K. Successive rubblization and combustion
   L. Thermomechanical fracturing
   M. Water leaching and explosive fracturing
   N. Inlet gas means
   O. Fluid communication
   P. Cementation to minimize plastic flow
   Q. Near-surface cavity preparation
   R. Dielectric heating
2. Retorting techniques
   A. Ignition techniques
   B. Multistage operation
   C. Steam leaching and combustion
   D. Pressure swing recovery
   E. Multistratum reservoir
   F. Production well throttling
   G. Combined combustion techniques
   H. Laser retorting
   I. Low-heat fans for frontal advance units
   J. Gas introduction and blockage
   K. Water injection
   L. Oil collection system
   M. Handling system for feed and products
   N. Uniform gas flow
   O. Postretorting flow
   P. Sound monitoring
   Q. Underground weir separator
   R. Emulsion breaking technique
   S. Offgas recycling
   T. Prevention of offgas leakage

3. Others
   A. Molecular sulfur and benzene recovery
   B. Hydrogen sulfide and carbon dioxide treatment
   C. Hot-fluid injection into solvent-leached shale
   D. Steam treatment and extended soak period
   E. Steam-driven excavating unit
   F. Anaerobic microorganisms
   G. Hot aqueous alkaline liquids and fluid circulation
   H. Plasma arc

In the second half of the 20th century, extensive research and development efforts were devoted to the commercialization of the *in situ* pyrolysis of oil shale. However, most of these efforts were either shelved, halted, or scaled down in the late 20th century because of the unfavorable process economics in the short term. As mentioned earlier in the chapter, the comparative economics of shale oil has become substantially more favorable in the 21st century. Several noteworthy processes are described in the following sections.

8.5.2.1 Sinclair Oil and Gas Company Process

In 1953, Sinclair Oil and Gas Co. performed one of the earliest experiments on *in situ* oil shale retorting. Their process concept was similar to that shown in Figure 8.26. Their study found that: (1) communication between wells could be established through induced or natural fracture systems, (2) wells could be ignited successfully, and (3) combustion could be established and maintained in the oil shale bed. They also realized that high pressures were required to maintain injection rates during the heating period. These tests were conducted near the outcrop in the southern part of the Piceance Creek Basin.[50] Additional tests were done several years later at a depth of about 365 m in the north-central part of the Piceance Creek Basin with some limited success, which was believed to be due to the inability to obtain the required surface area for the heat transfer. However, their experiments established the basic technology required for *in situ* retorting of oil shale and suggested further study areas.

8.5.2.2 Equity Oil Co. Process

The Equity Oil Co. of Salt Lake City[51] studied an *in situ* process that is somewhat different from the Sinclair process. This process involves injecting hot natural gas into the shale bed to retort the shale. One injecting well and four producing wells were drilled into the oil shale formation in an area of the Piceance Creek Basin. The natural gas was compressed to about 85 atm, heated to approximately 480°C, and delivered through insulated tubing to the retorting zone. Based on the experimental results and a mathematical model developed from them, it was concluded that this technique was feasible and potentially an economically viable method for extracting shale oil. However, the process economics is undoubtedly strongly dependent on the cost of natural gas and the amount required for makeup of natural gas. The cost fluctuations of natural gas experienced at the beginning of the 21st century may make this process less attractive than in the previous decades.

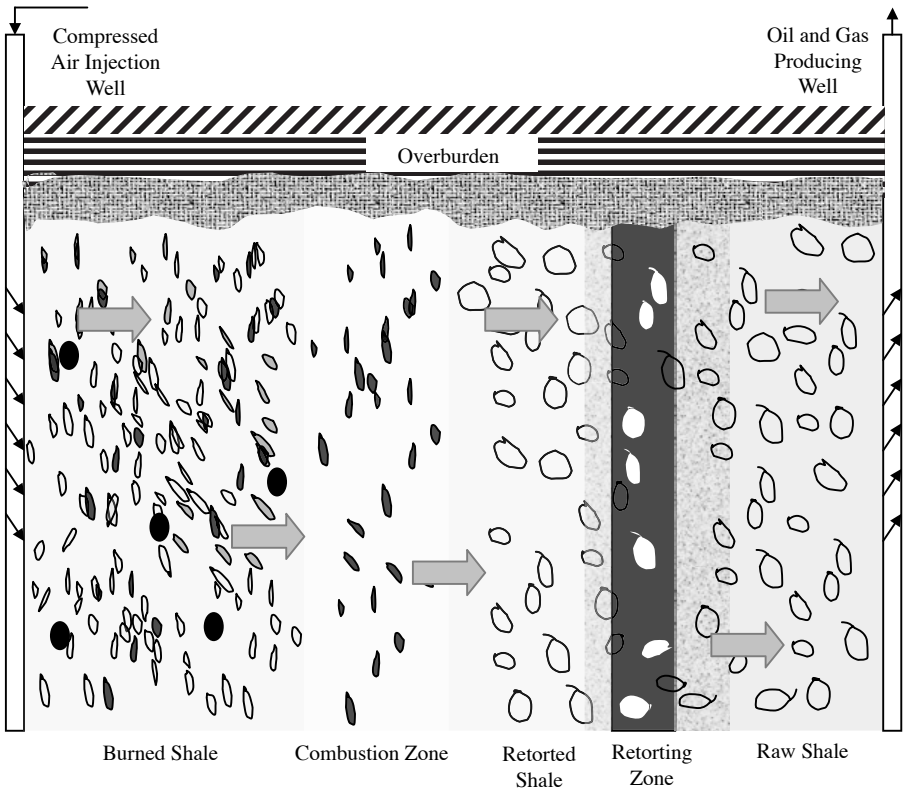

FIGURE 8.26 An *in situ* oil shale retorting process.

8.5.2.3 Occidental Petroleum Process

Occidental Petroleum developed a MIS process in which conventional explosives are used to expand solid blocks of shale into a vertical mined-out cavity, creating underground chimneys of fractured shale. Figure 8.27 shows a schematic of this retort design. To improve the fluid communication, about 10 to 25% of the shale in the chimney is removed. Air is then blown down through the remaining crushed shale, and the top ignited with a burner that can be fueled with shale oil or offgas from other retorts. On ignition, the burner is withdrawn and the steam is mixed with the inlet air to control the process.[45] The liquid and gaseous products flow to the bottom of the chimney, leaving the char in the shale behind as the main source of fuel for the slowly advancing flame front.

Occidental Petroleum did a series of field tests on this process at Logan's Wash in Debeque, CO, with 3 retorts — 30 ft. across and 72 ft. deep — each containing 6,000 to 10,000 tons of oil shale. Based on their experimental success, full-scale production of 57,000 bbl/d was very seriously considered.

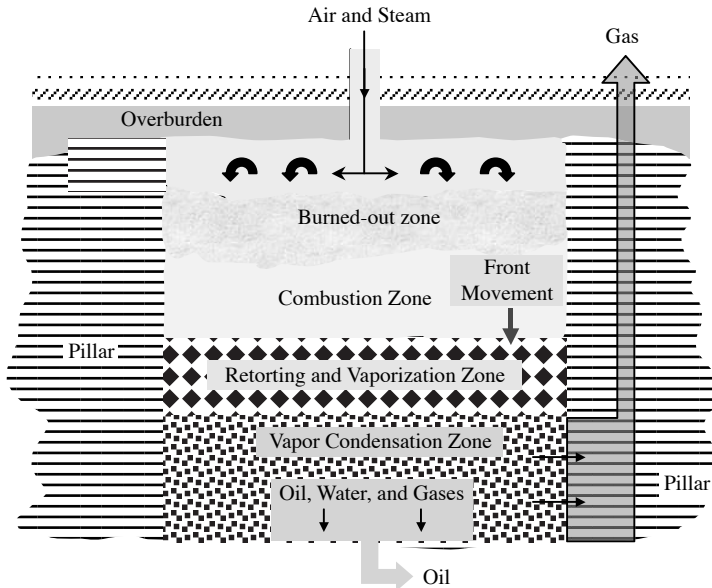

FIGURE 8.27 A modified *in situ* retort of Occidental Petroleum.

8.5.2.4 LETC Process (LERC Process)

Laramie Energy Technology Center (LETC), currently Western Research Institute, has been sponsoring several field projects to demonstrate the technical and economic feasibility of shale oil recovery by *in situ* technology.

LETC initiated their study on *in situ* retorting in the early 1960s with laboratory tests, simulated pilot plant tests on 10-ton and 150-ton retorts, and field tests at Rock Spring, WY. The test results demonstrated that it was possible to move a self-sustaining combustion zone through an oil shale formation and to produce shale oil.

The underground shale bed is prepared for the LETC process by first boring injection and production wells into the shale, and then increasing the permeability of formation by conventional fracturing techniques. Based on the LETC tests, the sequential use of hydraulic fracturing and explosives worked best. Once the formation is fractured, hot gases are forced into it to heat the area surrounding the injection point. As the desired temperature is reached and air is substituted for the hot gas, combustion begins and becomes self-sustaining across a front that gradually moves through the bed. As retorting progresses, oil and gas products are pumped out through the predrilled production wells. A schematic[52] for the LETC process is shown in Figure 8.28.

8.5.2.5 Dow Chemical Co.'s Process

The Dow Chemical Co., under contract with the U.S. DOE, conducted a 4-year research program to test the feasibility of deep *in situ* recovery of low-heat content gas from Michigan Antrim Shale.[53]

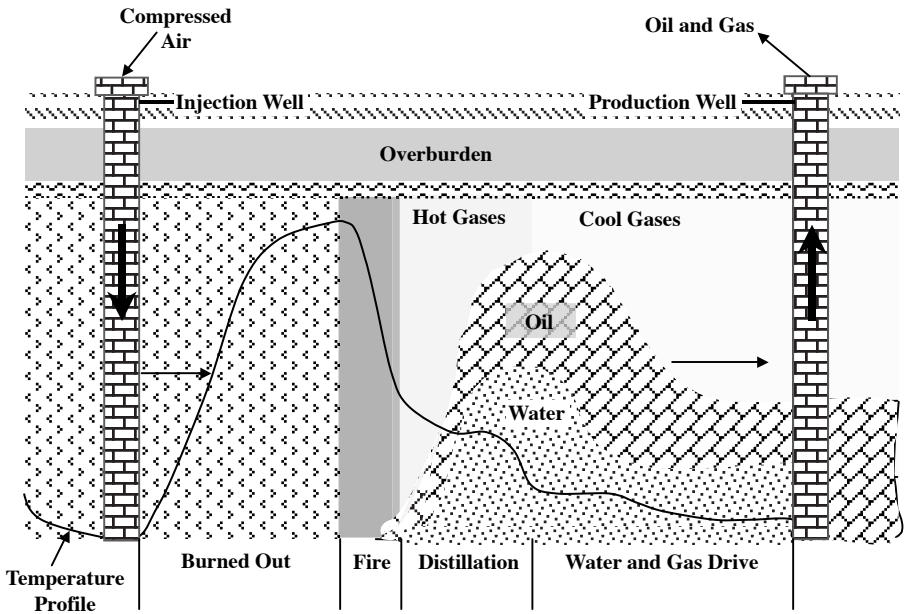

FIGURE 8.28 The Laramie Energy Technology Center (LETC) *in situ* retorting process. (From Cook, W.E., *Q. Colo. Sch. Mines*, 65(4), 133, 1970.)

The Antrim shale is part of the eastern and midwestern oil shale deposits, formed some 260 million years ago during the Devonian and Mississippian ages. These oil shales underlie an area of 400,000 mi^2 (1.07×10^{12}). In Michigan, the oil shale is approximately 61 m thick and is in a basin at depths ranging from about 0.8 km to outcroppings in three northern counties. The Michigan Antrim shale is believed to contain an equivalent hydrocarbon volume of 2,500 bbl barrels. Even applying a 10% recovery factor, this resource is about 9 times the amount of the U.S. proven oil reserves.

Extensive fracturing (rubblizing) of the oil shale is considered essential for adequate *in situ* retorting and recovery of energy from the Antrim shale. Two wells were explosively fractured using 19,000 kg of metalized ammonium nitrate slurry. Their test facility was located 75 mi north east of Detroit, MI, over 1 acre of field. The process used was TIS retorting.

Combustion of the shale was started using a 440-V electric heater (52 kW) and a propane burner (250,000 Btu/h). The special features of this process include shale gasification and tolerance to severe operating conditions. Their tests also showed that explosive fracturing in mechanically underreamed wells did not produce extensive rubblization. They also tested hydrofracturing, chemical underreaming, and explosive underreaming.

8.5.2.6 Talley Energy Systems Process

Talley Energy Systems Inc. carried out a U.S. DOE-Industry Cooperative oil shale project at 11 mi. west of Rock Springs, WY. The shale in this area is part of the

Green River shale formation, which is about 50 million years old. This process is also based on TIS processing, and uses explosive fracturing, additional hydraulic fracturing, and no mining.

8.5.2.7 Geokinetics Process

Geokinetics Inc. developed an *in situ* process that may be best described by modified horizontal technology. Explosive fracturing is used and the process can be used even for the shallow thin-seam recovery. This was one of the U.S. DOE–industry cooperative oil shale projects, and was located 61 mi. northwest of Grand Junction, CO. The geological formation used for this process study was Green River formation, Parachute Creek member, and Mahogany zone, which was the same as for the Occidental Oil process. The only difference between the two is that the Geokinetics process is *modified horizontal*, whereas the Occident oil process is *modified vertical*. Therefore, the Geokinetics process is good for shallow thin-seam recovery, whereas the Occidental Oil process is better suited for deep thick-seam recovery.

8.5.2.8 Osborne's *In Situ* Process

This process was developed by Osborne in 1983; a U.S. patent[54] describing the process has been assigned to Synfuel (an Indiana limited partnership). The process is unique, and enhanced oil recovery is achieved by forming generally horizontal electrodes from the injection of molten metal into preheated or unheated fractures of formation. A nonconductive spacing material is positioned in the casing of the borehole between the electrodes. A fracture horizontally intermediate between the metallic electrodes is propped up with a nonconductive granular material. Unterminated standing waves from a radio frequency (RF) generator are passed between the electrodes to heat the oil shale formation. The hydrocarbons in the formation are vaporized and recovered at the surface by their transport through the intermediate fracture and tubing. By this method, radial metallic electrodes can be formed at various depths throughout a subterranean oil shale formation to devolatilize the hydrocarbons contained within the oil shale formation.[54]

One advantage of this process is in the uniform heating of the rock formation that can be achieved by using RF electrical energy that corresponds to the dielectric absorption characteristics of the rock formation. An example of such techniques is described in U.S. Patent numbers 4,140,180 and 4,144,935, in which many vertical conductors are inserted into the rock formation and bound to a particular volume of the formation. A frequency of electrical excitation is selected to attain a relatively uniform heating of the rock formation. The energy efficiency of the process is very good; however, the economics of the process strongly depends on the cost of the electrodes and RF generation. The other merits of the process include the relative ease of controlling the retort size.

The difficulty, however, with this process is in the necessity of implanting an electrode within the subterranean rock formation at a precise distance. A schematic of this process is shown in Figure 8.29.

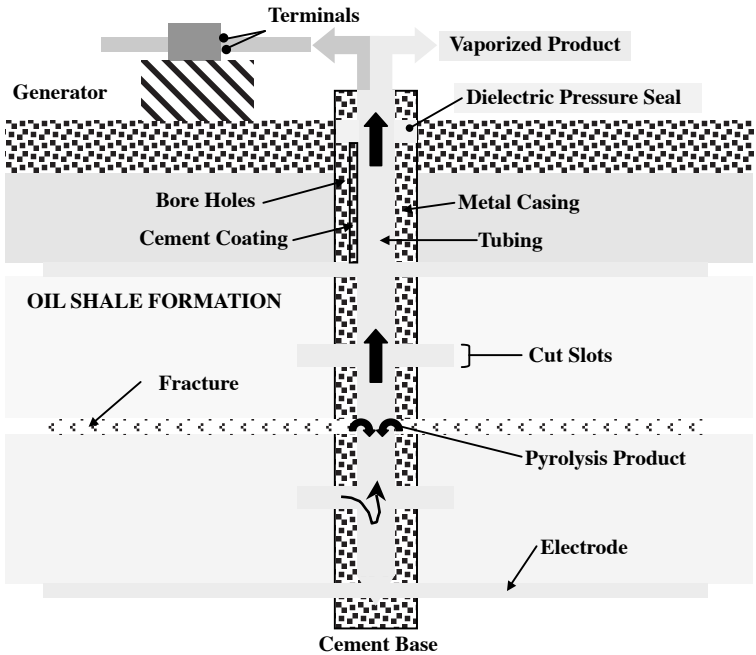

FIGURE 8.29 A vertical sectional view of a borehole penetrating a subterranean oil shale formation in completed condition for the recovery of hydrocarbons from oil shale — the Osborne process. (From Osborne, J., U.S. Patent No. 4,401,162, August 30, 1983.)

8.5.2.9 Shell Oil's Thermally Conductive *In Situ* Conversion Process

Shell Oil is currently developing an *in situ* retorting process known as *thermally conductive in situ conversion*.[71] This process involves *in situ* heating of underground oil shale using electric heaters placed in deep vertical holes drilled through a section of oil shale. The entire volume of oil shale is heated over a period of 2 to 3 years until it reaches 650 to 700°F, at which point oil is released from the shale. The released product is gathered in collection wells positioned within the heated zone. Shell's current plan also involves use of ground-freezing technology to establish an underground barrier called a *freeze wall* around the perimeter of the extraction zone. The freeze wall is created by pumping refrigerated fluid through a series of wells drilled around the extraction zone. The freeze wall prevents groundwater from entering the extraction zone, and keeps hydrocarbons and other products generated by the *in situ* retorting from leaving the project perimeter and contaminating the surrounding soil.

In 1997, Shell Oil successfully conducted small-scale field tests of this novel *in situ* process based on slow underground heating via thermal conduction, on Mahogany property. After deferring further tests because of economic reasons, Shell returned to Mahogany for further tests in 2000, and the R & D program is currently in operation. Larger-scale operations need to be conducted to establish technical viability, espe-

cially with regard to eliminating or alleviating any adverse impacts on groundwater quality.[71] The process has a number of merits that can contribute to lowering the processing cost of oil shale, as well as toward environmentally benign processing of this vast energy resource. The Shell Oil process is technologically classified as one of the TIS retorting processes, as there is no mining of shale involved.

8.5.2.10 True *In Situ* (TIS) and Modified *In Situ* (MIS) Retorting

In situ retorting of oil shale is often classified into TIS and MIS cases, as briefly mentioned earlier. In this section, these two terms are further clarified.

TIS retorting involves drilling wells and fracturing oil shale rock to increase its permeability. It, however, does not involve any mining of oil shale. Typically, a hot gas mixture is used to heat the oil shale rubble. Forced air then helps burn the oil shale. A flame front is formed and gradually moves through the bed, and the produced oil and gas are drawn through the production wells to the surface. As mentioned earlier, the Shell *in situ* process does not use a hot-gas heating technique to initiate retorting, but is classified as TIS process.

In TIS modified underground retorting, a blocked-out area is mined to remove approximately 10 to 25% of the oil shale. Vertical or horizontal wells are drilled through the remaining portion and are detonated. The produced voids help fracture and rubblize the oil shale. This is a modification of the TIS conversion process and was first developed by Occidental Oil.

8.5.3 Shale Oil Refining and Upgrading

As the demand for light hydrocarbon fractions constantly increases, there is much interest in developing economical methods for recovering liquid hydrocarbons from oil shale on a commercial scale. However, the recovered hydrocarbons from oil shale are not yet economically competitive against the petroleum crude produced. Furthermore, the value of hydrocarbons recovered from oil shale is diminished because of the presence of undesirable contaminants. The major contaminants are sulfurous, nitrogenous, and metallic (and organometallic) compounds, which cause detrimental effects to various catalysts used in the subsequent refining processes. These contaminants are also undesirable because of their disagreeable odor, corrosive characteristics, and combustion products that further cause environmental problems.

Accordingly, there is great interest in developing more efficient methods for converting the heavier hydrocarbon fractions obtained in a form of shale oil into lighter-molecular-weight hydrocarbons. The conventional processes include catalytic cracking,[73,74] thermal cracking,[72] coking, etc.

It is known that heavier hydrocarbon fractions and refractory materials can be converted to lighter materials by hydrocracking. These processes are most commonly used on liquefied coals or heavy residual or distillate oils for the production of substantial yields of low-boiling saturated products, and to some extent on intermediates that are used as domestic fuels, and still heavier cuts that are used as lubricants. These destructive hydrogenation or hydrocracking processes may be operated on a strictly thermal basis or in the presence of a catalyst. Thermodynamically speaking,

larger hydrocarbon molecules are broken into lighter species when subjected to heat. The H-to-C ratio of such molecules is lower than that of saturated hydrocarbons, and abundantly supplied hydrogen improves this ratio by saturating reactions, thus producing liquid species. These two steps may occur simultaneously.

However, the application of hydrocracking process has been hampered by the presence of certain contaminants in such hydrocarbons. The presence of sulfur- and nitrogen-containing compounds along with organometallics in crude shale oils and various refined petroleum products has long been considered undesirable. Desulfurization and denitrification processes have been developed for this purpose.

8.5.3.1 Thermal Cracking Process

Gulf Research & Development[55,56] developed a process for the noncatalytic thermal cracking of shale oil in the presence of a gaseous diluent and an entrained stream of inert heat carrier solids. The cracking process is directed toward the recovery of gaseous olefins as the primarily desired cracked product, in preference to gasoline-range liquids. By this process, it is claimed that at least 15 to 20% of the feed shale oil is converted to ethylene, which is the most common gaseous product. Most of the feed shale oil is converted to other gaseous and liquid products. Other important gaseous products are propylene, l,3-butadiene, ethane, and other C_4's. Hydrogen is also recovered as a valuable nonhydrocarbon gaseous product. Liquid products can comprise 40 to 50 wt% or more of the total product. Recovered liquid products include benzene, toluene, xylene, gasoline-boiling-range liquids, and light and heavy oils.

Coke is a solid product of the process and is produced by polymerization of unsaturated materials. Coke is typically formed in an oxygen-deficient environment via dehydrogenation and aromatization.[72] Most of the formed coke is removed from the process as a deposit on the entrained inert heat carrier solids.

The thermal cracking reactor does not require a gaseous hydrogen feed. In the reactor, entrained solids flow concurrently through the thermal riser at an average riser temperature of 700 to 1400°C. The preferred high L-to-D ratio is in the range of a high 4:l to 40:l, or 5:l to 20:l preferably.

8.5.3.2 Moving Bed Hydroprocessing Reactor

This process was developed by Universal Oil Products Co.[57] for deriving crude oil from oil shale or tar sands containing large amounts of highly abrasive particulate matter, such as rock dust and ash. The hydroprocessing takes place in a dual-function moving bed reactor, which simultaneously removes particulate matter by the filter action of the catalyst bed. The effluent from the moving bed reactor is then separated and further hydroprocessed in fixed bed reactors with fresh hydrogen added to the heavier hydrocarbon fraction to promote desulfurization.

A preferred way of treating the shale oil involves using a moving bed reactor followed by a fractionation step to divide the wide-boiling-range crude oil produced from the shale oil into two separate fractions. The lighter fraction is hydrotreated for the removal of residual metals, sulfur, and nitrogen, whereas the heavier fraction is cracked in a second fixed bed reactor normally operated under high-severity conditions.

Hydrotreating (HDT) reactions are generally carried out at high pressures (100–3000 psi) and high temperatures (270–350°C). During hydrotreating, the following reactions take place: hydrodesulfurization,[77] hydrodenitrogenation, hydrodemetalization, hydrodeoxygenation, and hydrogenation.[73]

8.5.3.3 Fluidized Bed Hydroretort Process

This process was developed by Cities Service Co.[58] in 1978. The process eliminates the retorting stage of conventional shale upgrading, by directly subjecting crushed oil shale to a hydroretorting treatment in an upflow, fluidized bed reactor such as that used for the hydrocracking of heavy petroleum residues. This process is a *single-stage retorting and upgrading* process. Therefore, the process involves: (1) crushing oil shale, (2) mixing the crushed oil shale with a hydrocarbon liquid to provide a pumpable slurry, (3) introducing the slurry along with a hydrogen-containing gas into an upflow, fluidized bed reactor at a superficial fluid velocity sufficient to move the mixture upwardly through the reactor, (4) hydroretorting the oil shale, (5) removing the reaction mixture from the reactor, and (6) separating the reactor effluent into several components.[59]

The mineral carbonate decomposition is minimized, as the process operating temperature is lower than that used in retorting. Therefore, the gaseous product of this process has a greater heating value than that of other conventional methods. In addition, owing to the exothermic nature of the hydroretorting reactions, less energy input is required per barrel of product obtained. Furthermore, there is practically no upper or lower limit on the grade of oil shale that can be treated.

8.5.3.4 Hydrocracking Process

Hydrocracking is essentially a cracking process in which higher-molecular-weight hydrocarbons pyrolyze to lower-molecular-weight paraffins and olefins in the presence of hydrogen.[74] The hydrogen saturates the olefins formed during the cracking process. Hydrocracking is used to process low-value stocks with a high heavy metal content. It is also suitable for highly aromatic feeds that cannot be processed easily by conventional catalytic cracking. Shale oils are not highly aromatic, whereas coal liquids are very highly aromatic.

Middle-distillate (often called *mid-distillate*) hydrocracking is carried out with a noble metal catalyst. The average reactor temperature is 480°C, and the average pressure is around 130 to 140 atm. The most common form of hydrocracking is carried out as a two-stage operation.[74] The first stage is to remove nitrogen compounds and heavy aromatics from the raw crude, whereas the second stage is to carry out selective hydrocracking reactions on the cleaner oil from the first stage. Both stages are processed catalytically. Once the hydrocracking stages are over, the products go to a distillation section that consists of a hydrogen sulfide stripper and a recycle splitter. Commercial hydrocracking processes include Gulf HDS, H-Oil, IFP Hydrocracking, Isocracking, LC-Fining, Microcat-RC (also known as M-Coke), Mild Hydrocracking, Mild Resid Hydrocracking (MRH), Residfining, Unicracking, and Veba Combi-Cracking (VCC).[74]

REFERENCES

1. Taylor, R.B., Oil Shale Commercialization: The Risks and the Potential, *Chemical Engineering*, September 7, 1981.
2. Thumann, A., *The Emerging Synthetic Fuel Industry*, Fairmont Press, Lilburn, GA, 1981.
3. Tisot, P.R. and Murphy, W.I.R., *Chem. Eng. Prog. Symp. Ser.*, 61(54), 25, 1965.
4. Tisot, P.R., *J. Chem. Eng. Data*, 12(3), 405, 1967.
5. Nottenburg, R., Rajeshwar, K., Rosenvold, R., and Dubow, J., *Fuel*, 58, 144, 1979.
6. Prats, M. and O'Brien, S.M., *J. Pet. Technol.*, 97, 1975.
7. Nottenburg, R., Rajeshwar, K., Rosenvold, R., and Dubow, J., *Fuel*, 57, 789, 1978.
8. Tihen, S.S., Carpenter, H.C., and Sohns, H.W., Thermal Conductivity and Thermal Diffusivity of Green River Oil Shale, Conf. Thermal Conductivity Proc. 7th, NBS Special Publ. 302, p. 529, Sept. 1968.
9. Lee, S., *Oil Shale Technology*, CRC Press, Boca Raton, FL, 1991.
10. Barnes, A.L. and Ellington, R.T., *Q. Colo. Sch. Mines,* 63(4), 827, 1968.
11. Sladek, T., Ph.D. thesis, A Determination of the Composition and Temperature Dependencies of Thermal Conductivity Factors for Green River Oil Shale, Colorado School of Mines, Golden, CO, 1970.
12. Dubow, J., Nottenburg, R., Rajeshwar, K., and Wang, Y., The Effects of Moisture and Organic Content on the Thermophysical Properties of Green River Oil Shale, *11th Oil Shale Symposium Proc.*, Colorado School of Mines, Golden, CO, 1978, p. 350.
13. Johnson, W.F., Walton, D.K., Keller, H.H., and Couch, E.J., *Q. Colo. Sch. Mines*, 70(3), 237, 1975.
14. McKee, R.H. and Lyder, E.E., *J. Ind. Eng. Chem.*, 13, 613, 1921.
15. Wang, Y., Rajeshwar, K., Rosenvold, R., and Dubow, J., *Thermochim. Acta*, 30, 141, 1979.
16. Shih, S.-M. and Sohn, H.Y., *Fuel*, 57, 662, 1978.
17. Wise, R.L., Miller, R.C., and Sohns, H.W., *U.S. Bur. Mines Rep. Invest.*, 7482, 1971.
18. Shaw, R.J., *U.S. Bur. Mines Rep. Invest.*, 4151, 1947.
19. Sohns, H.W., Mitchell, L.E., Cox, R.J., Burnet, W.I., and Murphy, W.I.R., *Ind. Eng. Chem.*, 43, 33, 1951.
20. Cook, W.E., *Q. Colo. Sch. Mines*, 65(4), 133, 1970.
21. Johnson, P.R., Young, N.B., and Robb, W.A., *Fuel*, 54, 249, 1975.
22. Gregg, M.L., Campbell, J.H., and Taylor, J.R., *Fuel*, 60, 179, 1981.
23. Wang, Y., M.S. thesis, A Single Particle Model for Pyrolysis of Oil Shale, University of Akron, Akron, OH, 1982.
24. Smith, J.W., *U.S. Bur. Mines Rep. Invest.*, 7248, 1969.
25. Allred, V.D., *Q. Colo. Sch. Mines*, 59(3), 47, 1964.
26. Branch. M.C., *Prog. Energy Combust. Sci.*, 5, 193, 1979.
27. Joshi, R., M.S. thesis, A Comparative Study between the Kinetics of Retorting of Ohio and Colorado Shale, University of Akron, Akron, OH, 1983.
28. Yen, Y.F., Structural investigations on Green River oil shale, in *Science and Technology of Oil Shale*, Yen, Y.F., Ed., Ann Arbor Publishers, Ann Arbor, MI, 1976.
29. Cook, E.W., *Fuel*, 53, 16, 1976.
30. Eggertsen, F.T., Groennings, S., and Holst, J.J., *Anal. Chem.*, 32(8), 904, 1960.
31. ASTM Standards D2887-06, Standard Test Method for Boiling Range Distribution of Petroleum Fractions of Gas Chromatography, ASTM International, 2006.
32. Rajeshwar, K., Nottenburg, R., and Dubow, J., *J. Mater. Sci.*, 14, 2025–2052, 1979.

33. Wang, Y., Dubow, J., Rajeshwar, K., and Nottenburg, R., *Thermochim. Acta*, 28, 23, 1979.
34. Johnson, D.R., Young, N.B., and Smith, J.W., LERC/Rl, Laramie Energy Research Center, Laramie, Wyoming, June 1977.
35. Dyni, J.R., Mountjoy, W., Hauff, P.L., and Blackman, P.D., U.S. Geological Survey, Professional Paper No. 750B, 1971.
36. Loughman, F.C. and See, G.T., *Am. Miner.*, 52, 1216, 1967.
37. Huggins, C.W. and Green, T.E., *Am. Miner.*, 58, 548, 1973.
38. Skrynnikova, G.N., Avdonina, E.S., Golyand, M.M., and Akhmedova, L. Ya., Trudy Vsesoyuz Nauch-Issledovatel Inst. *Pererab. Slants.*, 7, 80, 1959.
39. Agroskin, A.A. and Petrenko, I.G., *Zavodskaya Lab.*, 14, 807, 1948.
40. Scott, J.H., Carroll, R.D., and Cunningham, D.R., *J. Geophys. Res.*, 72, 5101, 1967.
41. Nottenburg, R., Rajeshwar, K., Freeman, M., and Dubow, J., *Thermochim. Acta*, 31, 39, 1979.
42. Rajeshwar, K., Nottenburg, R., Dubow, J., and Rosenvold, R., *Thermochim. Acta*, 27, 357, 1978.
43. Matzick, A., Dannenburg, R.O., Ruark, J.R., Phillips, J.E., Lankford, J.D., and Guthrie, B., *U.S. Bureau of Mines Bulletin*, 635, 99, 1966.
44. Whitcombe, J.A. and Vawter, R.G., The TOSCO-II oil shale process, in *Science and Technology of Oil Shale*, Yen, Y.F., Ed., Ann Arbor Science, Ann Arbor, MI, 1976, chap. 4.
45. National Research Council (U.S.), Panel on R&D Needs in Refining of Coal and Shale Liquids, *Refining Synthetic Liquids from Coal and Shale*, National Academy Press, Washington, D.C., 1980, chap. 5, pp. 78–135.
46. Rammler, R.W., *Q. Colo. Sch. Mines*, 65(4), 141–168, 1970.
47. Matar, S., *Synfuels: Hydrocarbons of the Future*, Pennwell Publishing Co., Tulsa, OK, 1982.
48. Lee, S. and Joshi, R., U.S. Patent No. 4,502,942, March 5, 1985.
49. Yen, T.F., Oil shales of United States: a review, in *Science and Technology of Oil Shale*, Yen, T.F., Ed., Ann Arbor Science, Ann Arbor, MI, 1976, pp. 1–17.
50. Dinneen, G.U., Retorting technology of oil shale, in *Oil Shale*, Yen, T.F. and Chilingarran, G.V., Eds., Elsevier, Amsterdam, Netherlands, 1976, chap. 9, pp. 181–197.
51. Dougan, P.M., Reynolds, F.S., and Root, P.J., The potential for *in situ* retorting of oil shale in the Piceance Creek Basin of northwestern Colorado, *Q. Colo. Sch. Mines*, 65(4), 57–72, 1970.
52. Sladek, T.A., Recent Trends in Oil Shale — Part 2: Mining and Shale Oil Extraction Processes, *Colorado School of Mines Mineral Industries Bulletin*, 18(1), pp. 1–20, 1975.
53. McNamara, P.H. and Humphrey, J.P., Hydrocarbons from Eastern Oil Shale, *Chemical Engineering Progress*, September 1979, p. 88.
54. Osborne, J., U.S. Patent No. 4,401,162, August 30, 1983.
55. Wynne, F.E., Jr., U.S. Patent No. 4,057,490, November 8, 1977.
56. McKinney, J.D., Sebulsky, R.T., and Wynne, F.E., Jr., U.S. Patent No. 4,080,285, March 21, 1978.
57. Anderson, R.F., U.S. Patent No. 3,910,834, October 7, 1975.
58. Gregoli, A.A., U.S. Patent No. 4,075,081, February 21, 1978.
59. Ranney, M.W., *Oil Shale and Tar Sands Technology-Recent Developments*, Noyes Data Corporation, NJ, 1979, p. 238.
60. Barcellos, E.D., U.S. Patent No. 4,060,479, November 29, 1977.
61. Qian, J., Wang, J., and Li, S., Oil shale development in China, *Oil Shale*, Vol. 20, No. e Special, 356–359, 2003.

62. Web site of Energy Minerals Division, American Association of Petroleum Geologists, http://emd.aapg.org/technical_areas/oil_shale.cfm.
63. Web site of World Energy Council, Survey of Energy Resources, http://www.worldenergy.org/wec-geis/publications/reports/ser/shale/shale.asp.
64. Hill, J.O., Thermogravimetric analysis, in *Encyclopedia of Chemical Processing (EChP)*, Lee, S., Ed., Vol. 5, Taylor & Francis, New York, 2005, pp. 3017–3029.
65. Laherrere, J., Review on Oil Shale Data, September 2005, www.oilcrisis.com/laherrere/OilShaleReview200509.pdf.
66. Lukens, L.A., Asphalt Rejuvenater and Recycled Asphalt Composition, U.S. Patent No. 5,755,865, May 1998.
67. Reeves, T.L. and Elgezawi, S.M., Time domain reflectometry for measuring volumetric water content in processed oil shale waste, *Water Resources Research*, 28(3), 769–776, 1992.
68. Kennedy, C.R. and Krambeck, F.J., Surge Bin Retorting Solid Feed Material, U.S. Patent No. 4,481,100, 1984.
69. Petrobras Web site about Petrosix process (2006), http://www2.petrobras.com.br/minisite/refinarias/ingles/six/conheca/ProcPetrosix.html.
70. Poulson, R.E., Jensen, H.B., and Cook, G.L., *ACS Div. Pet. Chem. Prepr.*, 15(1), A49–A55, 1971.
71. Bartis, J.T., LaTourrette, T., Dixon, L., Peterson, D.J., and Cecchine, G., O*il Shale Development in the United States: Prospects and Policy Issues*, MG-414-NETL, report prepared for National Energy Technology Laboratory, U.S. Department of Energy, part of RAND Corporation *Monograph Series,* 2005.
72. Tsai, T.C. and Albright, L.F., Thermal cracking of hydrocarbons, in *Encyclopedia of Chemical Processing (EChP)*, Lee, S., Ed., Vol. 5, Taylor & Francis, New York, 2006, pp. 2975–2986.
73. Kundu, A., Dwivedi, N., Singh, A., and Nigam, K.D.P., Hydrotreating catalysts and processes — current status and path forward, in *Encyclopedia of Chemical Processing (EChP)*, Lee, S., Ed., Vol. 2, Taylor & Francis, New York, 2006, pp.1357–1366.
74. Speight, J.G., Hydrocracking, in *Encyclopedia of Chemical Processing (EChP)*, Lee, S., Ed., Vol. 2, Taylor & Francis, New York, 2005, pp.1281–1288.
75. Chilingarian, G.V. and Yen, T.F., *Bitumens, Asphalts, and Tar Sands*, Elsevier, Amsterdam, 1978, chap. 1.
76. Hill, J.O., Thermal analysis techniques, in *Encyclopedia of Chemical Processing (EChP)*, Lee, S., Ed., Vol. 5, Taylor & Francis, New York, 2005, pp. 2965–2974.
77. Song, C. and Turaga, U.T., Desulfurization, in *Encyclopedia of Chemical Processing (EChP)*, Lee, S., Ed., Vol. 1, 2005, pp.651–661.
78. Kesavan, S.K. and Lee, S., *Fuel Sci. Technol. Int.*, 6(5), 505, 1988.

9 Methanol Synthesis from Syngas

Sunggyu Lee

CONTENTS

9.1 INTRODUCTION

The catalytic synthesis of methanol has continuously attracted substantial interest from industry, academia, and government, even though the technology for commercial synthesis of methanol has been quite mature and readily available since the 1920s.

Over the decades, scientists and engineers have tried to develop better catalysts that would enable the synthesis reaction to be carried out at less severe conditions with higher efficiencies. Efforts have also been made to diversify the raw material sources from mainly natural gas to coal and others, including biomass. Owing to the enormous volume of methanol demands in a variety of industrial sectors, the size of commercial production units has been ever increasing, thus making process efficiency of utmost importance for process economics and viability. The environmental constraints on the process have also played a major role in the production and utilization of methanol.[1]

Even though methanol is very widely used in chemical, petrochemical, pharmaceutical, and polymer industries as raw materials for synthesis reactions as well as solvents for other chemicals, market demand and interest have long been tied to global politics and contemporary issues. It is also true that whenever the petroleum price is uncontrollably high, interest in methanol becomes more intense. It may be recalled that the movement toward oxygenated fuel for cleaner air pushed methanol demand very high, for the manufacture of *methyl-tert-butyl ether (MTBE)*[12]; however, this boom did not last too long after the harmful health effects of MTBE were discovered and challenged. This chemical, MTBE, as a gasoline-blending oxygenate, was once the fastest-growing chemical commodity of the world market, in the 1990s.

Methanol is very toxic and fatal if taken internally by humans or animals. Methanol is far more toxic than ethanol, which is a homologue of the former. Even though the methanol molecule contains only one carbon and has a low molecular weight (of only 32) that is about the same as oxygen, its synthesis chemistry is quite complex and controversial. Methanol itself has a high octane value, 105, and burns cleanly. Similar to ethanol, methanol raises the octane rating of gasoline and reduces engine "knock" or "ping" without affecting the efficiency of the conventional catalytic converter. A 5% blend of methanol in unleaded gasoline may raise the octane rating at the pump by 1–1.5. However, its use as a gasoline-blending fuel to enhance the oxygenate content of gasoline has not been popular, owing to the relatively high volatility of the methanol-blended gasoline. Methanol has outstanding chemical properties as an excellent solvent as well as chemical reactant in a number of important chemical syntheses. In recent years, it has become a popular choice for the development of fuel cell technologies, in particular, direct methanol fuel cells (DMFCs).[4]

The *methanol economy* is a hypothetical future economy in which methanol fuel would have replaced fossil fuels as a means of transportation of energy. It offers an alternative to the hydrogen economy and the ethanol economy. Many arguments are offered for preferring the methanol economy against the hydrogen economy, in terms of the cost of energy generation, cleanness of conversion processes, continued dependence on fossil fuel sources, volumetric power density, infrastructural cost, safety associated with the fuel in various aspects of synthesis, distribution, storage, etc. *DMFCs* are being very actively developed to power portable electronics. They can be a very viable power source in many applications if their power density and energy conversion efficiency can be increased.[4] As such, methanol in DMFC can be a contributing player in consumer electronics and many other domestic applications.

Methanol synthesis is also a good subject for academic research and teaching. A number of process design problems have been developed for students as well as for textbook examples. Methanol synthesis involves a great deal of model and practical problems in a variety of topics including classical thermodynamics, condensed phase thermodynamics, reaction mechanisms, reactor design, reactor modeling, reactor configuration, catalyst design, catalyst life management, pore diffusion and external mass transfer, recycling of unreacted feed stream, separation, energy integration, process integration, process economics, environmental engineering, and cost accounting.

In this chapter, a comprehensive overview of methanol chemistry and synthesis technology is presented with a particular emphasis placed on its value as an alternative fuel and petrochemical feedstock.

9.2 CHEMISTRY OF METHANOL SYNTHESIS

The catalytic synthesis of methanol has been commercially available since 1923, when the first commercial plant for the synthesis of methanol from syngas was built by BASF.[1] The technology of manufacturing methanol has gone through constant improvements and major modifications, among which the biggest change was undoubtedly a transition from high-pressure synthesis to low-pressure synthesis. Both process technologies adopted heterogeneous catalytic conversion to methanol from synthesis gas typically originated from natural gas or, alternatively, from coal. The quality and composition of synthesis gas differ very widely, depending on the process of conversion as well as the type and quality of the feedstock. Therefore, a variety of commercial process designs reflected and encompassed these differences. Accordingly, it is imperative that the chemistry of synthesis gas conversion be fully elucidated in the synthesis of methanol and further conversion of methanol into other petrochemicals, including alternative hydrocarbon fuels.

9.2.1 Conversion of Syngas to Methanol

Synthesis gas is a mixture that contains hydrogen, carbon monoxide, and carbon dioxide as principal components, and methane and steam (moisture) as secondary components. Synthesis gas is also called *syngas*. Syngas is typically produced via steam reforming of natural gas, gasification or partial oxidation of coal, gasification of biomass, gasification of municipal solid wastes (MSWs), coke oven gas, etc. The synthesis of methanol from syngas is typically conducted over a heterogeneous catalyst system, most popularly coprecipitated $Cu/ZnO/Al_2O_3$, which is a reduced form of $CuO/ZnO/Al_2O_3$. In such a catalyst formulation, alumina (Al_2O_3) is a support that can be replaced by other similar supports such as ThO_2. The principal stoichiometric reactions involved in this chemical conversion are:

$$CO_2 + 3H_2 = CH_3OH + H_2O$$
$$CO + 2H_2 = CH_3OH$$
$$CO + H_2O = CO_2 + H_2$$

As can be seen from the preceding stoichiometric representation, only two of these three reaction equations are stoichiometrically independent. Stoichiometric independence can be very easily verified either by Gauss elimination type of mathematical procedure as well as by derivability of the third equation from a linear combination of the other two. In this specific case, a linear combination of any two stoichiometric equations would result in the third equation, thus leaving the system with only two independent stoichiometric reactions. If the stoichiometry and material balances are the only problems, there is very little difference with regard to which two are to be chosen as principal reactions. However, if the mechanistic view of the process synthesis is involved, then the choice of the two principal reactions needs to be in line with real-world situations. This is where a controversy exists regarding the synthesis of methanol over a $Cu/ZnO/Al_2O_3$ catalyst system.[1,5,7,9,19] There are two major mechanistic views regarding the principal reactions in methanol synthesis from syngas over a $Cu/ZnO/Al_2O_3$ system.

9.2.1.1 CO Hydrogenation as Principal Reaction for Synthesis of Methanol

In this mechanistic view, the principal reactions have been taken as:

$$CO + 2H_2 = CH_3OH$$
$$CO_2 + H_2 = CO + H_2O$$

According to this view, methanol is predominantly synthesized via direct hydrogenation of carbon monoxide. The second reaction is the reverse water gas shift reaction (RWGS), which proceeds in the reverse direction. Thus, the direction of the WGS reaction is determined from material balance considerations, not necessarily from chemical thermodynamic considerations. Experimental reaction data involving typical syngas mixtures that contain 3 to 9% CO_2 show a decrease in carbon dioxide concentration in the reactor effluent stream; thus, we intuitively infer that the WGS reaction proceeds in the direction of reducing carbon dioxide concentration, i.e., in the reverse direction. However, it must be noted that this explanation is consistent only when the principal reaction is believed to be hydrogenation of carbon monoxide.

It should also be noted that the first reaction of the methanol synthesis is exothermic, whereas the second reaction of reverse water gas shift is endothermic. According to this mechanism, via depletion of carbon dioxide in the reverse WGS reaction, more reactant carbon monoxide is produced to boost the synthesis of methanol. The role of carbon dioxide in the overall synthesis was crucially important for reasons other than participation in the WGS reaction, as evidenced consistently by various investigators in the laboratory as well as engineers in the field. Deficiency of carbon dioxide in the feed composition can be extremely detrimental to the overall synthesis, very rapidly deactivating the catalysts and immediately lowering methanol productivity by the process. Typically, 2 to 4% of carbon dioxide is present in the syngas mixture for the vapor-phase synthesis of methanol, whereas this value is somewhat higher, 4 to 8%, for the liquid-phase synthesis.[1,5]

9.2.1.2 CO_2 Hydrogenation as Principal Reaction for Methanol Synthesis

In this view, the principal chemical reactions that lead to the synthesis of methanol are:

$$CO_2 + 3H_2 = CH_3OH + H_2O$$
$$CO + H_2O = CO_2 + H_2$$

It should be noted that according to this view, the synthesis of methanol proceeds predominantly via direct hydrogenation of carbon dioxide, not carbon monoxide. It should also be noted that the WGS reaction proceeds in the forward direction, consuming carbon monoxide to produce the principal reactant of carbon dioxide and hydrogen, thus boosting the eventual methanol productivity. A number of different authors have tried a variety of reaction experiments to elucidate the true reaction pathways or mechanistic pathways, including isotope labeling studies and kinetic studies involving complete absence of one of the syngas components.[1,5–7,9]

9.2.1.3 Chemical Reactions under Extreme Syngas Conditions

As a case study, the following extreme conditions are examined using the aforementioned mechanistic postulates.[19]

9.2.1.3.1 CO-Free Syngas Feed

If the feed syngas is free of carbon monoxide, experimental observations show that the methanol productivity is very low and slowly decreases even further. This reaction phenomenon can be explained, using the CO_2 hydrogenation reaction mechanism as:

$$CO_2 + 3H_2 = CH_3OH + H_2O$$
$$CO_2 + H_2 = CO + H_2O$$

Owing to the total absence of CO, the WGS reaction proceeds in the reverse direction, i.e., in the direction that will generate more CO. Thus, the main reactant, CO_2, is wanted by both reactions. Considering that the RWGS reaction is a faster reaction than methanol synthesis reaction, the methanol production rate will have to suffer. Furthermore, both the RWGS reaction and the methanol synthesis reaction produce H_2O, whose concentration buildup in the system adversely affects the conversion of CO_2 toward methanol by pushing the chemical system closer to the equilibrium condition. Moreover, too high a water concentration in the catalyst pore is detrimental to the longevity of the catalyst.[13] Therefore, methanol productivity further decreases.

The same observation can also be explained by the CO hydrogenation mechanism as:

$$CO + 3H_2 = CH_3OH$$
$$CO_2 + H_2 = CO + H_2O$$

In this case, the WGS reaction proceeds also in the reverse direction, because of the total lack of carbon monoxide. According to the CO hydrogenation mechanism, carbon monoxide is the essential reactant for methanol formation; however, the only source for this reactant would be coming from the RWGS reaction, because there is no CO in the feed. Therefore, the reaction is very seriously limited by lack of the essential reactant. As shown, both the mechanisms can explain the situation more or less properly. Therefore, the experiments conducted under these conditions alone do not confirm which of the two mechanisms is the right one for the synthesis of methanol over the $Cu/ZnO/Al_2O_3$ catalyst.

9.2.1.3.2 CO_2-Free Syngas Feed Conditions

If methanol synthesis is practiced over the $Cu/ZnO/Al_2O_3$ catalyst system using the CO_2-free syngas, methanol productivity is also significantly lower than under normal syngas feed conditions, and it rapidly decreases even further.[19]

According to the CO_2 hydrogenation mechanism, the following stoichiometric equations can be written:

$$CO_2 + 3H_2 = CH_3OH + H_2O \quad (1)$$

$$CO + H_2O = CO_2 + H_2 \quad (3)$$

Owing to the total absence of CO_2 in the feed syngas, the WGS reaction proceeds in the forward direction, resulting in carbon dioxide, which is the essential reactant for the methanol synthesis reaction utilizing this mechanism. Because of the unavailability and limited supply of carbon dioxide, the principal reaction of methanol synthesis does not proceed properly, resulting in poor methanol productivity. Further, the lack of carbon dioxide makes the Boudouard reaction also proceed in its reverse direction as:

$$2\ CO(g) = CO_2(g) + C\ (s)$$

As can be expected, this reaction takes place on heterogeneous surfaces and involves carbon deposition. This reaction is responsible for catalyst deactivation via fouling by carbon deposition. This may be the reason for the rapid decrease of methanol productivity. However, the conditions promoting carbon deposition may be quite different between vapor-phase and liquid-phase synthesis. In this regard, carbon dioxide is a crucially important ingredient of the syngas mixture for the stability of catalytic activity. It is also found that the CO_2 deficiency in the feed syngas composition can be supplemented by H_2O input to a certain degree. Because H_2O is directly involved in generation of CO_2 in CO_2-starved conditions, this is also explainable. Complete absence of CO_2 in the feed syngas has been known to result in irreversible damage to the catalyst.

If CO hydrogenation is taken as the mechanism, the reaction of CO_2-free syngas would be represented by:

$$CO + 2H_2 = CH_3OH \quad (2)$$

$$CO + H_2O = CO_2 + H_2 \quad (3)$$

As can be seen, carbon monoxide is required by both reactions. The WGS reaction is faster under these conditions and proceeds in the forward direction as long as there is some H_2O in the system. Because carbon monoxide is abundantly available in the system, this alone would not explain the low methanol productivity. However, the explanation using the Boudouard reaction holds for this mechanism. When there is no CO_2 in the feed gas, carbon deposition via Boudouard reaction can be more active. Water promotes and participates in the WGS reaction, thereby producing H_2, which is a key reactant methanol synthesis, and CO_2, which inhibits the carbon deposition reaction.

9.2.1.3.3 H_2O-Free Syngas Feed Conditions

In this case, let us assume that the syngas mixture still contains typical amounts of H_2, CO, and CO_2. Then, if we adopt CO_2 hydrogenation as the principal reaction for methanol formation, the reaction system may be described as follows:

$$CO_2 + 3H_2 = CH_3OH + H_2O$$
$$CO_2 + H_2 = CO + H_2O$$

As written, the WGS reaction proceeds in the reverse direction, at least in the beginning, when H_2O is totally absent in the feed. Accordingly, CO_2 is the reactant for both the methanol synthesis reaction via CO_2 hydrogenation as well as the RWGS reaction. The two reactions occur in a competitive manner, thus resulting in a lower productivity of CH_3OH. Further, both reactions generate H_2O, whose concentration builds up in the reactor and eventually approaches the reaction equilibrium of the two reactions. Once the H_2O concentration reaches a certain level in the system, the WGS reaction is likely to go in the forward rather than the reverse direction. The system will quickly restore order.

The same phenomenon can also be explained by the CO hydrogenation mechanism.

$$CO + 2H_2 = CH_3OH$$
$$CO_2 + H_2 = CO + H_2O$$

In this case, it is rather obvious that the WGS reaction proceeds in the reverse direction, at least in the beginning, until it reaches WGS equilibrium and, eventually, the two-reaction equilibrium. Other than that, hydrogen is a reactant for both reactions, at least in the initial stage, and it is not very clear how the final methanol productivity will be impacted. The reaction is likely to proceed without much difficulty.

Water in the reformer effluent gas needs to be removed for initiation of and high conversion in the methanol synthesis reaction. As implied by the reaction chemistry, water in the reactant mixture is detrimental to conversion, regardless of whichever mechanism we may choose to explain the chemistry. However, if the CO_2 level in the syngas is excessively low, water does exhibit some compensating and complementing functions.[1,13]

Therefore, there are several factors of significance among most of the low-pressure methanol synthesis technologies. They are[1,7]:

1. The presence of carbon dioxide in the feed syngas mixture is essential. Different designs and processes may set this CO_2 concentration differently. However, there is a minimum threshold value of this concentration for the process to be functional. If CO_2 is absent or deficient in the system, the catalyst deactivation is greatly promoted.
2. The presence of carbon monoxide in the syngas feed composition is also very important. Lack of CO in the syngas feed not only results in low methanol productivity, but also in a continuous decrease in productivity.
3. There is an optimal value for the temperature of methanol synthesis reaction from the standpoint of optimal conversion of syngas as well as the kinetic reaction rate. The rate of reaction is increased with an increase in the temperature by following the Arrhenius-type of temperature dependency, whereas the equilibrium conversion is thermodynamically unfavored with an increase in the reaction temperature. Furthermore, there is also a limit for the maximum temperature at which the process can be operated. This ceiling is mostly governed by the temperature tolerance of catalyst ingredients, in particular, the copper component of the catalyst. This temperature is about 280–300°C. Beyond this temperature, the catalyst would be subjected to sintering and fusing, which would result in permanent damage to the catalyst.

Even though the sensitivity of overall methanol productivity to CO_2 concentration variation is not as pronounced as that of a typical principal reactant of general chemical reaction systems, it has to be noted that the true picture regarding the role of carbon dioxide is inevitably masked by the presence of very active WGS reaction. Conversely, a total lack of CO_2 in the feed syngas would cause irreversible damage to the catalyst. There are different views regarding the mechanism of catalyst deactivation in cases when carbon dioxide is lacking in the syngas feed.[5]

9.2.2 Active Form of Methanol Synthesis Catalyst

The commercial methanol synthesis catalyst is prepared by a coprecipitation technique in which both CuO and ZnO are precipitated onto porous structure of support, typically alumina, Al_2O_3. The formula of this catalyst is most frequently expressed as $CuO/ZnO/Al_2O_3$. This is in an oxidized form that is stable upon exposure to air or other oxidizing environments, and a reason why all catalysts of this type are shipped in oxidized form for safety and storage. Therefore, this catalyst must be reduced before use in a hydrogenation reaction such as methanol synthesis.[8] If not, hydrogen as a reactant in the hydrogenation reactor would be first consumed in reduction of this oxidized form of catalyst. During this process, which is highly exothermic, sintering of catalyst would occur and induce irreversible damage. Most catalyst manufacturers provide their customers with the detailed reduction procedure.

However, reduction of this catalyst also provides a couple of possibilities that are the source of another controversy regarding which is the active phase of the catalyst, Cu^0 or Cu^{+1}, i.e., $Cu/ZnO/Al_2O_3$ vs. $Cu_2O/ZnO/Al_2O_3$.

Reduction of the methanol synthesis catalyst is described in Lee's work.[1,8] The basic procedure follows a stepwise reduction strategy, thereby preventing the exothermic heat of reaction for reduction treatment from sintering or thermally annealing the catalyst. The procedure is basically the same for the vapor-phase or the liquid-phase process. Many pieces of evidence and counterevidence have been presented in the literature regarding the active form of copper in the reduced catalyst. Among them, the most striking evidence may be the one obtained by Lee and his coworkers.[10] They used a liquid-phase reduction treatment on their $CuO/ZnO/Al_2O_3$ catalyst in a mechanically agitated slurry reactor, and the active catalyst was analyzed by x-ray diffraction (XRD) technique. Because the analyzed catalyst was coated by the protective film of high-boiling white mineral oil (Witco-70 or Freezene-100 oil), the catalyst analyzed was not allowed to go through any atmospheric reoxidation to either CuO or Cu_2O before the intended analysis. They found ample presence of Cu^0 and, at the same time, total absence of Cu^{+1}.

Deactivation of methanol synthesis catalysts may be attributed to the following four principal causes, namely: (1) poisoning by sulfur or carbonyls; (2) sintering, thermal deactivation, or annealing; (3) copper crystallite size growth;[11] and (4) catalyst fouling by carbon deposition. Advances have been made, and all or most of these causes are avoidable in well-designed processes. A regeneration process was developed for the deactivated catalyst whose crystallite size has grown. The regeneration process is based on repeated oxidation and reduction steps that constitute renucleation and redispersion of catalyst crystallites via successive phase changes. Lee and his coworkers reported that their process is able to recover most of the lost activity due to crystallite size growth via the repeated oxidation–reduction cycles.[11]

9.2.3 Chemical Equilibrium

Methanol synthesis reactions, both CO and CO_2 hydrogenation, are thermodynamically not favored at low pressure and high temperature, as shown by a plot of K_p vs. T in Figure 9.1. Reducing the temperature of reaction is kinetically undesirable, because it significantly reduces the reaction rate. Therefore, the synthesis reaction must be carried out at a relatively high temperature, which further pushes the pressure requirement even higher. Higher-pressure operation, on the other hand, may represent higher capital investment, greater energy demands, and more severe operational conditions. Furthermore, a higher temperature increases the potential likelihood for thermal deactivation of the catalyst, and the risk is further complicated by the exothermic heat of the reaction. Owing to the unfavorable equilibrium nature, the once-through conversion (or single-pass conversion) of the synthesis reaction is typically low, thus making recycle duty higher. All the commercial processes recycle the unconverted syngas back to the methanol converter for enhancement of overall conversion, thus improving the process economics. The typical operating conditions for the methanol synthesis reaction are 220 to 270°C and 50 to 100 bars. It is quite interesting to note that the low-pressure process conditions are in the vicinity of the critical points of pure methanol, i.e., about 240°C and 80 atm.

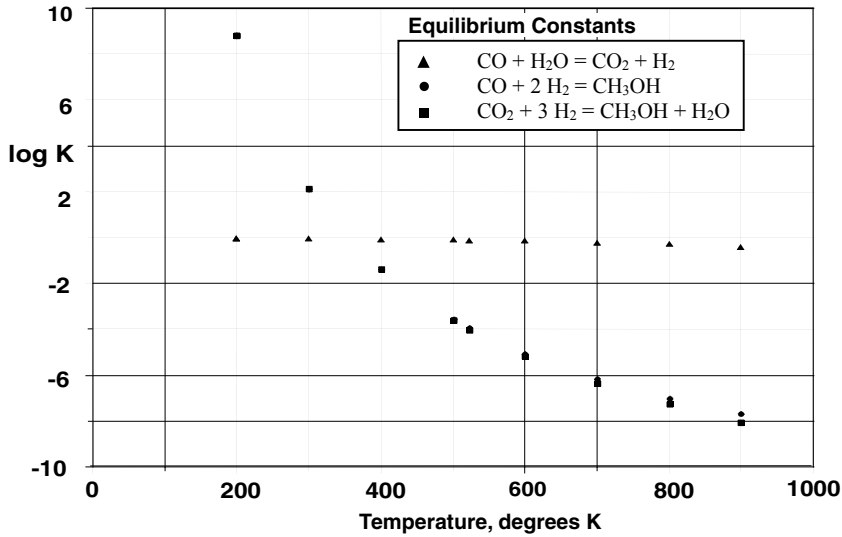

FIGURE 9.1 Temperature dependence of equilibrium constants for principal reactions.

The WGS reaction is particularly worthy of note in all processes dealing with any syngas mixture in reactive environments. It has been understood that the reaction takes place predominantly on the heterogeneous surfaces of the catalyst, whenever a catalytic system is employed. It should be also noted that the WGS reaction has a relatively flat functional relation between the equilibrium constant and the temperature, i.e., the temperature dependency of equilibrium constant for the WGS reaction is weak compared to other syngas reactions, as shown in Figure 9.1. This means that the WGS reaction has a very wide temperature range of significance, namely, from room temperature to as high as 1000°C, thus affecting nearly all syngas-related processes. Another significance of its relatively low equilibrium constant over a wide range of temperatures is that the reaction equilibrium can be easily reversed in direction by changing the compositions (or partial pressures) of the involved species. More than often, this fact obscures the true picture of the intrinsic mechanism of process chemistry.

Furthermore, typical WGS reaction catalysts also have very similar compositions to those of the methanol synthesis reaction. This also means that the catalysts used for methanol synthesis will also catalyze the WGS reaction. Owing to its reversibility over a wide range of process conditions as well as its high impact on the final product compositions, the WGS reaction equilibrium is an important issue in designing both steam reformer as well as methanol synthesis reactors.

9.2.4 Properties of Methanol

Methanol is also known as methyl alcohol, carbinol, methyl hydroxide, methylol, monohydroxymethane, wood alcohol, colonial spirit, Columbian spirit, hydroxymethane, or

wood naphtha. The CAS number for methanol is 67-56-1. The RCRA (Resource Conservation and Recovery Act) waste number of methanol is U154 and UN 1230.

The density of methanol at room temperature, of 25°C, is 0.7918 g/cm^3. The heat of formation for methanol as gas ($\Delta H°_{f,\ gas}$) is –201.1 ± 0.2 kJ/mol, whereas that for liquid methanol ($\Delta H°_{f,\ liquid}$) is –239.5 ± 0.2 kJ/mol. The constant-pressure heat capacity of methanol as gas ($C_{p,\ gas}$) at room temperature is 44 J/K-mol, whereas that for liquid methanol is 80 ± 1 J/K-mol. The Henry's law constant ($K°_H$) for solubility of methanol in water at 298.15 K is 210 ± 10 mol/kg-bar.

The critical temperature and pressure of methanol are 513 ± 1.2 K and 81 ± 1.0 bars, respectively, whereas the normal boiling and melting temperatures are 337.8 ± 0.3 K and 176.0 ± 1.0 K, respectively. The triple point of methanol is 175.5 ± 0.5 K. The flash point of methanol is 11°C. The enthalpy of vaporization[2] of methanol at room temperature ($\Delta H°_{vap}$) is 37.83 kJ/mol. Methanol can be used as a supercritical solvent or cosolvent for a variety of modern processes. The hydroxyl group in its molecular structure makes possible unique properties that are normally not attainable from carbon dioxide. Its critical point is harsher than CO_2's, but milder than H_2O's.

Methanol's acidity is pKa = ~15.5, and viscosity is 0.59 mPa·sec at 20°C. Owing to its low freezing point, methanol has been popularly used as a cold-weather windshield washer fluid. A concentration of 30% by weight can provide antifreezing protection of –20°C. Because of the hydroxyl group in methanol, it has a strong tendency to hydrogen-bond. A hydrogen bond is not a true bond, but a particularly strong form of dipole–dipole interaction. The O-H bonds are strongly polarized, leaving the hydrogen atom with a partially positive charge, which is electrophilic hydrogen. This hydrogen has a strong affinity for nonbonding electrons and, as such, it forms intermolecular attachments with the nonbonding electrons on the oxygen atom. Comparing the two isomers between ethanol (C_2H_5OH) and dimethylether (CH_3OCH_3), both of which have a formulation of C_2H_6O, a striking fact emerges: ethanol has a much higher boiling point (78°C) than dimethylether (–25°C). This significant difference of about 100°C in their boiling points is because ethanol has O-H hydrogen, which is extensively hydrogen-bonded, whereas dimethylether has no O-H hydrogen.

Methanol also reacts easily with carboxylic acids to produce esters, from which water is a by-product of the condensation-type reaction. Methanol is an important reactant in the manufacture of biodiesel via transesterification reaction. The presence of the methyl group in the formula provides chemical affinity toward hydrocarbons and, as such, methanol shows excellent solubility toward a variety of organic materials, and the hydroxyl group promotes excellent water miscibility. The dual nature of solubility makes methanol a good candidate for oxygenate fuel as well as a water remover from gasoline. As a water remover in gasoline fuel systems, methanol creates a miscible ternary mixture [gasoline-methanol-water] instead of an immiscible binary mixture [gasoline-water].

Methanol has an octane rating of 105 (Research Octane Number, RON) and can be used as an octane enhancer. Because high performance with a higher compression ratio requires a higher octane rating than its regular counterparts, methanol is used as a racing fuel. Because of the high oxygen content (50% by mass) in the methanol molecular

structure, it appears to be an excellent oxygenate fuel. However, it should be noted that its blending vapor pressure increase is substantially higher than other competing oxygenate blends such as MTBE (methyl-*t*-butylether) and ethanol, thus making it unpopular as a gasoline-blending fuel. The vapor pressure increase due to gasoline blending is typically measured by *Reid vapor pressure***.** High vapor pressure of blended gasoline can increase the chances for evaporative emission of the fuel as well as the risk of having "vapor lock" in the fuel line. Furthermore, methanol, if inhaled or consumed, is far more toxic than ethanol. Evaporative fuel emission is particularly of concern to environmental air quality during summer months, when the emitted hydrocarbon is directly linked with the environmental health problem of "high ozone level in the air."

The common method of measuring vapor pressure of petroleum products is the Reid vapor pressure test, or Rvp test. There are basically two methods approved by ASTM, i.e., Reid method (ASTM D323-99a) and Dry method (ASTM D4953-99a). The Reid method covers experimental measurements of vapor pressure of gasoline, volatile crude oil, and other volatile petroleum products, which include petroleum crude, gasoline, MTBE-blended gasoline, aviation fuel, and other petroleum products. There are four procedures provided by this method, depending on the types and vapor pressure ranges of the tested fuel. However, this method is not applicable to liquefied petroleum gas (LPG) and oxygenated gasoline except MTBE-blended gasoline. Determination of the vapor pressure of LPG is covered in ASTM D1267, whereas determination of the vapor pressure of gasoline-oxygenate blends is treated in ASTM D4953. The latter method is referred to as *Dry method*, which is applicable to most oxygenated gasoline, except MTBE-blended gasoline, with a vapor pressure range from 35 to 100 kPa (5 to 15 psi). There are thermodynamic algorithms developed for estimation of Rvp without performing actual measurement. An algorithm developed by Vazquez-Esparragoza et al.[3] used Gas Processors Association Soave-Redlich-Kwong equation of state and assumed that liquid and gas volumes are additive. They found excellent agreement between model prediction and experimental data.

9.2.5 Reaction with Methanol

Methanol is used to produce formaldehyde via oxidation reaction:

$$CH_3OH + \tfrac{1}{2}\, O_2 = HCHO + H_2O$$

About 40% of methanol is converted to formaldehyde (HCHO), and from there into products as diverse as thermosetting polymers, plywood, paints, explosives, and permanent press textiles.

Methanol is also used for making a variety of ethers including MTBE (methyl-*t*-butylether), ETBE (ethyl-*t*-butylether), TAME (*t*-amyl-methylether), DME (dimethylether), etc. The first three are normally synthesized by catalytic distillation (CD), whereas the fourth is produced by catalytic dehydration. As the name implies, catalytic distillation is a hybrid process between a well-established unit operation of distillation and a catalytic chemical reaction. Methanol also readily reacts with carboxylic acids to produce methyl esters of these acids. These esters, in particular

fatty acid esters, are quite important as ingredients for biodiesel, fuel additives, fuel system cleaners, octane enhancers, biodiesel formulations, etc.

Dimethylether (DME) is gaining importance as an alternative fuel. Dimethylether has always been considered a major derivative of methanol and its synthesis is based on the following stoichiometric equation:

$$2\ CH_3OH = CH_3OCH_3 + H_2O$$

Methanol serves as a direct reactant or as an intermediate in the synthesis of dimethylether, depending on the reaction routes.[18] The first process route is based on conventional dehydration of methanol over a dehydration catalyst, where methanol is a direct reactant, and dimethylether and water are recovered as products. This process is carried out as a stand-alone type of process. In recent years, however, the second process option, in which methanol is an intermediate in the conversion of syngas to dimethylether, i.e., single-stage synthesis of dimethylether from synthesis gas, has attracted a great deal of attention.

$$CO_2 + 3H_2 = CH_3OH + H_2O$$
$$CO + H_2 = CO_2 + H_2$$
$$2\ CH_3OH = CH_3OCH_3 + H_2O$$

The process benefits have been twofold: one, the direct synthesis of dimethylether from syngas can overcome the equilibrium limitation imposed by methanol synthesis reaction, and two, the reaction converting methanol into dimethylether is an important precursor step for methanol-to-hydrocarbon conversion processes[16,17] represented by *MTO* (Methanol-to-Olefin), *MTG* (Methanol-to-Gasoline), etc. Even if dimethylether itself is considered a final product, the direct route via single-stage synthesis is far more advantageous from the standpoints of both production cost and process efficiency. The single-stage DME synthesis exploits the equilibrium-unlimited dehydration of methanol to DME to its fullest extent by alleviating the equilibrium-limited nature of the methanol synthesis reaction.[15,18,19] This is accomplished via a dual catalytic system in which methanol produced *in situ* is selectively removed from the reaction equilibrium by converting the product methanol to dimethylether. In this process, methanol concentration in the reactor is kept low, thus keeping the methanol synthesis portion of the overall conversion process far from its chemical equilibrium. Catalyst 1, such as $Cu/ZnO/Al_2O_3$, catalyzes the first reaction of methanol synthesis, whereas Catalyst 2, e.g., γ-Al_2O_3, catalyzes dehydration of methanol. Both reactions are carried out in the very same reactor and, therefore, such a reaction system is called a *dual catalytic system*.[18] Obviously, as an advantage, a higher once-through conversion of syngas to dimethylether can be attained. This enhancement can also be successfully exploited for realignment of the syngas-to-hydrocarbon synthesis process.[20]

Consider MTG's alignment, which is basically composed of syngas conversion reactor and gasoline synthesis reactor as:

{Syngas-to-Methanol} + {Methanol-to-DME-to-Gasoline}
Syngas Conversion Gasoline Synthesis

where methanol-to-DME conversion takes place in the second reactor, i.e., the gasoline reactor. This methanol-to-DME reaction generates water, which is detrimental to gasoline synthesis. However, the reaction step of methanol-to-DME conversion can be very beneficially moved from the gasoline reactor to the syngas reactor; thereby, the methanol conversion step can be synergistically exploited to alleviating the equilibrium limitation of methanol synthesis. The resultant reaction alignment for syngas to gasoline[20] becomes as follows:

{Syngas-to-Methanol-to-DME} + {DME-to-Gasoline}
Syngas Conversion Gasoline Synthesis

This process concept was introduced by Lee et al.[15,20] Other benefits include catalyst life management, especially for zeolites catalysts such as ZSM-5. Even though the MTG plant in New Zealand terminated its successful commercial production in the late 1990s, the idea of production of clean liquid motor fuel via the synthesis route is remarkable. It not only diversifies the feedstock for gasoline, but also provides additional options for energy policy and planning.

DMFCs are unique in their low-temperature, atmospheric-pressure operation, allowing them to be miniaturized to an unprecedented degree. DMFC, combined with the relatively easy and safe storage and handling of methanol, may open the possibility of fuel-cell-powered consumer electronics.

9.3 METHANOL SYNTHESIS TECHNOLOGY

Pure methanol was first isolated as a chemical form in 1661 by Robert Boyle, who called it *spirit of box*, because he produced it via the distillation of boxwood.

However, the systematic synthesis of methanol has a history of about 100 years dating back to the early 1900s, when methanol was almost exclusively produced by the destructive distillation of wood wastes. This is why methanol was called *wood alcohol*. On the other hand, ethanol and isopropyl alcohol are called *grain alcohol* and *rubbing alcohol*, respectively. In 1923, BASF developed a catalytic synthesis process based on ZnO/Cr_2O_3 catalyst. Ever since, this commercial synthesis technology termed *high-pressure methanol synthesis technology* has been very popularly adopted by a number of industries for about 50 years. This process was quite successfully operated at a pressure of 250 to 350 atm and a temperature of 350 to 450°C. Because the operating pressure required by this catalytic process was substantially higher than that for the later version of the synthesis process using a different catalytic system, the process was called *high-pressure methanol synthesis.*

In 1963, ICI developed a new methanol synthesis technology termed *low-pressure methanol synthesis technology*, which has become an industrial successor to high-pressure synthesis.[1] This process is operated at a pressure of 50 to 100 atm and a temperature of 225 to 275°C over a catalyst of $Cu/ZnO/Al_2O_3$. The catalyst system used for this process is often referred to as *Cu-based catalyst.*

A number of different versions of low-pressure methanol synthesis technology have also been developed and are being successfully operated; however, most of these are based on very similar process concepts in terms of catalysts, synthesis chemistry, incorporation of steam reforming, etc. It should be noted that conventional low-pressure synthesis of methanol is carried out under conditions close to the critical temperature and pressure of methanol.

The reactants for methanol synthesis are carbon dioxide, carbon monoxide, and hydrogen. These species constitute the main ingredients of synthesis gas. Synthesis gas may be obtained from diverse sources including natural gas, coal, municipal wastes, coke oven gas, biomass, other hydrogen sources, etc. Industries have been predominantly using the steam reforming of methane to generate hydrogen and carbon monoxide in a proportion of $H_2/CO = 2–3$, as shown in the following stoichiometry:

$$CH_4 + H_2O = 3H_2 + CO$$

It should be noted here that hydrogen produced by steam reforming comes from both water and hydrocarbon. To synthesize methanol over a Cu-based catalytic system, carbon dioxide (CO_2) may have to be added to the syngas originating from the steam reforming of methane. The presence of carbon dioxide in the syngas composition is crucial, because it directly affects the catalytic activity and life. In the steam reformer, WGS reaction also takes place:

$$CO + H_2O = CO_2 + H_2$$

As mentioned earlier, the WGS reaction is typically limited by chemical equilibrium over a wide range of temperatures, thus affecting the reformer product compositions significantly. The optimal percentage of CO_2 in the syngas for methanol synthesis varies from process to process. However, it is generally in the range of 2 to 8%, with some exceptions that use substantially higher CO_2 contents in the feed syngas.

In methanol synthesis, scientists and engineers often use a term called *balanced gas* in referring to a 2:1 mixture of H_2 and CO. This 2:1 mixture is not an endorsement of a CO hydrogenation mechanistic path, rather a stoichiometric assessment of species balance that methanol as product has a molecular formula of direct addition of 1 molecule of CO and 2 molecules of H_2. This is also consistent with the experimental facts that the number of moles of hydrogen consumed vs. the number of moles of carbon monoxide consumed is slightly more than 2.[1,5] Although natural gas is an excellent source for such syngas, owing to its high hydrogen content, other carbonaceous and hydrocarbon-rich resources can also be viable sources, depending on the availability and local economy.

Some of the newer processes for methanol synthesis adopt CO-rich syngas rather than H_2-rich syngas. The CO-rich syngas is typically generated from a resource that is low in the H-to-C ratio, such as coal. Depending on the geological region, this option may prove to be an economically better option. This type of syngas is often termed as *unbalanced gas*, which means the H_2-to-CO ratio is much lower than 2:1. Second-generation coal gasifiers such as *Texaco* and *Shell* gasification processes, as

well as Koppers-Totzek gasifiers, yield syngas with low H_2-to-CO ratios, typically, 0.75–1.0. The *liquid-phase methanol synthesis process*, also known as the LPMeOH™ process, originally developed by Chem Systems Inc. in 1975, is a good example of the processes that are targeting CO-rich syngas as the feed stream. Owing to its low H_2 content in the feed gas, its H_2 conversion per pass has to be relatively high, thus making such a process more suitable for a once-through synthesis technology such as *once-through methanol (OTM)* process. As the name implies, this process is based on the synthesis of methanol without any recycling of unreacted syngas.

The pressure and temperature of the synthesis reaction are obviously two of the most important operating parameters from chemical kinetics and equilibrium conversion considerations. If the temperature is raised for the synthesis reaction, the kinetic rate of reaction increases while the conversion of carbon monoxide decreases. If the pressure of the reaction is increased, the conversion of CO also increases; but the increase is not very substantial above the pressure of 80 atm. The situation is also further complicated by the presence of WGS reaction, which is also limited by chemical equilibrium at a typical methanol synthesis reaction condition. This WGS equilibrium can be very easily reversed in terms of its direction by the concentration of water in the reactor feed stream. Even 5 mol% of water in the feed syngas stream of $H_2/CO = 3:1$ is more than sufficient to affect the direction of WGS reaction at 250ºC and 75 atm. Under this specific circumstance, the WGS reaction proceeds in the forward direction. In the case of H_2O-free feed, otherwise under nominally the same condition, the WGS reaction proceeds in the reverse direction.

A typical methanol process technology in the modern era involves several common process steps, namely: (1) feed purification, (2) steam reforming, (3) syngas compression, (4) catalytic synthesis, (5) crude methanol distillation, and (6) recycle and recovery. If the syngas is prepared from coal, as in the case of the liquid-phase methanol synthesis process, coal gasification becomes an important step for the overall process design and economics. Although the Lurgi gasifier yields hydrogen-rich syngas, Texaco, Shell, and Koppers-Totzek gasifiers yield carbon-monoxide-rich syngas.

As for the steam reforming, there are typically two types of processes, i.e., two-stage reforming and autothermal reforming (ATR). Although the two processes are very similar to each other, the ATR has a thermal balance over the reactor by adopting a hybrid combination of sacrificial partial oxidation with the subsequent steam reformation reaction. The former reaction of partial combustion generates exothermic heat, which can be utilized by the endothermic reforming reaction; as such, an energy balance is achieved for the reactor.

The process design varies largely based on the availability of feedstocks of different types, process energy efficiency and local energy economics, and financial restrictions related to capital investment. In the ensuing subsections, a number of methanol synthesis process technologies are explained and compared.

9.3.1 The Conventional ICI's 100-atm Methanol Synthesis Process

Even though it had long been desired in the mid-1900s to reduce the operating pressure of the methanol synthesis process, it was found that a process with a much

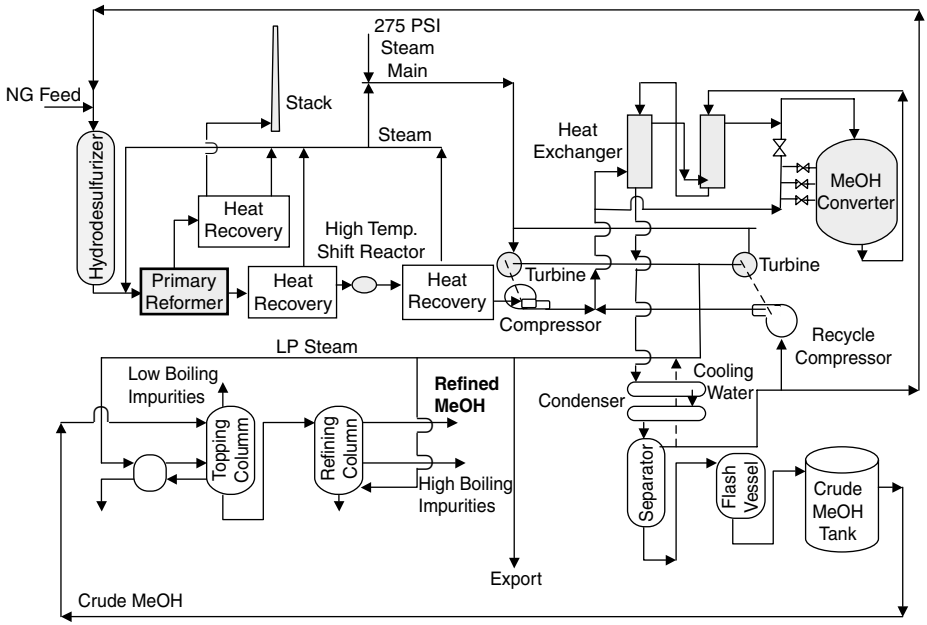

FIGURE 9.2 A schematic of ICI's low-pressure methanol synthesis process.

lower pressure would not be ideal for large-capacity units. A simple reason for this finding may be that under low-pressure conditions, the equipment has to be very large, and the chemical reaction is not as fast as desired. With the advancement and development of better materials and equipment design, a newly focused objective was the search for a catalytic synthesis system that would be more active at about 100 atm. The result of this effort was highlighted by the ICI's announcement of a $Cu/ZnO/Al_2O_3$ catalyst system. This novel process was tried in August 1972 with great success. This milestone process has been enhanced and modified with subsequent designs, especially in the areas of energy efficiency of the process as well as process optimization. A schematic of this process is given in Figure 9.2.

The original flowsheet includes two parts of the process, namely, reforming and synthesis sections. Even though unelaborated in Figure 9.2, process economics depends very heavily on the heat recovery and energy integration, recycle schemes, and refining and separation. Along with the efficient design, management of catalyst life has always been the principal issue of process maintenance and enhancement. Needless to say, catalyst life and efficiency are directly tied to the productivity of the plant.

9.3.2 Haldor Topsoe A/S Low-Pressure Methanol Synthesis Process

This process is designed to produce methanol from natural or associated gas feedstocks, utilizing a two-step reforming process to generate feed syngas mixture for the methanol synthesis.[21] Associated gas is natural gas produced with crude oil from the same reservoir. It is claimed that the total investment for this process is lower

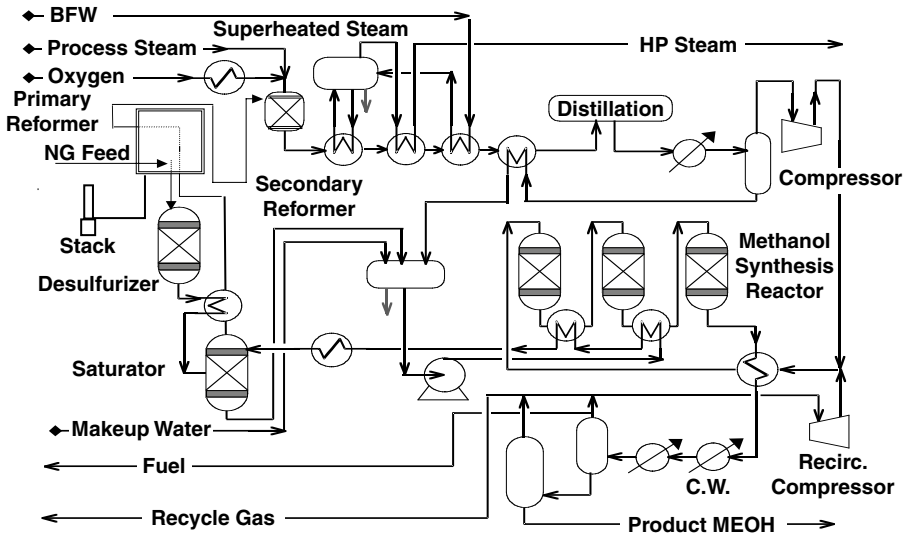

FIGURE 9.3 A schematic of Haldor Topsoe A/S methanol synthesis process.

than with the conventional flow scheme based on straight steam reforming of natural gas by approximately 10%, even after considering an oxygen plant.

As shown in Figure 9.3, the *two-stage reforming* is conducted by primary reforming, in which a preheated mixture of natural gas and steam is reacted, followed by secondary reforming, which further converts the exit gas from the primary reformer with the aid of oxygen that is fed separately. The amount of oxygen required as well as the balance of conversion between the primary and secondary reformers need to be properly adjusted so that a balanced syngas, i.e., in a stoichiometric ratio (2:1) of H_2/CO is obtained with a low inert content.

As an energy integration step, the heat content of flue gas is recovered for preheating reformer feed. Similarly, the heat content of the process gas is utilized for producing superheated high-pressure steam, preheating boiler feed water (BFW), and preheating process condensate before its entry into the saturator and reboiler of the distillation section. The synthesis section is composed of three adiabatic reactors with heat exchangers between the reactors; thus, exothermic heat of reaction is recovered and used for heating saturator water. Another energy integration is accomplished by cooling the effluent from the last reactor by preheating the feed to the first reactor. The total energy consumption for the process is claimed to be about 7.0 Gcal/ton of product methanol, including oxygen production. The process technology is suited for smaller as well as very large methanol plants up to 10,000 tpd. However, it has to be noted here that it is often very difficult to compare flowsheets for methanol synthesis among various commercial processes, because it is difficult to establish the common unbiased bases to compare reported design and operating data.

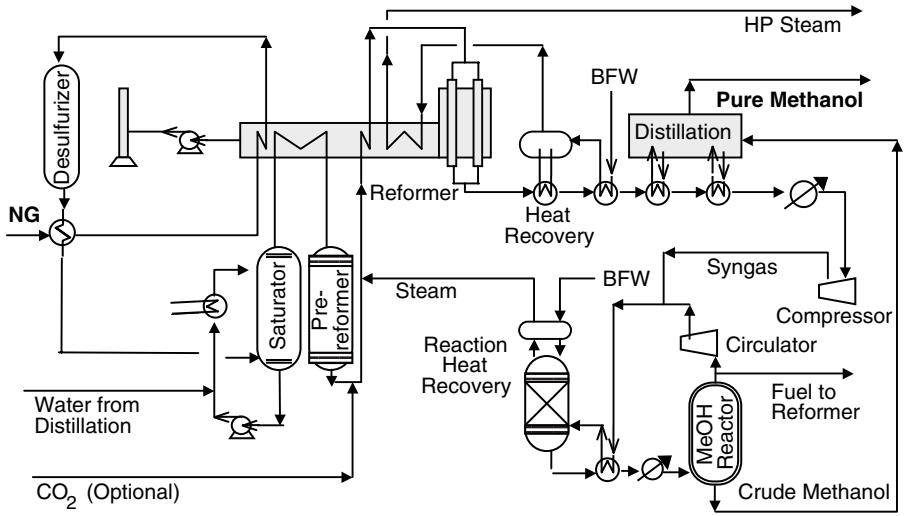

FIGURE 9.4 A schematic of the Kvaerner methanol synthesis process.

9.3.3 Kvaerner Methanol Synthesis Process

This process developed by Kvaerner Process Technology/Synetix, U.K., is based on a low-pressure methanol synthesis process and two-stage steam reforming, similar to the Haldor-Topsoe process. Figure 9.4 shows a schematic of the Kvaerner methanol synthesis process. The feed gas stock may be natural or associated gas. In this process, however, carbon dioxide can be used as a supplementary feedstock to adjust the stoichiometric ratio of the syngas. Recent plants based on this process have an energy efficiency of 7.2–7.8 Gcal/ton of product methanol,[31] which is lower than the Topsoe's published energy efficiency. However, this process is more suited for regions with high availability of low-cost gas such as CO_2-rich natural gas and financial restrictions of low capital investment. There are a number of commercial plants currently in operation based on this design and their typical sizes range from 2000 to 3000 mtpd.

9.3.4 Krupp Uhde's Methanol Synthesis Technology

The process, developed by Krupp Uhde GmbH, is based on the low-pressure synthesis chemistry of methanol as well as steam reforming for synthesis gas generation. A unique feature of this process is its flexibility of feedstock choice, which includes natural gas, liquefied petroleum gas, or heavy naphtha.[21]

The steam reformer is uniquely designed by Krupp Uhde and is a top-fired box-type furnace with a cold outlet header system. The steam reforming reaction takes place heterogeneously over a nickel catalyst system. The reformer effluent gas containing H_2, CO, CO_2, and CH_4 is cooled from 880°C to ambient temperature eventually, and most of the heat content is recovered by steam generation, BFW preheating, preheating of demineralized water, and heating of crude methanol for three-column distillation.

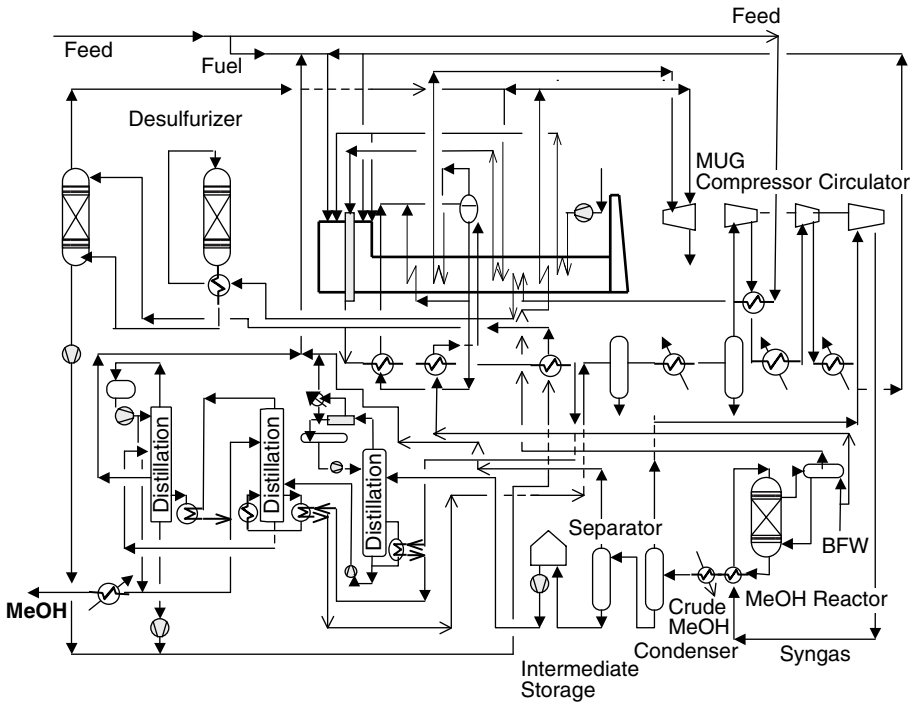

FIGURE 9.5 A schematic of Krupp Uhde's methanol synthesis process.

The typical energy consumption, including feed and fuel, ranges from 7 to 8 Gcal per metric ton of methanol, and is very much dependent on individual plant concepts and designs. Eleven plants have been built until 2005, using this technology. Figure 9.5 shows a schematic of Krupp Uhde's methanol synthesis process.

9.3.5 Lurgi Öl-Gas-Chemie GmbH Process

This process is meant to produce methanol in a single-train plant starting from natural gas or oil-associated gas with capacities up to 10,000 mtpd.[21] It can be used to increase the existing methanol plant based on steam reforming. Figure 9.6 shows a schematic of this process. Steam reforming of natural gas is accomplished in two stages, i.e., prereforming and ATR. In the prereformer, the mixture gas of desulfurized natural gas and steam is converted to H_2, CO_2, and CH_4, whereas in the autothermal reformer the gas is reformed with oxygen and steam, producing product gas containing H_2, CO, CO_2, and a small amount of unconverted CH_4 in addition to low-pressure steam. Oxygen is involved in this reaction scheme to generate exothermic heat by partial oxidation of sacrificial natural gas to provide the necessary endothermic heat for the subsequent reforming reaction.

The reformed gas, i.e., syngas, is mixed with hydrogen from the pressure swing adsorption (PSA) to increase the H_2-to-CO ratio. The produced synthesis gas is pressurized and mixed with recycled gas from the synthesis loop. The reaction takes

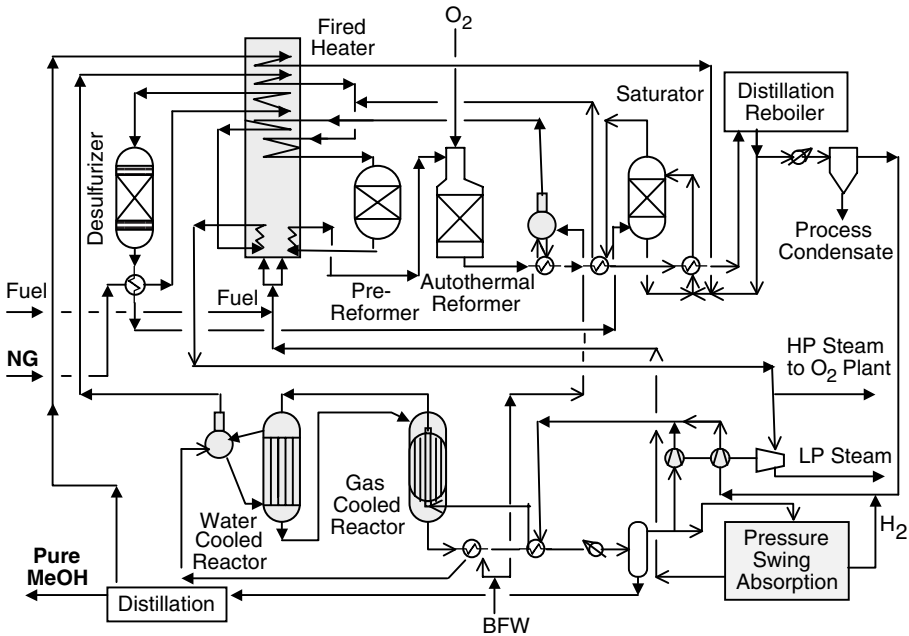

FIGURE 9.6 A schematic of the Lurgi Öl-Gas-Chemie GmbH process.

place under near-isothermal conditions in the Lurgi water-cooled methanol reactor, which houses a fixed bed of catalyst in vertical tubes surrounded by boiling water. The reactor effluent gas is cooled to 40°C to separate methanol and water from the unreacted syngas. Methanol and water are separated in distillation units, whereas the major portion of the gas is recycled back to the methanol synthesis reactor for higher overall conversion. As mentioned in the earlier subsection, the once-through conversion is typically low; therefore, recycling of the gas is imperative. Enhancements have been made, especially in the efficiency of the Lurgi combined converter (LCC), to reduce the recycle ratio down to about 2. The process water is preheated in a fired heater and used as a makeup water for the saturator, thus minimizing unnecessary water usage and treatment.

The reformed gas from the second-stage reformer contains a considerable amount of thermal energy that is recovered as high-pressure steam for energy required for preheater and reboiler. The energy consumption for the process including utilities and oxygen plant is about 7.1–7.2 Gcal/t of product methanol.

9.3.6 Synetix LPM Process

This is an improved version of the ICI's original low-pressure methanol (LPM) process.[21] This process is designed to produce a refined, high-purity methanol from natural gas, but it can also handle a variety of other hydrocarbon feedstocks, including naphtha, coal, and other petrochemical offgas streams. This process is ideal for large capacities where conventional processes may not be suitable. Figure 9.7 shows a schematic of the Synetix LPM process.

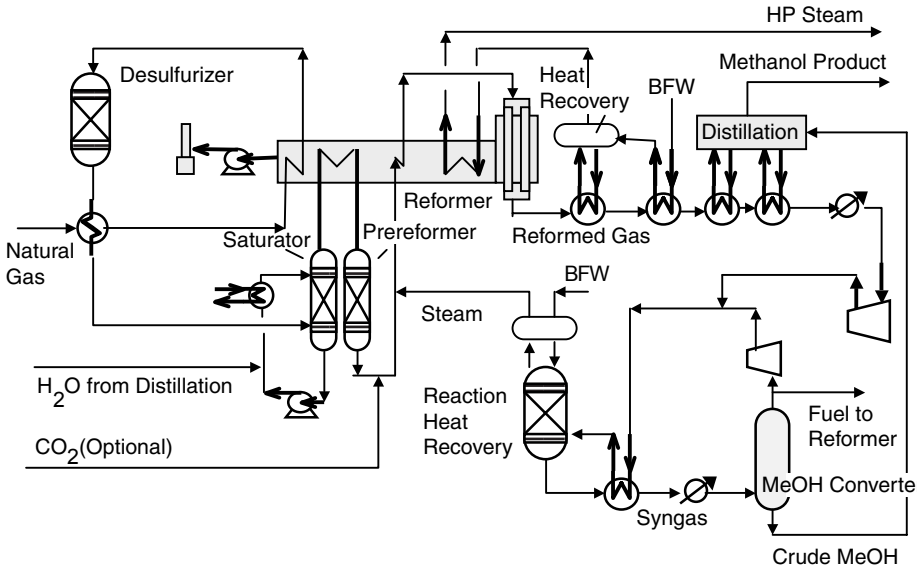

FIGURE 9.7 A schematic of Synetix LPM process.

The process consists of three principal sections, namely: (1) syngas preparation, (2) methanol synthesis, and (3) methanol purification. The process used for generation of syngas is the steam reforming process, whose product gas contains steam, hydrogen, carbon monoxide, and carbon dioxide. The reforming catalyst is nickel based and, therefore, the feed gas must be desulfurized before entering the reformer. The reforming catalyst is very sensitive to sulfur poisoning. The syngas leaving the reformer is typically at 880°C and up to 20 atm, similar to the Lurgi process. The peak temperature of the gas mixture in the reformer is significantly higher than this temperature.

The methanol synthesis section involves a circulator, methanol reactor, heat recovery and cooling unit, and methanol separator. The synthesis catalyst is copper based and typical operating conditions are 200 to 290°C and 50 to 100 atm. In the sense of reaction engineering, a temperature of close to 200°C is too low for a meaningful rate of chemical reaction, whereas a temperature of 290°C may be too high and too close to the potential catalyst-sintering range. As mentioned earlier, methanol formation is limited by chemical equilibrium, thus limiting the exit concentration only up to 7%. This value is higher at a lower reaction temperature, as can be predicted by the equilibrium constant for the conversion reaction. After condensing product methanol out by chilling, the unreacted syngas is recycled back to the methanol reactor for higher overall conversion.

The crude product methanol contains water and small amounts of undesired by-products, which are separated in a two-column distillation system. The two columns are a topping and a refining column. The former removes all light ends including dissolved gases, light hydrocarbons, low-molecular-weight ethers, esters, and acetone,

whereas the latter separates methanol from water and also eliminates higher hydrocarbons and alcohols by a side discharge from the column.

The total energy consumption for a self-contained plant is typically around 7.8 Gcal/t. The figure depends on the type of feedstock used.

9.3.7 Liquid-Phase Methanol Process

The liquid-phase methanol process was originally developed by Chem Systems Inc. in 1975. The R & D of this process was sponsored by the U.S. Department of Energy and Electric Power Research Institute. Commercialized by Air Products and Chemicals Inc. and Eastman Chemical Co. in the 1990s, the process is based on the low-pressure methanol synthesis process concept. The chemical reaction is carried out in a slurry reactor using $Cu/ZnO/Al_2O_3$ catalyst at 230 to 260°C and 50 to 100 atm. The commercial reactor used is a liquid entrained reactor in which fine powder catalyst is slurried in inert high-boiling oil, typically white mineral oil such as Witco-70 and Freezene-100. Fed gaseous reactants are dissolved in the oil, and the dissolved molecular species are reacted on the catalytic surface in a slurry. The process has enhanced heat transfer characteristics owing to the higher thermal mass of inert oil when compared to comparable vapor phase processes. To enhance the mass transfer properties of the process, specially developed, fine-powder catalysts are used. Special features of this process include its capability to handle unbalanced CO-rich syngas and high single-pass conversion of syngas. As a result, the process can be ideally packaged with advanced oxidation gasification technology. Figure 9.8 shows a schematic of the liquid-phase methanol synthesis process.

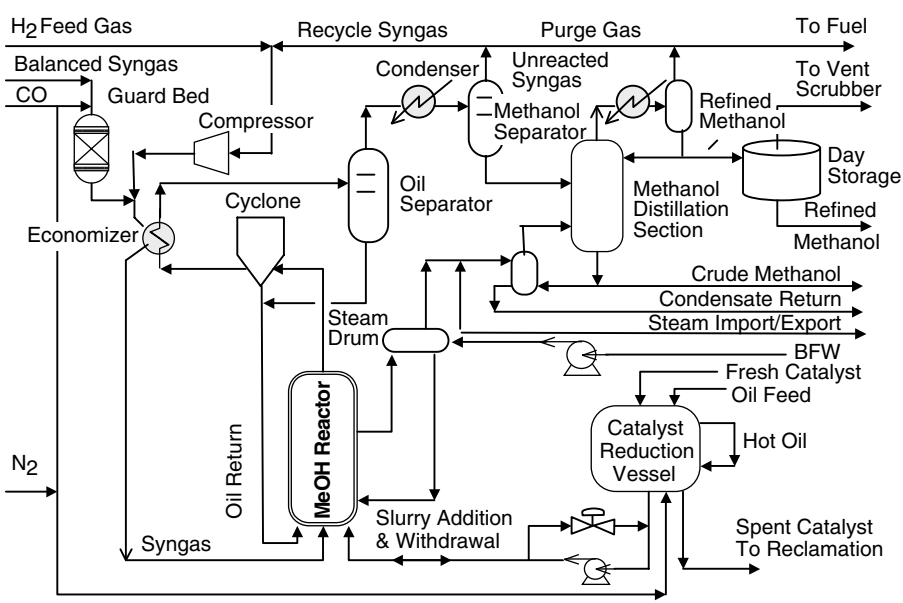

FIGURE 9.8 A schematic of the liquid-phase methanol synthesis process.

9.4 FUTURE OF METHANOL

Methanol can be produced from natural gas, coal, and biomass. The process technology is very mature and practiced on a large scale. The starting material for syngas production is expected to change at least partially from natural gas to coal, biomass, and mixed cofeed. In addition, comprehensive multifuel generation as well as cogeneration process concepts including methanol synthesis are becoming more attractive. Methanol can also be used efficiently as an *IGCC* (Integrated Gasification Combined Cycle) companion fuel as well. Development of efficient engines utilizing methanol or methanol blends is also highly conceivable. With advances in internal combustion engines based on methanol fuel, it is also conceivable that methanol can be used more popularly as *transportation fuel* for passenger vehicles, not just for race cars. Following development of the efficient *dimethylether (DME)* synthesis process as well as utilization of DME in internal combustion engines, methanol has good potential in the alternative fuel market. In the context of ever-rising cost of gasoline fuel throughout the world, processes like *MTG*[16,17] and MTO make much more sense now and in the future than before, thus making methanol a more valuable chemical commodity. As a result of recent developments in DMFC and its suggested use in consumer electronics, methanol has great potential in the future consumer electronics market. Further, methanol can play a more important role in the petrochemical industry as a *building-block chemical* of nonpetroleum origin.

REFERENCES

1. Lee, S., *Methanol Synthesis Technology*, CRC Press, Boca Raton, FL, 1990.
2. Majer, V. and Svoboda, V., *Enthalpies of Vaporization of Organic Compounds: A Critical Review and Data Compilation*, Blackwell Scientific Publications, Oxford, 1985, p. 300.
3. Vazquez-Esparragoza, J.J., Iglesias-silva, G.A., Hlavinka, M.W., and Bullin, J.A., How to estimate Reid vapor pressure (RVP) of blends, *Encyclopedia of Chemical Processing and Design*, Vol. 47, McKetta, J.J., Ed., Marcel Dekker, New York, 1994, pp. 415–424.
4. Larminie, J. and Dicks, A., *Fuel Cell Systems Explained*, 2nd ed., John Wiley & Sons, New York, 2003.
5. Cybulski, A., Liquid-phase methanol synthesis: catalysts, mechanism, kinetics, chemical equilibria, vapor-liquid equilibria, and modeling — review, *Catal. Rev.: Sci. Eng.*, 36(4), 557–615, 1994.
6. Klier, K., *Adv. Catal.*, 31, 243–313, 1982.
7. Lee, S., Parameswaran, V., Wender, I., and Kulik, C.J., The roles of carbon dioxide in methanol synthesis, *Fuel Sci. Technol. Int.*, 7(8), 1021–1057, 1989.
8. Sawant, A., Parameswaran, V., Lee, S., and Kulik, C.J., In-situ reduction of a methanol synthesis catalyst in a three-phase slurry reactor, *Fuel Sci. Technol. Int.*, 5(1), 77–88, 1987.
9. Chinchen, G.C., Mansfield, K., and Spencer, M.S., *CHEMTECH*, 29(11), 1990, pp. 692–699.
10. Lee, S., Sawant, A., and Kulik, C.J., Phases in the active liquid phase methanol synthesis catalyst, *Fuel Sci. Technol. Int.*, 6(2), 151–164, 1988.

11. Lee, S., Sawant, A., and Kulik, C.J., Process for Methanol Catalyst Regeneration Using Crystallite Redispersion, U.S. Patent No. 5,004,717, April 2, 1991.
12. Lee, S., *Methane and Its Derivatives*, Marcel Dekker, New York, 1997.
13. Sawant, A., Rodrigues, K., Kulik, C.J., and Lee, S., The effects of carbon dioxide and water on the methanol synthesis catalyst, *Energy Fuels*, 3(1), 2–7, 1989.
14. Lee, S. and Sardesai, A., Liquid phase methanol and dimethylether synthesis from syngas, *Top. Catal.*, 33(1–2), 2005.
15. Gogate, M.R., Kulik, C.J., and Lee, S., A novel single-step dimethyl ether (DME) synthesis in a three-phase slurry reactor from CO-rich syngas, *Chem. Eng. Sci.*, 47(13–14), 3769–3776, 1992.
16. Chang, C.D., Hydrocarbons from methanol, *Catal. Rev.: Sci. Eng.*, 25(1), 1–118, 1983.
17. Chang, C.D. and Silvestri, A.J., MTG Origin, Evolution, Operation, *CHEMTECH*, 10, 1987, pp. 624–631.
18. Lee, S. and Gogate, M.R., Development of a Single-Stage Liquid-Phase Synthesis Process of Dimethylether from Syngas, EPRI-TR-100246, 1–179, Electric Power Research Institute, Palo Alto, CA, 1992.
19. Lee, S. and Parameswaran, V., Reaction Mechanism in Liquid-Phase Methanol Synthesis, EPRI-ER/GS-6715, 1–206, Electric Power Research Institute, Palo Alto, CA, 1990.
20. Lee, S., Gogate, M.R., and Fullerton, K.L., Catalytic Process for Production of Gasoline from Synthesis Gas, U.S. Patent 5,459,166, 1995.
21. Petrochemical Processes Special Report, Hydrocarbon Processing, Vol. 82, No. 3, 105, 2003.

10 Ethanol from Corn

Sunggyu Lee

CONTENTS

10.1 FUEL ETHANOL FROM CORN

Ethanol is one of the simplest alcohols, which has long been used in human history. Ethanol can be readily produced by fermentation of simple sugars that are converted from starch crops. This has long been practiced throughout the world. Feedstocks for such fermentation include corn, barley, potato, rice, and wheat. This type of ethanol may be called *grain ethanol*, whereas ethanol produced from cellulose biomass such as trees and grasses is called *bioethanol* or *biomass ethanol*. Both grain ethanol and bioethanol are produced via biochemical processes, whereas *chemical ethanol* is synthesized by chemical synthesis routes that do not involve fermentation.

Ethanol, ethyl alcohol [C_2H_5OH], is a clear and colorless liquid. Ethanol has a substituted structure of ethane, with one hydrogen atom replaced by a hydroxyl group, -OH. Ethanol is a clean-burning fuel because of its oxygen content and has a high octane rating by itself. Therefore, ethanol is most commonly used to increase the octane rating of blend gasoline as well as to improve the emission quality of the gasoline engine. Owing to the presence of oxygen in its molecular structure, ethanol is classified as an oxygenated fuel. In many regions of the U.S., ethanol is blended up to 10% with conventional gasoline. The blend of 10% ethanol and 90% conventional gasoline is called *E10 blend* or simply *E10*. Ethanol is quite effective as an

oxygenated blending fuel, because its Reid vapor pressure (RVP) is low, i.e., it does not increase the volatility of the blend gasoline, unlike methanol.

As implied earlier, ethanol can be produced from any biological materials that contain appreciable amounts of sugar or feedstocks that can be converted into sugar. The former include sugar beets and sugar canes, whereas the latter include starch and cellulose. For example, corn contains starch that can be easily converted into sugar and is, therefore, an excellent feedstock for ethanol fermentation. Because corn can be grown and harvested repeatedly, this feedstock eminently qualifies as a *renewable feedstock*; i.e., this feedstock will not be easily depleted.

Fermentation of sugars produces ethanol, and this process technology has been practiced for well over 2000 years in practically all regions of the world. Sugars can also be derived from a variety of sources. In Brazil, as an example, sugar from sugar cane is the primary feedstock for the country's ethanol industry, which is very active. In North America, the sugar for ethanol production is usually obtained via enzymatic hydrolysis of starch-containing crops such as corn or wheat. The enzymatic hydrolysis of starch is a simple, inexpensive, and effective process, and is a mature commercial technology. Therefore, this process is used as a baseline or a benchmark that other hydrolysis processes can be compared against. Although the principal merit of ethanol production by fermentation of sugar and starch is in its technological simplicity and efficiency, its disadvantage is that the feedstock tends to be expensive and also competitively used for other applications. However, this high cost of feedstock can be favorably offset by the sale of by-products or coproducts such as distillers' dried grains. Many corn refineries produce both ethanol and other corn by-products such as starches and sweeteners so that the capital and manufacturing costs can be kept as low as possible, by increasing the overall process revenue. While manufacturing ethanol, corn refiners also produce valuable coproducts such as corn oil and corn gluten feed. The North American ethanol industry is, therefore, investing significant efforts in developing new by-products (coproducts) that are higher in value and minimize waste, thus making the grain ethanol industry more cost-competitive.

Corn refining in the U.S. has a relatively long history going back to the time of the civil war, with the development of cornstarch hydrolysis process. Before this event, the main sources for starch were wheat and potatoes. In 1844, the Wm. Colgate & Co.'s wheat starch plant in Jersey City, NJ, unofficially became the first dedicated cornstarch plant in the world. By 1857, the cornstarch industry accounted for a significant portion of the U.S. starch industry. However, for this era, cornstarch was the only principal product of the corn-refining industry, and its largest customer was the laundry business.

The industrial production of dextrose from cornstarch started in 1866. This industrial application and subsequent developments in the chemistry of sugars served as a major breakthrough in starch technology. Other product developments in corn sweeteners followed and occurred more than 15 years later with the first manufacture of refined corn sugar, or anhydrous sugar, in 1882.

In the 1920s, corn syrup technology advanced significantly with the introduction of enzyme-hydrolyzed products. Even though the production of ethanol by corn refiners had begun as early as after World War II, major quantities of ethanol via this process route were not produced until the 1970s, when several corn refiners

began fermenting dextrose to make beverage and industrial alcohol. Corn refiners' entry into the fermentation business has become a notable milestone for the major changes and transformation of the industry, especially in the fuel ethanol industry. The industry began to develop expertise in industrial microbiology, fermentation technology, and separation technology.

As of today, starch, glucose, and dextrose are still important products of the corn wet milling industry. However, the products of microbiology and biochemical engineering, including ethanol, fructose, food additives, and chemicals, have gradually overshadowed them. New R&D has significantly expanded the industry's product/by-product/coproduct portfolio, thus making the industry more profitable, competitive, and futuristic.

Lignocellulosic materials such as agricultural, hardwood, and softwood residues are also potential sources of sugars for ethanol production. The cellulose and hemicellulose components of these materials are essentially long and high-molecular-weight chains of sugars. They are protected by lignin, which functions more like "glue" that holds all of these materials together in the structure. Details of lignocellulosic ethanol technology are covered in Chapter 11, and therefore, not repeated here.

Ethanol plays three principal roles in today's economy and environment, and they are:

1. Ethanol replaces more than a billion dollars' worth of imported oil with a renewable domestic fuel. This value is also directly related to the import crude oil price.
2. Ethanol is an important oxygenated component of gasoline reformulation to reduce air pollution in many U.S. metropolitan areas, which are not achieving air quality standards mandated by the Clean Air Act Amendments (CAAA) of 1990. Ethanol is a cleaner-burning fuel because of its oxygen-containing molecular formula, and is also an excellent gasoline blend fuel owing to its low RVP.
3. Ethanol provides significant income to farmers and agricultural communities where most ethanol feedstock is produced.

Ethanol, blended with gasoline at a 10% level, or in the form of ethyl tertiary-butyl ether (ETBE) synthesized from ethanol, is effective in reducing carbon monoxide (CO) emission levels, ozone pollution, and NO_x emissions from automobile exhaust.

The U.S. ethanol industry is capable of expanding to meet the increased demand for oxygenated fuel that would result if there were a withdrawal of methyl-*t*-butyl ether (MTBE) from the domestic gasoline marketplace. In response to sharply rising national concerns about the presence of MTBE in groundwater as well as potential risk to public health and the environment, the U.S. Environmental Protection Agency (EPA) convened a Blue Ribbon Panel to assess policy options regarding MTBE. The Blue Ribbon Panel recommended that the use of MTBE be dramatically reduced or eliminated. EPA has subsequently stated that MTBE should be removed from all gasoline. Many U.S. states including California and New York mandated their own schedules of MTBE phase-outs and bans. It is a remarkable turnaround in the chemical and petrochemical marketplace, considering that MTBE used to be the

fastest-growing chemical in the U.S. in the 1990s. Recovering or retrofitting MTBE plant investments would become an issue to this industry for years to come.

According to the Renewable Fuels Association (RFA), U.S. ethanol production in 2002, 2003, and 2004 was 2.13, 2.80, and 3.40 billion gallons, respectively.[10] Considering that the production level of 2000 was 1.63 billion gallons, this is a more than twofold increase over 4 years. The replacement of MTBE with ethanol will increase the demand for ethanol even more. The increased national capacity will have to come principally from three sources, namely: (1) improvement in production efficiency leading to increased utilization of existing plants, (2) expansion of existing production facilities, and (3) construction of new plants.

In terms of product value, corn sweeteners are the most important refined corn product. In 2003, corn sweeteners supplied more than 55% of the U.S. nutritive sweetener market. The second major refined corn product was ethanol as blend fuel for gasoline. The third most important corn product, a very important part of the corn industry and also of the U.S. economy, is starch, i.e., cornstarch. Corn refiners fill more than 90% of the U.S. demand for starch. With the ever-increasing demand for fuel-grade ethanol from corn, changes in rankings for corn product utilization appear inevitable.

Corn refining has also become America's premier by-products industry. Increased production of amino acids, proteins, antibiotics, and biodegradable plastics has added further value to the U.S. corn crop.[1] In addition to cornstarches, sweeteners, and grain ethanol, corn refiners also produce corn oils as well as a variety of important feed products.

10.2 ETHANOL AS ALTERNATIVE FUEL

10.2.1 Industrial Significances of Grain Ethanol

Ethanol production and its utilization as automotive fuel received a major boost with the enforcement of the *Clean Air Act Amendments (CAAA) of 1990*. Blending gasoline with ethanol has become a popular method for gasoline producers to meet the new oxygenate requirements mandated by the CAAA. Provisions of the CAAA established the *Oxygenated Fuels Program (OFP)* and the *Reformulated Gasoline Program (RGP)* in an attempt to control carbon monoxide (CO) emission and ground-level ozone problems. Both programs require certain oxygen levels in gasoline, namely, 2.7% by weight for oxygenated fuel and 2.0% by weight for reformulated gasoline. Public policies aimed at encouraging ethanol development and production are largely motivated by the nation's desire to improve air quality as well as to enhance future energy supply security. In addition, agricultural policymakers keenly see the expansion of the ethanol industry as a means of stabilizing farm income and reducing farm subsidies. Increasing ethanol production stimulates a higher demand for corn crops and raises the average corn price. Higher corn prices and stronger demand of corns reduce farm commodity program payments and the participation rate in the Acreage Reduction Program. From technical and scientific viewpoints, use of ethanol as motor fuel or blend fuel makes sense, because corn ethanol can be produced in a renewable manner, i.e., as a nondepletable energy source.

10.2.2 Clean Air Act Amendments of 1990

The Clean Air Act Amendments of 1990 target automobile emissions as a major source of air pollution. The Act mandates the use of cleaner-burning fuels in U.S. cities with smog and air pollution problems. The oxygen requirements of CAAA spurred a market for oxygenates and created new market opportunities for ethanol. The Oxygenated Fuels Program (OFP) targets 39 cities that do not meet National Ambient Air Quality Standards (NAAQS) for carbon monoxide (CO). CAAA mandates the addition of oxygen to gasoline to reduce CO emissions. It requires an oxygen level in gasoline of 2.7% by weight. Control periods vary by city because most CO violations occur during the winter. The average control period is about 4 months. The most widely used oxygenate in the market has been a methanol-derived ether, MTBE, which is made mostly from natural gas and is being phased out in the 2000s.

Most major gasoline refiners are increasingly using ethanol to meet gasoline oxygenate content requirements. In 1993, about 300–350 million gallons of ethanol were blended with gasoline and sold in markets covered by the Oxygenated Fuels Program (OFP). In 2004, fuel ethanol consumption reached 3.4 billion gallons in the U.S. In about 10 years, U.S. production of grain ethanol has seen a tenfold increase. The CAAA also requires the use of oxygenated fuels as part of the reformulated gasoline (RFG) program for controlling ground-level ozone formation. This program requires an oxygen level in gasoline of 2.0% by weight. Beginning in January 1995, reformulated gasoline was required to be sold in 9 ozone nonattainment areas year-round. Other provisions in the act allow as many as 90 other cities with less severe ozone pollution to "opt in" to the RFG program. Under a total opt-in scenario, as much as 70% of the nation's gasoline could be reformulated.

An oxygen level of 2.0% by weight in gasoline means that at least 5.75% by weight of ethanol needs to be blended in gasoline, based on the stoichiometric calculation of $2.0 \times (46/16) = 5.75$. Therefore, 2.7% oxygen requirement pushes the required level of ethanol in gasoline to 7.76% as a minimum. Thus, 10% ethanol-blended gasoline, E10, sold in gas stations is consistent with this calculation. Even though ethanol is clean burning and has a low RVP of blending, it has substantially lower heating value than conventional gasoline. However, at a level of 10% blending, the reduced energy output is much less appreciable and could be compensated for by better engine performance.

Higher corn yields of modern agricultural industry, lower energy consumption per unit of output in the fertilizer industry, and recent advances in fuel conversion technologies have significantly enhanced the economic and technical feasibility of producing ethanol from corn, when compared with just a decade ago. Therefore, studies based on the older data may tend to overestimate energy use because the efficiency of growing corn as well as converting it to fuel ethanol has improved significantly over the past decade.[2] According to this study, the net energy value (NEV) of corn ethanol is calculated as 16,193 Btu/gal, assuming that: fertilizers are produced by modern processing plants, corn is converted in modern ethanol facilities, farmers achieve normal corn yields, and energy credits are allocated to coproducts.

10.2.3 Ethanol Production from Corn

Ethanol production facilities can be classified into two broad groups, i.e., *wet milling* and *dry milling* operations. Dry mills are usually smaller in size (capacity) and are built primarily to manufacture ethanol only. Wet mill facilities are called *corn refineries*, also producing a list of high-valued coproducts such as high-fructose corn syrup (HFCS), dextrose, and glucose syrup. Both wet and dry milling operations are used to convert corn to ethanol. Wet milling accounts for about two thirds of U.S. ethanol production from corn, whereas dry milling accounts for the remaining one third.

Thermal energy and electrical power are the main types of energy used in both types of milling plants. Currently, most corn-processing plants generate both electrical and thermal energy from burning coal. A few plants generate steam only, and electricity is also purchased from a utility. Electrical energy is used mostly for grinding and drying corn, whereas thermal energy is used for fermentation, ethanol recovery, and dehydration. On the other hand, flue gas is used for drying and stillage processing.

A large number of studies have been conducted to estimate the net energy value (NEV) of ethanol production. However, variations in data and model assumptions resulted in a wide range of estimated values, ranging from a very positive to a negative value. A net negative energy value would mean that it takes more energy to produce the energy content of ethanol. A recent comprehensive study conducted by Argonne National Laboratory shows that ethanol produces 35% more energy than it takes to generate.[11]

According to a study by Shapouri et al.,[2] modern wet milling plants are able to produce 1 gal of ethanol, while consuming 35,150 Btu of thermal energy and 2.134 kWh of electricity. If molecular sieves are used, the thermal input drops to 32,150 Btu/gal. DeSpiegelaere[3] reported that of the total thermal energy, 7,000 Btu/gal and 1.16 kWh were related to drying high-grade germ, fiber, and gluten. On average, wet mills produce 2.5 gal of ethanol per bushel. One U.S. bushel is equivalent to 35.23907 l.

A new dry milling plant requires 37,000 Btu of thermal energy and 1.2 kWh of electricity per gallon of ethanol produced.[2] The typical dry mill facility produces 2.6 gal of ethanol per bushel of corn. The total energy used for converting ethanol, weighted by milling process and adjusted by EPA's input efficiency factor[12] for the energy used to mine and transport coal, is 53,277 Btu/gal.[2]

Modern corn ethanol facilities use coal-based cogeneration. It has become common for modern wet and dry mill ethanol plants to employ cogeneration technology to produce steam and in-house power. In addition, in many operations, flue gas drying of products is also practiced as an energy integration scheme.

The ethanol fuel manufacturing process is a combination of biochemical and physical processes based on traditional unit operations. Ethanol is produced by fermentation of sugars with yeast. The fermentation crude product is concentrated to fuel-grade ethanol by distillation.

Feedstocks for ethanol fermentation are either sugar or starch-containing crops. These *biomass fuel crops* (tubers and grains) typically include sugar beets, potatoes, corn, wheat, barley, Jerusalem artichokes, and sweet sorghum. Sugar crops such as

sugar cane, sugar beets, or sweet sorghum are extracted to produce a sugar-containing solution or syrup that can be directly fermented by yeast. Starch feedstocks, however, must go through an additional step that involves starch-to-sugar conversion, as is the case for grain ethanol.

Starch may be regarded as a long-chain polymer of glucose (i.e., many glucose molecular units are bonded in a polymeric chain similar to a condensation polymerization product). As such, macromolecular starches cannot be directly fermented to ethanol by conventional fermentation technology. They must first be broken down into simpler and smaller glucose units through a chemical process called *hydrolysis*. In the hydrolysis step, starch feedstocks are ground and mixed with water to produce a mash typically containing 15 to 20% starch. The mash is then cooked at or above its boiling point and treated subsequently with two enzyme preparations. The first enzyme hydrolyzes starch molecules to short-chain molecules, and the second enzyme hydrolyzes the short chains to glucose. The first enzyme is amylase. Amylase liberates "maltodextrin" by the liquefaction process. Such maltodextrins are not very sweet as they contain dextrins and oligosaccharides. The dextrins and oligosaccharides are further hydrolyzed by enzymes such as pullulanase and glucoamylase in a process known as *saccharification*. Complete saccharification converts all the limit dextrans to glucose, maltose, and isomaltose. The mash is then cooled to 30ºC, and yeast is added for fermentation.

Yeasts are capable of converting sugar into alcohol by a biochemical process called *fermentation*. The yeasts of primary interest to industrial fermentation of ethanol include *Saccharomyces cerevisiae, Saccharomyces uvarum, Schizosaccharomyces pombe,* and *Kluyveromyces* sp. Under anaerobic conditions, yeasts metabolize glucose to ethanol primarily via the Embden–Meyerhof pathway. The *Embden–Meyerhof pathway* of glucose metabolism is the series of enzymatic reactions in the anaerobic conversion of glucose to lactic acid (or ethanol in this case), resulting in energy in the form of adenosine triphosphate (ATP).[13] The overall net reaction represented by a stoichiometric equation involves the production of 2 mol of ethanol from each mole of glucose as shown in the following text. However, the yield attained in practical fermentations does not usually exceed 90 to 95% of the theoretical value. In this case, the theoretical value, i.e., 100% of yield, means that exactly 2 mol of ethanol is produced from each mole of glucose input to the fermenter. Therefore, this 100% yield is equivalent to the mass conversion efficiency of 51%, which is defined later in this subsection. The following equation shows the basic biochemical reaction in the conversion by fermentation of glucose to ethanol, carbon dioxide, and endothermic heat.

$$C_6H_{12}O_6 = 2\ C_2H_5OH + 2\ CO_2 \qquad \Delta H^{o}_{298} = 92.3\ \text{kJ/mol}$$

Theoretically, the maximum conversion efficiency of glucose to ethanol is 51% on a weight basis, which comes from a stoichiometric calculation of $2 \times$ (Molecular Weight of Ethanol)/(Molecular Weight of Glucose) = $(2 \times 46)/(180) = 0.51$. However, some glucose is inevitably used by the yeast for production of cell mass and for metabolic products other than ethanol, thus reducing the conversion efficiency from its theoretical maximum. In practice, between 40 and 48% of glucose is actually converted to ethanol. With 46% fermentation efficiency, 1000 kg of fermentable

sugar would produce about 583 l of pure ethanol, after taking into account the density of ethanol (specific gravity at 20°C = 0.789). Or,

$$(1000 \text{ kg sugar}) \times (0.46 \text{ kg ethanol/kg sugar})/(0.789 \text{ kg ethanol/l}) = 583 \text{ l}$$

Conversely, about 1716 kg of fermentable sugar are required to produce 1000 l of ethanol, when 46% mass conversion efficiency is assumed. Mash typically contains between 50 and 100 g of ethanol per liter (about 5 to 10% by weight) when the fermentation step is complete. This is called *distilled mash* or *stillage*, which still contains a large amount of nonfermentable portions of fibers or proteins.

Ethanol is subsequently separated from mash by distillation, in which the components of a solution (in this case, water and ethanol) are separated by differences in boiling point (or individual vapor pressure). Separation is technically limited by the fact that ethanol and water form an *azeotrope*, or a constant boiling solution, of about 95.4% alcohol and 4.6% water. This azeotrope is of maximum boiling kind, for which the boiling temperature of the azeotrope is higher than that of the individual pure components, i.e., water and ethanol.

The 5%, more precisely 4.6 %, water cannot be separated by conventional distillation, because the maximum boiling temperature is attainable at the azeotropic concentration, not at the pure water concentration. Therefore, production of pure, water-free (anhydrous) ethanol requires an additional unit operation step following distillation. *Dehydration*, a relatively complex step in ethanol fuel production, is accomplished by one of two methods. The first method uses a third liquid, most commonly benzene, which is added to the ethanol-water mixture. This third component changes the boiling characteristics of the solution (now, a ternary instead of a binary system), allowing separation of anhydrous ethanol. In other words, this third component is used to break the azeotrope, thereby enabling conventional distillation to achieve the desired goal of separation. This type of distillation is also called *azeotropic distillation*, because the operation targets separating mixtures that form azeotropes. The second method employs molecular sieves that selectively absorb water based on the molecular size difference between water and ethanol. Molecular sieves are crystalline metal aluminosilicates having a three-dimensional interconnecting network of silica and alumina tetrahedra. Molecular sieves have long been known for their drying capacity (even to 90°C). There are different forms of molecular sieves that are based on the dimension of effective pore opening, and they include 3A, 4A, 5A, and 13X. Commercial molecular sieves are typically available in powder, bead, granule, or extrudate forms. Pressure Swing Adsorption (PSA) using molecular sieve offers economical and environmental advantages over the conventional ternary system distillation, and is gaining popularity in the field of ethanol dehydration.

The nonfermentable solids in distilled mash (stillage) contain variable amounts of fiber and protein, depending on the feedstock. The liquid also contains soluble protein and other nutrients and, as such, is still valuable. The recovery of the protein and other nutrients in stillage for use as livestock feed can be essential for the overall economic and profitability analysis of ethanol fuel production. Protein content in stillage varies with feedstock. Some grains such as corn and barley yield solid by-products called *distiller's dried grains (DDG)*. Protein content in DDG typically ranges from 25 to 30% by mass and makes an excellent feed for livestock.

The production of ethanol also generates liquid effluent, which may give rise to pollution concerns. About 9 l of liquid effluents are generated for each liter of ethanol produced. Some of the liquid effluent may be recycled. Effluent can have a high level of biological oxygen demand (BOD), which is a measure of organic water pollution potential, and it is also acidic. Therefore, the liquid effluent must be treated before being discharged into water stream. Specific treatment requirements depend on both feedstock quality (and type) as well as local pollution control regulations. Owing to the acidity of the effluent, precautions and care must be also taken if it is directly spread over fields.[4]

10.3 CHEMISTRY OF ETHANOL FERMENTATION

10.3.1 Sugar Contents of Biological Materials

Figure 10.1 shows a highly generalized view of plant cell wall composition. The base molecules that give plants their structure can be processed to produce sugars, which can be subsequently fermented to ethanol.

The principal components of most plant materials are commonly described as *lignocellulosic biomass*. This type of biomass is mainly composed of the compounds, cellulose, hemicellulose, and lignin. *Cellulose* is a primary component of most plant cell walls and is made up of long chains of the 6-carbon sugar, *glucose,* that are arranged in bundles (often described as crystalline bundles). The cellulose molecules in the plant cell wall are interconnected by another molecule called *hemicellulose*. The hemicellulose is primarily composed of the 5-carbon sugar, *xylose*. Besides cellulose and hemicellulose, another molecule called lignin is also present in significant

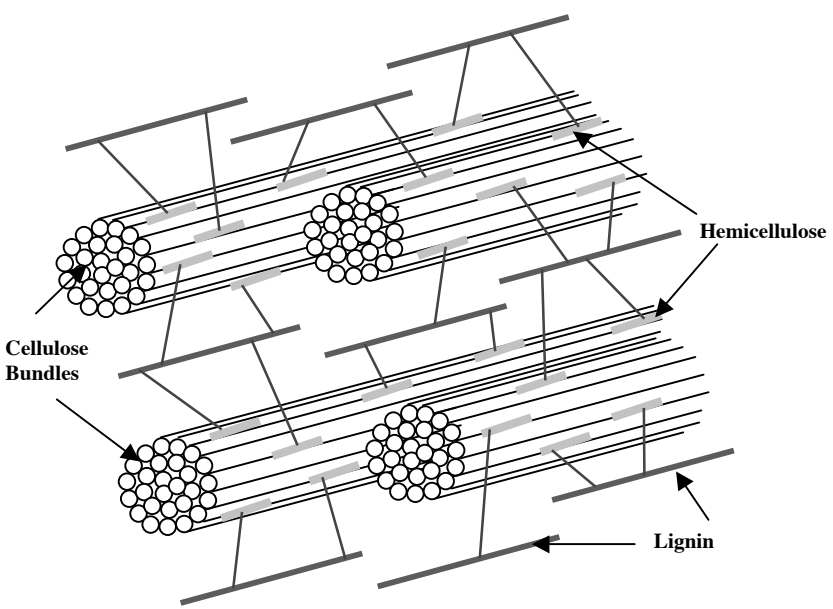

FIGURE 10.1 A generalized description of a plant cell wall.

amounts and provides the structural strength for the plant. Technological developments have recently introduced a variety of processes for extracting and dissolving the cellulose and hemicellulose to produce sugars in a form that can be readily fermented to ethanol. Generally speaking, appropriate pretreatment can liberate the cellulose and hemicellulose from the plant material. Further treatment using chemicals, enzymes, or microorganisms can also be applied to liberate simple sugars from the cellulose and hemicellulose, thus making them available to microorganisms for fermentation to ethanol.

10.3.2 Conversion of Sugars to Ethanol

Figure 10.2 illustrates the hydrolysis of cellulose.[5] The first step involves cellulose hydrolysis, which is essentially cleaving the chemical bonds in the cellulose to produce glucose.

Once the large molecules are extracted from plant cells, they can be broken down into their component sugars, using enzymes or acids. The sugars can be subsequently converted to ethanol, using appropriately selected microorganisms via fermentation. The fermentation of ethanol from 6-carbon sugars is represented by the following stoichiometric equation:

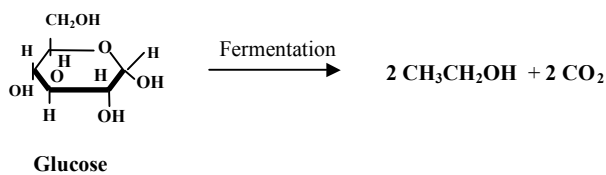

According to the stoichiometric equation, 1 mol of glucose produces 2 mol of ethanol and 2 mol of carbon dioxide. Considering the molecular weights of glucose, ethanol, and carbon dioxide, which are 180, 46, and 44, respectively, the maximum

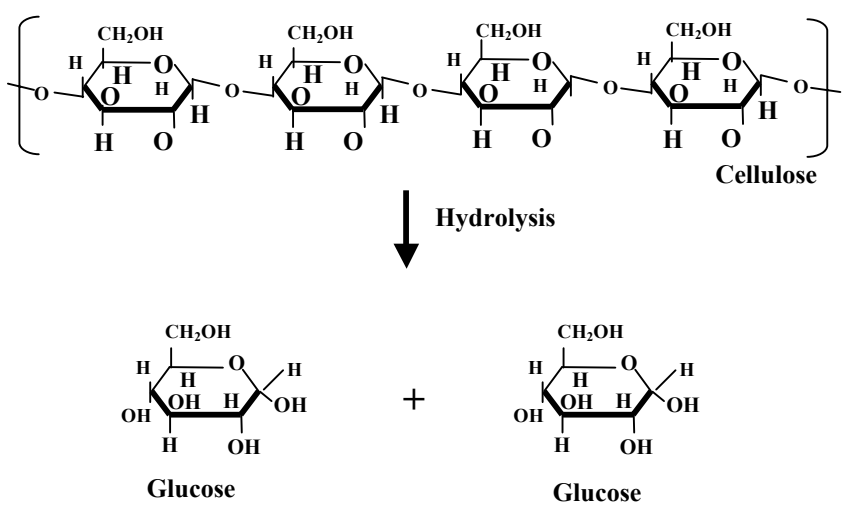

FIGURE 10.2 Hydrolysis of cellulose.

theoretical yield of ethanol by wt% from the process would be 92/180 = 51%. Nearly half the weight of the glucose (88/180 [49%]) is converted to carbon dioxide.

Hemicellulose is made up of the 5-carbon sugar, xylose, arranged in chains with other minor 5-carbon sugars interspersed as side chains. Similar to the cellulose case, the hemicellulose can also be extracted from the plant material and treated to liberate xylose that in turn can be fermented to produce ethanol. However, xylose fermentation is not as straightforward as glucose fermentation. Depending on the microorganism and conditions employed, a number of different fermentation paths are possible. The array of products can include ethanol, carbon dioxide, and water as:

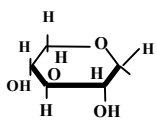

Xylose

Fermentation

$$2CH_3CH_2OH + CO_2 + H_2O$$

Actually, three different reactions have been documented with yields of ethanol ranging from 30 to 50% of the weight of xylose as the starting material (i.e., weight ethanol produced/weight xylose). They are:

$$3 \text{ Xylose} \rightarrow 5 \text{ Ethanol} + 5 \text{ Carbon Dioxide}$$
$$3 \text{ Xylose} \rightarrow 4 \text{ Ethanol} + 7 \text{ Carbon Dioxide}$$
$$\text{Xylose} \rightarrow 2 \text{ Ethanol} + \text{Carbon Dioxide} + \text{Water}$$

The first reaction yields a maximum of 51% $(5 \times 46/(3 \times 150))$, the second 41% $(4 \times 46/(3 \times 150))$, and the third 61% $(2 \times 46/150)$, respectively. Although the maximum theoretical ethanol yields from these fermentation reactions range between 41 and 61%, the practical yields of ethanol from xylose as starting material are in the range of 30–50%.

In the discussion of potential yields of ethanol from various starting materials, two different ranges of efficiencies of hemicellulose-to-xylose conversion and xylose-to-ethanol conversion have been combined to provide an overall conversion efficiency of hemicellulose to ethanol of about 50%. Just as with glucose fermentation, the conversion of carbon dioxide to value-added products would vastly improve the economics of ethanol production, because the yield of carbon dioxide is not only significant in amounts but also inevitable. It must be noted that even though xylose fermentation to ethanol is also mentioned in this chapter, the main focus of discussion for this chapter is on glucose fermentation. As conveyed earlier indirectly, ethanol-from-corn technology involves glucose fermentation, not xylose fermentation.

10.4 CORN-TO-ETHANOL PROCESS TECHNOLOGY

Fermentation of sugars to ethanol, using commercially available fermentation technology, provides a fairly simple, straightforward means of producing ethanol with little technological risk. The system modeled assumes that the molasses are clarified, and

then fermented via cascade fermentation with yeast recycle. The stillage is concentrated by multiple-effect evaporation, and a molecular sieve is used to dehydrate the ethanol.

For more than 150 years in the U.S., corn refiners have been perfecting the process of separating corn into its component parts to create a myriad of value-added corn products. The *corn wet milling process* separates corn into its four basic components, namely: *starch, germ, fiber,* and *protein*. There are eight basic steps involved in accomplishing this corn refining and alcohol fermentation process.[6]

These are:

1. The corn is *visually inspected and cleaned.* Refinery people inspect incoming corn shipments and clean them two or three times to remove cob, dust, chaff, and any other foreign materials before the next processing stage, *steeping*. Effective screening processes can save a great deal of trouble in the subsequent stages.
2. The corn is steeped to initiate bond breaking of starch and protein. *Steeping* is typically carried out in stainless steel tanks. Each steep tank (or steeping tank) holds about 3000 bushels of corn soaked in water at 50°C for 30–40 h. During steeping, the kernels absorb water, thereby increasing their moisture levels from 15 to 45% by weight and also more than doubling in size. The addition of 0.1% *sulfur dioxide* (SO_2) to the water suppresses excessive bacterial growth in the warm environment. As the corn swells and softens, the mild acidity of the steeping water begins to loosen the gluten bonds within the corn and eventually releases the starch. A bushel is a unit of volume measure used as a dry measure of grains and produce. *A bushel of corn* or milo weighs 56 lb, a bushel of wheat or soybeans weighs 60 lb, and a bushel of sunflowers weighs 25 lb. That is, a U.S. bushel is equivalent to 35.23907 l as a volume unit.
3. A coarse grind separates the germ from the rest of the kernel. Germ is the embryo of a kernel of grain. This is accomplished in *cyclone separators*, which spin the low-density corn germ out of the slurry. Therefore, this cyclone separator is called a *germ separator.* The germs, which contain about 85% of corn's oil, are pumped onto screens and washed repeatedly to remove any starch left in the mixture. A combination of mechanical and solvent processes extracts the oil from the germ. The oil is then refined and filtered into finished *corn oil.* The germ residue is saved as another useful component of animal feeds. Both corn oil and germ residue are important by-products of this process.
4. As the fourth step, the remaining slurry, consisting of fiber, starch, and protein, is finely ground and screened to separate the fiber from the starch and protein. After the germ separation step (step 3), corn and water slurry goes through a more thorough grinding in an impact or attrition-impact mill to release the starch and gluten from the fiber in the kernel. The suspension of starch, gluten, and fiber flows over fixed concave screens, which catch fiber but allow starch and gluten to pass through. The fiber is collected, slurried, and screened again to reclaim any residual starch or protein, then piped or sent to the feed house as a major ingredient of

animal feeds. The starch-gluten suspension, called *mill starch*, is piped or sent to the starch separators.

5. Starch is separated from the remaining slurry in *hydrocyclones*. By centrifuging mill starch, the gluten is readily spun out owing to the density difference between starch and gluten. Starch is denser than gluten. Separated gluten can be used for animal feeds. The starch, with just 1 to 2% protein remaining, is diluted, washed 8 to 14 times, rediluted and rewashed in hydrocyclones to remove the last trace of protein and produce high-quality starch, typically more than 99.5% pure. Some of the starch is dried and marketed as *unmodified cornstarch*, some is modified into *specialty starches*, but most is converted into corn syrups and dextrose. Cornstarch has a variety of industrial and domestic uses. All these are important by-products of the process, which improve the corn distillers' profitability.
6. The cornstarch then is converted to syrup, and this stage is called *starch conversion* step. Starch-water suspension is liquefied in the presence of acid and enzymes. Enzymes help convert the starch to *dextrose***,** which is soluble in water as an aqueous solution. Treatment with another enzyme is usually carried out, depending on the desired process outcome. The process of acid and enzyme reactions can be stopped or terminated anytime throughout the process to produce a right mixture of sugars such as dextrose and maltose for syrups to meet desired specifications. For example, in some cases, the conversion of starch to sugars can be halted at an early stage to produce low- to medium-sweetness syrups. In other cases, however, the starch conversion process is allowed to proceed until the syrup becomes nearly all dextrose. After this conversion process, the syrup is refined in filters, centrifuges or ion-exchange columns, and excess water is evaporated, producing concentrated syrup. Syrup can be sold directly as is, crystallized into pure dextrose, or processed further to produce high-fructose corn syrup.
7. Syrups can be made into several other products through a *fermentation* process. Dextrose is one of the most fermentable forms of all the sugars. Dextrose is also called *corn sugar* and *grape sugar*, and dextrose is a naturally occurring form of glucose. Dextrose is better known today as *glucose*. Following the conversion of starch to dextrose, corn refiners pipe and send dextrose to fermentation units and facilities, where dextrose is converted to ethanol by traditional yeast fermentation. Using a continuous process, the fermenting mash is allowed to flow, or cascade, through several fermenters in series until the mash is fully fermented and then leaves the final tank. In a batch fermentation process, the mash stays in one fermenter for about 48 h before the distillation process is initiated. Generally speaking, a continuous mode is more effective with a higher fermenter throughput, whereas higher-quality product may be obtained from a batch mode.
8. *Ethanol separation* follows the fermentation step. The resulting broth is distilled to recover ethanol or concentrated through membrane separation to produce other by-products. Carbon dioxide generated from fermentation is recaptured for sale, and nutrients still remaining in the broth after fermentation are used as components of animal feed ingredients. These by-products also help the overall economics of the corn refineries.

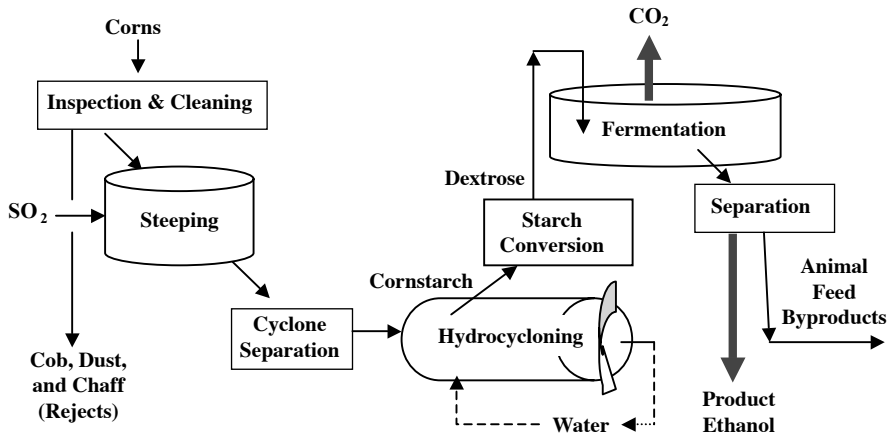

FIGURE 10.3 A typical schematic of corn-to-alcohol process.

Even though the term *by-product* was used throughout the process description, *coproduct* may be a better term, because these products are not only valuable but also targeted in the master plan of corn distillers. The *corn-to-alcohol process* detailed earlier can be summarized in a schematic process diagram, as shown in Figure 10.3.

10.5 ETHANOL AS OXYGENATED FUEL

Oxygenated fuel is conventional gasoline that has been blended with an oxygenated hydrocarbon to achieve a certain concentration level of oxygen in the blended fuel. Oxygenated fuel is required by the CAAA of 1990 for areas that do not meet federal air quality standards, especially for carbon monoxide. The oxygen present in the blended fuel helps the engine burn the fuel more completely, thus emitting less carbon monoxide. Extra oxygen already present *in situ* in the fuel formulation helps efficient conversion into carbon dioxide rather than carbon monoxide.

Reformulated gasoline (RFG) is a new formulation of gasoline that has lower controlled amounts of certain chemical compounds that are known to contribute to the formation of ozone and toxic air pollutants. It is less evaporative than conventional gasoline during the summer months, thus reducing evaporative fuel emission and leading to reduced volatile organic compound (VOC) emission. It also contains oxygenates, which increase the combustion efficiency of the fuel and reduce carbon monoxide emission. The CAAA of 1990 require RFG to contain oxygenates and have a minimum oxygen content of 2.0% oxygen by weight. RFG is required in the most severe ozone nonattainment areas of the U.S. Other areas with ozone problems have voluntarily opted into the program. The EPA has implemented the RFG program in two phases, i.e., Phase I for 1995 to 1999 and Phase II, which began in 2000.

To be more specific, the CAAA mandated the sale of reformulated gasoline (RFG) in the nine worst ozone nonattainment areas beginning January 1, 1995. Initially, the EPA determined the nine regulated areas to be the metropolitan areas of Baltimore,

Chicago, Hartford, Houston, Los Angeles, Milwaukee, New York City, Philadelphia, and San Diego. The important parameters for RFG by the CAAA of 1990 are:

1. At least 2% oxygen by weight
2. A maximum benzene content of 1% by volume
3. A maximum of 25% by volume of aromatic hydrocarbons

Methyl-tert-butyl ether (MTBE) was the most commonly used oxygenate, until recent claims of health problems associated with MTBE use as a blending fuel emerged. Tertiary-amyl methyl ether (TAME), ethyl tertiary-butyl ether (ETBE), and ethanol have also been used in reformulated fuels. Among these, ethanol has been gaining popularity as a blending fuel, based on its clean-burning nature, low *Reid vapor pressure*, renewability, minimal or no health concerns, and relatively low cost.

The RFG should have no adverse effects on vehicle performance or the durability of engine and fuel system components. However, there may be a slight decrease in fuel mileage (1–3% or 0.2–0.5 mi/gal) with well-tuned automobiles owing to the higher concentrations of oxygenates that have lower heating values. Nevertheless, RFG burns more completely, thereby reducing formation of engine deposits and often boosting the actual gas mileage.

The RVP is crucially important information for blended gasoline from practical and regulatory standpoints. Evaporated gasoline compounds combine with other pollutants on hot summer days to form ground-level ozone, commonly referred to as *smog*. Ozone pollution is of particular concern because of its harmful effects on lung tissue and breathing passages. Therefore, the government, both federal and state, imposes an upper limit as a requirement, which restricts the maximum level reformulated gasoline can have as its Reid vapor pressure. By such regulations, the government not only controls the carbon monoxide emission level, but also limits the evaporative emission of the fuel. Because of this limit, certain oxygenates may not qualify as a gasoline-blending fuel even if they possess excellent combustion efficiency and high octane rating. Further, the legal limits for the Reid vapor pressure depend on many factors, including current environmental conditions, geographical regions, climates, time of the year (such as summer months vs. winter months), etc. It should be also noted that ground-level ozone is harmful to humans, whereas stratospheric ozone is essential for global environmental safety.

The *oxygenated fuel program (OFP)* is a winter-time program for areas with problems of carbon monoxide air pollution. The oxygenated winter fuel program uses normal gasoline with oxygenates added. On the other hand, the reformulated gasoline program is for year-round use to help reduce ozone, CO, and air toxins. Although both programs use oxygenates to reduce CO, RFG builds on the benefit of oxygenated fuel and uses improvements in the actual formulation of gasoline to reduce pollutants, including *volatile organic compounds (VOCs).*

Although MTBE was widely credited with significantly improving the nation's air quality, it has been found to be a major contributor to groundwater pollution. Publicity about the leaking of MTBE from gasoline storage tanks into aquifers, as well as its adverse health effects, has prompted legislators from the Midwest to push for a federal endorsement of corn-derived ethanol as a substitute oxygenate. Oil

refineries in the state of California have been required to phase out MTBE, and replace it by ethanol, by the year 2004. This may serve as an incentive for corn ethanol industries, as they can market their products as being environmentally more acceptable than other alternatives and at the same time, it is renewable.

Ethanol can be used directly as fuel for internal combustion engines. In this case, the ethanol content is far more than that for blended fuel. In the U.S., the National Ethanol Vehicle Coalition (NEVC) is actively promoting expanded use of 85% ethanol (E85) motor fuel. NEVC is advocating E85, based on its clean burning as well as renewability of the fuel. E85 fuel can achieve a very high octane rating of 105. The major automakers of the world are producing vehicles that are E85 compatible. They include Daimler Chrysler, Ford, General Motors, Isuzu, Mazda, Mercedes, Mercury, and Nissan. Many of their late-model pick-up trucks are compatible with E85, and more passenger cars are being added to the list of E85-compatible vehicles. As an extra incentive plan for the E85 users, the U.S. federal government provides federal income tax credits for the use of E85 as a form of alternative transportation fuel. The E85 vehicles undoubtedly help alleviate the petroleum dependence of the world by using a renewable alternative fuel source.

10.6 ETHANOL VEHICLES

Fuel ethanol is most commonly used as a fuel for internal combustion, four-cycle, spark-ignition engines in transportation and agriculture. It can be used as a direct replacement for gasoline, or can be blended with gasoline as an extender and octane enhancer. The *research octane number (RON)* of ethanol is about 113 and, as such, ethanol blending enhances the octane rating of the fuel. The octane number is a quantitative measure of the maximum compression ratio at which a particular fuel can be utilized in an engine without some of the fuel-air mixture "knocking." By defining octane number of 100 for iso-octane and 0 for *n*-heptane, linear combinations of these two components are used to measure the octane number of a particular fuel. Therefore, a fuel with octane number of 90 would have the same ignition characteristics at the same compression ratio as a 90/10 mixture of iso-octane and *n*-heptane. It should be noted that there are several different rating schemes for octane numbers of fuels, namely, research octane number (RON), motor octane number (MON), and the average of the two ((R + M)/2). The RON, or F1, simulates fuel performance under low-severity engine operation, whereas the MON, or F2, simulates more severe operation that might be incurred at high speed or high load. Therefore, RON is nearly always higher in value than MON for the same fuel. In practice, the octane of a gasoline is reported as the average of RON and MON, or (R + M)/2.

The use of ethanol to replace gasoline requires modifications to the carburetor, fuel injection system components and, often, the compression ratio. Therefore, efficient and safe conversion of existing gasoline engines is a complex matter. Engines specifically designed and manufactured to operate on ethanol fuel, or predominantly ethanol fuel, will generally be more efficient than modified gasoline

engines. Ethanol concentrations of between 80 and 95% can be used as fuel, which eliminates the need for a cumbersome dehydration processing step, thus simplifying the distillation step. This complication comes from the fact that an ethanol-water solution makes an azeotropic mixture at 95.4% of ethanol (by mass), i.e., a maximum boiling mixture. In many cases, the conversion of engines for azeotropic ethanol operation may be simpler and more cost-effective than ethanol dehydration as an effort to produce 99+% purity ethanol.

In the U.S., *E85* is a federally designated alternative fuel that contains 85% ethanol and 15% gasoline. As of 2003, there are hundreds of thousands of E85 vehicles on the roads in the U.S. E85 vehicles are *flexible-fuel vehicles*, which can run on a very wide range of fuels, ranging from 100% gasoline to 85% ethanol; however, they run best on E85.[7] Nearly all the major automobile makers offer many models of passenger cars and sports utility vehicles (SUVs) with E85 engines.

In unmodified engines, ethanol can replace up to 20% of the gasoline. In the U.S., up to 10% blend of ethanol is quite popularly used. Blending ethanol with gasoline extends the gasoline supply, and improves the quality of gasoline by increasing its octane value as well as adding clean-burning properties of oxygenates. There are advantages to using gasoline–ethanol blends rather than pure (or very-high-concentration) ethanol. Blends do not require engine modification. Therefore, ethanol can be integrated rapidly with existing gasoline supply and distribution systems.

Even though the use of ethanol in specially designed two-cycle engines has been demonstrated on a number of occasions, it is not yet commercialized. One of the major issues has been in the fact that ethanol does not mix well with the lubricating oil typically used for such engines. Therefore, development of lubricating oils that are not affected by ethanol is an important step for this application.

Similarly, the use of ethanol in diesel-fueled engines is quite feasible but is not practiced much, because of a number of technical difficulties. These limitations are based on ethanol's inability to ignite in compression ignition engines and poor miscibility with diesel. However, ethanol can be used in supercharged diesel engines for up to about 25% of the total fuel, the rest preferably being diesel. This can be achieved by delivering ethanol from a separate fuel tank and injecting it into the diesel engine through a supercharger air stream. This mode of fuel delivery system may be called *dual fuel system* in comparison to blended fuel, which is delivered preblended from a single fuel tank. Ethanol can also replace aviation fuel in aircraft engines, even though this potential is not commercially exploited.

As a recent effort, a dual-fuel internal combustion engine technology has been developed and demonstrated, in which ethanol is used as a cofuel with acetylene, which is the principal fuel. The dual-fuel system has been very favorably demonstrated on modified gasoline and diesel engines originally designed for cars, trucks, fork lifts, tractors, and power generators. Up to 25% of ethanol in acetylene-based dual-fuel systems has been successfully tested. Ethanol was found to be very effective in eliminating knocking/pinging and lowering the combustion temperatures, thus reducing NO_x emissions.[8,9]

10.7 USE OF ETHANOL OTHER THAN AS RENEWABLE FUEL

In the presence of an acid catalyst (typically sulfuric acid) ethanol reacts with carboxylic acids to produce ethyl esters: the two largest-volume ethyl esters are ethyl acrylate (from ethanol and acrylic acid) and ethyl acetate (from ethanol and acetic acid).

Ethyl acetate is used as a common solvent used in paints, coatings, and in the pharmaceutical industry. The most familiar application of ethyl acetate in the household is as a solvent for nail polish. The typical reaction that synthesizes ethyl acetate is based on esterification:

$$C_2H_5OH + CH_3COOH = C_2H_5OOCCH_3 + H_2O$$

This chemical reaction very closely follows second-order reaction kinetics, and is often used as an example problem in chemical reaction engineering textbooks. Recently, Kvaerner Process Technology developed a process that produces ethyl acetate directly from ethanol without acetic acid or other cofeeds. Considering that both acetic acid and formaldehyde can also be produced from ethanol, this innovative process idea is not only understandable, but also quite significant. Further, the process elegantly combines both dehydrogenation and selective hydrogenation in its process scheme, thus producing hydrogen as a process by-product, which makes the process economics even better.

Ethyl acrylate, which is synthesized by reacting ethanol and acrylic acid, is a monomer used to prepare acrylate polymers for use in coatings and adhesives.

Ethanol is a reactant for ETBE, as is the case for methanol to MTBE. ETBE is produced by reaction between isobutylene and ethanol as:

$$C_2H_5OH + CH_3C(CH_3)=CH_2 \leftrightarrows C(CH_3)_3\,OC_2H_5$$

Vinegar is a dilute aqueous solution of acetic acid prepared by the action of *Acetobacter* bacteria on ethanol solutions. Ethanol is used to manufacture ethylamines by reacting ethanol and ammonia over a silica- or alumina-supported nickel catalyst at 150–220°C. First, ethylamine with a single amino group in the molecule is formed, and further reactions create diethylamine and triethyamine. The ethylamines are used in the synthesis of pharmaceuticals, agricultural chemicals, and surfactants.

Ethanol can also be used as feedstock to synthesize petrochemicals that are also derived from a petroleum source. Such chemicals include ethylene and butadiene, but are not limited to these. This option may become viable for regions and countries where petrochemical infrastructure is weak, but agricultural produce is vastly abundant. This is particularly true for the times when the petroleum price is very high. Ethanol can also be converted into hydrogen via a reforming reaction, i.e., chemical reaction with water at an elevated temperature, typically with the aid of a catalyst. Even though this method of generation may be economically less favorable than either steam reforming of methane or electrolysis, it can be used for special applications, where specialty demands exist, or where other infrastructure is lacking.

REFERENCES

1. National Corn Growers Association, homepage, http://www.ncga.com/WorldOfCorn/main/, 2005.
2. Shapouri, H., Duffield, J.A., and Graboski, M.S., Estimating the Net Energy Balance of Corn Ethanol, U.S. Department of Agriculture, Agricultural Economic Report Number 721, July 1995.
3. DeSpiegelaere, T., Energy Consumption in Fuel Alcohol Production for a Corn Wet Milling Process, IBIS 1992 Fuel Ethanol Workshop, Wichita, Kansas, June 1992.
4. Bradley, C. and Runnion, K., Understanding Ethanol Fuel Production and Use, Technical Paper #3, Understanding Technology Series, Volunteers in Technical Assistance (VITA), Arlington, VA, 1984.
5. Ethanol Production in Hawaii Report, http://www.state.hi.us/dbedt/ert/ethanol/ethano94.html, 1994.
6. Corn Refiners Association, homepage, http://www.corn.org/, 2005.
7. American Coalition for Ethanol, homepage, http://www.ethanol.org/, 2004.
8. Wulff, J.W., Hulett, M., and Lee, S., Internal Combustion System Using Acetylene Fuel, U.S. Patent No. 6,076,487, 2000.
9. Wulff, J.W., Hulett, M., and Lee, S., A Dual Fuel Composition Including Acetylene for Use with Diesel and Other Internal Combustion Engines, U.S. Patent No. 6,287,351, 2001.
10. Renewable Fuels Association Web site, http://www.ethanolrfa.org/industry/statistics, November 2005.
11. Office of Energy Efficiency and Renewable Energy, U.S. Department of Energy, http://www.ncga.com/public_policy/PDF/03_28_05ArgonneNatlLabEthanolStudy.pdf, 2005.
12. Spurr, M., Comments of the International District Energy Association on the NESCAUM Draft Model Rule on Generation Performance Standards, April 21, 1999, http://www.nescaum.org/pdf/energy_GPScommp/IntlDistrictEnergy.pdf [NESCAUM: Northeast States for Coordinated Air Use Management].
13. Dorland, W.A.N., *Dorland's Illustrated Medical Dictionary*, 30th ed., W.B. Saunders Company, Elsevier Health Sciences Division, Philadelphia, PA, 2003.

11 Ethanol from Lignocellulosics

Sunggyu Lee

CONTENTS

11.1 INTRODUCTION

Developing countries with characteristically weak economies and precarious industrial infrastructures have been seriously hit by the energy crisis. To fully tap the potential of fossil-based fuels and other new renewable sources, huge capital outlays are required that these countries do not have. The trend has thus been toward the small-scale utilization of resources. One area in which developing countries can succeed relatively quickly is fossil fuel supplementation with alternative fuels derived from food and agricultural crops such as sugarcane, cassava, maize, and sorghum. Although the focus has primarily been on the petroleum products as a primary source of transportation fuels, ethanol has attracted a great deal of attention all over the world as an alternative source to petrol or as a blend with petrol to reduce the consumption of petrol. In Brazil, all cars are run on either a 22 to 25% mixture of ethanol with gasoline or pure ethanol. In Brazil, the National Program of Alcohol, *PROALCOOL*, started in November 1975, was created in response to the first petroleum crisis of 1973. This program effectively changed the profile of transportation fuels in the country. For the period 1979–2004, about 5.4 million ethanol-powered cars were produced. In 1998, these ethanol-powered cars consumed about 2 billion gallons of ethanol per year and about 1.4 billion gallons of ethanol was additionally used for producing gasohol (22% ethanol and 78% gasoline) for other cars.[46] Brazil produces about 4 billion gallons of ethanol annually,[1] whereas the U.S produces just over 3.5 billion gallons (as of 2004). The U.S. production of ethanol is increasing very sharply. The Brazilian program has successfully demonstrated large-scale production of ethanol from sugarcanes and successful use of ethanol as a motor fuel.

Regarding the atmospheric concentrations of so-called greenhouse gases, the National Research Council (NRC), responding to a request from Congress and with funding from the U.S Department of Energy, emphasizes substantially increased research on renewable energy sources, improved methods of employing fossil fuels, energy conservation, and energy-efficient technologies.[28] The *Energy Policy Act* of 1992 (EPAct) was passed by Congress to reduce the nation's dependence on imported petroleum by requiring certain fleets to acquire alternative-fuel vehicles, which are capable of operating on nonpetroleum fuels. Alternative fuels for vehicular purposes, as defined by the Energy Policy Act, include ethanol, natural gas, propane, hydrogen, biodiesel, electricity, methanol, and p-series fuels.

It is not that the U.S. suffers from a lack of energy resources; it has plenty of coal and oil shale reserves, but it needs transportation fuels. The market for transportation fuels has been dominated by petroleum-based fuels until very recently. Gaddy[13] and his colleagues have worked on the biological production of liquid fuels from biomass and coal. They have found microorganisms that can produce ethanol

from biomass, convert natural gas into ethanol, and convert syngas from coal gasification into liquid fuels. These microorganisms, Gaddy says, are very energy efficient. The microbial process works at ordinary temperature and pressure and offers significant advantages over chemical processes for production of liquid fuels from coal. Naae (1990)[30] focuses on using a renewable resource, lignin, to recover a nonrenewable resource, oil. Lignins are produced in large quantities, approximately 250 billion pounds per year in the U.S., as by-products of the paper and pulp industry. As a consequence, the prices of some lignin products, such as lignosulfonates, are as low as 2 to 3 cents a pound.

11.1.1 Ethanol

Ethanol, C_2H_5OH, is one of the most significant synthetic oxygen-containing organic chemicals because of its unique combination of properties as a solvent, fuel, germicide, beverage, antifreeze, and especially because of its versatility as an intermediate to other chemicals. Ethanol is one of the largest-volume chemicals used in industrial and consumer products. The main uses for ethanol are as an intermediate in the production of other chemicals and as a solvent. As a solvent, ethanol is second only to water. Ethanol is a key raw material in the manufacture of plastics, lacquers, polishes, plasticizers, perfume, and cosmetics. The physical and chemical properties of ethanol are primarily dependent on the hydroxyl group, which imparts polarity to the molecule and also gives rise to intermediate hydrogen bonding. In the liquid state, hydrogen bonds are formed by the attraction of the hydroxyl hydrogen of one molecule and the hydroxyl oxygen of another.[18] This makes liquid alcohol behave as though it were largely dimerized. Its association is confined to the liquid state; in the vapor state it is monomeric.

11.1.2 Manufacture of Industrial Alcohol

Industrial alcohol can be produced either: (1) synthetically from ethylene, (2) as a by-product of certain industrial operations, or (3) by the fermentation of sugars, starch, or cellulose. There are two main processes for the synthesis of alcohol from ethylene. The earlier one (in the 1930s by Union Carbide) was the indirect hydration process, otherwise called the *strong sulfuric acid-ethylene process*, the *ethyl sulfate process*, the *esterification hydrolysis process*, or the *sulfation hydrolysis process*. The other synthetic process designed to eliminate the use of sulfuric acid is the direct hydration process. In the direct hydration process, ethanol is manufactured by reacting ethylene with steam. The hydration reaction is exothermic and reversible, i.e., the maximum conversion is limited by chemical equilibrium.

$$CH_2{=}CH_{2(g)} + H_2O_{(g)} \leftrightarrows CH_3CH_2OH_{(g)} \qquad \Delta H = -45 kJmol^{-1}$$

Only about 5% of the reactant ethylene is converted into ethanol per pass through the reactor. By selectively removing ethanol from the equilibrium product mixture and recycling the unreacted ethylene, it is possible to achieve an overall 95% conversion. Typical reaction conditions are 300°C, 6–7 MPa, and phosphoric (V) acid catalyst.

In addition to the direct hydration process, the sulfuric acid process, and fermentation routes to manufacture, several other processes have been suggested.[11,22,26,29] None of these have been successfully implemented on a commercial scale.

11.1.3 Fermentation Ethanol

Fermentation, one of the oldest and most widely practiced chemical processes known to humans, is used to make a variety of useful products and chemicals. At present, however, many of the products that can be produced by fermentation are also synthesized from petroleum feedstocks, often at lower costs. The future of the fermentation industry, therefore, depends on its ability to utilize the high efficiency and specificity of enzymatic catalysis to synthesize complex products and also on its ability to overcome variations in the quality and availability of the raw materials.

Ethanol can be derived by fermentation processes from any material that contains sugars or sugar precursors. The raw materials used in the manufacture of ethanol via fermentation are classified as sugars, starches, and cellulosic materials.[2] Sugars can be directly converted to ethanol, as discussed in detail in Chapter 10. Starches must first be hydrolyzed to fermentable sugars by the action of enzymes. Cellulose must likewise be converted to sugars, generally by the action of mineral acids (i.e., inorganic acids). Once the simple sugars are formed, enzymes from yeasts can readily ferment them to ethanol.

11.1.4 Sugars

The most widely used form of sugar for ethanol fermentation is the black-strap molasses, which contain about 30–40 wt% sucrose, 15–20 wt% invert sugars such as glucose and fructose, and 28–35 wt% of nonsugar solids. The direct fermentations of sugarcane juice, sugarbeat juice, beat molasses, fresh and dried fruits, sorghum, whey, and skim milk have been considered, but none of these could compete economically with molasses. As far as industrial ethanol production is concerned, sucrose-based substances such as sugarcane and sugarbeat juices offer many advantages, including their relative abundance and renewable nature. Molasses, the noncrystallizable residue that remains after the sucrose purification, has additional advantages: it is relatively inexpensive raw material, readily available, and already used for industrial ethanol production. Park and Baratti[34] have studied the batch fermentation kinetics of sugar beat molasses by *zymomonos mobilis*. This bacterium has several interesting properties that make it competitive with the yeasts, the most important being higher ethanol yields and specific productivity. However, when cultivated on molasses, *Z. mobilis* generally shows poor growth and low ethanol production in comparison to those in glucose media.[34] The low ethanol yield is explained by the formation of by-products such as levan and sorbital. Other components of molasses such as organic salts, nitrates, or the phenolic compounds could also be inhibitory for growth. Park and Baratti found that in spite of good growth and prevention of levan formation, the ethanol yield and concentration were not sufficient for the development of an industrial process.[34] Yeasts of the *saccharomyces* genus are mainly used in industrial processes. However,

there are continued efforts to develop mutant strains of *Z. mobilis* to avoid the costly addition of yeast extract.

11.1.5 Starches

The grains generally provide cheaper ethanol feedstocks, and the conversion is less expensive because they can be stored more easily than most sugar crops, which often must be reduced to a form of syrup prior to the storage. Furthermore, grain distillation produces a by-product that can be used for protein meal in the animal feeds.[41] Fermentation of starch from grains is somewhat more complex than sugars because the starch must first be converted to sugar and then to ethanol. The simplified equations for the conversion of starch to ethanol can be written as:

$$C_6H_{10}O_5 + H_2O \xrightarrow[\text{Fungal amylase}]{\text{Enzyme}} C_6H_{12}O_6 \xrightarrow{\text{Yeast}} 2C_2H_5OH + 2CO_2$$

As shown in Figure 11.1, in making grain alcohol, the distiller produces a sugar solution from feedstock, ferments the sugar to ethanol, and then separates the ethanol from water through distillation. A more detailed discussion can be found in Chapter 10.

Among the disadvantages of the use of grain are the fluctuations in its price. Whenever the price of grain falls, there is intense interest in the use of grain alcohol

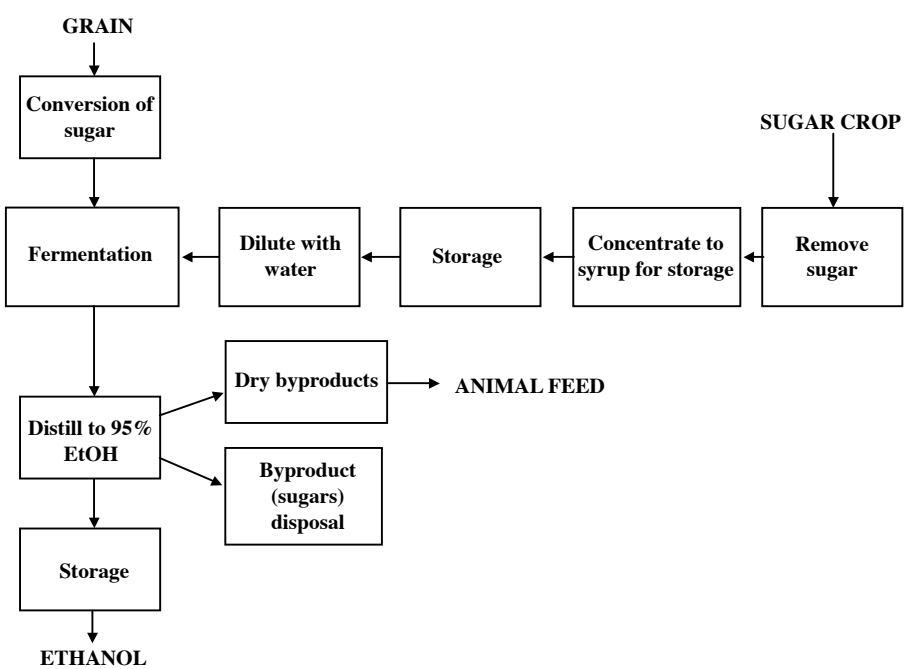

FIGURE 11.1 Synthesis of ethanol from grains and sugar crops. (From U.S. Congress, *Energy from Biological Processes*, Vol. 2, Office of Technology Assessment, Washington, D.C., 1980, 142–177.)

as an automotive fuel additive. Obviously, a very similar trend is also observed whenever petroleum crude price goes up. Ethanol in the petrol boosts the fuel's octane rating and also helps cleaner burning. More detailed discussions can be found in Chapter 10.

European farms produce more food than they can consume. Farmers and oil companies have been lobbying[9] in the European parliament for a scheme to blend petrol with 5% bioethanol. They insist that farmers grow energy crops so that alcohol can replace petrol. In Western Europe and the U.S., agricultural policies no longer concern themselves with the problem of producing enough food. Instead, they struggle with the problem of storing the food from increasingly abundant harvests. It costs them as much to store as it would to promote ethanol as a fuel. In producing ethanol from crops, the European Community may have several advantages over the U.S. and Japan. Europe has more land than Japan and unlike the U.S., there is no shortage of water. Furthermore, Europe now has the highest yields of grain in the world.

11.1.6 Alcohol without Pollution

Alfa-Laval's ethanol fermenter in Sweden has brewed 20,000 l of ethanol a day from surplus grain since 1983. In the 1990s, Alfa-Laval refined the *wide-gap heat exchanger* for ethanol plants, and set industry standards for a variety of processing equipment, from welded heat exchangers to wide-gap heat exchangers

All the products from Alfa-Laval's process, which runs continuously, are recovered and most are solids. The products include animal feed, bran, and CO_2. The company reports that this process does not pollute the environment, because it requires only a little amount of water to keep functioning.[9] A schematic flowsheet of the process system is shown in Figure 11.2. The process begins when the weak beer and the process water from the fermenter and the still are mixed with the ground grain. The starch of liquid feed is converted into fermentable sugars by the enzymes in large-sized stirred tank reactors. The reactors operate at a temperature of about 60 to 90°C. The effluent stream now consists of suspended solids and fibers. This stream is continuously fed to the fermenter. On its way to the fermenter, it heats up the fresh feed to the reactors, as an energy integration scheme. The air enters the reactor to enable growth of yeast. The beer is continuously removed from the fermenter by a process that keeps the level of beer in the fermenter at about 7% by volume. This constant concentration of ethanol helps prevent unwanted by-product formation and suppresses bacterial growth, obviating the need for feedstock pasteurization.

The beer from the fermenter passes through a sieve that removes the fibers. The fibers are washed and sent straight to the bottom part of the still, where steam removes any remaining ethanol. The beer then enters a centrifuge that removes the yeast and passes the cells back to the fermenter. The recycled yeast consumes significantly less sugar to stay alive and to grow than the fresh yeast.

Newly fermented beer passes through the still. A 40% solution of ethanol exits the top of the still and leaves the weak beer behind. The weak beer passes out of the side of the still, warms up the newly fermented one, and then moves to the start of the process. The weak beer is already pasteurized, which means it is better than the fresh water for mixing with the feedstock. Heat for the distillation comes from

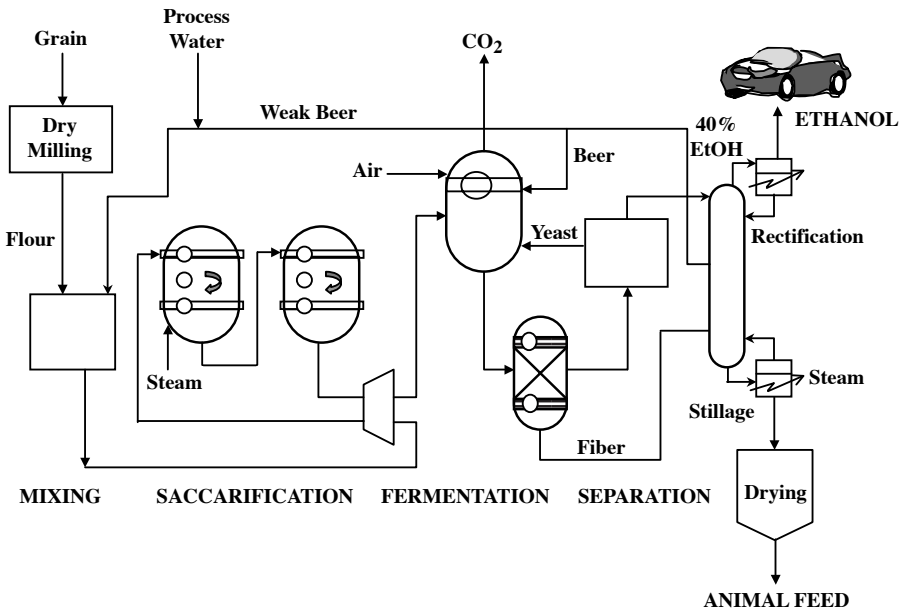

FIGURE 11.2 A flow sheet of Alfa-Laval's ethanol fermenter. (From de Groot, P. and Hall, D. *New Scientist*, 112, 1986, 50–55.)

the steam that cleans the ethanol from the fibers. The fibers (stillage) from the bottom of the still are passed to a dryer, which turns them into the animal feed. The dryer operates at 70°C, hot enough to dry the stillage and cool enough not to destroy the proteins in the fiber. The process is highly automated.

11.1.7 Cellulosic Materials

Cellulose from wood, agricultural residue, and waste sulfite liquor from pulp and paper mills must first be converted to *sugar* before it can be fermented. Enormous amounts of carbohydrate-containing cellulosic waste is generated every year throughout the world from agricultural production. The technology for converting this material into ethanol is available, but the stoichiometry of the process is unfavorable. About two thirds of the mass disappears during the conversion of cellulose to ethanol, most of it as CO_2 in the fermentation of glucose to ethanol. This amount of CO_2, rather than constituting a raw material credit, leads to a disposal problem. Another problem is that the aqueous acid used to hydrolyze the cellulose in wood to glucose and other simple sugars destroys much of the sugar in the process. New ways of reducing the cost of ethanol include the use of less corrosive acids and reduced hydrolysis time.[40]

The conversion of cellulosic wastes proceeds via a two-step process, i.e., *hydrolysis and fermentation.* The two steps are sequential. Regardless of whether the process is conducted on a batch or continuous basis, the two steps can be separated. Of the two steps, hydrolysis is more critical and rate determining, as in this process

cellulose is transformed into the glucose that is made available to the microbes responsible for the ethanol fermentation.

Among the several forms of *cellulose hydrolysis (saccharification),* the chemical and biological types are the most commonly applied. Because the actual hydrolysis is accomplished enzymatically, the biological hydrolysis is termed *enzymatic hydrolysis.* Although the use of enzymes avoids the corrosion problems and the loss of fuel product associated with acid hydrolysis, enzymes have their own drawbacks. Enzymatic hydrolysis slows as the glucose product accumulates in the reactor vessel. The end product inhibition eventually halts the hydrolysis unless some way is found to draw off the glucose as it is formed.

In 1978, Gulf Oil researchers[40] designed a commercial-scale plant producing 95×10^6 liters per year of ethanol by simultaneous enzymatic hydrolysis of cellulose and fermentation of resulting glucose as it is formed and overcoming the problem of product inhibition. The method consists of a pretreatment developed for this process that involves the grinding and heating of the feedstock followed by hydrolysis with a mutant bacterium, also specially developed for this purpose. Mutated strains of the common soil mold *Trichoderma viride* can process 15 times as much glucose as natural strains. Simultaneous hydrolysis and fermentation reduces the time requirement for the separate hydrolysis step, thus reducing the cost and increasing the yield. Also, the process does not use acids, which would increase the equipment costs. The sugar yields from the cellulose are about 80% of what is theoretically achievable, but the small amount of hemicellulose in the sawdust does not get converted.

11.2 CONVERSION OF AGRICULTURAL LIGNOCELLULOSIC FEEDSTOCKS

One reason that the world has depended so heavily up to now on natural gas and petroleum for energy and for the manufacture of most organic materials is that the gases and liquids are relatively easy to handle. Solid materials like wood, on the other hand, are difficult to collect, transport, and process into components that can make desired products for energy.

In simple terms, agricultural lignocellulose is inexpensive and renewable because it is made with the aid of solar energy. In addition, the quantity of biological materials available for conversion to fuel, chemicals, and other materials is virtually unlimited. Greater biomass utilization can also help ameliorate solid waste disposal problems. About 180 million tons of municipal waste is generated annually in the U.S. About 50% of this is cellulosic and could be converted to useful chemicals and fuels.[16]

Although lignocellulose is inexpensive, it is difficult to convert it to fermentable sugars. Furthermore, as shown in Figure 11.3, lignocellulose has a complex chemical structure with three major components, each of which must be processed separately to make the best use of high efficiencies inherent in the biological process. The three major components of lignocellulose are crystalline cellulose, hemicellulose, and lignin. A general scheme for the conversion of lignocellulose to ethanol is shown in Figure 11.4. The lignocellulose is pretreated to separate the xylose and, sometimes,

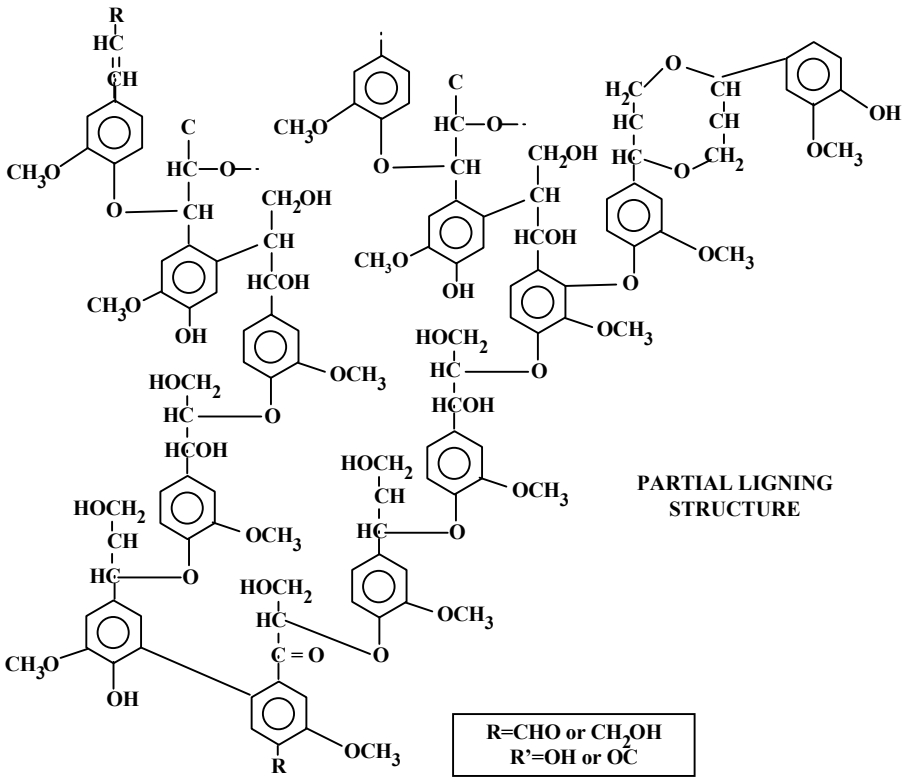

FIGURE 11.3 Major polymeric components of plant materials (C&EN., Sept. 10, 1990).

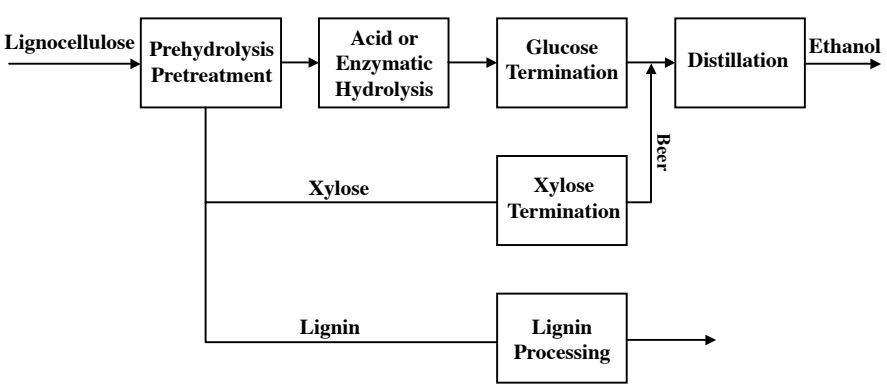

FIGURE 11.4 Conversion of lignocellulose to ethanol. (From Wright, J.D. *Chem. Eng. Prog.*, 84, 62–74, 1988.)

the lignin from the crystalline cellulose. The xylose can then be fermented to ethanol, and the lignin can be further processed to produce other liquid fuels. The crystalline cellulose, the largest (around 50%) and most difficult fraction, remains behind as a solid after the pretreatment and is sent to an enzymatic hydrolysis process that breaks

the cellulose down into glucose. Enzymes, the biological catalysts, are highly specific and, hence, the hydrolysis of cellulose to sugar does not further break down the sugars. Enzymatic processes are capable of achieving a nearly 100% yield. The glucose is then fermented to ethanol and combined with the ethanol from xylose fermentation. This dilute beer, i.e., an ethanol–water solution, is then concentrated to fuel-grade ethanol via distillation.

The hemicellulose fraction, the second major component at around 25%, is primarily composed of xylan, which is simple to convert to the simple sugar xylose; but the xylose is difficult to convert to ethanol. Methods have been identified using new yeasts, bacteria, and processes combining enzymes and yeasts. Although none of these fermentation processes are yet fully ready for commercial use, considerable progress has been made.

Lignin, the third major component of lignocellulose (around 25%), is a large, random phenolic polymer. In lignin processing, the polymer is broken down into fragments containing one or two phenolic rings. Extra oxygen and side chains are stripped from the molecules by catalytic methods and the resulting phenol groups are reacted with methanol to produce methyl aryl ethers. Methyl-aryl ethers are high-value octane enhancers that can be blended with gasoline.

11.2.1 Acid or Chemical Hydrolysis

Among the important specific factors in chemical hydrolysis are surface-to-volume ratio, acid concentration, temperature, and time. The surface-to-volume ratio is especially important in that it also determines the magnitude of the yield of glucose. Therefore, the smaller the particle size, the better the hydrolysis in terms of the extent and rate of reaction.[10] With respect to the liquid-to-solids ratio, the higher the ratio, the faster the reaction. A trade-off must be made between the optimum ratio and economic feasibility because the increase in the cost of equipment parallels the increase in the ratio of liquid to solids. For chemical hydrolysis, a ratio of *10:1* seems to be most suitable.[10]

In a typical system for chemically hydrolyzing cellulosic wastes, the wastes are milled to micron-sized particles. The milled material is immersed in a weak acid (0.2 to 10%), the temperature of the suspension is elevated to 180 to 230°C, and moderate pressure is applied. Eventually, the hydrolyzable cellulose is transformed into sugar. However, this reaction has no effect on the lignin that may be present. The yield of glucose varies depending on the nature of raw waste. For example, 84 to 86% of kraft paper or 38 to 53% of the weight of the ground refuse may be recovered as sugar. The sugar yield increases with the acid concentration as well as the elevation of temperature. A suitable concentration of acid (H_2SO_4) is about 0.5% of the charge.

A two-stage low-temperature and ambient-pressure acid hydrolysis process that utilizes separate unit operations to convert the hemicellulose and cellulose to fermentable sugars is being developed[12] and tested by the Tennessee Valley Authority (TVA) and the U.S. Department of Energy (DOE). Laboratory- and bench-scale evaluations showed more than 90% recovery and conversion efficiencies of sugar from corn stover. Sugar product concentrations of more than 10% glucose and 10%

xylose were achieved. The inhibitor levels in the sugar solutions never exceeded 0.02 g/100 ml, which is far below the level shown to inhibit fermentation. An experimental plant was designed and built in 1984. The acid hydrolysis plant provides fermentable sugars to a 38 l/h fermentation and distillation facility built in 1980. The results of their studies are summarized as follows:

- Corn stover ground to 2.5 cm was adequate for the hydrolysis of hemicellulose.
- The time required for optimum hydrolysis in 10% acid at 100°C was 2 h.
- Overall xylose yields of 86 and 93% were obtained in a bench-scale study at 1- and 3-h reaction times, respectively.
- Recycled leachate, dilute acid, and prehydrolysis acid solutions were stable during storage for several days.
- Vacuum drying was adequate in the acid concentration step.
- Cellulose hydrolysis was successfully accomplished by cooking stover containing 66 to 78% acid for 6 h at 100°C. Yields of 75 to 99% cellulose conversion to glucose were obtained in the laboratory studies.
- Vinyl ester resin fiberglass-reinforced plastics were used for construction of process vessels and pipings.

11.2.1.1 Process Description

The process involves two-stage sulfuric acid hydrolysis, relatively low temperature, and a cellulose prehydrolysis treatment with concentrated acid. Figure 11.5 is a flow diagram of the TVA process. Corn stover is ground and mixed with dilute sulfuric acid (about 10% by weight). The hemicellulose fraction of the stover is converted to pentose sugars by heating the solution to 100°C for 2 h in the first hydrolysis reactor. Raw corn stover contains, on a dry basis, about 40% cellulose, 25% hemicellulose, and 25% lignin. Sulfuric acid for the hydrolysis reaction is provided by recycling the product stream from the second hydrolysis step, which contains the sulfuric acid and hexose sugars. The pentose and hexose sugars, which are primarily xylose and glucose, respectively, are leached from the reactor with warm water. The sugar-rich leachate is then neutralized with lime, filtered to remove precipitated material, and fermented to produce ethanol.

Residue stover from the first hydrolysis step (hemicellulose conversion) is dewatered and prepared for the second hydrolysis step (cellulose conversion) by soaking (prehydrolysis treatment step) in sulfuric acid (about 20 to 30% concentration) from 1 to 2 h. The residue is then screened, mechanically dewatered, and vacuum-dried to increase the acid concentration to 75 to 80% in the liquid phase before entering the cellulose reactor. The second hydrolysis reactor operates at 100°C and requires a time of 4 h. The reactor product is filtered to remove solids (primarily lignin and unreacted cellulose). As the second hydrolysis reactor product stream contains about 10% acid, it is used in the first hydrolysis step to supply the acid required for hemicellulose hydrolysis. Residue from the reactor is washed to recover the remaining sulfuric acid and the sugar not removed in the filtration step.

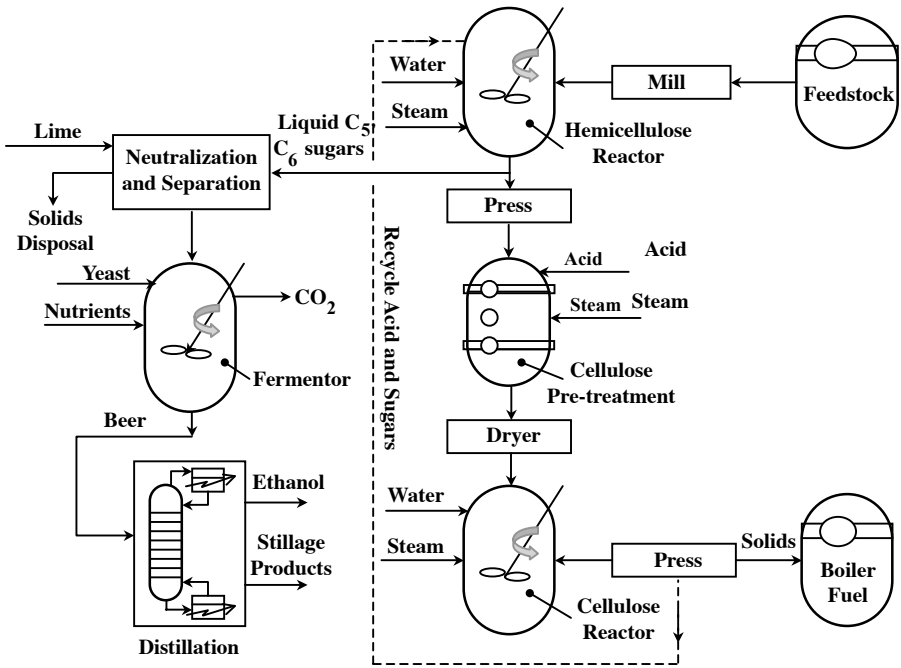

FIGURE 11.5 Low-temperature, low-pressure, two-stage acid hydrolysis concept for conversion of nonwoody feedstocks to ethanol. (Form Farina, G.E. et al., *Energy Sources*, 10, 231–237, 1988.)

Lignin is the unreacted fraction of the feedstock, which can be burned as a boiler fuel. It has a heating value of about 5270 kcal/kg, which is comparable to that of subbituminous coal. Other products, such as surfactants and adhesives, can be made from lignin. Stillage can be used to produce several products, including methane. Preliminary research has shown that 30 l of biogas containing 60% methane gas is produced from a liter of corn stover stillage. For each liter of ethanol produced, 10 l of stillage is produced.

All process piping, vessels, and reactors in contact with corrosive sulfuric acid are made of vinyl ester resin fiberglass-reinforced plastic. The dryer is made of carbon steel and lined with Kynar®, which is a trade mark of Archema (formerly, Atofina) for polyvinylidenefluoride. Conveyor belts are made of acid-resistant material. Mild steel agitator shafts are coated with Kynar® or Teflon® which is a DuPont trade mark for polytetrafluoroethylene. Heat exchangers are made with chlorinated polyvinylchloride (CPVC) pipe shells and Carpenter 20 stainless steel coils. Pumps are made with nonmetallic compound Teflon lining, or Carpenter 20 stainless steel. The two filter press units have plates made of polypropylene.

11.2.2 Enzymatic Hydrolysis

As a fermentable carbohydrate, cellulose differs from other carbohydrates generally used as substrate for fermentation. Cellulose is insoluble and is polymerized

as 1,4-β-glucosidic linkage. Cellulose is solubilized so that an entry can be made into cellular metabolic pathways. Solubilization is brought about by enzymatic hydrolysis catalyzed by the cellulase system of certain bacteria and fungi.

11.2.2.1 Enzyme System

Each cellulolytic microbial group has an enzyme system unique to it. The enzymes range from those that can hydrolyze only soluble derivatives of cellulose to those that can disrupt a cellulose complex. Based on the enzymatic capability, the cellulase is characterized into two groups: C_1 enzyme or factor, and C_X enzyme or factor.[10] The C_1 factor is regarded as an affinity or prehydrolysis factor that transforms cotton cellulose into linear and hydroglucose chains. Raw *cotton* is composed of 91% pure cellulose**.** As such, it serves as an essential precursor to the action of the C_X factor. The C_X (hydrolytic) factor breaks down the linear chains into soluble carbohydrates, usually cellobiose (a disaccharide) and glucose (a monosaccharide).

Microbes rich in C_1 are more useful in the production of glucose from the cellulose. Moreover, as the C_1 phase proceeds more slowly than the subsequent step, it is the rate-determining step. Among the many microbes, *Trichoderma reesei* surpasses all others in the possession of the C_1 complex. *Trichoderma reesei* is an industrially important cellulolytic filamentous fungus and is capable of secreting large amounts of cellulases and hemicellulases. The site of action of cellulolytic enzymes is important in the design of hydrolytic systems (the C_X factor). If the enzyme is within the cell mass, material to be reacted must diffuse into it. Therefore, enzymatic hydrolysis of cellulose usually takes place extracellularily, where enzyme is diffused from the cell mass into the external medium.

Another important factor in the enzymatic reaction is whether the enzyme is adaptive or constitutive. A *constitutive enzyme* is the one that is present in the cell all the time. *Adaptive enzymes* are found only in the presence of a given substance, and the synthesis of the enzyme is triggered by an inducing agent. Most of the fungal cellulases are adaptive.[2,10]

Cellobiose is an inducing agent with respect to *Trichoderma reesei*. In fact, depending on the circumstances, cellobiose can be either an inhibitor or an inducing agent. It is inhibitory when its concentration exceeds 0.5 to 1.0%. Cellobiose is an intermediate product and is generally present in concentrations low enough to permit it to serve as a continuous inducer.[42]

11.3 ENZYMATIC PROCESSES

All enzymatic processes consist of four major steps that may be combined in a variety of ways: *pretreatment, enzyme production, hydrolysis,* and *fermentation* as represented in Figure 11.6.

11.3.1 Pretreatment

It has long been recognized that some form of treatment is necessary to achieve reasonable rates and yields in the enzymatic hydrolysis of biomass. Pretreatment has

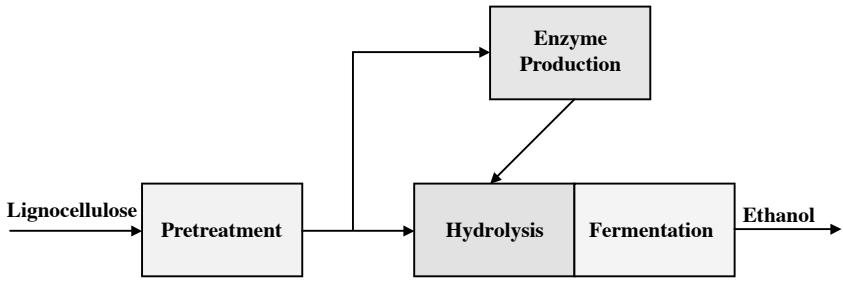

FIGURE 11.6 Fungal enzyme hydrolysis. (From Wright, J.D. *Chem. Eng. Prog.*, 84, 62–74, 1988.)

generally been practiced to reduce the crystallinity of cellulose, to lessen the average polymerization of the cellulose and the lignin–hemicellulose sheath that surround the cellulose, and to increase available surface area for the enzymes to attack.

Mechanical pretreatments such as intensive ball milling and roll milling have been investigated as means of increasing the surface area, but they require exorbitant amounts of energy. The efficiency of a chemical process can be understood by considering the interaction between the enzymes and the substrate. The hydrolysis of cellulose into sugars and other oligomers is a solid-phase reaction in which the enzymes must bind to the surface to catalyze the reaction. Cellulase enzymes are large proteins, with molecular weights ranging from 30,000 to 60,000 and are thought to be ellipsoidal with major and minor dimensions of 30 to 200 Å. The internal surface area of wood is very large, but only 20% of the pore volume is accessible to cellulase-sized molecules. By breaking down the hemicellulose–lignin matrix, hemicellulose or lignin can be separated and the accessible volume greatly increased. This removal of material greatly enhances enzymatic digestibility.

The hemicellulose–lignin sheath can be disrupted by either acidic or basic catalysts. Basic catalysts simultaneously remove both lignin and hemicellulose, but suffer large consumption of base through neutralization by ash and acid groups in the hemicellulose. In recent years attention has been focused on acidic catalysts. They can be mineral acids or organic acids generated *in situ* by autohydrolysis of hemicellulose.

Various types of pretreatments are used for biomass conversion. The pretreatments that have been studied in recent years are steam explosion autohydrolysis, wet oxidation, organosolv, and rapid steam hydrolysis (RASH). The major objective of most pretreatments is to increase the susceptibility of cellulose and lignocellulose material to acid and enzymatic hydrolysis. Enzymatic hydrolysis is a very sensitive indicator of lignin depolymerization and cellulose accessibility. Cellulose enzyme systems react very slowly with untreated material; however, if the lignin barrier around the plant cell is partially disrupted, then the rates of enzymatic hydrolysis are increased dramatically.

Most pretreatment approaches are not intended to actually hydrolyze cellulose to soluble sugars, but rather to generate a pretreated cellulosic residue that is more readily hydrolyzable by cellulase enzymes than native biomass. *Dilute acid hydrolysis* processes are currently being proposed for several near-term commercialization

ventures until lower-cost commercial cellulase preparations become available. Such dilute acid hydrolysis processes typically result in no more than 60% yields of glucose from cellulose.

11.3.1.1 Autohydrolysis Steam Explosion

The process is represented as shown in Figure 11.7. Very-high-temperature processes may lead to significant pyrolysis, which produces inhibitory compounds. The ratio of the rate of hemicellulose hydrolysis to that of sugar degradation is greater at higher temperatures. Low-temperature processes have lower xylose yields and produce more degradation products than a well-controlled high-temperature process using small particles.

In general, xylose yields in autohydrolysis are low (30 to 50%). An autohydrolysis system is used as the pretreatment in separate hydrolysis and fermentation (SHF). The reaction conditions are 200°C for 10 min, with a xylose yield of 35%.

Steam consumption in autohydrolysis is strongly dependent on the moisture content of the starting material. Wet feedstocks require considerably more energy because of the high heat capacity of water. An important advantage of autohydrolysis is that it breaks the lignin into relatively small fragments that can be easily solubilized in either base or organic solvents.

11.3.1.2 Dilute Acid Prehydrolysis

Lower-temperature operation with reduced sugar degradation is achieved by adding a small amount of mineral acid to the pretreatment process. The acid increases the reaction rates at a given temperature; also, the ratio of hydrolysis rate to degradation rate is increased.

A compromise between the reaction temperature and reaction time exists for acid-catalyzed reactions. As for autohydrolysis, however, operating conditions ranged from

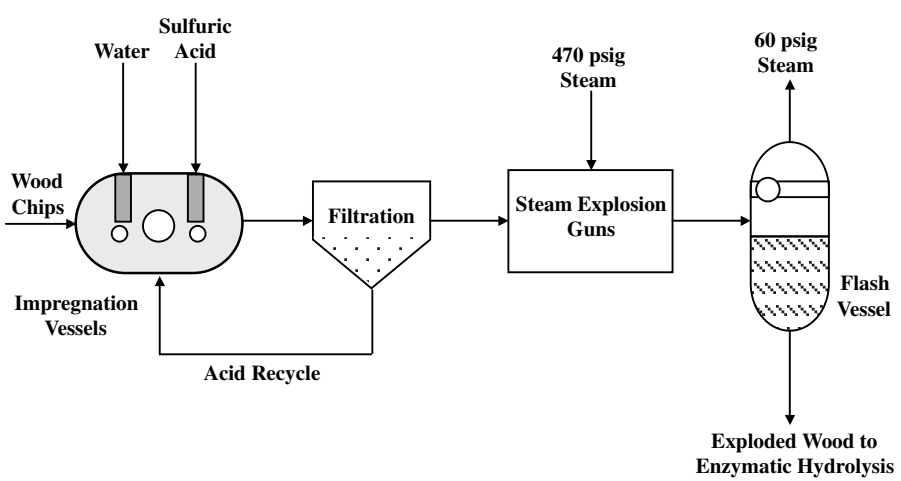

FIGURE 11.7 Steam explosion pretreatment process flow diagram. (From Wright, J.D. *Chem. Eng. Prog.*, 84, 62–74, 1988.)

several hours at 100°C to 10 sec at 200°C with sulfuric acid concentration of 0.5 to 4.0%. Acid catalysts have also been used in steam explosion systems with similar results. Xylose yields generally range from 70 to 95%. However, sulfuric acid processes produce lignin that is more condensed (52% of the lignin extractable in dilute NaOH) than that produced by autohydrolysis system. Sulfur dioxide has also been investigated as a catalyst to improve the efficiency of the pretreatments. Use of excess water increases energy consumption and decreases the concentration of xylose in the hydrolysate, thus decreasing the concentration of ethanol that can be produced in the xylose fermentation step. In a recent study by Ojumu and Ogunkunle,[47] production of glucose was achieved in batch reactors from hydrolysis of lignocellulose under extremely low acid (ELA) and high-temperature conditions by pretreating the sawdust by autohydrolysis *ab initio*.

11.3.1.3 Organosolv Pretreatment

In this type of pretreatment, an organic solvent (ethanol or methanol) is added to the pretreatment reaction to dissolve and remove the lignin fraction. In the pretreatment reactor, the internal lignin and hemicellulose bonds are broken and both fractions are solubilized, whereas the cellulose remains as a solid. After leaving the reactor, the organic fraction is removed by evaporation in the liquid phase, and the lignin precipitates and can be removed by filtration or centrifugation. Thus, this process cleanly separates the feedstock into a solid cellulose residue, a solid lignin that has undergone a few condensation reactions, and a liquid stream containing xylon, as shown in Figure 11.8.

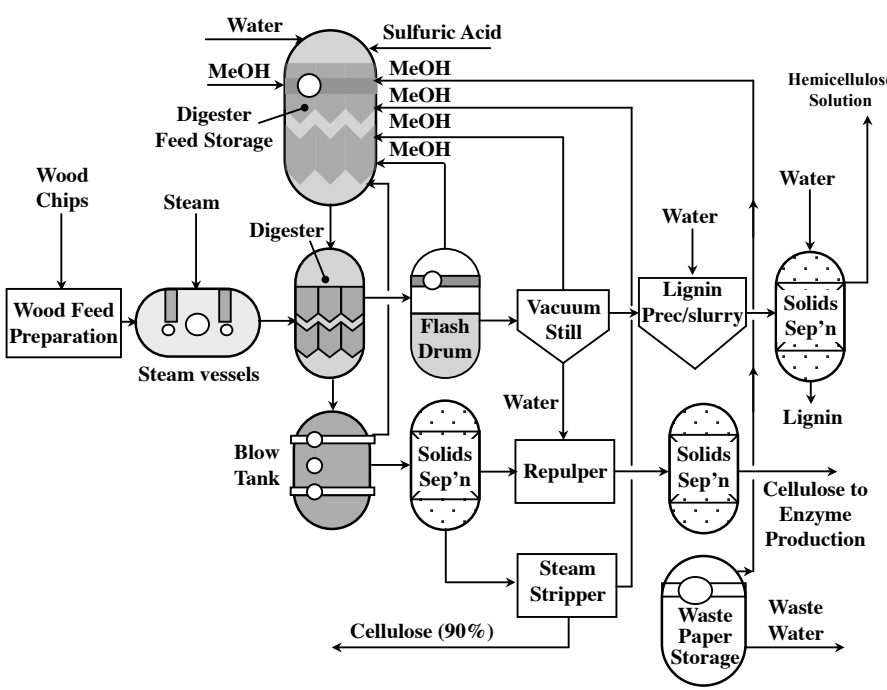

FIGURE 11.8 Organosolv pretreatment process. (From Wright, J.D. *Chem. Eng. Prog.*, 84, 62–74, 1988.)

Results have shown[36] that there are some reactions occurring during the Organosolv process that strongly affect the enzymatic rate. These reactions could be due to the physical or chemical changes in lignin or cellulose. In general, Organosolv processes have higher xylose yields than the other processes because of the influence of organic solvent on hydrolysis kinetics. However, a major concern in these processes is the complete recovery of the solvent, which affects the process economics.

11.3.1.4 Combined RASH and Organosolv Pretreatment

Attempts have been made to improve the overall process efficiency by combining the two individual pretreatments. Rughani and McGinnis[36] have studied the effect of a combined RASH–Organosolv process on the rate of enzymatic hydrolysis and the yield of solubilized lignin and hemicellulose. A schematic diagram of the process is shown in Figure 11.9. For the Organosolv pretreatment, the steam generator is disconnected and the condensate valve closed. The rest of the reactor setup is similar to the RASH procedure. The Organosolv processes at low temperature are generally ineffective in removing lignin; however, combining the two processes leads to increased solubilization of lignin and hemicellulose. RASH temperature is the major factor in maximizing the percentage of cellulose in the final product. The maximum yield of solubilized lignin was obtained at a temperature of 240°C for RASH and 160°C for the Organosolv process.

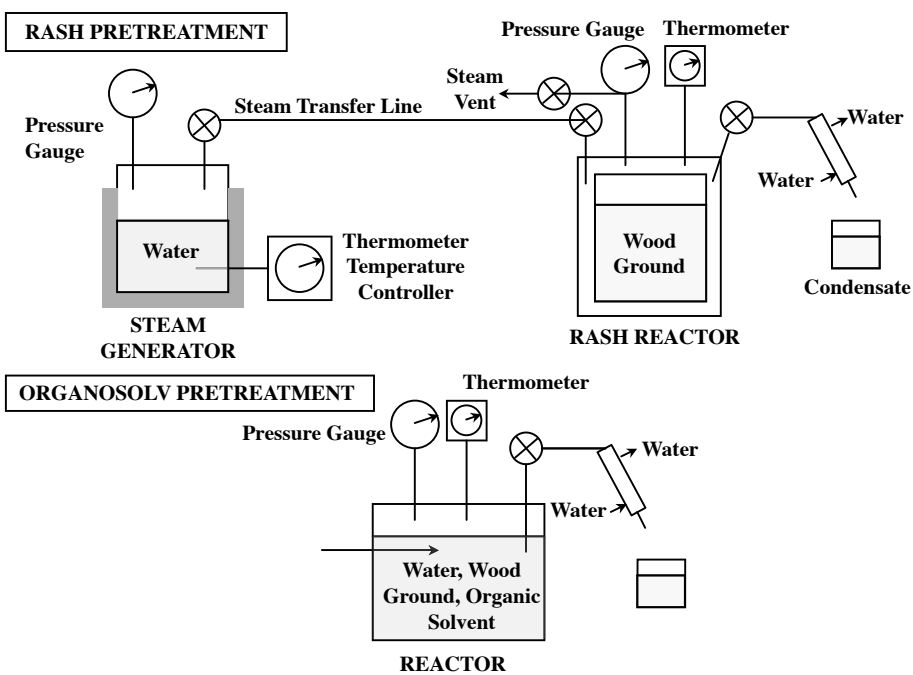

FIGURE 11.9 RASH and Organosolv pretreatment scheme. (From Rughani, J. and McGinnis, G.D., *Biotechnol. Bioeng.*, 33, 681–686, 1989.)

11.3.2 Enzyme Production and Inhibition

The enzyme of interest is the cellulase, which is needed for the hydrolysis of the cellulose. Cellulase is a multicomponent enzyme system consisting of: endo-β-1,4-glycanases; exo-β-1,4-glucan gluco hydrolases; and exo-β-1,4-glucan cellobiohydrolase. Cellobiose is the dominant product of this system but is highly inhibitory to the enzymes and is not usable by most organisms. Cellobiase hydrolyzes cellobiose to glucose, which is much less inhibitory and highly fermentable. Many of the fungi produce this, and most of the work that is presently going on is on *Trichoderma reesei* (viride). This cellulase is much less inhibited than other cellulases, which is a major advantage for industrial purposes.[20]

The type of inhibition exhibited by cellulases is the subject of much confusion. Although most researchers favor competitive inhibition,[5,6,17,31,32,37] some cellulases are noncompetitively[19,32,44] inhibited.[5] *Trichoderma reesei* enzyme on substrates like solka floc (purified cellulose), wheat straw, and bagasse (biomass remaining after sugarcane stalks are crushed to extract their juice) is competitively inhibited by glucose and cellobiose. On the other hand, some enzyme is noncompetitively inhibited by cellobiose, using other substrates like rice straw and avicel. *Trichoderma viride* is uncompetitively inhibited by glucose in a cotton waste substrate.[5]

Many mutants have been produced following *Trichoderma reesei*. The most prominent among these is the Rut C-30, the first mutant with β-glucosidase production.[45] 0ther advantages of the strain are that it is hyperproducing and is carbolite-repression resistant.

Cellulases from thermophilic bacteria have also been extensively examined. Among these, *Clostridium thermocellum* is perhaps the most extensively characterized organism; it is *an* anaerobic, thermophilic, cellulolytic, and ethanogenic bacterium capable of directly converting cellulosic substrate into ethanol. The enzymes isolated from thermophilic bacteria may have superior thermostability and hence will have longer half-lives at high temperatures. Although this is not always the case, cellulases isolated from *Clostridium thermocellum* have high specific activities,[3] especially against crystalline form of cellulose that have proved to be resistant to other cellulase preparations.

Enzyme production with *trichoderma reesei* is difficult because cellulase production terminates in the presence of easily metabolizable substrates. Thus, most production work has been carried out on insoluble carbon sources such as steam-exploded biomass or Solka-Floc®. In such systems, the rate of growth and cellulase production is limited because the fungi must secrete the cellulase and carry out slow enzymatic hydrolysis of the solid to obtain the necessary carbon. Average productivities have been approximately l00 IU/l/h (Hydrolytic activity of cellulose is generally in terms of international filter unit [IU]. This is a unit defined in terms of the amount of sugar produced per unit time from a strip of Whatman filter paper.) The filter paper unit is a measure of the combined activities of all three enzymes on the substrate. High productivities have been reported with *Trichoderma reesei* mutant in a fed-batch system using lactose as carbon source and steam-exploded aspen as an inducer. Although lactose is not available in quantities required to supply a large

ethanol industry, this does suggest that it may be possible to develop strains that can produce cellulases with soluble carbon sources such as xylose and glucose

Increases in productivities dramatically reduce the size and cost of the fermenters used to produce the enzyme. More rapid fermentations would also decrease the risk of contamination and might allow for less expensive construction. Alternatively, using a soluble substrate may allow simplification of fermenter design or allow the design of a continuous enzyme production system.

Low-cost but efficient enzymes for lignocellulosic ethanol technology must be developed to reduce the operational cost and improve the productivity of the process.

11.3.3 Cellulose Hydrolysis

11.3.3.1 Cellulase Adsorption

The enzymatic hydrolysis of cellulose proceeds by adsorption of cellulase enzyme on the lignacious residue as well as the cellulose fraction. The adsorption on the lignacious residue is an attractive factor from the viewpoint of the recovery of enzyme after the reaction and recycling it for use on the fresh substrate. Obviously, the recovery is reduced by the adsorption of enzyme on lignacious residue, an important consideration, because a large fraction of the total operating cost is due to the production of enzyme. As the capacity of lignacious residue to adsorb the enzyme is influenced by the pretreatment conditions, the pretreatment should be evaluated, in part, by how much enzyme adsorbs on the lignacious residue at the end of hydrolysis, as well as its effect on the rate and extent of the hydrolysis reaction.

The adsorption of cellulase on cellulose and lignacious residue has been investigated by Ooshima et al.[33] using cellulase from *Trichoderma reesei* and hardwood pretreated by dilute sulfuric acid with explosive decomposition. The cellulase was found to adsorb on the lignacious residue as well as on the cellulose during hydrolysis of the pretreated wood. A decrease in the enzyme recovery in the liquid phase with an increase in the substrate concentration has been reported owing to the adsorption on the lignacious residue. The enzyme adsorption capacity of the lignacious residue decreases as the pretreatment temperature is increased, whereas the capacity of the cellulose increases. The reduction of the enzyme adsorbed on the lignacious residue as the pretreatment temperature increases is important in increasing the ultimate recovery of the enzyme, as well as enhancing the enzyme hydrolysis rate and extent.

An enzymatic hydrolysis process involving solid lignocellulosic materials can be designed in many ways. The common features are that the substrates and the enzyme are fed into the process, and the product stream (sugar solution) along with a solid residue leaves it at various points. The residue contains adsorbed enzymes that are lost when the residue is removed from the system.

To ensure that the enzymatic hydrolysis process is economically efficient, a certain degree of enzyme recovery is essential. Both the soluble enzymes and the enzyme adsorbed onto the substrate residue must be reutilized. It is expected that the loss of enzyme is influenced by the selection of the stages at which the enzymes in the solution and adsorbed enzymes are recirculated and the point at which the residue is removed from the system. Vallander and Erikkson[43] defined an enzyme loss function, L, assuming that no loss occurs through filtration:

$$L = \frac{\text{The amount of enzyme lost through removal of residue}}{\text{The amount of enzyme at the start of hydrolysis}}$$

They developed a number of theoretical models, finally concluding that increased enzyme adsorption leads to increased enzyme loss. The enzyme loss decreases if the solid residue is removed late in the process. Both the adsorbed and dissolved enzymes should be reintroduced at the starting point of the process. This is particularly important for the dissolved enzymes. Washing of the entire residue is likely to result in significantly lower recovery of adsorbed enzymes than if a major part (60% or more) of the residue with adsorbed enzymes is recirculated. Uninterrupted hydrolysis over a given time period leads to a lower degree of saccharification than when hydrolysate is withdrawn several times. Saccharification is also favored if the residue is removed at a late stage. Experimental investigations of the theoretical hydrolysis models have recovered more than 70% of the enzymes.[43]

11.3.3.2 Mechanism of Hydrolysis

The overall hydrolysis is based on the synergistic action of three distinct cellulase enzymes, depending on the concentration ratio and the adsorption ratio of the component enzymes: endo-β-gluconases, exo-β-gluconases, and β-glucosidases. Endo-β-gluconases attack the interior of the cellulose polymer in a random fashion,[45] exposing new chain ends. Because this enzyme catalyzes a solid-phase reaction, it adsorbs strongly but reversibly to the microcrystalline cellulose (also known as *avicel*). The strength of the adsorption is greater at lower temperatures. This enzyme is necessary for the hydrolysis of crystalline substrates. The hydrolysis of cellulose results in a considerable accumulation of reducing sugars, mainly cellobiose, because the extracellular cellulase complex does not possess cellobiose activity. Sugars that contain aldehyde groups that are oxidized to carboxylic acids are classified as *reducing sugars*.

Exo-β-gluconases remove cellobiose units (two glucose units) from the nonreducing ends of cellulose chains. This is also a solid-phase reaction, and the exogluconases adsorb strongly on both crystalline and amorphous substrates. The mechanism of the reaction is complicated because there are two distinct forms of both endo- and exo-enzymes, each with a different type of synergism with the other members of the complex. As these enzymes continue to split off cellobiose units, the concentration of cellobiose in solution may increase. The action of exo-gluconases may be severely inhibited or even stopped by the accumulation of cellobiose in the solution.

The cellobiose is hydrolyzed to glucose by action of β-glucosidase. Glucosidase is any enzyme that catalyzes hydrolysis of glucoside. β-Glucosidase catalyzes the hydrolysis of terminal, nonreducing beta-D-glucose residues with release of beta-D-glucose. The effect of β-glucosidase on the ability of the cellulase complex to degrade avicel has been investigated by Kadam and Demain.[23]

They determined the substrate specificity of the β-glucosidase and demonstrated that its addition to the cellulase complex enhances the hydrolysis of avicel specifically by removing the accumulated cellobiose. A thermostable β-glucosidase form, *Clostridium thermocellum*, which is expressed in *Escherichia coli*, was used to

determine the substrate specificity of the enzyme. The hydrolysis of cellobiose to glucose is a liquid-phase reaction, and β-glucosidase absorbs either quickly or not at all on cellulosic substrates. The action can be slow or halted by the inhibitive action of glucose accumulated in the solution. The accumulation may also induce the entire hydrolysis to a halt as inhibition of the β-glucosidase results in a buildup of cellobiose, which in turn inhibits the action of exo-gluconases. The hydrolysis of the cellulosic materials depends on the presence of all three enzymes in proper amounts. If any one of these enzymes is present in less than the required amount, the others will be inhibited or will lack the necessary substrates to act upon.

The hydrolysis rate increases with increasing temperature. However, because the catalytic activity of an enzyme is related to its shape, the deformation of the enzyme at high temperature can inactivate or destroy the enzyme. To strike a balance between increased activity and increased deactivation, it is preferable to run fungal enzymatic hydrolysis at approximately 40 to 50°C.

Researchers at the National Renewable Energy Laboratory reported results for a dilute acid hydrolysis of softwoods in which the conditions of the reactors were as follows[52]:

1. Stage 1: 0.7% sulfuric acid, 190°C, and a 3-min residence time
2. Stage 2: 0.4% sulfuric acid, 215°C, and a 3-min residence time

Their bench-scale tests also confirmed the potential of achieving yields of 89% for mannose, 82% for galactose, and 50% for glucose, respectively. Fermentation with *Saccharomyces cerevisiae* achieved ethanol conversion of 90% of the theoretical yield.[53]

11.3.4 Fermentation

Cellulose hydrolysis and fermentation can be achieved by two different process schemes, depending on where the fermentation is carried out: (l) separate hydrolysis and fermentation (SHF) or (2) simultaneous saccharification and fermentation (SSF).

11.3.4.1 Separate Hydrolysis and Fermentation

In SHF, the hydrolysis is carried out in one vessel and the hydrolysate is then fermented in a second reactor. The most expensive items in the overall process cost are the cost of feedstock, enzyme production, hydrolysis, and utilities. The feedstock and utility costs are high because only about 73% of the cellulose is converted to ethanol in 48 h, whereas the remainders of the cellulose, hemicellulose and lignin, are burned. Enzyme production is a costly step because of the large amount of the enzyme used in an attempt to overcome the end product inhibition, as well as its slow rate of production. The hydrolysis step is also expensive, owing to the large capital and operating costs associated with large-size tanks and agitators. The most important parameters are the hydrolysis section yield, product quality, and the required enzyme loading, which are all interrelated. Yields are typically higher in more dilute systems, where inhibition of enzymes by glucose and cellobiose is minimized. Increasing the amount of enzyme loading can help overcome inhibition

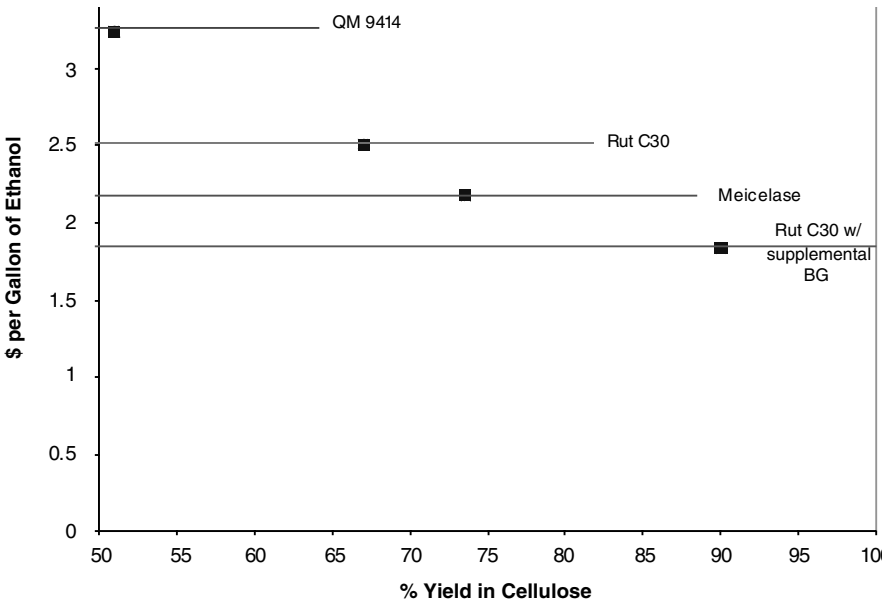

FIGURE 11.10 Effect of yield on selling price of ethanol (βG, β-Gluconase). (From Wright, J.D. *Chem. Eng. Prog.*, 84, 62–74, 1988.)

and increase yield and concentration. Increased reaction time also leads to higher yields and concentrations. Cellulase enzymes from different organisms can result in markedly different performances. Figure 11.10 shows the effect of yield at constant solid and enzyme loading and the performance of different enzyme loadings. Increase in enzyme loading beyond a particular point is of no value. It would be economical to operate at a minimum enzyme loading level, or the enzyme could be recycled by appropriate methods. As the cellulose is hydrolyzed, the endo- and exogluconase components are released back into the solution. Because of their affinity for cellulose, these enzymes can be recovered and reused by contacting the hydrolysate with fresh feed. The amount of recovery is limited because of β-glucosidase, which does not adsorb on the feed. Some of the enzyme remains attached to the lignin, and unreacted cellulose and enzymes are thermally denatured during hydrolysis. A major difficulty in this type of process is maintaining the sterility, which would otherwise be contaminated. The power consumed in agitation is also significant and does affect the economics of this process.[45]

11.3.4.2 Simultaneous Saccharification and Fermentation

The operating cost of this process is generally lower than that of SHF. As the name implies, both hydrolysis and fermentation are carried out in the same vessel. In this process, yeast ferments the glucose to ethanol as soon as the glucose is produced, preventing the sugars from accumulating and inhibiting the end product. Using the yeast, *Candida brassicae* and the Genencor enzyme (by Genencor International), the yield is increased to 79% and the ethanol concentration produced is 3.7%.[45]

Even in SSF, cellobiose (the soluble sugar) inhibition occurs to an appreciable extent. The enzyme loading for SSF is only 7 IU/g of cellulose, compared to 33 IU/g in SHF. The cost of energy and feedstock is somewhat reduced because of the improved yield, and the increased ethanol concentration significantly reduces the cost of distillation and utilities. The cost of SSF process is slightly less than the combined cost of hydrolysis and fermentation in the SHF process. The decreasing factor of the reactor volume due to the higher concentration of ethanol offsets the increasing factor in the reactor size caused by the longer reaction times (7 d for SSF vs. 2 d for hydrolysis and 2 d for fermentation). Experiments show that fermentation is the rate-controlling step and not the enzymatic hydrolysis process. The hydrolysis is carried out at 37°C and increasing the temperature increases the reaction rate; however, the ceiling temperature is limited by yeast cell viability. The concentration of ethanol is also a limiting factor. (This was tested by connecting a flash unit to the SSF reactor and removing the ethanol periodically. This technique showed higher productivities up to 44%.) Recycling the residual solids may also increase process yield. However, the most important limitation in enzyme recycling comes from the presence of lignin, which is inert to the enzyme. High recycling rates increase the fraction of lignin in the reactor and cause handling difficulties.

Two major types of enzyme-recycling schemes have been proposed, one in which enzymes are recovered in the liquid phase and the other in which enzymes are recovered by recycling unreacted solids.[45] Systems of the first type have been recommended for SHF processes, which operate at 50°C. These systems are favored at such a high temperature because increasing temperature increases the proportion of enzyme that remains in the liquid phase. Conversely, as the temperature is decreased, the amount of enzyme adsorbed on the solid increases. Therefore, at the lower temperatures encountered in SSF processes, solid recycling appears to be more effective.

11.3.4.3 Comparison between SSF and SHF Processes

SSF systems offer large advantages over SHF processes, thanks to their reduction of end product inhibition of the cellulase enzyme complex. The SSF process shows a higher yield (88% vs. 73%) and greatly increases product concentrations (equivalent glucose concentration of 10% vs. 4.4%). The most significant advantage is the enzyme loading, which can be reduced from 33 to 7 IU/g cellulose, and this cuts down the cost of ethanol appreciably. With constant development of low-cost enzymes, the comparative analysis of the two processes is in flux. A comparative study of the approximate costs of the two processes was reported in Wright's article.[45] The results show that based on the estimated ethanol selling price from a production capacity of 25,000,000 gallons per year, SSF is more cost-effective than SHF by a factor of 1:1.49, i.e., $\$_{SHF}/\$_{SSF} = 1.49$. It has to be clearly noted that the number quoted here is the ratio of the two prices, not the direct dollar value of the ethanol selling price.

From the very same process for economic reasons, it is anticipated that a hybrid hydrolysis and fermentation (HHF) process configuration is going to be widely accepted as a process of choice for production of lignocellulosic fuel ethanol, which begins with a separate hydrolysis step and ends with simultaneous saccharification (hydrolysis) and fermentation (SSF) step. In the first stage of hydrolysis,

higher-temperature enzymatic cellular saccharification takes place, whereas in the second stage of SSF, mesophilic enzymatic hydrolysis and biomass sugar fermentation occur simultaneously.

11.3.4.4 Xylose Fermentation

As xylose accounts for 30 to 60% of the fermentable sugars in hardwood and herbaceous biomass, it becomes an important issue to ferment it to ethanol. The efficient fermentation of xylose and other hemicellulose constituents is essential for the development of an economically viable process to produce ethanol from biomass. Xylose fermentation using *pentose yeasts* has proved to be difficult, owing to the requirement for O_2 during ethanol production, acetate toxicity, and production of xylitol as a by-product. Xylitol (or xyletol) is a naturally occurring low-calorie sugar substitute with anticariogenic (preventing production of dental caries) properties.

Other approaches to xylose fermentation include the conversion of xylose to xylulose (a pentose sugar that is a part of carbohydrate metabolism and is found in the urine in pentosuria[50]) using xylose isomerase prior to fermentation by *Saccharomyces cerevisiae* and the development of genetically engineered strains.[38]

The method of integrating xylose fermentation into the overall process is shown in Figure 11.11. The liquid stream is neutralized to remove any mineral acids or organic acids liberated in the pretreatment process and then sent to xylose fermentation. Water is added before the fermentation, if necessary, so that organisms can make full use of the substrate without having the yield limited by end-product inhibition. The dilute ethanol stream from xylose fermentation is then used to provide the dilution water for the cellulose-lignin mixture entering SSF. Thus, the water that enters during the pretreatment process is used in both xylose fermentation and the SSF process.

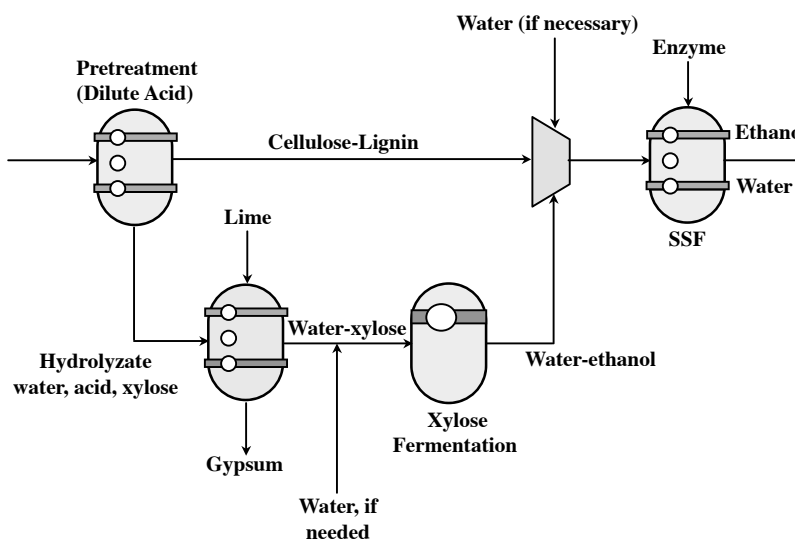

FIGURE 11.11 Integration of xylose fermentation and SSF. (From Wright, J.D. *Chem. Eng. Prog.*, 84, 62–74, 1988.)

The conversion of xylose to ethanol by recombinant *E. coli* has been investigated in pH-controlled batch fermentations.[4] Relatively high concentrations of ethanol (56 g/l) were produced from xylose with excellent efficiencies. In addition to xylose, all other sugar constituents of biomass can be efficiently converted to ethanol by recombinant *E. coli*.[4] Neither oxygen nor strict maintenance of anaerobic conditions is required for ethanol production by *E. coli*. However, the addition of base to prevent excessive acidification is essential. Although less base is needed to maintain low-pH conditions, poor ethanol yields and slower fermentations are observed below a pH of 6. Also, the addition of metal ions stimulates ethanol production. In general, xylose fermentation does not require precise temperature control, provided the broth temperature is maintained between 25 and 40°C. Xylose concentrations as high as 140 g/l have been positively tested to evaluate the extent to which this sugar inhibits the growth and fermentation. Higher concentrations considerably slow down growth and fermentation.

11.3.4.5 Ethanol Extraction during Fermentation

In spite of the considerable efforts given to the fermentative alcohols, industrial applications have been delayed because of the high cost of production, which depends primarily on the energy input to the purification of dilute end products and on the low productivities of cultures. These two points are directly linked to inhibition phenomena.

Along with the conventional unit operations, liquid–liquid extraction with biocompatible organic solvents, distillation under vacuum, and selective adsorption on the solids have demonstrated the technical feasibility of the extractive fermentation concept. Of late, membrane separation processes, which decrease biocompatibility constraints, have been proposed. These include dialysis,[25] and reverse osmosis.[14] More recently, the concept of supported liquid membranes has also been reported. This method minimizes the amount of organic solvents involved and permits simultaneous realization of the extraction and recovery phases. Enhanced volumetric productivity and high substrate conversion yields have been reported,[7] using a porous Teflon sheet as support (soaked with isotridecanol) for the extraction of ethanol during semicontinuous fermentation of *Saccharomyces bayanus*. This selective process results in ethanol purification and combines three operations: fermentation, extraction, and reextraction (stripping), as schematically represented in Figure 11.12.

11.4 LIGNIN CONVERSION

Lignin is produced in large quantities, approximately 250 billion pounds per year in the U.S., as by-products of the paper and pulp industry. Lignins are complex amorphous phenolic polymers, not sugar based, and hence cannot be fermented into ethanol. Lignin is a random polymer made up of phenyl propane units, where the phenol unit may be either a guaiacyl or syringyl unit (Figure 11.13). These units are bonded together in many ways, the most common of which are α- or β-ether linkages. A variety of C–C linkages are also present, but are less common (Figure 11.14). The distribution of linkage in lignin is random because lignin formation is a free

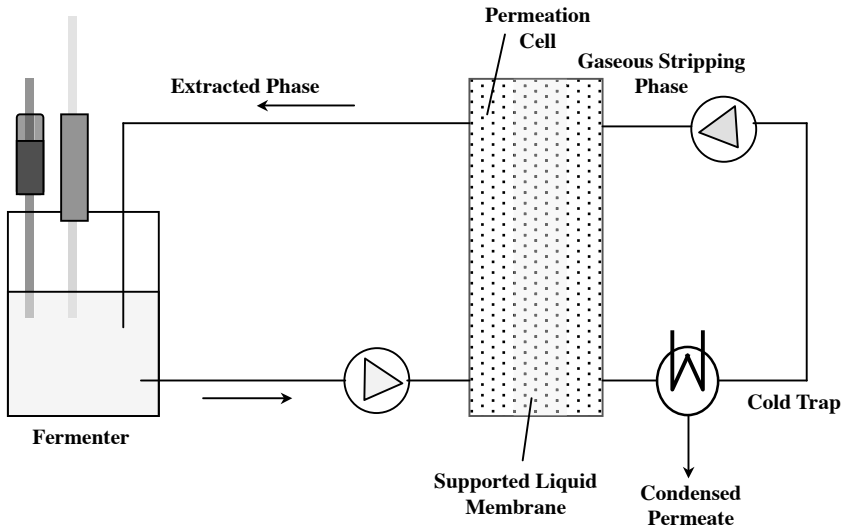

FIGURE 11.12 Extractive fermentation system: (1) fermenter, (2) permeation cell, (3) supported liquid membrane, (4) extracted phase, (5) gaseous stripping phase, (6) cold trap, (7) condensed permeate. (From Christen, P. et al., *Biotechnol. Bioeng.*, 36, 116–123, 1990.)

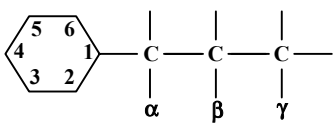

PHENYLPROPANE UNIT

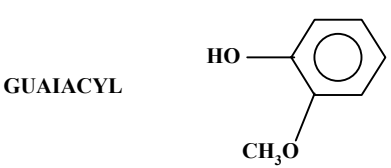

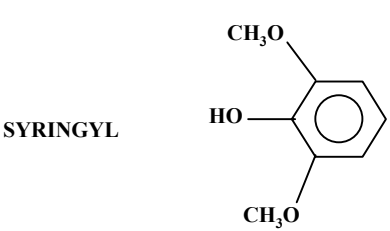

FIGURE 11.13 Monomer units in lignin. (From Wright, J.D. *Chem. Eng. Prog.*, 84, 62–74, 1988.)

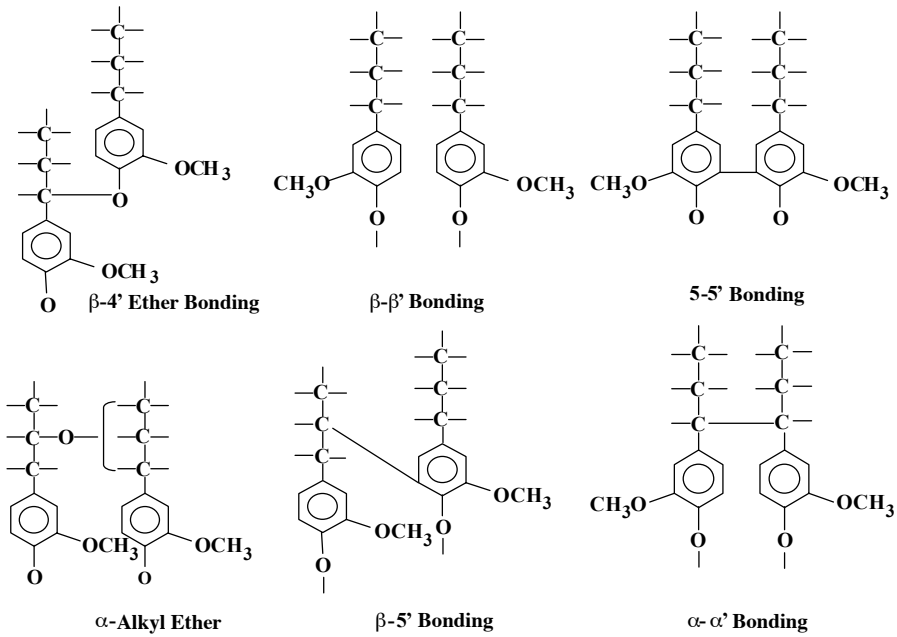

FIGURE 11.14 Ether and C–C bonds in lignin. (From Wright, J.D. *Chem. Eng. Prog.*, 84, 62–74, 1988.)

radical reaction that is not under enzymatic control. Lignin is highly resistant to chemical, enzymatic, or microbial hydrolysis, owing to extensive cross-linking. Therefore, lignin is frequently removed simply to gain access to cellulose.

Lignin monomer units are similar to gasoline, which has a high octane number; thus, breaking the lignin molecules into monomers and removing the oxygen makes them useful as liquid fuels. The process for lignin conversion consists of mild hydrotreating to produce a mixture of phenolic and hydrocarbon materials, followed by reaction with methanol to produce methyl aryl ether. The first step usually consists of two parts: (1) hydrodeoxygenation (removal of oxygen and oxygen-containing groups from the phenol ring) and (2) dealkylation (removal of ethyl or large side chains from the rings). One must be careful in carrying out these reactions to remove the unwanted chains without carrying the reaction too far, which would lead to excessive consumption of hydrogen and produce saturated hydrocarbons, which are not as good octane enhancers as the aromatic compounds. Catalysts that carry out these reactions have dual functions. Metals such as molybdenum and molybdenum/nickel catalyze the deoxygenation, whereas the acidic alumina support promotes the carbon–carbon bond cleavage.

Although lignin chemicals have many applications such as in drilling muds, as binders for animal feed, and as the base for artificial vanilla, they have not been previously used as surfactants for oil recovery. According to Naae,[30] lignin chemicals can be used in two ways in chemical floods for enhanced oil recovery. In one method, lignosulfonates are blended with tallow amines and conventional petroleum sulfonates

to form a unique mixture that costs about 40% less to use than chemicals made solely from petroleum or petroleum-based products. In the second method, lignin is reacted with hydrogen or carbon monoxide to form a new class of chemicals called lignin phenols. These phenols, because they are soluble in organic solvents, but not in water, are good candidates for further conversion to chemicals useful in enhanced oil recovery.

11.5 COPRODUCTS

To reduce ethanol production cost, it is imperative to expand the market for the process coproducts. Unlike the mature corn ethanol industry, the by-product (or coproduct) industry for lignocellulosic ethanol industry is not yet very well defined or established. Potential coproducts include hemicellulose hydrolysate (xylose), cellulose hydrolysate (glucose of mixed sugars), cell mass, enzymes, soluble and insoluble lignins, solid residues, etc.

11.6 ENERGY BALANCE FOR ETHANOL PRODUCTION FROM BIOMASS

Biomass process development depends on the economics of the conversion processes, be it chemical, enzymatic, or a combination of both. A number of estimates have been computed based on existing or potential technologies. One obvious factor is that, regardless of the process, transportation of the biomass material from its source to the site of conversion must be kept to an absolute minimum. Approximately 35% of the expected energy is consumed in transporting the substrate a distance of 15 mi.[3] This considerable expenditure of energy just to transport the starting material dictates that any conversion plant be of moderate size in close proximity to the production source of the starting material.

There are some objections to the production and use of ethanol as a fuel. Most important is the criticism that producing ethanol can consume more energy than is present in finished ethanol. The European analysis takes wheat as the feedstock and includes estimates of the energy expended in growing the wheat, transporting it to the distillery, making the alcohol, and transporting it to a refinery for blending with petrol. It allows credit for by-product, such as animal feed from wheat, for savings on petrol that comes from replacing 5% with alcohol, and from the energy gained from the increase of 1.25 octane points. Yet, to confine debates on biomass fuels solely to energy balance is misleading. At least 13 plants of a variety of designs, like the Swedish one, are working or are under construction in Europe, South America, and Asia.[9]

The greatest opposition to bioethanol, not surprisingly, comes from the oil industry, where the preference is to produce low-octane petrol together with octane boosters based on oil. This would reduce the investment needed at the refinery. They would also sell more petrol because the reduction of 1 octane point increases a car's fuel consumption by 1 to 1.5%.[9]

Energy requirements to produce ethanol from different crops were evaluated by Da Silva et al.[8] The industrial phase is always more energy intensive, consuming from 60 to 75% of the total energy. The energy expended in crop production includes

all the forms of energy used in agricultural and industrial processing, except the solar energy that plants use for growth. The industrial stage, including extraction and hydrolysis, alcohol fermentation, and distillation, requires about 6.5 kg of steam per liter of alcohol. It is possible to furnish the total industrial energy requirements from the by-products of some of the crops. Thus, it is also informative to consider a simplified energy balance in which only agricultural energy is taken as input and only ethanol is taken as the output, the bagasse supplying energy for the industrial stage, for example. Furthermore, it is often very difficult, or nearly impossible, to compare data associated with different technologies, because of the wide variety of feedstock crops as starting lignocellulose. Therefore, the U.S. Department of Energy–sponsored projects chose corn stover as the model feedstock.[49] This selection is based on the fact that corn stover is the most abundant and concentrated biomass resource in the U.S., and its collection can leverage the existing corn ethanol infrastructure, including corn harvesting and ethanol production.[49]

There have been several energy analyses for ethanol production from food crops, and they have been characterized by confusion. For example, results from Brazil show that sugarcane has a very favorable energy balance for ethanol production.[8] In contrast, at Iowa State University,[35] it was concluded: "It cannot be claimed that ethanol fermentation produces energy, the opposite is instead true." The dichotomous nature of these analyses shows the need for more site-specific studies. It is also important to resolve this matter as the very existence of alcohol plants in some countries could be threatened.

The energy balance results in Zimbabwe have shown that the energy ratio is 1.52 if all the major outputs are considered, and 1.15 if ethanol is considered as the only output. The reported values of the net energy ratio in Brazil[8] is 2.41 and in Louisiana[21] is 1.85. The low ratio in Zimbabwe is due to: (1) the large energy input in the agricultural phase, arising from a large fertilizer need and (2) the large fossil-based fuel consumption in the sugarcane processing.

Generally speaking, the cost of production of ethanol decreases with an increase in capacity of the production facility. However, the minimum total cost corresponds to a point of inflection, at which point an increase in the production cost for every increase in the plant capacity is seen. The possibility of existence of an empirical relationship between the plant size or output and the production costs has also been examined using various production functions and the computed F values at level of significance taken as 5%.[15] It is also conceivable that if the average distance of raw material transportation and acquisition becomes excessively long owing to the increased plant capacity, then the production cost can be adversely affected by the plant size.

Xylose fermentation is being carried out by bacteria, fungi, yeast, or enzyme-yeast systems. This would reduce the cost by 25% or more in the case of herbaceous-type materials. Efforts are being made to achieve the yield of 100% and an increased ethanol concentration.

Lignin, another major component of the biomass, accounts for the large energy contents of biomass because it has much higher energy per pound than the carbohydrates. As it is a phenolic polymer, it cannot be fermented to sugar and converted to materials like methyl-aryl ethers, which are compatible with gasoline as a high-octane

enhancer. The combination of the preceding processes has the potential to produce fuels for a competitive price.

11.7 PROCESS ECONOMICS AND STRATEGIC DIRECTION

McAloon et al.[51] studied the cost of ethanol production from lignocellulosic materials in comparison to that from corn starch. As correctly pointed out in their study, the cost comparison was made between the mature corn-ethanol industry and the emerging lignocellulosic ethanol industry. Based on the fixed price of year 2000, the cost of fuel ethanol production from lignocellulose processes was determined to be \$1.50/gal, whereas that from corn processes was \$0.88/gal.[89] Needless to say, the cost values determined in year 2000 cannot be considered to be still valid for the current year because of significant changes during the period in infrastructural costs as well as variable operating costs.

To make the lignocellulosic biorefinery technology a success, the following must be resolved:

1. Lignocellulose feedstock and delivery system has to be established on an economically sound basis.
2. Each step of the process technology needs to be separately investigated for various options, and the interactions and connectivity between the steps must be completely evaluated.
3. An exhaustive database for a variety of different feedstocks must be established. For issue 2, the idea of model feedstock such as corn stover is a very good idea. A different feedstock can be chosen as a model feedstock for different countries and regions, depending on local availability and infrastructural benefits. Further, conversion technologies should be adaptable to other lignocellulosic feedstocks and agricultural residues.[87]
4. Large-scale demonstration is crucially important for commercial operational experience as well as for minimized risk involved in scale-up efforts. Further, such an operation on a large scale helps demonstrate environmental life cycle benefits.
5. Low-cost but efficient enzymes for the technology must be developed to reduce operational cost and improve productivity. Current efforts by Genencor International and Novozymes Biotech are very significant and noteworthy in this regard.

REFERENCES

1. Web site http://www.earth-policy.org/Updates/2005/Update49_data.htm.
2. Bailey, J.E. and Ollis, D.F., *Biochemical Engineering Fundamentals*, 2nd ed., McGraw-Hill, New York, 1986.
3. Batt, C.A., Moses, V., and Cape, R.E., *Biotechnology, The Science and The Business*, Harwood Academic, Chur, Switzerland, 1991, pp. 521–536.

4. Beall, D.S., Ohta, K., and Ingram, L.O., Parametric studies of ethanol production from xylose and other sugars by recombinant Escherichia coli, *Biotechnol. Bioeng.*, 38, 296–303, 1991.
5. Beltrame, P.L., Carniti, P., Focher, B., Marzetti, A., and Sarto, V., Enzymatic hydrolysis of cellulosic materials: a kinetic study, *Biotechnol. Bioeng.*, 26, 1233–1238, 1984.
6. Blotkamp, P.J., Takagi, M., Pemberton, M.S., and Emert, G.H., *Biochemical Engineering: Renewable Sources of Energy and Chemical Feedstocks*, Nystrom, J.M. and Barnett, S.M., Eds., AICHE Symposium Series No.181, 74, AICHE, New York, 1978.
7. Christen, P., Minier, M., and Renon, H., Ethanol extraction by supported liquid membrane during fermentation, *Biotechnol. Bioeng.*, 36, 116–123, 1990.
8. Da Silva, J.G., Serra, G.E., Moreira, J.R., Concalves, J.C., and Goldenberg, J., Energy balance for ethyl alcohol production from crops, *Science*, 201, 903–906, 1978.
9. de Groot, P. and Hall, D., Power from the Farmers, *New Scientist*, 112, 1986, pp. 50–55.
10. Diaz, L.F., Savage, G.M., and Golueke, C.G., Critical review of energy recovery from solid wastes, *CRC Crit. Rev. Environ. Control*, 14(3), 285–288, 1984.
11. Ellis, C., *Chemistry of Petroleum Derivatives*, Vol. 2, Reinhold Publishing Corp., New York, 1937.
12. Farina, G.E., Barrier, J.W., and Forsythe, M.L., Fuel alcohol production from agricultural lignocellulosic feedstocks, *Energy Sources*, 10, 231–237, 1988.
13. Gaddy, J.L., Renewable energy sources and improved methods of employing fossil fuels, *Proceedings of the 200th National Meeting of ACS*, in Symposium on Fuel Chemistry, Washington, D.C., August 1990.
14. Garcia, A., Lannotti, E.L., and Fischer, J.L., Butanol fermentation liquor production and separation by reverse osmosis, *Biotechnol. Bioeng.*, 28, 785–791, 1986.
15. Gladius, L., Some aspects of the production of ethanol from sugar cane residues in Zimbabwe, *Solar Energy*, 33(3/4), 379–382, 1984.
16. Goldstein, I.S., Department of Wood and Paper Science, North Carolina State University, *Chemical and Engineering News*, 68, 20, September 10, 1990.
17. Gonzales, G., Caminal, G., de Mas, C., and Santin, J.L., *J. Chem. Technol. Biotechnol.*, 44, 275, 1989.
18. Hodzi, D., *Hydrogen Bonding*, Pergamon Press, London, 1957.
19. Holtzapple, M.T., Caram, H.S., and Humphrey, A.E., The HCH-1 model of enzymatic cellulose hydrolysis, *Biotechnol. Bioeng.*, 26, 775–780, 1984.
20. Holtzapple, M.T., Cognata, M., Shu, Y., and Hendrickson, C., Inhibition of Trichoderma reesei cellulase by sugars and solvents, *Biotechnol. Bioeng.*, 38, 296–303, 1991.
21. Hopkinson, C.S. and Davy, J.W., Net energy analysis of alcohol production from sugarcane, *Science*, 207, 302–304, 1980.
22. Judice, C.A. and Pirkle, L.E., U.S. Patent No. 3,095,458, June 25, 1963, to Esso Research and Eng. Co.
23. Kadam, S. and Demain, A., Addition of cloned β-glucosidase enhances the degradation of crystalline cellulose by the clostridium thermocellum cellulase comolex, *Biochem. Biophvs. Res. Commun.*, 161(2), 706–711, 1989.
24. *Kirk-Othmer Encyclopedia of Chemical Technology*, 3rd ed., Vol. 9, John Wiley & Sons, 1978, pp. 342–351.
25. Kyung, K.H. and Gerhardt, P., Continuous production of ethanol by yeast "immobilized" in membrane-contained fermentor, *Biotechnol. Bioeng.*, 26, 252, 1984.
26. Lewis, W.K., U.S. Patent No. 2,045,785, June 30, 1936, to Standard Oil Dev. Co.
27. L'Italien, Y., Thibault, J., and Le Duy, A., Improvement of ethanol fermentation under hyperbaric conditions, *Biotechnol. Bioeng.*, 33, 471–476, 1989.

28. Long, J.R., More Energy Research Called for to Stem Oil, Climate Change Crises, *Chemical and Engineering News*, 68, 16–17, September 10, 1990.
29. Miller, S.A., *Ethylene and Its Industrial Derivatives*, Ernest Benn Std., London, 1969.
30. Naae, D.G., ACS Press Conference, 200th National Meeting of the ACS, August, 1990, Washington D.C., *Chemical and Engineering News*, 68, 17, September 10, 1990.
31. Ohmine, K., Ooshima, H., and Harano, Y., Kinetic study on enzymatic hydrolysis of cellulose by cellulase from Trichoderma viride, *Biotechnol. Bioeng.*, 25, 2041–2053, 1983.
32. Okazaki, M. and Young, M., Kinetics of enzymatic hydrolysis of cellulose: analytical description of mechanistic model, *Biotechnol. Bioeng.*, 20, 637–663, 1978.
33. Ooshima, H., Burns, D.S., and Converse, A.O., Adsorption of cellulase from Trichoderma reesei on cellulose and Lignacious residue in wood pretreated by dilute sulfuric acid with explosive decompression, *Biotechnol. Bioeng.*, 36, 446–452, 1990.
34. Park, S.C. and Baratti, J., Batch fermentation kinetics of sugar beet molasses by Zymomonas mobilis, *Biotechnol. Bioeng.*, 38, 304–313, 1991.
35. Reilly, P., Economics and Energy Requirements for Ethanol Production, Department of Chemical and Nuclear Engineering, Iowa State University, Ames, IA, 1978.
36. Rughani, J. and McGinnis, G.D., Combined rapid–steam hydrolysis and organosolv pretreatment of mixed southern hardwoods, *Biotechnol. Bioeng.*, 33, 681–686, 1989.
37. Ryu, D.Y. and Lee, S.B., Enzymatic hydrolysis of cellulose: determination of kinetic parameters, *Chem. Eng. Commun.*, 45, 119–134, 1986.
38. Sarthy, A., McConaughy, L., Lobo, Z., Sundstorm, A., Furlong, E., and Hall, B., Expression of the Escherichia coli xylose isomerase gene in Saccharomyces cerevisiae, *Appl. Environ. Microbiol.*, 53, 1996–2000, 1987.
39. Sperling, D., An analytical framework for siting and sizing biomass fuel plants, *Energy*, 9(11–12), 1033–1040, 1984.
40. Szamant, H., Big push for a biomass bonanza, *Chem. Week*, 122(14), 40, 1978.
41. U.S. Congress, *Energy from Biological Processes*, Vol. 2, Office of Technology Assessment, Washington, D.C., 1980, pp. 142–177.
42. Vallander, L. and Erikkson, K., Enzymatic hydrolysis of lignocellulosic materials: I. Models for the hydrolysis process — a theoretical study, *Biotechnol. Bioeng.*, 38, 35–138, 1991.
43. Vallander, L. and Erikkson, K., Enzymatic hydrolysis of lignocellulosic materials: II. Experimental investigations of theoretical hydrolysis process models for an increased enzvme recovery, *Biotechnol. Bioeng.*, 38, 139–144, 1991.
44. Wald, S., Wilke, C.R., and Blanch, H.W., Kinetics of the enzymatic hydrolysis of cellulose, *Biotechnol. Bioeng.*, 26, 221–230, 1984.
45. Wright, J.D., Ethanol from biomass by enzymatic hydrolysis, *Chem. Eng. Prog.*, 84, 62–74, 1988.
46. La Rovere, E. L., The Brazilian Ethanol Program: Biofuels for Transport, a paper presented at International Conference for Renewable Energies, Bonn, Germany, June 1–4, 2004. Presentation view graphs are available through http://www.renewables2004.de/ppt/Presentation4-SessionIVB(11-12.30h)-LaRovere.pdf.
47. Ojumu, T.V. and Ogunkunle, O.A., Production of glucose from lignocellulosic under extremely low acid and high temperature in batch process, auto-hydrolysis approach, *J. Appl. Sci.*, 5(1), 15–17, 2005.
48. Torget, R., Kim, J.S., and Lee, Y.Y., Fundamental aspects of dilute acid hydrolysis/fractionation kinetics of hardwood carbohydrates. 1. Cellulose hydrolysis, *Ind. Eng. Chem. Res.*, 39, 2817–2825, 2000.

49. Web site http://www.eere.energy.gov/biomass/pdfs/sugar_enzyme.pdf.
50. *The American Heritage® Stedman's Medical Dictionary*, 2nd ed., Houghton Mifflin Company, New York, 2004.
51. McAloon, A., Taylor, F., Yee, W., Ibsen, K., and Wooley, R., Determining the Cost of Producing Ethanol from Corn Starch and Lignocellulosic Feedstocks, Technical Report, NREL/TP-580-28893, National Renewable Energy Laboratory, Golden, CO, October 2000.
52. Torget, R., Milestone Completion Report: Process Economic Evaluation of the Total Hydrolysis Option for Producing Monomeric Sugars Using Hardwood Sawdust for the NREL Bioconversion Process for Ethanol Production, Internal Report, National Renewable Energy Laboratory, Golden, CO, 1996.
53. Nguyen, Q., Milestone Completion Report: Evaluation of a Two-Stage Dilute Sulfuric Acid Hydrolysis Process, Internal Report, National Renewable Energy Laboratory, Golden, CO, 1998.
54. C&EN, Vol. 68, Sept. 10, 1990.

12 Energy from Biomass Conversion

Sunggyu Lee

CONTENTS

12.1 INTRODUCTION

The term *biomass* is defined as "different materials of biological origin that can be used as a primary source of energy."[1,2] Merriam-Webster OnLine Dictionary[38] defines biomass as "plant materials and animal waste used especially as a source of fuel." An attractive aspect of biomass utilization is its renewability, which ultimately guarantees that the source will not be depleted. With plant and plant-derived materials, all energy is originally captured by photosynthesis. Going by these definitions of biomass, it can be safely said that energy from biomass has been exploited by humans for a very long time. The burning, or incineration, of biological substances such as wooden materials has long been used to provide warmth. It has been estimated that, in the late 1700s, approximately two thirds of the volume of wood removed from the American forest was for energy generation.[3] Because wood was one of the few renewable energy sources readily exploitable at the time, its use continued to grow. During the 1800s, single households consumed 70 to 145 m^3 of wood annually for heating and cooking.[4,5] A small percentage of the rural communities in the U.S. still use biomass for these purposes. Other countries such as Finland use the direct combustion of wood for a percentage of their total energy use.[6] Finland and the U.S. are not the only countries that use biomass consumption to supplement their total energy usage. In fact, the share of biomass energy in the total energy consumption of a country is far greater in African nations and many other developing countries. Table 12.1 shows the percentages of biomass consumption by several

TABLE 12.1
Biomass Utilization for Energy in Various Countries

Country	Energy from Biomass Utilization (%)
Austria	4.0
Belgium	0.2
Canada	3.0
Denmark	1.0
Ireland	13.0
New Zealand	0.4
Norway	4.0
Sweden	13.0
Switzerland	1.6
U.S.	2.8

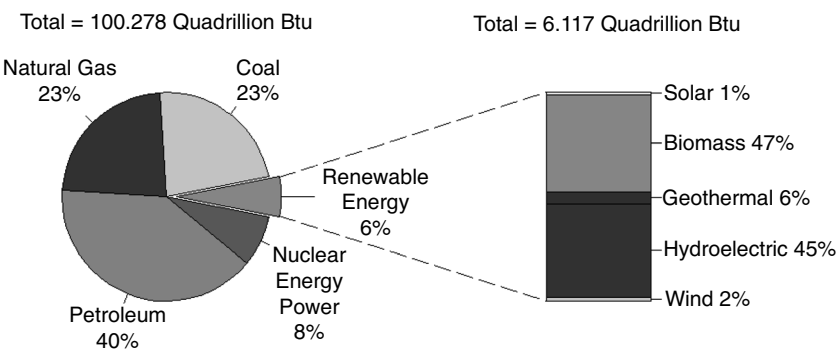

FIGURE 12.1 U.S. renewable energy consumption for the year 2004.

"developed" countries.[7] The data shown include all biomass consumption for energy generation, which includes, for example, corn for ethanol as well as wood for combustion.

On a larger scale, biomass is currently the primary fuel in the residential sector in many developing countries. For instance, it accounts for over 90% of total household use in the poorer countries of Africa and Central America[8] and 35% in Latin America and Asia.[9] The biomass resource may be in the form of wood, charcoal, crop waste, or animal waste. For these countries, its most critical function is cooking, with the other principal uses being lighting and heating. The dependence on biomass for critical energy supply for these countries is generally decreasing, whereas that for developed countries is strategically refocused.

Figure 12.1 shows a pie chart for U.S. renewable energy consumption in the national energy supply for the year 2004.[40] As shown, biomass accounts for about 2.8% of the total energy supply, which is the largest among all renewable energy sources.[40] This percentage also tops the hydroelectric contribution, and the gap between the two is expected to grow. Further, biomass consumption increased by

4%, or 105 trillion Btu, in 2004, whereas the total renewable energy consumption increased slightly less than 1%.[40] This faster rate of increase for biomass is attributed to rapid usage growth of fuel ethanol in transportation sectors owing to the phaseout of MTBE as well as regulatory demand of oxygenated fuel.

Although the direct combustion of charcoal and animal waste is extensively used in developing countries, this usage of biomass may not be generally considered "suitable" or "efficient" for direct energy applications.[10] There are three broad categories of biomass feedstocks that have been deemed suitable for energy production applications as well as for industrial processing:

1. Vegetable oils
2. Pure carbohydrates, such as sugar and starch
3. Heterogeneous "woody" materials, collectively termed *lignocelluloses*

Typically targeted fuel products from the preceding feedstocks are biodiesel and ethanol. The annual world production of biomass for these three categories is estimated at 146 billion metric tons. Approximately 80% of this amount is attributed to uncontrolled plant growth. Trees and farm crop wastes can produce 10 to 20 tons/acre/year of dry biomass. Certain genera of algae and grass can produce up to 50 metric tons/year of biomass, whose heating value is 5000 to 8000 Btu/lb.[11] This heating value per unit mass is lower than that for typical bituminous coal by about 30 to 50%. Compared to coal, however, fuel from biomass has essentially no or very little sulfur (0.1 to 0.2%) or ash content.[12,13] In addition, it does not add any significant net CO_2 to the atmosphere, because CO_2 is consumed for renewable generation of biomass.[14]

Meeting U.S. demands for oil and gas by the direct combustion of lignocellulose materials would require 6–8% of the land area of the 50 states to be cultivated solely for biomass production.[15] Although the direct combustion of biomass is not an efficient or economical alternative, the conversion of biomass feedstocks into a gaseous or liquid fuel is not only feasible, but also quite promising. Biomass could be used to replace the very large amounts of petroleum and natural gas currently consumed in the manufacture of primary chemicals in the U.S. annually. Especially for the countries that depend heavily on imported petroleum and petroleum products, this option may be even more valuable for both short- and long-term future. Among the sources of biomass that could be used for chemical production are grains and sugar crops for ethanol manufacture, oil seeds for oil extraction, soy beans for soy oil and soy alcohol, animal by-products and wastes, manure and sewage for methane generation, and wood and straw for biogas and liquid fuel generation. Biomass can be used for generation of synthesis gas (hydrogen and carbon monoxide) and hydrogen by pyrolysis or gasification. These options are becoming even more attractive owing to the very high market price of natural gas that has been prevailing in the 21st century. Significant R & D accomplishments have been made in Europe, especially in Germany and Sweden, through a variety of industrial efforts to generate syngas and liquid fuels. Many of these efforts have resulted in commercial-scale demonstration plants that are currently in operation. It is particularly noteworthy

that the efforts in Europe did not let up even when the petroleum and natural gas prices on the international market were stable and low.

Regardless of whether the biomass feedstock is from lignocellulose, crop waste, or animal waste, several factors must be addressed when considering a large-scale biomass program[16]:

1. Short- and long-term land availability
2. Productivities, species involved, and mixtures
3. Environmental sustainability
4. Social and socioeconomic factors
5. Economic feasibility
6. Ancillary benefits
7. Disadvantages and perceived problems

Although item 1 is primarily applicable to lignocellulose materials, all the remaining factors apply to each of the biomass feedstocks. Many of the disadvantages and perceived problems diminish if biomass energy is viewed as a long-term entrepreneurial opportunity.

Each of the aforementioned biomass feedstocks can be converted into a viable fuel by three primary routes. As indicated in Figure 12.2, these routes are categorized as thermal, biological, and extractive. Extraction processes, which supply oils for food and industrial uses, have been in commercial use for over 100 years. Therefore, conventional extraction processes will not be elaborated any further in this chapter. The following sections will therefore discuss the thermal and biological methods for the conversion of biomass to fuel.

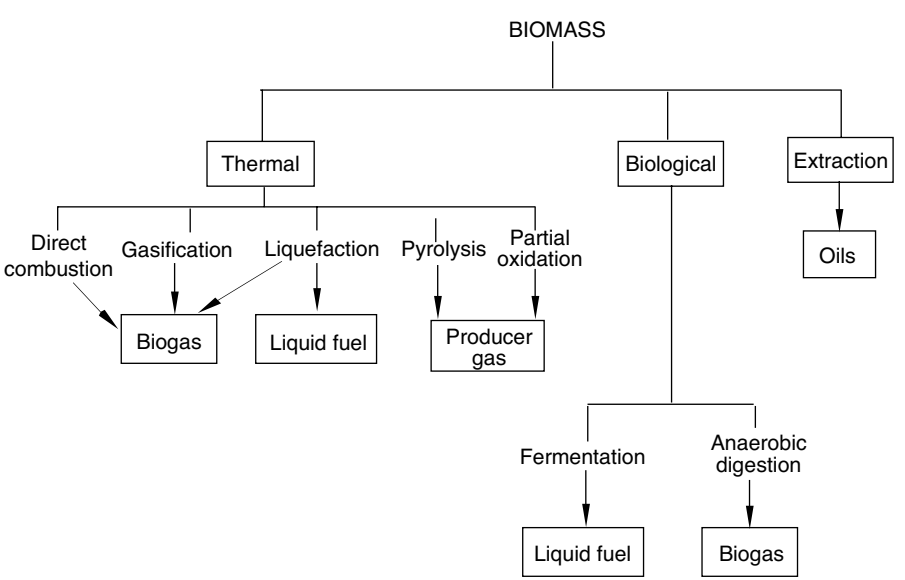

FIGURE 12.2 Conversion routes of biomass.

12.2 THERMAL CONVERSION

There are five thermal approaches that are commonly used to convert biomass into an alternative fuel: direct combustion, gasification, liquefaction, pyrolysis, and partial oxidation.

When biomass is heated under oxygen-deficient conditions, it generates synthesis gas, or syngas, which consists primarily of hydrogen and carbon monoxide. This syngas can be directly burned or further processed for other gaseous or liquid products. In this sense, thermal or chemical conversion of biomass is very similar to that of coal.

12.2.1 Direct Combustion

Indoor combustion of biomass fuels in unvented cooking and heating spaces has caused considerable health problems to the direct users, primarily the women and children of developing countries.[17] Biomass fuels, when used improperly in this manner, release considerable amounts of toxic or hazardous gases into the unvented area. These gases are, typically, carbon monoxide (CO), nitrogen oxides (NO_x), hydrocarbons, organics, aldehydes, and trace amounts of aromatics and ketones. As the moisture content of the wood increases, and as other biomass fuels of lower energy content (such as animal and crop waste) are used, the emissions increase. The woody components of biomass burn much more efficiently during complete combustion. In the earthen kilns of developing countries, the wood undergoes incomplete combustion, which causes the release of carbon monoxide, carbon dioxide, and nitrous oxide.

When the direct combustion of biomass is conducted in a well-vented area, biomass burning used for domestic stoves and boilers can be a sound substitute for combustion of conventional fossil fuel.[17] Sulfur emissions (0.05 to 0.2 wt%) are much lower and the formation of particulates can be controlled at the source.[18] On a larger scale, the biomass is reduced into fine pieces for combustion in a *close-coupled turbine*. In a close-coupled system, the turbine is separated from the combustion chamber by a filter. Energy Performance Systems Inc. of Minneapolis has demonstrated 87% efficiency with a close-coupled system using lignocellulose material. The company states that the process is feasible for 25 to 400 MW plants.[39]

Most electrical power generation systems are relatively inefficient, owing to the loss of a significant portion of energy, as much as half to two thirds, in a form of waste heat. If this heat is used efficiently for industrial manufacture, space heating, district heating, or other purposes, the overall efficiency can be greatly enhanced. Therefore, smaller biopower systems are more suitable for cogeneration-type processes than much larger counterparts.

12.2.2 Gasification

Gasification is not a new technology; however, its use for the conversion of biomass into a viable fuel has only been investigated for the past 30 years.[19,20] Production of syngas from biomass can be accomplished by basically two broad categories of the chemical and thermal processes, namely, catalytic routes and noncatalytic processes.

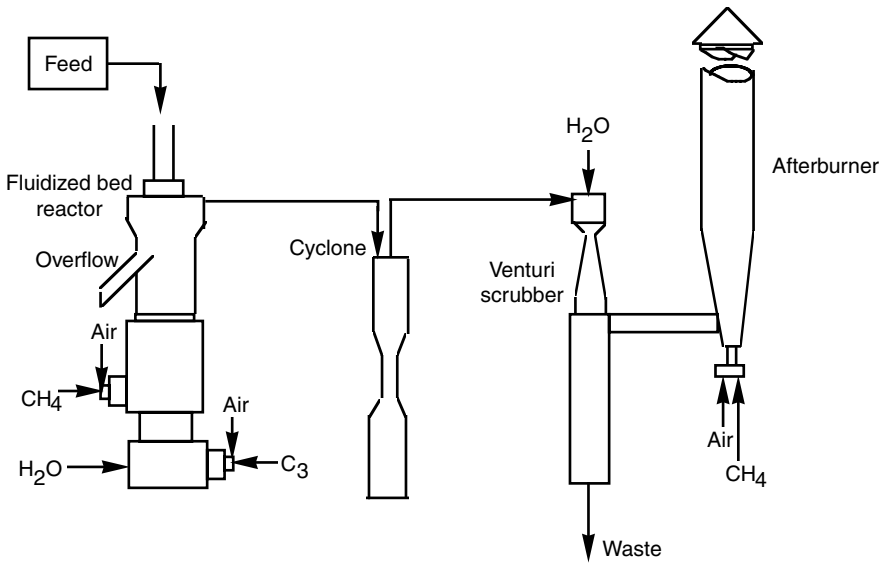

FIGURE 12.3 Pilot-plant fluidized bed for the gasification of corn stover.

Typically, noncatalytic processes require a very high temperature of operation, as high as 1300°C, whereas catalytic processes can be operated at substantially lower temperatures. With advances in catalysis, the temperature requirement is expected to go downward further from the current value of about 900°C.

The first system to be investigated at the pilot scale was a fluidized bed that incorporated dry ash-free (DAF) corn stover as the feed. Corn stover has been selected as the feed since 1977, when the annual production of "corn crop wastes" exceeded 300 million tons.[20] The corn stover, if treated properly, has the potential to be converted into an energy source that would supply up to 2% of the U.S. energy needs. The pilot-scale system, shown in Figure 12.3, has a 45.5-kg bed capacity.[21] Fluidizing gas and heat for the gasification were supplied by the combustion of propane in the absence of air. The particulates and char were removed using a high-temperature cyclone. A Venturi scrubber was then used to separate the volatile material into noncondensable gas, a tar-oil fraction, and an aqueous waste fraction. Raman et al.[21] conducted a series of tests with temperatures ranging from 840 to 1020 K. The optimal gas production was obtained using a feed rate of 27 kg/h and a temperature of 930 K. At these conditions, 0.25×10^6 BTU/h of gas was produced. This is enough to operate a 25-hp internal combustion engine operating at 25% efficiency.[21]

Another extensively studied gasification system for biomass conversion is Sweden's VEGA gasification system. Skydkraft AB, a Swedish power company, decided in June 1991 to build a cogeneration power plant in Vämamo, Sweden, to demonstrate integrated gasification combined cycle (IGCC) technology. Bioflow was formed in 1992 as a joint venture between Skydkraft and Alstrom to develop pressurized air-blown circulating fluidized bed gasifier technology for biomass. The biomass integrated gasification combined cycle (*BIGCC*) was commissioned in 1993

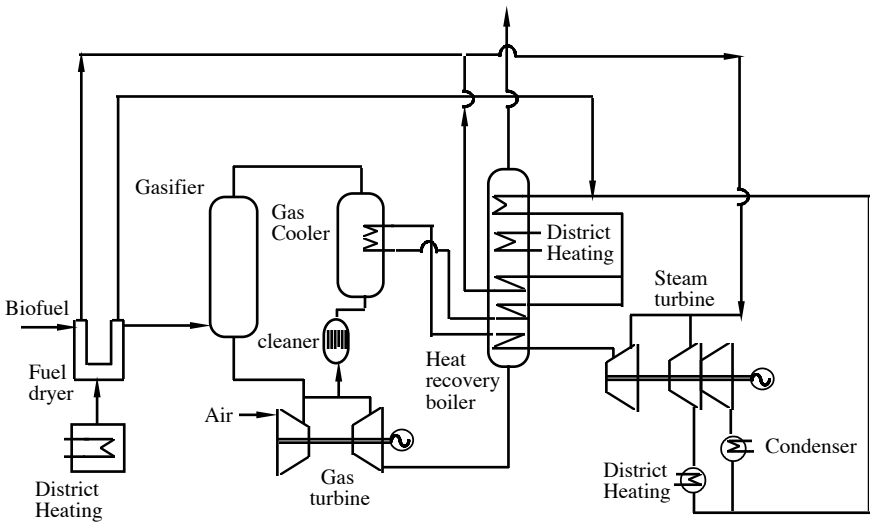

FIGURE 12.4 Schematic of Vega process gasification of biomass.

and fully completed in 1995. VEGA is a biomass-fuel-based IGCC system that combines heat and power (CHP) for a district heating system.[22] It generates 6.0 MW and 9.0 MWth for district heating of the city of Vämamo, Sweden. As indicated in Figure 12.4, the moisture of the entering biomass feedstock is removed via a "biofuel dryer" to decrease gaseous emissions.[22] The dried biomass is then converted into a "biofuel" in a combined cycle gasifier. The resulting gas is cooled before it enters the heat recovery boiler and distribution to the district heating. The gasifier is known as the *Bioflow Gasifier.*

The most common method of gasifying biomass is using an *air-blown circulating fluidized bed gasifier with a catalytic reformer*, though there are many different variations. Most fluidized bed gasification processes use closed-coupled combustion with very little or no intermediate gas cleaning.[42] This type of process is typically operated at around 900°C, and the product gas from the gasifier contains H_2, CO, CO_2, H_2O, and CH_4, C_2H_4, benzene, and tars. Gasification uses oxygen (or air) and steam to help the process conversion, similar to coal gasification. The effluent gas from the fluidized bed gasifier contains a decent amount of syngas compositions, and the hydrocarbon content is also quite substantial. Therefore, the gasifier effluent gas cannot be directly used as syngas for further processing for other liquid fuels or chemicals without major purification steps. This is the reason why the gasifier is coupled with a catalytic reformer, where hydrocarbons are further reformed to synthesis gas. In this stage, the hydrocarbon content including methane is reduced by 95% or better. A very successful example is Chrisgas, an EU-funded project, which operates an 18-MWth circulating fluidized gasifier reactor at Värnamo, Sweden. They use a pressurized circulating fluidized bed gasifier operating on oxygen/steam, a catalytic reformer, and a water gas shift (WGS) conversion reactor that enriches hydrogen content of the product gas. The process also uses a high-temperature filter. The project has been carried out by the VVBGC (Växjö Värnamo

Biomass Gasification Centre). The use of oxygen instead of air is to avoid nitrogen dilution that, if not avoided, would add the additional burden of nitrogen removal to downstream processing.

Indirect gasification is another gasification process technology that takes advantage of the unique properties associated with biomass. As such, indirect gasification of biomass is substantially different from most coal-based gasification process technologies. For example, biomass is low in sulfur and ash, and highly reactive and volatile. In an indirect gasification process, biomass is heated indirectly using an external means such as heated sands in Battelle's process. A typical gaseous product from an indirect gasifier is close to medium-Btu gas, explained in Chapter 2. Battelle began this process R&D in 1980 and has continued up to the present, accumulating very valuable data regarding biomass gasification and utilization through long hours of their demonstration plant operation. Battelle's process is known as *FERCO SilvaGas process,* which is commercialized by FERCO Enterprise. A commercial-scale demonstration plant of the SilvaGas process was constructed in 1997 at Burlington, VT, at a Burlington Electric Department (BED) McNeil Station.[43] The design capacity of this plant is 200 tons/d of biomass feed (dry basis). McNeil station uses conventional biomass combustion technology, a stoker gate, conventional steam power cycle, and electrostatic precipitator (ESP)-based particulate matter removal system. The gas produced by the SilvaGas gasifier is used as a cofired fuel in the existing McNeil power boilers.[43] The product gas has a heating value of about 450 to 500 Btu/scf.

CUTEC, a German institute, recently constructed an oxygen-blown circulating fluidized bed gasifier of 0.4-MW_{th} capacity coupled with a catalytic reformer. Part of their product gas is after compression directly sent to a Fischer–Tropsch reactor for liquid hydrocarbon synthesis. This process, once fully developed, has good potential for a single-train biomass-to-liquid fuel conversion process.[44]

Another important process option for biomass gasification for syngas production involves the use of an entrained flow reactor. This type of process is operated at a very high temperature, around 1300°C, and without the use of a catalyst. The high temperature is necessary because of the fast reaction rate required for an entrained reactor whose reactor residence time is inherently very short. If a specific biomass feed has high ash content, which is not very typical for biomass, slag can be formed at such a high temperature. Learning from the research developments in coal gasification, a slagging entrained flow gasifier may be adopted for high-ash biomass conversion. Another important process requirement besides high temperature and short residence time is the particle size of solid feed, which must be very fine for efficient entrainment as well as for better conversion without mass transfer limitations. However, pulverization or milling of biomass is energy intensive and costly. To facilitate efficient size reduction of biomass feed, two options are most commonly adopted, namely, torrefaction and pyrolysis. *Torrefaction* is a mild thermal treatment at a temperature of 250 to 300°C, which converts solid biomass into a more brittle and easily pulverizable material that can be treated and handled just like coal. This torrefied product is often called *biocoal*. Thus, pulverized torrefied biomass can be treated like coal, and most entrained flow gasifiers designed for coal can be smoothly converted for torrefied biocoal without much adaptation. Torrefaction as a process

has long been utilized in many applications, including the coffee industry. However, more study is needed by the biomass industry to tune the process for biomass and optimize it as an efficient pretreatment technique. Gases produced during the torrefaction process may be used for torrefaction, thus accomplishing a self-energy supply cycle. An example of entrained flow biomass gasification can be found from the *Buggenum IGCC* plant, whose capacity is 250 MW_e.[45] NUON has operated this process, and their test program used for a period of 2001 through 2004, 6000 M/T of sewage sludge, 1200 M/T of chicken litter, 1200 M/T of wood, 3200 M/T of paper pulp, 50 M/T of coffee, and 40 M/T of carbon black as cofeeds with coal. A typical particle size of biomass feed was smaller than 1 mm, and pulverizing wood was more difficult than pulverizing chicken litter and sewage.[45] In their test program, they also mention torrefaction as a pretreatment option. Their experience with a variety of biomass feedstocks provides valuable operational data for future development in this area.

Pyrolysis of biomass is an important process option, either as a pretreatment for gasification or as an independent process treatment. Pyrolysis takes place actively at around 500°C and produces a liquid product, which is called *bio-oil*. As can be seen from the prevailing pyrolysis temperature, pyrolysis of biomass is quite similar, as a process treatment, to oil shale pyrolysis and coal pyrolysis. Bio-oil production via biomass pyrolysis is typically carried out via *flash pyrolysis*. The produced oil can be mixed with char to produce a *bioslurry*. Bioslurry can be more easily fed to the gasifier for efficient conversion. A viable example is the *FZK process*.[46] FZK (Forschungszentrum Karlsruhe) developed a process that produces syngas from agricultural waste feeds such as straws. They developed a flash pyrolysis process that includes twin screws for pyrolysis. The process concept is based on the Lurgi-Ruhrgas coal gasification process, as discussed in Chapter 2. A 5–10 kg/h PDU (process development unit) is available at the FZK company site. In this process, straw is flash-pyrolyzed into a liquid that is mixed with char to form a bio-oil/char slurry. The slurry is pumpable and alleviates technical difficulties involved in solid biomass handling. This slurry is transported and added to a pressurized oxygen-blown entrained gasifier. The operating conditions of the gasifier at Freiberg involve a slurry throughput of 0.35 to 0.6 tons/d, 26 bars, and 1200 to 1600°C. The current FZK process concepts involve gasification of flash-pyrolyzed wood products, slow-pyrolyzed straw char slurry (with water condensate), and slow-pyrolyzed straw char slurry (with fast pyrolysis oil).[46] Slurries from straws have been efficiently converted into syngas with high conversion and near-zero methane content.[42] Their ultimate objective is development of an efficient *biomass-to-liquid (BtL)* plant. A schematic representation of the FZK process concept leading to BtL is shown in Figure 12.5.

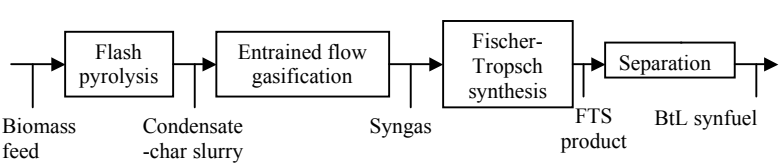

FIGURE 12.5 FZK process concept of BtL synfuel.

Canadian developments in biomass gasification for the production of medium- and high-Btu gases have also received worldwide technical acclaim. The *BIOSYN gasification* process was developed by Biosyn Inc., a subsidiary of Nouveler Inc., a division of Hydro-Quebec. The process is based on a bubbling fluidized bed gasifier containing a bed of silica (or alumina) and can be operated at a pressure as high as 1.6 MPa. They tested the process extensively from 1984 to 1988 on a 10 ton/h demonstration plant comprising a pressurized air- or oxygen-fed fluidized bed gasifier.[23] The system has the ability to utilize a diversified array of feedstock including whole biomass, fractionated biomass, peat, and MSW. The primary end use for biogas is replacing the oil currently used in industrial boilers. It also has the added capability of producing synthesis gas for methanol or low-energy gas production. In the following years, they used a 50 kg/h BIOSYN gasification PDU, and it has also proved the feasibility of gasifying a variety of other feedstocks, such as primary sludges, RDF, rubber residues containing 5–15% Kevlar, granulated polyethylene, and polypropylene.[41]

12.2.3 Liquefaction

During the mid-to-late 1980s, commercial interest of the thermochemical conversion of biomass focused on liquefaction. Unlike the initial gasification studies, the preliminary liquefaction studies utilized woody biomass, or lignocellulose material, as the feedstock. Woody biomass was considered superior to corn stover biomass owing to its potentially lower cost and greater availability.[24]

The first documented "successful" production of ethanol from the liquefaction of woody material was at McGill University in Canada. Researchers at McGill used aqueous hydrogen iodide at mild conditions for the ethanol production. Because the operating temperatures were mild (125°C), char production was minimal.[23] Dr. Boocock and associates from the University of Toronto have also contributed to the understanding of biomass liquefaction. Their research determined that the size of the wood chips used for liquefaction was directly related to the amount of ethanol produced. As chip size increased, the product yield also increased.[23] This led to research of the combined process of liquefaction, fermentation, and distillation.

The pilot plant process, shown in Figure 12.6, was designed based on a feed rate of 579,270 Mg/year of wood chips. The mixed wood feedstock comprises

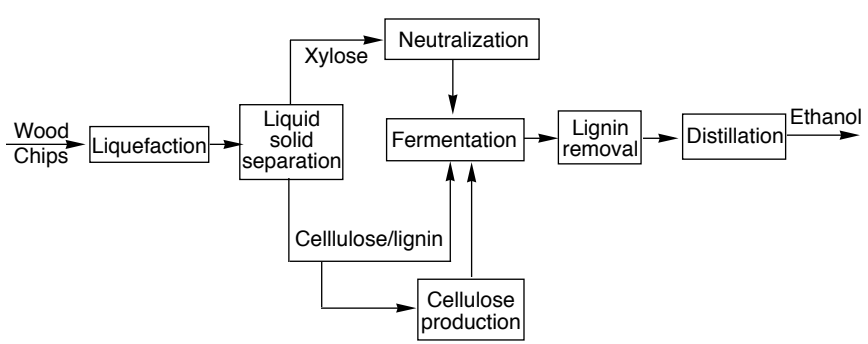

FIGURE 12.6 Combined wood-to-ethanol process.

cellulose, xylose, and lignin. Liquefaction converts the wood chips into a liquid and solid fraction. The liquid fraction, comprising xylose, is passed through a neutralization unit before it enters the fermentation step. The solid fraction, cellulose and lignin material, is sent directly to the fermentation unit. After leaving the fermentation unit, the lignin components are removed for the generation of process heat and electricity. The remaining material is then sent to the distillation unit. From the pilot plant results, the yield of ethanol from cellulose and hemicellulose feedstocks is approximately 110 gal of ethanol per ton of wood.[25] A more detailed discussion on the liquefaction of lignocellulosic materials is presented in Chapter 11.

12.2.4 Pyrolysis

Biomass can be converted into gas, liquid, and char via pyrolysis. The exact proportion of the end products is dependent on the pyrolysis process used (i.e., temperature, pressure, etc.).[26] During the early 1980s, the National Renewable Energy Laboratory (NREL) investigated the use of ablative pyrolysis for biomass conversion. The technology behind the biomass pyrolysis is identical to that used in the petroleum industry.

The first biocrude was produced at a 30 kg/h scale.[18] At operating conditions of 500°C and a residence time of 1 sec, the biocrude had the same oxygen and energy content as its "natural crude" counterpart. Since then, Canadian researchers have converted woody biomass into fuel via pyrolysis in a 200 kg/h pilot plant.[27] The fuel oil substitute was produced (on 1000 ton/d dry basis) at approximately $3.4/GJ. At the time, the cost for light fuel oil was $4.0–4.6/GJ,[28] thus indicating that the pyrolyzed biomass fuel was a more economical alternative. However, the apprehension that high transportation costs of the biomass to the pyrolyzer would outweigh potential profits limited research funding for the next 2 years. This was when the petroleum-based liquid fuel price was considerably lower than that in the 21st century. To circumvent this problem, the Energy Resources Company (ERCO) in Massachusetts developed a mobile pyrolysis prototype for the U.S. EPA.

ERCO's unit was designed to accept biomass with a 10% moisture content at a rate of 100 tons/d. At this rate, the system had a minimal net energy efficiency of 70% and produced gaseous, liquid, and char end products. The process, which is initially started using an outside fuel, is completely self-sufficient shortly after start-up. This was achieved by implementing a cogeneration system to convert the pyrolysis gas into the electricity required for operation. A small fraction of the pyrolysis gas is also used to dry the entering feedstock to the required 10% moisture. A simplified version of ERCO's mobile unit is shown in Figure 12.7.

The end products are pyrolytic oil and pyrolytic char, both of which are more economical to transport than the original biomass feedstock. The average heating values for the pyrolytic oil and char are 10,000 Btu/lb and 12,000 Btu/lb, respectively.[29] The pyrolysis gas, which has a nominal heating value of 150 Btu/scf, is not considered an end product because it is directly used in the cogeneration system. The mobility, self-sufficiency, and profitability of the system removed some of the hesitancy of funding research on the pyrolysis of biomass. In addition, ERCO's success led to the additional investigation of "dual," or cogeneration systems.

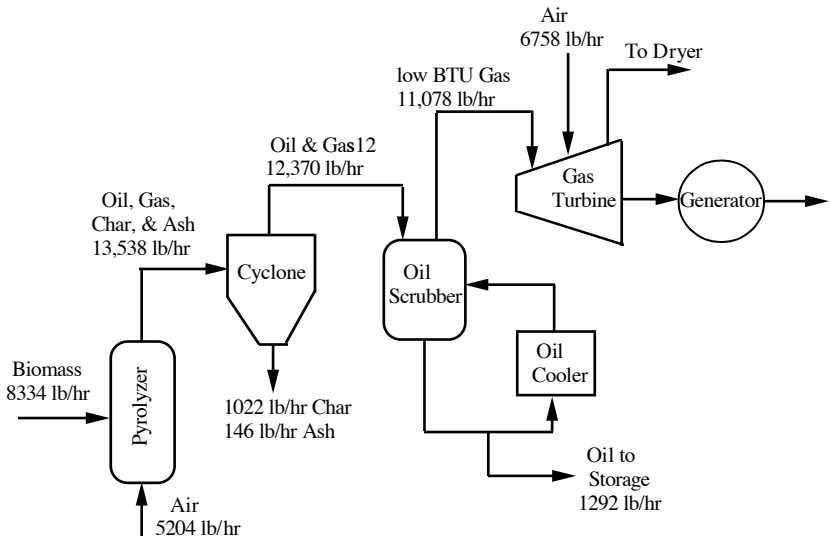

FIGURE 12.7 Simplified schematic and material balance for ERCO's mobile pyrolysis unit. (From Skelley, W.W. et al., The Energy Resources Fluidized Bed Process for Converting Biomass to Electricity, symposium on Energy from Biomass and Wastes VI, January 25–29, 1982, pp. 665–705.)

The most widely studied dual gasification-pyrolysis system is the Hydrocarb process.[29–31] The Hydrocarb process focuses on the configuration of gasification and pyrolysis systems to convert a mixed biomass and natural gas feedstock into methanol, gasoline, and char. The process combines three basic steps: (1) a hydropyrolyzer in which the biomass is gasified with a recycled hydrogen-rich gas to form a methane-rich gas, (2) a methane pyrolyzer in which methane is decomposed to carbon and hydrogen, and (3) a methanol synthesis reactor in which carbon monoxide is catalytically combined with hydrogen to form methanol.[32] Preliminary studies maintained the gasifier at 800°C, the methanol converter at 260°C, and the pyrolysis reactor at 1100°C. When process step 3 had a system pressure of 50 atm at the corresponding temperatures, the equilibrium compositions shown in Figure 12.8 were obtained. For every 100 kg of biomass and 18 kg of methane fed to the gasifier, approximately 67 kg of methanol and 40 kg of char were produced.[33]

One advantage of this process is that the char produced is essentially "pure" carbon. In other words, it is free of sulfur, ash, and nitrogen. Therefore, it can be used as a clean fuel by the industrial sector. Second, the conversion of methane to methanol in the presence of biomass decreases the carbon dioxide emissions typically associated with the gasification of methane. Another advantage is the potential to replace the feedstocks with other materials. The biomass component can be replaced with other carbonaceous materials, such as MSW. Methane could be replaced with coal. Although feedstock replacement is still in the preliminary stages, researchers at Brookhaven National Lab (BNL) anticipate similar results.

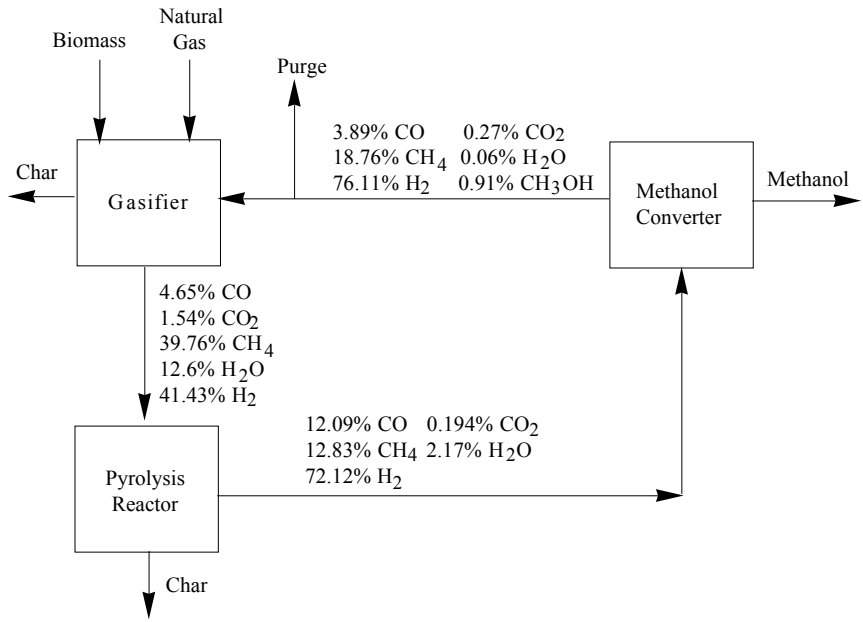

FIGURE 12.8 Typical equilibrium compositions for the Hydrocarb process. (From Borgwardt, R.H. et al., Biomass and Fossil Fuel to Methanol and Carbon via the Hydrocarb Process: A Potential New Source of Transportation and Utility Fuels, presented at: Energy from Biomass and Wastes XV, IGT, Washington, D.C., 1991.)

12.3 BIOLOGICAL CONVERSION: ANAEROBIC DIGESTION

Although the process of anaerobic digestion has been well known for the past 100 years, researchers have been recently reinvestigating the process for use as a potential fuel source.[9,10] Specifically, the focus is on hastening the natural process of biomass conversion to a gaseous fuel referred to as *biogas*. Since 1977, universities and research institutes have been conducting experiments to ascertain the optimal conditions (feedstock, temperature, pressure, etc.) for the most efficient operations. Most of the biomass feedstocks studied have produced a biogas rich in methane. This medium-to-high-BTU gas can, in some instances, be upgraded to a substitute natural gas (SNG).[34] However, depending on the feedstock, nonnegligible amounts of sulfur are also produced.[35] Table 12.2 contains a listing of different feedstocks, initial sulfur content, final sulfur percentage, and the projected power generation for studies conducted in Germany.

The first anaerobic digester studies, conducted at Penn State University, utilized cow manure for biogas production. During the anaerobic process, organically bound materials are mineralized to methane and carbon dioxide. The Penn State University digester was operated for a total of 450 d to treat 1200 tons of manure. The digester

TABLE 12.2
Comparison of Different Biogas Feedstocks

Feedstock	Power Generation (MW_e/ton of biomass)	Original Sulfur Content (mg/m^3)	Final Sulfur Percentage
Liquid and solid manure	0.2–0.5	300–500	0.5
Organic waste	0.5–2.0	100–300	0.3
Wood chips	5–50	300–1000	0.3
Sewage sludge	100–500	300–500	0.6

Source: From Ellegard, A. and Egenéus, H., *Energy Policy*, 21(5): 625–622, 1993; Wendt, H. et al., Conversion of Biomass-Obtained Gases in Solid Oxide Fuel Cells, Luxembourg Report No. 13564, 1991.

TABLE 12.3
Capacity Tests for 100 m^3 Digester

Manure Input kg/d	Retention Time d	Total Biogas m^3/d	Production (m^3/m^3) digester/d
346	35	67	0.67
554	21	129	1.29
1030	11	202	2.02

Source: From Bartlett, H.D., *Biomass as a Nonfossil Fuel Source I*, American Chemical Society, Washington, D.C., 1981.

was started up using activated municipal sludge, then fed twice a day with manure. Digester retention times were varied to determine the optimal biogas production, as shown in Table 12.3.

The biogas produced was approximately 60% methane, 32–34% carbon dioxide, 6–8% nitrogen, and trace amounts of hydrogen sulfide.[36] Based on a methane content of 60%, the biogas had a total energy generation of 44 kW. This preliminary success led to the investigation of other feedstocks for anaerobic digesters.

Ghosh and Klass conducted a series of anaerobic digestion experiments using a mixed biomass waste feedstock.[37] The mixed waste contained various ratios of *Eichhornia crassipies* (water hyacinth), *Cynodon dactylon* (Bermuda grass), sewage sludge, and MSW. All the experiments were conducted in cylindrical Plexiglass® digesters. The optimal "blend" was determined to be 32.3:32.3:32.3:3.1 of hyacinth:grass:sludge:MSW. Once the optimal waste blend had been determined, studies were conducted that varied the temperature and pH of the digester. Their final results are given in Table 12.4.

At first glance, the results indicate that varying the temperature and pH had very little effect on the amount of methane produced. However, the thermophilic digester had a higher pH and approximately 3 times the loading rate of its mesophilic counterpart. This indicates that additional experiments are required to determine the

TABLE 12.4
Mesophilic (35°C) and Thermophilic (55°C) Digestion of Mixed Biomass Waste

	Mesophilic (pH not measured)	Digester Feed (pH = 8.0–8.4)	Thermophilic (pH = 9.0)	Digester Feed (pH = 10.0)
Operating conditions				
Loading (lb/ft^3 d)	0.1	0.1	0.4	0.43
Detention time (d)	12	12	6.0	5.5
Gas production rate (vol/vol/d)	0.61	0.67	2.85	2.91
CH_4 content (mol%)	59.5	58.1	56.4	56.0
CH_4 yield (scf/lb)	4.10	3.92	4.00	3.68
% CH_4 collected	46.1	44.1	45.0	41.4

Source: From Ghosh, S. and Klass, D.L., *Biomass as a Nonfossil Fuel Source I*, American Chemical Society, Washington, D.C., 1981.

"optimal" operating conditions. Regardless of the operating conditions used, the anaerobic digestion of biomass is a promising alternative for supplementing the world's energy needs.

REFERENCES

1. Sampson, R.N. et al., Biomass management and energy, *Water Air Soil Pollut.*, 70(1–4): 139–159, 1993.
2. Trebbi, G., Power-production options from biomass: The vision of a southern Euorpean utility, *Bioresour. Technol.*, 46: 23–29, 1993.
3. MacCleery, D.W., *American Forests: A History of Resiliency and Recovery*, U.S. Department of Agriculture Forest Service, 1993, p. 59.
4. Reese, R.A. et al., Herbaceous biomass feedstock production, *Energy Policy*, 21(7): 726–734, 1993.
5. Sampson, R.N., Forest management and biomass in the U.S., *Water Air Soil Pollut.*, 70(1–4): 519–532, 1993.
6. Nurmi, J., Heating values of the above ground biomass of small-sized trees, *Acta For. Fenn.*, 236: 2–30, 1993.
7. Sipilä, K., New power-production technologies: various options for biomass and cogeneration, *Bioresour. Technol.*, 46: 5–12, 1993.
8. Ramsay, W., Biomass energy in developing countries, *Energy Policy*, 326–329, August 1985.
9. Elliot, P., Biomass-energy overview in the context of Brazilian biomass powered demonstration, *Bioresour. Technol.*, 46: 13–22, 1993.
10. Ellegard, A. and Egenéus, H., Urban energy: exposure to biomass fuel pollution in Lusaka, *Energy Policy*, 21(5): 625–622, 1993.
11. Bylinsky, G., Biomass: The Self-Replacing Energy Source, *Fortune*, 100(6): 78–81, 1979.
12. Lapidus, A. et al., Synthesis of liquid fuels from products of biomass gasification, *Fuel*, 73(4): 583–589, 1994.

13. Randolph, J.C. and Fowler, G.L., Energy policies and biomass resources in the Asia-Pacific region, *Public Adm. Rev.*, 43(6): 528–536, 1983.
14. Wright, L.L. and Hughes, E.E., U.S. carbon offset potential using biomass energy systems, *Water Air Soil Pollut.*, 70(1–4): 483–497, 1993.
15. Rahmer, B.A., Alternative Energy: towards Fuel Farming, *Petroleum Economist*, 1978, pp. 59–60.
16. Scurlock, J.M.O., Hall, D.O., House, J.I., and Howes, R., Utilizing biomass crops as an energy source: A European perspective, *Water Air Soil Pollut.*, 70(1–4): 499–518, 1993.
17. Pastor, J. and Kristoferson, L., *Bioenergy and the Environment — the Challenge*, Westview Press, Boulder, CO, 1990.
18. Bain, R.L., Electricity from biomass in the United States: status and future direction, *Bioresour. Technol.*, 46(1–2): 86–93, 1993.
19. Freeman, H.M., Ed., *Standard Handbook of Hazardous Waste Treatment and Disposal*, McGraw-Hill, New York, 1989.
20. Benson, W.R., Biomass potential from agricultural production, Proceedings: Biomass — A Cash Crop for the Future?, Midwest Research Institute, Kansas City, MO, 1977.
21. Raman, K.P., Walawender, W.P., Shimizu, Y., and Fan, L.T., Gasification of Corn Stover in a Fluidized Bed, presented at Bio-Energy 80, Atlanta, GA, April 1980.
22. Bodland, B. and Bergman, J., Bioenergy in Sweden: potential, technology, and application, *Bioresour. Technol.*, 46(1–2): 31–36, 1993.
23. Hayes, R.D., Overview of thermochemical conversion of biomass in Canada, in *Biomass Pyrolysis Liquids: Upgrading and Utilization*, Elsevier Science, New York, 1991.
24. Farrell, K., Fighting OPEC with Biomass: The European Counteroffensive, Europe, May–June, 1981, pp. 18–20.
25. Bergeron, P.W. and Hinman, N.D., Fuel Ethanol Usage and Environmental Carbon Dioxide Production, in Energy From Biomass and Wastes XIV, Klass, D.L., Ed., Institute of Gas Technology, Chicago, IL, 14, 1991, pp. 153–167.
26. Borgwardt, R.H., Steinberg, M., and Grohse, E.W., Biomass and Fossil Fuel to Methanol and Carbon Via the Hydrocarb Proces: A Potential New Source of Transportation and Utility Fuels, in Energy From Biomass and Wastes XIV, Klass, D.L., Ed., Institute of Gas Technology, Chicago, IL, 15, 1991, pp. 823–853.
27. Solantausta, Y. et al., Wood-pyrolysis oil as fuel in a diesel-power plant, *Bioresour. Technol.*, 46: 177–188, 1993.
28. Rick, F. and Vix, U., Product standards for pyrolysis products for use as a fuel, in *Biomass Pyrolysis Liquids Upgrading and Utilization*, Bridgwater, A.V. and Grassi, G., Eds., Elsevier, London, 1991, pp. 177–218.
29. Skelley, W.W., Chrostowki, J.W., and Davis, R.S., The Energy Resources Fluidized Bed Process for Converting Biomass to Electricity, symposium on Energy from Biomass and Wastes VI, January 25–29, 1982, pp. 665–705.
30. Brown, R.F. et al., Economic Evaluation of the Coproduction of Methanol and Electricity with Texaco Gasification-Combined-Cycle Systems, EPRI AP-2212, 1983.
31. Ismail, A. and Quick, R., Advances in Biomass Fuel Technologies, presented at: Energy from Biomass and Wastes XV, IGT, Washington, D.C., 1991.
32. Keuster, J.L., Liquid hydrocarbons fuels from biomass, in *Biomass as a Nonfossil Fuel Source*, American Chemical Society, Washington, D.C., 1991, pp. 163–184.
33. Borgwardt, R.H., Steinberg, M., Grohse, E.W., and Tung, Y., Biomass and Fossil Fuel to Methanol and Carbon via the Hydrocarb Process: A Potential New Source of Transportation and Utility Fuels, presented at: Energy from Biomass and Wastes XV, IGT, Washington, D.C., 1991.

34. Schaefer, G.P., Industrial development of biomass energy sources, in *Biomass as a Nonfossil Fuel Source -I,* Symposium by Division of Petroleum Chemistry, American Chemical Society, Washington, D.C., 1981, pp. 1–17.
35. Wendt, H., Plzak, V., and Rohland, B., Conversion of Biomass-Obtained Gases in Solid Oxide Fuel Cells, Luxembourg Report No. 13564, 1991.
36. Bartlett, H.D., Energy production of a 100 m^3 biogas generator, in *Biomass as a Nonfossil Fuel Source -I,* Symposium by Division of Petroleum Chemistry, American Chemical Society, Washington, D.C., 1981, pp. 373–378.
37. Ghosh, S. and Klass, D.L., Advanced digestion process development for methane production from biomass — waste blends, in *Biomass as a Nonfossil Fuel Source -I,* Symposium by Division of Petroleum Chemistry, American Chemical Society, Washington, D.C., 1981, pp. 251–278.
38. Merriam and Webster On-line Dictionary, 2006.
39. Ragland, K.W., Ostlie, L.D., and Berg, D.A., WTE Biomass Power Plant in Central Wisconsin, Grant No. 89029, Final Report submitted to Wisconsin Energy Bureau, November 2000.
40. Energy Information Administration, Renewable Energy Trends 2004 Edition, U.S. Department of Energy, release date: August 2005.
41. Babu, S., Biomass Gasification for Hydrogen Production — Process Description and Research Needs, www.ieahia.org/pdfs/gasification_report_sureshbabu.pdf, accessed April 2006.
42. van der Drift, A. and Boerrigter, H., Synthesis Gas from Biomass for Fuels and Chemicals, Report of Workshop on Hydrogen and Synthesis Gas for Fuels and Chemicals, Organized IEA Bioenergy Task 33, SYNBIOS Conference, Stockholm, Sweden, May 2005, published January 2006, available through http://www.gastechnology.org/webroot/downloads/en/IEA/syngasFromBiomassvanderDrift.pdf.
43. FERCO homepage, The Vermont Gasification Project, http://www.fercoenterprises.com/proj-vgp.htm, accessed on April 23, 2006.
44. Claussen, M. and Vodegel, S. The CUTEC concept to produce BtL-fuels for advanced power trains, a paper presented at International Freiberg Conference on IGCC and XtL TECHNOLOGIES, Freiberg, Germany, June 16–18, 2005.
45. Wolters, C., Canaar, M., and Kiel, J., Co-gasification of Biomass in 250 MW_e IGCC Plant 'Willem-Alexander-Centrale', a paper presented at Biomass Basification Workshop at Rome, Italy, May 10, 2004, available through http://www.gastechnology.org/webroot/downloads/en/IEA/IEARomeWSKiel.pdf.
46. Dinjus, E., German Developments in Biomass Gasification, a paper presented at IEA Renewable Working Party Bioenergy Task 33: Thermal Gasification, Innsbruck, Austria, September 26, 2005, also available through http://www.gastechnology.org/webroot/downloads/en/IEA/Fall05AustriaTaskMeeting/GermanyGasificationActivities.pdf.

13 Energy Generation from Waste Sources

Sunggyu Lee

CONTENTS

13.1 INTRODUCTION

Solid wastes are by definition, any wastes other than liquids or gases that are no longer deemed valuable, and therefore discarded.[1] Such wastes typically originate

TABLE 13.1
Comparison of Heating Values of Various Waste-Derived Fuels

Fuel Source	Btu/lb
Yard wastes	3,000
Municipal solid waste	6,000
Combustible paper products	8,500
Textiles and plastics	8,000
Bituminous coal (average)	11,300
Anthracite coal (average)	12,000
Spent tires	13,000–15,000
Crude oil (average)	17,000
Natural gas (425 ft^3)	13,500

from either the residential community (i.e., municipal solid waste or *MSW*) or commercial and light-industrial communities. Wastes generated from manufacturing activities of heavy-industrial and chemical industries are typically classified as hazardous wastes. As regulations continue to get stricter with decreasing land availability, alternative uses for the waste must be found in order to recover the residual heating values as well as to alleviate landfill-overburdening problems. As indicated from the heating values listed in Table 13.1, the generation of waste-derived fuels appears to be very promising from both the environmental and energy points of view.[2,3]

In a landfill, the biodegradable components of the MSW decompose over time and emit methane. Methane is a very potent *greenhouse gas* that is known to be 23 times more potent than carbon dioxide. Therefore, the biodegradable components in MSW, such as food and paper wastes that end up in landfills, must be reduced in a good waste management plan. Many nations have implemented regulations and specific efforts to significantly reduce this level. A good example is the European Union's (EU's) *landfill directive of 1999*, which targets reducing the amount of biodegradable materials going to landfills by 65% of the 1995 level by 2016. From this perspective, energy generation from MSW is regarded as one of the very few options to efficiently cope with the greenhouse gas emission problem from landfills.

Although *refuse-derived fuel (RDF)* is attractive from the standpoints of resource conservation as well as waste reduction, there are serious concerns that waste treatment for energy generation may cause new environmental problems. Most of the processing difficulties arise from the heterogeneous and nonuniform nature of the waste feed itself, which in turn generates a very widely varying spectrum of treated intermediates and by-products.

This chapter will address the development of alternative energy sources from various solid waste classifications, except biological and agricultural wastes, which are covered separately in Chapter 12.

13.2 ENERGY RECOVERY FROM MSW

13.2.1 Introduction

The recovery of energy from MSW has been practiced for centuries. The burning, or incineration, of wastes such as wooden planks and miscellaneous household products was first used to produce warmth. This idea has become the basis for energy generation from today's MSW. For instance, each year Sweden burns 1.5 million tons of MSW to meet approximately 15% of its *district heating* requirements.[4] The heating value of this MSW incineration is approximately one-third the heating value of coal combustion. Besides incineration, "gaseous fuels" can also be obtained by *anaerobic digestion* in conjunction with landfill gas recovery. Anaerobic digestion is discussed in detail in Chapter 12.

13.2.2 Gasification of MSW

One method of recovering usable energy from MSW is gasification. The U.S. EPA is currently investigating the use of the *Texaco gasification process* for generating a medium-Btu gas from MSW.[5] A simplified Texaco process (Figure 13.1) gasifies the MSW under high pressure by the injection of air and steam with concurrent gas/solid flow. After separation of the noncombustible waste, water or oil is added to the combustible MSW to form a pumpable slurry. This is then pumped under pressure to the gasifier. In the gasifier, the slurry is reacted with air at high temperatures. The resultant gaseous product is then sent to a scrubbing system to remove any pollutants and impurities.

The Texaco gasification process was originally developed for gasification of coal (refer to Chapter 2). Recently it has been modified to treat soils contaminated with hydrocarbons, as well as to recover usable energy from MSW and polymeric wastes.

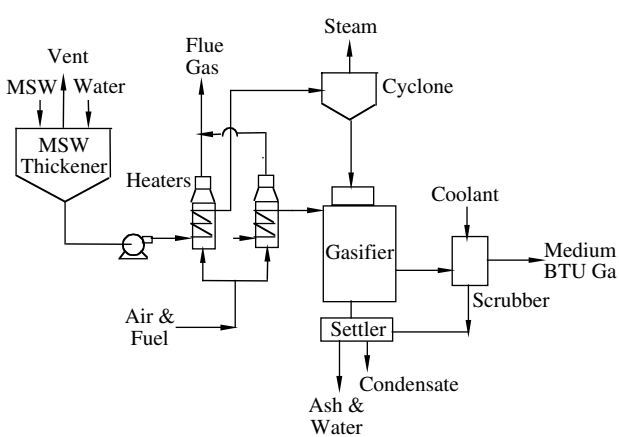

FIGURE 13.1 Simplified Texaco gasification process for the conversion of MSW to a medium-Btu gas.

Although the process has demonstrated 85% remediation efficiency for contaminated soils, it is still in the preliminary experimental stages for the MSW-to-energy application.[5] A demonstration of the MSW-to-energy process has been scheduled for July 1995 at Texaco's Montebello Research Laboratory in South El Monte, CA.[5]

13.2.3 Anaerobic Digestion of MSW

Anaerobic digestion of solid wastes is a process very similar to that used at *wastewater treatment* facilities and also to that used in *biogas production*. Anaerobic bacteria, in the absence of oxygen, are used to break down the organic matter of the waste. Frequently, the MSW is mixed with sewage sludge from the treatment plant to enhance the efficiency of the digestion. During the "conversion," a mixture of methane and carbon dioxide gases is produced. The typical ratio of the gas mixture is 70% methane and 30% carbon dioxide. Even without further treatment, the offgas has a heating value of 650 to 750 Btu/ft^3. It should be noted that the principal ingredients of the offgas are major greenhouse gases. Therefore, its efficient capture and recovery is very important from the environmental standpoint.

With rising energy costs and diminishing landfill space, the use of anaerobic digestion to generate a potential fuel source from MSW is an attractive alternative. A relatively new technology of landfill gas recovery has been developed to aid in the collection of gases generated from the anaerobic digestion of solid wastes. In 1980, 23 landfills were used as a source of methane production.[6] However, the vast majority of current research focuses on the generation of liquid fuels instead of the gaseous fuels from anaerobic digestion owing to the high capital cost associated with methane collection.

Production of liquid fuels has several advantages. First, low-sulfur, low-ash fuels can be made for commercial use.[7] Second, liquid fuels are traditionally much easier to store, handle, and transport than their gaseous counterparts. Finally, the production of the fuel aids in the battle against pollution by municipal wastes.[8,9] By utilizing the waste as an alternative source to generate fuel, less MSW will have to be disposed of in landfills. Although this statement holds true for the production of gaseous fuel, the generation of liquid fuels utilizes more MSW. In fact, processes have been developed that are capable of producing over a barrel of pyrolytic fuel oil from a ton of MSW.[7]

13.2.4 Pyrolysis of MSW

Figure 13.2 contains typical material distribution data for MSW generation in the U.S. in the early 1990s. Figure 13.3 shows more recent data for the early 2000s on MSW distribution in the U.S. by relative percentages. Because raw MSW contains both noncombustible and combustible components, the first step in producing a liquid fuel is to concentrate the combustible components. This is usually achieved with a rotating screen to remove noncombustible materials such as glass and dirt. An air classifier is used to remove the "light-ends" such as plastics, wood, and small metals. Heavier components, ceramics, heavy metals, and aluminum are routed for disposal in the landfill. By removing these noncombustible materials, the heating value of

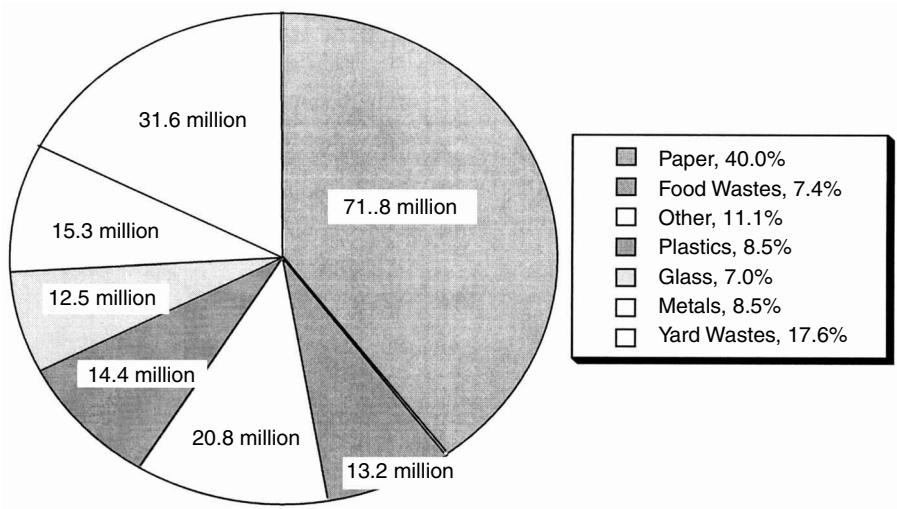

FIGURE 13.2 Material distribution of MSW collected in the U.S. by weight (tons) in the early 1990s.

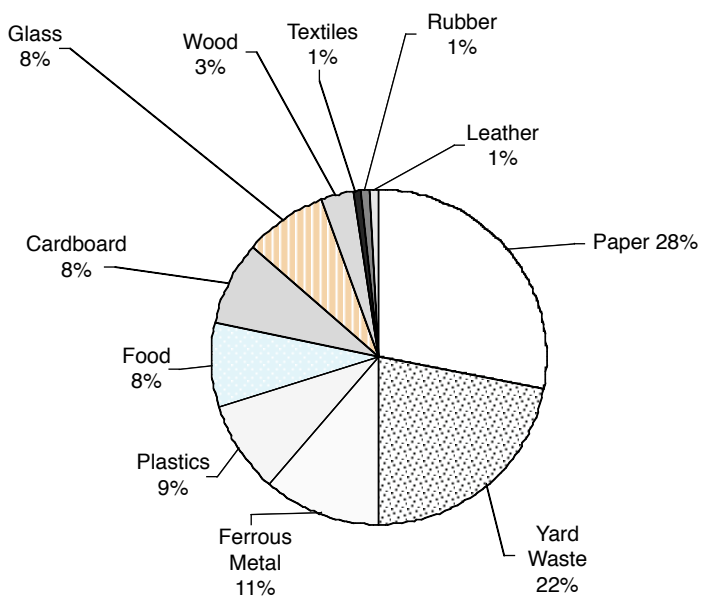

FIGURE 13.3 Breakdown of material distribution of MSW collected in the U.S. in 2002.

the raw MSW becomes approximately 7000 Btu/lb on a wet basis. The combustible components are sent to a shredder to reduce their size, and then to a pyrolysis unit to generate the fuel by *pyrolysis reactions*.

In the past, pyrolysis of MSW was mainly used to generate a gaseous fuel. However, recent research has found that pyrolyzing a cellulose-based waste at 116°C

and atmospheric pressure will generate a liquid fuel. In 1988, approximately 80% of the 180 million tons of waste generated in the U.S. had a cellulose base.[10] The estimated percentages of cellulosic components of MSW did not change much in the 1990s and 2000s, as shown in Figure 13.2 and Figure 13.3. Pober et al.[7] was able to utilize this particular type of waste to obtain a fuel that contained 77% of the heating value of typical petroleum fuels. The cellulosic components of the refuse comprise papers, newsprints, packing materials, wood clippings, and yard wastes.[11]

A typical pyrolytic reaction for the cellulose component of MSW may be written as:

$$C_8H_{10}O_5 \xrightarrow{\Delta} 8H_2O + 2CO + 2CO_2 + CH_4 + H_2 + 7C + C_6H_8O \qquad (1)$$

where C_6H_8O represents a "family" of liquid products. The exact composition of C_6H_8O is dependent on feedstock composition and reaction temperature. Research conducted by the U.S. Bureau of Mines has further demonstrated the successful pyrolysis of 1 ton of MSW at temperatures ranging from 500 to 900°C.[12] At these conditions, the end product composition is similar to that given in Table 13.2.

The light oil primarily comprises benzene, whereas the liquor contains dissolved organics in water. The gaseous product resembles that of a typical *town gas*. The heating value of the gas is 447 Btu/ft^3, which translates into a heat recovery of 82%.[13] Town gas is also known as *manufactured gas*, which typically contains hydrogen, carbon monoxide, methane, and volatile hydrocarbons. Prior to natural gas supplies and transmission in the U.S., town gas played a major role in providing gaseous fuel for lighting and heating in both residential and industrial sectors.

When the pyrolysis temperature is higher than 350°C, small quantities of polyethylene chips can be added to the cellulose feedstock. Operating temperatures ranging from 100 to 400°C decrease the amount of gaseous product and increase the formation of the liquid product (i.e., C_6H_8O family).

In addition to the liquid fuel or oil, pyrolysis generates a medium-BTU gas stream that, after purification, can be recycled as a supplemental fuel within the plant. Process water and char are also generated. The process water may have to be treated before discharge or can be used in the plant as heat exchanger water. All the pyrolysis products have the potential of being useful fuels or intermediates for

TABLE 13.2
Final Product Composition from the Pyrolysis of 1 Ton of MSW

Component	Mass or Volume
Char	154–424 lb
Tar	0.5–6 gal
Light oil	1–4 gal
Liquor	97–133 gal
Gas	7.38–18 scf

Source: From Bell, P.R. and Varjavandi, J.J., *Waste Management, Control, Recovery and Reuse*, Ann Arbor Science, MI, 1974.

producing other valuable products for use in the petrochemical industry. A simplified schematic of the pyrolysis process such as the one developed by Pober et al. and the full-scale plant in Ames, IA, is shown in Figure 13.4. A schematic of the pilot plant used to demonstrate the pyrolysis of MSW, which generated the results presented in Table 13.2, is shown in Figure 13.5.[12]

An example of a successful commercial-scale MSW pyrolysis plants in full operation is the Müllpyrolyseanlage (MPA) MSW pyrolysis plant, which is located outside of the City of Burgau, Germany.[65] The plant is on a 3-acre lot adjacent to a closed landfill, surrounded by farmlands. The plant was commissioned in mid-1984 and is currently in full operation, serving 120,000 residents and processing about 38,580 tons/year of MSW, which include both residential and industrial wastes as well as sewage sludge. The process utilizes a thermal pyrolysis process designed by WasteGen U.K. Ltd. The process is typically operated at 400–900°C in the complete absence of oxygen. The produced syngas mainly contains hydrogen, carbon monoxide, carbon dioxide, and methane, and the air emission control system removes most of the air pollutants. The syngas is used in boilers, gas turbines, and internal combustion engines

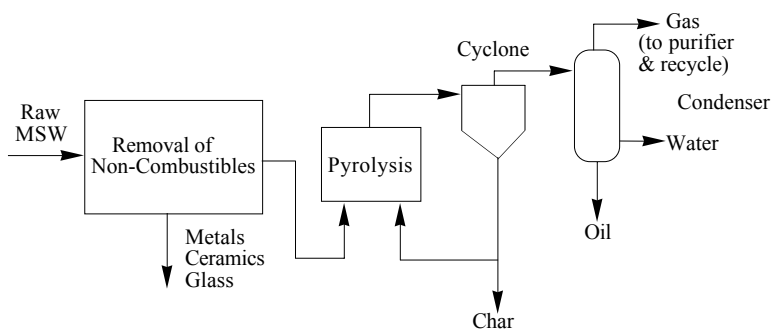

FIGURE 13.4 A simplified process schematic for the pyrolysis of MSW.

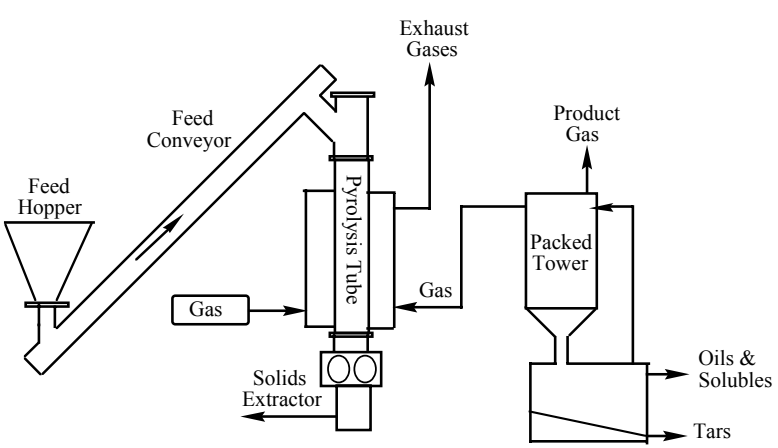

FIGURE 13.5 A solid waste pyrolysis system. (From Bell, P.R. and Varjavandi, J.J., *Waste Management, Control, Recovery and Reuse*, Ann Arbor Science, Ann Arbor, MI, 1974.)

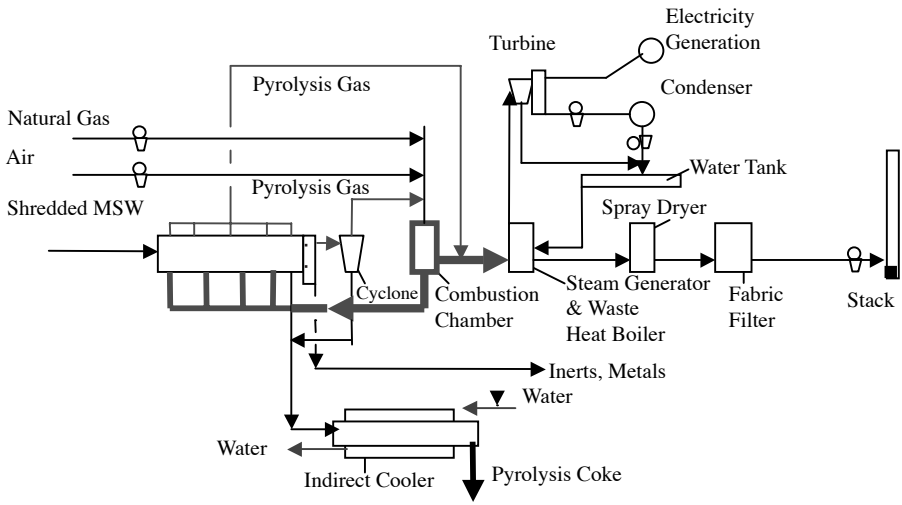

FIGURE 13.6 A schematic of the Müllpyrolyseanlage (MPA) MSW pyrolysis process.

to generate electricity, or it is used for the manufacture of chemicals. The solid char material is used as an absorbent and the inorganic ash is for disposal. The process does not require any special presegregation or pretreatment of MSW feedstock. However, MSW must be shredded to maximum size of 12 in. The average heating value of MSW feedstock is about 3660 Btu/lb, ranging between 2150 Btu/lb and about 6000 Btu/lb. A schematic of the *MPA MSW Pyrolysis Process* is shown in Figure 13.6[65]

Although there are a number of MSW-derived fuel systems in full operation or being started up throughout the world, there are still developmental issues in regard to process design and engineering, pollution control and monitoring, equipment design and selection, and application-related information.[14] The cost–benefit analysis along with the environmental impact analysis must be carefully conducted for any chosen process and site.

13.3 ENERGY GENERATION FROM POLYMERIC WASTES

13.3.1 Introduction

A significantly important component of MSW is polymeric materials. Although polymer waste only accounts for 8.5% by mass of the total MSW disposed of in the U.S., plastics represent over 28% by volume.[15] Furthermore, most plastic wastes are not biodegradable and constitute a long-term waste management problem. The high volume-to-mass ratio and the inertness to biological reactions make plastics and polymeric wastes the most important target for recycling, not for disposal. Polymeric wastes range from packaging materials used in the food industry to various parts in automobiles to high-density polyethylene (HDPE) containers such as pop bottles, laundry detergent bottles, milk jugs, etc. In 1993, over 50% of all the food packaged

in Europe for distribution utilized plastics.[4] It is estimated that over 65% of the food packaging in the U.S. is from plastics. As of 1978, the Ford Motor Company estimated that the average junked car contained 80 kg of plastic and nontire rubber.[16] The Ford Motor Co. also stated that the number was expected to rise at the rate of 4% per year. Metallic parts were replaced by plastic ones to reduce the vehicle weight as well as the component cost. About 7.5% by weight of an automobile comes from plastic components in 1998, which is a substantial increase from 4.6% in 1977.[66] The same trend is also observed in the computer and electronics industry, which depends very heavily on plastics for their fabrication materials. Moreover, the expected usable life of electronic or computer components is typically quite short, thus generating an enormous amount of scrap polymeric wastes.

Over the next few decades, the use of polymeric materials will continue to increase, owing to their versatility, functional values, and low energy requirements for production. Current technology enables over 200 million kg of plastic and rubber materials (excluding tire rubber) to be recovered from shredded automobiles.[16] The impetus to reuse polymeric wastes instead of disposing of them in landfills is primarily owing to the inability of polymers to rapidly degrade once dumped or buried at landfills.

13.3.2 Mechanical Recycling

The manufacture of bottle containers from HDPE, is perhaps the largest use of polymeric materials. Some of the more common items manufactured from HDPE are soft drink bottles, juice containers, milk jugs, laundry detergent bottles, spring water bottles, and motor oil cans. Austria introduced a regulation in October 1993 stating that over 90% of all HDPE containers must be recycled instead of placed in landfills.[17] Germany has been the most aggressive in its demand for plastics recycling. In 1993, over 12% of all German municipalities were active in collecting 12,000 tons of polymeric containers.[18,19] Officials have projected that this number will increase to 80,000 tons of containers from 62% of the municipalities by 1996, and nearly 100% by the early 2000s.

Most other countries have also jumped on the recycling bandwagon. The Netherlands plans to recycle 35% of all plastics and to recover energy by incinerating another 45%.[20] Italy currently recycles over 40% of its containers. Several states within the U.S. have also enforced mandatory recycling of HDPE. In order to ensure consumer involvement, states such as Michigan impose a deposit "tax" on all their HDPE bottles. The consumer is able to recover the deposit only if the item is returned to designated stores or distributors. Other states have developed a recycling "lottery."[1] Sanitary officials randomly pick an area and check for proper recycling of domestic waste. The homeowners complying with all recycling guidelines receive $200.

There are a great many different types of plastics. The American Society of Plastics Industry (SPI) has developed a standard code system to help consumers identify and sort the main types of plastics. There are seven designated types and each type is represented by a number: "1" for polyethylene terephthalate (PET), "2" for high-density polyethylene (HDPE), "3" for polyvinyl chloride (PVC), "4" for

low-density polyethylene (LDPE), "5" for polypropylene (PP), "6" for polystyrene (PS), and "7" for all others, such as melamine and polycarbonate (PC).

However, recycling alone is not the solution to polymeric waste. Research conducted at DOW Chemical Co. has shown that more than 52% of all HDPE bottles would have to be recovered before mechanical recycling could save more energy than employing a waste-to-energy process such as incineration.[21] For this reason, scientists are striving to develop processes to generate fuel from polymeric wastes.

13.3.3 Waste-To-Energy Processes

There are a number of technologies available for the generation of fuel energy, either in gaseous or liquid form, from polymeric waste. These technologies include pyrolysis, thermal cracking, catalytic cracking, and degradative extrusion followed by partial oxidation. Brief descriptions of these technologies follow. However, it is important to note that these are not the only processes available. As the technology advances, so do the processes used for the recovery of energy from wastes.

13.3.3.1 Pyrolysis

Pyrolysis of polymers is, by definition, the thermal decomposition of plastic waste back into oil or gas using heating processes in oxygen-starved or oxygen-deprived environments. This is the process typically used for waste-to energy generation because it has several advantages. Besides being a proven technology, pyrolysis has relatively good adaptability to fluctuations in the quality of the feedstock, is simple to operate, and is also economical. In addition, refineries, which will utilize the chemically recycled polymers, already have pyrolysis units in operation. SPI's Council for Solid Waste Solutions originally comprised three of the leading petroleum companies, Amoco, Mobil, and Chevron, even though all these companies went through corporate mergers with other leading companies. The council investigated the use of oil refineries equipped with pyrolysis units for the conversion of mixed plastics into hydrocarbons.[22] Ideally, these hydrocarbons would be identical to those split from petroleum oils.

Research conducted by Chambers et al.[16] implements the pyrolysis of polymeric wastes in the presence of molten salts. The molten salts are used to enhance the production of a particular desired oil–gas mix based on their excellent heat transfer properties. For instance, when a mixture of LiCl-KCl and 10% CuCl was used as the pyrolysis medium at 520°C, over 35% of the shredded polymer was converted to fuel oil.[16]

Molten salts have also been successful at slightly lower operating temperatures. When the salts are used during a standard pyrolysis operation at 420°C, the gaseous fraction is minimized. This enables higher liquid and solid fractions to be recovered. Although the nature of chemical reactions between the molten salts and polymeric waste is not yet completely understood, it does appear that production of a particular product mix is optimized by the presence of the salts. Typically, the recovered fractions consist of light oils, aromatics, paraffin waxes, and monomers.[23] When pyrolysis utilizes molten salts, care must be taken to decrease the amount of corrosion and contamination of the pyrolysis chamber due to the salts.

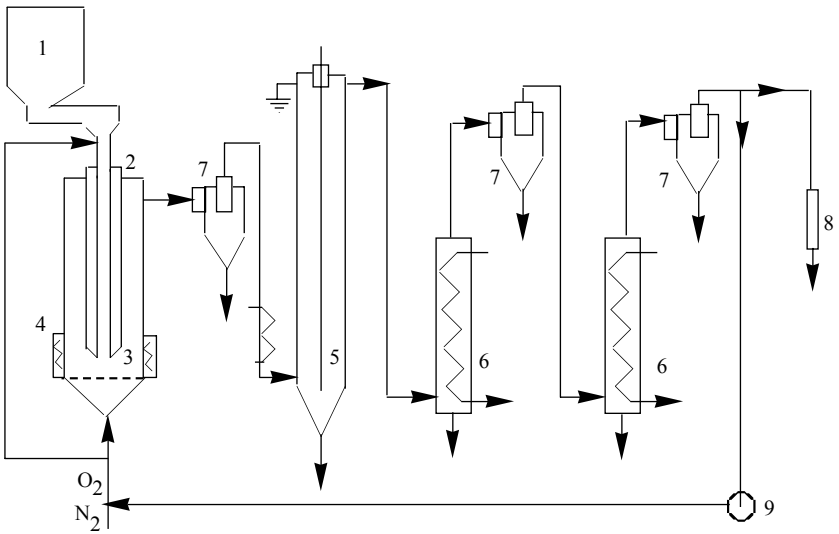

FIGURE 13.7 A simplified flow diagram of the FMRT laboratory test plant — 1: feed hopper, 2: downpipe and cooling jacket, 3: fluidized bed reactor, 4: heater, 5: electrostatic precipitator, 6: intensive cooler, 7: cyclone, 8: gas sampler, 9: compressor. (From Kaminsky, W., *Resour. Recovery Conserv.*, 5: 205–216, 1980.)

In 1980, researchers at Germany's Federal Ministry of Research and Technology (FMRT) demonstrated the success of pyrolyzing polymeric wastes in a 10 kg/h pilot plant. Figure 13.7 shows a simplified flow diagram of the laboratory test plant used in the development of the full-scale pilot plant. The main body of the FMRT pilot plant is a fluidized bed reactor with a space–time ratio of 0.4 kg/h/l. Preliminary experiments with the pilot plant enabled 40 to 60% of polymeric feed to be recovered as a usable liquid product.[24] The major components of this liquid product were benzene, toluene, styrene, and C_3-C_4 hydrocarbons. Table 13.3 presents the data for all of the end products for two pyrolysis experiments. These experiments utilized waste polyethylene and spent syringes as the feed at pyrolysis temperatures of 810°C and 720°C, respectively.

As of 1981, the pilot plant had accumulated over 600 h of successful operation. The researchers at FMRT have also demonstrated that the plant was self-sufficient in regard to energy needs. In other words, FMRT's facility was able to utilize one half of the pyrolysis gas produced.[24]

13.3.3.2 Thermal Cracking

Thermal cracking is similar to pyrolysis in that it is a high-temperature process. When polymeric wastes are cracked in an oxygen-free environment at temperatures above 480°C, a mixture of gas-liquid hydrocarbon is produced. At higher temperatures (650 to 760°C), more of the gaseous product is generated. Conversely, at lower temperatures, up to 85% of the product is a liquid hydrocarbon.[25] Both the gas and liquid form of the converted mixed-polymeric waste can be utilized as a feed stream by petroleum facilities.

TABLE 13.3
Composition of Pyrolysis Products from Preliminary Pilot Plant Studies

Identified Products	Polyethylene (wt%)	Spent Syringes (wt%)
Hydrogen	1.2	0.49
Methane	18.8	18.82
Ethane	6.2	7.75
Ethylene	17.9	13.73
Propane	0.2	0.08
Propene	7.2	10.67
Butene	1.0	3.32
Butadiene	1.5	1.39
Cyclopentadiene	0.8	2.79
Other aliphatics	1.3	3.46
Benzene	21.6	13.62
Toluene	3.8	3.84
Xylene, ethylbenzene	0.2	Trace
Styrene	0.4	0.43
Indane, indene	0.6	0.46
Naphthalene	3.7	2.46
Methylnaphthalene	0.6	0.92
Diphenyl	0.3	0.33
Fluorene	0.1	0.14
Phenanthrene	0.6	0.33
Other aromatics	0.7	1.15
Carbon dioxide	0.0	Trace
Carbon monoxide	0.0	Trace
Water	0.0	Trace
Acetonitrile	0.0	Trace
Waxes, tars	9.3	5.07
Carbon residue, fillers	1.8	5.80
Balance	99.8	97.05

13.3.3.3 Catalytic Cracking

Scientifically speaking, catalytic cracking is an extrapolation of thermal cracking. The same operating principles apply; the primary difference is the addition of a catalyst to enhance the cracking process. A typical catalytic cracker consists of two large reactor vessels, one to react the feed over the hot catalyst and the other to regenerate the spent catalyst by burning off carbon (fouled carbon on the catalytic surface) with air. Using two catalytic reactors enables the process to be run on a continuous basis. Figure 13.8 is a simplified schematic of *Mobil Oil's* process for the generation of gasoline from polymeric wastes via catalytic cracking.[26] Because the theory behind catalytic cracking is not new, the main focus of research is to determine the optimum catalyst for the cracking of the waste polymers.

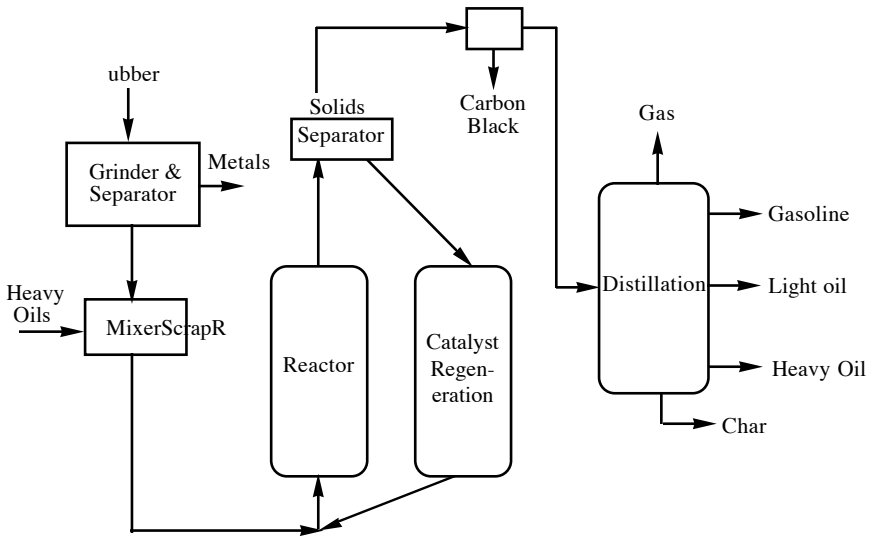

FIGURE 13.8 A simplified schematic of the Mobil Oil Corp. process for gasoline production from polymeric waste.

Studies using *organotin* compounds have shown promise for generation of fuel from polyurethanes. However, the highest activity was exhibited when used for glycolysis (oxidation of glucose), not cracking.[27] The use of chromium compounds has also been investigated. Sheirs and associates have demonstrated the feasibility of the use of chromium to aid in the cracking and pyrolysis of HDPE.[28] Although chromium compounds appear to be relatively effective, more research needs to be done to determine the optimum solubility of the catalyst for each polymeric compound. The addition of platinum and iron over activated carbon has also been investigated. Specifically, the activity of the catalysts for the degradation of polypropylene (PP) waste into aromatic hydrocarbons was studied. The addition of these metals increased the yield of the aromatics from polypropylene. It has been speculated that the increase in activity is influenced by the methyl branching of the polypropylene. However, the exact mechanism is still not clearly understood. Especially, aromatization from aliphatic polymeric materials needs to be investigated mechanistically.

Perhaps the most widely studied classification of catalysts for cracking operations is that of solid acid catalysts.[29–31] Specifically, HZSM-5, HY, and rare earth metal-exchanged Y-type (REY) zeolites and silica-alumina have been investigated.[31] Only HZSM-5 was found to be unsuitable for cracking polymeric wastes. HY, REY, and silica-alumina were all capable of producing at least 30% gasoline (or gasoline-range hydrocarbons) and 20% heavy oil. The differences between the catalysts arise in the production of the coke and gas fractions. Formation of coke is not desirable, because it causes catalytic deactivation by fouling and plugging the pore paths. Songip et al. found that the incorporation of rare-earth metals in HY zeolite increased the gasoline yield and decreased coke formation.[31] Regardless of the catalyst used,

catalytic cracking, owing to lower-temperature operation, appears to be more technologically sound than pyrolysis. However, catalytic processes are often costlier than noncatalytic counterparts because of the costs involved in catalysts, catalytic reactors, and catalyst regeneration steps.

13.3.3.4 Degradative Extrusion

Degradative extrusion is, in principle, not a new technology; however, its use as a process for energy generation is a new technology. The basis of the technology is that at high temperatures, under the simultaneous effect of shearing, it is possible to break down complex mixtures of plastics into homogeneous low-molecular weighted polymer melts.[32] These polymer melts could replace the heavy oils used in the production of synthesis gas. The polymer-derived heavy oil would be fed directly into a partial-oxidation fluidized bed chamber. The end product from the extruded waste at 800°C would include methanol, one of the primary feedstocks for the chemical industry.[33] Depending on the operating conditions, the methanol could be sent directly to a chemical plant as feedstock without undergoing any subsequent treatment. However, if the gas undergoes low-temperature decomposition, then carbon dioxide and hydrogen would be the end products. Figure 13.9 contains a possible process schematic for the generation of methanol from polymeric wastes. Degradative extrusion is the reverse of reactive extrusion, in which a specially desired chemical reaction is carried out on the polymeric backbone, such as graft copolymerization.

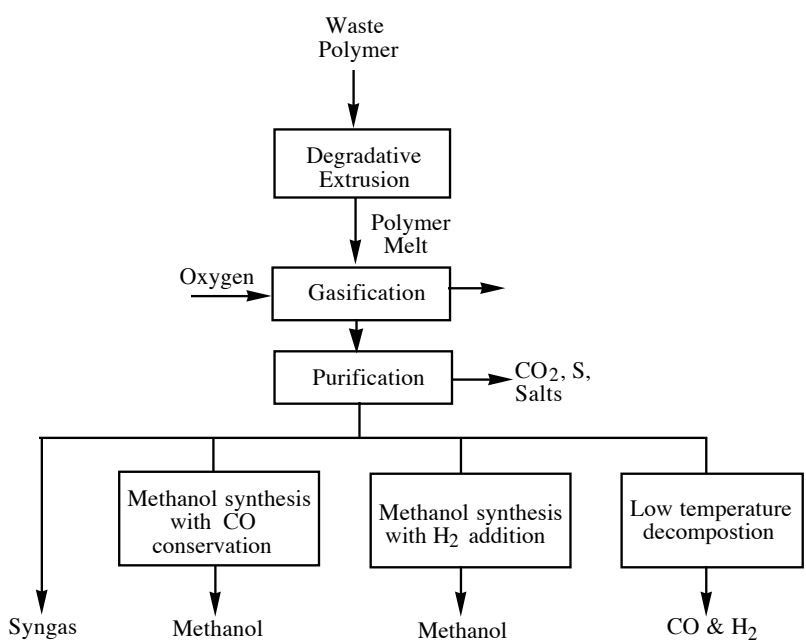

FIGURE 13.9 A process scheme for the degradative extrusion and partial oxidation of polymeric wastes for methanol generation.

13.4 FUEL PRODUCTION FROM SPENT TIRES

13.4.1 Introduction

Scrap tire disposal has become a global problem of epidemic proportions. In 1977, the number of tires scrapped in Japan was 47 million a year.[34] More alarming is the fact that this number has doubled over the past 5 years. In 1992, the U.K. scrapped over 25 million tires per year.[35] Add the annual scrapping of 250 million passenger tires in the U.S., and the outlook becomes even grimmer.[36]

Traditional handling of the scrap tires was by landfills; however, the acute shortage of viable landfills has all but eliminated this as a means of disposal. In fact, several of the midwestern U.S. states have issued laws that close landfills to tires.[37] State-registered private collectors must dispose of the tires at approved, legal dumps and recyclers. But even the number of legal landfills is dwindling. This has forced researchers to find an economical and efficient alternative for the spent tires.

Currently there are four key areas for "marketing" the spent tires. The first uses shredded tires as a "clean dirt" for road embankments and landfill liners.[38] The second use is as a rubber-modified asphalt. The asphalt, or tire crumb, can be used for playgrounds, running tracks, or as an ingredient of highway-paving material. The third use of spent tires is for electric power generation by combusting ground tire chips together with coal. The fourth, and most important area, is for tire-derived fuels (TDFs).[39] Although this may seem far-fetched, under proper conditions, spent tires are a clean fuel with a 15% higher Btu value than coal.[40] In fact, it was estimated that by 1997, over 150 million scrap tires would be used for the generation of TDFs.[41]

TDFs can be obtained by several methods. The first is by incineration.[39,42] Britain's tire incinerator burns approximately 90,000 tons of rubber a year. With this amount, the Wolverhampton facility will generate 25 MW of energy, which is enough to power a small town.[43] In the U.S., Illinois Power incinerates shredded tire chips to supplement their soft coal. This cocombustion of tire chips and coal is practiced widely in the U.S. The direct incineration of the chips will utilize approximately 15.6 million tires per year and will make up 2% of the total fuel consumed at the plant. Other processes, such as thermal cracking and depolymerization, recover the oil, char, and gases from the tires as separate "product" streams.[44,45] However, the most well-known method for the generation of TDFs is from pyrolysis.[36,38,46–49]

13.4.2 Pyrolysis of Spent Tires

The recovery of energy from spent tires is not a new process. In 1974, the U.K. Department of Industry's Warren Spring Laboratory conducted the first tests to recover energy from spent passenger tires.[47] These initial experiments demonstrate that it was possible to break the tires down into oil and gas by heating it in a closed retort, followed by distillation of the gaseous products. As research continued, it was found that the final bottoms product, or char, could be further treated for the manufacture of activated carbon (as shown in Figure 13.10).[50] During the late 1980s, the use of pyrolysis for making TDFs became common. A number of U.S. and European patents have been granted for the pyrolysis of scrap tires.[51–54] Although each patent is somewhat different, the main operating principles and conditions are quite similar.

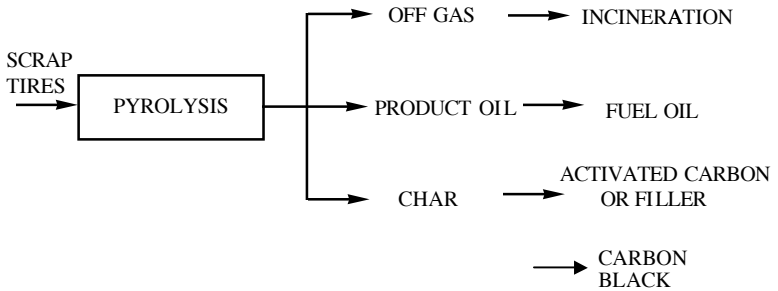

FIGURE 13.10 Possible end products from the pyrolysis of scrap tires.

In each instance, the scrap tires are first reduced in size, either by grinding, chipping, or pelletizing, then sent to a clarifier for the removal of the scrap metal. The method presented by Williams et al. represents the basic process utilized as the "starting block" by most research.[55] The temperature is initially at 100°C while the rubber is loaded into the reactor. After 1 h, the temperature is ramped up to 300–500°C, depending on the process. The reactor is held at the final temperature for a minimum of 2 h. The gas fraction is sent to a distillation apparatus for subsequent purification and analysis. The oil and char are separated using a second column. The slight variations on the pyrolysis process and their end products are presented in the following sections.

13.4.2.1 Occidental Flash Pyrolysis

Occidental Chemical's flash pyrolysis system was first demonstrated in late 1971. The process was able to produce a high-quality fuel oil at a moderate temperature and pressure. The advantage of the process was that the pyrolysis reaction was achieved without having to introduce hydrogen or using a catalyst. The process was divided into three main sections: feed preparation, flash pyrolysis, and product collection. A simplified schematic of the overall process is shown in Figure 13.11.[55]

The most time-consuming aspect of Occidental's process is the feed preparation. During this stage, the tires are debeaded and shredded to approximately 3 in. A magnet is then used to remove all the metal components. The remaining material is further shredded to 1 in. before being ground to -24 mesh. The grinding of the tires to such fine particles enabled the flash pyrolysis to occur at a quicker rate. The quick vulcanization of the ground rubber enabled a shorter residence time, which in turn decreased product cracking.[57]

After leaving the pyrolysis reactor, the gaseous stream was sent to a quench tower to separate the two end products. The product oil was collected and sent to a storage facility. The recovered gas was recycled to the char fluidizer and pyrolysis reactor as a supplemental process fuel. The solid components that remained in the bottom of the pyrolysis reactor were sent through three cyclones. The cyclones were used to separate the solid particles by size, as well as to cool the material back down to room temperature. At the end of the process, a 35 wt% carbon black was obtained. Analysis conducted on the carbon black showed that it had high enough quality for direct reuse in the rubber industry.[55]

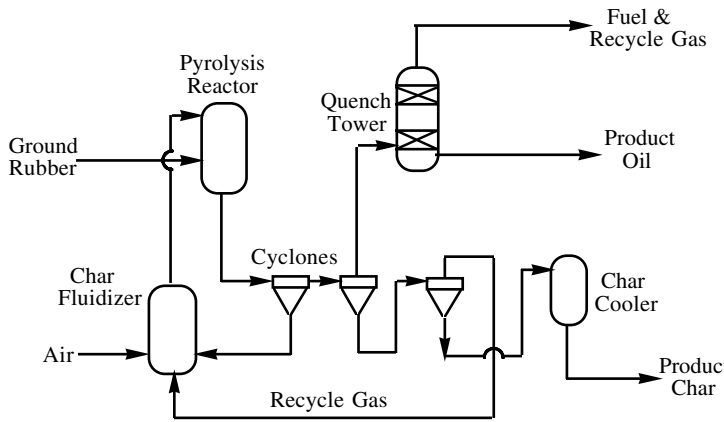

FIGURE 13.11 A simplified schematic of Occidental's flash pyrolysis system.

13.4.2.2 Fluidized Thermal Cracking

The first commercial use for *fluidized thermal cracking (FTC)* dates back to the 1930s for coal gasification. Similar to other pyrolysis processes, the FTC process burns waste with high combustion efficiency; however, it has a few other added advantages. Because it is a fluidized bed process, there is a rapid mixing of solid particles, which enables uniform temperature distribution; thus, the operation can be simply controlled. Fluidization also enhances the heat and mass transfer rates, which in turn decreases the amount of CO emitted. Researchers have been able to adjust the FTC operating conditions to decrease the SO_x and NO_x emissions.[58]

The Nippon Zeon Company has conducted extensive studies on TDFs via thermal cracking. The precommercial process feeds crushed tire chips to the fluidized bed using a screw feeder. Air heated by a preheating furnace is fed to the reactor bottom to elevate the reactor temperature near cracking conditions, 400 to 600°C, before the chips are introduced. This enables the tire chips themselves to maintain the cracking temperature. A continuous cyclone is used to remove the char. The cracked gases are brought into contact with the recovered oil from the quench tower. Part of the recovered oil is recycled to the quench tower and the remainder sent to an oil storage tank for further purification. The uncondensed gas is sent to a treatment process to remove the hydrogen sulfide. A simplified flowchart of the Nippon Zeon plant in Tokuyama is shown in Figure 13.12. The estimated break-even cost of the pyrolysis plant is $0.25 per tire.[59]

The preliminary studies used for the development of the Tokuyama plant had very promising results. All the end products produced could either be used directly as a supplemental fuel source at the plant or sent off-site for petroleum and chemical industries. A typical end product distribution of the FTC process is given in Table 13.4.[60]

13.4.2.3 Carbonization

Carbonization is another form of pyrolysis, which can convert over one half of a scrap tire into usable products. Carbonization processes operate at much higher temperatures than typical pyrolysis units. At this higher-temperature condition, the

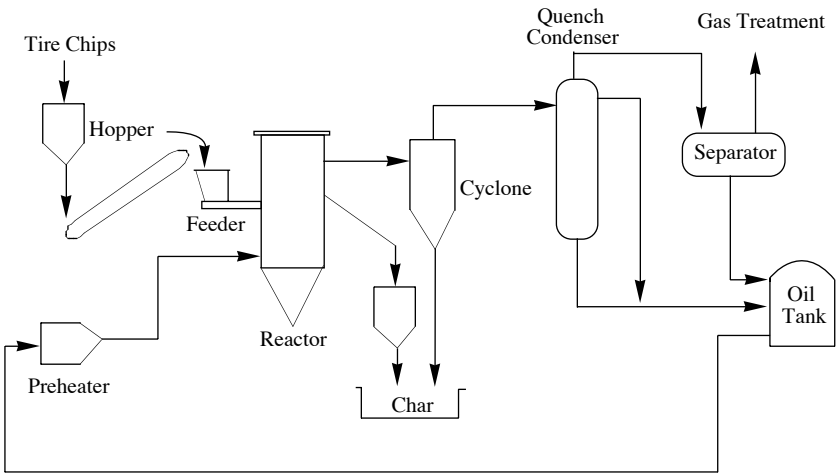

FIGURE 13.12 Nippon Zeon scrap tire fluidized cracking process. (From Saeki, Y. and Suzuki, G., *Rubber Age*, 108(2), 33–40, 1976.)

TABLE 13.4
End Product Distribution for Tires Cracked at 450°C

Product	Amount Produced (kg)	Percent
Oil	257	52.0
Char	166	33.6
Gas	72	14.4
Total	495	100.0

main product is char. The char is purified into carbon black, one of the main components in the manufacture of tires. In 1974, the cost of carbonization was approximately 3 times the cost of making carbon black from standard petroleum operations.[61] Although this number decreased by only 15% in the next decade, the incentive of utilizing a waste material offsets the remaining cost.[62]

13.4.3 Cocombustion of Scrap Tires and TDFs

Tire rubber can be combusted together with other fossil fuels as well as biomass without major alteration of an existing combustion facility. Energy generation using scrap tires and TDFs as a supplemental fuel to coal is of particular interest and is being practiced throughout the world. The rationale behind the use of tire rubber as a supplemental fuel to conventional coal in power generation is based on the following[64,69,70]:

1. Excellent combustion characteristics and high heating value
2. Lower cost and good availability

3. Relatively low sulfur content, especially on a Btu basis
4. Reducing the environmental burden and health effects of tire stockpiles

Typical heating values of tires are 15,000 to 16,000 Btu/lb, whereas typical bituminous coal (washed) has a heating value of 12,000 to 13,000 Btu/lb. Further, both carbon and hydrogen contents[69] are excellent, namely, 89 to 90 wt% for C and 7.5 wt% for H. These values are substantially better than those for coals. Typically, the sulfur content of scrap tires and TDFs is 1.5 to 2%. Considering the sulfur dioxide (SO_2) emission potential per fuel's generated energy value (pound SO_2 produced per million Btu generated), the result is closer to that for low-sulfur-containing coals.

However, cocombustion of tire and TDF may alter the emission characteristics of the combustion facility.[64,69,70] Some studies showed that using TDF resulted in slight increases in pollutant emissions, whereas others showed slight decreases in the mass emission rates of these pollutants.[69] There is no consistent trend. Based on the Purdue University Wade Utility Plant Facility test runs[64] comparing pure coal combustion and combustion of coal (95%) + TDF(5%), the atmospheric emissions of most trace metals increase when TDF is cocombusted with coal. In particular, zinc and cadmium emissions were drastically higher with TDF-blended fuel feed, whereas mercury emission was about the same. A comprehensive recent study of the effect of TDF supplement to fuel on air emissions was performed at Riverside Cement Inc. in Oro Grande, CA.[69] Based on the testing of 41 specific air toxins potentially emitted from a cement kiln, the average of three runs with and without TDF supplement (about 4.5% TDF by weight) showed that the mass emission rates of 22 air toxics were lower with TDF supplement, whereas the mass emission rates of only two compounds, zinc and anthracene, were higher with TDF-supplemented coal feed.[69] The two compounds are not classified as hazardous air pollutants (HAPs).

As can be seen, results of the effects on pollutant emission with TDF-supplemented fuel can be quite conflicting and point toward different directions.[69] Therefore, results of one plant study should not be generalized to another, because the prevailing conditions may differ very widely. Environmental impacts and health effects of tire cocombustion need to be carefully assessed for each plant with all relevant factors taken into account, namely, the combustion process itself, combustion conditions, plant design, control equipment and its efficiency with respect to specific trace elements, feed material properties, blend ratios, and analysis techniques.

13.4.4 IFP Spent Tire Depolymerization Process

A relatively new approach to the decomposition of used tires is the IFP process developed by the French Institute of Petroleum.[35] Unlike the other process, IFP does not require pretreatment of the scrap tire. The whole tires are placed in a basket and lowered into a 600-l reactor. Hot oil at 380°C is sprinkled onto the tire's surface. A chemical reaction between the hot oil and tires causes the depolymerization of the rubber. After the tires have been completely depolymerized, the reactor is cooled to 100°C. The offgases are sent to a distillation column. The column separates the gas and light hydrocarbon fractions. The resultant gas is sent for further purification into a C_4-C_6 fraction and gasoline (C_8-C_{10}), and the light hydrocarbons are recycled to

the reactor. The recycled hydrocarbon fraction is used to dilute the viscous fuel oil generated during the depolymerization process. Upon evacuating the reactor, the scrap metal is removed and sent off-site for salvage.

The IFP process is different in that it is a batch process.[44] Because it is operated batchwise, the concern over having enough tires for continuous feed is eliminated. Depolymerizing 4000 tons per year of waste tires has been estimated to generate over 15,200 tons of fuel oil, 360 tons of gasoline, 560 tons of gas, and 600 tons of metallic waste.

13.4.5 Dry Distillation of Spent Tires

Researchers have investigated the use of a specialty dry distillation apparatus for producing a gaseous fuel from spent tires. The process can be operated with either shredded or whole tires without removing metallic wires. The tires enter the top of the distillation tower via a conveyor belt. Once filled, the tower is sealed to prevent the gaseous product from escaping. Combustion is initiated by burners located at the bottom of the tower and then sustained by the introduction of process air. As combustion continues, the hot gas rises to the top of the tower. The rising gas has a dual purpose. The first is to assist in the combustion of the tires located at the top of the tower. Second, the rising of the gas acts in the same manner as a traditional distillation column for the separation of the end products. The gas is cooled down by the gas cooler. Part of the gas is liquefied and recovered in the form of oil. Recovered oil is equivalent to Class B heavy oil.[71] The residue (char and tire cord) is removed from the bottom tower by a conveyor. Once cooled, the residue is separated into individual components.

Hiroshi and Haruhiko[63] operated a pilot plant scale of the tower continuously for 250 h. At the end of the process time, it was found that approximately 40 wt% of the tires were converted into usable gaseous fuel. The remaining 60% was composed of char and tire cord. Research is being conducted on improving the amount and purity of the recovered gas. In addition, Hiroshi and Haruhiko are also investigating the potential uses for the recovered char.

A process schematic of the *Direct Dry Distillation of Tire* by Fujikasui Engineering Co. is shown in Figure 13.13.[71]

13.4.6 Goodyear's Devulcanization Process

Goodyear Rubber and Tire Co. has developed a unique process for devulcanizing scrap tire rubber using a novel supercritical fluid technology.[67,68] The technology uses sec-butanol as a supercritical fluid, which functions as a pyrolysis medium and also as a chain cleavage agent.[67] The solvent is unique in the sense that it not only facilitates C-S and C-C bond cleavage reaction in a near-homogeneous state, but also dissolves the reacted fragments and takes them away from other reactive intermediates. The solvent, sec-butanol, is fully recoverable and reusable in the process. Furthermore, the objective of the process is quite different from that of other processes in the sense that the product of the process treatment is intended for use in manufacturing tires as a tread-compounding ingredient. Laboratory test of 20 phr (parts per hundred parts of rubber) of the process reclaimed materials has shown

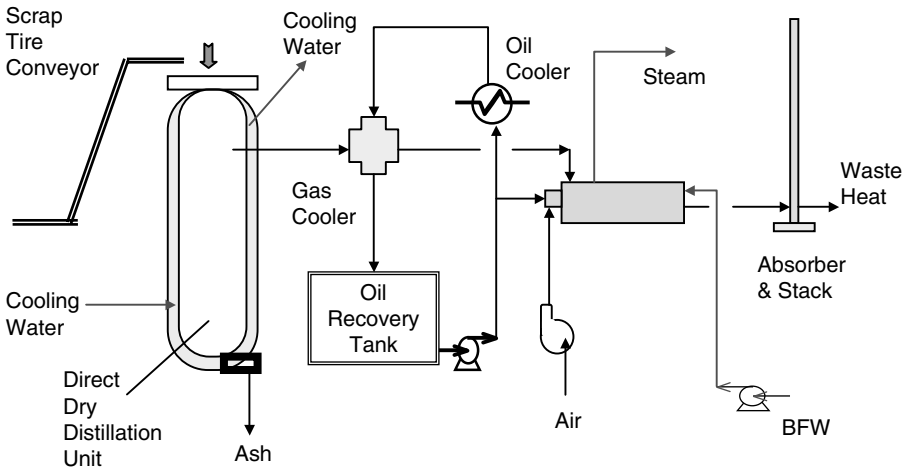

FIGURE 13.13 A process schematic of the direct dry distillation of tire.

equal mechanical properties and cure characteristics, when compared with fresh tread-compounding formulations (i.e., without any reclaimed material).[68] The process achieves devulcanization in the truest sense without altering basic polymeric properties. They have tested an exhaustive list of other solvents that are intuitively promising and structurally attractive for the similar process application. Their results showed that sec-butanol in its supercritical condition was at least severalfold better than all other fluids. It is noteworthy that even the closest isomer such as iso-butanol did not yield any comparable results. This strong supercritical behavior of sec-butanol may be attributed to its unique molecular structure, which has the center carbon connected to all four different functional fragments, thereby maximizing the quadruple moments. They further enhanced their process by employing a cosolvent process, by which the amount of sec-butanol needed can be significantly reduced for the process without loss of efficiency. As a cosolvent to this process, carbon dioxide (CO_2) was found to be very effective.[67]

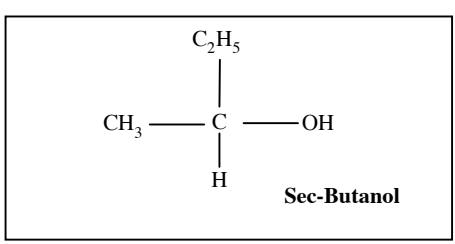

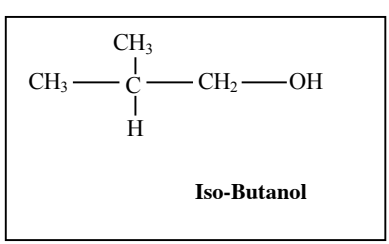

13.4.7 Hydrogenation of Spent Tire Rubber

Hydrogenation, unlike pyrolysis or similar processes, is a chemical synthesis process. In simple terms, it entails the addition of hydrogen, the element that is removed from oil, to make synthetic rubber. By adding the appropriate amount of hydrogen to the

waste tires, the rubber can be returned to its original form. By adding hydrogen, devulcanization, saturation, and carbon–carbon bond cleavage reactions are induced. In a sense, the process is quite similar to the hydrotreating process of heavy oil and resids.

REFERENCES

1. Corbitt, R.A., Ed., *Standard Handbook of Environmental Engineering*, McGraw-Hill, New York, 1990.
2. Fisher, P.M. and Evans, L.R., Jr., Whole tyre recycling: the elm energy approach, *Rubber Europe Conference Proceedings*, No. 6.012, June 1993, pp. 1–6.
3. Frederick, W.J. et al., Energy and Materials from Recycled Paper Sludge, AIChE Summer National Meeting, Denver Co., August 14–17, 1994.
4. Association of Plastics Manufacturers in Europe, Plastics: A Vital Ingredient for the Food Industry, RAPRA Technology, Ltd., 1993, pp. 12–30.
5. Richards, M.K., USEPA's evaluation of a texaco gasification technology, *Proceedings: ACS Emerging Technologies in Hazardous Waste Managemen*t, VI, Atlanta, GA., September 1994, pp. 19–21.
6. Stearns, R.P., Landfill methane: 23 sites are developing recovery systems, *Solid Wastes Manage./Resour. Recovery J.*, 1980, pp. 56–59.
7. Pober, K. and Bauer, H., From Garbage — Oil, *CHEMTECH*, 1(3), 1977, pp. 164–169.
8. Kagayama, M., Igarashi, M., Hasegawa, M., and Fukuda, J., Gasification of Solid Waste in Dual Fluidized-Bed Reactors, *ACS Symposium*, Ser. No. 130, 38, 1980, pp. 525–540.
9. Henry, J.G. and Heinke, G.W., *Environmental Science and Engineering*, Prentice Hall, NJ, 1989, p. 560.
10. Green, A.E.S., Overview of fuel conversion, *Fuel Combust. Technol.*, 12: 3–15, 1991.
11. Helt, J.E. and Mallya, N., Pyrolysis experiments with municipal solid waste components, *Proceedings of 23rd Intersociety Energy Conversion Engineering*, IEEE Service Society, NJ, 1988.
12. Bell, P.R. and Varjavandi, J.J., Pyrolysis — Resource from Solid Waste, Proceeds, *Waste Management, Control, Recovery and Reuse*, Ann Arbor Science, MI, 1974, pp. 207–210.
13. Schlesinger, M.D. et al., Pyrolysis of waste materials from urban and rural sources, *Proceedings of Third Mineral Waste Utilization Symposium*, Chicago, IL, March 14–16, 1972, pp. 423–428.
14. Davis, M.L. and Cornwell, D.A., *Introduction to Environmental Engineering*, 2nd ed., McGraw-Hill, New York, 1991.
15. Scott, D.S., Czernik, S.R., Piskorz, J., and Radlein, A.G., Fast pyrolysis of plastic wastes, *Energy Fuels*, 4: 407–411, 1990.
16. Chambers, C., Larsen, J.W., Li, W., and Wiesen, B., Polymer waste reclamation by pyrolysis in molten salts, *Ind. Eng. Chem. Process Des. Dev.*, 23: 648–654, 1984.
17. Producer Responsibility for Packaging Waste in Austria, *ENDS Rep.*, 224: 18, 1993.
18. Baker, J., Unravelling the Recycling Targets, *European Chemical News*, 60(1596), 1993, pp. 16–17.
19. Topfer Extends Plastics Recycling Deadlines, *European Chemical News*, 60(1595), 1993, p. 25.
20. McMahon, P., Plastics Reborn, *Chemical Engineering*, 1992, pp. 37–43.

21. Hunt, J., LCA Endorses Use of HDPE Waste, *Packaging Week*, 9(22), 1993, p.1.
22. Leaversuch, R.D., Chemical recycling brings real versatility to solid-waste management, *Mod. Plast.*, July 1991, pp. 40–43.
23. Bertolini, G.E. and Fontaine, J., Value recovery from plastics wastes by pyrolysis in molten salts, *Conserv. Recycling*, 10(4): 331–343, 1987.
24. Kaminsky, W., Pyrolysis of plastic waste and scrap tires in a fluid bed reactor, *Resour. Recovery Conserv.*, 5: 205–216, 1980.
25. Romanow-Garcia, S., Plastics-planning for the future, *Hydrocarbon Processing*, 72(10): 15, 1993.
26. Sittig, M., *Organic and Polymer Waste Reclaiming Encyclopedia*, Noyce Data Corp., NJ, 1981, p. 178.
27. Vohwinkel., F., Approach to recycling polyurethane waste, *Tin and Its Uses*, 149: 7–10, 1986.
28. Scheirs, J., Bigger, S.W., and Billingham, N.C., Effect of chromium on the oxidative pyrolysis of gas-phase HDPE as determined by dynamic thermogravimetry, *Polym. Degradation Stability*, 38(2): 139–145, 1992.
29. Venuto, P.B. and Habib, E.T., Jr., *Fluid Catalytic Cracking with Zeolite Catalysts*, Marcel Dekker, New York, 1979.
30. Hashimoto, K. et al., *New Developments in Zeolite Science and Technology*, Elsevier, Amsterdam, 1986, pp. 505–510.
31. Songip, A.R., Masuda, T., Kuwahara, H., and Hashimoto, K., Test to screen catalysts for reforming heavy oil from plastic wastes, *Appl. Catal. B: Environ.*, 2: 153–164, 1993.
32. Menges, G., Basis and technology for plastics recycling, *Int. Polym. Sci. Technol.*, 20(8):10–15, 1993.
33. Semel, G., Study of Gasification of Plastic Waste, *UAPG Symposium*, Ser. No. 19, 9, 1991.
34. Kawakami, S., Inoue, K., Tanaka, H., and Sakai, T., Pyrolysis Process for Scrap Tires, *ACS Symposium* Ser. No. 130, 40, 557–572, 1980.
35. Used Tyres: A Crumb of Comfort, *Recycling and Resource Management*, 1992, pp. 25–26.
36. English, D., Scrap Tire Problem Could Be Gone by 2003, *Tire Business*, 11(7), 1993, pp. 34–35.
37. Greenhut, S., Dealers, Retreaders Confront Growing Scrap Tire Problem, *NTDRA Dealer News*, 49(1), 1986, pp. 36–40.
38. Clark, T., Scrap Tyres: Energy for the Asking, *British Plastics and Rubber*, 1985, pp. 35–37.
39. McCarron, K., Maker of Scrap-Tire Boilers Sees Bright Future, *Tire Business*, 11(17), 1993, p. 14.
40. Sikora, M.C., Ed., Whitewall Cement Fires Kiln with Scrap Tires: Tires-to-Fuel Process Becomes a Reality at LaFarge Cement, *Scrap Tire News*, 7(11), 1993, pp. 1–10.
41. Kokish, B., Organization Seeks Scrap Tire Solutions, *Rubber Plastics News*, 23(6), 1993, pp. 44–46.
42. SSI: Lucas Furnaces — Tyres Disposal by Incineration, *Tyres and Accessories*, 11, 1992, pp. 68–69.
43. Pearce, F., Scrap Tyres: A Burning Issue, *New Scientist*, 140(1900), 1993, pp. 13–14.
44. Audibert, F. and Beaufils, J.P., Thermal Depolymerization of Waste Tires by Heavy Oils: Conversion into Fuels, Final Report EUR 8907 EN, Commission of European Communities: Energy, 1984.

45. Saeki, Y. and Suzuki, G., Fluidized Thermal Cracking Processes for Waste Tires, *Rubber Age*, 108(2), 1976, pp. 33–40.
46. Braslaw, J., Gealar, R.L., and Wingfield, R.C., Jr., Hydrocarbon generation during the inert gas pyrolysis of automobile shredder waste, *Polym. Prep.*, 24(2): 434–435, 1983.
47. Reed, D., Tyre pyrolysis comes on stream, *Eur. Rubber J.*, 166(6): 29–33, 1984.
48. Earle, B.A., Dallas Investors Purchase Tire Pyrolysis Plant, *Rubber Plastic News*, 23(2), 1993, p. 3.
49. Wyman, V., Turning a Profit from Old Tyres, *The Engineer*, 273(7066/7), 1991, p. 36.
50. Jackson, D.V., Resource Recovery, Warren Spring Laboratory Report No. C95/85, 1985.
51. Apffel, F., Recovery Process, U.S. Patent No. 4,647,443, 1987.
52. Reu, R.A., Pyrolyric Conversion System, European Patent No. 446,930,A1, 1991.
53. Grispin, C.W., Jr., Pyrolytic Process and Apparatus, European Patent No. 162,802, 1984.
54. Roy, C., Vacuum Pyrolysis of Scrap Tires, U.S. Patent No. 4,740,270, 1988.
55. Williams, P.T., Besler, S., and Taylor, D.T., The pyrolysis of scrap automotive tires: influence of temperature and heating rate on product composition, *Fuel*, 69, 1474–1481, 1990.
56. Che, S.C., Deslate, W.D., and Duraiswamy, K., The Occidental Flash Pyrolysis Process for Recovering Carbon Black and Oil from Scrap Rubber Tires, *ASME*, 76-ENAs-42, 1976.
57. Nag, D.P., Nath, K.C., Mitra, D.C., and Raja, K., A laboratory study on the utilization of waste tire for the production of fuel oil and gas of high calorific value, *J. Mines Met. Fuels*, 473–476, 1983.
58. Chang, Y.M. and Chen, M.Y., Industrial waste to energy by circulating fluidized bed combustion, *Resour. Conserv. Recycling*, 9(4): 281–294, 1993.
59. Kroschwitz, J.I., Ed., *Encyclopedia of Polymer Science and Engineering*, Vol. 14, Wiley & Sons, New York, 1988, pp. 787–904.
60. Saeki, Y. and Suzuki, G., Fluidized Thermal Cracking Process For Waste Tires, *Rubber Age*, 108(2), 1976, pp. 33–40.
61. Kiefer, I., U.S. EPA Report No. SW-32c.1, 1974.
62. Jarrell, J., International Patent, WO 93/12198, 1993.
63. Hiroshi, K. and Haruhiko, A., Process and Apparatus for Dry Distillation of Discarded Rubber Tires, European Patent No. 0,072,387, 1982.
64. Carleton, L.E., Giere, R., Lafree, S.T., and Tishmack, J.K., Investigation of Atmospheric Emissions from Co-combustion of Tire and Coal, paper presented at the Annual Meeting of the Geological Society of America, Seattle, WA, November 2–5, 2003.
65. Official Web site of the City of Los Angeles, accessed in May 2006, http://www.lacity.org/council/cd12/pdf/Landfilling_Resources_MPA_Pyrolysis_Facility.pdf.
66. Web site of automotive learning center, accessed in May 2006, http://www.drivinginnovation.com/glossary/faq.html.
67. Benko, D.A., Beers, R.N., Lee, S., and Clark, K., Devulcanization of Cured Rubber, U.S. Patent No. 6,992,116, January 31, 2006.
68. Beers, R.N. and Benko, D.A., Recycling of spent tires, *Encyclopedia of Chemical Processing*, Lee, S., Ed., Taylor & Francis, New York, 2005, pp. 2613–2623.
69. Karell, M., Regulation Impacts on Scrap Tire Combustion: Part II, MALCOM PIRNIE Web site, http://www.pirnie.com/resources_pubs_air_feb00_3.html.

70. Alvarez, R., Callén, M.S., Clemente, C., Gómez-Limón, D., López, J.M., Mastral, A.M., and Murillo, R., Soil, water, and air environmental impact from tire rubber/coal fluidized-bed cocombustion, *Energy Fuels,* 18(6), 1633–1639, 2004.
71. Web site by Japanese Advanced Environment Equipment, Waste Tires Direct Dry Distillation System; accessed May 2006, http://nett21.gec.jp/JSIM_DATA/WASTE/WASTE_6/html/Doc_541.html.

14 Geothermal Energy

Sunggyu Lee and H. Bryan Lanterman

CONTENTS

14.1 INTRODUCTION

The natural heat of the earth is called geothermal energy. *Geothermal* is a hybrid word, combining *geo* (earth) and *thermal* (of heat). The term *geothermal energy* denotes the total thermal energy contained beneath the relatively thin and comparatively cool outer surface of the earth. This represents about 260 billion cubic miles of rocks and metallic alloys at or near their melting temperatures. Geothermal resources range from shallow ground to hot rock and water several miles below the earth's outer surface, and even farther down toward the earth's core, in the region of extremely high temperatures of molten rock called *magma*.

Geothermal energy, the second most abundant source of heat on earth after solar energy, is accessible using current technology, and is concentrated in underground reservoirs, usually in the forms of steam, hot water, and hot rocks. The three applicable technology categories are geothermal heat pumps, direct-use applications, and electric power plants. Geothermal heat pumps use the earth's surface as a heat sink and heat source for both heating and cooling. Direct-use applications utilize the naturally occurring geothermally heated water for heating. Electric power plants use electric turbines fed by geysers to generate electricity. As in solar energy, the utility of geothermal energy is hampered by the extent of its distribution over the earth's surface in amounts that are often too small or too dispersed.[1] This is especially serious for the generation of electricity.

The most obvious forms of geothermal energy are *geysers*, boiling pools of mud, fumaroles, and hot springs. However, a greater potential does exist in regions not yet recognized for their energy possibilities — they are *hot dry rocks* (*HDRs*).

Besides the vast availability and the unique distribution pattern of these resources, geothermal energy is very clean and environmentally friendly. Geothermal energy generates no (or minimal) greenhouse gases because the conversion or utilization process does not involve any chemical reaction, in particular, combustion. Geothermal fields produce only about one sixth of the carbon dioxide that a natural-gas-fueled power plant produces and very little, if any, of the nitrous oxide or sulfur-bearing gases. Furthermore, geothermal energy is available 24 hours a day, and 365 days a year, whatever the external weather conditions may be. This is in sharp contrast to other green energy technologies such as wind and solar. In fact, geothermal power plants typically have average availabilities of 95% or higher, much higher than most coal and nuclear plants. Even this high availability can be further enhanced to a level that is practically near 100%, with advances and enhancements in the process technology.

14.2 GEOTHERMAL ENERGY AS RENEWABLE ENERGY

14.2.1 Need for Geothermal Energy

The development and importance of new, clean energy sources such as geothermal energy gather pace because of not only the depletion of petroleum resources but also the environmental problems associated with conventional energy processes. Environmental problems associated with the utilization of fossil fuel sources involve: (1) emission of greenhouse gases such as CO_2, CH_4, and N_2O; (2) emission of SO_x

and H_2S; (3) discharge of nitrogen oxides; (4) potential emission of mercury and selenium; (5) emission of volatile and semivolatile organic compounds (*VOCs* and *SVOCs*)[22]; (6) emission of particulate matter (*PM*); and (7) contamination of soils and groundwater resources with hazardous wastes.

At a depth of about 6 mi from the earth's surface, the temperature is higher than 100°C; thus, the total amount of geothermal energy in storage far exceeds, by several orders of magnitude, the total thermal energy accountable in all forms of nuclear and fossil fuel resources of this planet. Solar energy is the only comparable resource in terms of such vast quantities. Therefore, it is very logical, if not imperative, that our energy priorities incorporate a vital resource such as geothermal energy.

14.2.2 Renewability and Sustainability of Geothermal Energy

The U.S. Department of Energy classifies geothermal energy as *renewable*. Its source is the continuously emanating thermal energy generated by the earth's core. Each year, rainfall and snowmelt maintain the supply of requisite water to geothermal reservoirs, and production from individual geothermal fields can be sustained for decades and perhaps centuries. An accurate prediction of the sustainable service life of each field is, however, very difficult.

14.2.3 Occurrence of Geothermal Energy

The occurrence of geothermal heat (also known as geoheat) can be explained by one of the following theories[2]:

1. The first theory is that about 6 billion years ago the earth was a hot molten mass of rock, and this mass has been cooling through the epochs of time, with the outer crust formed as a result of a faster cooling rate.
2. The second theory presupposes that the earth is like a giant furnace. The decaying of radioactive material within the earth provides a constant heat source.
3. The third theory is based on the presumption that geothermal heat originates from the earth's fiery consolidation of dust and gas over 4 billion years ago.

Even though a generally agreed explanation for the natural occurrence of geothermal energy is unavailable, a combination of the aforementioned theories is widely offered.

The interior of the earth consists of a molten fluid of extremely high-temperature rocks called *magma*, which cools and expels heat to the earth's surface according to the second law of thermodynamics. The flow of heat is from the hot source (earth core) toward the cold sink (earth surface). The cold sink (i.e., heat sink in thermodynamics) consists of the earth's crust, surface, and atmosphere. This may be considered a very slow process of heat transfer.

Figure 14.1 shows a typical geological setting of a geothermal energy source. Thermal energy from the earth's core continuously flows outward. The heat transfer from the core to the surrounding layers of rock, the *mantle*, is principally via conduction. As the temperature and pressure of the system become high enough,

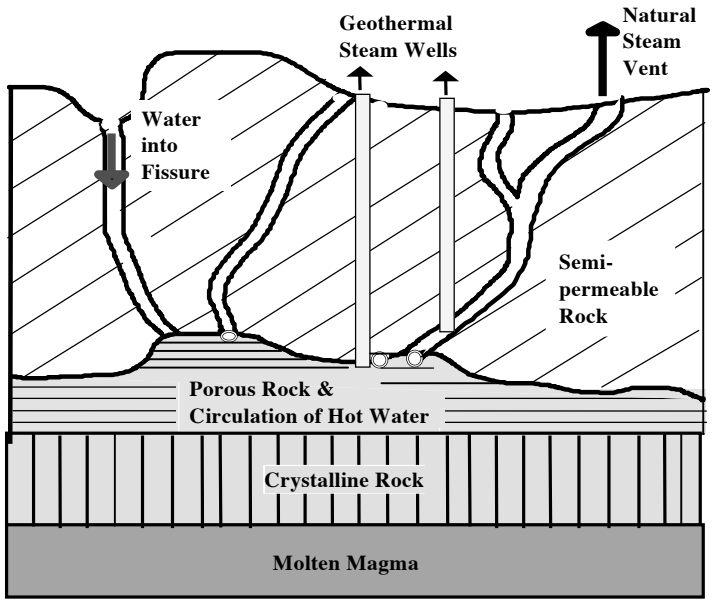

FIGURE 14.1 Geothermal energy source.

some mantle rocks melt and form *magma*. Because the magma as a liquid phase is less dense and more fluidlike than the surrounding rock, it slowly rises and moves toward the earth's crust, thus convecting the heat from the core. This is why a slow convective heat transfer often represents the overall heat transfer process. Sometimes, the hot molten magma reaches all the way to the earth's surface, where it is known as *lava*. However, in most cases, the magma remains well below the earth's crust, heating neighboring rocks and water, which originates from rainwater seepage deep into the earth. The temperature of the water can be as hot as 380°C, which is even higher than the critical temperature of water, 374°C.

The water at this depth is subjected to high pressure and temperature. Depending on the imposed conditions, it may exist as a supercritical fluid. It then rises to the surface through fissures as a result of its density change and, in effect, it vents from the system, thereby reducing the pressure of the system. When the pressure decreases, the water boils, turns into steam and rises to the surface through fissures and wells. Some of the best-known examples of hot geothermal water are hot springs or *geysers*. However, most of the hot geothermal water remains deep underground, typically trapped in cracks and porous rocks. This natural collection of hot underground water is called a *geothermal reservoir.*

The gross quantity of geothermal energy cannot be properly determined. The total energy content of the rocks down to a depth of 10 km has been estimated to be 3×10^{26} cal. At the earth's core, i.e., 6400 km deep, the temperature may reach over 5000°C. However, based on current technology, only a fraction of this heat is available as a recoverable resource. A mere 0.03%, or 10^{23} cal, of this energy is considered hot enough and near enough to the earth's surface to be recoverable; the rest of the energy is too widely dispersed over the crust or too deep to be practical.

TABLE 14.1
Classification of Geothermal Resources

Types of Geothermal Resources	Temperature (approximate; °C)
(a) Convective hydrothermal resource	
Vapor-dominated	240
Hot-water-dominated	30–350
(b) Other hydrothermal resources	
Sedimentary basins/regional aquifers (hot fluid in sedimentary rocks)	30–150
Geopressured (hot fluid under pressure that is greater than hydrostatic)	90–200
Radiogenic (heat generated by radioactive decay)	30–150
(c) Hot rock resources	
Part still molten (magma)	>600
Solidified (hot, dry rock)	90–650

Geothermal resources may be classified into several categories, principally based on their phases and forms, as shown in Table 14.1.

Although all resources shown in the table cannot be used to produce electricity, they can still be utilized in many industrial, agricultural, and domestic areas. Research conducted by the U.S. Geological Survey[3] has identified the significant research problems that need to be solved for full utilization of geothermal resources.

14.2.4 Advantages of Geothermal Energy

Geothermal energy resources are continuous, reliable, sustainable, clean, and can be cost-competitive in meeting baseload capacity needs. Specific advantages of geothermal systems include:

1. Indigenous energy — Geothermal energy helps reduce dependence on fossil or nuclear fuels and, as such, helps boost the economic benefits in the region.
2. Clean energy — Use of geothermal energy helps reduce combustion-related emissions.
3. Diversity of use — Geothermal energy has three common economic uses: electricity generation, direct use of heat, and geothermal heat pumps.
4. Long-term resource potential — With optimum development strategies, geothermal energy can provide a significant portion of a nation's long-term energy needs.
5. Flexible system sizing — Current power generation projects range in capacity from a 200-kW system in China to 1200-MW at The Geysers in California. Additional units can be installed in increments depending on the growth of the electricity demand.
6. Power plant longevity — Geothermal power plants are designed for a life span of 20 to 30 years. With proper resource management strategies, life spans can exceed design periods.
7. High availability and reliability — "Availability" is defined as the percentage of the time that a system is capable of producing electricity.

Availability of 95 to 99% is typical for modern geothermal plants, compared to a maximum 80 to 85% for coal and nuclear plants.[6]

8. Combined use — Geothermal energy can be simultaneously used for both power generation and direct-use applications.
9. Low operating and maintenance costs — The annual operation and maintenance costs of a geothermal electric system are typically 5 to 8% of the capital cost.
10. Land area requirement — The land area required for geothermal power plants is smaller per megawatt than for almost every other type of power generation plant.
11. Enhanced standard of living — Geothermal systems can be installed at remote locations without requiring other industrial infrastructure. The region can prosper without pollution.

14.2.5 Global Geothermal Energy

The current total installed capacity of geothermal power stations throughout the world is over 8200 MW.[4] The U.S. remains the biggest producer of electricity from geothermal energy, as shown in Table 14.2. The developing countries accounted for

TABLE 14.2
Installed Geothermal Electricity Generation Capacity

Country	1990	1995	1998
Argentina[a]	0.67	0.67	0
Australia	0	0.17	0.4
China	19.2	28.78	32
Costa Rica	0	55	120
El Salvador	95	105	105
France (Guadeloupe)	4.2	4.2	4.2
Greece[a]	0	0	0
Guatemala	0	0	5
Iceland	44.6	49.4	140
Indonesia	144.75	309.75	589.5
Italy	545	631.7	768.5
Japan	214.6	413.7	530
Kenya	45	45	45
Mexico	700	753	743
New Zealand	283.2	286	345
Nicaragua	70	70	70
Philippines	891	1191	1848
Portugal (Azores)	3	5	11
Russia	11	11	11
Thailand	0.3	0.3	0.3
Turkey	20.4	20.4	20.4
U.S.	2774.6	2816.7	2850
Total	5866.72	6796.98	8240

[a] Argentina and Greece closed their pilot plants.

TABLE 14.3
Major Geothermal Power Plants in the U.S.

Location	Capacity Installed (MW)
The Geysers, CA	2115
East Mesa, CA	119
Salton Sea	198
Heber, CA	94
Mammoth, CA	7
Coso. CA	225
Amadee, CA	2
Wendel, CA	0.6
Puna, HI	18
Steamboat, NV	31
Beowave, NV	17
Brady, NV	6
Desert Peak, NV	9
Wabuska, NV	1.2
Soda Lake, NV	3.6
Stillwater, NV	14
Empire Farms, NV	4.8
Roosevelt, UT	20
Cove Fort, UT	4.2
Total	2889.4

Source: From Wright, P.M., *The American Association of Petroleum Geologists Bulletin*, Vol. 23, No. 12, 366, October 1989.

35% of the total for 1995, and 46% for 1999. About 2850 MW of electricity generation capacity is available from geothermal power plants in the western U.S. The major geothermal fields along with their capacities are shown in Table 14.3.[5] Direct-use geothermal technologies utilize naturally hot geothermal water for commercial greenhouses, crop dehydration, fish farming, bathing, and district community heating. *Geothermal heat pumps* (*GHPs*) use the constant temperature of the top 50 ft of the earth's surface to heat buildings in winter and cool them in summer. Table 14.4 shows the direct-use of geothermal heat in various categories in the U.S.[6,7]

Fossil fuels, namely oil, coal, and gas, provide 86% of all the energy used in the U.S. In 2004, renewable energy sources supplied just 6.1% of the total U.S. energy consumption. Most of the renewable energy consumption was provided by hydroelectric power (44.5%) and biomass utilization (46.5%), whereas only 5.6% came from geothermal sources. Figure 14.2 shows the history and projections for U.S. energy consumption from fuel sources during the period 1980–2030.[23]

As shown in the figure, the projected future growth in the area of nonhydro and nonnuclear renewable energies is substantial. When the relative cost of electricity generation from geothermal sources decreases, the popularity of geothermal power generation will undoubtedly increase. Figure 14.3 shows a cost comparison among various modes of power generation.

TABLE 14.4
U.S. Geothermal Direct-Use Projects

Applications	Number of Sites	Thermal Capacity (MW)	Annual Energy (GWh)
Geothermal heat pumps	most states	2072	2402
Space and district heating	126	188	433
Greenhouses	39	66	166
Aquaculture	21	66	346
Resorts/pools	115	68	426
Industrial processes	13	43	216
Total		2503	3989

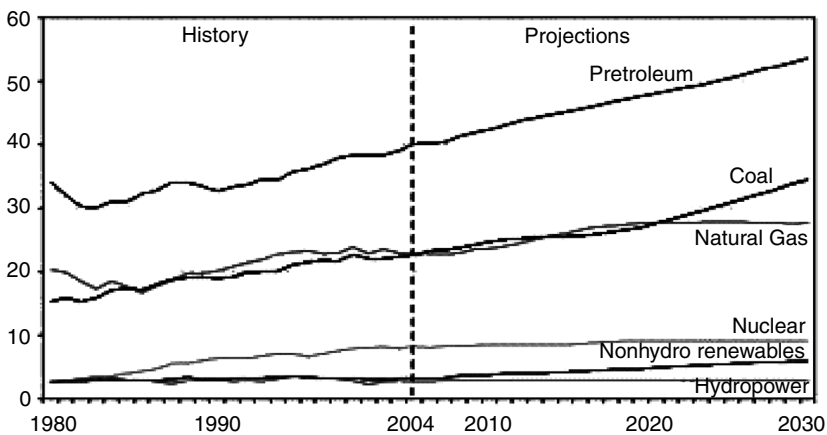

FIGURE 14.2 U.S. energy consumption by fuel sources: past, current, and future forecast. Unit used is in quadrillion Btus. (From U.S. Department of Energy, 2006.)

14.3 HISTORY OF GEOTHERMAL ENERGY DEVELOPMENTS

Ancient people regarded the depths of the earth with horror as hell, the seat of malignant gods, who were responsible for natural phenomena like earthquakes and volcanic eruptions. Nevertheless, in ancient times the Romans, and in modern times the Icelanders, Japanese, Turks, Koreans, and others, have used its potential for baths and space heating.

The Larderello field in Tuscany, Italy, first began to produce electricity in 1904, which developed over the next 10 years to a capacity of 250 KW. In Japan, Beppu was the first site for experimental geothermal work in 1919, and these experiments led to a pilot plant in 1924 producing 1 KW of electricity. Somewhat earlier than this, the Japanese had begun to use geoheat to warm their greenhouses. In Iceland, municipal heating was provided using hot thermal waters in the 1930s, and it is still the major source of heating today.

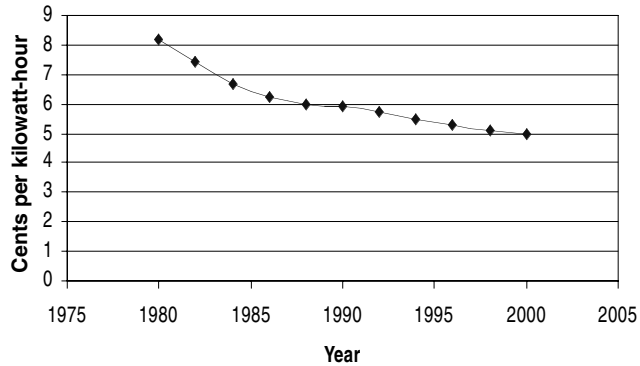

(a) Geothermal Energy

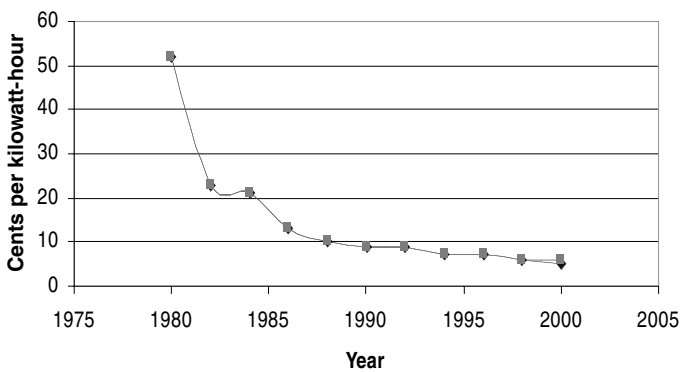

(b) Solar Thermal Energy

FIGURE 14.3 Cost comparison of electricity generation between (a) geothermal energy and (b) solar thermal energy.

It was not until the early 1920s that the U.S. examined the possibilities of commercial usage of geothermal steam. However, the competition from hydroelectric power was too keen to promote further development at that time. Today, the largest geothermal power plant in the world is located in California at The Geysers, which is probably the largest reservoir of geothermal steam in the world.[8] In recent years, U.S. DOE's *GeoPowering the West* (*GPW*) program has been working to further geothermal energy efforts.[9]

Growing concerns about the environmental effects of increasing CO_2 and methane in the atmosphere are working to enhance the role of geothermal resources worldwide. Hence, the utilization of geothermal energy to generate electric power dominates all other applications.

A number of factors that have boosted the production of geothermal energy are[10]:

1. The economics of geothermal energy became more favorable, owing to the increase in petroleum and natural gas prices.

2. The cost of producing geothermal energy decreased during 1980–2000.
3. Legislative actions and measures encouraging geothermal developments have been in place for many countries. Examples in the U.S. include the Energy Policy Act and the National Geologic Mapping Act in the early 1990s.[11]
4. The implementation of the Clean Air Act Amendments of 1990 also provides an economic benefit because of the well-developed technology for control of gas emissions from geothermal power plants.
5. Amendment of the Public Utilities Regulatory Act removed the 80-MW limit from independent power plants selling electricity to utilities and is expected to improve the competitiveness of geothermal energy.

14.4 GEOTHERMAL PROCESSES AND APPLICATIONS

14.4.1 Geothermal Power Plants

Geothermal resources may be described as hydrothermal, hot dry rock, or geopressured. Hydrothermal resources contain hot water, steam, or a mixture of water and steam. Although research into ways of efficiently extracting and using the energy contained in hot dry rock and geopressured resources continues, virtually all current geothermal power plants operate on hydrothermal resources.

The characteristics of the hydrothermal resource determine the power cycle of the geothermal power plant. A resource that produces dry steam uses a direct steam

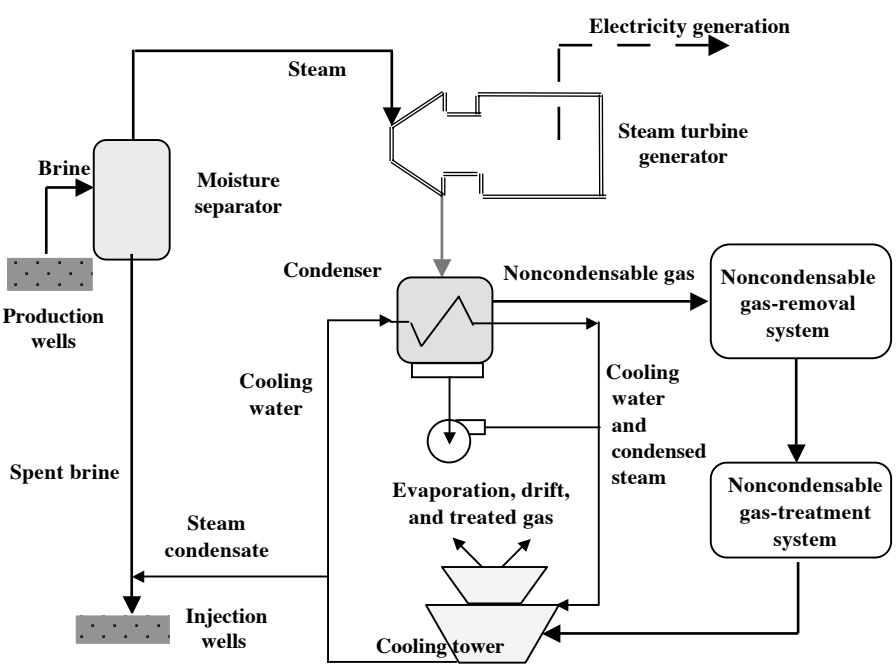

FIGURE 14.4 Direct steam cycle geothermal power plant.

cycle. A power plant for a liquid-dominated resource with a temperature above 165°C typically uses a flash steam cycle. For liquid-dominated resources with temperatures below 165°C, a binary cycle is the best choice for power generation. Power plants on liquid-dominated resources often benefit from combined cycles, using both flash and binary energy-conversion cycles.

14.4.1.1 Direct Steam Cycle[12]

Direct steam is also referred to as *dry steam*. As the term implies, steam is routed directly to the turbines, thus eliminating the need for the boilers used by conventional natural gas and coal power plants. Figure 14.4 shows a schematic of a direct steam cycle power generation process. In a direct steam cycle power plant, a geothermal turbine can operate with steam that is far from pure. Chemicals and compounds in solid, liquid, and gaseous phases are transported with the steam to the power plant. At the power plant, the steam passes through a separator that removes water droplets and particulate before it is delivered to the steam turbine. The turbines are of conventional design with special materials, such as 12Cr steel and precipitation-hardened stainless steel, to improve reliability in geothermal services.

The other components present in the direct steam geothermal cycle include:

1. A condenser used to condense turbine exhaust steam. Both direct-contact and surface condensers are used in direct-steam geothermal power plants.
2. Noncondensable gas-removal system, to remove and compress the non-condensable gases. A typical system uses two stages of compression. The first stage is a steam jet ejector. The second stage is another steam jet ejector, a liquid ring vacuum pump, or a centrifugal compressor.
3. The cooling tower employs a multicell wet mechanical draft design. Cooling is accomplished primarily by evaporation. Water that is lost from the cooling system to evaporation and drift is replaced by steam condensate from the condenser.
4. An injection well: Excess water is returned to the geothermal resource in an injection well.

The direct steam cycle is typical of power plants at The Geysers in northern California, the largest geothermal field in the world. The primary operator of The Geysers is Calpine Corporation.

14.4.1.2 Flash Steam Cycle[12]

Flash steam is the steam produced when the pressure on a geothermal fluid is reduced. A flash steam cycle for a high-temperature liquid-dominated resource is shown in Figure 14.5. This dual-flash cycle is typical of most larger flash steam geothermal power plants. Single-flash cycles are frequently selected for smaller facilities.

Geothermal brine, or a mixture of brine and steam, is delivered to a flash vessel at the power plant by either natural circulation or pumps in the production wells. At the entrance to the flash vessel, the pressure is reduced to produce flash steam. The steam is delivered to the high-pressure inlet to the turbine. The remaining brine

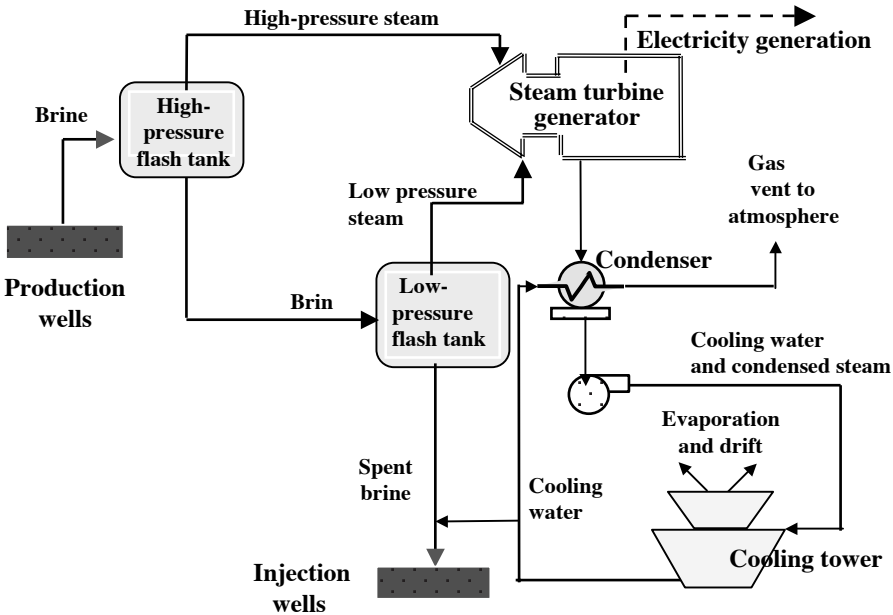

FIGURE 14.5 Double-flash steam cycle geothermal power plant.

drains to another flash vessel in which the pressure is again reduced to produce low-pressure flash steam.

The other components present in the double-flash steam geothermal cycle include:

1. Direct-contact condenser: As hydrogen sulfide is not produced in large quantities.
2. A cooling tower: This cycle also uses a multicell wet mechanical draft cooling tower. The water lost because of evaporation and drift is replaced by steam condensate.
3. The excess water and spent brine from the flash vessels are injected back into the geothermal resource in an injection well.

14.4.1.3 Binary Cycle[4]

A binary-cycle geothermal power plant employs a closed-loop heat exchange system in which the heat of geothermal fluid (*primary fluid*) is transferred to a lower-boiling heat transfer fluid (*secondary fluid*) that is thereby vaporized and used to drive a turbine or generator set. In other words, a binary cycle uses a secondary heat transfer fluid instead of steam in the power generation equipment. Binary geothermal plants have been in service since the late 1980s. A binary cycle is the economic choice for hydrothermal resources, with temperatures below approximately 165°C. A typical binary cycle is shown in Figure 14.6.

The binary cycle shown in Figure 14.6 uses isobutane (i-C_4H_{10}) as the binary heat transfer fluid. Heat from geothermal brine vaporizes the binary fluid in the brine

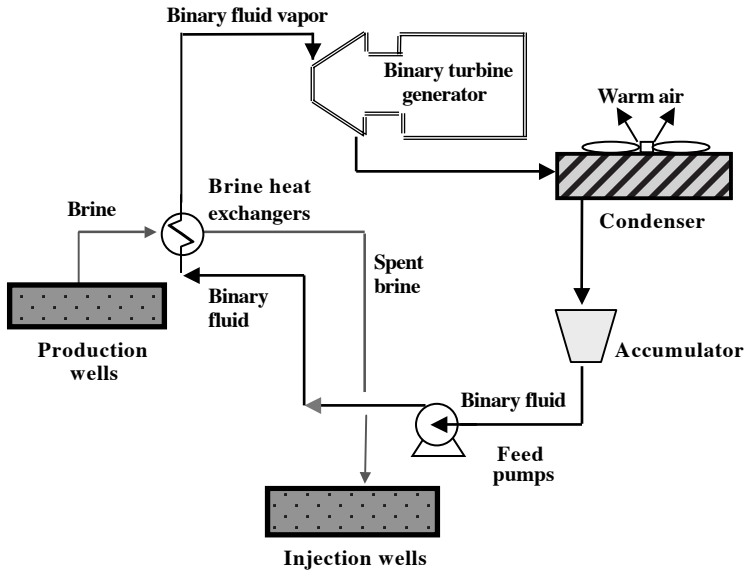

FIGURE 14.6 Binary cycle geothermal power plant.

heat exchanger. Spent brine is returned to the resource in injection wells, and the binary fluid vapor drives a turbine generator. The turbine exhaust vapor is delivered to an air-cooled condenser, in which the vapor is condensed. Liquid binary fluid drains to an accumulator vessel before being pumped back to the brine heat exchangers to repeat the cycle. The brine heat exchangers are typically shell-and-tube units fabricated from carbon steel.

14.4.1.4 Hot Dry Rock (Dry Geothermal Sources) Systems[2,13,14]

Because the vast majority of the geothermal heat resources of the world exist as hot dry rocks (HDR) sources rather than water (hydrothermal) systems, it is only natural for this energy source to receive more attention from geothermalists. The more accessible HDR resources in the U.S. alone would provide an estimated 650,000 quads of heat, one quad (one quadrillion Btu's) being equivalent to the amount of energy contained in 171.5 million barrels of oil. Because annual U.S. energy consumption is approximately 84 quads, whoever figures out how to economically tap even a fraction of the potential in HDR could earn a place in history.

HDR is a deeply buried crystal rock at a usefully high temperature. Current engineering designs plan to tap its heat by drilling a wellbore, fracturing or stimulating pre-existing joints around the wellbore, and directionally drilling another wellbore through the fracture network. Cold water then flows down one wellbore, pushes through the fractured rock, warms, returns up the other wellbore, and drives a power plant. The major technical uncertainty is establishing the fracture network between the two wellbores. If adequate connectivity can be established and a sufficiently large fracture surface area can be exposed between the two welbores, HDR can be a very competitive source of energy.

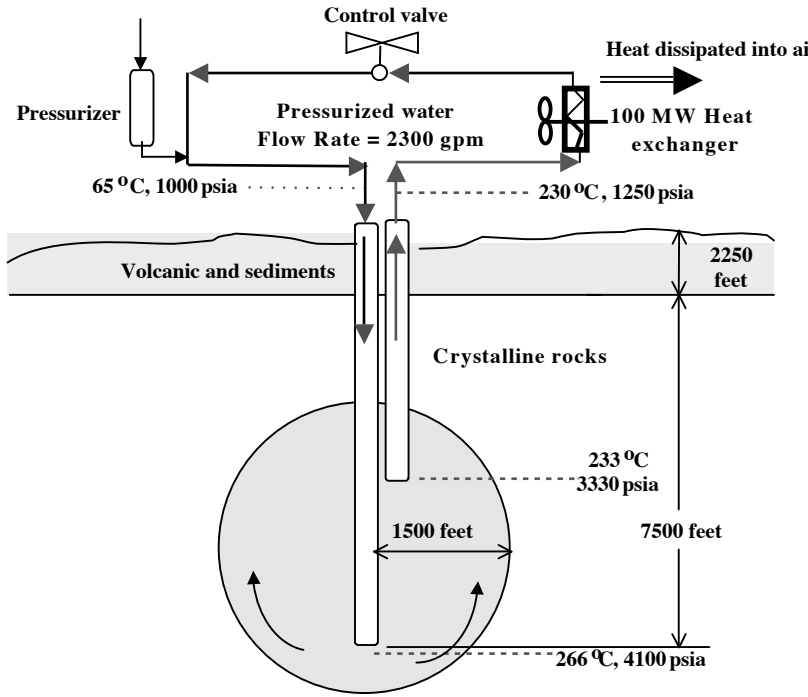

FIGURE 14.7 Experimental configuration and operating conditions Los Alamos hydraulic fracture network.

Figure 14.7 is a schematic diagram of the experimental Los Alamos System in New Mexico. Water at 65°C and 1000 psia is pumped into the hydraulic fracture network, approximately 3000 ft in diameter and circulated at 7500 ft, where temperatures range between 260 and 320°C. The pressure is around 4100 psia. The water is then pumped out of the ground, and when it reaches the surface, its temperature is 230°C at 1250 psia.

In this experimental system, the hot water is circulated through an air-cooled heat exchanger with the extracted heat dissipated to the atmosphere.

14.4.1.5 Fresh Water Production

Less than 2% of the earth's retained water supply is available for drinking. The oceans, atmosphere, rocks or rock formations, and polluted resources contain the remaining 98%. From the standpoint of water shortage, all the systems recognized to date (desalination, recycling, and transportation over long distances) consume enormous amounts of energy and have also proved to be uneconomical. Geothermal resources, on the other hand, contain vast reservoirs of hot water and steam, and some of these produce electricity and fresh water as by-products. The geothermal resource satisfies two main criteria for alleviating water shortages, namely:

1. An energy source for distillation process such as multistage flash (MSF) and vertical tube evaporator (VTE)
2. An ample supply of water

14.4.2 Direct Use of Geothermal Heat

Direct-heat use is one of the oldest, most versatile, and also the most common form of utilization of geothermal energy. The term *direct use* means that geothermal heat is used directly without first converting it to electricity. The warm water or steam exiting the ground will be piped into the dwelling or structure to provide warmth. Direct heating is obviously an older technology than geothermal power generation and is widely practiced.

14.4.2.1 Space and District Heating

Direct heating can be applied in what are known as either district or space heating systems, the distinction being that space heating systems serve only one building, whereas district heating systems serve many structures from a common set of wells. Direct heating has made the greatest progress and development in Iceland, where the total capacity of the operating geothermal district heating system is 800 MW.[15] Figure 14.8 shows an example of a district heating system.

Each system has to be adapted to the local situation, depending on the type of geothermal resource available, the population density of the area and the predicted population growth, the type of buildings requiring heating or cooling and, above all, the local climate. Geothermal district heating pumps are capital intensive in the early

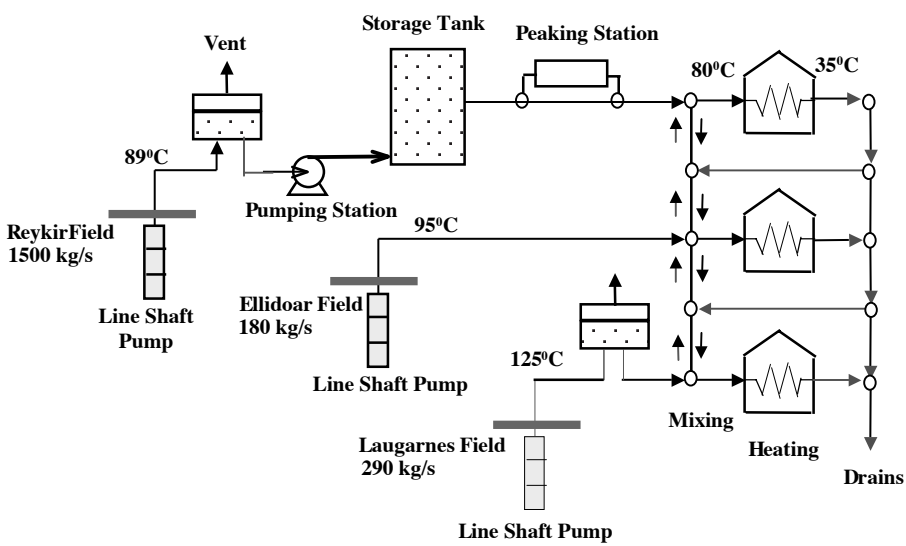

FIGURE 14.8 A schematic of Hitaveita Reykjavikur (Reykjavik district heating system).

stages. The principal costs are initial investments for production and injection wells, down-hole and circulation pumps, heat exchangers, and pipelines, as well as the distribution network. A high load density usually makes district heating economically more feasible, because the cost of the distribution network transporting hot water to consumers is shared. Importantly, operating costs are comparatively low, thus making the long-term cost much more favorable. Geothermal district heating systems offer significant life cycle cost savings to consumers, as much as 30 to 50% of the cost of using natural gas or oil.

At present, a very successful district heating system exists in San Bernardino, CA. The water production system, consisting of two wells, yields an average flow of 5200 l/min at 54°C water. The system currently serves 33 buildings, including government centers, a prison, a new blood bank facility, and other private buildings.

14.4.2.2 Agricultural Applications

One specific application of direct heating is greenhouse heating. This is one of the most common worldwide applications of geothermal energy. Fruits, vegetables, flowers, and ornamental plants are successfully grown year-round, in geothermally heated greenhouses using low-temperature sources (<38°C). Geothermal energy can extend short growing seasons and significantly reduce fuel costs. One example is a 650-m^2 greenhouse in California, utilizing a geothermal well 150 m deep that supplies 67°C water. The well is capable of supplying heat for an additional 1800–3700 m^2 of greenhouse. It is noteworthy that the energy crisis experienced in California in 2001 posed a very severe threat to greenhouse farmers who relied on electricity or natural gas heating. As of 2003, there were at least 37 greenhouse operations based on the geothermal energy in the United States.[24]

Another direct-heating application involves aquaculture, which is the raising of freshwater or marine organisms in a controlled environment. Geothermally heated water produces excellent yields of high-quality fish and crustaceans under accelerated growth conditions. Furthermore, geothermal aquaculture permits breeding in the winter, allowing fish farmers to harvest their products when product availability is low, and market prices are high. As of 2003, there were at least 58 aquaculture sites using geothermal energy in the U.S.[24] About 15 aquaculture operations were clustered in the southern California area.

14.4.2.3 Balneology

Balneology involves the use of geologically heated water/brine/mud sources for bathing purposes and is also said to possess healing and prophylactic properties. Balneology is centuries old and has been practiced by Etruscans, Romans, Greeks, Turks, Mexicans, Japanese, Koreans, Americans and, undoubtedly, others.

14.4.2.4 Industrial Process Heat

Industrial processes can be heat intensive, and commonly use either steam or superheated water with temperatures of 150°C or higher. This makes industrial processes the highest-temperature users of geothermal direct-heat applications. However, lower temperatures can suffice in some cases, especially for some drying applications. Two

of the largest industrial users of geothermal heat are a diatomaceous-earth drying plant in Iceland and a paper and pulp processing plant in New Zealand.

14.4.3 Geothermal Heat Pumps

The *geothermal heat pump* (*GHP*), also referred to as the *ground source heat pump* (*GSHP*), uses the earth as a heat source for heating and as a heat sink for cooling. The GSHP uses a reversible refrigeration cycle combined with a circulating ground loop to efficiently provide either heating or cooling from electricity. The basic mechanism is the same as that of an air source heat pump but operates more efficiently because the temperature of the ground is more favorable than that of the air, i.e., the ground is warmer in the winter and cooler in the summer than the air. Additionally, the ground temperature is fairly constant throughout the year, even at depths of as little as 5 to 10 ft.

The typical components of a residential GSHP during heating and cooling cycles are shown in Figure 14.9 and Figure 14.10. The major components of the system are the ground loop and a refrigeration unit composed of the compressor, primary heat exchanger, expansion valve, and secondary heat exchanger. The refrigeration cycle utilizes the same unit operation steps as an air source heat pump or typical home air conditioning unit. In what is referred to as a closed-loop system, a water and antifreeze mixture circulates through a pipe buried in the ground and transfers thermal energy between the ground and the primary heat exchanger in the heat pump. Depending on the mode of operation, either heating or cooling is provided based on the reversible valve that allows the refrigerant to reverse the order of the operations of the cycle. Therefore, the primary heat exchanger, which consists of a water-to-refrigerant loop, can act as an evaporator or condenser. Also included in this system is a heat exchanger

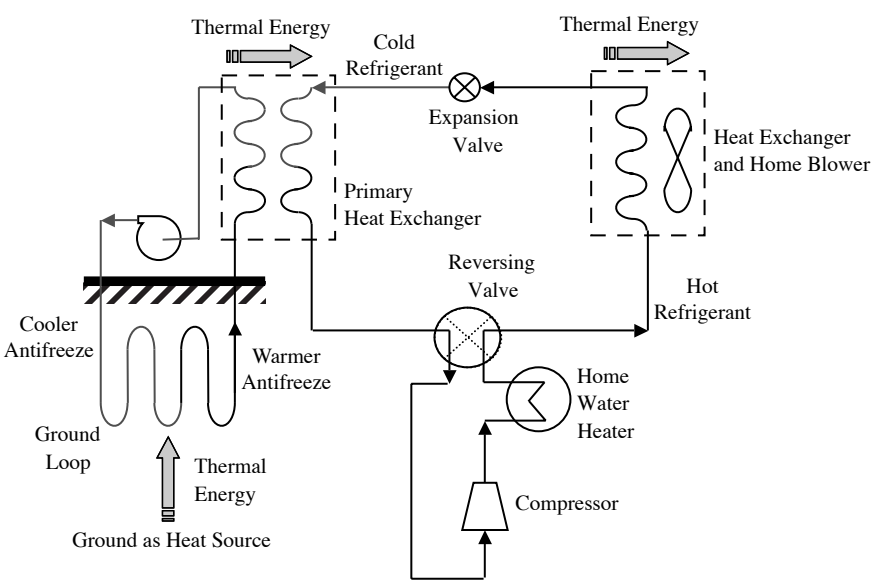

FIGURE 14.9 GSHP during heating cycle.

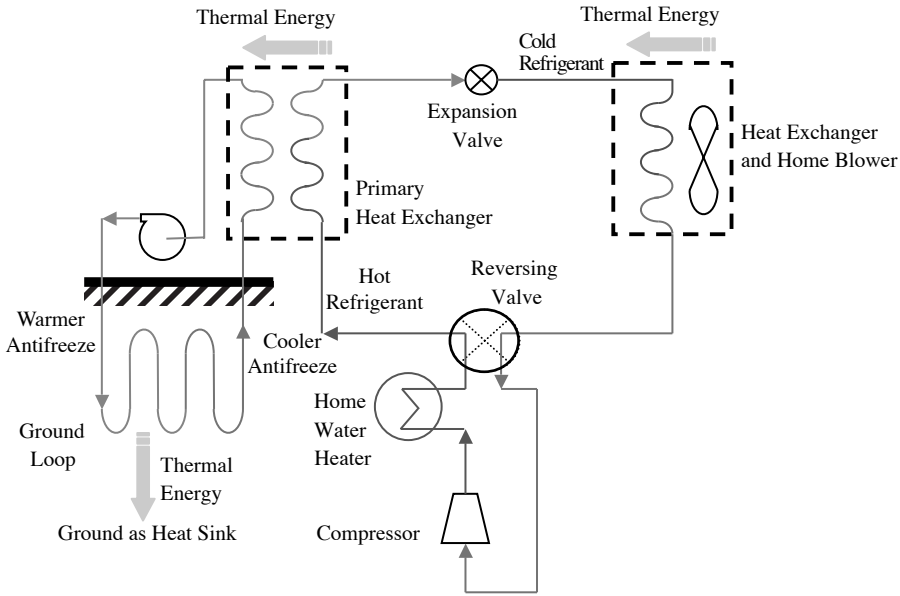

FIGURE 14.10 GSHP during cooling cycle.

following the compressor that provides heat to a hot water heater; this is often referred to as a de-superheater. The Geothermal Heat Pump Consortium Inc. offers technical, educational, and promotional support for Geoexchange systems.[16]

Geothermal heat pumps offer a distinct advantage over the use of air as a source or sink, because the ground is at a more favorable temperature. Compared to atmospheric air, the ground is warmer in winter and cooler in summer. Therefore, GHPs demonstrate better performance over air-source heat pumps. GHPs also reduce electricity consumption by approximately 30% compared to air-source heat pumps. Aided by utility-sponsored programs, GHPs are becoming increasingly popular throughout the world. In the U.S., the GHP industry is expanding at a growth rate of 10 to 20% annually. As of 2004, more than 200,000 GHPs are being operated in U.S. homes, schools, and commercial buildings.[17]

The industrial and other potential applications of geothermal energy suggest that great economic advantages could be gained from dual or multipurpose plants combining power production with one or more other applications. Such plants would enable the costs of exploration drilling and certain other items to be shared among two or more end users.

14.5 SCIENTIFIC AND TECHNOLOGICAL DEVELOPMENTS

14.5.1 Major Research Efforts

The following major activities are examples of U.S.-Government-funded research being conducted in accordance with its R&D strategy:[6,9]

1. Advanced techniques to detect and delineate hidden geothermal resources are being developed, including remote-sensing techniques and improvements of various electric and acoustic methods.
2. Slim-hole drilling and coring, a cost-effective option for exploratory drilling, needs to be improved. This research includes developing slim-hole reservoir engineering techniques and logging tools.
3. Improved materials that are capable of withstanding the high temperature and corrosive nature of geothermal brines are being developed.
4. Methods to increase the net brine effectiveness of geothermal power plants are being pursued, as are ways to reduce power plant costs.

Significant research activities in progress at national laboratories and universities in the U.S. and the world include those of Sandia National Laboratory,[18,9] Lawrence Berkeley National Laboratory,[9] Brookhaven National Laboratory,[4,9] National Renewable Energy Laboratory,[17] Los Alamos National Laboratory,[19,20,21] The Geysers,[10] Camborne School of Mines,[4] European Hot Dry Rock Industries,[4] Stanford University and Leningrad's Mining Institute,[4] Electric Power Research Institute (EPRI), Geo-Heat Center of the Oregon Institute of Technology, Southern Methodist University Geothermal Laboratory, and Virginia Polytechnic Institute and State University.

14.5.2 Technology Updates

The development of a successful geothermal energy project relies on a variety of specialized technologies as well as their cost-effectiveness.

14.5.2.1 Exploration Technology

Exploration is key to the discovery of new geothermal resources. It identifies geothermal resources, estimates resource potential, and establishes resource size, depth, and potential production. It relies on surface measurements of subsurface geological, geochemical, and geophysical conditions to develop a conceptual model of the system. Geothermal exploration of unmapped regions typically proceeds in two basic phases, reconnaissance and detailed exploration. During the reconnaissance phase, regional geology and fracture systems are studied, such as young volcanic features, tectonically active fault zones (as deduced from seismic information), and overt or subtle geothermal manifestations. If the reconnaissance phase confirms that the province has geothermal potential and that specific sites in the province should be explored further, the second phase focuses on one or more individual prospects covered in the reconnaissance phase.

14.5.2.2 Brine-Handling Technology

Brine is a geothermal solution containing appreciable concentrations of sodium chloride or other salts. The chemical composition, including the salinity of geothermal fluids, varies greatly from one reservoir to another. Variations in chemistry and salinity affect the design, maintenance, and longevity of wells and surface equipments. Recent advances in this area include[6]:

1. Use of scale-inhibiting chemicals to reduce carbonate scaling of flashing wells
2. Development of pH modification to control silica scaling in power plants
3. Development of highly effective computer programs to estimate and predict chemistry effects in geothermal systems
4. Continued development of polymeric cement coating to reduce corrosion in heat exchangers and process piping

14.5.2.3 Environmental Issues of Geothermal Energy Utilization

Even though geothermal energy is one of the cleanest and safest means of generating electric power, its effects on water resources, air quality, and noise during geothermal development and operation must be understood and mitigated. Among these are emissions to air (particularly of hydrogen sulfide), land use, and disposal of solid wastes. Effects can vary greatly from site to site.

Steam and flash plants emit mostly water vapor (steam). Binary power plants run on a closed-loop system, therefore zero discharge of gases is accomplished. Geothermal industries have developed advanced technologies to recycle minerals in geothermal fluid so that little or no disposal or emissions occur. The examples are found from The Geysers power plants in northern California that separate and use sulfur for sulfuric acid production, and also from the Salton Sea power plants in southern California recycling salts from geothermal brine, recovering silica from mineralized brine for use as fillers in concrete, and extracting zinc for additional plant profitability.

14.6 CONCLUSION

Geothermal resources are continuously renewable sources of energy regardless of climate or weather conditions, unlike wind or solar energy. Reliability, sustainability, and cleanness make geothermal energy especially attractive as a source of baseload electricity generation or for direct-use applications that need constant heat or energy. Geothermal power plants compete economically with coal, oil, and nuclear plants in meeting baseload capacity needs, with significant environmental advantages. The next generation of geothermal power plants will be designed using long-term projections for resource production as the basis for cycle selection, optimization, and system design.

Current HDR technology is competitive with modern coal-fired plants in regions with geothermal gradients exceeding 60°C/km.[13] Reasonable improvements in reservoir performance or reductions in drilling and completion costs may substantially lower the effective cost of HDR power. In areas with steep geothermal gradients, the use of HDR may demonstrate a substantial cost advantage over coal. This advantage may increase over time, allowing the use of HDR to produce a significant portion of the future electricity of the world.

Owing to its practicality and low operating costs, direct application of geothermal energy is expected to grow in popularity, especially in geothermally favored regions.

Diverse applications are expected to be developed in this field, and more advances in geothermal heat pump technology are also expected. Advances in materials, process integration and design, resource management, instrumentation, and drilling technology will undoubtedly enhance the global utilization of geothermal energy.

REFERENCES

1. Geothermal Resource Group, Geothermal Resource and Technology in the United States, National Academy of Sciences, Washington, D.C., 1, 1979.
2. Chermisinoff, P.N. and Morresi, A.C., *Geothermal Energy Technology Assessment*, Technomic Publishing Co., CT, 1970.
3. Griffin, R.D., *CQ Researcher*, Vol. 2, No. 25, July 10, 1992, pp. 575–588.
4. Lynn, M. and Reed, M.J., *Energy Sources*, Vol. 14, 443, 1992.
5. Wright, P.M., *The American Association of Petroleum Geologists Bulletin*, Vol. 23, No. 12, 366, October 1989.
6. U.S. Department of Energy, United States Geothermal Energy — Equipment and Services for Worldwide Application, 1994, DOE/EE — 0044.
7. U.S. Department of Energy, Geothermal Energy: 1992 Program Overview, 1992.
8. Hadfield, P., *New Scientist*, February 17, 1990, p. 58.
9. Web site of Geothermal Technologies Program, Energy Efficiency and Renewable Energy, U.S. Department of Energy, 2004, http://www.eere.energy.gov/geothermal/deployment_gpw.html.
10. Reed, M.J., *Geotimes*, Vol. 36, No. 2, 1991, p.16.
11. Reed, M.J., *Geotimes*, Vol. 38, No. 2, February 1993, p. 12.
12. Phair, K.A., *Mechanical Engineering*, September 1994, p. 76.
13. Harden, J., *Energy*, Vol. 17, No. 8, 777, 1992.
14. Tenenbaum, D., *Technology Review*, Vol. 98, January 1995, p. 38.
15. Dickson, M.H. and Fanelli, M., *Energy Sources*, Vol. 6, 349, 1994.
16. Web site of Geothermal Heat Pump Consortium, Inc., 2004, http://www.geoexchange.org/about/how.html.
17. Web site of National Renewable Energy Laboratory, 2004, http://www.nrel.gov/documents/geothermal_energy.html.
18. Feature Article, *Power Engineering*, Vol. 93, October 1989, p. 50.
19. Joyce, C., *New Scientist*, February 4, 1989, p. 58.
20. Anderson, I., *New Scientist*, Vol. 111, July 24, 1986, p. 22.
21. Feature Article, *Mechanical Engineering,* Vol. 113, January 1991, p. 10.
22. Speight, J.G. and Lee, S., *Handbook of Environmental Technology*, 2nd ed., Taylor & Francis, New York, 2000.
23. Annual Energy Outlook 2006, Energy Information Administration, U.S. Department of Energy, Washington, D.C., 2006.
24. Boyd, T.L. and Lund, J.W., Geothermal Heating of Greenhouses and Aquaculture Facilities, paper presented at International Geothermal Conference, Session #14, Reykjavik, Iceland, September 2003: accessible through http://jardhitafelag.is/papers/PDF_Session_14/S14Paper029.pdf.

15 Nuclear Energy

Sudarshan K. Loyalka

CONTENTS

15.1 NUCLEAR FISSION AND NUCLEAR REACTOR PHYSICS

The neutron was discovered in 1932. The following years witnessed intense studies of its properties and interactions with matter. This neutral particle is about 2000 times the mass of an electron, and is scattered and absorbed by different materials. The nature and rate of its reaction are determined by the nuclei of the host material and the energy of the neutron. Moreover, the nuclei that absorb neutrons can become radioactive and be transmuted to other types of nuclei, through radioactive decays. Neutrons can also split (fission) some nuclei (the fissile isotopes such as U-233, U-235, and Pu-239). Such fission is a complex process that produces new nuclei, beta and gamma radiation, and a few neutrons themselves. The products are energetic (the kinetic energy of fission products, energy of the radiation), deriving their energy from the binding energy of the nucleus. Consequently, the new neutrons (2 to 3 on average) released in fission provide the basis for a chain reaction. This chain reaction can be sustained (each successive generation has the same number of neutrons) or multiplied (each successive generation has more neutrons), and it can be used for a controlled and a sustained as well as an explosive release of energy.[1–21]

TABLE 15.1
Distribution of Fission Generated Energy in Time and Position

Type	Process	Percent of total released energy	Principal position of energy deposition
Fission			
I: instantaneous energy	Kinetic energy of fission fragments	80.5	Fuel material
	Kinetic energy of newly born fast neutrons	2.5	Moderator
	γ energy released at time of fission	2.5	Fuel and structures
II: delayed energy	Kinetic energy of delayed neutrons	0.02	Moderator
	β-decay energy of fission products	3.0	Fuel materials
	Neutrinos associated with β decay	5.0	Nonrecoverable
	γ-decay energy of fission products	3.0	Fuel and structures
Neutron capture			
III: instantaneous and delayed energy	Nonfission reactions due to excess neutrons plus β- and γ-decay energy of (n,γ) products	3.5	Fuel and structures
Total		100	

Source: From El-Wakil, M.M., *Nuclear Heat Transport*, International Textbook Company, now available from the American Nuclear Society, 1971. With permssion.

Fission of a single nucleus releases about 200 MeV ($3.2\ 10^{-11}$ J) of energy. This energy is distributed, in a power reactor of modern design, approximately as shown in Table 15.1 and Figure 15.1.

Of this 200 MeV, about 190 MeV, or 95%, is recoverable energy, as the neutrinos do not interact with matter, and escape from the system without depositing energy. One kilogram of U-235 contains 2.563×10^{24} U-235 nuclei, and its fission would release energy of about 78×10^6 MJ (which is the same as 21.6×10^6 kWh or 2.47 MWyr).

The fission products and beta and alpha particles are mostly deposited within a fraction of centimeter from the point of birth (in a solid or a liquid), whereas neutrons and gammas travel a greater distance depending on their energy and the material. The prompt radiation is emitted within 10^{-17} to 10^{-6} sec from an interaction, whereas the delayed radiation can be emitted within a few milliseconds to thousands of years (e.g., the long-lived isotopes).

The U-235 and neutron fission reaction can thus be described as:

$$U^{235} + n \rightarrow A + B + \nu\, n \tag{15.1}$$

in which A and B can be, for example, nuclei of cesium and strontium, and ν is the number of neutrons produced. The reaction is in accordance with generalized laws of conservation, but A, B, and ν are not necessarily the same for each fission. In fact, a

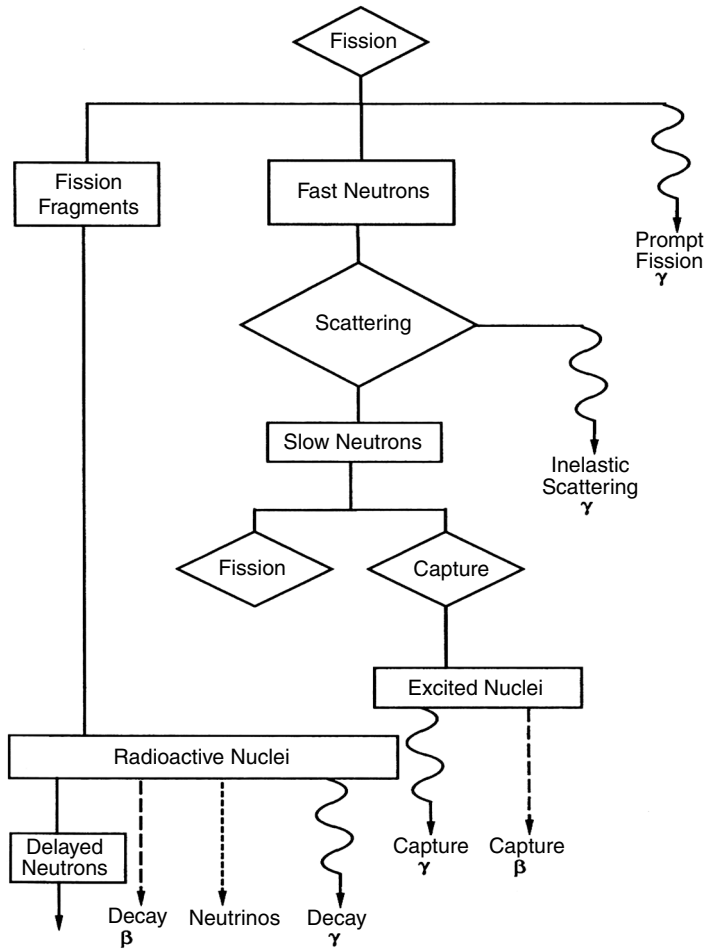

FIGURE 15.1 Distribution of fission energy in energy and time. (From Ott, K.O. and Neuhold, R.J., *Introductory Nuclear Reactor Dynamics*, American Nuclear Society, 1985. With permission.)

number of species are produced, and both ν and the energy (kinetic) of product neutrons vary. Furthermore, the fission reaction rate is strongly dependent on the energy (kinetic) of the reacting neutron (and also on the kinetic energy of the reacting U-235 in certain energy ranges). Figure 15.2 and Figure 15.3 show, respectively, the distribution of fission products and the distribution in energy of the neutrons produced in fission.

It is useful to note here that in a nuclear reactor the overall neutron density (#/cm^3) is smaller than the nuclei density (#/cm^3) by about 10 orders of magnitude. Thus, the nuclei distribution is determined by nuclei–nuclei interactions, and the neutron distribution in space, direction, energy, and time is determined by neutron–nuclei interaction. In the long term, the fission products, actinides, and lattice suffer damage because the energetic products and neutrons affect the nuclei–nuclei interactions. Incidentally, both microscopic and macroscopic experiments have been

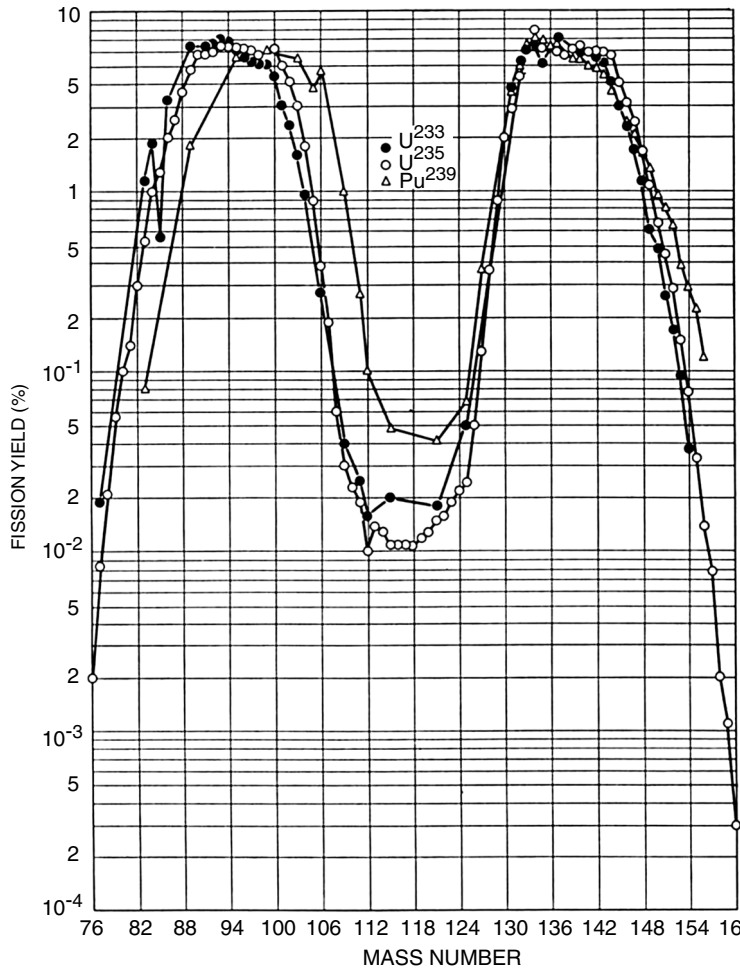

FIGURE 15.2 Fission product distribution. (From Weinberg, A.M. and Wigner, E.P., *The Physical theory of Neutron Chain Reactors*, University of Chicago Press, 1958. With permission.)

used to study neutron–nuclei interactions, and a wealth of information on the nature of these interactions and their rates is now available. The rate R_i(#/sec) for a reaction of type "i" (absorption, fission, scattering) is expressed as:

$$R_i\left(\mathbf{r},E,\Omega,t\right)d\mathbf{r}\,d\Omega\,dE=\Sigma_i\left(\mathbf{r},E,t\right)\phi\left(\mathbf{r},E,\Omega,t\right)d\mathbf{r}\,d\Omega\,dE \tag{15.2}$$

in which,

$\Sigma_i\left(\mathbf{r},E,t\right)$ = *Macroscopic* cross section (1/length) at $\mathbf{r}$ at E at time t,
$\phi\left(\mathbf{r},E,\Omega,t\right)dE\,d\Omega$ = "Neutron Flux," (#/area time) at $\mathbf{r}$ at E in dE at Ω in $d\Omega$ at time t,

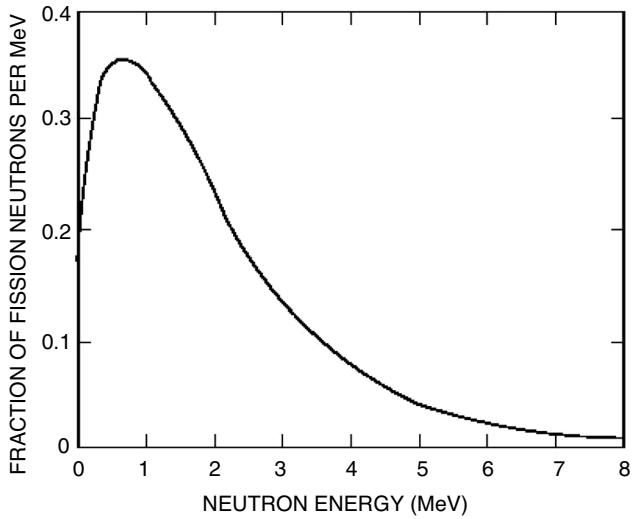

FIGURE 15.3 Energy distribution of neutrons produced in fission (the fission spectrum).

$d\mathbf{r}$ is a volume element at location $\mathbf{r}$, and $d\Omega$ is an elemental solid angle in direction Ω. E indicates energy, and t is the time. A neutron balance equation can thus be constructed as:

$$\frac{1}{v}\frac{\partial\phi(\mathbf{r},E,\Omega,t)}{\partial t} = -\Omega.\nabla\phi(\mathbf{r},E,\Omega,t) - \Sigma_t(\mathbf{r},E,t)\phi(\mathbf{r},E,\Omega,t) + \int dE' \int d\Omega'\Sigma_s(\mathbf{r},E'\to E,\Omega'\to\Omega,t)\phi(\mathbf{r},E',\Omega',t) + S(\mathbf{r},E,\Omega,t) \qquad (15.3)$$

This is often known as the *Linear Boltzmann Equation* for neutron transport, or just the *Transport Equation*, as it follows directly from the *Nonlinear Boltzmann Equation* for molecular distribution in the kinetic theory of gases. Note that v is the speed of neutrons, the integral includes scattering as well as neutrons born in fission, and S is a source term. Subscript t indicates "total." The gradient is with respect to $\mathbf{r}$, and the gradient term indicates free streaming or drift. The boundary conditions for this equation are usually those of no inward neutron flow for a convex surface for a body situated in a vacuum. The initial conditions just prescribe the initial flux.

We should note that the neutron flux is related to the neutron density n by

$$\phi(\mathbf{r},E,\Omega,t) = vn(\mathbf{r},E,\Omega,t)$$

and that the flux in the nuclear nomenclature is a scalar quantity. Thus,

$$\phi(\mathbf{r},E,\Omega,t)\,d\mathbf{r}dE\,d\Omega$$

should be understood as the path length traveled per unit time by neutrons in the elemental phase space volume $d\mathbf{r}dEd\Omega$. Thus, the inverse of the macroscopic cross section is the neutron mean free path ℓ for that particular reaction, and we have $\ell = 1/\sum$.

Progress of the last few years enables us now to compute the neutron flux for complicated geometries and reactor configurations by using combinations of analytical, deterministic, and Monte Carlo methods,[11–18] and this task has been greatly aided by advances in computational hardware. In a simplified picture, we note that for any given mass, the neutron multiplication factor (the ratio of neutrons in a generation to the previous generation) can be written as:

$$k = \frac{neutrons\ produced}{neutrons\ absorbed + neutrons\ lost\ due\ to\ leakage} \tag{15.4}$$

and is a measure of the criticality of the mass ($k > 1$, supercritical; $k = 1$, critical; $k < 1$, subcritical. $k >= 1$ is needed to sustain a chain reaction). The associated rate equation can be written as:

$$\frac{\mathrm{dn(t)}}{\mathrm{dt}} = \frac{\mathrm{k\text{-}1}}{\ell}\mathrm{n(t)} + \mathrm{s(t)} \tag{15.5}$$

where $n(t)$ is the number density of neutrons (#/cm^3), ℓ is known as the neutron lifetime (~10^{-3} to10^{-6} sec) , and "s" (#/cm^3 sec) is a source of neutrons. For a non-re-entrant mass (surface), the factor k is approximately expressed as:

$$k = \frac{\int d\mathbf{r}\int dE\int d\Omega\nu(E)\Sigma_f(\mathbf{r},E)\phi(\mathbf{r},E,\Omega)}{\int d\mathbf{r}\int dE\int d\Omega\Sigma_a(\mathbf{r},E)\phi(\mathbf{r},E,\Omega) + \int d\mathbf{r}_s\int dE\int\limits_{\Omega.n(\mathbf{r}_s)>0} d\Omega\,\Omega.n(\mathbf{r}_s)\phi(\mathbf{r},E,\Omega)} \tag{15.6}$$

Here, the second term in the denominator relates to the leakage from the system, with $\mathbf{r}_s$ a point on the surface, and $n(\mathbf{r}_s)$ a unit normal to the surface directed outward to vacuum. This term is more important for small assemblies (with respect to the neutron mean free path) and less so for larger assemblies. Small assemblies generally correspond to weapons and research reactors, and the larger assemblies to cores of nuclear power plants. The macroscopic cross section is represented (we suppress the position dependence) as:

$$\Sigma(E) = N\sigma(E) \tag{15.7}$$

where N, the number density of the nuclei (#/cm^3) in the mass, is expressed as:

$$N = \frac{0.6023\times10^{24}\rho}{M} \tag{15.8}$$

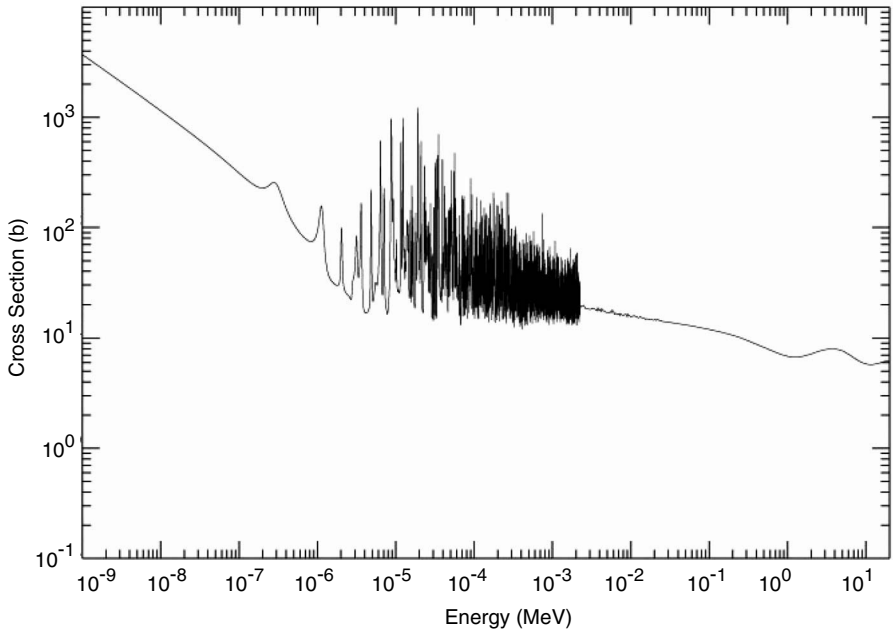

FIGURE 15.4 U-235 total cross section. (ENDFB-VI cross-section files, obtained from www.nndc.bnl.gov.)

in which ρ is the density of the mass (gm/cm^3), and M is the molecular weight (gm/gmol). σ(cm^2) is known as the microscopic cross section for interaction with neutrons. It is different for different processes (fission, absorption, scattering) and generally has a complex dependence on the material and the energy. We have shown a typical cross section in Figure 15.4 (note, a barn = 10^{-24} cm^2).

For large reactors and design purposes, k can be approximately expressed as:

$$k_\infty = \frac{\int_{all} d\mathbf{r} \int_0^\infty dE \nu(E) \Sigma_f(\mathbf{r}, E) \phi(\mathbf{r}, E)}{\int_{all} d\mathbf{r} \int_0^\infty dE \Sigma_a(\mathbf{r}, E) \phi(\mathbf{r}, E)} \tag{15.9}$$

where an integral on the solid angle is understood. Further, it is conveniently expressed as:

$$k_\infty = \varepsilon \eta f p$$

where the four factors are defined in Table 15.2.

We also define E_c as some cutoff energy (about 1 eV), below which neutrons are regarded as "thermal" in that they have kinetic energy comparable to those of the nuclei, and both gain and lose energy while interacting with nuclei (above the cutoff, the analysis can be simplified by assuming that the neutrons lose energy in

TABLE 15.2
The Four Factors

Factor	Approximate Calculation or Measurement	Values (Typical of Natural-Uranium Water)	
		Homogeneous Assembly	Heterogeneous Lattice
$\varepsilon = \dfrac{\int_{fuel} d\mathbf{r} \int_0^{\infty} dE \nu(E) \Sigma_f(\mathbf{r}, E) \phi(\mathbf{r}, E)}{\int_{fuel} d\mathbf{r} \int_0^{E_c} dE \nu(E) \Sigma_f(\mathbf{r}, E) \phi(\mathbf{r}, E)}$	Insensitive to geometry. Can be estimated using approximate shapes of the neutron spectrum and cross sections	1.03	1.03
$\eta = \dfrac{\int_{fuel} d\mathbf{r} \int_0^{E_c} dE \nu(E) \Sigma_f(\mathbf{r}, E) \phi(\mathbf{r}, E)}{\int_{fuel} d\mathbf{r} \int_0^{E_c} dE \Sigma_a(\mathbf{r}, E) \phi(\mathbf{r}, E)}$	Insensitive to geometry. Can be estimated using $\phi(\mathbf{r}, E) \sim \psi_M(E)$, thermal cross sections, and a thermal neutron beam incident on a foil in a manganese bath	1.34	1.34
$f = \dfrac{\int_{fuel} d\mathbf{r} \int_0^{E_c} dE \Sigma_a(\mathbf{r}, E) \phi(\mathbf{r}, E)}{\int_{all} d\mathbf{r} \int_0^{E_c} dE \Sigma_a(\mathbf{r}, E) \phi(\mathbf{r}, E)}$	Assuming $\phi(\mathbf{r}, E) \sim R(\mathbf{r}) \psi_M(E)$) R can be measured through use of bare and cadmium-covered gold foils embedded at different points in a typical cell	0.9	0.8
$p = \dfrac{\int_{all} d\mathbf{r} \int_0^{E_c} dE \Sigma_a(\mathbf{r}, E) \phi(\mathbf{r}, E)}{\int_{all} d\mathbf{r} \int_0^{\infty} dE \Sigma_a(\mathbf{r}, E) \phi(\mathbf{r}, E)}$	Neutron absorption in thermal and resonance regions can be measured through use of bare and cadmium-covered U-238 foils.	0.7	0.9

collisions, scattering, with nuclei, but do not gain energy). Each of these four factors (known as the fast fission factor, reproduction factor, thermal utilization factor, and the resonance escape probability, respectively) can be experimentally measured or estimated (computed). They aid greatly in understanding the role of various nuclear and material properties, thermal conditions, and geometrical arrangements of fuel (UO_2, etc.) and moderators, absorbers, and coolants in influencing k. Use of these four factors was quite important in early design of heterogeneous reactors, and it is still useful today. For example, it was found that arrangement of fuel in lumps or lattices leads to a higher value of k over a homogeneous distribution. Also, whereas a critical reactor cannot be constructed with just natural uranium (of enrichment currently available) and light water even in the most favorable geometry, it is possible to construct critical reactors with natural uranium and graphite or heavy water as moderators, and with a gas, heavy water, or light water as coolants. Indeed, the earliest reactors were constructed with just natural uranium. We have shown typical values of the four factors in Table 15.2, and noted how each of these can be measured or calculated approximately.

Clearly, knowledge of the neutron flux is crucial to the design of a reactor as the criticality and heat generation are directly dependent on it. The flux can be calculated if the geometry and material distribution are defined, and the relevant neutron cross sections are known (from experiments or theory). The nuclear enterprise has paid detailed and careful attention to the cross sections from the beginning of the nuclear age, and extensive and carefully assessed values are available for almost all materials of interest in the open literature and through government-sponsored research centers (for example, the National Nuclear Data Center at the Brookhaven National Laboratory). The geometry and material information can be used to create an input file for a Monte Carlo computer program such as MCNP[24] that has the cross sections libraries integral to it, and one can obtain the flux distribution in the reactor as well as compute the reactor's multiplication factor, power distribution, and other needed quantities. Computer programs are also available for computation of space–time variation of the fission products that accumulate in the reactor core, and for devising fuel management strategies to obtain optimum power from the fuel consistent with applicable safety standards and regulations.

15.2 ELECTRICITY GENERATION FROM NUCLEAR REACTORS

As we have noted earlier, the energy released in a nuclear reactor is that associated with fission of fissile nuclei by neutrons, and also by emissions of beta, gamma, alpha, and neutrons by radioactive or unstable nuclei that are created by fission or absorption of neutrons by nuclei. Not all neutrons are released at the moment of fission; some are released later from the fission products, and some are also emitted by the actinides or because of photon or alpha particle reactions. The rate of this energy release (that is, the power, P) can be expressed as:

$$P(\mathbf{r},t) = G_{f,p}\int_0^\infty dE\Sigma_f(\mathbf{r},E,t)\phi(\mathbf{r},E,t) + \sum_i G_i\lambda_i\int d\mathbf{r}'\int_0^t dt' K_i(\mathbf{r},\mathbf{r}';t,t')N_i(\mathbf{r}',t') \quad (15.10)$$

in which we have made the simplifying assumption that a part of the energy is deposited locally (the first term) and is directly related to the local and instantaneous value of the neutron flux, and the rest is from the decays of the radioactive isotopes. The kernel K is a measure of the contribution to power at **r** at time t from a decay at **r** and t. In practice, computer programs are used to calculate space–time distributions of all important isotopes and the power production. For our purposes, it is sufficient to note that in an operating reactor 95% or more of the energy is deposited in nuclear fuel, and the rest in reactor coolant and structural material. In a steady state, this energy is continuously removed to produce electricity and maintain the reactor at the desired neutronic, thermophysical, and structural conditions. We should also note that for a reactor that has operated for some time, not all the power production will stop if the neutron flux is reduced to a zero value (reactor shutdown) at the end of the operation, in that the radioactive isotopes would have accumulated and these will continue to produce power (the decay heat). This accumulation of isotopes depends on the reactor power history. The decay power after reactor shutdown for a reactor that has been operated for a long time at some steady state power P_0 can be approximately represented as:

$$P(t)/P_0 = 0.066\ t^{-0.2} \tag{15.11}$$

in which t is the time in seconds after the shutdown. We have shown a plot of the decay power in Figure 15.5.

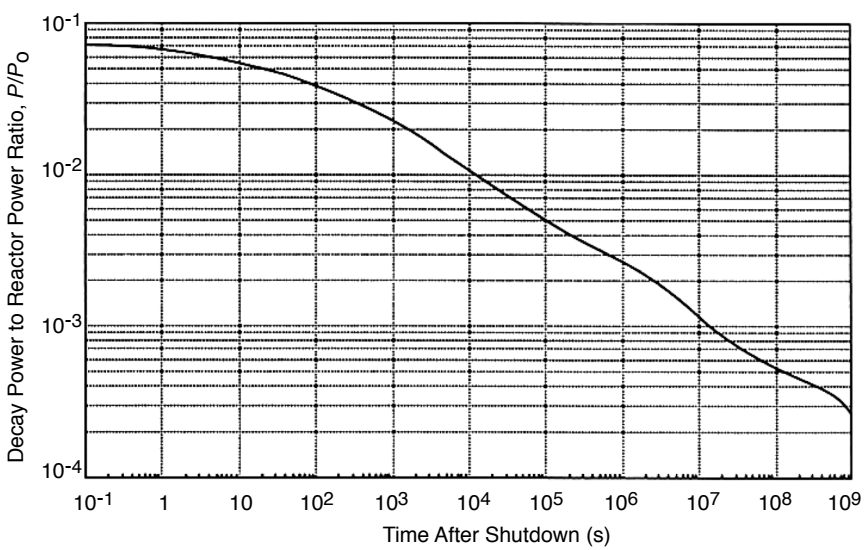

FIGURE 15.5 Decay heat after shutdown for a reactor that had been operated for a very long time. (From American Nuclear Society Standard, ANS 5.1.)

Thus, the decay power is a significant factor in that adequate cooling must be maintained even after the reactor is shut down, as otherwise the reactor fuel could melt and fission products may be released.

Nuclear reactor power plants typically have three essential parts:

a. Nuclear reactor core, where the nuclear fuel is fissioned, and energy and associated radiation is produced. The core must be designed to contain the radiation and fission products.
b. A coolant system (the primary), which removes energy from the core.
c. A coolant system (the secondary), which transfers the energy (removed by the primary from the core) to an electricity generator through a turbine, and to the environment through a condenser and associated cooling tower or system. Some designs do not use a secondary coolant system at all and transfer energy from the primary to the turbine directly, whereas other designs require use of a tertiary system. Generally, about $\frac{1}{3}$ of the energy generated in the core is converted to electricity and about $\frac{2}{3}$ is dissipated (lost) to the environment.

We have shown a typical nuclear power plant schematic in Figure 15.6.

A considerable portion of "b" and all of "c" are similar to those in coal-fired steam plants, and do not require any special elaboration here. We will hence focus more on part "a," and we will also discuss parts of "b."

The reactor core of a modern 1000-MW_e reactor is generally composed of about 250 reactor fuel assemblies ("bundle"), with each assembly consisting of about 200 fuel rods. Thus, there may be about 50,000 fuel rods in the reactor core. Generally, the fuel is UO_2, in which the fresh fuel, the uranium, has been enriched to 2 to 4% (by weight) in U-235. The pencil-thin fuel rods are each about 4 m long, and are contained in individual Zircaloy cans. There is some small spacing (filled with helium at the beginning) between a rod and its Zircaloy can ("cladding") to hold xenon, krypton, iodine, and other gases that are released during fission in the fuel. The core is placed in a thick pressure vessel, and coolant (water) is pumped through the core at high velocities. Each fuel rod can thus be envisaged as central to a cooling channel, in which the colder water (~573 K) enters the bottom, is heated by the fuel, and exits relatively hot (~610 K) at the top. The high coolant temperature at exit is required by 2-T Carnot cycle thermal efficiency considerations, and this in turn dictates the choice of coolants, the fuel material, the operating pressure (which can be as high as 15 MPa to prevent boiling), structural materials, etc. Once the coolant and the fuel are chosen, other design aspects depend on these choices.

During steady operation, there are typical drops in temperature of about 500, 200, 30, and 30 K (radial), respectively, across the fuel (from its centerline to surface), the gap, the clad, and the coolant. Obviously, these drops depend on thermophysical properties (thermal conductivity) of the materials, the structural conditions of the fuel and clad, the hydrodynamic conditions (the Reynolds and Prandtl numbers), and the heat generation rate in the fuel, and are different at different locations in the

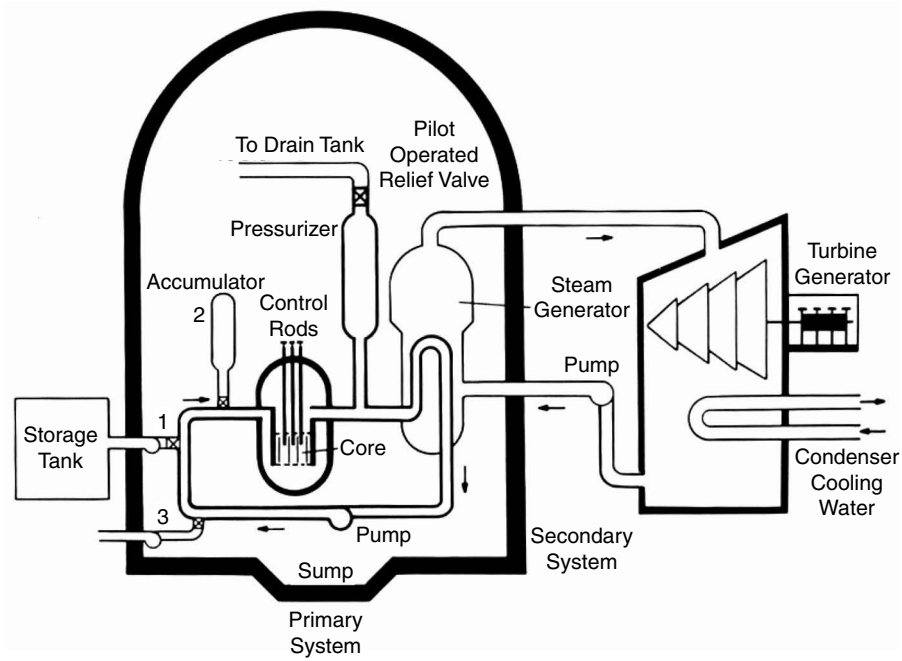

FIGURE 15.6 Schematic of a pressurized water reactor (PWR) plant. (From LANL report.)

core. A useful quantity here is the linear heat generation rate, which is typically about 15 to 20 kW/m of a fuel rod. Thus, each fuel rod generates 60 to 80 kW, and 50,000 or so fuel rods generate 3,000 to 4,000 MW_{th} (Mega Watt thermal) power. With an overall thermal efficiency of 33% or so, this corresponds to 1000 to 1300 MW_e (Mega Watt electric) of power generation, with the rest rejected to the atmosphere via cooling towers, etc.

We have shown a view of a PWR core and pressure vessel in Figure 15.7, and schematics of a fuel assembly and rod in Figure 15.8. Typical fuel rod arrangement and the temperature drop across a fuel rod are shown in Figure 15.9.

As a nuclear reactor generates power, U-233, U-235, Pu-239, and other fissile isotopes are fissioned (consumed), and fertile isotopes such as Th-232 and U-238 are converted to fissile isotopes U-233 and Pu-239. The space–time concentrations of all the isotopes are controlled through reactor designs and fuel management strategies. Typically, because of neutronic and structural considerations, one third of the fuel assemblies are replaced with fresh fuel assemblies each year, requiring reactor shutdowns for the refueling period. In a typical pressurized water reactor (PWR) that has been operating for a longtime, most of the power is generated from U-235, whereas the rest derives from Pu-239 that is continuously generated from U-238. Some reactor designs also permit online refueling of reactors, and shutdowns for refueling are then not necessary. There is considerable interest at this time to design and employ high and ultrahigh burn-up fuels that have refueling times of 10 to 15 years.

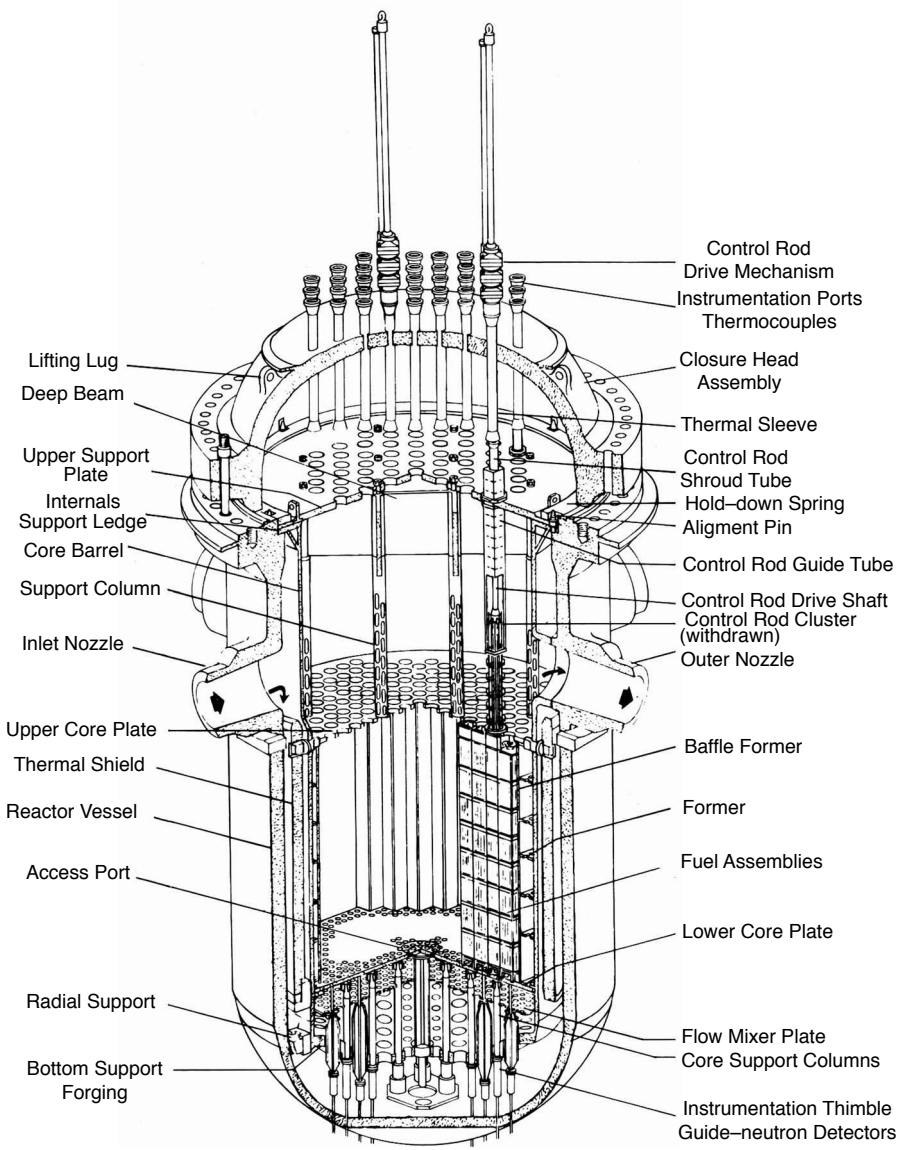

FIGURE 15.7 A view of a pressurized water reactor (PWR) core and pressure vessel. (Westinghouse, from Connolly, T.J., *Foundations of Nuclear Engineering*, John Wiley & Sons, 1978. With permission.)

15.2.1 Reactor Control and a Toy Model

The reactor control requires careful attention to details. Equation 15.5 does not tell the entire story in that not all neutrons are emitted at the same time, and some neutrons are born "delayed" through some fission products. Also, some fission

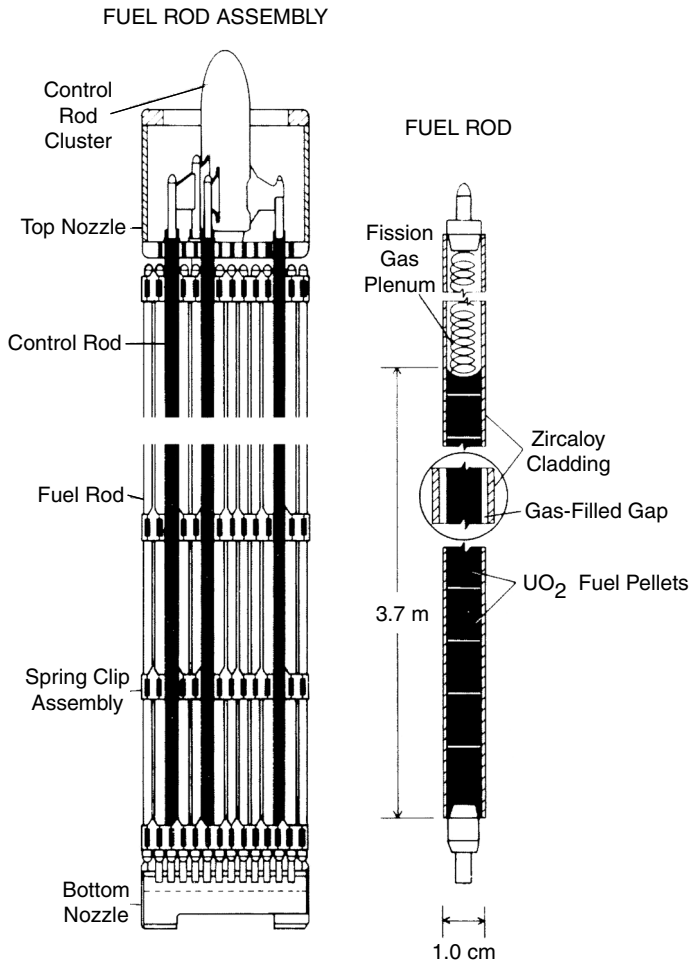

FIGURE 15.8 Schematic of a fuel assembly and rod. (From LANL report.)

products (such as xenon) are strong neutron absorbents, and they have both local and global effects on the reactor criticality, as they are both born (through fission products and their transmutation) and destroyed (through decay and neutron capture) continuously during the reactor operation. The multiplication factor k is further dependent on the reactor temperature (for example, there is an increase in neutron absorption in U-238 resonances as the temperature goes up, leading to a decrease in k) and coolant conditions (an increase in temperature leads to lower density or phase change from liquid to vapor, and these changes known as the density and void effects, respectively, both lead to a decrease in k). A simple model (a point kinetics, or a toy model) that captures effects of some of these phenomena could be written as:

$$\frac{dn(t)}{dt}=\frac{\left(k(t,U(t))\text{-}1\right)\text{-}\beta}{\ell}n(t)+\lambda^{c}c(t)-\sigma_{a}^{Xe}Xe(t)vn(t)+s(t)$$

$$\frac{dc(t)}{dt}=\frac{\beta^{c}}{\ell}n(t)-\lambda^{c}c(t)$$

$$\frac{dI(t)}{dt}=\frac{\beta^{I}}{\ell}n(t)-\lambda^{I}I(t) \tag{15.12}$$

$$\frac{dXe(t)}{dt}=\lambda^{I}I(t)-\lambda^{Xe}Xe(t)-\sigma_{a}^{Xe}Xe(t)vn(t)$$

$$\frac{dU(t)}{dt}=P(t)-\dot{m}(t)\left(h_{out}(t)-h_{in}(t)\right)$$

with appropriate initial conditions. Here, U is the internal energy of the core, $\dot{m}$ is the coolant mass flow rate through the core, h is the enthalpy of the coolant, and P is the power generation in the core. We have,

$$P(t)=VG_{f}\,\Sigma_{f}\,vn(t) \tag{15.13}$$

in which V is the total volume of the core (assuming the cross sections are for the homogenized core in some sense). Also, βs are fractional coefficients that indicate generation due to fissions of the delayed neutron precursor "c" (actually there are several, but we have shown only one), iodine-135 (I), and xenon-135 (Xe). The

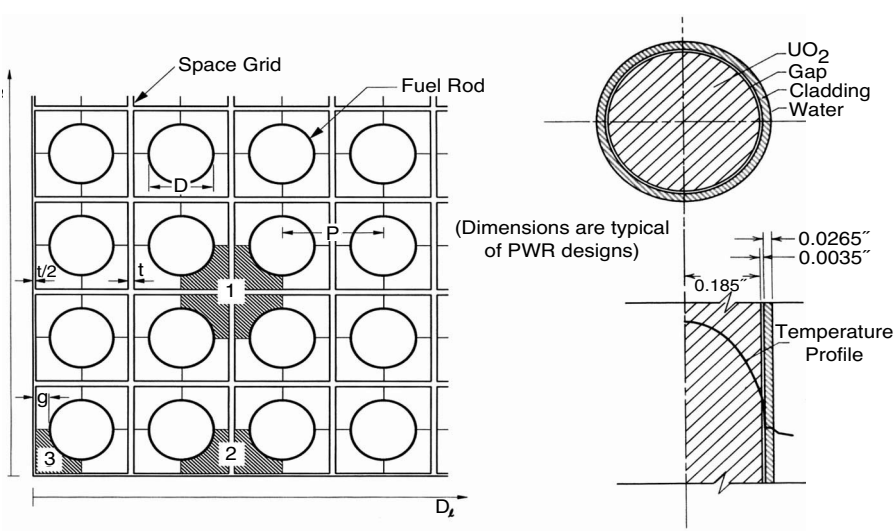

FIGURE 15.9 Fuel rod arrangement with coolant channels in a PWR, and typical temperature drop across a fuel rod.

delayed neutron effects are most important for the routine short-term control of the reactor, whereas other effects are important for both short-term and long-term control of the reactor.

The multiplication factor k has a complex dependence on the internal energy of the core, but this dependence can be expressed in some simple ways through use of a summation of contributions from separate effects via coefficients that provide a measure of the change in k with respect to these effects. For example, one constructs the equation:

$$\frac{dk\left(t,U\left(t\right)\right)}{dt}=\left(\frac{\partial k}{\partial U}\right)\frac{dU}{dt}+.. \tag{15.14}$$

and develops it as dictated by insights and measurements or calculations. The nonlinear system of ordinary differential equations then can be numerically solved, and considerable insights can be gained in the overall working of the system through simulations. In fact, simulators based on similar principles have played a very significant role in reactor operator training, just as they have been crucial in the aircraft industry.

15.3 NUCLEAR FUEL CYCLE

Natural uranium and thorium, and their compounds and transmuted products (Pu-239 and U-233, respectively) are the fuel resources for nuclear reactors. At present, natural uranium contains 99.3% U-238 and 0.7% U-235 in its compounds. Natural thorium occurs mainly as Th-232 in its compounds. Th-232 is not fissile, but through neutron absorption and subsequent decays of products, it can be converted to U-233, which is fissile. As we have noted earlier, through similar processes U-238 is converted to Pu-239, which is also fissile. Thus, fertile materials such as U-238 and Th-232 can be converted or "bred" into fissile materials. Because both U-238 and Th-232 are plentiful in the earth's crust, the nuclear fuel resource can be expanded 100-fold or more through breeding over the ones that are naturally available in the fissile form. Although all nuclear reactors convert fertile materials into fissile materials, special designs can enhance the breeding ratio (BR), which is defined as:

$$\text{BR}=\frac{\text{Average rate of production of fissile isotopes}}{\text{Average rate of loss of fissile isotopes}} \tag{15.15}$$

And it is possible to achieve BR > 1, guaranteeing long-term nuclear fuel supply (thousands of years). BR depends on the neutron spectrum (thermal, epithermal or fast) in the reactor, and the fuel (mainly the fertile content of uranium and thorium, that is U-238 or Th-232 content in the fuel). Note that fast neutrons produce a larger number of neutrons per fission as compared to thermal neutrons, as shown in Figure 15.10.

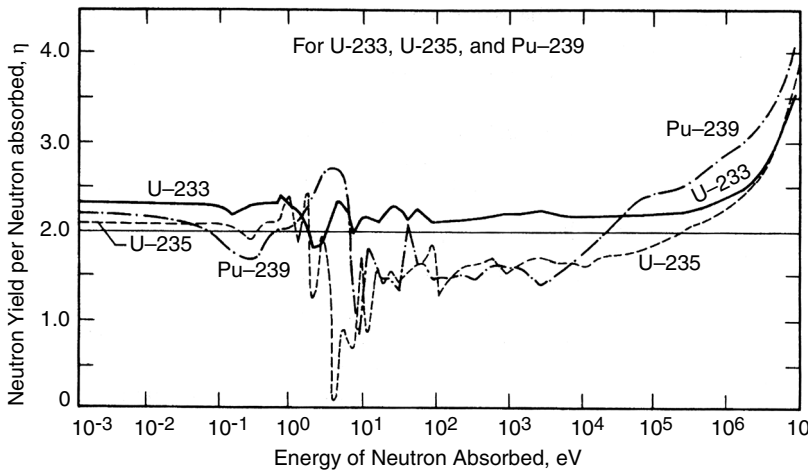

FIGURE 15.10 Net neutrons produced per absorption in fissile isotopes, as a function of the energy of the neutron absorbed. (From ERDA-1541, June 1976.)

The effect is, however, dependent on the isotope. Significantly, for a fast-neutron spectrum, there is a greater availability of fission-produced neutrons for capture by the fertile isotopes, which results in a greater production of fissile isotopes. Thus, fast reactors (these are reactors in which neutron spectrum is rich in fast-neutron content through avoidance of light moderating materials) can lead to a BR > 1, though certain thermal reactors based on U-233 (and thorium) can also lead to a BR > 1. Generally, however, for all light water reactors BR < 1, and such reactors are known as converters rather than breeders (for which by definition, BR > 1).

Indeed, as we have noted earlier, nuclear power plants can be built with reactor cores that are either natural uranium based or that use enriched uranium. One can also use mixed fuels, which are based on various combinations of thorium, uranium, and plutonium. The fissile materials produced in reactors can thus be recycled, either through special reactors or through most reactors of present designs, with appropriate adjustments.

Because nuclear reactors initially developed in the same time frame as nuclear weapons, the development of nuclear reactor power plants in various countries largely followed the expertise and resources that were developed in conjunction with nuclear weapons programs. Almost all present-day power plant designs derive from the initial work in the U.S., Canada, U.K., Russia (the Soviet Union), France, and Sweden. The countries that developed or used uranium technologies for weapons work preferred slightly enriched uranium (as the technology was already available to them and the enriched uranium leads to higher power densities, smaller cores, and longer fuel replacement times), whereas the other countries preferred (or had no other realistic choice) to use natural uranium with graphite or heavy water, with water or a gas as a coolant. The fuel resource needs for the former are more complicated, as the enrichment at the scales needed is an expensive process, and is available now only in a few nations.

The nuclear fuel cycle initially involves exploration and mining of uranium and thorium ores. These ores are widely available, and the principal resources are in the U.S., Russia, China, Australia, South Africa, Gabon, Congo, Niger, India, etc. After mining (through open pit mining or *in situ* leaching from the ground or rocks), the uranium ore (~0.1% uranium oxide content) is milled (and leached and precipitated out in an acid solution) to an oxide powder. In this form, the powder is known as *yellowcake* (~80% uranium oxide content). The remainder of the ore is known as the *tailings*; it is slightly radioactive and toxic, and is a waste that must be properly disposed of.

At a conversion facility, the yellowcake is first refined to uranium dioxide, which can be used as the fuel in reactors that use natural uranium. Further processing, however, is needed if this uranium were to be enriched in U-235 for the reactors that require such uranium. For enrichment, the yellowcake is converted into uranium hexafluoride gas through use of hydrogen fluoride and is shipped in containers to an enrichment facility where either a diffusion or a centrifuge process is used (other methods such as Laser Isotope Separation are still not in commercial use). The first process relies on a slight difference in the diffusion of the U-235 hexafluoride molecule from that of the U-238 hexafluoride molecule through a membrane (the diffusion coefficient is inversely proportional to the square root of the molecular mass), whereas the second method relies on the mass difference (inertia) between the two molecules.

In practice, thousands of stages are used. The diffusion process is highly energy intensive because of the pumping requirements, whereas the centrifuge process requires special rotor materials, motors, bearings, etc. (the practical details are not in the public domain but are reported to have been clandestinely disseminated to a number of countries in the last few years). The enriched uranium hexafluoride is next reconverted to produce enriched uranium oxide. This oxide then is sintered (baked) at a high temperature (over 1400°C) to produce pellets, which are then used in fuel rods and assemblies. In all this processing, great care is taken to ensure quality control with respect to content of fuel and its size and shape. Extensive efforts are also made to avoid accidental criticality.

As the reactor fuel is used in a reactor, it undergoes enormous transformations. The fissile isotopes are fissioned and lead to fission products, neutrons, other radiation, and heat (as discussed earlier). The neutrons transmute the fission products and also produce many actinide species through absorption in the fertile isotopes (some of which will fission again). The fuel cracks because of heat and stresses, the fission products migrate within the fuel, and gases such as xenon and iodine accumulate in the gap between a fuel rod and its cladding. The degradation in the fuel thermophysical properties requires that the fuel be taken out of the reactor after a certain time period, and that fresh fuel replace it. This generally is a batch process in that in most reactors, this "refueling" is done once a year when a reactor is shut down for a couple of weeks, and approximately one third of the reactor core is replaced. The fuel that is taken out of the reactor would have been generally used for a period of about 3 years, and is known as the *spent fuel*. There are certain reactors in operation (the CANDU reactor, which we will discuss later) in which the refueling is done online, and a shutdown is not required.

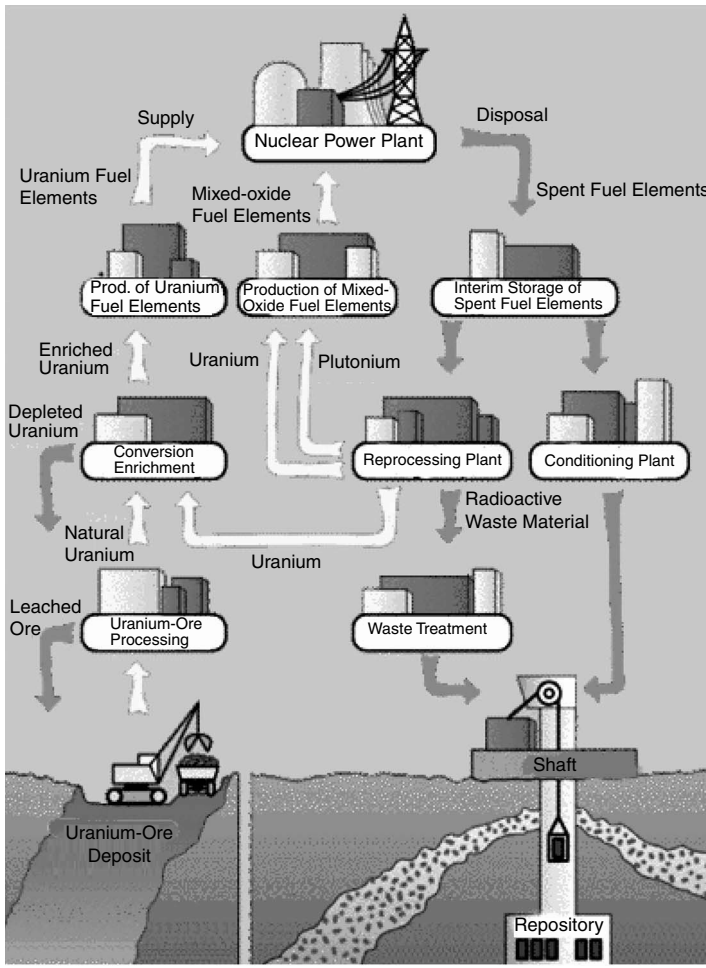

FIGURE 15.11 Nuclear fuel cycle. (From http://www.infokreis-kernenergie.org/e/brennst-offkreislauf.cfm.)

The spent fuel contains fission products, actinides (both minor and major), original fissile isotopes, and other material. It is both radioactive and hot, and is stored at the reactor site in concrete-lined and cooled water pools for 6 months or longer. This storage is temporary, as eventually the fuel must be reprocessed for extraction of the fissile isotopes (chiefly U-235 and Pu-239) and shipped for longer-term storage and disposal at remote sites. Figure 15.11 is a schematic of the fuel cycle.

The reprocessing permits recycling of unused U-235, enables use of Pu in a reactor, and reduces the volume of the waste that needs to be disposed. Although these actions are very desirable from an economic viewpoint and the technology has been demonstrated, both the recycling of Pu and waste disposal issues have been very controversial. It has been contended that the availability of Pu can lead to weapons proliferation, and that it is very difficult to demonstrate long-term safe storage of the nuclear waste (even in geological sites such as the Yucca mountain site in the U.S.).

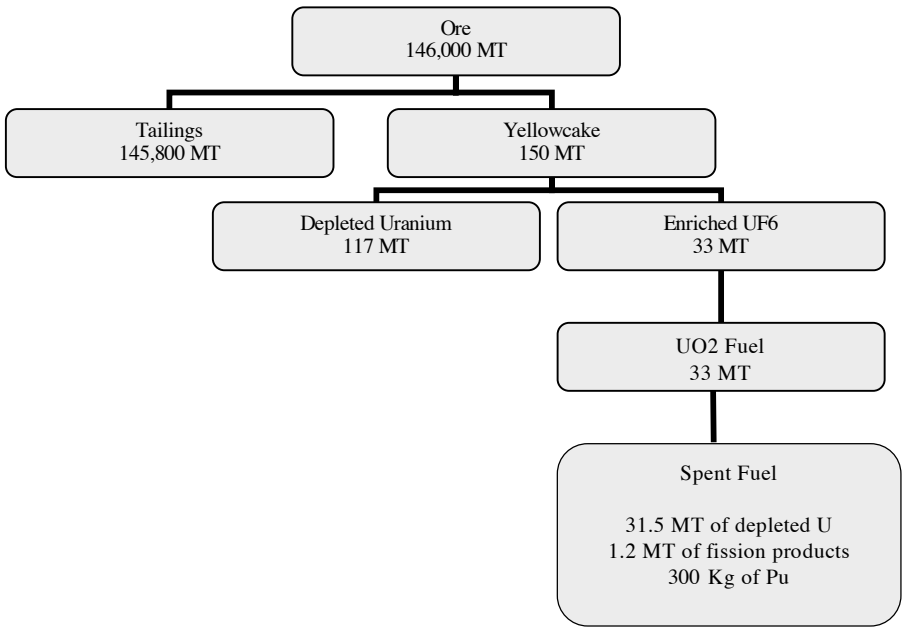

FIGURE 15.12 Uranium ore needed for annual operation of a 1000-MW_{th} reactor and the associated material balance and waste.

We have shown a typical material balance for the fuel needed for the annual operation of a 1000 MW_{th} reactor in Figure 15.12.

15.4 TYPES OF REACTORS

We have discussed the PWR design earlier. Other types of reactors in present use are as follows:

The boiling water reactor (*BWR*): This type of reactor differs from a PWR in that water is allowed to boil fully in the upper portions of the reactor core, and no heat exchanger loop (the secondary) is used. The water is maintained at about 6–7 MPa (instead of 15.5 MPa as in a PWR). The steam passes through a separator at the top of the core and then goes on to drive turbines; the condensed water is pumped back to the core. The steam does contain some radioactive material, and so a modest shielding on the turbine side is required. Lower pressures and avoidance of steam generators simplify the plant design, but then there is the additional complication of two phase flows in the core. Also, the pressure vessel is larger (it needs to accommodate the separator) and the control blades are inserted from the bottom, thereby precluding gravitational insertion of control rods in an emergency. Several different designs of BWRs and their containments are presently in existence, but in the U.S. these reactors are designed only by the General Electric Co. We have shown a schematic of a BWR in Figure 15.13.

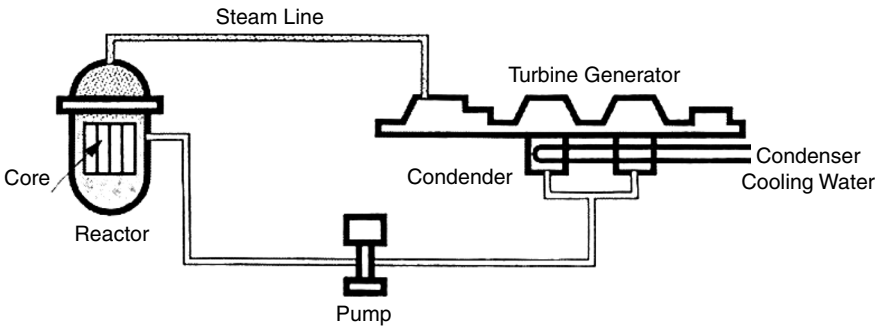

FIGURE 15.13 Schematic of a boiling water reactor. (Courtesy U.S. Department of Energy.)

The pressurized heavy water reactor (*PHWR*): These reactors, sometimes also known as CANDU because of their primary development in Canada, employ heavy water as a moderator and either the heavy water or light water or both as a coolant. These reactors use natural uranium or slightly enriched uranium and pressurized tubes for the coolant, thereby avoiding large pressure vessels. Because of the use of the tubes, fuel can be replaced "online" without a reactor shutdown for refueling.

The graphite-moderated gas cooled reactors (*Magnox and HTGR*): These reactors use graphite as a moderator and a gas (CO_2 or Helium) as a coolant. Because, like heavy water, graphite is a good moderator and a poor neutron absorber, graphite-moderated reactors can use natural uranium as fuel. Note that a gas, because of its low density, is quite transparent to neutrons. Gases are, however, poor coolants as compared to liquids, and these reactors have low specific heat generation and comparatively large surface areas and, hence, large volumes. But one can achieve very high temperatures (hence the name *high-temperature gas reactor*) as phase changes and dissociations or surface reactions can be avoided, particularly with the use of a noble gas such as helium. However, helium does pose a difficulty both in terms of its cost (in countries other than U.S.) and the ease of its leakage from the system.

The graphite-moderated water-cooled reactors (*RBMK types*): These reactors use graphite as a moderator and light water as a coolant. Natural uranium or slightly enriched uranium can be used as fuel. The Chernobyl reactor was this type. These reactors are more compact as compared to the gas-cooled reactors, and also put less demands on coolant pumping power. These reactors, however, can have a positive temperature coefficient in that under certain circumstances an increase in reactor power can lead to an additional automatic increase in power (a positive feedback). Thus, if other means of automatic or manual control of the reactor are disabled, an increase in reactor power could potentially occur that would terminate only after an excursion and reactor core disassembly, resulting in serious damage to the plant and, possibly, its surroundings.

Liquid metal fast breeder reactors (*LMFBR*): The breeding ratio depends on average neutron energy as the cross sections for absorption and fission are

functions of neutron energy. For uranium-fueled reactors, a fast spectrum (that is, the neutrons are mostly at energies higher than 100 keV or so) can lead to a breeding higher than unity. The need for a fast spectrum precludes use of low atomic mass materials in the reactor core (excepting gases, which, because of their low density, have large mean free paths for neutrons at all energies). This requires consideration of liquid metals or their alloys. Sodium, lead-bismuth, and mercury have all merited consideration, and several power reactors have been built, tested, and extensively used with sodium as a coolant. Generally, the cores are designed with zones of different fuel compositions (seed and blanket) to maximize breeding and facilitate fuel reprocessing. Sodium does pose challenges because of its corrosiveness and high melting point (it is solid at room temperature), but it is an excellent coolant. One of the earliest reactors to produce electric power was the Experimental Breeder Reactor-I. The Experimental Breeder Reactor-II (EBR-II) operated for a long time. The Fast Fuel Test Facility (FFTF) was a sodium-cooled test reactor, and so is the Kalpakkam reactor in India. The French Phoenix and Super Phoenix reactors both have been LMFBRs, and have produced power. In the U.S., the experience has been mixed. The Fermi-I, the first commercial LMFBR built near Detroit, was eventually shut down because of a flow blockage and consequent temperature rise that damaged the core. The Clinch River reactor was aborted because of economic and political considerations. We have shown a schematic of a LMFBR in Figure 15.14.

We have summarized the basic features of these reactor types and their thermodynamic parameters in Table 15.3 and Table 15.4, respectively.

The nationwide distribution of nuclear power plants is shown in Table 15.5. Table 15.6 shows the distribution of reactors by their types. These data are current as of April 2003.

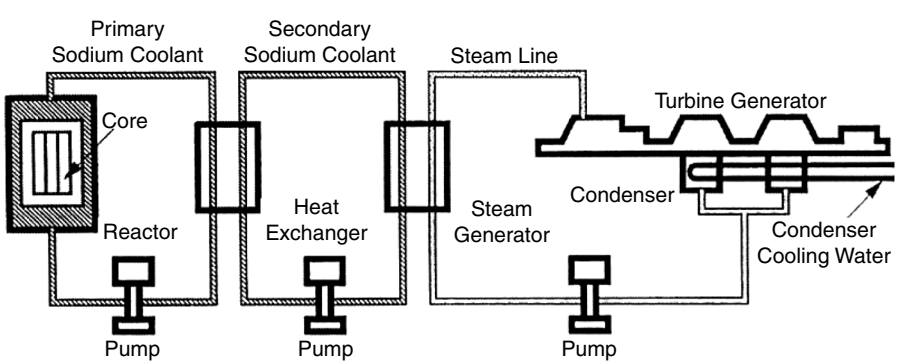

FIGURE 15.14 Schematic of a liquid metal fast breeder reactor. (Courtesy U. S. Department of Energy.)

TABLE 15.3
Basic Features of Major Power Reactor Types

Reactor type	Neutron spectrum	Moderator	Coolant	Fuel	
				Chemical form	Approximate fissile content (all ^{235}U except LMFBR)
Water-cooled	Thermal				
PWR		H_2O	H_2O	UO_2	~3% enrichment
BWR		H_2O	H_2O	UO_2	~3% enrichment
PHWR (CANDU)		D_2O	D_2O	UO_2	Natural
SGHWR		D_2O	H_2O	UO_2	~3% enrichment
Gas-cooled	Thermal	Graphite			
Magnox			CO_2	U metal	Natural
AGR			CO_2	UO_2	~3% enrichment
HTGR			Helium	UC ThO_2	~7–20% enrichment[a]
Liquid-metal-cooled	Fast	None	Sodium		
LMR				U/Pu metal; UO_2/PuO_2	~15–20% Pu
LMFBR				UO_2/PuO_2	~15–20% Pu

[a] Older operating plants have enrichments of more than 90%.

Source: From Ott, K.O. and Neuhold, R.J., *Introductory Nuclear Reactor Dynamics*, American Nuclear Society, 1985. With permission.

TABLE 15.4
Typical Characteristics of the Thermodynamic Cycles for Six Reference Power Reactor Types

Characteristic	BWR	PWR(W)	PHWR	HTGR	AGR	LMFBR
Reference design						
Manufacturer	General Electric	Westinghouse	Atomic Energy of Canada, Ltd.	General Atomic	National Nuclear Corp.	Novatome
System (reactor station)	BWR/6	(Sequoyah)	CANDU-600	(Fulton)	HEYSHAM 2	(Superphenix)
Steam-cycle						
No. coolant systems	1	2	2	2	2	3
Primary coolant	H_2O	H_2O	D_2O	He	CO_2	Liq. Na
Secondary coolant	—	H_2O	H_2O	H_2O	H_2O	Liq. Na/H_2O
Energy conversion						
Gross thermal power, $MW_{(th)}$	3579	3411	2180	3000	1550	3000
Net electric power, $MW_{(e)}$	1178	1148	638	1160	618	1200
Efficiency (%)	32.9	33.5	29.3	38.7	40.0	40.0
Heat transport system						
No. primary loops and pumps	2	4	2	6	8	4
No. intermediate loops	—		—	—	—	8
No. steam generators	—	4	4	6	4	8
Steam generator type	—	U tube	U tube	Helical coil	Helical coil	Helical coil
Thermal hydraulics						
Primary coolant						
Pressure (MPa)	7.17	15.5	10.0	4.90	4.30	~0.1
Inlet temp. (°C)	278	286	267	318	334	395
Average outlet temp. (°C)	288	324	310	741	635	545
Core flow rate (Mg/s)	13.1	17.4	7.6	1.42	3.91	16.4
Volume (L) or mass (kg)	—	3.06×10^5	1.20×10^5	(9550 kg)	5.3×10^6	$(3.20 \times 10^6$ kg)
Secondary coolant						
Pressure (MPa)	—	5.7	4.7	17.2	16.0	~0.1/17.7
Inlet temp. (°C)	—	224	187	188	156.0	345/235
Outlet temp. (°C)	—	273	260	513	541.0	525/487

TABLE 15.5
Nuclear Power Units by Nation

	In operation		Total	
Nation	**# units**	**Net MWs**	**# units**	**Net MWs**
Argentina	2	1,018	3	1,710
Belgium	7	5,680	7	5,680
Brazil	2	1,901	3	3,176
Bulgaria	4	2,722	4	2,722
Canada	22	15,113	22	15,113
China	7	5,426	11	8,764
China (Taiwan)	6	4,884	8	7,584
Czech Republic	4	1,648	6	3,610
Finland	4	2,656	4	2,656
France	59	63,203	59	63,203
Germany	20	22,594	20	22,594
Hungary	4	1,755	4	1,755
India	14	2,548	22	6,128
Iran	0	0	1	916
Japan	53	44,041	58	48,883
Lithuania	2	2,370	2	2,370
Mexico	2	1,364	2	1,364
Netherlands	1	452	1	452
North Korea	0	0	2	2,000
Pakistan	2	425	2	425
Romania	1	655	5	3,135
Russia	27	20,799	33	26,074
Slovakia	6	2,512	8	3,392
Slovenia	1	656	1	656
South Africa	2	1,800	2	1,800
South Korea	18	14,970	22	18,970
Spain	9	7,565	9	7,565
Sweden	11	9,460	11	9,460
Switzerland	5	3,220	5	3,220
Ukraine	13	11,195	18	15,945
United Kingdom	31	11,802	31	11,802
United States	104	99,034	107	102,637
Totals	**443**	**363,468**	**493**	**405,761**

15.4.1 Advanced Reactors and Concepts

Over the past 60 years, many nuclear reactor designs have been considered. Many have been utilized for commercial and routine production of electric power. Considering that France produces almost 70% of its electric power needs through existing nuclear reactor designs, it should be clear that given the political will and public acceptance, power plants based on the existing designs can provide electric power to most countries in the immediate future.

TABLE 15.6
Nuclear Power Units by Reactor Type

	In operation		Total	
Reactor type	**# units**	**Net MW_e**	**# units**	**Net MW_e**
Pressurized light-water reactors (PWR)	262	236,236	293	264,169
Boiling light-water reactors (BWR)	93	81,071	98	87,467
Gas-cooled reactors, all types	30	10,614	30	10,614
Heavy-water reactors, all types	44	22,614	54	27,818
Graphite-moderated light-water reactors (LGR)	13	12,545	14	13,470
Liquid metal-cooled fast-breeder reactors (LMFBR)	2	793	5	2,573
Totals	**444**	**363,873**	**494**	**406,111**

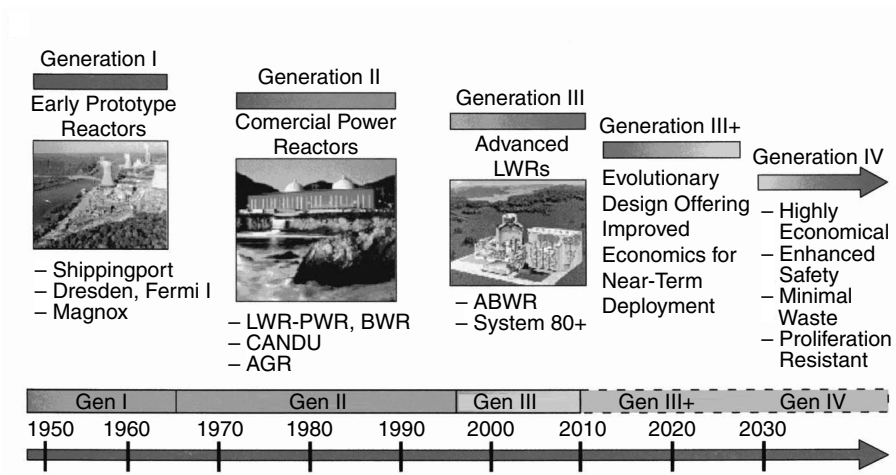

FIGURE 15.15 Historical progression of nuclear reactor development. (From *A Technology Road Map for Generation IV Nuclear Energy Systems*, USDOE, 2002.)

However, from a long-range technical point of view, as well as current and anticipated socioeconomic and political viewpoints, it is important to consider new reactor designs. The historical development of nuclear power plants is well depicted by Figure 15.15.

A major consideration in the new developments is the desire to extend the utilization of fuel resources through breeding of fertile material (which are plentiful but do not directly produce energy) to fissile material (which are not plentiful but produce energy), and minimization of nuclear waste material. Figure 15.16 shows how the advancements would lead to less waste and more sustainable energy production.

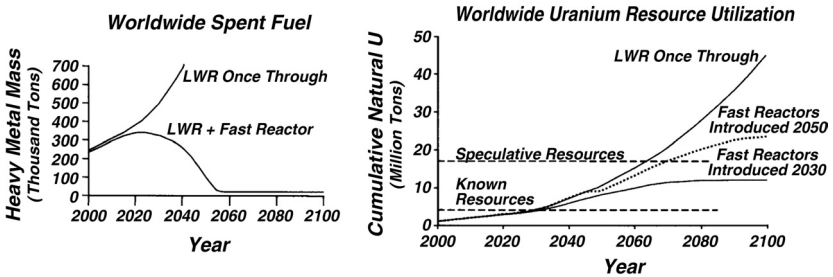

FIGURE 15.16 Gain in sustainable nuclear resources with Pu-recycling. (From *A Technology Road Map for Generation IV Nuclear Energy Systems*, USDOE, 2002.)

Two types of initiatives have received broad industrial and government support in this regard:

1. The first initiative consists of some incremental but important modifications of the existing designs. These modifications are based on the criteria of credible plans for regulatory acceptance, existence of industrial infrastructure, commercialization, cost-sharing between industry and government, demonstration of economic competitiveness, and reliance on existing fuel cycle industrial structure. The reactor designs that have emerged are the Advanced Boiling Water Reactor (ABWR-1000, ESBWR), the Advanced Pressurized Water Reactor (AP600, AP1000, SWR-1000), Pebble Bed Modular Reactor (PBMR), International Reactor and Innovative and Secure (IRIS), and Gas-Turbine Modular Helium Reactor (GT-MHR). These reactors, and the demonstration plants, could come in operation by the year 2010.
2. The second initiative,[22] known as the Generation IV Initiative (the GEN-IV Initiative), has the goals of *sustainability* (the ability to meet the needs of present generations while enhancing and not jeopardizing the ability of future generations to meet society's needs indefinitely into the future), *Safety and Reliability, Economics*, and *Proliferation Resistance and Physical Protection*. The emphasis here is on reactor concepts and associated nuclear energy systems that will satisfy the following criteria:
   a. Meet clean air objectives
   b. Promote long-term availability of systems and effective fuel utilization for worldwide energy production
   c. Excel in safety and reliability
   d. Have very low likelihood and degree of reactor core damage
   e. Eliminate the need for off-site emergency response
   f. Have a clear life-cycle cost advantage over other energy sources
   g. Have a level of financial risk comparable to other energy sources
   h. Provide assurance against diversion or theft of weapons-usable materials
   i. Provide physical security of the reactor and facilities

Nearly 100 concepts that can be generally classified in the broad categories of water cooled, gas cooled, liquid metal cooled, and nonclassical (molten salt, gas-core, heat pipe, and direct energy conversion) have been proposed and considered. Six leading candidates that have been identified for research funding by the U.S. Department of Energy are:

- Gas-cooled fast reactor (GFR)
- Lead-cooled fast reactor (LFR)
- Molten salt reactor (MSR)
- Sodium-cooled fast reactor (SFR)
- Supercritical water-cooled reactor (SWCR)
- Very-high-temperature reactor (VHTR)

We have shown their schematics in Figure 15.17 and summarized important parameters in Table 15.7.

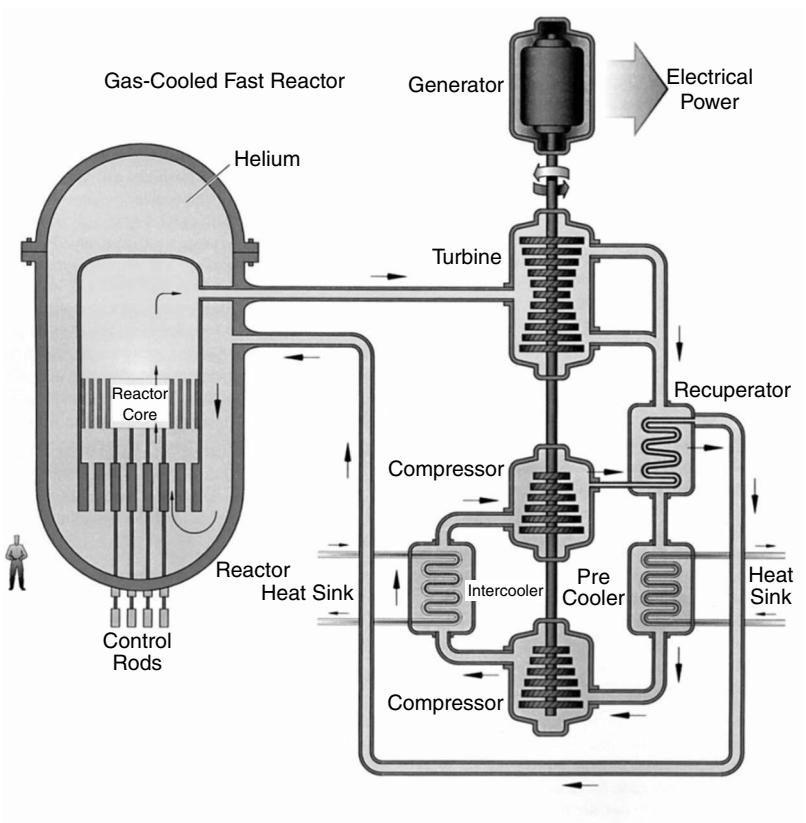

FIGURE 15.17A Schematics of GEN-IV reactors. (a) Gas-cooled fast reactor (GFR) (From *A Technology Road Map for Generation IV Nuclear Energy Systems*, USDOE, 2002.)

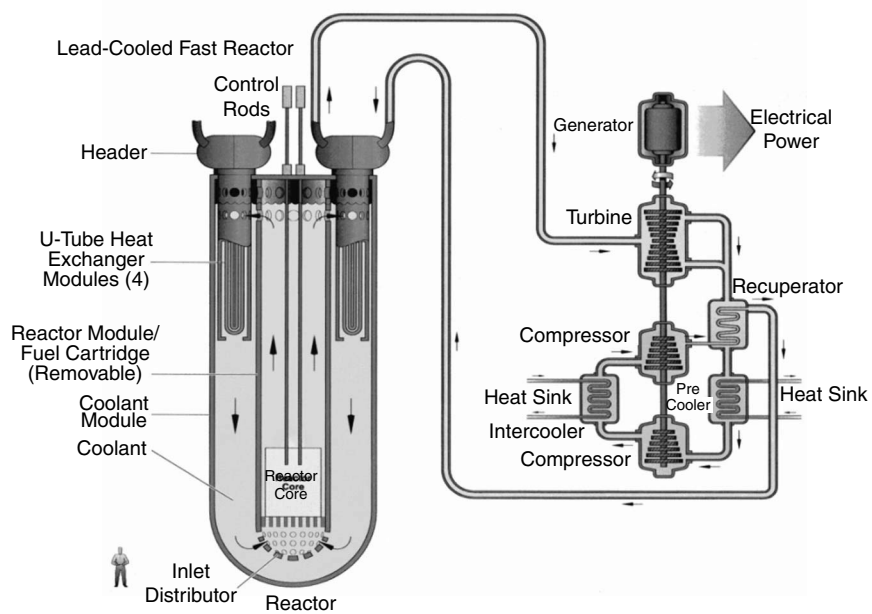

FIGURE 15.17B Schematics of GEN-IV reactors. (b) Lead-cooled fast reactor (LFR) (From Lapeyre, B., Pardoux, E., and Sentis, R., *Introduction to Monte-Carlo Methods for Transport and Diffusion Equations*, Oxford, 2003, original in French, 1998. With permission.)

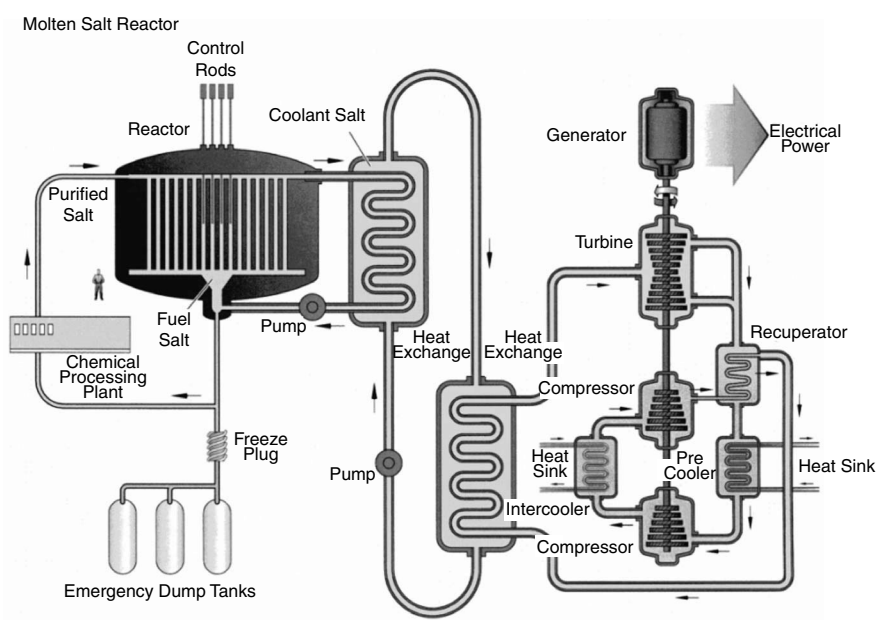

FIGURE 15.17C Schematics of GEN-IV reactors. (c) Molten salt reactor (MSR) (From Lapeyre, B., Pardoux, E., and Sentis, R., *Introduction to Monte-Carlo Methods for Transport and Diffusion Equations*, Oxford, 2003, original in French, 1998. With permission.)

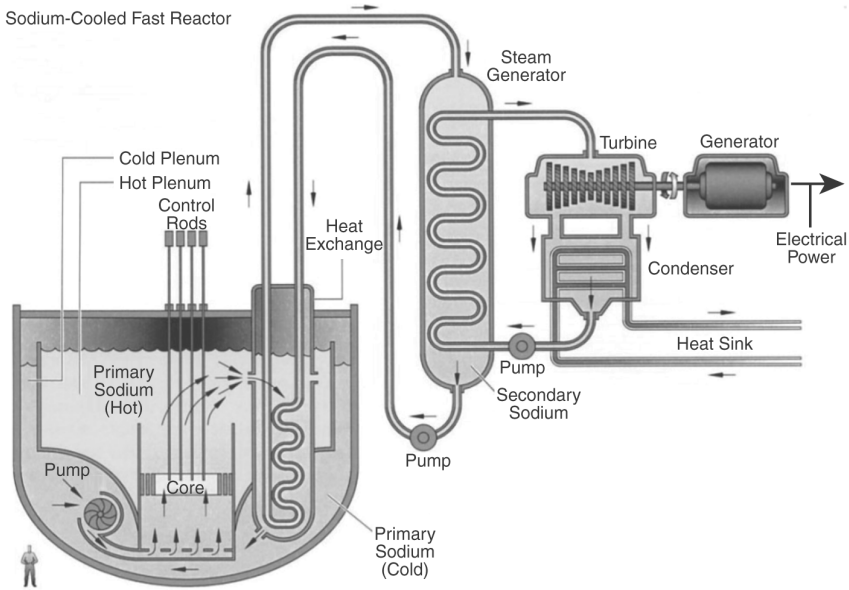

FIGURE 15.17D Schematics of GEN-IV reactors. (d) Sodium-cooled fast reactor (SFR) (From Lapeyre, B., Pardoux, E., and Sentis, R., *Introduction to Monte-Carlo Methods for Transport and Diffusion Equations*, Oxford, 2003, original in French, 1998. With permission.)

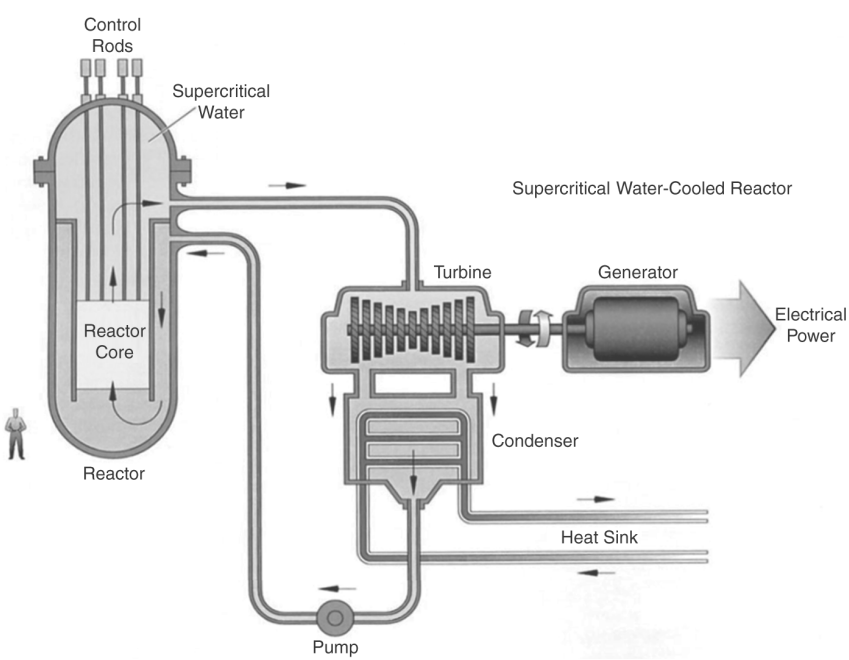

FIGURE 15.17E Schematics of GEN-IV reactors. (e) Supercritical water-cooled reactor (SWCR) (From Lapeyre, B., Pardoux, E., and Sentis, R., *Introduction to Monte-Carlo Methods for Transport and Diffusion Equations*, Oxford, 2003, original in French, 1998. With permission.)

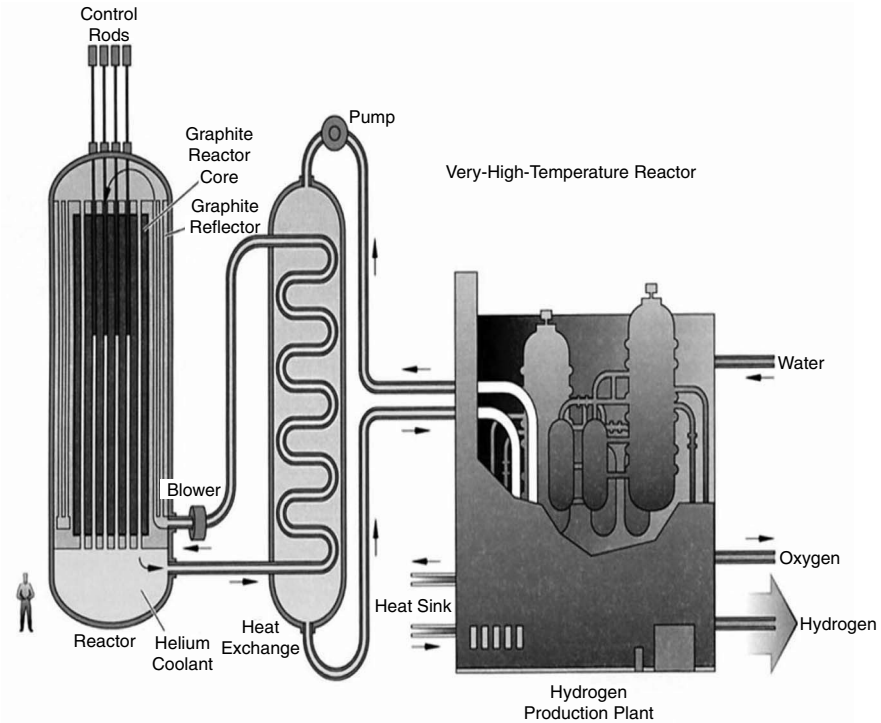

FIGURE 15.17F Schematics of GEN-IV reactors. (f) Very-high-temperature reactor. (From *A Technology Road Map for Generation IV Nuclear Energy Systems*, USDOE, 2002.)

Interesting as these concepts are, they do not constitute a radical departure from the reactor designs of the past. The research and development issues with these GEN-IV reactors are mostly related to long-term operations at high temperatures, and thus concern materials compatibility, corrosion and damage, safety (particularly for fast spectra), and fuel processing and recycling. But basically, the GEN-IV reactors are recycles of old designs, and no new physics is involved.

An interesting design concept under exploration is the accelerator-driven reactor.[34] In this design a proton beam is used to strike a lead or other heavy target, creating high-energy (fast) neutrons (known as *spallation neutrons*). These neutrons drive an otherwise subcritical reactor, and a steady state of neutron population is maintained in a subcritical ($k < 1$) reactor (see Equation 15.5, where $dn/dt = 0$, but $s \neq 0$, leads to $n = (s\ell)/(k-1)$). These reactors avoid any chances of large reactivity insertions and, hence, large reactor accidents. These reactors can use any fissile material and have breeding ratios because of fast spallation neutrons. These designs are receiving some attention in the international community.

We should also note that all the preceding designs rely on conversion of fission heat through a thermodynamic steam or gas cycle to electricity and thus have low conversion efficiencies (maximum of about 50%). There are research efforts underway to explore direct conversion schemes in which the fission energy can be first

TABLE 15.7
Some Technical Specifications of GEN-IV Reactors

	Reactor Type					
Reactor Parameter	**GFR**	**LFR**	**MSR**	**SFR**	**SCWR**	**VHTR**
Power	600 MW_{th}	125–400 MW_{th}	1000 MW_e	1000–5000 MW_{th}	1700 MW_e	600 MW_{th}
Net plant efficiency %	48		44 to 50		44	>50
Reference fuel compound	UPuC/SiC with about 20% Pu	Metal alloy or nitride	U or Pu fluorides dissolved in Na/ZR fluorides	Oxide or metal alloy	UO2 with stainless-steel or Ni-alloy cladding	ZrC-coated particles in blocks, pins or pebbles
Moderator	N/A	N/A	Graphite	N/A	Water	Graphite
Coolant	Helium	Lead-eutectic		Sodium	Water	Helium
Coolant inlet/outlet temperature °C	490/850	NA/550	565/700(850)	NA/550	280/510	640/1000
Coolant pressure (bar)	90	1		1	250	Variable
Neutron spectrum	Fast	Fast	Thermal	Fast	Thermal/fast	Thermal
Conversion (breeding) ratio	Self-sufficient	1.0	Burner	0.5–1.30		
Average power density (MW_{th}/m^3)	100		22	350	100	6–10
Burnup[a] Damage	5% FIMA: 60 dpa	100 GWD/MTHM		150–200 GWD/MTHM	45 GWD/MTH 10–30 dpa	
Earliest deployment	2025	2025	2025	2015	2025	2020

[a] GWD = Giga Watt days; MTHM = metric tonne heavy metal; dpa = displacements per atom; FIMA = fissions of initial metal atoms; N/A = not applicable; NA = not available.

Source: From *A Technology Road Map for Generation IV Nuclear Energy Systems*, USDOE, 2002.

converted to photonic energy through formation of excimers and photonic emissions by these excimers, and then the conversion of this photon energy to electric energy through the use of photoelectronic devices. In principle, one might then be able to get higher conversion efficiencies as a 2T Carnot cycle is avoided.[36]

15.4.2 Hydrogen Production

Fuel cells for automotive transport will require hydrogen. It has been suggested that nuclear energy (reactors) may provide a very effective means of generating hydrogen. The schemes under consideration include[37]:

- Steam methane reforming, using nuclear energy for the endothermic heat of reaction
- Conventional electrolysis, using nuclear-generated electricity
- Thermochemical cycles for water splitting
- Hybrid cycles combining thermochemical and electrolytic steps
- High-temperature electrolysis using nuclear electricity and heat

The steam–methane reformation is based on the reaction

$$CH_4 + 2H_2O + 185\ \text{kJ} \rightarrow CO_2 + 4H_2 \tag{15.16}$$

The advantage of using nuclear energy to produce steam for this above process is that the process itself has been extensively studied. The use of nuclear energy to produce steam avoids the need of methane combustion to produce steam, and the CO_2 so produced is easier to sequester than CO_2 resulting from methane burning. The disadvantages are that the CO_2 is nevertheless produced and needs to be sequestered. Also, a large amount of methane (natural gas) is used.

In the thermochemical cycle under consideration (see Figure 15.18), the nuclear-generated heat is used to split hydrogen from water through use of sulfur dioxide and iodine reactions. The process has the advantage that the raw stocks (iodine and sulfur dioxide) are not consumed, and are recycled. Its disadvantages are that a high-temperature reactor must be built to test the idea.

The high-temperature electrolysis process is quite straightforward as shown in Figure 15.19, but it has a lower conversion efficiency than that of the thermochemical cycle.

Note that both the VHTR of the GEN-IV designs would also be quite suitable for hydrogen production because of the high temperature of the exiting helium.

15.5 PUBLIC CONCERNS OF SAFETY AND HEALTH

Public concerns regarding safety and health issues associated with the operation of nuclear reactors have their genesis in the dread of nuclear weapons, and the fact that the developments of the weapons and the nuclear reactors have overlapped and proceeded in a coincident time frame. Fission weapons are, however, characterized by small size; the explosive part is only a few centimeters in diameter. Power density

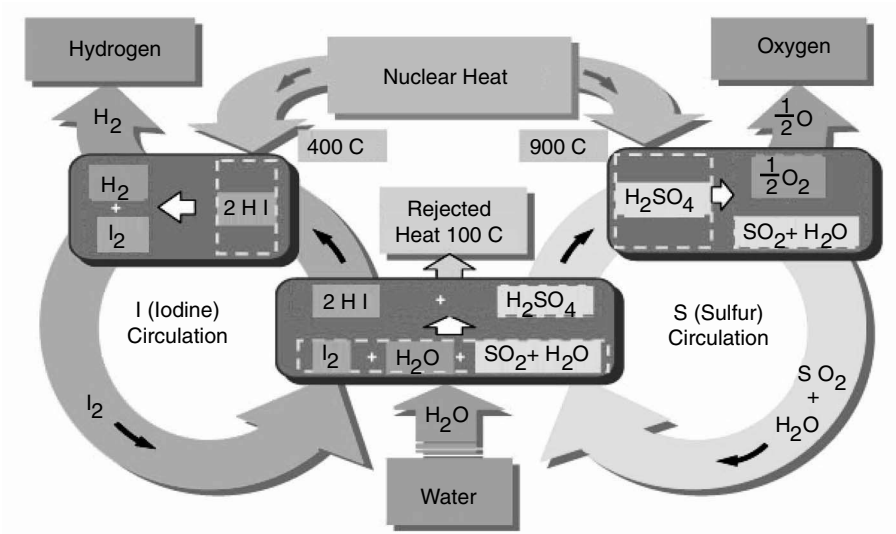

FIGURE 15.18 The thermochemical cycle for producing hydrogen from water and nuclear energy. (Courtesy of INEL.)

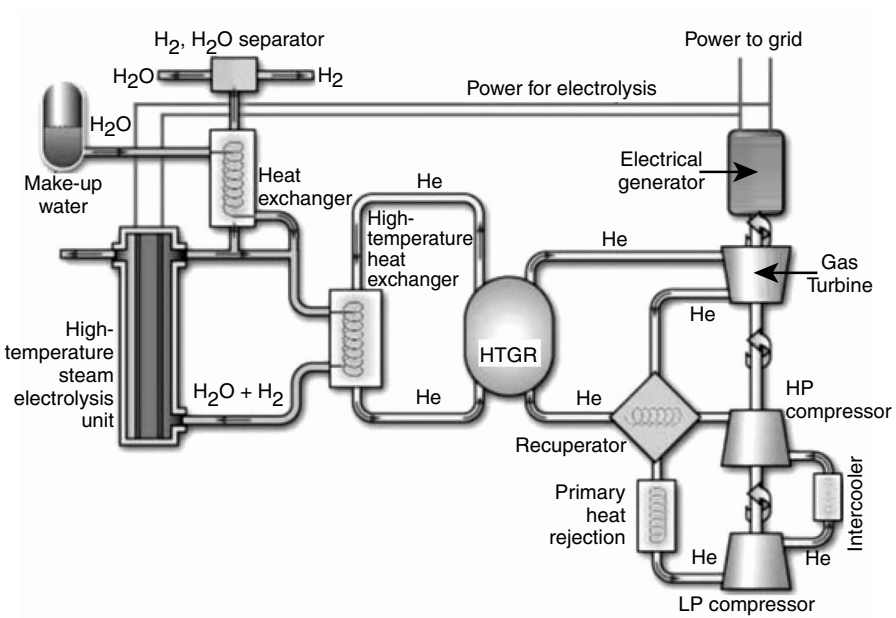

FIGURE 15.19 High-temperature electrolysis using heat and electricity generated from a high-temperature gas reactor. (From *A Technology Road Map for Generation IV Nuclear Energy Systems*, USDOE, 2002.)

is extremely high, and explosion time is a few microseconds. The design is specific to achieving the explosion in that the fissile material is compressed and brought to supercriticality and kept supercritical for a short time frame in a specific fashion, and the neutrons are introduced at an appropriate time to get the desired explosive energy release. Commercial nuclear reactors, on the other hand, are large with cores that are approximately 12 ft in diameter. Their power density is low. Also, energy is produced over a long period of time. Design safeguards protect against power excursions of the type the weapons are designed for.

Generally, in a nuclear explosion 50% of the damage comes from thermal radiation, 35% from the blast, and only the remaining 15% comes from the short term and delayed radiation (beta, gamma, and alpha radiation associated with decay of radioisotopes). The radiation can cause cellular, glandular, and DNA damage and induce cancer through inhalation or other means of exposure (digestion or skin exposure). The thermal radiation and the blast are not the causes of concern with respect to nuclear reactors, as the reactors cannot explode like weapons. But all reactors can encounter circumstances in which the rate of heat generation in the reactor core exceeds the heat removal rate. Let us consider the first law of thermodynamics as applied to the entire reactor core (we neglect conduction and radiation losses, etc., to simplify the arguments):

$$\frac{dU(t)}{dt} = -\dot{m}(t)\left(h_{out}(t) - h_{in}(t)\right) + P(t) \tag{15.17}$$

where U is the internal energy of the core, $\dot{m}$ is the coolant mass flow rate through the core, h is the enthalpy, and P is the power generation in the core. The steady state corresponds to the two terms on the right balancing out, but obviously if the second term exceeds the first, the core will heat up. For example, if the coolant flow slows down or stops owing to a breakage of piping or loss of power to a pump, and P is not reduced correspondingly, the core will heat up. Similarly, if P is increased, but $\dot{m}$ is not (or if h_{out} is not, which relates to conditions at the exit and, hence, the convective heat transfer coefficient between the fuel and the coolant), the core can again heat up.

Under normal operations, these imbalances are adjusted through passive and active controls. Most reactors are also designed to be somewhat inherently safe in that an increase in fuel or coolant temperature leads to an automatic reduction in k and, hence, the power generation P. Also, expansion of the core leads to a reduction in k and, hence, P. The rate constants are affected by delayed emission of neutrons, and thermal reactors have most neutrons at relatively slow speeds, thus reducing the overall rate of increase of neutron populations should k be increased accidentally. Thus, generally with most reactors, concerns are focused more on accidents that start with loss of coolant flow or the coolant itself, and rapid increase in power P that, for example, could result from sudden withdrawal or lack of insertion of a control rod.

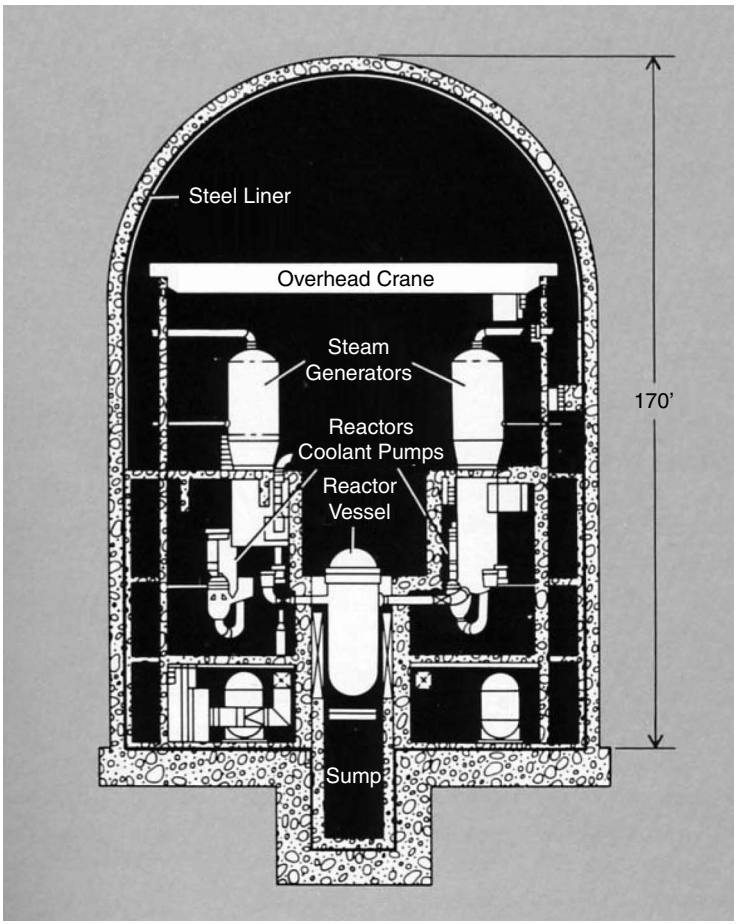

FIGURE 15.20 Cross section of a typical containment building for a pressurized water reactor (PWR). The concrete building houses the entire primary system, the pressure control system, ventilation equipment, and part of the emergency core-cooling system. The various components are encased in concrete and surrounded by a 0.63 cm thick steel liner. (From *Los Alamos Science*, Vol. 2, No. 2., Los Alamos Scientific Laboratory, 1981. With permission.)

Under normal conditions, radioactive isotopes are contained in the fuel rods. The cladding, water coolant system, piping and pressure vessel, containment, and engineered safety features (sprays, ice condensers, suppression pools, etc.) are designed to limit the release of radioactive isotopes during accidents (see Figure 15.20). Natural processes (physicochemical reactions, deposition, settling, coagulation, fragmentation, aerosol growth, etc.) may act to reduce or enhance the release fractions.

Overall, there are several aspects of the nuclear fuel cycle that have been causes of public concern:

- Release of radioactive material to the environment during the mining, processing, and transport (shipping) of fresh or used nuclear fuel

- Releases of radioactive material during normal operation or accidents at nuclear power plants
- Short-term and long-term storage of nuclear waste, and releases from the storage sites
- Proliferation of technology and the attendant risk of terrorism

Nuclear industry, utility groups, national governments, and the International Atomic Energy Agency (IAEA) have all addressed these issues in depth, and stringent regulations at national levels, as well as guidance at international levels, have been formulated. These are enforced or followed to reduce risks to the public from postulated or real accidents. Yet, it must be realized that accidents have occurred, and will occur, and neither accidents nor releases of radionuclides can be completely prevented. The best one can do is reduce the probabilities of accidents, and then when the accidents do occur, reduce the consequences associated with them. But risk management is expensive, and good risk–benefit and cost–benefit analysis are needed to arrive at regulatory requirements that would find public and institutional support.[38–45] This support has varied greatly in different countries and at different times.

Table 15.8 gives the half-lives and radioactive inventories of some important isotopes that are produced in a nuclear power plant. Health hazards are largely associated with the longer-lived, volatile isotopes of I, Cs, Sr, Pu, Ru, and Te, which emit beta and gamma radiation, and Pu and other actinides that emit alpha particles and neutrons also.

Accident sequences that can cause vaporization of reactor inventory are those initiated by a loss of coolant, accidents, and severe transients (primary coolant pipe break, main steam line break in a PWR, control rod ejection, pressure vessel failure, etc.). Details of such sequences are discussed in Reactor Safety Study (WASH-1400).

The amount and timing of the release of radioactive substances from a reactor plant to the environment is referred to as a *nuclear source term.* More broadly, source terms are characterized by the radionuclides that are released to the environment as well as the time dependence of the release, the size distributions of the aerosols released, the location (elevation) of the release, the time of containment failure, the warning time, and the energy and momentum released with the radioactive material. The definition of the source term is slightly loose as different computer programs may require different inputs. Still, it is clear that source terms will be closely related to the vapors, gases, and particles in suspension in the reactor containment (or building) at a given time, and the states of this suspension and the containment. If a containment does not fail (and is not bypassed) then, regardless of the complicated phenomenology that takes place inside the containment during the accident, the source term would be zero, and no direct harmful effects to the public would result.

The determination of source terms within well-defined bounds is not simple. First, a range of severe accident scenarios, with corresponding initiating events, must be studied. Using probabilistic methods (fault and event trees), a probability of occurrence can then be assigned to the given accident scenario. Next, an integrated analysis of all that occurs in the plant needs to be carried out. Detailed physicochemical, neutronic, and thermal hydraulic models with an extensive database (separate effects) and integrated computer programs (as verified against a range of integral experiments)

TABLE 15.8
Important Radioactive Nuclides (in a 3412-MW_{th} PWR operated for 3 years, as predicted by computations)

Radionuclide	Half-Life (days)	Inventory (Ci × 10^{-8})	Radionuclide	Half-Life (days)	Inventory (Ci × 10^{-8})
		Iodine isotopes			
I-131	8.05	0.87	I-133	0.875	1.8
I-132	0.0958	1.3	I-135	0.280	1.7
		Noble gases			
Kr-85	3.950	0.0066	Kr-88	0.117	0.77
Kr-85m	0.183	0.32	Xe-133	5.28	1.8
Kr-87	0.0528	0.57	Xe-135	0.384	0.38
		Cesium isotopes			
Cs-134	7.5×10^2	0.13	Cs-137	1.1×10^4	0.065
		Other fission products			
Sr-90	1.103×10^4	0.048	Ba-140	1.28×10^1	1.7
Ru-106	3.66×10^2	0.29	Ce-144	2.84×10^2	0.92
Te-132	3.25	1.3			
		Actinide isotopes			
Pu-238	3.25×10^4	0.0012	Pu-241	5.35×10^3	0.052
Pu-239	8.9×10^6	0.00026	Cm-242	1.63×10^2	0.014
Pu-240	2.4×10^6	0.00028	Cm-244	6.63×10^3	0.0084

Note: A Curie, Ci, signifies 3.7×10^{10} emissions of a radioactive particle per second, and is often used in describing radioactivity.

Source: From Williams, M.M.R. and Loyalka, S.K., *Aerosol Science: Theory and Practice with Special Applications to the Nuclear Industry*, Pergamon, Oxford, 1991. With permission.

are required. This task can be quite overwhelming as the number of molecular species involved is large, temperatures and pressures can be high, and the associated flows can be quite complex. High radiation fields are also present and, depending on the specific type of accident, the situation can be very dynamic.

Note that in 1957, the WASH-740 reports recommended an exclusion zone of radius R (miles) around a nuclear plant of power P (MW_{th}), based on the formula:

$$R = \left(\frac{P}{10}\right)^{1/2} \sim 17 \text{ mi for a 3000-MW}_{th} \text{ plant}$$

This formula is not based on realistic estimates. Rather, all material from the plant is assumed to disperse without any mitigating mechanisms. In 1957, the Windscale accident occurred, in which 100% of the noble gases, 12% of the I inventory, and 10% of Cs inventory of the core were released to the environment. This accident was the

basis for the TID-14844 criteria for licensing ([1962], regulatory guides 1.3 and 1.4), which stipulates that release from the core to the environment will consist of 100% of noble gas, 50% of I (in gaseous form), and 10% of the nonvolatile (solids) inventory. It was also specified that the containment would retain half of the I (of that released), and all of the solids. Further retentions could occur because of particular containment designs and engineered safety features. In these guidelines, containment is assumed not to fail, but to leak.

The year 1975 was significant in the history of reactor safety analysis and the source term. The WASH-1400 report provided estimates on frequency of accidents and related consequences. The analysis was specific to a PWR and a BWR. The report showed that reactors are very safe and pose only an extremely small risk.

The March 28, 1979, accident at the Three Mile Island-2 (TMI-2) plant near Harrisburg, PA was rather serious. In the WASH-1400 nomenclature, the accident sequence was TMLQ (transient with loss of flow), initiated by a pressure relief valve stuck in an open position, and later exacerbated by operator actions that shut down emergency cooling water. The source terms, however, were a matter of great surprise. Whereas all the noble gases were released (no surprise), the releases of volatiles (I, Cs) were 3 to 4 orders of magnitude smaller than predicted by a TID-14844 type of analysis. These observations and their implications for safety analysis were noted in a series of papers. It was argued that in wet reducing environments, iodine and cesium are quite reactive and do not stay in the vapor phase but either plate out or react with aerosols that settle or deposit on the walls. Thus, the chemistry of the environment and the aerosol dynamics clearly play a vital role in the estimation of source terms.

The Chernobyl accident (April 26, 1986) was characterized by a large source term (large releases). At Chernobyl, however, the situation was quite different in that the reactor design was not inherently safe (there could be a rapid increase in power), and the building was not designed to be a containment. Also, chemical explosions rendered any containment possibilities ineffective.

In the past, several nuclear reactors (SL-1, SNAPTRAN, Crystal River-3, Windscale-1, KIWI-TNT, HTRE-3, SPERT-1, TMI-2) have, unintentionally or otherwise, experienced core damage accidents. A common observation is that large releases to the atmosphere occurred only when "dry" situations prevailed (Windscale-1, a graphite-moderated reactor, and HTRE-3, a zirconium-hybrid-moderated reactor). In all light water reactor accidents, releases to the atmosphere were rather small.

The Chernobyl accident is in contrast to the other accidents mentioned earlier. The RBMK reactor #4 was destroyed, lives were lost, and sizeable releases of radioactivity occurred, extending over a period of several days. The Chernobyl reactor started operating in December 1983 and by April 1986 had an average fuel burnup of 10.3 MWd/kgU. The accident on April 26, 1986, was caused by operator errors that led to a prompt critical excursion exacerbated by positive void coefficients. It is estimated that within a second (1:23:44 a.m. to 1:23:45 a.m. local time) the fuel went from about 330°C to 2000°C and, during the next second, a substantial part of the fuel melted and vaporized (above 2760°C). The reactor core then disassembled violently and the excursion was terminated. In the following hours, the heat from the excursion and the radioactive decay was redistributed in the fuel and the relatively

cooler graphite. Eventually, the graphite began to burn and continued to burn for several days. This exothermic reaction heated the core further. Sand and other materials (boron carbide, dolomite, Pb, etc.) were dropped on the core and eventually, by May 6, the fire was effectively extinguished, and the release terminated. The violent disassembly of the core and the graphite fire led to some 30 additional fires in and around the reactor. Firefighting efforts were carried out in a radioactive environment, leading to 2 immediate and 29 subsequent deaths of site personnel. The radioactive releases occurred over a 10-d period. The releases contained noble gases, fuel and core debris including fuel fragments and large chunks of metal and graphite, a large number of large-sized particles (tens to hundreds of micrometers), and an even larger number of submicron aerosol particles. The latter were transported through the air over large distances within the northern hemisphere.

Since the Chernobyl accident, there has been no reactor accident worldwide. There was, however, an accident in Japan at the Tokaimura fuel processing facility, where some fissile materials in solution were poured in excess in a tank. The tank became critical, and a small nuclear excursion and radiation release took place. A worker lost his life because of radiation exposure, and a few other workers were also affected. Release of radiation external to the plant was small. There have been additional instances, for example, in the U.S., which have shown that reactor pressure vessels and their components can suffer greater structural damage during operation than previously envisaged, but so far it has been possible to detect major problems in time and to take corrective actions.

15.5.1 Nuclear Weapons Proliferation

Fission of 1 kg of U-235 or Pu-239 releases an energy equivalent to that obtained in explosion of about 20 kT of TNT. World War II imperatives led to the Manhattan Project in the U.S. and construction, testing, and use of the first nuclear weapon in 1945. There has been no other combat use of nuclear weapons, but there have been many other detonations, both aboveground and underground. The fission bombs have been surpassed with vastly more powerful (~50 MT, 1 MT = 1000 kT) hydrogen or thermonuclear bombs where a fission bomb is used to create a fusion reaction. The U.S., Russia (Soviet Union), U.K., France, China, India, and Pakistan have tested nuclear weapons. It is also widely accepted that Israel has produced and stockpiled nuclear weapons and that South Africa had also produced nuclear weapons and perhaps detonated one. Many other nations (Argentina, Brazil, Iraq, Iran, Libya, and North Korea) have pursued nuclear weapons technology clandestinely at one time or another, and several of them are currently pursuing it (it detonated one in October, 2006). It is also widely accepted that North Korea has a few nuclear weapons, and it is working on more. Nuclear weapons are comparatively compact, and these can be delivered by airplanes, missiles, ships, barges, or even trucks. There is speculation that suitcase-size nuclear weapons exist.

Nuclear weapons technology was born in wartime, and many of its practical aspects have since been well guarded (classified) not only by the U.S. but by other nations also. Many Manhattan Project documents, and the subsequent nuclear literature, however, provide considerable insights into the basic technology. Aspects of

the technology acquired with respect to power production, including uranium enrichment, fuel processing for plutonium production, experience with radiation and its detection, neutronics, metallurgy, specialized electronics, and theoretical understanding and computational capabilities have direct applications in the weapons area. Although it is far-fetched to imagine homemade nuclear bombs, a determined nation or a well-financed group can hide a weapons program under the guise of a power program and, indeed, some nations have already done so. Concerns remain that nuclear material and weapons can be stolen also, or nuclear shipments can be hijacked. These are all legitimate concerns, and similar concerns now surround biotechnology and aspects of chemical technology. The most effective means of alleviating concerns here can only be international understanding and control, and arms reduction. There are, however, no simple answers to the issue of proliferation, as the political parts of it overwhelm any technical fixes one might attempt. Also, the knowledge (for example, with respect to the centrifuge technology) has diffused to an extent that the proliferation is occurring from secondary and tertiary sources over which little control is being exercised.

15.5.2 Nuclear Waste Disposal

As challenging as the problems of reactor safety and the nuclear weapons proliferation are, nothing has caught the public attention more than the problems of nuclear waste disposal, whether it be the uranium mill tailings or the spent reactor fuel. This is a bit unfortunate as good technical solutions to the waste disposal problems are either available, or can be formulated. Uranium (together with several of its decay products) is naturally radioactive, and it is possible to reduce much of the fuel cycle products to a radioactive state that has a life span of about 1000 years only. This, for example, can be done by separating major actinides from the spent fuel and recycling them for fission (power production) in the standard or specialized reactors. The Integrated Fast Reactor (IFR) is an example of such a reactor concept, wherein pyroprocessing (electrolytic separation at high temperatures) can be used to process spent fuel on site. Mixed oxide fuel reactors are another example, where Pu-based fuel is used together with U-based fuel.

The problem, however, is presently being addressed through two stages:

1. On-site storage, for several years, of the spent fuel
2. Relocation to temporary or permanent storage sites in the future

These permanent sites are to be geologically stable, and safe from water percolation and other climactic factors that might lead to radioactive material dispersal. In the U.S., a site is being constructed at Yucca Mountains in the State of Nevada, and spent reactor fuel (assemblies) will be transported via trucks from nuclear power plant fuel storage pools to this site contingent on the results of a drawn-out regulatory and public or political process.

Other nations have made progress, both with respect to reprocessing and recycling of the spent fuel in reactors, as well as long-term storage and disposal. For example, in France, the fuel is reprocessed and recycled, as well as stored after

reprocessing (wherein the waste is encapsulated in vitreous material that is impervious to fluids and is environmentally stable) in salt formations.

15.5.3 Terrorism

Most recently, there has been considerable concern regarding "dirty bombs," or radioactive material dispersion, in which, for example, a reactor fuel assembly is exploded with dynamite, and the material is dispersed in a dense population. Sabotage of nuclear reactor power plants is also feared. These aspects have required, and will require, enhanced security at nuclear power plants, and improved safeguards on nuclear materials.[46]

In conclusion, we should note that at least one natural reactor had existed millions of years ago in Africa. As Lammarsh[2] has stated,

> . . . Oklo is the name of a uranium mine in the African nation of Gabon, where France obtains much of the uranium for her nuclear program. When uranium from this mine was introduced into a French gaseous diffusion plant, it was discovered that the feed uranium was already depleted below the 0.711 wt% of ordinary natural uranium. It was as if the uranium had already been used to fuel some unknown reactor.
>
> And so it had. French scientists found traces of fission products and Trans Uranic (TRU) waste at various locations within the mine. These observations were puzzling at first, because it is not possible to make a reactor go critical with natural uranium, except under very special circumstances with a graphite or heavy water moderator, neither of which could reasonably be expected to have ever been present in the vicinity of Oklo. The explanation of the phenomenon is to be found in the fact that the half-life of U-235, 7.13E8 years, is considerably shorter than the half-life of U-238, 4.51E9 years. Since the original formation of the Earth, more U-235 has therefore decayed than U-238. This, in turn, means that the enrichment of natural uranium was greater years ago than it is today. Indeed . . . about 3 billion years ago this enrichment was in the neighborhood of 3 wt%, sufficiently high to form a critical assembly with ordinary water, which is known to have been present near Oklo at that time. . . .

Thus, nuclear energy from fission is really not that new! Our challenge is to recognize that we have an amazing source of energy that with good institutional safeguards can provide, in environmentally safe ways, abundant energy to humankind for thousands of years to come.

15.6 NUCLEAR FUSION

Fusion is the inverse of fission in that certain light nuclei can combine together to create a pair of new nuclei that have a greater stability than the reactants. Fusion reactions are the primary source of power in stars, including the sun.[47–50] To understand conditions under which fusion can occur, let us look at a much-studied[1,47–58] reaction:

$$D+T \rightarrow He^4 + n + 17.6MeV \tag{15.18}$$

where D indicates a deuteron or deuterium nucleus (H_1^2), T indicates a triton or tritium nucleus (H_1^3), and "n" indicates a neutron. Because 1 kg of D contains 3.0115×10^{26} D nuclei, its fusion with an equal number of T nuclei (1.5 kg) would release about 8.5×10^8 MJ (or expressed differently, 2.36×10^8 kWh or 26.9 MWyr). This is about 10 times the energy released from the fission of 1 kg U-235.

Note that both D and T are positively charged particles; their interaction is governed by repulsive coulombic forces. Large gravitational or inertial (acceleration) forces, or high temperatures are needed to overcome this repulsion for any significant fusion reaction to occur. This is a crucial difference from fission, where such special conditions for the reaction are not needed. The 17.6 MeV that is released in this reaction, is associated with the kinetic energy of the neutron (14.1 MeV) and the He^4 (3.5 MeV). The rate equations for this reaction, and the associated energy balance (the first law of thermodynamics) can be approximately described by a point kinetics model as:

$$\begin{aligned}
\frac{dN_D}{dt} &= -R_{DT}(T)N_D N_T + \dot{N}_{D,netgain} \\
\frac{dN_T}{dt} &= -R_{DT}(T)N_D N_T + \dot{N}_{T,netgain} \\
\frac{dN_{He^4}}{dt} &= R_{DT}(T)N_D N_T - \dot{N}_{He^4,netloss} \\
\frac{dN_n}{dt} &= R_{DT}(T)N_D N_T - \dot{N}_{n,netloss} \\
\frac{dU}{dt} &= V\left(f_n G_n \frac{dN_n}{dt} + f_{He^4} G_{He^4} \frac{dN_{He^4}}{dt}\right) - \dot{Q}_{loss}
\end{aligned} \tag{15.19}$$

Here N indicates the concentration of the subscripted species, U the internal energy of the system, V its volume, f the fraction of energy G (14.1 MeV or 3.5 MeV) that is deposited in the system, and Q_{loss} the power removed from the system through losses or that is removed through cooling to drive a turbine and generate electricity. R (m^3/sec) is a measure of the reaction rate (here T indicates the temperature, and it should not cause any confusion with the symbol for triton, as they are used in different contexts), and it is approximately given by[1,53]:

$$R_{DT}(T) = 3.7 \times 10^{-18} \frac{\exp\left(-20/(k_B T)^{1/3}\right)}{(k_B T)^{2/3}} \tag{15.20}$$

in which kT has been expressed in units of keV (note that the Boltzmann constant, $k_B = 0.861735 \times 10^{-7}$ keV/K). We have shown in Figure 15.21 a plot of this expression.

Note that R is significant only at very high temperatures that are not realizable. But, because at the high temperatures that are needed, the material will be in a state

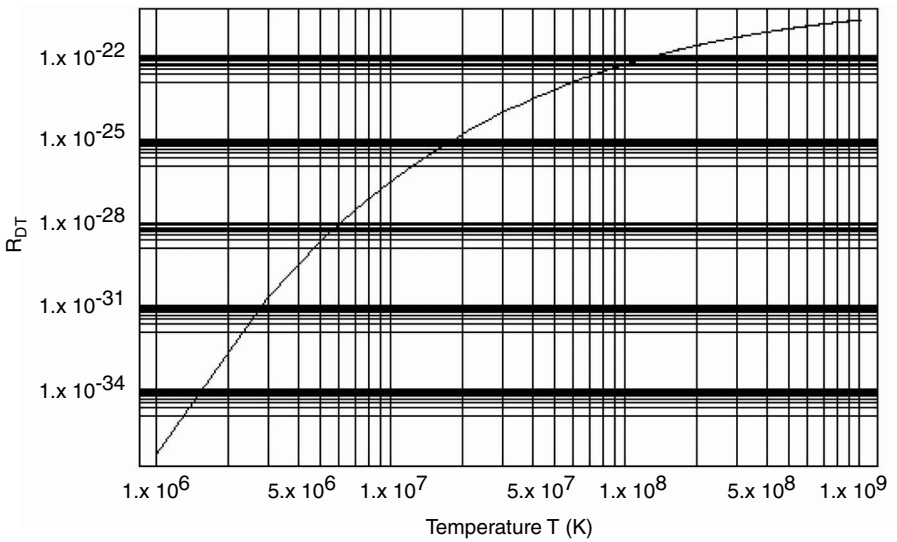

FIGURE 15.21 The reaction parameter as a function of temperature.

of plasma (mixture of ions, electrons, and neutrals) with very low densities, the perfect gas equation of state applies, and we have:

$$n_D \sim \frac{1}{T}, \quad n_T \sim \frac{1}{T} \tag{15.21}$$

A plot of the expression $R_{DT}n_Dn_T$ (Figure 15.22), shows that the D + T reaction has a maximum at about 45×10^6 K.

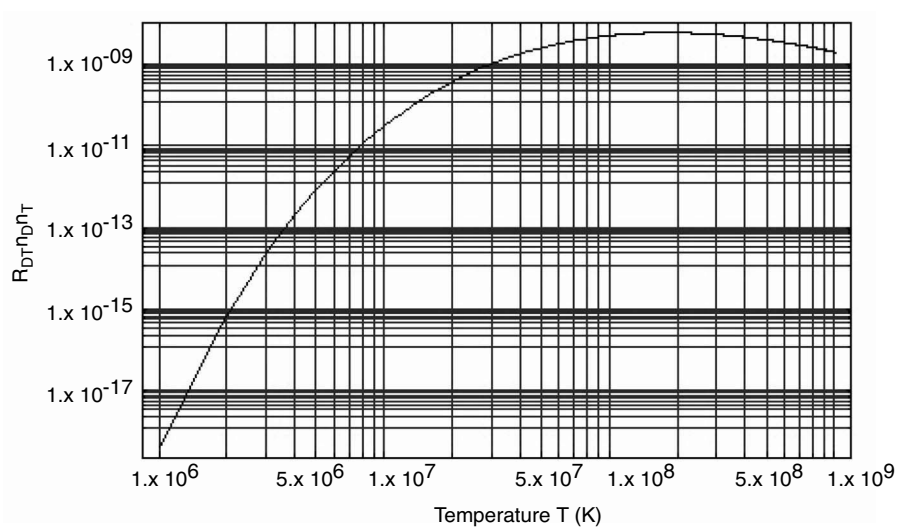

FIGURE 15.22 The normalized reaction rate as a function of temperature.

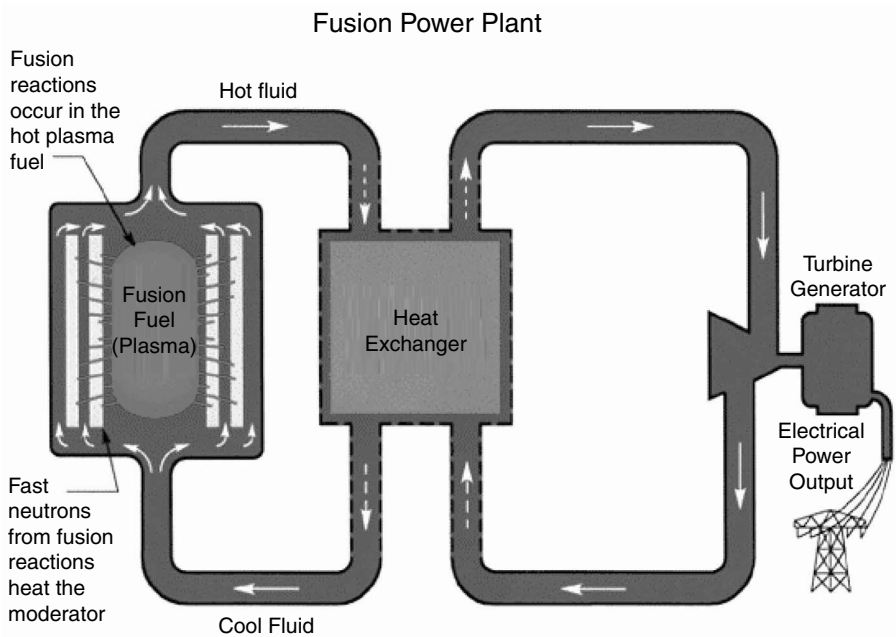

FIGURE 15.23 A schematic of a fusion power plant.

It also turns out that for a D + D reaction, the reaction rate is about 1/25 of that for the D + T reaction for a given temperature. Overall then, the focus has been on the D + T reaction. What is clear is that we need temperatures in the millions of degrees to get reaction rates that would enable significant energy generation. The deuterium needed for the system can be obtained from heavy water, whereas the tritium can be generated from a reaction of the neutrons with lithium.

The physics and engineering challenges of achieving such high temperatures and still confining the plasma for any significant time in a fusion reactor are enormous (the ions that move at very high speeds, are light, and leak). Note that the plasma (because of its very low density) is essentially transparent to neutrons, and only the alpha energy is available for the plasma heating and maintenance of a high temperature in the plasma. A schematic of the fusion power plant is given in Figure 15.23, and it shows some of the engineering concepts involved.

Although there have been efforts to investigate engineering designs of the fusion plants, much of the focus so far has been on achieving plasma confinement, and toward investigations of conditions that could lead to break even (that is $dU/dt = 0$, at a significant temperature with external energy input for plasma heating). There are two concepts that are playing the major role in current research:

1. Magnetic confinement (Mirror and Tokamak)
2. Laser-driven inertial fusion

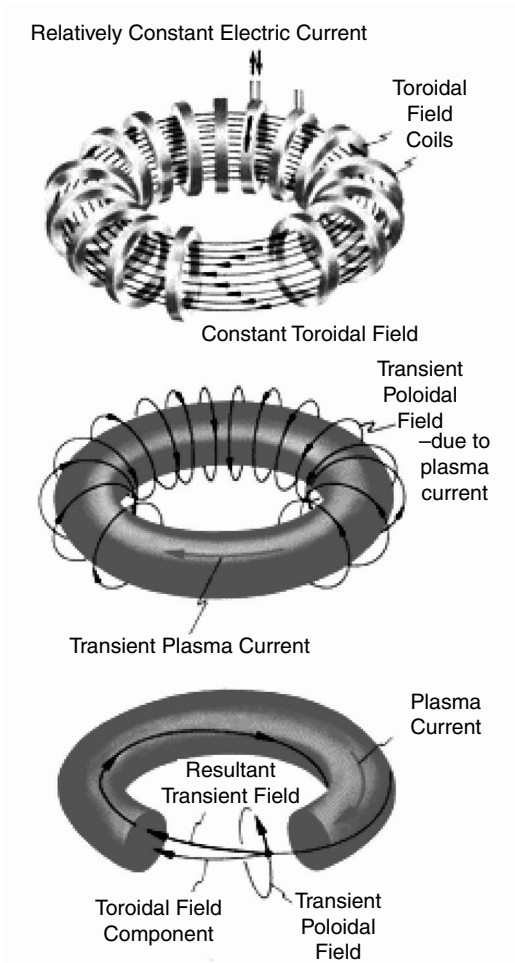

FIGURE 15.24 Toroidal confinement.

In magnetic confinement, the charged particles are sought to be confined through the use of high magnetic fields. The fields alter ion trajectories, and in a mirror (an open system) reflect the particles back towards the plasma at the two ends. In the tokamak (which comprises a toroidal geometry and is a closed system), the ions move in loops within the plasma. Because of the high temperature of the plasma, it is essential to keep the plasma away from surfaces. Schematics of the tokamak concept are shown in Figure 15.24. At present, there is a substantial international effort (known as the ITER program) on tokamaks.

Laser-driven inertial confinement uses laser ablation and resulting compression of a small hollow glass sphere to create very high densities for the reactants (D + T, where the sphere is filled with D and some T, and most of the T is obtained from

Li + n reaction. Li is coated on the inside surface of the hollow sphere). Very-high-energy lasers and precise focusing of the laser beams (from several directions) on the sphere are needed to achieve uniform compression.

The challenges of controlled fusion for electricity generation are enormous: plasma confinement, high temperatures, very-high-powered lasers, precise and economic target fabrication, damage from high-energy neutrons, etc. But the promises are also huge: unlimited raw material supply, very little stored energy in the system, and negligible possibilities of catastrophic accidents, lower radioactive material and waste, etc., as compared to fission-based reactors. We hope that eventually the challenges will be met, as every year there is some progress in our understanding of the physics and engineering of fusion. There has been, however, a significant reduction in government research funding in this area as the realizable benefits are distant.

REFERENCES

1. Connolly, T.J., *Foundations of Nuclear Engineering*, John Wiley & Sons, New York, NY, 1978.
2. Lamarsh, J., *Introduction to Nuclear Engineering*, Addison-Wesley, Reading, MA, 1983, p. 181.
3. Glasstone, S. and Sesonske, A., *Nuclear Reactor Engineering*, Van Nostrand Reinhold, New York, NY, 1981.
4. Lamarsh, J., *Nuclear Reactor Theory*, Addison-Wesley, Reading, MA, 1966.
5. Henry, A., *Nuclear Reactor Analysis*, MIT Press, Cambridge, MA, 1975.
6. Duderstadt, J., *Nuclear Reactor Theory*, John Wiley & Sons, New York, NY, 1976.
7. Ott, K.O. and Bezella, W.A., *Introductory Nuclear Statistics*, American Nuclear Society, La Grange Park, IL, 1989.
8. Ott, K.O. and Neuhold, R.J., *Introductory Nuclear Reactor Dynamics*, American Nuclear Society, La Grange Park, IL, 1985.
9. Stacey, W.M., *Nuclear Reactor Physics*, John Wiley & Sons, New York, NY, 2001.
10. El-Wakil, M.M., *Nuclear Heat Transport*, International Textbook Company, now available from the American Nuclear Society, La Grange Park, IL, 1971.
11. Todreas, N.E. and Kazimi, M.S., *Nuclear Systems*, Vol. I, Hemisphere, New York, NY, 1990.
12. Lahey, R.T. and Moody, F.J., *The Thermal Hydraulics of a Boiling Nuclear Reactor*, American Nuclear Society, La Grange Park, IL, 1977.
13. Weinberg, A.M. and Wigner, E.P., *The Physical Theory of Neutron Chain Reactors*, University of Chicago Press, Chicago, IL, 1958.
14. *Reactor Physics Constants*, ANL-5800, U.S. Govt., Washington, DC, 1963.
15. Davison, B., *Neutron Transport Theory*, Oxford University Press, London, UK, 1957.
16. Bell, G.I. and Glasstone, S., *Nuclear Reactor Theory*, Van Nostrand, New York, NY, 1974.
17. Williams, M.M.R., *The Slowing Down and Thermalization of Neutrons*, John Wiley & Sons, New York, NY, 1966.
18. Willaims, M.M.R., *Mathematical Methods in Particle Transport Theory*, Butterworths, London, UK, 1971.

19. Case, K.M. and Zweifel, P.F., *Linear Transport Theory*, Addison-Wesley, Reading, MA, 1967.
20. Duderstadt, J. and Martin, W., *Transport Theory*, John Wiley & Sons, New York, NY, 1982.
21. Lewis, E.E. and Miller, W.F., *Computational Methods of Neutron Transport*, American Nuclear Society, La Grange Park, IL, 1993.
22. Lapeyre, B., Pardoux, E., and Sentis, R., *Introduction to Monte-Carlo Methods for Transport and Diffusion Equations*, Oxford University Press, London, UK, 2003, original in French, 1998.
23. Loyalka, S.K., Transport theory, in *Encyclopedia of Physics*, Vol. 2, 3rd ed., Trigg, L. and Lerner, R., Eds., Wiley-VCH, Weinheim, Germany, 2005.
24. MCNP — A General Monte Carlo N-Particle Transport Code, Version 5, Los Alamos National Laboratory, Los Alamos, NM 2003.
25. Wirtz, K., *Lectures on Fast Reactors*, American Nuclear Society, La Grange Park, IL 1982.
26. *Controlled Nuclear Chain Reaction: The First Fifty Years*, American Nuclear Society, La Grange Park, IL, 1992.
27. Glasstone, S., *The Effects of Nuclear Weapons*, U.S. Atomic Energy Commission, Washington, DC, first published 1950, 1964.
28. Till, C.E., Nuclear fission reactors, in *More Things in Heaven and Earth: A Celebration of Physics at the Millennium*, Bederson, B., Ed., Springer, New York, NY, 1999.
29. *Los Alamos Science*, Vol. 2, No. 2., Los Alamos Scientific Laboratory, Las Alamos, NM, 1981.
30. Knief, R., *Nuclear Energy Technology: Theory and Practice of Commercial Nuclear Power*, McGraw-Hill, New York, NY, 1981.
31. Melese, G. and Katz, R., *Thermal and Flow Design of Helium Cooled Reactors*, American Nuclear Society, La Grange Park, IL, 1984.
32. Simpson, J.W., *Nuclear Power from Underseas to Outer Space*, American Nuclear Society, La Grange Park, IL, 1994.
33. Serber, R., *The Los Alamos Primer*, U.S. Govt., first published as LA-1, April 1943, declassified 1965, annotated book, University of California Press, Berkeley, CA, 1992.
34. Garwin, R.L. and Charpak, G., *Megawatts and Megatons*, Knopf, New York, NY, 2001.
35. A Technology Roadmap for Generation IV Nuclear Energy Systems, U.S. DOE Nuclear Energy Research Advisory Committee and the Generation IV International Forum, December, 2002.
36. Steinfelds, E.V., Ghosh, T.K., Prelas, M.A., Tompson, R.V., Loyalka, S.K., Development of radioisotope energy conversion systems, *ICAPP Conference Proceeding*, Space Nuclear Power, 2003.
37. Lake, J.A., Nuclear Hydrogen Production, Idaho National Engineering and Environmental Laboratory, paper available at http://nuclear.inel.gov, 2003.
38. Cochran, R. and Tsoulfanidis, N., *The Nuclear Fuel Cycle: Analysis and Management,* American Nuclear Society, La Grange Park, IL, 1999.
39. Faw, R.E. and Shultis, J.K., *Radiological Assessment: Sources and Doses*, American Nuclear Society, La Grange Park, IL, 1999.
40. Shultis, J.K. and Faw, R.E., *Radiation Shielding*, American Nuclear Society, La Grange Park, IL, 2000.
41. U.S. Nuclear Regulatory Commission, Reactor Safety Study: An Assessment of Accident Risks in U.S. Power Plants, Report No. WASH-1400, NUREG-75/014, 1975.

42. McCormick, N.J., *Reliability and Risk Analysis: Methods and Nuclear Power Applications*, Academic Press, New York, NY, 1981.
43. Wilson, R., Araj, A., Allen, O., Auer, P., Boulware, D.G., Finlayson, F., Goren, S., Ice, C., Lidofsky, L., Seesoms, A.L., Shoaf, M.L., Spiewak, I., and Tombrello, T., Report to the American Physical Society of the study group on radionuclide release from severe accidents at nuclear power plants, *Rev. Mod. Phys.*, 57(3), Part II, S1–S154, 1985.
44. U.S. Nuclear Regulatory Commission, Severe Accident Risks: An Assessment For Five U.S. Nuclear Power Plants, (Final Summary Report) NUREG-1150, Vol. 1–2, 1990.
45. Williams, M.M.R. and Loyalka, S.K., *Aerosol Science: Theory and Practice with Special Applications to the Nuclear Industry*, Pergamon, Oxford, UK, 1991.
46. Ghosh, T.K., Prelas, M.A., Viswanath, D.S., and Loyalka, S.K., *Science and Technology of Terrorism and Counter-Terrorism*, Marcel Dekker, New York, NY, 2002.
47. von Weizsacker, C.F., *Phys. Z.*, 38, 176, 1937.
48. Gamow, G. and Teller, E., *Phys. Rev.*, 53, 608, 1938.
49. Bethe, H.A. and Critchfield, C.H., *Phys. Rev.*, 54, 248, 1938.
50. Bethe, H.A., Energy production in stars, *Phys. Rev.*, 55, 434, 1939.
51. Rose, D.J. and Clarke, M., *Plasma and Controlled Fusion*, MIT Press, Cambridge, MA, 1961.
52. Glasstone, S., *Controlled Nuclear Fusion*, U.S. Atomic Energy Commission, Washington, DC, 1965.
53. Kamash, T., *Fusion Reactor Physics*, Ann Arbor Science, Ann Arbor, MI, 1973.
54. Miley, G.H., *Fusion Energy Conversion*, American Nuclear Society, La Grange Park, IL, 1976.
55. Dolan, T.J., *Fusion Research: Principles, Experiments and Technology*, Pergamon, Oxford, UK, 1982.
56. Stacey, W.M., *Fusion: An Introduction to the Physics and Technology of Magnetic Confinement Fusion*, John Wiley & Sons, New York, NY, 1984.
57. Duderstadt, J.E. and Moses, G.R., *Inertial Confinement Fusion*, John Wiley & Sons, New York, NY, 1982.
58. Fowler, T.K., Nuclear power: fusion, in *More Things in Heaven and Earth: A Celebration of Physics at the Millennium*, Bederson, B., Ed., Springer, New York, NY, 1999.

16 Fuel Cells

Mihaela F. Ion and Sudarshan K. Loyalka

CONTENTS

16.1 INTRODUCTION

Fuel cells are devices that produce electrical energy through electrochemical processes, without combusting fuel and generating pollution of the environment. They represent a potential source of energy for a wide variety of applications.

Sir William Robert Grove invented the fuel cell in 1839, and further improvements have been added over the years by many investigators, a significant contribution being made by Francis Bacon in the 1930s. By the 1960s, fuel cells were already being used in NASA's space exploration missions. Over the next few decades, the interest in fuel cells declined considerably due to their extremely high associated costs and relatively poor performance for daily applications. More recently, the increasing demand for cleaner energy sources has brought the fuel cells back into public attention. At present, there is a major push for commercialization of fuel cells, with a potential for applications from portable to automotive and even power-generating stations.

16.2 BASIC CONCEPTS

16.2.1 Design Characteristics

The core structure of a generic fuel cell includes two thin *electrodes* (anode and cathode), located on the opposite sides of an *electrolyte* layer (Figure 16.1).

The electrochemical reactions occur at the *electrodes*. For most fuel cells, the catalytic fuel decomposition occurs at the anode, where ions and electrons split. They recombine at the cathode, where by-products of the reaction are created (i.e., water or CO_2). As high rates of reaction are desired in functioning of the fuel cell, thin layers of catalysts are applied to the electrodes. Furthermore, materials used for electrodes require specific properties such as high conductivity and high ionization and deionization properties, and they must have sufficient permeability to the fuel/oxidant and electrolyte (i.e., they have to be made of porous materials).

The electrolyte layer is made of either a solute or a solid material and plays an important role during operation, as a conductor for the ions between the two electrodes. Characterized by strong insulating properties, the electrolyte does not allow the transfer of electrons. These are conducted through one of the electrodes via an external pathway to the other electrode, closing the electric circuit of the cell.

16.2.2 Operation

Fuel cells are a type of galvanic cell, and they operate similarly to conventional batteries, converting the chemical energy of the reactants directly into electrical energy. However, there is an important difference between them, which lies in the way the chemical energy is transformed into electrical energy. A battery uses the

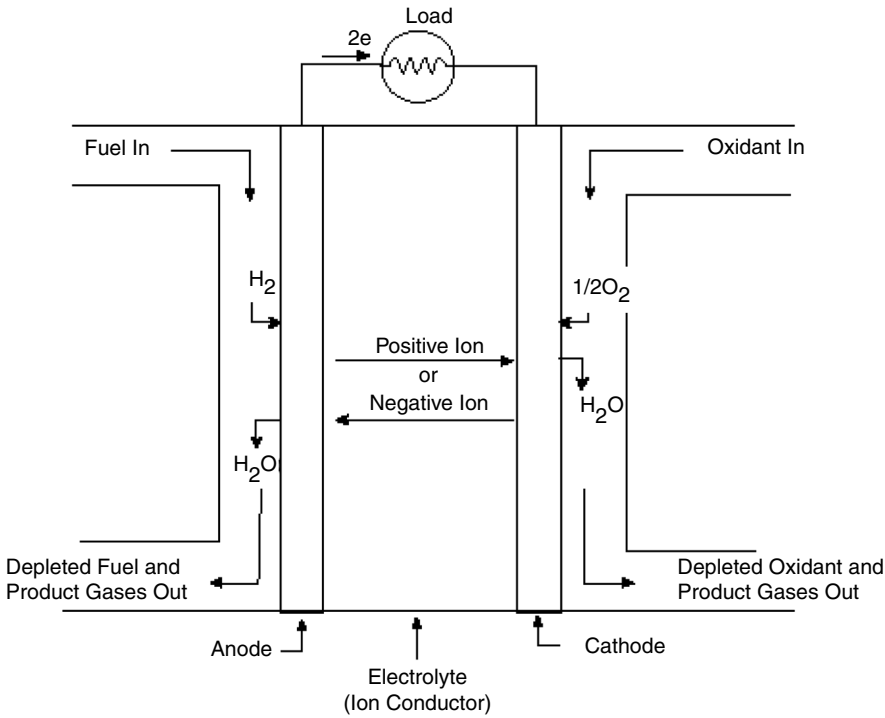

FIGURE 16.1 Design of a generic fuel cell (EG&G Services, Parsons Inc. and Science Applications International Corporation, *Fuel Cell Handbook* (Fifth Edition), Contract No. DE–AM26–99FT40575, for U.S. Department of Energy, October 2000.)

chemical energy *stored* within the reactants inside the battery, whereas a fuel cell *converts* the chemical energy provided by an external fuel/oxidant mixture into electrical energy. Thus, batteries use chemical energy until the reactants are completely depleted and, at the end of their lifetime, they can either be recharged or just thrown away. Fuel cells, on the other hand, can provide electrical output as long as the supply of fuel and oxidant is maintained.

Typically, hydrogen-rich fuels are used for operation, and the most common fuels include gases (i.e., hydrogen, natural gas, or ammonia), liquids (i.e., methanol, hydrocarbons, hydrazine), or coal. A preliminary conversion (*reforming*) process is required for all fuels, except for direct hydrogen. The oxidant used at the cathode is usually oxygen or air.[1,2]

During operation, both hydrogen-rich fuel and oxygen/air are supplied to the electrodes. Hydrogen undergoes catalytic oxidation at one of the electrodes and splits into ions and electrons. Oxygen undergoes a reduction reaction at the other electrode. Both ions and electrons travel from one electrode to the other, using different pathways. Ions travel through the electrolyte and electrons are forced through a separate pathway via the current collectors to the other electrode, where they combine with oxygen to create water or other by-products, such as CO_2.

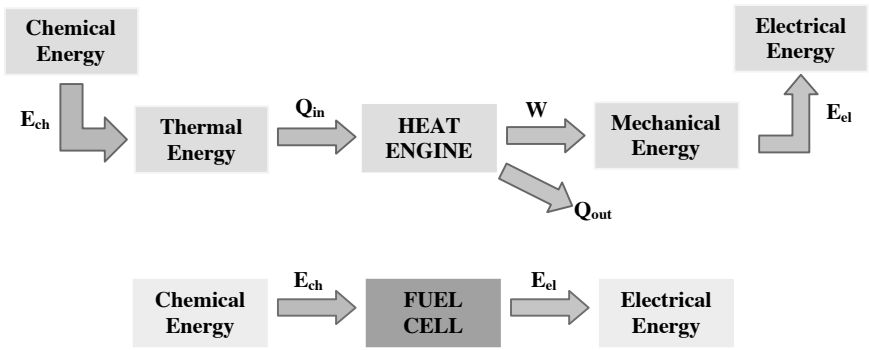

FIGURE 16.2 Energy conversion processes for heat engine and fuel cell.

16.2.3 Thermal Efficiency

Although the input (chemical energy, E_{ch}) and output (electrical energy, E_e) of the operation are the same for fuel cells and heat engines, the conversion process is different. Heat engines use chemical energy to produce intermediate heat, which is subsequently transformed into mechanical energy, which in turn leads to electrical energy. Fuel cells use a direct conversion process, transforming the chemical energy directly into electrical energy (see Figure 16.2). Thus, when comparing fuel cells with heat engines, two aspects of the second law of thermodynamics have to be considered: heat absorption from a reservoir to use for operation, and energy losses to the surroundings.

16.2.3.1 Heat Absorption from a Reservoir to Use for Operation

Fuel cell operation does not require two different temperature reservoirs, and thus any temperature restrictions associated with the Carnot cycle are eliminated. In comparison, heat engines operate between a hot source and a cold sink. Their thermal efficiency (η) is calculated as the amount of net work (W) done for the heat (Q_{in}) absorbed by the engine. The amount of net work is determined as the difference between the absorbed (Q_{in}) and the rejected (Q_{out}) heat. In case of an ideal, reversible heat engine, the entropy remains constant, and

$$\frac{Q_{out}}{Q_{in}} = \frac{T_{out}}{T_{in}}.$$

The maximum efficiency of such an engine is given by

$$\eta_{HE,\max} = 1 - \frac{T_{out}}{T_{in}}.$$

A high value is therefore obtained using either a very low T_{out} (for an ideal machine, this can be zero) or a very high combustion temperature, T_{in}. In reality, T_{out} is approximately 300 K, which is the ambient temperature. At the other end, the

combustion temperature cannot be too high (i.e., 2000–3000 K), owing to temperature restrictions of the materials.

16.2.3.2 Energy Losses to the Surroundings

Processes in real heat engines or fuel cells are irreversible, and losses occur. The real efficiency is always less than the theoretical efficiency. To properly compare the efficiency of heat engines and fuel cells, the theoretical values have to be considered in each case. For fuel cells, this is calculated as the maximum electrical work (W_{el}) done for the total thermal energy available or the enthalpy of the fuel (ΔH_0). W_{el} is given by the change in the chemical energy, or the Gibbs free energy of the electrochemical process, and it is calculated as the difference between the total heat available and the heat produced during operation. The maximum efficiency can be written as:

$$\eta_{FC,\max} = 1 - \frac{T\,\Delta S_0}{\Delta H_0}$$

where ΔS_0 represents the entropy change of the system.

16.2.4 Cell Voltage

Under ideal conditions, operation of fuel cells is performed without any losses. This can be seen in Figure 16.3, which presents the cell voltage and current characteristics for ideal and real situations. The most important losses that occur during normal operation are:

- Activation losses, which are directly dependent on the reaction rates
- Ohmic losses, caused by resistance to flows of ions and electrons through media
- Concentration losses, due to changes in the concentration of reactants

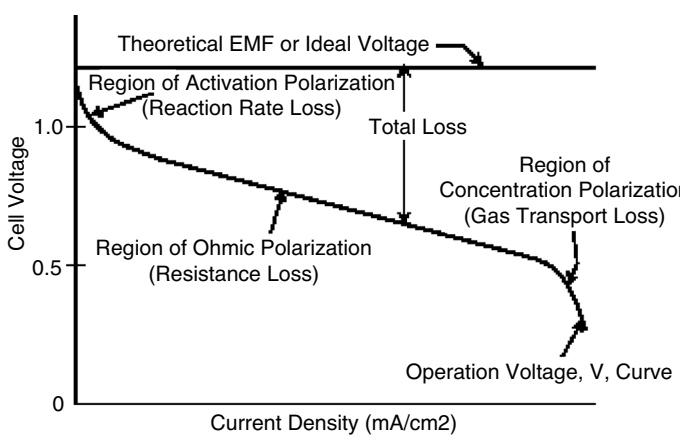

FIGURE 16.3 Fuel cell voltage/current characteristic. (From EG&G Services, Parsons Inc. and Science Applications International Corporation, *Fuel Cell Handbook* (Fifth Edition), Contract No. DE–AM26–99FT40575, for U.S. Department of Energy, October 2000.)

16.3 FUEL CELL SYSTEM

16.3.1 General Description

Major applications require power input that is far above the output produced by a single fuel cell unit (i.e., approximately 1 W/cm^2 electrode area for hydrogen fuel cells). Multiple fuel cells are therefore arranged in stacks to produce the desired power output. Preliminary conversion processes are required to supply the fuel cells with the appropriate fuel for operation and after the electrochemical reactions occur, further conversion processes are required to transform the electrical output from the fuel cells into a form accessible to various applications. The whole ensemble comprising the fuel processor, stack of fuel cells, and power conditioner represents the *fuel cell system*. A schematic representation of a typical fuel cell system configuration is shown in Figure 16.4.

The component playing the major role in the whole system is the *fuel cell stack* (or *power section*). A fuel cell stack is usually made of at least 50 fuel cell units of various configurations. Here, the electrochemical reactions that transform chemical energy directly into electrical energy occur (see Figure 16.5). This structure, which resembles a sandwich, is further placed between two *bipolar separator plates*. The bipolar plates have two important operating functions as current collectors and separator plates: as *current collectors* they conduct the electrons produced by the oxidation of hydrogen, and *as separator plates* they provide the necessary physical separation of the flows for adjacent cells as well as the required electrical connections.[4]

Typically, hydrogen-rich gas is used for fuel cell operation. Because only the hydrogen component of these fuels reacts at the electrodes, a reforming process is performed in the *fuel processor* for all the fuels, except for the direct hydrogen, before the gas enters the fuel cell.

The *power conditioner* is the section of the fuel cell system where the direct current (DC) obtained from the fuel cell stack is converted into alternating current (AC), when required. It is also designed to adjust the current and voltage of the stack to produce the desired power output.

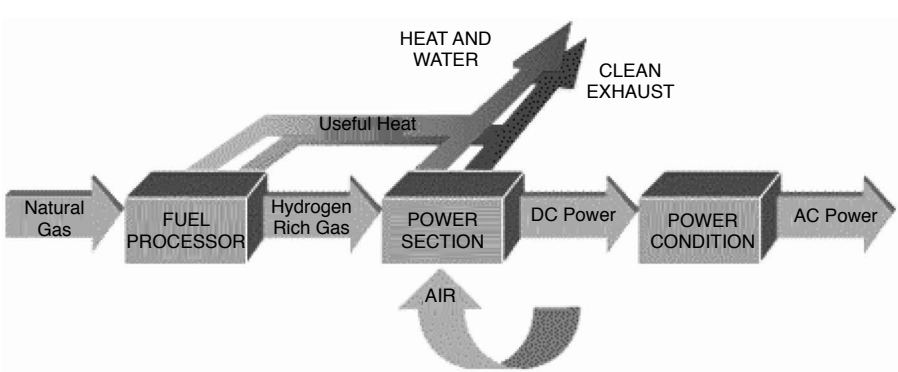

FIGURE 16.4 Fuel cell system. (From U.S. Department of Defense Fuel Cell Demonstration Program, Fuel Cell Descriptions, www.dodfuelcell.com/fcdescriptions.html.)

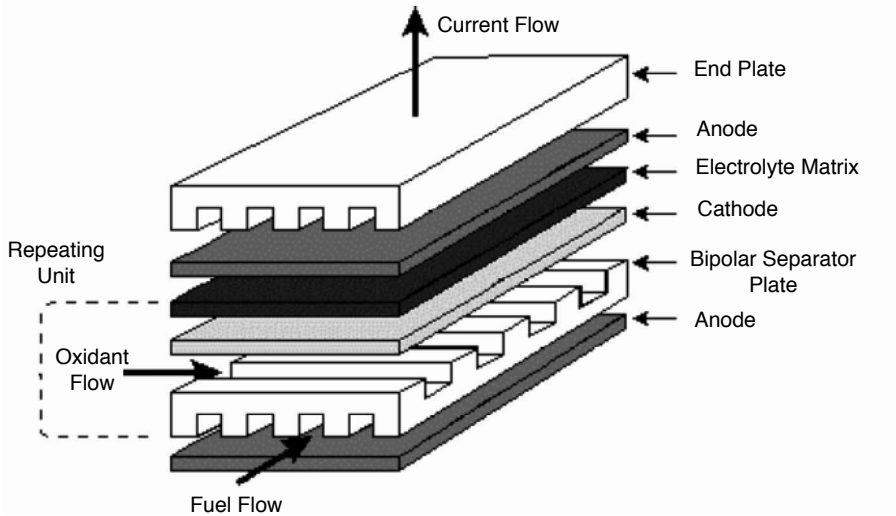

FIGURE 16.5 Fuel cell stack components. (From Energy Center of Wisconsin Fuel Cells for Distributed Generation. A Technology and Marketing Summary Report, 193-1, 2000.)

16.3.2 Fuel Cells Classification

Fuel cells can be classified according to various criteria, based on electrolyte, operating temperature, fuel or oxidant used, reforming process, etc. The most common criterion, also used to name these devices, is the type of the electrolyte used for operation. Five major categories can be identified, based on the type of the electrolyte:

- Proton exchange membrane fuel cells (PEMFC).
- Alkaline fuel cells (AFC).
- Phosphoric acid fuel cells (PAFC).
- Molten carbonate fuel cells (MCFC).
- Solid oxide fuel cells (SOFC), can be further divided into two subcategories, respectively the intermediate temperature solid oxide fuel cells (ITSOFC), with operating temperatures less than 800°C, and the tubular solid oxide fuel cells (TSOFC), with temperatures over 800°C (EG&G Services, Parsons Inc. and Science Applications International Corporation, *Fuel Cell Handbook* (Fifth Edition), Contract No. DE–AM26–99FT40575, for U.S. Department of Energy, October 2000).

A summary of the characteristics of fuel cells is presented in Table 16.1. The PEMFC and AFC operate at lower temperatures and are mainly developed for transportation and small utilities. The PAFC operate at higher temperatures, being designed for medium-scale power applications. The MCFC and SOFC operate at high temperatures and are intended for large power utilities.[5]

TABLE 16.1
Fuel Cell Characteristics

Characteristics	PEMFC	AFC	PAFC	MCFC	SOFC	
					ITSOFC	TSOFC
Operating Parameters						
Temperature[a] (°C)	80	65–220	150–220	~ 650	600–800	800–1000
Pressure[b] (atm)	1–5		1–8	1–3	1–15	
Efficiency[e] (%)	40–50	40–50	40–50	50-60	45–55	
Power density[f] (kW/kg)	0.1–1.5	0.1–1.5	0.12	—	1–8	
Cell Components[c]						
Electrolyte	Proton exchange membrane (solid)	Potassium hydroxide (liquid)	Phosphoric acid (liquid)	Molten carbonate salt (liquid)	Ceramic (solid)	
Electrodes	Carbon-based	Carbon-based	Graphite-based	Nickel and stainless steel-based	Ceramic	
Catalyst	Platinum	Platinum	Platinum	Nickel	Perovskites	
Reactants[d]						
Charge carrier	H^+	OH^-	H^+	CO_3^{2-}	O^{2-}	
Fuel	H_2 (reformate)	H_2 (pure)	H_2 (reformate)	$H_2/CO/CH_4$ (reformate)	$H_2/CO/CH_4$ (reformate)	
Reforming process	External	—	External	External/internal	External/internal	
Oxidant	O_2/air	O_2	O_2/air	CO_2/O_2/air	O_2/air	
Operation						
Water management[g]	Evaporative	Evaporative	Evaporative	Gaseous product	Gaseous product	
Heat management[g]	Process gas Independent cooling medium	Process gas Electrolyte calculation	Process gas Independent cooling medium	Internal reforming Process gas	Internal reforming Process gas	

Advantages/Disadvantages[h]					
Advantages	High current and power density; long operating life	High current and power density; high efficiency	Advanced technology	High efficiency; internal fuel processing; high-grade waste heat	Internal fuel processing; high-grade waste heat; potentially inexpensive
Disadvantages	CO intolerance; water management; noble metal catalyst	CO_2 intolerance	Efficiency; lifetime; noble metal catalyst	Electrolyte instability; lifetime	High temperature; efficiency; low ionic conductivity
Applications[i]					
Type	Motive/small utility	Aerospace	Small utility	Utility	Utility
Scale	0.1 kW–10 MW	0.1–20 kW	200 kW–10 MW	>100 MW	>100 MW

Source: [a]Adapted from EG&G Services, Parsons Inc. and Science Applications International Corporation, *Fuel Cell Handbook* (Fifth Edition), Contract No. DE–AM26–99FT40575, for U.S. Department of Energy, October 2000.

[b]Adapted from Penner, S.S., Ed., Commercialization of fuel cells, *Energy: Int. J.*, 20(5), Pergamon Press, New York, 1995; Energy Center of Wisconsin Fuel Cells for Distributed Generation. A Technology and Marketing Summary Report, 193-1, 2000.

[c]Adapted from EG&G Services, Parsons Inc. and Science Applications International Corporation, *Fuel Cell Handbook* (Fifth Edition), Contract No. DE–AM26–99FT40575, for U.S. Department of Energy, October 2000; Mehta, S.K. and Bose, T.K., Ed., *Proceedings of the Workshop on Hydrogen Energy Systems*, presented at the Official Opening of the Hydrogen Research Institute, in collaboration with Canadian Hydrogen Association, Canada, 1996; Energy Center of Wisconsin Fuel Cells for Distributed Generation. A Technology and Marketing Summary Report, 193-1, 2000.

[d]Adapted from EG&G Services, Parsons Inc. and Science Applications International Corporation, *Fuel Cell Handbook* (Fifth Edition), Contract No. DE–AM26–99FT40575, for U.S. Department of Energy, October 2000; Mehta, S.K. and Bose, T.K., Ed., *Proceedings of the Workshop on Hydrogen Energy Systems*, presented at the Official Opening of the Hydrogen Research Institute, in collaboration with Canadian Hydrogen Association, Canada, 1996. With permission.

[e]Adapted from European Commission, A Fuel Cell Research, Development and Demonstration Strategy for Europe up to 2005, 1998 ed., Belgium, 1998. With permission.

[f]Adapted from Norbeck, J.M., *Hydrogen Fuel for Surface Transportation*, Society of Automotive Engineers, Warrendale, PA, 1996..

[g]Adapted from EG&G Services, Parsons Inc. and Science Applications International Corporation, *Fuel Cell Handbook* (Fifth Edition), Contract No. DE–AM26–99FT40575, for U.S. Department of Energy, October 2000.

[h]Adapted from Decher, R., *Direct Energy Conversion — Fundamentals of Electric Power Production*, Oxford University Press, 1997. With permission.

[i]Adapted from Mehta, S.K. and Bose, T.K., Ed., *Proceedings of the Workshop on Hydrogen Energy Systems*, presented at the Official Opening of the Hydrogen Research Institute, in collaboration with Canadian Hydrogen Association, Canada, 1996. With permission.

16.4 LOW-TEMPERATURE FUEL CELLS

16.4.1 Proton Exchange Membrane Fuel Cells

The PEMFCs were developed originally by General Electric in the 1960s for NASA's space explorations. Over the years, these fuel cells have been known under various names, such as *ion exchange membrane*, *solid polymer electrolyte, proton exchange membrane*, or simply, *polymer electrolyte* fuel cells. They use hydrogen as fuel, oxygen or air as oxidant, and a solid polymer membrane as electrolyte.

16.4.1.1 Design Characteristics

The core of the PEMFC design consists of a proton conducting membrane (the electrolyte), located between two platinum-impregnated porous electrodes. Teflon gaskets and current collectors are added to these components to complete a single fuel cell unit. The core of the fuel cell is usually less than a millimeter thick and is referred to as the *membrane-electrode assembly* (MEA). Depending on the mode of fabrication, MEA can include either the membrane along with the catalyst layers only, or the whole ensemble of the previously mentioned components plus the carbon electrodes. Figure 16.6 shows a schematic representation of the PEMFC manufactured by Ballard Power Systems. A general view of the cell hardware and its cross section are presented in Figure 16.7.

16.4.1.1.1 Electrolyte

Various electrolyte materials have been developed over the years for use in PEMFC, and there is still extensive ongoing research focused on improving the materials currently used or finding new solutions. Currently, the thickness of the membrane is approximately 50–175 μm, and recent developments show that stable operation conditions can be obtained with membranes only 10–25 μm thick.[10]

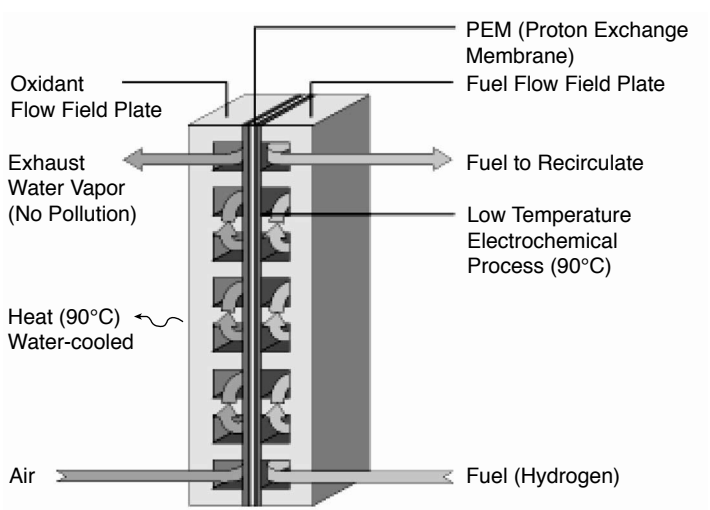

FIGURE 16.6 PEMFC, Ballard Power systems. (From Ballard Power Systems, How the Ballard® fuel cell works, www.ballard.com.)

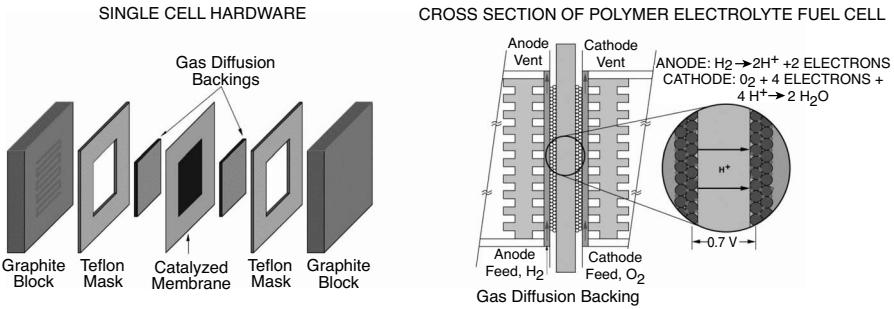

FIGURE 16.7 PEMFC design. (Gottesfeld, S., "The Polymer Electrolyte Fuel Cell, Materials Issues in a Hydrogen Fueled Power Source," Los Alamos National Laboratory, Materials Science and Technology Division, White Paper on LANL Hydrogen Education Web site: http://education.lanl.gov/RESOURCES/h2/gottesfeld/education.html.

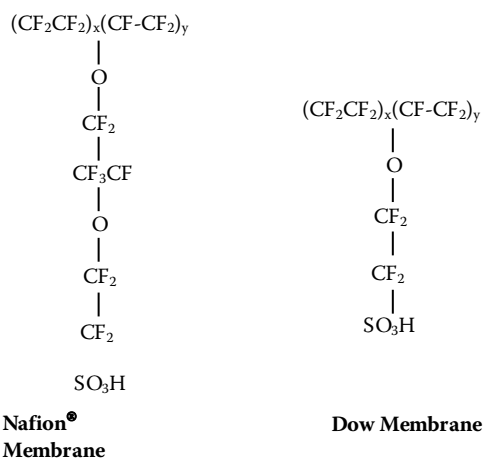

FIGURE 16.8 Structural characteristics of PEMFC membranes. (Bloemen, L.J. and Mugerwa, M.N., (Eds.), "Fuel Cell Systems," Plenum Press, New York, 1994)

Most of the membranes used to date in PEMFC have a fluorocarbon-polymer-based structure to which sulfonic acid groups are attached. The key characteristic of these materials is that, although the acid molecules are fixed to the polymer, the protons on these acid groups are free to travel through the membrane. The most well known are the Nafion® membranes, which have been developed by DuPont over more than three decades. These types of membranes are thin, nonreinforced films based on the Nafion® resin, a perfluorinated polymer.[11] The structure of the Nafion membranes is given in Figure 16.8.

This type of membrane is usually prepared by modifying a basic polymer (polyethylene) through a process called *perfluorination*, where the hydrogen is substituted with fluorine. The modified polymer is the polytetrafluoroethylene (PTFE) or Teflon. A side chain of sulphonic acid HSO_3 is then added to PTFE through the "sulphonation" process. The end of the chain is an SO_3^- ion, and the

HSO_3 group is ionically bonded. The resulting structure combines strong hydrophobic properties of the fluorocarbon polymer backbone with strong hydrophilic properties of the terminal sulfonic acid function. It is an excellent proton conductor, durable (owing to strong bonds between the fluorine and carbon) and shows good chemical resistance.[2,9]

Tests showed that the PEMFC performance levels improved with the membrane developed by Dow Chemical.[13,14] Although this membrane remains a perfluorosulfonic acid membrane, its structure is characterized by a shorter side chain and thus a lower equivalent weight compared to Nafion®. Conductivity and hydrophilic properties are slightly enhanced, and durability is still maintained. The Dow membrane was tested in 1987–1988 at Ballard Power Systems, and the results showed significant increases in PEMFC performance levels (Figure 16.9).

16.4.1.1.2 Electrodes

The anode and cathode have an identical structure, consisting of two layers in close contact with each other and with the membrane. The roles of the electrodes in operation of the fuel cell are summarized in Table 16.2.

The layer situated adjacent to the membrane is the *catalyst layer*, which provides the area where the electrochemical reactions occur (Figure 16.7). It is a platinum carbon

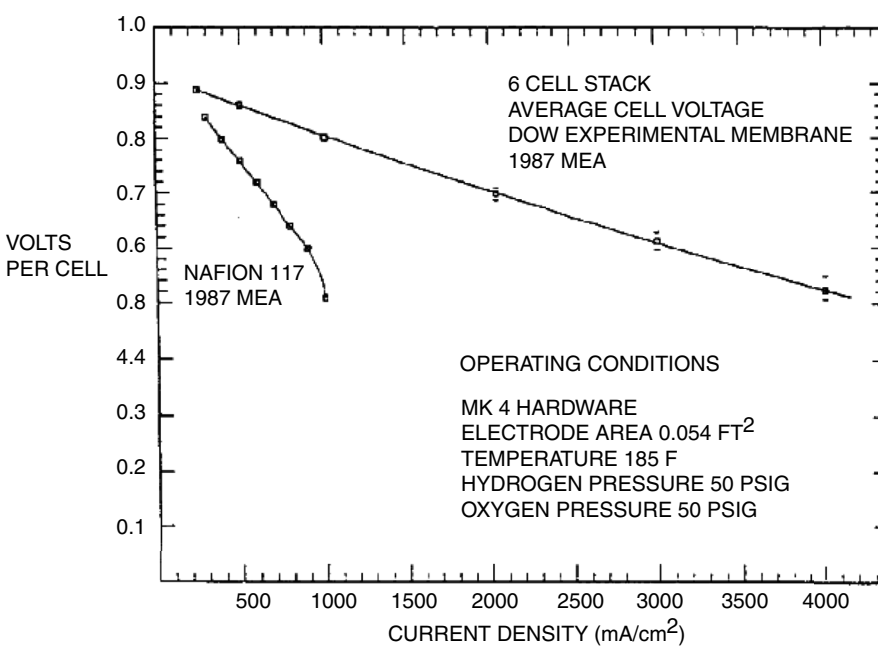

FIGURE 16.9 PEMFC performance using Nafion® and Dow membranes. (EG&G Services, Parsons Inc. and Science Applications International Corporation, *Fuel Cell Handbook* (Fifth Edition), Contract No. DE–AM26–99FT40575, for U.S. Department of Energy, October 2000.)

TABLE 16.2
Roles of Electrodes in PEMFC Operation

Electrode	Layer	Role
Anode	Catalyst	Catalysis of anode reaction
		Proton conduction into membrane
		Electron conduction into gas-diffusion layer
		Water transport
		Heat transport
	Gas diffusion	Fuel supply and distribution (hydrogen/fuel gas)
		Electron conduction
		Heat removal from reaction zone
		Water supply (vapor) into electrocatalyst
Cathode	Catalyst	Catalysis of cathode reaction
		Oxygen transport to reaction sites
		Proton conduction from membrane to reaction sites
		Electron conduction from gas-diffusion layer to reaction zone
		Water removal from reactive zone into gas-diffusion layer
		Heat generation/removal
	Gas diffusion	Oxidant supply and distribution (air/oxygen)
		Electron conduction towards reaction zone
		Heat removal
		Water transport (liquid/vapor)

Source: Adapted from Hoogers, G., Ed., *Fuel Cell Technology Handbook*, CRC Press, Boca Raton, FL, 2003. With permission.

composite film, about 5–10 μm thick, used to increase the reaction rates. Because of the high cost of platinum, sustained technological efforts were focused on reduction of the platinum load, originally about 4 mg Pt/cm^2, but currently almost 0.2 mg Pt/cm^2 and even lower values, with high performance levels.[15,16]

Typically, carbon paper is used when a compact design of fuel cells is desired; the most used brand is Toray® paper. However, if only a simple assembly is preferred, carbon cloth is sufficient. Thickness of the backing layer is typically between 100 and 300 μm. Figure 16.10 shows details of the MEA structure with the catalyst and backing layers.[17]

16.4.1.1.3 Teflon Masks and Current Collectors

The single-cell structure is completed by two Teflon masks and two high-density graphite plates. The Teflon masks are gaskets that confine the gas flow to the active area, providing an effective seal along the periphery of the membrane. The graphite plates are current collectors, and they also contain gas flow fields at the same time. In a fuel cell stack, the current collector plates contain gas flow fields on both sides, and they become *bipolar plates*.

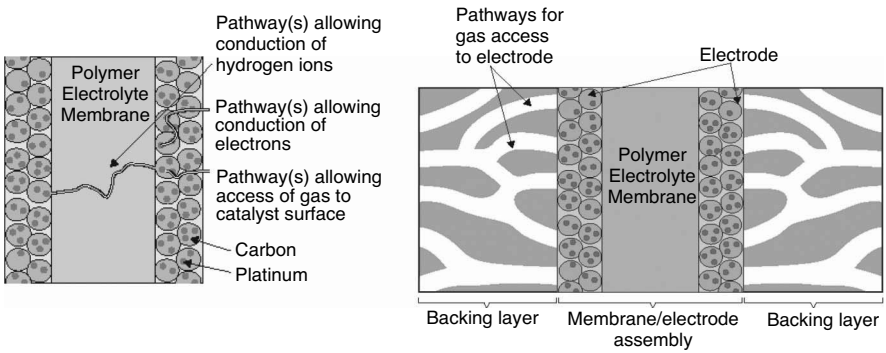

FIGURE 16.10 MEA structure design details. (From Thomas, S., and Zalbowitz, M., Fuel Cells — Green Power, LA–UR–99–3231, Los Alamos National Laboratory, 1999. With permission.)

16.4.1.2 Operation Characteristics

Hydrogen gas is supplied to the anode, where it dissociates into hydrogen atoms in the presence of the platinum catalyst. The atoms further split into protons and electrons, which travel separate ways from the anode to the cathode. Protons are conducted through the electrolyte membrane, and electrons are forced to go via an external circuit to the cathode, producing electricity. Oxygen is supplied to the cathode, where a reduction process occurs and water and heat are created as by-products. Figure 16.11 shows an illustration of the PEMFC principle of operation. The basic reactions for the PEMFC are:

$$\text{Anode: } 2\,H_2 \rightarrow 4\,H^+ + 4\,e^-$$
$$\text{Cathode: } O_2 + 4\,H^+ + 4\,e^- \rightarrow 2\,H_2O$$
$$\text{Cell reaction: } 2H_2 + O_2 \rightarrow 2\,H_2O$$

Continuous research efforts over the years have led to significant improvements in the performance levels of the PEMFC (Figure 16.12).

The typical output is approximately 0.7 V per cell unit, and the power density is usually higher compared to other fuel cells, which translates into a smaller size of the fuel cell stack. For transport applications, Asia Pacific Fuel Technologies produces 3-kW 64-cell stacks, which are 25 cm high and have an active area of 150 cm^2. The Mark 902 fuel cell module produced by Ballard Power Systems has the dimensions of $80.5 \times 37.5 \times 25.0$ cm and yields an 85-kW rated net output.[19] The Nexa™ power module, Ballard's first volume-produced PEMFC designed to be integrated into stationary and portable applications, is $56 \times 25 \times 33$ cm, with a rated net output of 1200 W (see Figure 16.13).

PEMFCs are intended to be used also in small applications, such as portable devices (i.e., laptops; see Figure 16.14) and electronics, etc.

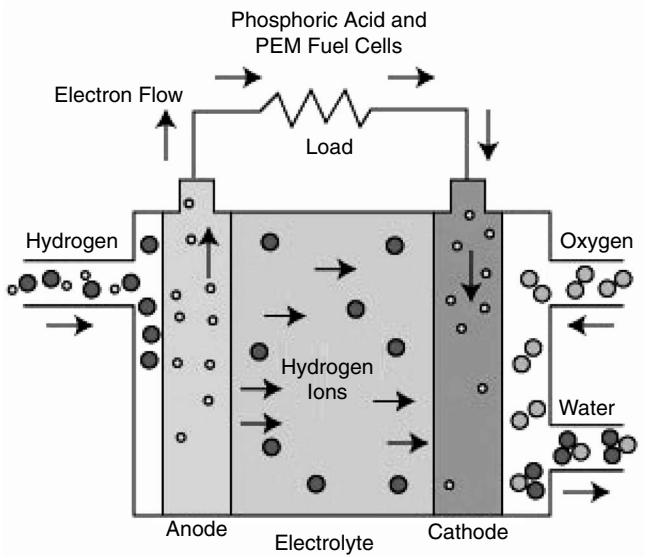

FIGURE 16.11 PEMFC and PAFC operation principle. (U.S. Department of Defense Fuel Cell Test and Evaluation Center, "Fuel Cell Basics," www.fctec.com/index.html.)

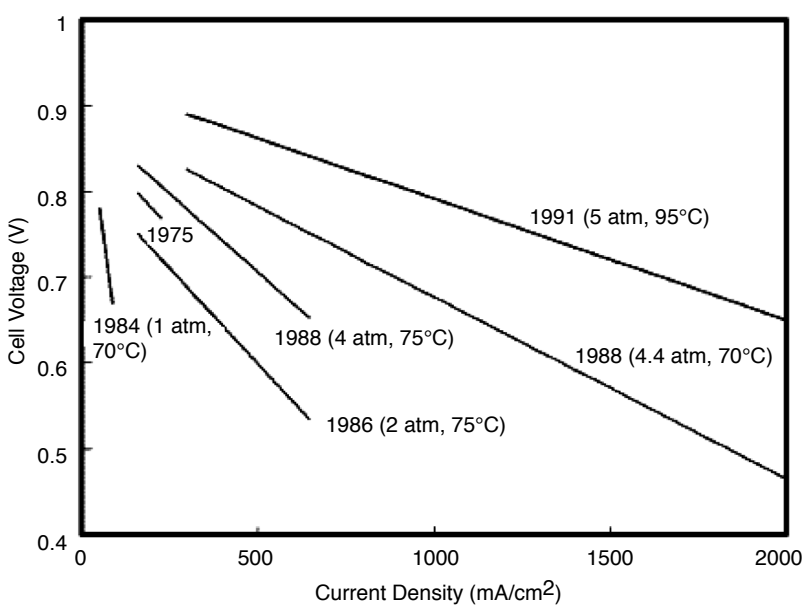

FIGURE 16.12 PEMFC performances. (EG&G Services, Parsons Inc. and Science Applications International Corporation, *Fuel Cell Handbook* (Fifth Edition), Contract No. DE–AM26–99FT40575, for U.S. Department of Energy, October 2000)

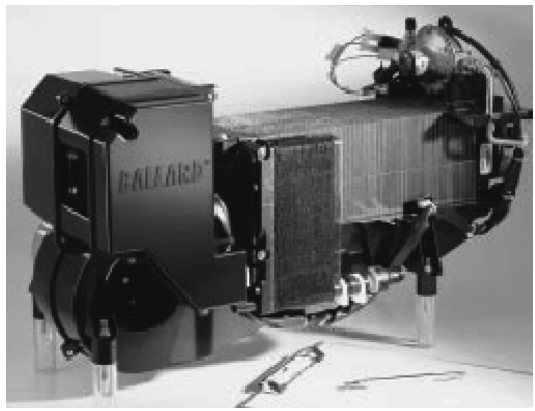

FIGURE 16.13 Nexa™ power module. (Ballard Power Systems, "Ballard® Fuel Cell Power Module Nexa™," www.ballard.com, 2002.)

FIGURE 16.14 Ballard fuel cell. (Fuel Cells 2000, "Transportation Fuel Cells — Technical Info," www.fuelcells.org.)

16.4.2 Alkaline Fuel Cells

The development of the AFC started almost seven decades ago, when researchers started to realize that hydrogen fuel cells with alkaline electrolytes can be used in commercial applications. The first notable solution was the high-power-density AFC developed by Sir Francis Bacon, with an output of 0.6 V at 1.11 A/cm^2 current density and 240°C operating temperature.[20] AFCs have been used by NASA on their space explorations during the 1960s and 1970s.

The AFCs utilize potassium hydroxide (KOH) as an electrolyte of variable concentration, either in aqueous solution or stabilized matrix form. The KOH concentration varies with the operating temperature, increasing from 35 wt% for low temperatures to about 85 wt% for high temperatures. The electrolyte is contained in

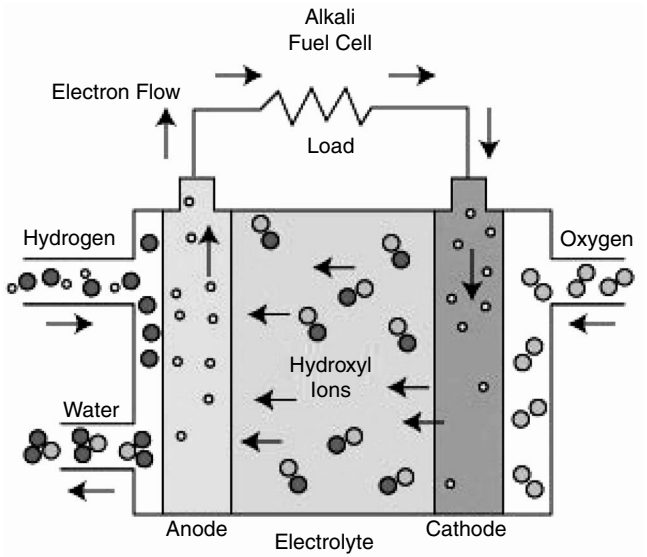

FIGURE 16.15 AFC operation principle. (U.S. Department of Defense Fuel Cell Test and Evaluation Center, "Fuel Cell Basics," www.fctec.com/index.html.)

a porous asbestos matrix, and the catalysts are typically made of nickel (Ni) and silver (Ag). Noble metals, metal oxides, or spinels are also considered among the materials used to fabricate the catalysts.[21] Further details of the AFC components used for the space applications are given in EG&G Services, Parsons Inc. and Science Applications International Corporation, *Fuel Cell Handbook* (Fifth Edition), Contract No. DE–AM26–99FT40575, for U.S. Department of Energy, October 2000.

Hydrogen and oxygen are supplied to the electrodes similarly to PEMFCs. The KOH electrolyte is extremely sensitive to potential poisoning with CO or reaction with CO_2 and, thus, only pure hydrogen and oxygen can be used as reactants for the electrochemical processes. The carrier in this case is the hydroxyl ion (OH), which travels from the cathode to the anode, where it combines with H_2 and creates water and electrons (Figure 16.15). If the electrolyte is in a solution form, it mixes up with the water created at the anode. To ensure proper operation of the fuel cell unit, it is required that water be continuously removed from the electrolyte. Electrons formed at the anode are conducted to the external circuit to create the electrical output and then forced to the cathode, closing the circuit. The basic electrochemical reactions for the AFC are:

$$\text{Anode: } 2\,H_2 + 4\,OH^- \rightarrow 4\,H_2O + 4\,e^-$$
$$\text{Cathode: } O_2 + 2\,H_2O + 4\,e^- \rightarrow 4\,OH^-$$
$$\text{Cell reaction: } 2H_2 + O_2 \rightarrow 2\,H_2O$$

Owing to the fact that only pure fuel or oxidant can be used in operation, the AFC is used for specialized applications. Space explorations, military use, and research are among the few areas in which these fuel cells are utilized. Efforts are

being made to broaden the spectrum of terrestrial daily applications. Tests and demonstrations have shown that AFC hybrid vehicles are potential technological solutions for the near future in transportation. In the 1970s, an AFC-based hybrid vehicle was tested for 3 years, using liquid hydrogen and oxygen, and KOH liquid electrolyte.[22] The improved version of this vehicle was tested again in 1998, using a system consisting of AFC and rechargeable alkaline manganese dioxide-zinc (RAM™) batteries. The operating lifetime of these AFCs is anticipated to be about 4000 h, and the mass production cost is expected to become comparable to the cost of the currently used heat engines ($50 to $100 per kW).[23]

16.4.3 Phosphoric Acid Fuel Cells

These cells have been developed for medium-scale stationary applications and are the only commercialized type of fuel cells. The technology employed for the PAFC is the most well-known technology developed to date for fuel cells.

The PAFC have a similar design with the PEMFC. The electrolyte used for PAFC is concentrated phosphoric acid (H_3PO_4), allowing operation at temperatures higher than the PEMFC (i.e., over 100°C). This electrolyte is contained in a silicon carbide matrix, and catalysts are typically made of Pt. Technological advances of the components of this type of fuel cells have been extensively documented over the last 40 years, and a brief summary is presented in Table 16.3.

Operation of PAFC is similar to PEMFC, as can be seen in Figure 16.11. Hydrogen-rich fuel is supplied to the anode, where protons and electrons split and start traveling to the cathode, following different pathways through the membrane layer (protons) and via an external circuit, producing electricity (electrons). At the

TABLE 16.3
PAFC Component Characteristics

Component	ca. 1965	ca. 1975	Current Status
Anode	PTFE-bonded Pt black	PTFE-bonded Pt/C Vulcan XC-72[a]	PTFE-bonded Pt/C Vulcan XC-72[a]
	9 mg/cm^2	0.25 mg Pt/cm^2	0.1 mg Pt/cm^2
Cathode	PTFE-bonded Pt black	PTFE-bonded Pt/C Vulcan XC-72[a]	PTFE-bonded Pt/C Vulcan XC-72[a]
	9 mg/cm^2	0.5 mg Pt/cm^2	0.5 mg Pt/cm^2
Electrode Support	Ta mesh screen	Carbon paper	Carbon paper
Electrolyte Support	Glass fiber paper	PTFE-bonded SIC	PTFE-bonded SIC
Electrolyte	85% H_3PO_4	95% H_3PO_4	100% H_3PO_4

[a]Conductive oil furnace black, product of Cabot Corp. (Typical properties: 002 d-spacing of 3.6 Å by x-ray diffusion, surface area of 220 m^2/g by nitrogen adsorption, and average particle size of 30 μm by electron microscopy.)

Source: [a]Adapted from EG&G Services, Parsons Inc. and Science Applications International Corporation, *Fuel Cell Handbook* (Fifth Edition), Contract No. DE–AM26–99FT40575, for U.S. Department of Energy, October 2000.

TABLE 16.4
PC25 System Performance Data

Feature	Characteristics
Rated electrical capacity	200 kW/235kVA
Voltage and frequency	480/277 V, 60 Hz, 3 phase
	400/230 V, 50 Hz, 3 phase
Fuel consumption	Natural gas: 2,050 cft/h @ 4–14" water pressure
	Anaerobic digester gas: 3200 cft/hr at 60% CH_4
Efficiency (LHV basis)	~90% Total: 40% Electrical, 50% Thermal
Emissions	<2 ppmv CO, <1 ppmv NO_x and negligible SO_x (on 15% O_2, dry basis)
Thermal energy available	
standard	900,000 Btu/hr @ 140°F
high heat options	450,000 Btu/hr @ 140°F and 450,000 Btu/hr @ 250°F
Sound profile	Conversational level (60dBA @ 30 ft.), acceptable for indoor installation.
Modular power	Flexibility to meet redundancy requirements as well as future growth in power requirements.
Flexible siting options	Indoor or outdoor installation, small footprint
Power module	
Dimensions and weight	10' × 10' × 18'; 40,000 lbs.
Cooling module	
Dimensions and weight	4' × 14' × 4'; 1,700 lbs.

cathode, they will combine with oxygen, and water and heat are obtained as by-products. The basic reactions for PAFC are the same as for PEMFC.

Currently, the only commercially available fuel power system is the 200 kW PC25™ system, produced by UTC Fuel Cells, which is a unit of United Technologies Corporation. Each unit of this system provides more than 900,000 Btu's per hour of heat, and more than 250 are already being used throughout the world. Table 16.4 presents performance data of this system.[24]

16.5 HIGH TEMPERATURE FUEL CELLS

16.5.1 Molten Carbonate Fuel Cells

The electrolyte is a mixture of lithium carbonate (~68%) and potassium carbonate (~32%), contained in a lithium-aluminum oxide ($LiAlO_2$) matrix. Hydrogen and CO are used for the electrochemical reactions, and water and CO_2 result as by-products. Catalysts are typically made of nickel.

Operation of MCFC is shown in Figure 16.16. CO_2 and O_2 are supplied at cathode, and they react with the available electrons. The resulting carbonate ions travel to the anode, where they combine with the hydrogen to produce water, CO_2, and electrons. These electrons are then forced to go back to the cathode through the external pathway to create electricity. The basic reactions for MCFC are:

$$\text{Anode: } CO_3^{2-} + H_2 \rightarrow H_2O + CO_2 + 2\,e^-$$
$$\text{Cathode: } CO_2 + \tfrac{1}{2}\,O_2 + 2\,e^- \rightarrow CO_3^{2-}$$

$$\text{Cell reaction: } H_2 + \tfrac{1}{2}\,O_2 + CO_2\ (\text{cathode}) \rightarrow H_2O + CO_2\ (\text{anode})$$

The MCFC operates at much higher temperatures (about 650°C) compared to PEMFC and PAFC, which makes it possible to process the fuel internally, thus increasing the overall efficiency of the fuel cell and minimizing emissions. They are intended to be used for power plant applications. Over the years, various attempts have been made to commercially develop plants based on MCFC. In the 1990s, companies such as MC Power and FuelCell Energy (formerly known as Energy Research Corp.) installed MCFC power plants for testing and development purposes. For example, a 2-MW unit was installed in 1996 in California by FuelCell Energy to test the design of commercial units. FuelCell Energy has recently signed a number of agreements to build several MCFC systems in the U.S., Europe, and Japan.[25]

16.5.2 Solid Oxide Fuel Cells

The least mature technology of the fuel cells, SOFCs are characterized by extremely high operating temperatures. The fuel/oxidant mixture is less restricted, compared to all the other fuel cells, owing to the high operating temperature of the cell, which allows for more combinations. Fuel can be hydrogen, CO, or CH_4, and the oxidant can be CO_2, O_2, or air; catalysts are made of perovskites materials. A solid coated zirconia oxide ceramic (Y_2O_3-stabilized ZrO_2) is used as electrolyte.

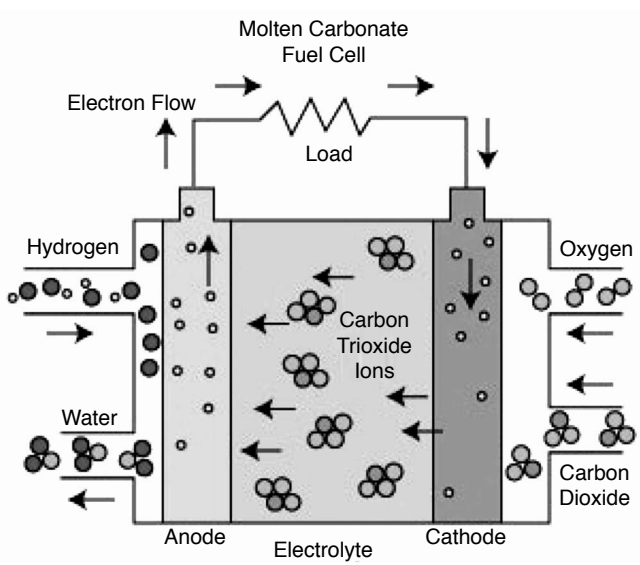

FIGURE 16.16 MCFC operation principle. (U.S. Department of Defense Fuel Cell Test and Evaluation Center, "Fuel Cell Basics," www.fctec.com/index.html.)

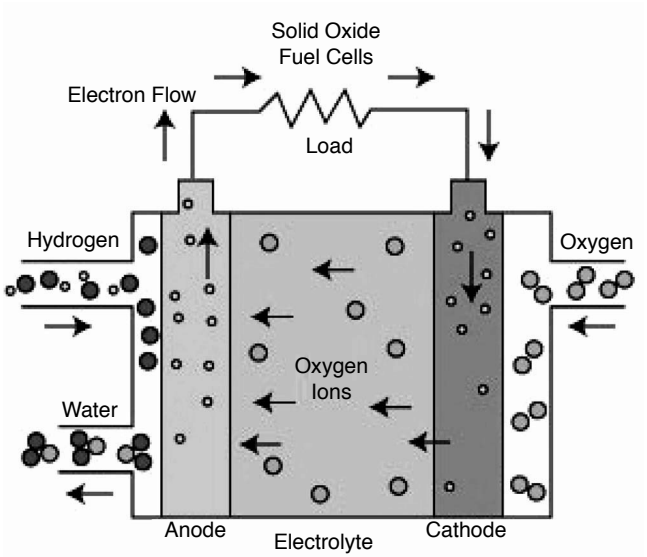

FIGURE 16.17 SOFC operation principle. (U.S. Department of Defense Fuel Cell Test and Evaluation Center, "Fuel Cell Basics," www.fctec.com/index.html.)

Operation of SOFC is shown in Figure 16.17. In this case, oxygen ions formed at the cathode from reaction of oxygen and electrons travel through the electrolyte to the anode. There they combine with fuel, creating by-products (i.e., water) and electrons. These electrons travel to the cathode through an external circuit, producing electricity. The basic reactions are:

$$\text{Anode: } 2\,H_2 + 2\,O^{2-} \rightarrow 2\,H_2O + 4\,e^-$$
$$\text{Cathode: } O_2 + 4\,e^- \rightarrow 2\,O^{2-}$$
$$\text{Cell reaction: } 2H_2 + O_2 \rightarrow 2\,H_2O$$

SOFCs are intended to be used for large power and cogeneration utilities. A number of 25-kW SOFC-based systems are already in testing, such as those developed by Siemens Westinghouse Power Corp., which operated for more than 9,000 and 13,000 h continuously. The longest operating time of more than 16,600 h was obtained in 2000 by Siemens Westinghouse with a 100-kW SOFC. After the testing period ended, the prototype was moved and restarted; it continues to operate at the Fuel Cell Pavilion at the Meteorit Park site in Germany.[26]

Currently, separate tests are being performed at the National Fuel Cell Research Center in California on a 220-kW hybrid system, which would be used in cogeneration plants. This system is based on a combination of a 200-kW fuel cell and a 20-kW gas turbine, and it is anticipated that the electrical efficiency will be around 55%.[26]

16.6 HYDROGEN PRODUCTION AND STORAGE

16.6.1 Hydrogen Production

Fuel cells operate with hydrogen-rich fuels, and either direct hydrogen or reformed fuels are typically used. Currently, industrial production of hydrogen is designed to accommodate the required supply for producing ammonia, which is largely used in agriculture as fertilizer and in oil refineries to produce automotive fuels. A number of methods can be used to obtain hydrogen, as illustrated in Figure 16.18; the most notable example is extraction from fossil fuels. Other technologies, such as water electrolysis, are employed only on a much smaller scale because of their high costs, etc.

16.6.1.1 Fossil Fuels

Hydrogen is extracted from fossil fuels through various techniques, such as steam reforming, partial oxidation (or a combination of them), and gasification.

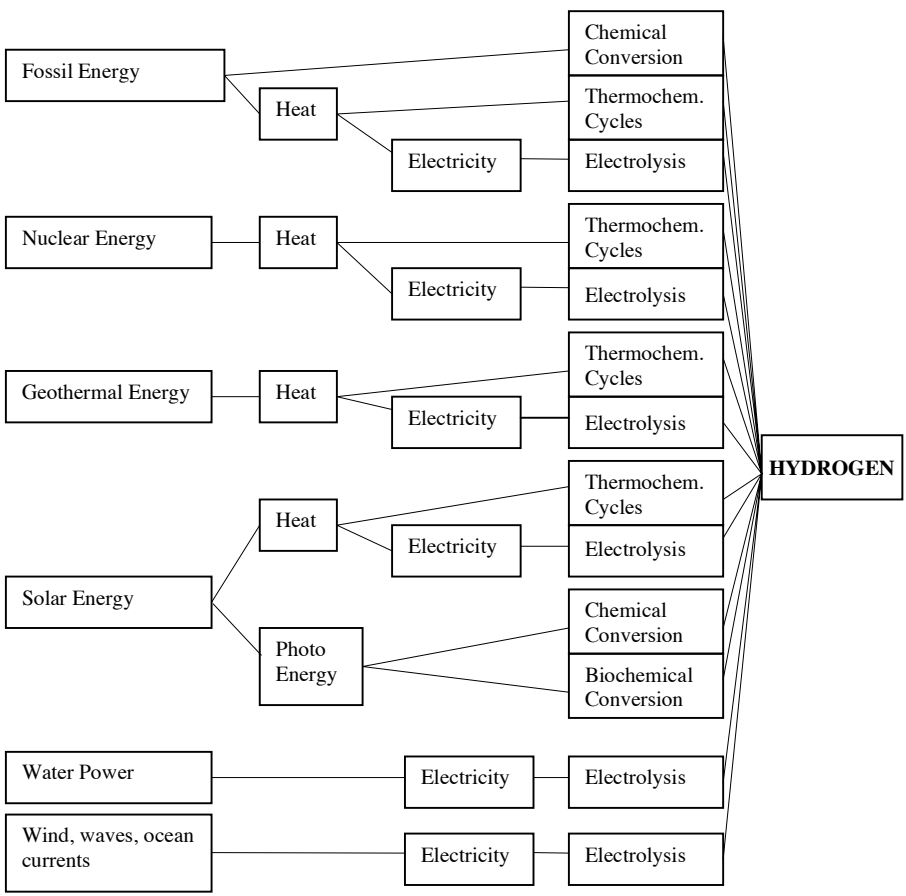

FIGURE 16.18 Hydrogen production sources.

Steam reforming is a well-established technology, which uses natural gas as feedstock. This process takes place at temperatures between 750 and 1000°C. Methane reacts with water over a catalyst (usually nickel, supported by alumina) and produces the hydrogen-rich gas that is further used by fuel cells. The overall process takes place in two steps:

- Steam reforming: $CH_4 + HO_2 \rightarrow CO + 3\ H_2$
- Shift reaction: $CO + H_2O \rightarrow CO_2 + H_2$

Methanol is also used for producing hydrogen, and the reaction takes place at temperatures between 200 and 300°C, the catalyst being made of copper, supported by zinc oxide:

- Steam reforming: $CH_3OH + H_2O \rightarrow CO_2 + 3\ H_2$
- Shift reaction: $CO + H_2O \rightarrow CO_2 + H_2$

Partial oxidation is typically used to process heavy oil fractions; the exothermic reaction in this case does not require the presence of a catalyst. If applied to natural gas or methane, presence of a catalyst becomes necessary. The following reactions for methane are given as an example:

- Partial oxidation: $CH_4 + \frac{1}{2}\,O_2 \rightarrow CO + H_2$
- Shift reaction: $CO + H_2O \rightarrow CO_2 + H_2$

The advantage of steam reforming technology is that its output has the highest hydrogen concentration compared to other technologies based on fossil fuel. However, it does not offer fast start-up and dynamic response. Partial oxidation, on the other hand, produces only low concentrations of hydrogen combined with a fast start-up and dynamic response. A natural question is thus, what would happen if we try to combine both these technologies, using the advantages of each of them? This combination is known as *autothermal reforming*, and efforts have been made to develop various reformers, such as the HotSpot fuel processor developed by Johnson Matthey.[27] Table 16.5 shows a comparison of the gas compositions obtained after using different options for the reforming process, using methanol as fuel.

TABLE 16.5
Gas Composition of Reformer Outputs

Composition (dry gas, %)	Steam Reforming	Partial Oxidation	Autothermal Reforming
H_2	67	45	55
CO_2	22	20	22
N_2	—	22	21
CO	—	—	2

Source: From Hoogers, G., Ed., *Fuel Cell Technology Handbook*, CRC Press, Boca Raton, FL, 2003. With permission.

The third technology, *coal gasification*, is achieved through coal reaction with oxygen and steam at high temperatures, and uses all types of coals for the process.

A disadvantage common to all these technologies is that one of the by-products of the reforming reactions is CO_2, a significant contributor to the environment pollution. To eliminate this, various other technologies are being developed as potential solutions for "CO_2-free" hydrogen production from fossil fuels, such as the *pyrolytic cracking* of natural gas[28]:

$$CH_4 \rightarrow C + 2\ H_2$$

16.6.1.2 Water Electrolysis

Another way of obtaining hydrogen is through water electrolysis. This technology is based on decomposition of water into hydrogen and oxygen with the help of electricity. Although its development began with the 19th century, water electrolysis has never reached the level of large-scale production because it uses electricity as input, and this has a direct impact on the overall cost of producing hydrogen. Costs associated with this technology are considerably higher than for obtaining hydrogen directly from the fossil fuels.[3] The contribution of water electrolysis technology to the total production of hydrogen represents only about 0.5%.

16.6.1.3 Other Sources

Nuclear or renewable energies are also considered potentially "CO_2-free" sources of hydrogen production.

16.6.2 Hydrogen Storage

Hydrogen storage represents one of the difficult issues associated with operation of the fuel cell systems. This is because hydrogen is characterized by low energy density and high specific energy. There are a number of technologies currently used for storage, such as liquefaction or compression. Other storage methods based on carbon nanofibers, metal hydrides, or glass microspheres are currently under investigation.

Hydrogen liquefaction can be done through several techniques. For small-scale systems, the Stirling process is considered an important solution. An alternative to the Stirling refrigerator is the magnetocaloric refrigeration process, based on the isentropic demagnetization of a ferromagnetic material near its Curie point temperature. For large-scale applications, the Claude process represents a viable economic solution.[37]

Different types of pressure cylinders or tanks are currently used for storing compressed hydrogen with a typical maximum pressure up to 30 MPa. Cylinders are made of lightweight composite materials, which reduce the overall weight of the storage. It is also proposed to design pressure cylinders or tanks with better space filling of hydrogen compared to the current solutions. A "conformable technology" has been developed by Sleegers and Thiokol Propulsion's Group, which allows storing more fuel in pressure tanks while reducing the overall tank weight. This

technology uses a combination of multicell conformable tanks located such that maximum fuel storage is obtained.[29]

Other technologies, such as hydrogen storage in solid forms, are being researched, and recent results have been reported using carbon (nanotubes, activated carbon, Fullerenes), metal hydrides, and glass microspheres. Carbon storage is a very attractive technology, which provides the overall system with high energy density, reliability, and safety. This technology is based on gas-on-solids adsorption of hydrogen, and it is being developed for small applications, in which safety and weight of the device are key characteristics.[30] Metal hydrides are another interesting option currently explored for hydrogen storage, where hydrogen reacts chemically with a metal. Table 16.6 shows the characteristics of a number of metal hydride systems. The third option, glass microspheres, takes advantage of the variation of glass permeability with temperature, and fills the microspheres with hydrogen to trap it inside.

TABLE 16.6
Hydrogen Storage Properties of Metal Hydrides

Metal Hydride System	Mg/MgH_2	Ti/TiH_2	V/VH_2	Mg_2Ni/Mg_2NiH_4	$FeTi/FeTiH_{1.95}$	$LaNi_5/LaNi_5H_{5.9}$	LH_2
Hydrogen content as mass fraction (%)	7.7	4.0	2.1	3.2	1.8	1.4	100.0
Hydrogen content by volume (kg/dm^3)	0.101	0.15	0.09	0.08	0.096	0.09	0.077
Energy content (based on HHV) (MJ/kg)	9.9	5.7	3.0	4.5	2.5	1.95	143.0
Energy content (based on LHV) (MJ/kg)	8.4	4.8	2.5	3.8	2.1	1.6	120.0
Heat of reaction (kJ/Nm^3)	3360	5600	—	2800	1330	1340	—
Heat of reaction (kJ/mol)	76.3	127.2	—	63.6	30.2	30.4	—
Heat of reaction (as fraction of HHV) (%)	26.7	44.5	—	22.2	10.6	10.6	—
Heat of reaction (as fraction of LHV) (%)	31.6	52.6	—	26.3	12.5	12.6	—

Source: From Hoogers, G., Ed., *Fuel Cell Technology Handbook*, CRC Press, Boca Raton, FL, 2003. With permission.

16.7 CURRENT PERFORMANCES

16.7.1 Operational Issues

16.7.1.1 Water and Heat Management

Although good results have been obtained using solid polymers as membranes, there are a number of issues that require special attention during PEMFC operation, such as the water and heat management. Conductivity properties are extremely sensitive to the level of hydration of membranes, and maintaining adequate humidity conditions is a challenging task. A fine balance of equilibrium has to be maintained to avoid either flooding or dehydration of the membrane. Water management depends on several factors, such as operating parameters (temperature and pressure), water content, and the presence of the impurity ions in the membranes. PEMFC typically operate efficiently at approximately 80°C at atmospheric pressure; if increased above 100°C, dehydration of the membrane occurs, and conductivity of the membrane decreases significantly. The water content depends on the water transport, which is a complex phenomenon still not very well understood. Diffusion and electro-osmosis are considered to be the processes responsible for the water transport, and various models have been developed describing the mechanism and the factors influencing it.[31–34] Impurities in membranes are due to the impurities present in the fuel or oxidant, or to the corrosion of materials, and water management can be seriously affected by their presence.[35,36]

16.7.1.2 CO Poisoning

Hydrogen-rich fuels used for fuel cells are either pure hydrogen or reformed fuel. As briefly described in Subsection 16.6.1, during the reforming process CO is produced, and trace amounts of carbon monoxide remain present in the flow fed to the electrodes. For low-temperature fuel cells using platinum catalysts, the presence of carbon monoxide even in trace levels is detrimental, with CO having an affinity for platinum and thus poisoning the catalysts. The overall performance of fuel cells deteriorates as hydrogen is blocked from reaching the catalysts. Although further fuel processing with complete removal of CO is critical for fuel cell operation, these additional processes require design modifications of the system which, in the end, translate into higher overall costs.

16.7.1.3 Hydrogen Safety

Handling of hydrogen, similar to any other flammable fuel, entails a number of hazards. Although since the Hindenburg incident in 1937 the public has considered hydrogen to be extremely dangerous, it has been demonstrated that risks associated with it are manageable and are similar to those with other gaseous fuels. Hydrogen is indeed characterized by high volatility and flammability, but it also has very low density, which means that it disperses extremely rapidly, and the ignition and detonation levels are not easily reached.

16.7.2 Cost

Despite numerous improvements over the years (i.e., reducing of the membrane thickness), the cost of the PEMFC membranes remains high, the price of Nafion

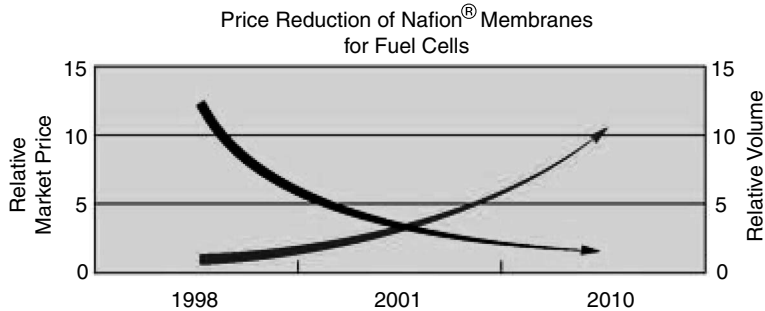

FIGURE 16.19 Price/volume trends for Nafion membranes. (From DuPont Fuel Cells, DuPont™ Nafion® Membranes and Dispersions, http://www.dupont.com/fuelcells. With permission.)

membranes, for example, being $500 to $1000 per m^2 based on quantity acquired, or approximately $100 per kW electric power.[27,37] It is estimated, however, that the cost of the membranes will decrease with the increasing of the production volume; their relative trends are shown in Figure 16.19. To achieve lower costs and improve performance of the membranes, different technologies have been investigated during the last few years. Summary descriptions of these investigations are presented in Reference 27 and 38.

16.7.3 Environmental Impact

The most attractive feature of fuel cells is their minimum impact on the environment during operation. An interesting comparison is shown in Figure 16.20, where drastic reductions in greenhouse gas emissions can be observed when comparing fuel cells with internal combustion engines. If direct hydrogen is used as primary fuel for fuel cell operation, greenhouse gas emissions are practically zero.

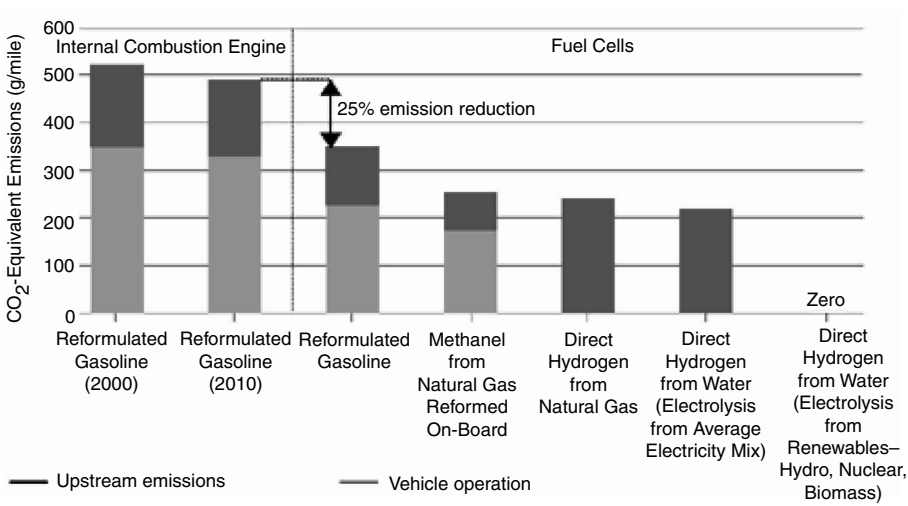

FIGURE 16.20 Greenhouse gas emissions. (Industry Canada, "Canadian Fuel Cell Commercialization Roadmap," March, 2003.

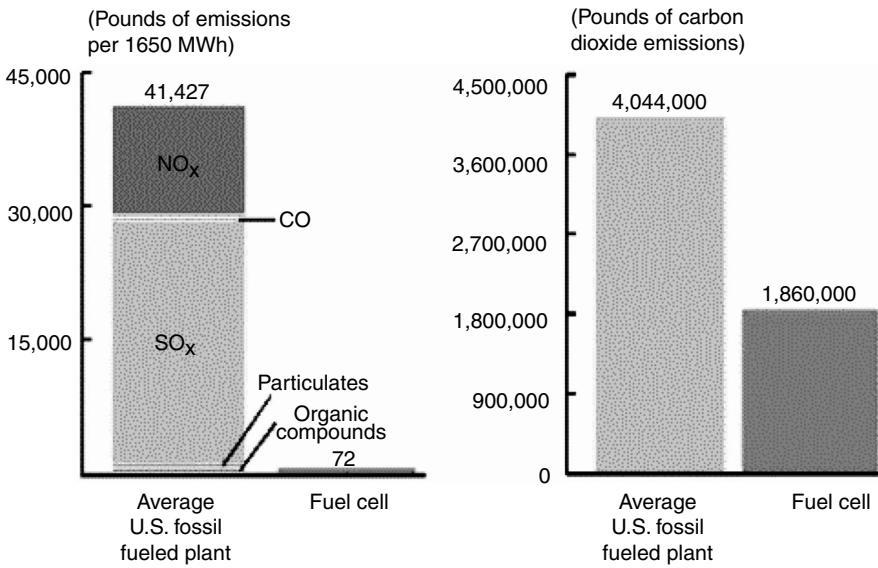

FIGURE 16.21 PC25 greenhouse emissions after 1 year of operation. (From UTC Fuel Cells, Commercial Power Systems, Experience and Proven Performance in Fuel Cell Power, http://www.utcfuelcells.com/commercial/pc25summary.shtml. With permission.)

As mentioned previously, the 200-kW PC25™ system produced by UTC Fuel Cells is the only commercially available fuel power system. It is estimated that after 1 year of operation this system will generate less than half of the total CO_2 emissions compared to an average fossil fuel plant. The remaining greenhouse emissions are estimated to be negligible compared to the same average fossil fuel plant (see Figure 16.21).

16.8 RESEARCH AND DEVELOPMENT ISSUES

Extensive efforts are currently underway to improve fuel cell performance along with a reduction of the overall cost. To achieve this, issues like theoretical modeling, finding material and design alternatives for components or the entire fuel cell, and finding viable solutions for hydrogen storage are under intense scrutiny worldwide.

The diffusion mechanism of protons through water or the membrane of PEMFC is one of the theoretical aspects that has been under evaluation over the years, numerous attempts being made to identify the best model describing the phenomenon. These models are either deterministic[39,40] or statistical approaches.[38,41] The pore structure of the membranes is assumed to have different geometries. For example, a cylindrical pore structure is used in the model described in Reference 40, with either a uniform or variable pore radius and pore-wall distribution of fixed-charges. This model is an ion/solvent model that predicts the multicomponent salt separation by ion exchange membranes. Another example of the theoretical modeling developments is the mechanism describing the transport of the proton in water (*Grotthuss mechanism*), which considers that transport is done through consecutive proton

FIGURE 16.22 Direct methanol fuel cell stack (30 units). (Department of Energy, "Direct Methanol Fuel Cell," http://www.ott.doe.gov.)

migration steps between adjacent water (H_2O) molecules.[42] Other models assume that the diffusion process of the proton is facilitated through formation of complex structures, such as $H_5O_2^+$ (two H_2O molecules sharing the same proton) and $H_9O_4^+$ (three H_2O molecules strongly bonded to the H_3O^+ core).[43–45]

New types of membranes for PEMFC that would allow operation of the fuel cells at higher temperatures are also being investigated. Improved cathodes, advanced catalysts, and optimized gas diffusion layers are among the objectives of present contracts awarded in the U.S. and elsewhere.

New types of cells are being developed, such as direct methanol fuel cells (DMFC). The DMFCs (see Figure 16.22) are basically PEMFCs with a slightly modified anode catalyst made of platinum-ruthenium, and using methanol as fuel. These fuel cells eliminate the reforming process of the hydrogen-rich fuel of PEMFC but do not eliminate the CO_2 emissions produced through chemical reactions, which are greenhouse gas contributors.

REFERENCES

1. Appleby, A.J. and Foulkes, F.R., *Fuel Cell Handbook*, Van Nostrand Reinhold, New York, 1989.
2. Larminie, J. and Dicks, A., *Fuel Cell Systems Explained*, John Wiley & Sons, Chichester, U.K., 2000.
3. Norbeck, J.M., *Hydrogen Fuel for Surface Transportation*, Society of Automotive Engineers, Warrendale, PA, 1996.
4. Stobart, R., Ed., *Fuel Cell Technology for Vehicles*, PT-84, Society of Automotive Engineers, Warrendale, PA, 2001.

5. Holcomb, F.H., How a Fuel Cell Operates, U.S. Department of Defense Construction Engineering Research Laboratories, www.dodfuelcell.com/paper2.html.
6. Penner, S.S., Ed., Commercialization of fuel cells, *Energy: Int. J.*, 20(5), Pergamon Press, New York, 1995.
7. Mehta, S.K. and Bose, T.K., Ed., *Proceedings of the Workshop on Hydrogen Energy Systems*, presented at the Official Opening of the Hydrogen Research Institute, in collaboration with Canadian Hydrogen Association, Canada, 1996.
8. European Commission, A Fuel Cell Research, Development and Demonstration Strategy for Europe up to 2005, 1998 ed., Belgium, 1998.
9. Decher, R., *Direct Energy Conversion — Fundamentals of Electric Power Production*, Oxford University Press, 1997.
10. Gottesfeld, S. and Wilson, M.S., Polymer electrolyte fuel cells as potential power sources for portable electronic devices, in *Energy Storage Systems for Electronics*, Osaka, T. and Datta, M., Eds., Gordon and Breach Science Publishers, The Netherlands, 2000.
11. DuPont Fluoroproducts, DuPont™ Nafion® PSFA Membranes N-112, N-1135, N-115, N-117, N-1110 Perfluorosulfonic Acid Polymer, Product Information NAE101, November 2002.
12. Kreuer, K.D., On the development of proton conducting materials for technological applications, *Solid State Ionics*, 97(1–15), 1997.
13. Dow Chemical, http://www.dow.com/homepage/index.html.
14. Dow Chemical, DOWEX Ion Exchange Resins — Fundamentals of Ion Exchange, Dow Liquid Separations, June 2000.
15. Wakizoe, M. et al., Analysis of proton exchange membrane fuel cell performance with alternate membranes, *Electrochim. Acta*, 40(3), 335, 1995.
16. Wilson, M.S., Valerio, J.A., and Gottesfeld, S., Low platinum loading electrodes for polymer electrolyte fuel cells fabricated using thermoplastic ionomers, *Electrochim. Acta*, 40(3), 355, 1995.
17. Thomas, S., and Zalbowitz, M., Fuel Cells — Green Power, LA–UR–99–3231, Los Alamos National Laboratory, 1999.
18. Hoogers, G., Ed., *Fuel Cell Technology Handbook*, CRC Press, Boca Raton, FL, 2003.
19. Fuel Cells 2000, Transportation Fuel Cells — Technical Info, www.fuelcells.org.
20. Perry, M.L. and Fuller, T.F., A historical perspective of fuel cell technology in the 20th century, *J. Electrochem. Soc.*, 149(7), S59, July 2002.
21. Cabot, P.L., Guezala, E., Calpe, J.C., García, M.T., and Casado, J., Application of Pd-based electrodes as hydrogen diffusion anodes in alkaline fuel cells, *J. Electrochem. Soc.*, 147(1), 43, January 2000.
22. Kordesch, K. and Simader, G., *Fuel Cells and Their Applications*, John Wiley & Sons, New York, March 1996.
23. Kordesch, K. et al., Intermittent use of a low-cost alkaline fuel cell-hybrid system for electric vehicles, *J. Power Sources*, 80, 190, 1999.
24. UTC Fuel Cells, Commercial Power Systems, Experience and Proven Performance in Fuel Cell Power, http://www.utcfuelcells.com/commercial/pc25summary.shtml.
25. U.S. Department of Energy, Fuel Cell Technology — Molten Carbonate Fuel Cells, http://www.fe.doe.gov/coal_power/fuelcells/fuelcells_moltencarb.shtml.
26. U.S. Department of Energy, Fuel Cell Technology — Solid Oxide Fuel Cells, http://www.fe.doe.gov/coal_power/fuelcells/fuelcells_sofc.shtml.
27. Hoogers, G., Ed., *Fuel Cell Technology Handbook*, CRC Press, Boca Raton, FL, 2003.
28. Pohl, H.W., Ed., *Hydrogen and Other Alternative Fuels for Air and Ground Transportation*, John Wiley & Sons, Germany, 1995.

29. Sleegers Group, http://www.sleegers.on.ca/index.htm.
30. Workshop on Storage of Hydrogen on Carbon Nanostructured Materials: held at Institut de Recherche sur l'Hydrogene Trois-Rivieres, Canada, 2000.
31. Janssen, G.J.M., A phenomenological model of water transport in a proton exchange membrane fuel cell, *J. Electrochem. Soc.*, 148(12), A1313, 2001.
32. Motupally, S. et al., Diffusion of water in Nafion 115 membranes, *J. Electrochem. Soc.*, 147(9), 3171, 2000.
33. Zawodzinski, T.A., Jr., Springer, T.E., Davey, J., Lopez, R.C., Valerio, J., and Gottesfeld, S., A comparative study of water uptake by and transport through ionomeric fuel cell membranes, *J. Electrochem. Soc.*, 140(7), 1981, July 1993.
34. Nguyen, T.V. and White, R.E., A water and heat management model for proton-exchange-membrane fuel cells, *J. Electrochem. Soc.*, 140(8), 2178, August 1993.
35. Okada, T., Theory for water management in membranes for polymer electrolyte fuel cells — Part 1: The effect of impurity ions at the anode side on the membrane performances, *J. Electroanal. Chem.*, 465, 1, 1999.
36. Okada, T., Theory for water management in membranes for polymer electrolyte fuel cells — Part 2: The effect of impurity ions at the cathode side on the membrane performances, *J. Electroanal. Chem.*, 465, 18, 1999.
37. DuPont Fuel Cells, DuPont™ Nafion® Membranes and Dispersions, http://www.dupont.com/fuelcells.
38. Paddison, S.J., The modeling of molecular structure and ion transport in sulfonic acid based ionomer membranes, *J. New. Mater. Electrochem. Syst.*, 4, 197, 2001.
39. Thampan, T., Malhotra, S., Tang, H., and Datta, R., Modeling of conductive transport in proton–exchange membranes for fuel cells, *J. Electrochem. Soc.,* 147(9), 2000.
40. Pintauro, P.N. and Yang, Y., Mathematical Analysis of Transport in Ion–Exchange Membranes, in *Tutorials in Electrochemical Engineering — Mathematical Modeling*, Electrochemical Society Proceedings Vol. 99–14, Eds., Savinell, R.F., Fenton, J.M., West, A., Scanlon, S.L., and Weidner, J.W., The Electrochemical Society, Inc., 1999.
41. Paddison, S.J., Paul, R., and Zawodzinski, T.A., Jr., A statistical mechanical model of proton and water transport in a proton exchange membrane, *J. Electrochem. Soc.,* 147, 2000.
42. de Grotthuss, C.J.T., Sur la Décomposition de l'Eau et des Corps qu'Elle Tient en Dissolution à l'Aide de l'Électricité Galvanique, *Ann. Chim.*, LVIII, 1806.
43. Zundel, G., *The Hydrogen Bond — Recent Developments in Theory and Experiments. II. Structure and Spectroscopy*, Schuster, P., Zundel, G., and Sandorfy, C., Eds., North-Holland, Amsterdam, 1976.
44. Eigen, M., Proton transfer, acid-base catalysis and enzymatic hydrolysis, *Angew. Chem. Int. Ed. Engl.*, 3, 1964.
45. Marx, D., Tuckerman, M.E., Hutter, J., and Parrinello, M., The nature of the hydrated excess proton in water, *Nature*, 397, 1999.
46. EG&G Services, Parsons, Inc. and Science Applications International Corporation, Fuel Cell Handbook (Fifth Edition), Contract No. DE–AM26–99FT40575, for U.S. Department of Energy, October 2000.